DOCUMENTOS CONGRESUALES

Climate Change Perspectives from the Atlantic:

Past, Present and Future

JOSÉ MARÍA FERNÁNDEZ-PALACIOS,
LEA DE NASCIMENTO,
JOSÉ CARLOS HERNÁNDEZ,
SABRINA CLEMENTE
ALBANO GONZÁLEZ &
JUAN P. DÍAZ-GONZÁLEZ (eds.)

Climate Change Perspectives from the Atlantic:

Past, Present and Future

Climate Change Perspectives from the Atlantic:

Past, Present and Future

EDITED BY
José María Fernández-Palacios, Lea de Nascimento,
José Carlos Hernández, Sabrina Clemente,
Albano González & Juan P. Díaz-González

SERVICIO DE PUBLICACIONES
UNIVERSIDAD DE LA LAGUNA, 2013

CLIMATE change perspectives from the Atlantic : past, present and future / Edited by José María Fernández-Palacios ... [et al.]. – 1ª ed. – La Laguna : Servicio de Publicaciones, Universidad de La Laguna, 2013. – 727 p. : il. col. ; 24 cm. – (Documentos congresuales ; 33)
Bibliografía por cap.
D.L. TF 911-2013. – ISBN 978-84-15910-54-1
1. Climatología-Cambios-Atlántico (Región) 2. Climatología-Cambios-Aspectos ambientales I. Fernández-Palacios, José María (1958-), (ed.) II. Universidad de La Laguna. Servicio de Publicaciones III. Serie
551.583

Colección:
DOCUMENTOS CONGRESUALES/33

Edita:
Servicio de Publicaciones
UNIVERSIDAD DE LA LAGUNA
Campus Central
38200 La Laguna. Santa Cruz de Tenerife
Teléfono: 34 922 31 91 98

Diseño Editorial:
Jaime H. Vera
Javier Torres. Cristóbal Ruiz

1ª Edición 2013

Maquetación y preimpresión:
SERVICIO DE PUBLICACIONES

Impresión:
FABRICACIÓN CANARIA DEL DISCO, S.L.

I.S.B.N.: 978-84-15910-54-1
Depósito Legal: TF 911-2013

INDEX

PAST: MACARONESIAN PALAEOCLIMATE

CHAPTERS

PRESENT: RESPONSES OF KEY SEA URCHIN POPULATIONS TO CLIMATE CHANGE PROCESSES: FROM LARVAE TO ECOSYSTEMS

CHAPTERS: http://ullmedia.udv.ull.es/view_collection.php?cid=33&type=videos

ABSTRACTS

FUTURE: CORDEX WEATHER RESEARCH AND FORECASTING

CHAPTERS

ABSTRACTS

FOREWORD

Two major challenges are faced by Mankind on the 21st century: human beings' health, in a broad sense —from disease to poverty—, and, the health of the planet —from the more specific problem, such as waste management, to the more general, such as global warming. Mankind attempts to manage them with a single tool: science.

The Tri-continental Atlantic Campus, Regional Campus of International Excellence «CEI Canarias» (Canary Islands CIE) has given us the opportunity to approach both challenges. This book records what is possibly most significant for future generations: the health of the planet. Approaching this problem from a region such as the Canary Islands —a paradigm of biodiversity— teaches us all what we will lose, what we must not neglect, and what we have to preserve.

Talking about the economic crisis —with the fall of the countries that we have witnessed during this decade—, talking about a humanitarian crisis —with the terrible tragedies that immigration or wars show us day after day—, and not getting all to talk at once about planetary crisis —with regards to what we are doing to our living environment— is a sign of selfishness that we cannot afford. Only relying on science can save us, because saving the future for our offspring will be our own salvation.

This book is a compendium of science. A present full of knowledge, generated by Mankind to help us; with a look at the present moment, back and forth in time, a look at what we were —and what we can become— if we don't pay attention to science. I highly value as an achievement being able to offer such a large and varied range of reflections –at a time when economy, social differences and politics seems to be the only thing that citizens are interested on.

The year 2012 was a hive of ideas for the Canary Islands CIE. The Canary Islands draw the attention of scientists between October and November. For a time, they met with the idea of looking at the sky, land and sea, and wonder what is happening, why happened and what will happen. In addition, what pleases scientists best: to share knowledge and experience.

Sitting all scientists who attended these three workshops in the same room meant, for the author of these lines, a pleasure that makes up for everything that's bad with academic administration. Having the opportunity to help science grow is a luxury available to few: from the land where one had the privilege to be born, where we want our offspring to live, and where future generations require us to act with prudence and responsibility. This wonderful land does not deserve what we are doing to her.

I hope, and that's also my wish, that the result of these meetings —gathered in this volume— will provide the reader with enough satisfaction to meet their expectations, their thirst for knowledge and will open the door to find out more.

Finally, I cannot fail to mention the work of the editors. I greatly appreciate their effort to organize these workshops; to be able to combine interests of scientists from all continents; to concentrate in this Atlantic garden so much talent and passion for science —and make it accessible to the entire scientific community through this publication. It was an honour to support these projects from the beginning, to let me present them, to welcome all participants, and now, to author these forewords.

Rodrigo TRUJILLO GONZÁLEZ
Vice-chancellor of Internationalization and Excellence
Universidad de La Laguna
November, 2013

INTRODUCTION

Within the framework of the *Campus de Excelencia Internacional* (CEI), an award given by the Spanish Education Ministry to the University of La Laguna (Tenerife, Spain) for the period 2010–2012, the Atlantic Centre of Environmental and Climate Change Research [*Centro de Investigaciones Medio Ambientales y del Cambio Climático del Atlántico (CIMACCA)*] was launched. Among other activities, in autumn 2012, three different scientific workshops dealing, respectively, with the past, present and future impacts of climate change took place.

WORKSHOP I: PERSPECTIVES FROM THE PAST

This workshop, entitled «First Macaronesian Palaeoclimate Workshop», organized by the Island Ecology and Biogeography Group of the University of La Laguna took place between the 24th and 27th of October 2012. It was held in a charming venue; the historical building that houses the Vice-Rector's Office for Internationalization and Excellence of the University of La Laguna in *Poeta Viana* street, in the centre of this UNESCO World Heritage city. The main goal of this Workshop was to get together to facilitate contacts and promote discussion among scientists and researchers, who although involved in different lines of research, all have a common interest in the reconstruction of the ancient (i.e., the Last Glaciation Cycle, from 130 ka to the Holocene) climate of the Macaronesian Biogeographical Region *sensu lato*, including the oceanic archipelagos of Azores, Madeira, the Canary Islands and Cape Verde, as well as the Western Mediterranean Area (Iberian Peninsula and North Africa).

We managed to bring together some 30 researchers from different institutions and countries (Australia, Belgium, France, Germany, Portugal, Spain, Netherlands, and United Kingdom) with research profiles that included palaeoecologists, geomorphologists, palaeontologists, palaeoclimatologists, palaeobiogeographists, etc. This yielded a very multi- and trans-disciplinary workshop, specially designed for the discussion among specialists about the ancient climate of the North Eastern Atlantic Region.

The workshop was scheduled over three days (plus post-workshop excursion). Half the time was used for presentations of research works that we include in this book. The second half of the workshop was used for the discussion of several questions regarding our current knowledge, certainties and uncertainties, and especially our lack of knowledge regarding the Macaronesian palaeoclimate. These topics were selected by all the participants following a participatory appraisal methodology (de Nascimento *et al.*, 2013).

The presentations dealt with either the whole Macaronesian realm (Hooghiemstra *et al.*, 2013; Rijsdijk *et al.*, 2013) or with palaeoevidence extracted from different individual islands of specific archipelagos, such as Santa María (Ávila, 2013), and Pico and Flores (Connor *et al.*, 2013) in the Azores; La Palma (Rubiales *et al.*, 2013), La Gomera and Tenerife (Nogué *et al.*, 2013), Fuerteventura and Lanzarote (Criado *et al.*, 2013; von Suchodoletz *et al.*, 2013; Yanes *et al.*, 2013) in the Canary Islands, or finally Sal (Cabero *et al.*, 2013) in Cape Verde. In addition, other palaeoevidence from mainland territories off Macaronesia, such as the Atlas Chain in Morocco (Cheddadi, 2013) or the Western Mediterranean Alborán Sea Basin (Martínez-Ruiz *et al.*, 2013) were presented.

In these contributions, different proxies that may shed light on the reconstruction of the Last Glaciation Cycle's palaeoclimate in the Macaronesian realm were used, including fossil pollen assemblages (Cheddadi, 2013; Connor *et al.*, 2013; Hooghiemstra *et al.*, 2013; Nogué *et al.*, 2013), woody macrofossils (Rubiales *et al.*, 2013), palaeosoils and palaeodunes stratigraphy (Criado *et al.*, 2013; von Suchodoletz *et al.*, 2013), marine (Ávila, 2013; Cabero *et al.*, 2013) or terrestrial fossils (Yanes *et al.*, 2013) gastropods assemblages, archipelagos geographic configuration hindcasting models (Rijsdijk *et al.*, 2013) or the geochemical composition of submarine sediments (Martínez-Ruiz *et al.*, 2013).

In relation to the temporal framework, several of the contributions focused on the entire Last Glaciation Cycle (Ávila, 2013; Cabero *et al.*, 2013; Martínez-Ruiz *et al.*, 2013; Rijsdijk *et al.*, 2013; von Suchodoletz *et al.*, 2013; Yanes *et al.*, 2013); whereas others referred exclusively to the Holocene climatic variation (Cheddadi, 2013; Connor *et al.*, 2013; Hooghiemstra *et al.*, 2013; Nogué *et al.* 2013; Rubiales *et al.*, 2013) or even to historical times (Criado *et al.*, 2013).

Finally, two additional and very interesting presentations were also part of the scientific content in this workshop, the first of them by Kathy J. Willis (University of Oxford) was the introductory presentation, entitled, «Biodiversity futures: Scenario setting for Africa using lessons from the past» and a further contribution by Francisco la Roche and Carolina Castillo (University of La Laguna) entitled, «Environmental meaning of the faunistic changes detected in the Quaternary of the Canary Islands».

One of the main goals of the organizers of this First Macaronesian Palaeoclimate Workshop was to launch a scientific initiative that would have continuity in the near future. We hope this will become a reality within the next few years!

WORKSHOP II: PERSPECTIVES IN THE PRESENT

This workshop focused on how climate change processes are currently affecting marine ecosystems and was entitled, «Responses of Key Sea Urchin Populations to Climate Change Processes: From Larvae to Ecosystems». This international meeting was organized by the Biodiversity, Marine Ecology and Conservation Research Group of the University of La Laguna and was held in the Canary Islands from 14th to 18th November 2012. The organizing committee came up with a dynamic venue consisting of a two-day meeting held at the University of La Laguna (conference rooms at the Faculty of Physics) on the island of Tenerife, followed by a two-day trip to El Hierro island (Restingolita Museum conference room, La Restinga). Activities included plenary conferences, short presentations, field trips and post-presentation discussions. In order to assess such a broad subject as the effects of climate change processes on marine ecosystems, we focused on recent knowledge about the influence of climate-related variables on the dynamics of habitat modifier species in coastal environments. Given that sea urchin-generated barren grounds are a global phenomenon of general concern for the conservation of marine ecosystems and their services worldwide, the main goal of the workshop was to bring together researchers working on different issues of the influence of environmental change on the biology and ecology of these key species.

Since the very first announcement of this workshop, it attracted the attention of both the national and international research communities in the field. The event brought together 34 researchers from 15 research institutions from all around the world (Australia, Canada, Japan, Mexico, Norway, Panama, Puerto Rico, Sweden, Spain and USA). These researchers had a wide area of expertise ranging from the impact of global changes on sea urchin larval ecophysiology (Dupont and Thorndyke, 2013) to ecosystem dynamics (Hernández *et al.*, 2013). It also included the assessment of baseline data of how populations change in response to natural and anthropogenic causes (Ebert, 2013) on the basis of both long-term data on population parameters and genetic diversity of populations (Lessios, 2013); causes and consequences of recurrent mass mortality events (Scheibling *et al.*, 2013); geographical range expansions (Ling, 2013); as well as forces acting on different temporal scales that drive changes in urchin populations in highly conserved marine protected areas (Hereu *et al.*, 2013). It is also worth highlighting the participation of about 20 undergraduate students from the University of La Laguna, who registered for the event and attended the conference.

The workshop was structured into six plenary talks from invited speakers plus one video-conference (thanks to the technical assistance of ULL-media department), all of them are included as full papers in this book, followed by eight short oral communications, which we are presenting as abstracts. The rest of the workshop was devoted to two field trips, where participants had the opportunity to dive both at an urchin barren off the coast of Tenerife and at an algae-dominated system at El Hierro island. Field trips provided a quick view of how marine ecosystems work in the eastern Atlantic Islands (Canary Islands) and facilitated discussion about general patterns of the functioning of these alternative states in benthic ecosystems and common processes with other regions worldwide. The workshop in El Hierro ended with a general discussion on the main conclusions and with the commitment of writing an opinion paper about them. An early result of this workshop is the publication of some of the field data regarding catastrophic changes in temperate benthic communities (urchin barrens *vs.* macroalgae stands) as an invited paper that will be published in the journal *Philosophical Transaction of the Royal Society B: Biological Sciences* during this year (Ling *et al.,* 2014).

Plenary talks dealt with populations of several sea urchin species and the influence of climate change on several aspects of their dynamics: population fluctuations of *Strongylocentrotus droebachiensis* on the east coast of North America (Scheibling *et al.*, 2013); *Strongylocentrotus purpuratus* on the west coast of North America (Ebert, 2013); *Paracentrotus lividus* and *Arbacia lixula* in the Mediterranean (Hereu *et al.*, 2013); *Centrostephanus rodgersii* in Tasmania (Ling, 2013); *Diadema africanum* in the Canary Islands (Hernández *et al.*, 2013) and other sea urchin species (Lessios, 2013). Short presentations focused on several specific topics such as the effect of sea water warming on sea urchin recruitment in the north-eastern Atlantic Ocean (Fagerli *et al.*, 2013), the effect of different climatic events on population fluctuations of *Strongylocentrotus nudus* in Japan (Fujita, 2013), phylogeographic and past demographic patterns of *Arbacia lixula* in the Mediterranean Sea (Wangensteen *et al.*, 2013), recent sea urchin diseases in the eastern Atlantic Archipelagos (Lorenzo-Morales, 2013), as well as effects of ocean acidification and warming on *Paracentrotus lividus* fertilization and larvae development at its southernmost limit of distribution in the Canary Islands (García *et al.*, 2013). Finally, a special session of the workshop was devoted to the effects of the recent underwater volcanic eruption in El Hierro as examples of natural experiments to elucidate the effects of global change on benthic assemblages (Haroun *et al.*, 2013; Clemente *et al.*, 2013; Navarro *et al.*, 2013).

The general aim of all contributions was to collect existing data and evidence about the nature of fluctuations in sea urchin dynamics that drive alternative community states in marine systems, and to elucidate whether current knowledge permits any predictions regarding the future of echinoid populations under the current ocean global change scenario.

We hope everyone enjoyed the workshop «Responses of Key Sea Urchin Populations to Climate Change Processes: From Larvae to Ecosystems» as well as its compendium of proceedings, which included a fascinating foreword by Dr. J.M. Lawrence (Department of Integrative Biology, University of South Florida). We also hope this initiative provides a forum for critical reflection on the effects of climate change processes on benthic ecosystems for future actions.

WORKSHOP III: PERSPECTIVES FOR THE FUTURE

Finally, the third workshop, focusing on the regional modelling of the climate change and entitled «First CORDEX-WRF Workshop and CORWES/WRF4G hands-on tutorial», was organized by the Group of Observation of Earth and Atmosphere (GOTA, University of La Laguna), Santander Meteorological Group (University of Cantabria) and Group of Regional Modelling of Atmosphere (University of Murcia). The workshop and the tutorial took place in the School of Computer Science, University of La Laguna, from 1st to 5th October 2012. This meeting was organized in close collaboration with the research projects «Coordinated regional climate downscaling experiment using WRF: a contribution to the CORDEX initiative by the Spanish WRF community» and «High resolution climate regionalization and aerobiological analysis for the Canary Islands» (projects funded by the Spanish Ministry of Economy and Competitiveness, ref: CGL2010-21366-C04-01/CLI and CGL2010-22158-C02, respectively). The Insular Government of the Island of Tenerife also collaborated in the development of this event.

The conference consisted of two different parts. The first (1st-3rd October) was devoted to a review of the status and main issues of regional climate modelling using WRF. It included both invited and contributed papers, and aimed to foster open discussions in a friendly environment. The second segment (4th-5th October) consisted of hands-on laboratory sessions for training in WRF management frameworks, such as WRF for GRID (WRF4G), WRF code modifications for regional climate purposes like Climate WRF (CLWRF) and post-processing tools.

The main goal of the workshop was to bring together scientists using the WRF model in the CORDEX initiative or, more generally, using it as a dynamical downscaling tool in climate modelling. At all times, knowledge transfer and coordination among research groups using WRF was encouraged, both through presentations and a social program. The main task was to produce a rigorous state-of-the-knowledge framework to improve the coordination of the different efforts for every CORDEX region and engage in collaboration. The following aspects were highlighted:

- Current state of the simulations in the different regions
- Coordination needs
- State of database
- Common problems to be addressed and future plans
- Tools and data to be shared
- Synergies between different user communities: modelling, impacts, policymakers...

The program sessions were organized following the Coordinated Regional Climate Downscaling Experiment (CORDEX) regions. Keynote speakers presented either the main results of their own research or a review of recent results.

The efforts of coordination of the CORDEX-Africa community and the preliminary results were presented by Chris Lennard (Lennard *et al.*, 2013), with special emphasis on analysing CORDEX data for integration into community impacts. The use of WRF-ARW to simulate an extreme case that occurred in January 2002 on the Africa western coast, causing huge damage in Senegal and Mauritania, was presented by A. Sarr (Sarr, 2013). The discussion on current problems with modelling clouds was also a key point. Comparisons, in the Africa-CORDEX domain, between cloud cover data obtained from ISCCP and CRU databases, reanalysis of NCEP/DOE AMIP-II, ERA-40 and ERA-Interim data, and different simulation results from global climate models included in the Coupled Model Intercomparison Project Phase 5 (CMIP5) were presented by the Group of Observation of Atmospheres and Earth (GOTA) of the University of La Laguna (Pérez *et al.*, 2013).

Applications of dynamical downscaling to topographically complex archipelagos were discussed by Yuqing Wang, who talked about the configuration of the Weather Research and Forecasting model as a dynamical downscaling tool for the Hawaiian region and presented an evaluation of the model's performance based on a continuous ten-year simulation forced by observed boundary conditions with 3-km horizontal grid spacing (Wang *et al.*, 2013).

Lluis Fita presented the initiative, NSW/ACT Regional Climate Modelling project, which aims to provide a comprehensive dynamically downscaled climate dataset for the CORDEX-Austral Asia region at 50km, and South-East Australia at a resolution of 10km. These data will be used by governments to design their climate change adaptation plans (Fita *et al.*, 2013).

The situation in the CORDEX initiative in South America was presented by Silvina A. Solman, who summarized the progress achieved over the last decade on regional climate modelling activities over South America. The remaining challenges in modelling South American climate features were also discussed (Solman, 2013).

The situation for the Coordinated Downscaling Experiment in Europe (EURO-CORDEX) was presented by Kirsten Warrach-Sagi, who showed the results of an ensemble of regional climate model simulations at spatial resolutions of 0.11°, 0.22° and 0.44°, completed in 2012 (Kirsten *et al.*, 2013). The development of the project named EC-EARTH (see http://ecearth.knmi.nl) and the applications over Ireland to provide dynamically downscaled RCM output data for use in other disciplines such as biodiversity mapping, forestry pest and disease control, water resource management, etc., was presented by R.F. Teck (Teck and Sweeney, 2013). Results from the hindcast simulation 1990–2008 performed with the WRF3.3.1 model within the framework of the EURO-CORDEX initiative and the comparison with the E-OBS observational dataset for two key climatic variables, 2m temperature and precipitation were discussed by E. Katragkou (Katragkou *et al.*, 2013). Dynamical downscaling simulations using the PRECIS (Providing Regional Climates for Impact Studies) regional climate model, based on the United

Kingdom (UK) Met Office Hadley Centre HadRM3P model for the 20th and 21st centuries, in the eastern Mediterranean and the Middle East regions were also discussed (Zittis *et al.*, 2013)

Other activities, connected with the above presentations, were the discussion sessions for the coordination of the different CORDEX domains and the definition of strategies to solve previously detected common problems as well as the definition of a matrix of configurations, access to the GCM data, validations datasets, post-processing tools, etc.

In conclusion, we wish to thank all those who attended this event and that the presentations and contacts you made will be of value to you. We hope you have fond memories of these workshops, and consider that they were fruitful both personally as well as professionally. Finally, for the readers of this book, we sincerely hope you find its contents interesting.

J.M. Fernández-Palacios, L. de Nascimento,
J.C. Hernández, S. Clemente,
A. González & J.P. Díaz-González

PAST:
MACARONESIAN PALAEOCLIMATE

LIST OF AUTHORS

María R. Alonso
Departamento de Biología Animal, Faculty of Biology, University of La Laguna,
Avda. Astrofísico Francisco Sánchez, s/n, 38206 La Laguna, Canary Islands, Spain.

Sérgio P. Ávila
Facultade de Ciências da Universidade do Porto, Portugal.
Centro de Investigação em Biodiversidade e Recursos Genéticos (CIBIO), InBIO
Laboratório Associado, Pólo dos Açores, Açores, Portugal.
Departamento de Biologia, Universidade dos Açores, 9501-801 Ponta Delgada,
Açores, Portugal.
MPB-Marine PalaeoBiogeography Working Group of the University of the Azores,
Rua da Mãe de Deus, 9501-801 Ponta Delgada, Açores, Portugal.
E-mail: avila@uac.pt

Cláudia Baider
The Mauritius Herbarium, R.E. Vaughan Building, Ministry of Agro-Industry and
Food Security, Réduit, Mauritius.

Juan Antonio Ballesteros-Cánovas
Departamento de Investigación y Prospectiva Geocientífica, Instituto Geológico
y Minero de España, Ríos Rosas 23, 28003 Madrid, Spain.

Teresa Bardají
Departamento de Geología, Universidad de Alcalá, Edificio de Ciencias, Campus
Externo, Carretera A-II km 33,600, 28871 Alcalá de Henares, Madrid, Spain.

Luis A. Bermejo
Department of Agricultural Engineering, Production and Economy, Technical
School of Agricultural Engineering, University of La Laguna, Carretera de Geneto
nº 2, 38201 La Laguna, Canary Islands, Spain.

José Bethencourt
Department of Geography, Faculty of Geography and History, University of La
Laguna, Campus de Guajara, s/n, 38071 La Laguna, Canary Islands, Spain.

ANA CABERO
Facultad de Ciencias, Universidad Nacional de Educación a Distancia UNED, Paseo Senda del Rey nº 9, 28040 Madrid, Spain.
E-mail: acabero@ccia.uned.es

RACHID CHEDDADI
Institut des Sciences de l'Évolution (ISEM), CNRS UMR 5554, Université de Montpellier II, Place Eugène Bataillon F-34095 Montpellier, France.
E-mail: rachid.cheddadi@um2.fr

SIMON E. CONNOR
Centro de Investigação Marinha e Ambiental, FCT Campus Gambelas, Universidade do Algarve, 8005-139 Faro, Portugal.
E-mail: sconnor@ualg.pt

CONSTANTINO CRIADO
Department of Geography, Faculty of Geography and History, University of La Laguna, Campus de Guajara, s/n, 38071 La Laguna, Canary Islands, Spain.
E-mail: ccriado@ull.es

CRISTINO J. DABRIO
Departamento de Estratigrafía, Facultad de Ciencias Geológicas, Universidad Complutense, José Antonio Novais, 12, 28040 Madrid, Spain.

ERIK DE BOER
Institute for Biodiversity and Ecosystem Dynamics, University of Amsterdam, Science Park 904, 1098 XH Amsterdam, The Netherlands.

LEA DE NASCIMENTO
Island Ecology and Biogeography Group, Instituto de Enfermedades Tropicales y Salud Pública de Canarias (IUETSPC), University of La Laguna, Avda. Astrofísico Francisco Sánchez, s/n, 38206 La Laguna, Canary Islands, Spain.
E-mail: leadenas@ull.es

ANDRÉS DÍEZ-HERRERO
Departamento de Investigación y Prospectiva Geocientífica, Instituto Geológico y Minero de España, Ríos Rosas 23, 28003 Madrid, Spain.

PEDRO DORTA
Department of Geography, Faculty of Geography and History, University of La Laguna, Campus de Guajara, s/n, 38071 La Laguna, Canary Islands, Spain.

Dominik Faust
Institute of Geography, University of Technology Dresden, Helmholtzstrasse 10, D–01069 Dresden, Germany.

Silvia Fernández-Lugo
Island Ecology and Biogeography Group, Instituto de Enfermedades Tropicales y Salud Pública de Canarias (IUETSPC), University of La Laguna, Avda. Astrofísico Francisco Sánchez, s/n, 38206 La Laguna, Canary Islands, Spain.

José María Fernández-Palacios
Island Ecology and Biogeography Group, Instituto de Enfermedades Tropicales y Salud Pública de Canarias (IUETSPC), University of La Laguna, Avda. Astrofísico Francisco Sánchez, s/n, 38206 La Laguna, Canary Islands, Spain.

F.B. Vincent Florens
Department of Biosciences, Faculty of Science, University of Mauritius, Réduit, Mauritius.

David Gallego-Torres
Instituto Andaluz de Ciencias de la Tierra (CSIC-UGR), Avda. de Las Palmeras nº4, 18100 Armilla, Granada, Spain.
Departamento de Mineralogía y Petrología, Facultad de Ciencias, Universidad de Granada, Campus Fuentenueva s/n, E-18002 Granada, Spain.

Mar Génova
Escuela de Ingeniería Forestal y del Medio Natural, Universidad Politécnica de Madrid, Ciudad Universitaria s/n, 28040 Madrid, Spain.

Bassam Ghaleb
GEOTOP, Université du Québec à Montréal (UQAM), Succ. Centre-Ville, H3C 3P8 Montréal, Québec, Canada.

José Á. González-Delgado
Departamento de Geología, Facultad de Ciencias, Universidad de Salamanca, Plaza de los Caídos, s/n, 37008 Salamanca, Spain.

José L. Goy
Departamento de Geología, Facultad de Ciencias, Universidad de Salamanca, Plaza de los Caídos, s/n, 37008 Salamanca, Spain.

Tom Hengl
Global Soil Information Facilities ISRIC, Droevendaalsesteeg 3, 6708 PB Wageningen, The Netherlands.

ALEXANDRA HILGERS
Institute of Geography, University of Cologne, Albertus-Magnus-Platz, D–50923 Köln, Germany.

CLAUDE HILLAIRE-MARCEL
GEOTOP, Université du Québec à Montréal (UQAM), Succ. Centre-Ville, H3C 3P8 Montréal, Québec, Canada.

HENRY HOOGHIEMSTRA
Institute for Biodiversity and Ecosystem Dynamics, University of Amsterdam, Science Park 904, 1098 XH Amsterdam, The Netherlands.
E-mail: H.Hooghiemstra@uva.nl

MIGUEL IBÁÑEZ
Departamento de Biología Animal, Faculty of Biology, University of La Laguna, Avda. Astrofísico Francisco Sánchez, s/n, 38206 La Laguna, Canary Islands, Spain.

FRANCISCO J. JIMÉNEZ-ESPEJO
Instituto Andaluz de Ciencias de la Tierra (CSIC-UGR), Avda. de Las Palmeras nº 4, 18100 Armilla, Granada, Spain.

PETR KUNEŠ
Department of Botany, Faculty of Science, Charles University in Prague, Benátská 2, CZ-128 01 Praha 2, Czech Republic.

JAVIER LARIO
Facultad de Ciencias, Universidad Nacional de Educación a Distancia UNED, Paseo Senda del Rey nº 9, 28040 Madrid, Spain.

FRANCISCA MARTÍNEZ-RUIZ
Instituto Andaluz de Ciencias de la Tierra (CSIC-UGR), Avda. de Las Palmeras nº4, 18100 Armilla, Granada, Spain.
E-mail: fmruiz@ugr.es

JUAN F. NAVARRO
Department of Archaeology, Prehistory, Anthropology and Ancient History, Faculty of Geography and History, University of La Laguna, Campus de Guajara, s/n, 38071 La Laguna, Canary Islands, Spain.

VANESA NIETO-MORENO
Instituto Andaluz de Ciencias de la Tierra (CSIC-UGR), Avda. de Las Palmeras nº 4, 18100 Armilla, Granada, Spain.
Departamento de Mineralogía y Petrología, Facultad de Ciencias, Universidad de Granada, Campus Fuentenueva s/n, E-18002 Granada, Spain.
present address: Biodiversität und Klima Forschungszentrum, Senckenberganlage 25, D-60325 Frankfurt am Main, Germany.

SANDRA NOGUÉ
Long-term Ecology Laboratory, Biodiversity Institute, Department of Zoology, University of Oxford, South Parks Road, OX1 3PS Oxford, United Kingdom.
E-mail: Sandra.noguebosch@zoo.ox.ac.uk

SIETZE NORDER
Computation GeoEcology Group IBED, University of Amsterdam, Nieuwe Achtergracht 166, 1018 WV Amsterdam, The Netherlands.

ULRICH RADTKE
Institute of Geography, University of Cologne, Albertus-Magnus-Platz, D–50923 Köln, Germany.
Rectorate of the University Duisburg-Essen, Universitätsstraße 2, D–45117 Essen, Germany.

KENNETH F. RIJSDIJK
Computation GeoEcology Group IBED, University of Amsterdam, Nieuwe Achtergracht 166, 1018 WV Amsterdam, The Netherlands.
Institute for Biodiversity and Ecosystem Dynamics, University of Amsterdam, Science Park 904, 1098 XH Amsterdam, The Netherlands.
E-mail: K.F.Rijsdijk@uva.nl

MARTA RODRIGO-GÁMIZ,
Instituto Andaluz de Ciencias de la Tierra (CSIC-UGR), Avda. de Las Palmeras nº4, 18100 Armilla, Granada, Spain.
Department of Marine Organic Biogeochemistry, Royal Netherlands Institute for Sea Research (NIOZ), 59 NL-1790 AB Den Burg, Texel, The Netherlands.

CARMEN ROMERO
Department of Geography, Faculty of Geography and History, University of La Laguna, Campus de Guajara, s/n, 38071 La Laguna, Canary Islands, Spain.

Juan Manuel Rubiales
Escuela de Ingeniería Forestal y del Medio Natural, Universidad Politécnica de Madrid, Ciudad Universitaria s/n, 28040 Madrid, Spain.
E-mail: jm.rubiales@upm.es

Willem O. van der Knaap
Institute of Plant Sciences and Oeschger Centre for Climate Change Research, University of Bern, Altenbergrain 21, 3013 Bern, Switzerland.

Jacqueline F.N. van Leeuwen
Institute of Plant Sciences and Oeschger Centre for Climate Change Research, University of Bern, Altenbergrain 21, 3013 Bern, Switzerland.

Hans von Suchodoletz
Institute of Geography, University of Technology Dresden, Helmholtzstrasse 10, D–01069 Dresden, Germany.
Institute of Geography, University of Leipzig, Johannisallee 19a, D–04103 Leipzig, Germany.
E-mail: hans.von.suchodoletz@uni-leipzig.de

Kathy J. Willis
Long-term Ecology Laboratory, Biodiversity Institute, Department of Zoology, University of Oxford, South Parks Road, OX1 3PS Oxford, United Kingdom.

Yurena Yanes
Department of Geology, University of Cincinnati, OH 45221 Cincinnati, USA.
E-mail: yanesya@ucmail.uc.edu

Caridad Zazo
Departamento de Geología, Museo Nacional Ciencias Naturales (CSIC), Calle José Gutiérrez Abascal, 2, 28006 Madrid, Spain.
E-mail: mcnzc65@mncn.csic.es

Ludwig Zöller
Institute of Geography, University of Bayreuth, Universitätsstrasse 30, D–95440 Bayreuth, Germany.

WESTERN MEDITERRANEAN RESPONSES TO CLIMATE VARIABILITY SINCE THE LAST GLACIAL MAXIMUM: A HIGH-RESOLUTION MULTI-PROXY GEOCHEMICAL APPROACH

Francisca Martínez-Ruiz, Marta Rodrigo-Gámiz,
Vanesa Nieto-Moreno, Francisco J. Jiménez-Espejo, David Gallego-Torres

CLIMATE CHANGE PERSPECTIVES FROM THE ATLANTIC:
PAST, PRESENT AND FUTURE
Jose María Fernández-Palacios, Lea de Nascimento, José Carlos Hernández,
Sabrina Clemente, Albano González & Juan P. Díaz-González (eds.)
Servicio de Publicaciones, Universidad de La Laguna – 2013

ISBN: 978-84-15910-54-1 pp. 29-50

Abstract

The Mediterranean Sea has been especially sensitive to climate variability due to its semi-enclosed nature and latitudinal position. Marine records from diverse Mediterranean basins have provided excellent archives for palaeoclimate and palaeoceanographic reconstructions. In particular, the westernmost Mediterranean (Alborán Sea basin) has offered valuable information for understanding climate responses at millennial-to-centennial time scales due to high sedimentation rates in this basin, which have allowed exceptional analysis resolution. Thus, high-resolution analyses of selected records spanning the last 20,000 years within this basin have provided new insights into rapid climate variability and potential forcing mechanisms during this time interval. This work bases on a multi-proxy geochemical approach including mineral composition, major and trace element-contents, grain size distribution and isotopic composition. Geochemical and mineralogical proxies have served to characterize major climate oscillations, as well as to establish detrital input fluctuations (aeolian and fluvial), marine palaeoproductivity, palaeocirculation patterns and oxygen conditions during these periods of abrupt climate change, such as the last Heinrich event, the Bölling-Alleröd, the Younger Dryas, and further Holocene climate variations. These oscillations have also been correlated with terrestrial and Greenland ice records, supporting the strong connection between the western Mediterranean and the North Atlantic climate. Additionally, spectral periodicities further support the extreme sensitivity of this region to cyclic climate changes, being the North Atlantic Oscillation, the migration of the Inter-Tropical Convergence Zone and solar irradiance variations the main climate forcing mechanisms driving natural climate variability during this time.

Keywords: Alborán Sea basin, climate variability, geochemical approach, palaeoceanography, western Mediterranean.

INTRODUCTION

The Mediterranean has been the focus of an intensive palaeoclimate research spanning different time-scales. It is well known that it has been traditionally considered as an excellent natural laboratory (e.g., Krijgsman, 2002) since it is particularly sensitive to climate variability due to its semi-enclosed nature and latitudinal position (e.g., Lionello *et al.*, 2006; Durrieu de Madron *et al.*, 2011; Lionello, 2012). As an example, during the last five millions years the eastern Mediterranean basins have registered the cyclic deposition of sapropel layers as a consequence of climate changes involving higher precipitation and nutrient input that led to enhanced productivity and decreasing bottom water ventilation due to oxygen consumption (e.g., Rossignol-Strick *et al.*, 1982; Thomson *et al.*, 1995; Nijenhuis and de Lange, 2000; Slomp *et al.*, 2002; de Lange *et al.*, 2008; Gallego-Torres *et al.*, 2010). The western Mediterranean have also offered excellent records of past climate variability, in particular those from the westernmost Mediterranean (Alborán Sea basin), where high sedimentation rates have allowed an exceptional high-resolution analysis of climate changes (e.g., Cacho *et al.*, 1999; Moreno *et al.*, 2002; 2012; Martínez-Ruiz *et al.*, 2003; Sierro *et al.*, 2005; Bout-Roumazeilles *et al.*, 2007; Jiménez-Espejo *et al.*, 2007; 2008; Martín-Puertas *et al.*, 2010; Nieto-Moreno *et al.*, 2011; 2013a; 2013b; Rodrigo-Gámiz *et al.*, 2011). A detailed reconstruction of high-frequency climate oscillations at millennial-to-centennial time scales based on these records is thus the main objective of our work. In terms of time windows, we focus on the last 20,000 years because other than availability of excellent records, it is also a key period for understanding rapid climate variability. The Last Glacial Maximum (LGM) is the most recent maximum in global ice volume (e.g., Mix *et al.*, 2001), which was followed by other known abrupt climate fluctuations as the last Heinrich event (H1, 16,500–15,700 cal. years BP) (Heinrich, 1988), the Bölling-Alleröd period (B-A, 14,670–12,890 cal. years BP) (e.g., Brauer *et al.*, 2000; Liu *et al.*, 2009), the Younger Dryas (YD, 12,890–11,650 cal. years BP) (e.g., Dansgaard *et al.*, 1989; Alley *et al.*, 1993; Peteet, 1995) and short-term variations during the Holocene (e.g., Alley *et al.*, 1997; Mayewsky *et al.*, 2004; Wanner *et al.*, 2008), such as the widely known «8200 years» event (e.g., Mayewsky *et al.*, 2004; Wanner *et al.*, 2008) and the end of the African Humid Period (AHP) (deMenocal *et al.*, 2000). During the Late Holocene the best recognized climate fluctuations are the Late Bronze Age–Iron Age (LBA, 3600–2600 cal. years BP) (Van Geel *et al.*, 1996), the Roman Humid Period (RHP, 2600–1600 cal. years BP) (Issar, 2003), the Dark Ages (DA, 1600–1150 cal. years BP) (Berglund, 2003), the Medieval Climate Anomaly (MCA, 1150–650 cal. years BP) (Hughes *et al.*, 1994) and the Little Ice Age (LIA 650–150 cal. years BP) (Bradley and Jones, 1993). Further insights into these rapid fluctuations will contribute to better understanding of the complex interactions among the components of the climate system, which are still poorly unstated.

In general, patterns of rapid climate variability still remain largely unknown and so diverse proxies have been developed in order to afford detailed reconstruction of past climate conditions and interactions between the different components of the climate system. Among these proxies, both organic and inorganic proxies have been revealed as reliable indicators of palaeoenvironmental conditions. For instance, organic fossil molecules preserved in marine sediments, i.e., biomarkers, have recorded fluctuations of sea surface temperature (SST), and in the particular case of the Alborán Sea basin have provided a detailed palaeotemperature reconstruction (Cacho *et al.*, 1999; 2000; 2002; Martrat *et al.*, 2004; 2007; Nieto-Moreno *et al.*, 2013a; Rodrigo-Gámiz *et al.*, submitted). Similarly, faunal assemblages and pollen records have also registered major climate fluctuations of SST (Pérez-Folgado

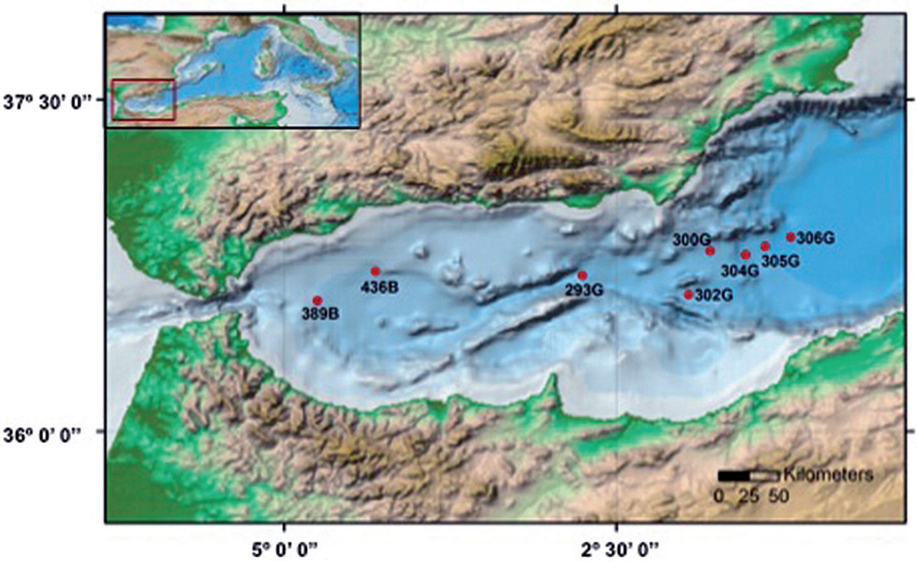

Figure 1. Map of the Alborán Basin showing the location of the studied cores.

et al., 2004; Sierro *et al.*, 2005; Cacho *et al.*, 2006) and reduction of the forest cover extent in the westernmost Mediterranean borderlands over the last deglaciation (Combourieu-Nebout *et al.*, 2002; Sánchez Goñi *et al.*, 2002; Fletcher and Sánchez Goñi, 2008; Combourieu-Nebout *et al.*, 2002; 2009; Fletcher *et al.*, 2010). The inorganic fraction of marine sediments has also been revealed as a reliable signature of climate variability since variations in past conditions have resulted in that of sediment composition in terms of major and trace elements concentrations as well as distribution of mineral components and sediment grain size. Here we centre on this inorganic fraction and show how climate oscillations since the LGM can be reconstructed at exceptional high resolution by a multi-proxy geochemical approach evidencing climate responses at millennial-to-centennial time scales.

Oceanographic and climatological setting

Analyzed marine sediment records were recovered in the Alborán Sea basin (Fig. 1). This basin is located in the westernmost Mediterranean Sea; it is connected with the Atlantic Ocean through the Strait of Gibraltar to the West and with the Algero-Balearic basin to the East. At present, its hydrodynamic framework is characterized by the entrance of the Atlantic Surface Water, which mixes with more saline water from the Mediterranean forming the Modified Atlantic Water

(MAW). This results in two anticyclonic gyres, the Western Alborán and the Eastern Alborán Gyres. The deeper water layers are fed by the Levantine Intermediate Waters (LIW) from the eastern Mediterranean and the Western Mediterranean Deep Water (WMDW) originated in the Gulf of Lion due to the northwesterly winds. Both water masses form the Mediterranean Modified Outflowing Water (MOW). The circulation patterns are as well largely controlled by climate conditions (e.g., Béthoux, 1979; 1980; Lacombe *et al.*, 1981), resulting from the continental and alpine climate regimes affecting surrounding continental areas in the northern regions and the semi-arid climates in the southern margins. In general, the North Atlantic Oscillation (NAO) and the migration of the Inter-Tropical Convergence Zone (ITCZ), inducing oscillations of the African monsoon rain belt, are major controls of present climate variability (e.g., Lionello *et al.*, 2006).

MATERIALS AND METHODS

We have analyzed diverse selected records that correspond to gravity and box cores recovered during several oceanographic cruises of the Training-Through-Research Programme, TTR-12, TTR-14 and TTR-17 (R/V Professor Logachev) (Comas and Ivanov, 2003; 2006) (Fig. 1, Table 1). The lithology of these marine sediments is characterized by homogeneous greenish-brownish hemipelagic mud-clays with foraminifera and some shell fragments. Cores were sampled every 1 cm or 1.5 cm obtaining a continuous record of samples, which provided an average temporal resolution of about 50 to 75 years per sample within the analyzed intervals. Samples were split into different representative portions. Thus, one portion was dried and homogenized in agate mortar for mineralogical and geochemical analyses; a second portion was used to separate marine planktonic foraminifera for stable isotope analyses and radiocarbon dating; and the third one was used for grain size analyses.

Bulk and clay mineral compositions were obtained by X-Ray Diffraction (XRD) following the international recommendations compiled by Kisch (1991). X-Ray diffractograms were obtained using a PANalytical X'Pert PRO diffractometer with Cu-K α radiation and automatic slit. Major elements and Zr were obtained by X-Ray Fluorescence (XRF). The quality of the analysis was monitored with reference materials showing high precision with 1 sigma 1.0–3.4% on 16 datasets at the 95% confidence level. Trace element concentrations were obtained by Inductively Coupled Plasma-Mass Spectrometry (ICP-MS), being the instrumental error ±2% and ±5% for elemental concentrations of 50 ppm and 5 ppm respectively (Bea, 1996). Selected major elements as well as trace elements have been normalized to Al concentration, which allows avoiding any lithological effect on elemental concentration (e.g., Calvert and Pedersen, 2007). Grain size distribution was obtained using a Micromeritics SediGraph 5100. The determination of Total Organic Carbon (TOC) was performed using a Horiba Carbon/Sulfur Analyzer EMIA-320V Series. The stable oxygen isotope ratio was measured by

TABLE 1. Coordinates of studied sediments cores and water depth.

Core	Latitude	Longitude	Depth (m b.s.l.)
293G	36°10.414’N	2°45.280’W	1840
300G	36°21.532’N	1°47.507’W	1860
302G	36°01.906’N	1°57.317’W	1989
304G	36°19.873’N	1°31.631’W	2382
384B	35°59.161’N	4°44.976’W	1022
436B	36°12.318’N	4°18.800’W	1108
305G	36°23.603’N	1°22.710’W	2512
306G	36°27.846’N	1°11.166’W	2574

mass spectrometry over approximately 10 specimens of monospecific planktonic foraminifera *Globigerina bulloides* from the >125 µm fraction avoiding senescent forms. Other than stable isotope stratigraphy, the age model has been based on ^{14}C AMS radiocarbon ages (Accelerator Mass Spectrometry, AMS) recorded in approximately 20 mg of *Globigerina bulloides* from the size fraction >125 µm, and in the most recent sediments on ^{210}Pb chronology.

RESULTS AND DISCUSSION

The geochemical composition of the analyzed core sediments has provided a detailed chronology of major climate oscillations over the last 20,000 years as well as insights on the response of climate system components. Atmosphere and lithosphere responses are registered by detrital input fluctuations, subsequently by those of typical fluvial and aeolian derived elements and mineral phases. Hence, Si, Ti, Zr, Rb, Mg, and K concentrations as well as detrital mineral such as clays and quartz allow establishing variations in river runoff and aeolian dust supply. Palaeoceanographic conditions in terms of marine productivity, bottom-currents and depositional oxygen conditions have also been tracked by geochemical proxies such as Ba, grain size distribution and concentration of redox sensitive elements, respectively.

Aeolian vs. fluvial input as record of dry/wet oscillations

The Alborán Sea basin is characterized by particularly high sedimentation rates. The active erosion over the prominent surroundings relieves has resulted in a massive supply of terrigenous fluvial-derived material to the marine catchment. Additionally, the proximity of this basin to the main dust source in Earth, the Sahara desert, has also led to a major contribution of aeolian dust to the sedimentary record. Thus, variations in fluvial vs. aeolian inputs have derived from a decrease vs. increase in aridity and dryness in southern Iberia and North Africa, accompanied by major oscillations in the intensity of Saharan winds. Sediments are subsequently characterized by high proportion of terrigenous minerals such as clay minerals, quartz, feldspars and accessory minerals such as apatite, zircon or biotite, which are present in the coarser fraction. Terrigenous components are over 50% of the sediment fraction, with clays up to 60%, while calcite is below 50% (e.g, Martínez-Ruiz *et al.*, 2003; Jiménez-Espejo *et al.*, 2007; 2008; Nieto-Moreno *et al.*, 2011; 2013b; Rodrigo-Gámiz *et al.*, 2011). Accordingly, as source areas are characterized by active and rapid erosion, typical detrital clays are abundant and clay mineral assemblages are dominated by high quantities of illite, up to 60%, and lower proportions of smectite, kaolinite, chlorite and palygorskite (Fig. 2). Within these assemblages, typical aeolian clays such as kaolinite and especially palygorskite have also served to indicate aeolian input fluctuations. Derived-aeolian minerals such as quartz and palygorskite evidence a significant increase in the eolian input from the LGM to the begining of the Bölling (18,000–14,670 cal. years BP), at the onset of the YD, and at the Early Holocene (Fig. 2). During the Holocene, palygorskite also started to increase at 4600 cal. years BP (Rodrigo-Gámiz *et al.*, 2011). Similarly, typical detrital proxies such as Si/Al, Mg/Al, K/Al, Rb/Al, Ti/Al, Zr/Al evidence fluvial and eolian input fluctuations over the last 20,000 years (Fig. 2). Zr/Al ratio shows a significant increase from the end of LGM to the begining of the Bölling (18,000–14,670 cal. years BP, Greenland Stadial 2 (GS-2) in NGRIP terminology, Lowe *et al.*, 2008). The Ti/Al and Si/Al ratios also show significant peaks featuring the H1. As expected, typical fluvial-derived elements and corresponding Rb/Al, Mg/Al and K/Al ratios display an opposite trend. The Rb/Al ratio shows a noteworthy increase from the Intra-Alleröd Cold Period (IACP) to the early YD. Both Mg/Al and K/Al ratios show similar profiles, with an increasing trend from the Bölling to the end of the intra-Alleröd period. The Early Holocene record supports a general trend towards more humid conditions, linked with greater insolation and moisture-flux from the ocean to the African continent. This trend is also punctuated by other short-term climate oscillations in connection with monsoonal activity (e.g., Mayewski *et al.*, 2004). In the Alborán Sea borderlands, such oscillations resulted in repeated declines of forest cover (APC 1 to 8) (Combourieu-Nebout *et al.*, 2009) and SST Mediterranean coolings (Cacho *et al.*, 2001), also correlated with the North Atlantic Bond events (Bond *et al.*, 2001). As an example, from 11,650 to 10,000 cal. years BP, the increase in palygorskite and quartz contents and declining trends in Mg/Al and K/Al ratios (Fig. 2) suggest an increase in eolian input during dryer conditions (Rodrigo-Gámiz *et al.*, 2011), likely related with the Preboreal oscillation recognized in the Alborán Sea record (Cacho *et al.*, 2001), and the Mediterranean declines in temperate forest (Carrión, 2002; Combourieu-Nebout *et al.*, 2009). Following this interval, a decrease in values of typical fluvial ratios suggests an early demise of the AHP; these ratios

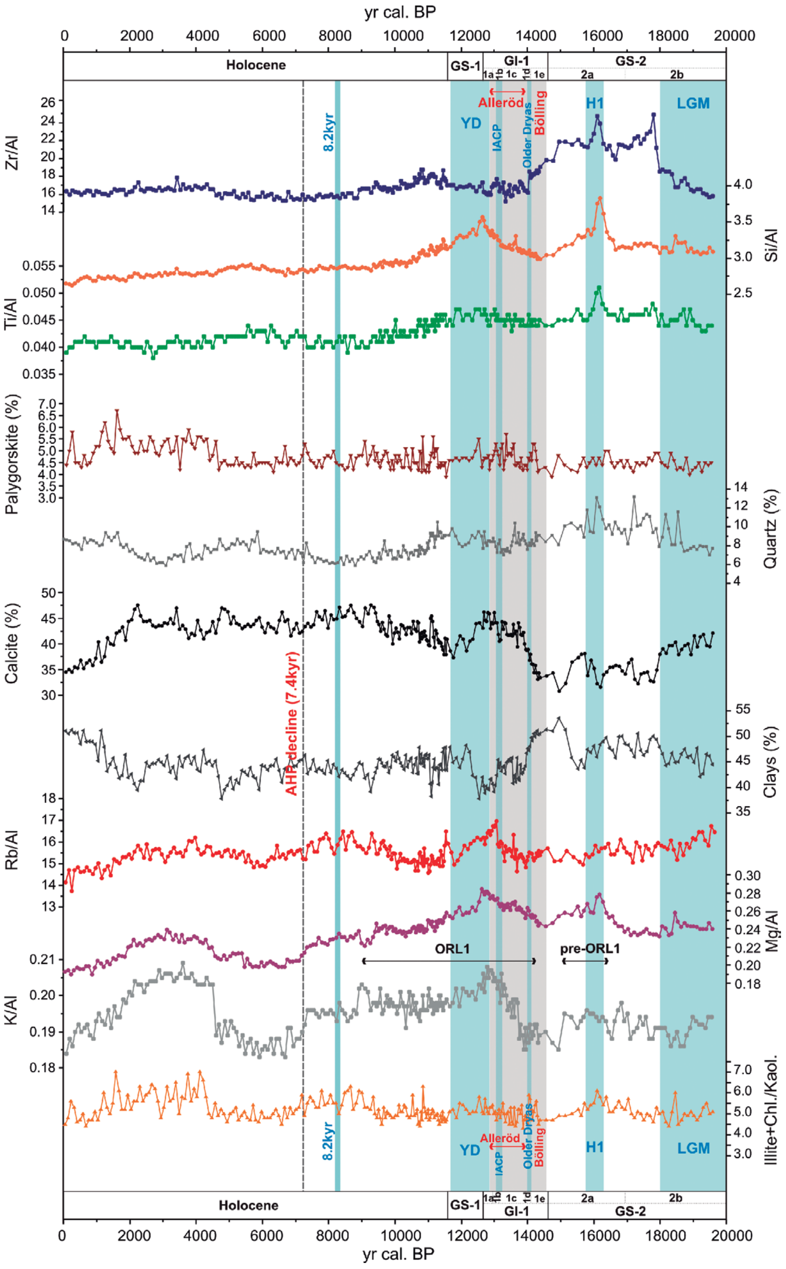

Figure 2. Age profiles of terrigenous proxies in 293G core, element/Al ratios (* 10^{-4} ppm for trace elements) and mineralogical proxies (bulk and clay mineral composition). Modified from Rodrigo-Gámiz *et al.* (2011), see details therein and in the text.

maintain relative low values until 4500 cal. years BP. Subsequently, the decreasing river discharge supports the progressive decline in humidity as evidenced by lower illite and chlorite supply in this region (Rodrigo-Gámiz *et al.*, 2011). This could be related with a southward displacement or weakening of the monsoonal rainfall system farther strengthened by a progressively lower insolation (Berger and Loutre, 1991). Such climate conditions are similar to those dominating during the YD period, when fluctuations in detrital proxies recorded an initial cold and dry phase characterized by high Zr/Al ratio, with a later decreasing trend (Fig. 2). Accordingly, an increase in aeolian dust transport with intense westerlies winds is followed by a more humid phase. North Africa monsoonal precipitations due to ITCZ migrations seem to play the major atmospheric role at this time. Accordingly, during the Late Holocene, detrital proxies have also allowed the characterization of humid (LIA and RHP) and dry (MCA, DA and LBA–IA) periods, as evidenced by typical fluvial derived elements (Rb/Al, Mg/Al and K/Al ratios) and eolian input proxies (Zr/Al ratio) (Nieto-Moreno *et al.*, 2011; 2012; 2013b).

Past productivity as indicated by Ba proxies

Barium enrichment in marine sediments has been revealed as a reliable proxy for reconstructing past productivity when such enrichment derives from authigenic marine barite originated in the water column and reducing conditions within the sediments did not compromise barite preservation (e.g., Dymond *et al.*, 1992; Paytan *et al.*, 1996; Dehairs *et al.*, 2000; Paytan and Griffith, 2007; Griffith and Paytan, 2012). Due to the insoluble nature of barite, when preserved, it has been extensively used in palaeoenvironmental studies as palaeoproductivity proxy. Even though seawater is largely under-saturated with respect to barite, it is ubiquitous in seawater and marine sediments deposited in high productivity areas. Mechanisms for barite precipitation are still poorly understood, it has been suggested that barite may be precipitated by organisms (e.g., Bishop, 1988). However, no living organisms that could account for abundance of barite in the present ocean have been identified. Recent investigations have shown that precipitation could be related to bacterial activity. In fact, Dehairs *et al.* (2008) proved that higher mesopelagic particulate Ba concentrations coincided with higher bacterial activity in the Pacific suggesting a potential relationship, and Gonzalez-Muñoz *et al.* (2012) have demonstrated that marine bacteria have the capability to precipitate barite. Regardless of the mechanisms responsible for barite precipitation and accumulation in marine sediments, over the geological record barite accumulation and Ba enrichments are supporting enhanced productivity. In the Alborán Sea basin, the high terrigenous input has also led to a detrital Ba contribution. However, when normalizing Ba concentrations to the terrigenous supply, i.e., considering the Ba/Al ratio or Ba excess (Jimenez-Espejo *et al.*, 2008; Rodrigo-Gámiz *et al.*, 2011), significant Ba enrichments are recognized. Thus,

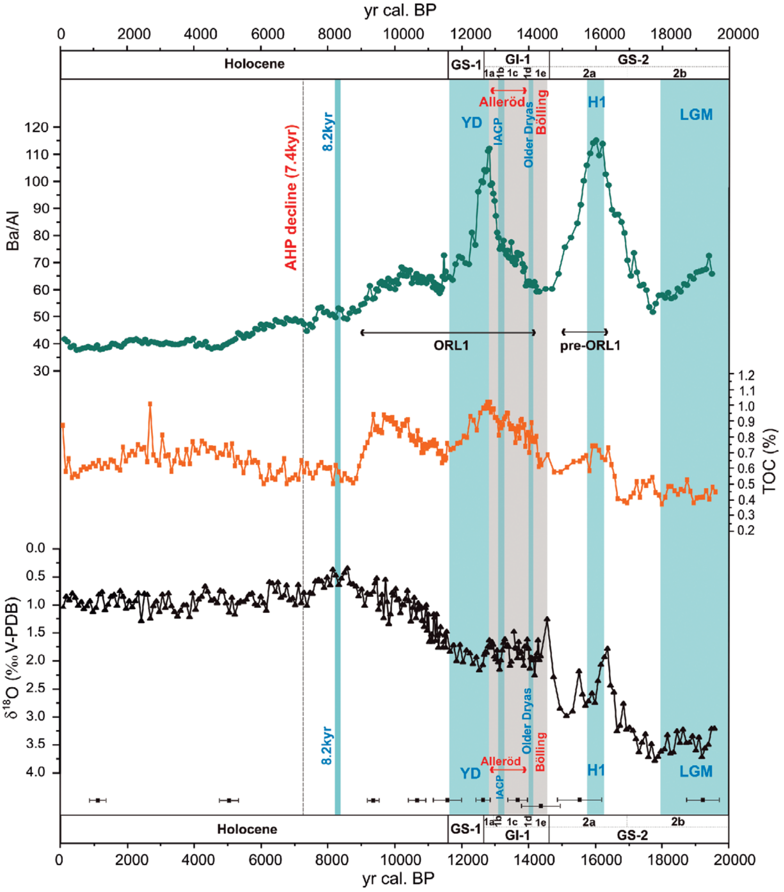

Figure 3. Ba/Al ratio (* 10^{-4} ppm) and total organic carbon content (TOC) used as palaeoproductivity proxies, and stable oxygen isotopes profile in 293G core. Modified from Rodrigo-Gámiz *et al.* (2011), see details therein and in the text.

over the analyzed time span, two major enrichments in Ba are recognized, which are related to cold events as the H1 and the boundary between the offset of the Alleröd period and the onset of YD (Fig. 3). Enhanced productivity during cold events as the YD has also been supported by other records such as diatoms from this same basin (Bárcena *et al.*, 2001). Furthermore, scanning electron microscope observations have showed the presence of authigenic marine barite within these intervals, thus corroborating enhanced productivity. Barite crystals showed typical sizes (<5 μm) and similar morphologies to those of marine barite originated in high productivity regions (Griffith and Paytan, 2012, and references herein).

Moreover, the enrichment in Ba is accompanied by higher contents in organic carbon (Fig. 3). This enrichment in organic carbon has been identified within the Alborán Sea basin as the Organic Rich Layer 1 (ORL1) (Cacho *et al.*, 2002; Jiménez-Espejo *et al.*, 2008), and physical oceanographic models explain the origin of this organic enrichment as a result of the strong reduction in surface water density and a shoaling of the interface between intermediate and deep water during the deglacial period (Rogerson *et al.*, 2008). Apart from changes in oxygen availability and enhanced preservation of the organic matter, increasing productivity is also considered a major control triggering organic carbon accumulation during this time. The onset of this ORL1 is also pointed out by a $\delta^{18}O$ decrease, resulting from the general northern atmospheric warming of the last Greenland Interstadial, in relation to the more humid conditions during the B-A period. These atmospheric conditions could be attributed to a negative NAO index with associated southward westerlies migration (Rodrigo-Gámiz *et al.*, 2011). Following productive intervals, the very Early Holocene is characterized by a considerable decrease in both organic carbon and Ba. Then a progressive decrease took place (initiated at about 8900 cal. years BP) until the present low productivity levels. In fact, in Late Holocene sediments from the Alborán Sea basin, no enrichments in Ba are recognized, being Ba mostly associated to the terrigenous input (Nieto-Moreno *et al.*, 2011; 2012; 2013b).

Palaeocirculation and deep-water ventilation

Concentration of redox sensitive elements has served to infer oxygen conditions at time of deposition as well as reventilation processes since fluctuations in the concentration of these elements above the content derived from the detrital input are controlled by oxygen availability in the water column and within the sediments. Diffusion from bottom waters, release to pore waters from degrading organic matter followed by precipitation or adsorption as well as dissolution of a solid phase and subsequent fixation, are the main mechanisms by which redox-sensitive elements accumulate in the solid phase of marine sediments (e.g., Calvert and Pedersen, 2007). Fluctuations in bottom water oxygenation are also indicated by grain size distribution since oscillations in the sortable silt (SS) proportion and silt/clay ratio (S/C) usually provides information about changes in palaeocurrent intensity (e.g., McCave *et al.*, 1995), being used as current speed proxies. In fact, the UP10 parameter, equivalent to SS, from some western Mediterranean records has showed significant oscillations in current intensity (e.g., Frigola *et al.*, 2007; 2008; Rogerson *et al.*, 2008). In this regard, the Aluminium normalized concentrations of redox-sensitive elements such as Zn/Al, Cu/Al, V/Al and Mn/Al ratios as well as grain size distribution have showed major fluctuations in bottom water oxygenation over the last 20,000 years (Fig. 4). Noteworthy changes to lower deep-water ventilation are registered during the

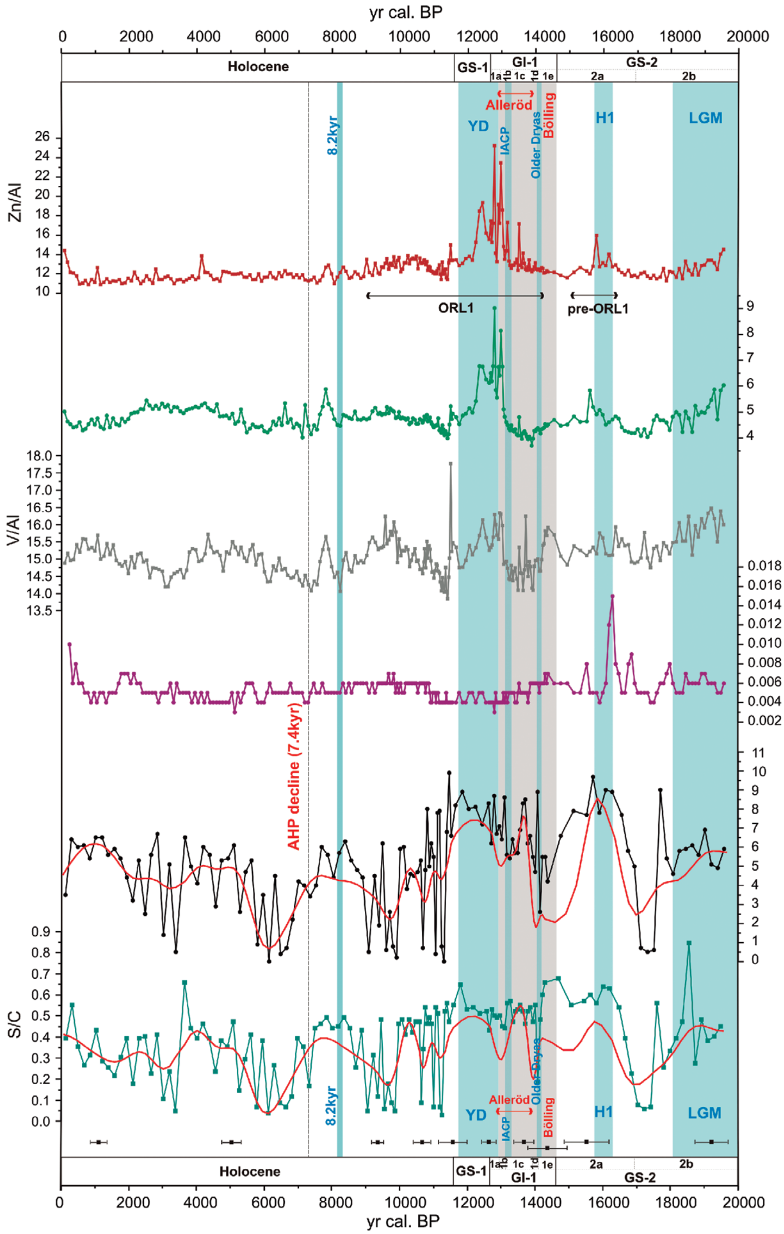

Figure 4. Age profiles of redox proxies/Al ratios in 293G core (* 10^{4} ppm for trace elements) and palaeocurrents indicators denoted by Sortable Silt (SS) and silt/clay ratios (S/C) with 3-point smoothing average (red line). Modified from Rodrigo-Gámiz *et al.* (2011), see details therein and in the text.

offset of the GS-2a and the YD, and from the Early Holocene to around 7800 cal. years BP, being the climate transition from the Alleröd to the YD characterized by the lowest oxygenation. A substantial decrease in SS and S/C ratios are also indicating a prominent decrease in bottom-water currents intensity. In contrast, well-ventilated conditions were reached just previous to the onset of the H1 as indicated by the Mn/Al ratio. SS and S/C ratios show high values during the GS-2a, further indicating intense bottom water circulation (Fig. 4). During this time, another significant feature is the depletion in δ^{18}O values (Fig. 3). Thus, all these observations point to an intense thermohaline circulation during the GS-2a triggered by strengthening of the north westerlies winds, with a complex pattern during the H1. At this time, a reduction of ventilation coexisting with anomalous light oxygen isotopes, agrees with the oceanographic situation triggered by freshwater inflow to the Mediterranean by North Atlantic iceberg melting, as described in other palaeoceanographic studies (Cacho *et al.*, 1999; 2006; Sierro *et al.*, 2005). Even though more stable conditions characterize the Holocene in comparison to major climate changes involving the deglaciation and the YD, the Holocene has also been punctuated by significant oscillations in bottom water oxygenation and palaeocurrent intensity. A sharp increase in palaeocurrent intensity is recognized for instance coinciding with the demise of ORL1 deposition. Following this event, the cold and dry phase that occurred at 8200 cal. years BP (e.g., Alley *et al.*, 1997; Lowe *et al.*, 2008), is also recorded by redox proxies and current intensification (Fig. 4). Similarly, these proxies also register significant changes at 7400 cal. years BP with low palaeocurrent intensity and substantial changes in oxygen conditions (Rodrigo-Gámiz *et al.*, 2011). During the Late Holocene notable changes in bottom water ventilation are also recognized. Thus, the RHP and the LIA are characterized by weaker bottom currents (lower SS) and reduced bottom water oxygenation (high V/Al, Cr/Al, Ni/Al and Zn/Al ratios), while opposite trends are recognized during the LBA–IA, the DA and the MCA (Nieto-Moreno *et al.*, 2011). Moreover, palaeoceanographic fluctuations involving changes in oxygen conditions recorded at 1450 and 1950 years AD have been related to variations in the Atlantic inflow into the Mediterranean Sea following those of the North Atlantic Deep Water (NADW) production (Nieto-Moreno *et al.*, 2012; 2013b). In fact, cold spells and reduced NADW have also been considered to explain fresh polar-derived waters reaching the Alborán Sea basin at different time intervals (e.g., Sierro *et al.*, 2005; Rogerson *et al.*, 2010).

CONCLUSIONS

A multiproxy geochemical approach including mineral composition, major and trace element-contents, grain size distribution and isotopic composition has allowed a detailed reconstruction of past climate variability in the western Mediterranean region over the last 20,000 years. The high sedimentation rates in the westernmost basin, the Alborán Sea basin, have resulted in excellent archives for high-resolution analyses. Thus, obtained results have provided valuable information for understanding climate responses at millennial-to-centennial time scales as well as forcing mechanisms. Geochemical and mineralogical proxies have been used to identify and characterize major climate oscillations. Subsequently we have established detrital input fluctuations (aeolian and fluvial), marine palaeoproductivity, palaeocirculation patterns and oxygen conditions during periods of abrupt climate change, such as the last Heinrich event, the Bölling-Alleröd, the Younger Dryas, as well as during rapid Holocene climate oscillations. Climate scenarios reconstructed from marine sediments are clearly correlated with terrestrial records from adjacent regions as well as with Greenland ice-cores, supporting the strong connection between the western Mediterranean and the North Atlantic climate variability. Main climate forcing mechanisms driving natural climate fluctuations over the studied time interval have been the North Atlantic Oscillation, the migration of the Inter-Tropical Convergence Zone and solar irradiance.

ACKNOWLEDGEMENTS

First of all, we would like to thank the Macaronesian Palaeoclimate Workshop organizing committee for their invitation to contribute on this volume. Our work is supported by Projects CGL2009-07603, CTM2009-07715 and CGL2012-32659 (Secretaría de Estado de Investigación), Project RNM 05212 and Research Group 0179 (Junta de Andalucía). We are also grateful to Projects 200800050084447 (MARM) and CSD2006-00041 (TOPOIBERIA) as well as to the Training-Through-Research Programme cruises, during which core sediments were recovered. Also thanks to the Centre for Scientific Instrumentation (CIC-University of Granada) for analytical facilities and to the National Centre for Accelerators (CNA, Sevilla, Spain), the Poznan Radiocarbon Laboratory (Poland) and J. Garcia-Orellana for age models and dating contributions. The Andalusian Institute of Earth Sciences (IACT, CSIC-UGR) and the Department of Mineralogy and Petrology (UGR) are also acknowledged for analytical facilities. Many special thanks to D. Ortega and E. Holanda, project technicians, for such a hard work preparing so many samples. Also thanks to C. Niembro, L. González, E. Abarca and J. Santamarina, as well as to the CIC personnel for their laboratory assistance, and to Alpiste for providing the maps. F.J. Jiménez-Espejo and D. Gallego-Torres also acknowledge funding from the CSIC «JAE-Doc» postdoctoral program.

REFERENCES

Alley, R.B., Meese, D.A., Shuman, C.A., Gow, A.J., Taylor, K.C., Grootes, P.M., White, J.W.C., Ram, M., Waddington, E.D., Mayewski, P.A. and Zielinski, G.A. (1993) Abrupt increase in Greenland snow accumulation at the end of the Younger Dryas event. *Nature*, 362, 527–529.

Alley, R.B., Mayewski, P.A., Sowers, T., Stuiver, M., Taylor, K.C. and Clark, P.U. (1997) Holocene climatic instability: A prominent, widespread event 8200 yr ago. *Geology*, 25, 483–486.

Bárcena, M.A., Cacho, I., Abrantes, F., Sierro, F.J., Grimalt, J.O. and Flores, J.A. (2001) Paleoproductivity variations related to climatic conditions in the Alboran Sea (western Mediterranean) during the last glacial-interglacial transition: the diatom record. *Palaeogeography, Palaeoclimatology, Palaeoecology*, 167, 337–357.

Bea, F. (1996) Residence of REE, Y, Th and U in granites and crustal protoliths; implications for the chemistry of crustal melts. *Journal of Petrology*, 37, 521–552.

Berger, A. and Loutre, M.F. (1991) Insolation values for the climate of the last 10 million years. *Quaternary Science Reviews*, 10, 297–317.

Berglund, B.E. (2003) Human impact and climate changes-synchronous events and a causal link? *Quaternary International*, 105, 7–12.

Béthoux, J.P. (1979) Budgets of the Mediterranean Sea. Their dependence on the local climate and on the characteristics of the Atlantic waters. *Oceanologica Acta*, 2, 157–163.

Béthoux, J.P. (1980) Mean water fluxes across sections in the Mediterranean Sea, evaluated in the basis of water and salt budgets and of observed salinities. *Oceanologica Acta*, 3, 79–88.

Bishop, J.K.B. (1988) The barite-opal-organic carbon association in oceanic particulate matter. *Nature*, 332, 341–343.

Bond, G., Kromer, B., Beer, J., Muscheler, R., Evans, M.N., Showers, W., Hoffmann, S., Lotti-Bond, R., Hajdas, I. and Bonani, G. (2001) Persistent solar influence on North Atlantic climate during the Holocene. *Science*, 294, 2130–2136.

Bout-Roumazeilles, V., Combourieu Nebout, N., Peyron, O., Cortijo, E., Landais, A. and Masson-Delmotte, V. (2007) Connection between South Mediterranean climate and North African atmospheric circulation during the last 50,000 yr BP North Atlantic cold events. *Quaternary Science Reviews*, 26, 3197–3215.

BRADLEY, R.S. and JONES, P.D. (1993) 'Little Ice Age' summer temperature variations: their nature and relevance to recent global warming trends. *The Holocene*, 3, 367–376.

BRAUER, A., GÜNTER, C., JOHNSEN, S.J. and NEGENDANK, J.F.W. (2000) Land-ice teleconnections of cold climatic periods during the last Glacial/Interglacial transition. *Climate Dynamics*, 16, 229–239.

CACHO, I., GRIMALT, J.O., PELEJERO, C., CANALS, M., SIERRO, F.J., FLORES, J.A. and SHACKLETON, N. (1999) Dansgaard-Oeschger and Heinrich Event Imprints in Alboran Sea Paleotemperatures. *Paleoceanography*, 14, 698–705.

CACHO, I., GRIMALT, J.O., SIERRO, F.J., SHACKLETON, N. and CANALS, M. (2000) Evidence for enhanced Mediterranean thermohaline circulation during rapid climatic coolings. *Earth and Planetary Science Letters*, 183, 417–429.

CACHO, I., GRIMALT, J.O. and CANALS, M. (2002) Response of the Western Mediterranean Sea to rapid climatic variability during the last 50,000 years: a molecular biomarker approach. *Journal of Marine Systems*, 33–34, 253–272.

CACHO, I., SHACKLETON, N., ELDERFIELD, H., SIERRO, F.J. and GRIMALT, J.O. (2006) Glacial rapid variability in deep-water temperature and δ18O from the Western Mediterranean Sea. *Quaternary Science Reviews*, 25, 3294–3311.

CALVERT, S.E. and PEDERSEN, T.F. (2007) Elemental proxies for palaeoclimatic and palaeoceanographic variability in marine sediments: interpretation and application. *Proxies in Late Cenozoic Paleoceanography* (ed. by HILLAIRE-MARCEL, C. and VERNAL, A.D.), pp. 567–644. Elsevier, Amsterdam.

CARRIÓN, J.S. (2002) Patterns and processes of Late Quaternary environmental change in a montane region of southwestern Europe. *Quaternary Science Reviews*, 21, 2047–2066.

COMAS, M.C. and IVANOV, M.K. (2003) Alboran basin (Leg 3). *Interdisciplinary geoscience research on the North East Atlantic margin, Mediterranean Sea and Mid-Atlantic Ridge* (ed. by KENYON, H., IVANOV, M.K., AKHMETZHANOV, A.M. and AKHMANOV. G.G.), pp. 51–71. IOC Technical Series UNESCO, Paris.

COMAS, M.C. and IVANOV, M.K. (2006) Eastern Alboran margin: the transition between the Alboran and the Balearic-Algerian basins. *Interdisciplinary geoscience studies of the Gulf of Cadiz and Western Mediterranean basins* (ed. by KENYON, N.H., IVANOV, M.K., AKHMETZHANOV, A.M. and KOZLOVA, E.V.), pp. 48–61. IOC Technical Series UNESCO, Paris.

COMBOURIEU-NEBOUT, N., TURON, J.L., ZAHN, R., CAPOTONDI, L., LONDEIX, L. and PAHNKE, K. (2002) Enhanced aridity and atmospheric high-pressure stability over the western Mediterranean during the North Atlantic cold events of the past 50 k.y. *Geology*, 30, 863–866.

COMBOURIEU-NEBOUT, N., PEYRON, O., DORMOY, I., DESPRAT, S., BEAUDOUIN, C., KOTTHOFF, U. and MARRET, F. (2009) Rapid climatic variability in the west Mediterranean during the last 25 000 years from high resolution pollen data. *Climate of the Past*, 5, 503–521.

DANSGAARD, W., WHITE, J.W.C. and JOHNSEN, S.J. (1989) The abrupt termination of the Younger Dryas climate event. *Nature*, 339, 532–534.

Dehairs, F., Fagel, N., Antia, A.N., Peinert, R., Elskens, M. and Goeyens, L. (2000) Export production in the Bay of Biscay as estimated from barium-barite in settling material: A comparison with new production: *Deep-Sea Research,* 47, 583–601.

Dehairs, F., Jacquet, S., Savoye, N., Van Mooy, B.A.S., Buesseler, K.O., Bishop, J.K.B., Lamborg, C.H., Elskens, M., Baeyens, W., Boyd, P.W., Casciotti, K.L. and Monnin, C. (2008) Barium in twilight zone suspended matter as a potential proxy for particulate organic carbon remineralization: Results for the North Pacific: *Deep-Sea Research,* 55, 1673–1683.

de Lange, G.J., Thomson, J., Reitz, A., Slomp, C.P., Principato, M.S., Erba, E. and Corselli, C. (2008) Synchronous basin-wide formation and redox-controlled preservation of a mediterranean sapropel. *Nature Geoscience,* 1, 606–610.

deMenocal, P.B., Ortiz, J., Guilderson, T., Adkins, J., Sarnthein, M., Baker, L. y Yarusinsky, M. (2000) Abrupt onset and termination of the African Humid Period: rapid climate responses to gradual insolation forcing. *Quaternary Science Reviews,* 19, 347–361.

Durrieu de Madron, X., Guieu, C., Sempéré, R., Conan, P., Cossa, D., D'Ortenzio, F., Estournel, C., Gazeau, F., Rabouille, C., Stemmann, L., Bonnet, S., Diaz, F., Koubbi, P., Radakovitch, O., Babin, M., Baklouti, M., Bancon-Montigny, C., Belviso, S., Bensoussan, N., Bonsang, B., Bouloubassi, I., Brunet, C., Cadiou, J.F., Carlotti, F., Chami, M., Charmasson, S., Charrière, B., Dachs, J., Doxaran, D., Dutay, J.C., Elbaz-Poulichet, F., Eléaume, M., Eyrolles, F., Fernandez, C., Fowler, S., Francour, P., Gaertner, J.C., Galzin, R., Gasparini, S., Ghiglione, J.F., Gonzalez, J.L., Goyet, C., Guidi, L., Guizien, K., Heimbürger, L.E., Jacquet, S.H.M., Jeffrey, W.H., Joux, F., Le Hir, P., Leblanc, K., Lefèvre, D., Lejeusne, C., Lemé, R., Loÿe-Pilot, M.D., Mallet, M., Méjanelle, L., Mélin, F., Mellon, C., Mérigot, B., Merle, P.L., Migon, C., Miller, W.L., Mortier, L., Mostajir, B., Mousseau, L., Moutin, T., Para, J., Pérez, T., Petrenko, A., Poggiale, J.C., Prieur, L., Pujo-Pay, M., Pulido, V., Raimbault, P., Rees, A.P., Ridame, C., Rontani, J.F., Ruiz Pino, D., Sicre, M.A., Taillandier, V., Tamburini, C., Tanaka, T., Taupier-Letage, I., Tedetti, M., Testor, P., Thébault, H., Thouvenin, B., Touratier, F., Tronczynski, J., Ulses, C., Van Wambeke, F., Vantrepotte, V., Vaz, S. and Verney, R. (2011) Marine ecosystems' responses to climatic and anthropogenic forcings in the Mediterranean. *Progress In Oceanography,* 91, 97–166.

Dymond, J., Suess, E. and Lyle, M. (1992) Barium in deep-sea sediment: a geochemical proxy for paleoproductivity. *Paleoceanography,* 7, 163–181.

Fletcher, W.J. and Sánchez Goñi, M.F. (2008) Orbital- and sub-orbital-scale climate impacts on vegetation of the western Mediterranean basin over the last 48,000 yr. *Quaternary Research,* 70, 451–464.

Fletcher, W.J., Sánchez Goñi, M.F., Peyron, O. and Dormoy, I. (2010) Abrupt climate changes of the last deglaciation detected in a Western Mediterranean forest record. *Climate of the Past,* 6, 245–264.

Frigola, J., Moreno, A., Cacho, I., Canals, M., Sierro, F.J., Flores, J.A., Grimalt, J.O., Hodell, D.A. and Curtis, J.H. (2007) Holocene climate variability in the western Mediterranean region from a deep water sediment record. *Paleoceanography,* 22, DOI: 10.1029/2006PA001307.

Frigola, J., Moreno, A., Cacho, I., Canals, M., Sierro, F.J., Flores, J.A. and Grimalt, J.O. (2008) Evidence of abrupt changes in Western Mediterranean Deep Water circulation during the last 50 kyr: a high-resolution marine record from the Balearic Sea. *Quaternary International*, 181, 88–104.

Gallego-Torres, D., Martínez-Ruiz, F., De Lange, G.J., Jiménez-Espejo, F.J. and Ortega-Huertas, M. (2010) Trace-elemental derived paleoceanographic and paleoclimatic conditions for pleistocene eastern mediterranean sapropels. *Palaeogeography, Palaeoclimatology, Palaeoecology*, 293, 76–89.

González-Muñoz, M.T., Martínez-Ruiz F., Morcillo, F., Martín-Ramos, J.D. and Paytan A. (2012) Precipitation of barite by marine bacteria: A possible mechanism for marine barite formation. *Geology*, 40, 675–678.

Griffith, E. and Paytan, A. (2012) Barite in the ocean-Occurrence, geochemistry, and palaeoceanographic applications: *Sedimentology*, 59, 1817–1835.

Heinrich, H. (1988) Origin and consequences of cyclic ice rafting in the Northeast Atlantic Ocean during the past 130,000 years. *Quaternary Research*, 29, 142–152.

Hughes, M.K. and Díaz, H.F. (1994) Was there a 'Medieval Warm Period', and if so, where and when? *Climatic Change*, 26, 109–142.

Issar, A. (2003) *Climate changes during The Holocene and their impact on hydrological systems.* Cambridge University Press, Cambridge, UK.

Jiménez-Espejo, F.J., Martínez-Ruiz, F., Sakamoto, T., Iijima, K., Gallego-Torres and D., Harada, N. (2007) Paleoenvironmental changes in the western Mediterranean since the last glacial maximum: High resolution multiproxy record from the Algero-Balearic basin. *Palaeogeography, Palaeoclimatology, Palaeoecology*, 246, 292–306.

Jiménez-Espejo, F.J., Martínez-Ruiz, F., Rogerson, M., González-Donoso, J.M., Romero, O.E., Linares, D., Sakamoto, T., Gallego-Torres, D., Rueda Ruiz, J.L., Ortega-Huertas, M. and Pérez Claros, J.A. (2008) Detrital input, productivity fluctuations, and water mass circulation in the westernmost Mediterranean Sea since the Last Glacial Maximum. *Geochemistry, Geophysics, Geosystems*, 9, DOI: 10.1029/2008GC002096.

Kisch, H.J. (1991) Illite crystallinity: recommendations on sample preparation, X-ray diffraction settings, and interlaboratory samples. *Journal of Metamorphic Geology*, 9, 665–670.

Krijgsman, W. (2002) The Mediterranean: Mare Nostrum of earth sciences. *Earth and Planetary Science Letters*, 205, 1–12.

Lacombe, H., Gascard, J.C., Cornella, J. and Béthoux, J.P. (1981) Response of the Mediterranean to the water and energy fluxes across its surface, on seasonal and interannual scales. *Oceanologica Acta*, 4, 247–255.

Lionello, P. (2012) *The Climate of the Mediterranean Region: From the Past to the Future.* Elsevier, Amsterdam.

Lionello, P., Malanotte-Rizzoli, P., Boscolo, R., Alpert, P., Artale, V., Li, L., Luterbacher, J., May, W., Trigo, R., Tsimplis, M., Ulbrich, U. and Xoplaki, E. (2006) The Mediterranean climate: An overview of the main characteristics and issues. *Mediterranean climate variability* (ed. by Lionello, P., Malanotte-Rizzoli, P. and Boscolo, R.), pp. 1–26. Elsevier, Amsterdam.

Liu, Z., Otto-Bliesner, B.L., He, F., Brady, E.C., Tomas, R., Clark, P.U., Carlson, A.E., Lynch-Stieglitz, J., Curry, W., Brook, E., Erickson, D., Jacob, R., Kutzbach, J. and Cheng, J. (2009) Transient simulation of last deglaciation with a new mechanism for Bolling-Allerod warming. *Science*, 325, 310–314.

Lowe, J.J., Rasmussen, S.O., Björck, S., Hoek, W.Z., Steffensen, J.P., Walker, M.J.C. and Yu, Z.C. (2008) Synchronisation of palaeoenvironmental events in the North Atlantic region during the Last Termination: a revised protocol recommended by the INTIMATE group. *Quaternary Science Reviews*, 27, 6–17.

Martínez-Ruiz, F., Paytan, A., Kastner, M., González-Donoso, J.M., Linares, D., Bernasconi, S.M. and Jiménez-Espejo, F.J. (2003) A comparative study of the geochemical and mineralogical characteristics of the S1 sapropel in the western and eastern Mediterranean. *Palaeogeography, Palaeoclimatology, Palaeoecology*, 190, 23–37.

Martín-Puertas, C., Jiménez-Espejo, F., Martínez-Ruiz, F., Nieto-Moreno, V., Rodrigo, M., Mata, M.P. and Valero-Garcés, B.L. (2010) Late Holocene climate variability in the southwestern Mediterranean region: an integrated marine and terrestrial geochemical approach. *Climate of the Past*, 6, 807–816.

Martrat, B., Grimalt, J.O., López-Martínez, C., Cacho, I., Sierro, F.J., Flores, J.A., Zahn, R., Canals, M., Curtis, J.H. and Hodell, D.A. (2004) Abrupt Temperature Changes in the Western Mediterranean over the Past 250,000 Years. *Science*, 306, 1762–1765.

Martrat, B., Grimalt, J.O., Shackleton, N.J., de Abreu, L., Hutterli, M.A. and Stocker, T.F. (2007) Four Climate Cycles of Recurring Deep and Surface Water Destabilizations on the Iberian Margin. *Science*, 317, 502–507.

Mayewski, P.A., Rohling, E.E., Curt Stager, J., Karlén, W., Maasch, K.A., David Meeker, L., Meyerson, E.A., Gasse, F., van Kreveld, S., Holmgren, K., Lee-Thorp, J., Rosqvist, G., Rack, F., Staubwasser, M., Schneider, R.R. and Steig, E.J. (2004) Holocene climate variability. *Quaternary Research*, 62, 243–255.

McCave, I.N., Manighetti, B. and Robinson, S.G. (1995) Sortable silt and fine sediment size/composition slicing: parameters for palaeocurrent speed and palaeoceanography. *Paleoceanography*, 10, 593–610.

Mix, A.C., Bard, E. and Schneider, R. (2001) Environmental processes of the ice age: Land, oceans, glaciers (EPILOG). *Quaternary Science Reviews*, 20, 627–657.

Moreno, A., Cacho, I., Canals, M., Prins, M.A., Sánchez-Goñi, M.-F., Grimalt, J.O. and Weltje, G.J. (2002) Saharan dust transport and high-latitude glacial climatic variability: The Alboran Sea record. *Quaternary Research*, 58, 318–328.

Moreno, A., Pérez, A., Frigola, J., Nieto-Moreno, V., Rodrigo-Gámiz, M., Martrat, B., González-Sampériz, P., Morellón, M., Martín-Puertas, C., Corella, J.P., Belmonte, A., Sancho, C., Cacho, I., Herrera, G., Canals, M., Grimalt, J.O., Jiménez-Espejo, F., Martínez Ruiz, F., Vegas, T. and Valero-Garcés, B.L. (2012) The Medieval Climate

Anomaly in the Iberian Peninsula reconstructed from marine and lake records. *Quaternary Science Reviews*, 43, 16–32.

Nieto-Moreno, V., Martínez-Ruiz, F., Giralt, S., Jiménez-Espejo, F., Gallego-Torres, D., Rodrigo-Gámiz, M., García-Orellana, J., Ortega-Huertas, M. and de Lange, G.J. (2011) Tracking climate variability in the western Mediterranean during the Late Holocene: A multiproxy approach. *Climate of the Past,* 7, 1395–1414.

Nieto-Moreno, V., Martínez-Ruiz, F., Giralt, S., Gallego-Torres, D., García-Orellana, J., Masqué, P. and Ortega-Huertas, M. (2012). Climate imprints during the Medieval Climate Anomaly and the Little Ice Age: a novel record from the Alboran Sea basin. *The Holocene*, accepted.

Nieto-Moreno, V., Martínez-Ruiz, F., Willmott, V., García-Orellana, J., Masqué, P. and Sinninghe Damsté, J.S. (2013a). Climate conditions in the westernmost Mediterranean over the last two millennia: a biomarker approach. *Organic Geochemistry*, 55, 1–10.

Nieto-Moreno, V., Martinez-Ruiz, F., Giralt, S., Gallego-Torres, D., García-Orellana, J., Masqué, P. and Ortega-Huertas, M. (2013b) Climate imprints during the 'Medieval Climate Anomaly' and the 'Little Ice Age' in marine records from the Alboran Sea basin. *The Holocene*, 23, 1227-1237.

Nijenhuis, I.A. and de Lange, G.J. (2000) Geochemical constraints on Pliocene sapropel formation in the eastern Mediterranean: *Marine Geology*, 163, 41–63.

Paytan, A. and Griffith, E.M. (2007) Marine barite: recorder of variations in ocean export productivity. *Deep-Sea Research,* 54, 687–705.

Paytan, A., Kastner, M. and Chávez F.P. (1996) Glacial to interglacial fluctuations in productivity in the equatorial pacific as indicated by marine barite. *Science,* 274, 1355–1357.

Pérez-Folgado, M., Sierro, F.J., Flores, J.A., Grimalt, J.O. and Zahn, R. (2004) Paleoclimatic variations in foraminifera assemblages from the Alborán Sea (Western Mediterranean) during the last 150 ka in ODP Site 977. *Marine Geology*, 212, 113–131.

Peteet, D. (1995) Global Younger Dryas? *Quaternary International*, 28, 93–104.

Rogerson, M., Cacho, I., Jimenez-Espejo, F., Reguera, M.I., Sierro, F.J., Martinez-Ruiz, F., Frigola, J. and Canals, M. (2008) A dynamic explanation for the origin of the western Mediterranean organic-rich layers. *Geochemistry, Geophysics, Geosystems*, 9, DOI: 10.1029/2007GC001936.

Rogerson, M., Colmenero-Hidalgo, E., Levine, R.C., Rohling, E.J., Voelker, A.H.L., Bigg, G.R., Schönfeld, J., Cacho, I., Sierro, F.J., Löwemark, L., Reguera, M.I., de Abreu, L. and Garrick, K. (2010) Enhanced Mediterranean-Atlantic exchange during Atlantic freshening phases. *Geochemistry, Geophysics, Geosystems,* 11, Q08013.

Rodrigo-Gámiz, M., Martínez-Ruiz, F., Jiménez -Espejo, F., Gallego-Torres, D., Nieto-Moreno, V., Romero, O. and Ariztegui, D. (2011) Impact of climate variability in the western Mediterranean during the last 20,000 years: oceanic and atmospheric responses. *Quaternary Science Reviews,* 30, 2018-2034.

Rodrigo-Gámiz, M., Martínez-Ruiz, F., Rampen, S.W., Schouten, S. and Sinninghe Damsté, J.S. (2012) Sea surface temperature variations in the western Mediterranean Sea over the last 20 kyr: a multi-organic proxy ($U^{k'}_{37}$, TEX^{H}_{86} and LDI) approach. *Paleoceanography*, submitted.

Rossignol-Strick, M., Nesteroff, W., Olive, P. and Vergnaud-Grazzini, C. (1982) After the deluge: Mediterranean stagnation and sapropel formation. *Nature*, 295, 105–110.

Sánchez-Goñi, M.F., Cacho, I., Turon, J.L., Guiot, J., Sierro, F.J., Peypouquet, J.P., Grimalt, J.O. and Shackleton, N.J. (2002) Synchroneity between marine and terrestrial responses to millennial scale climatic variability during the last glacial period in the Mediterranean region. *Climate Dynamics*, 19, 95–105.

Sierro, F.J., Hodell, D.A., Curtis, J.H., Flores, J.A., Reguera, I., Colmenero-Hidalgo, E., Bárcena, M.A., Grimalt, J.O., Cacho, I., Frigola, J. and Canals, M. (2005) Impact of iceberg melting on Mediterranean thermohaline circulation during Heinrich events. *Paleoceanography*, 20, DOI: 10.1029/2004PA001051.

Slomp, C.P., Thomson, J. and de Lange, G.J. (2002) Enhanced regeneration of phosphorus during formation of the most recent eastern Mediterranean sapropel (S1): *Geochimica et Cosmochimica Acta*, 66, 1171–1184.

Thomson, J., Higgs, N.C., Wilson, T.R.S., Croudace, I.W., De Lange, G.J. and van Santvoort, P.J.M. (1995) Redistribution and geochemical behaviour of redox-sensitive elements around S1, the most recent eastern Mediterranean sapropel. *Geochimica et Cosmochimica Acta*, 59, 3487–3501.

Van Geel, B., Buurman, J. and Waterbolk, H.T. (1996) Archaeological and palaeoecological indications of an abrupt climate change in The Netherlands, and evidence for climatological teleconnections around 2650 BP. *Journal of Quaternary Science*, 11, 451–460.

Wanner, H., Beer, J., Bütikofer, J., Crowley, T.J., Cubasch, U., Flückiger, J., Goosse, H., Grosjean, M., Joos, F., Kaplan, J.O., Küttel, M., Müller, S.A., Prentice, I.C., Solomina, O., Stocker, T.F., Tarasov, P., Wagner, M. and Widmann, M. (2008) Mid- to Late Holocene climate change: an overview. *Quaternary Science Reviews*, 27, 1791–1828.

INSULAR ENVIRONMENTAL CHANGE; CLIMATE-FORCED AND SYSTEM-DRIVEN

Henry Hooghiemstra, Kenneth F. Rijsdijk, Erik de Boer,
Lea de Nascimento, F.B. Vincent Florens, Cláudia Baider

CLIMATE CHANGE PERSPECTIVES FROM THE ATLANTIC:
PAST, PRESENT AND FUTURE
Jose María Fernández-Palacios, Lea de Nascimento, José Carlos Hernández,
Sabrina Clemente, Albano González & Juan P. Díaz-González (eds.)
Servicio de Publicaciones, Universidad de La Laguna – 2013

ISBN: 978-84-15910-54-1 pp. 51-73

Abstract

Vegetation dynamics since the last glacial maximum in small oceanic islands and in continental settings are compared. We selected the islands of Minorca (Western Mediterranean), Tenerife (Eastern Atlantic), the Azores (Central Atlantic) and Mauritius (Indian Ocean) and compared pollen-based dynamics with selected continental areas of southern Italy, the Atlas mountains, northwest Africa, and the East African mountains. We identified potential areas where plant diversity is conserved during unfavourable periods serving as refugial areas. Most pollen records from small oceanic islands with a low topography show, as far as the pollen records reach, stable forest compositions suggesting floral diversity is lodged within a mosaic-like structure. In mountainous islands data point to an altitudinal distribution of plant diversity and to altitudinal migration of plants as a response to climate change. In Mauritius we registered at 11.4 cal. ka a climate-forced change in forest composition which triggered a cascade of species turnover events considered as system-driven. In the small islands discussed we identified areas with a high potential to provide on a long-term shelter to insular floral diversity, thus serving as a refugium: 1) gallery forest located along the drainage system (topography constrained), 2) cloud forest located at the elevation where atmospheric moisture condensates and cloud formation takes place (sea surface temperature and atmospheric lapse rate constrained), 3) and deeply incised valleys, connecting diversity between all available elevations, where relatively humid conditions prevail such as the *barrancos* in Tenerife and the deeply incised valleys in Mauritius (geomorphology and sea-level constrained).

Keywords: *barrancos*, Macaronesia, Mauritius, oceanic islands, refugia, vegetation dynamics.

INTRODUCTION

Climatological gradients are responsible for large-scale spatial vegetation distribution (Knapp, 1973; White, 1983; Lovett and Wasser, 1993; Mistry, 2000; Shorrocks, 2007). On relatively flat continents in particular, biomes have ample opportunities to migrate when climatological conditions change. For example, the repeated expansions and contractions of the Saharan and Sahelian biomes (e.g. Dupont and Hooghiemstra, 1989; Kröpelin *et al.*, 2008) and the climate-forced altitudinal shifts of biomes in the East African mountains (Coetzee, 1967; Taylor, 1990; Kiage and Liu, 2006) are increasingly well documented. In small oceanic islands post-glacial sea-level rise may have had a larger impact than post-glacial temperature increase because of the capacity to buffer temperatures of ocean waters. Since the last glacial maximum (LGM) sea-levels rose ca. 120 m (Lister, 2004; Miller *et al.*, 2005; Zazo *et al.*, 2008; Warren *et al.*, 2010) causing relatively flat-domed oceanic islands to experience reductions in surface area affecting the area of coastal lowland vegetation and premontane vegetation in particular. In islands, reduction of the available surface area for biomes leads to higher species density and, potentially, to increased interspecific competition (Van Hengstum *et al.*, 2012). In small island settings, i.e. islands with a surface of ca. 2000 km^2, the potential capacity for plant migration is limited. The difference between arid lee side and a humid windward side may be pronounced. In addition small islands are characterized by limited hydraulic buffer capacities, short hydraulic transit times, short time hysteresis, and large effects of topographical and geomorphological variation. As a result, small changes in climate and sea-level stands may lead to relatively large changes in abiotic habitat parameters such as emerging fresh water volumes, soil water contents (e.g. Rijsdijk *et al.*, 2011) and vegetation distribution (e.g. Van der Plas *et al.*, 2012).

Migration of biomes implicitly assumes that the full diversity of species is able to follow the ecological niches along the migration route. Although plant species may have a larger genetic plasticity than required to occupy their present-day distribution area (Sexton *et al.*, 2002; Gienapp *et al.*, 2008), most plant taxa are ecologically constrained to a specific environmental range (e.g. Thompson *et al.*, 2000; Hooghiemstra *et al.*, 2012) forming the basis for palaeoecological reconstructions (Birks and Birks, 1980). Whereas flat continents allow significant migration, small oceanic islands and isolated hard rock formations (Porembski and Barthlott, 2000; Zinck and Huber, 2011) do not. For islands, the surface change across a glacial-interglacial transition is also of significant impact on the present-day distribution of diversity (Warren *et al.*, 2010; Osborne, 2012). After the post-glacial sea-level rise biomes migrated to their Holocene positions. In mountainous areas post-glacial temperature rise and concomitant upslope shift of biomes resulted in the Holocene configuration of altitudinally organised biomes. Biomes at highest elevations shrunk in surface (e.g. Hooghiemstra and Van der Hammen, 2004) or even became temporarily lost (e.g. González-Carranza *et al.*, 2012; Velásquez and Hooghiemstra, 2013).

Areas where biodiversity is temporarily able to survive unfavourable environmental conditions can be categorized as 'refugia'. The concept of a refugium is flexible and some examples are given: a) the limited residence area around the Mediterranean of the present-day West European semi-deciduous forest (e.g. Van der Hammen *et al.*, 1971); b) the limited residence area of C_4-vegetation during interglacial times when high atmospheric CO_2 pressure prevails and C_4-dominated vegetation is constrained to the lowermost parts of dry intramontane valleys (e.g. Boom *et al.*, 2002; Pagani *et al.*, 2009); c) the limited residence areas of alpine and tropical-alpine grasslands above the upper forest line on mountain tops. A refugium refers to a limited area where diversity is concentrated when surviving

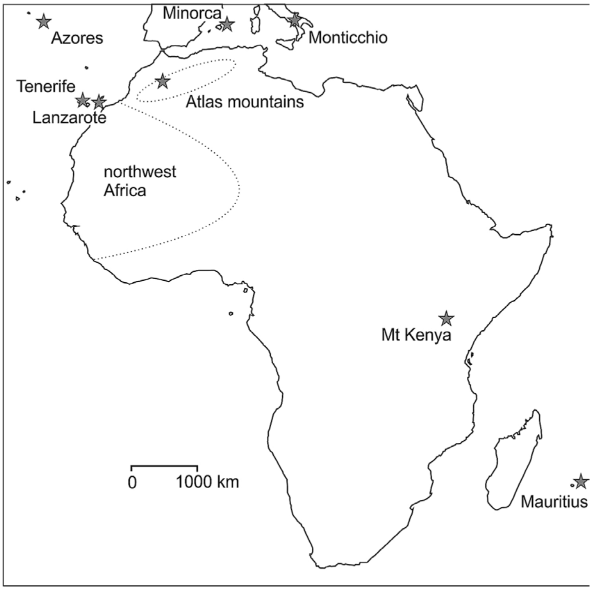

Figure 1. Map showing the location of sites discussed in the text.

a period of unfavourable environmental conditions. In example a, the refugial state is long and during glacial conditions; in examples b and c short and during interglacial conditions. Constraining parameters are temperature, atmospheric $p\mathrm{CO}_2$, sea-level stands, moisture, frequency of night frost, etc. The concept of refugia is much debated (e.g. Stewart *et al.*, 2010; Bennett *et al.*, 2012). Current interglacial refugia are 'discovered' only after the much larger residence area during glacial conditions has been realized (Boom *et al.*, 2002). The location of glacial refugia is often poorly understood, i.e. the location of the West European deciduous forest around the Mediterranean (e.g. Willis and Whittaker, 2000; Willis and Van Andel, 2004), and the location of rainforest around the equator in Africa and South America (Hooghiemstra and Van der Hammen, 1998; Bush and de Oliveira, 2006; Hoorn *et al.*, 2010). Pollen records reaching into the LGM are insufficiently available to contour the refugial area. Where in flat continents biomes can migrate latitudinally, and in mountainous continents biota can migrate altitudinally, we question where small oceanic islands do offer opportunities for developing refugia.

In the present paper we focus on pollen-based records with sufficient chronological control and temporal resolution of vegetation change in selected islands located around the African continent (Fig. 1). We explore the nature of dynamics shown in these Lateglacial and Holocene pollen records by evaluating if vegetation became most likely enriched by climate-forced latitudinal migration (flat continents) or altitudinal migration (mountains), or by alternative mechanisms in small and low elevation oceanic islands. In small islands with a low topography in particular, there may be little potential for migration and alternative processes of exchange of diversity between a source area ('refugium') and the regional vegetation may occur. Keeping in mind that biomes can migrate over large areas in flat continents but are coastline-locked in small oceanic islands, we focus on the last 15,000 years before present (15 ka) and we explore the pollen records on evidence how island biodiversity is 'recycled' and conserved. We selected pollen records from the islands of Minorca (Balearic Islands) (Yll *et al.*, 1997), Tenerife (Canary Islands) (de Nascimento *et al.*, 2009), the Azores (Connor *et al.*, 2012), and Mauritius (Mascarene Islands) (van der Plas *et al.*, 2012; de Boer *et al.*, 2013a, b). For pollen records reflecting a continental environment we selected a record from Southern Italy (Allen *et al.*, 2002), the Moroccan Atlas mountains (Lamb *et al.*, 1989), and the East African Mountains (Kiage and Liu, 2006). We discuss the potential of *barrancos* in southwest Tenerife, and deeply incised valleys in Mauritius as potential refugia.

RECORDS OF PAST ENVIRONMENTAL CHANGE

In this section we show aspects of vegetation dynamics from four island archipelagos. We explore where plant diversity potentially is conserved during periods of unfavourable climatic conditions, i.e. in oceanic islands coinciding with periods of drought. Subsequently, four selected continental areas are considered to compare island dynamics and continental dynamics.

Minorca (Balearic Islands, Western Mediterranean) – From the small Balearic island of Minorca (701 km^2) pollen-based records from coastal plain deposits in the littoral zone reflecting the last 8000 ^{14}C years were published by Yll *et al.* (1997). We refer to the Algendar pollen record showing in a 290 cm long core from 21 m above sea level (a.s.l.) the period from 8000 to ca. 2000 ^{14}C years BP. From 8000 to 5000 ^{14}C years BP forest with significant *Juniperus*, *Corylus*, *Quercus* and *Buxus* shows that seasonal climatic conditions prevailed. During the last millennium of this interval increasing *Ephedra*, Poaceae, Asteraceae tub. and Apiaceae are indicative of drier and seasonal climatic conditions. The period from 5000 to 4000 ^{14}C years BP shows in two steps a change in forest composition with a decline in *Corylus* and *Buxus* around 5000 ^{14}C years BP, and a marked increase of *Olea* and *Phillyrea* ca. 4000 ^{14}C years BP while the 1000-years interval in between shows a homogeneous forest and herbaceous vegetation cover. During the period from 4000 to ca. 3000 ^{14}C years BP the proportions of Ericaceae, Asteraceae lig., *Plantago* and Fabaceae increased markedly whereas during the period from ca. 3000 to ca. 2000 ^{14}C years BP evergreen oak, Ericaceae, *Artemisia*, Chenopodiaceae, Poaceae, Rubiaceae and aquatics all point to human impact on the landscape. The lower part of the record without human impact shows during four millennia little species turnover and the pollen record reflects a «steady-state» Holocene forest, followed by two pulses of species turnover at ca. 4000 and ca. 3000 ^{14}C years BP. Species turnover was approximately within 150 to 300 years. Vegetation changes suggest that changes in the length of the dry season reflect the most important climatic variable whereas evidence for temperature change is weak. The highest area in Minorca is 358 m a.s.l. which hardly allows for a temperature-stratified vegetation. It is assumed that evergreen and semi-deciduous taxa lodged in the gallery forests along the drainage systems while taxa more resistant to seasonal dryness occurred on the more exposed parts of the island. It is suggested that the pool of floral diversity lodged in the gallery forest and selected taxa became periodically abundant elsewhere.

Tenerife (Canary Islands, Eastern Atlantic Ocean) – Tenerife is a steeply sloped volcanic island with highest peaks up to over 3700 m and a small surface of only 2034 km^2. From a former lake bed in the city of La Laguna (Tenerife, Canary Islands) at 560 m elevation a 210-cm long sediment core reflecting the last 4.7 cal. kyr was analysed for pollen and charcoal (de Nascimento *et al.*, 2009). During the interval of ca. 4.7–2.9 cal. ka mixed forest was present dominated by *Quercus*, *Carpinus*, *Myrica* and *Pinus*. During the interval of ca. 2.9–2.0 cal. ka taxa of laurel forest increased, while *Pinus*, *Juniperus* and *Phoenix* declined. During the interval of 2.0–0.4 cal. ka the abundance of *Carpinus* and *Quercus* declined and laurel forest, including *Myrica,* established (de Nascimento *et al.*, 2009). Neither *Carpinus* nor *Quercus* was hitherto considered to be native to the Canary Islands. The decline of both taxa started ca. 2.0 cal. ka coinciding with microfossil charcoal evidence of increased burning and with archaeological evidence for first human settlement in Tenerife. It is suggested that in this island the pool of floral diversity was, and still is altitudinally stratified and plausibly lodged in relatively stable cloud forest from which taxa could spread over the island and reach temporarily high cover.

Azores (mid Atlantic Ocean) – Highest mountains in the archipelago of the Azores reach up to 2351 m. From the island of Flores a 330-cm sediment core was collected from Lake Rasa (530 m a.s.l.) reflecting the last 2.75 cal. kyr (Connor *et al.*, 2012). Apart from the last 500 years, the record shows forest with a stable taxonomic composition. From the island of Pico a 625-cm sediment core was collected from Lagoa do Caveiro reflecting the last 6 cal. kyr (Connor *et al.*, 2012). Neglecting the lowermost 175-cm with an impact of volcanic activity as well as the last 500 years showing human impact, the period from 5 to ca. 0.5 cal. ka shows a relatively stable forest composition. There is no hint to a reservoir of diversity supplying taxa episodically to change the floral composition of the main forests.

Mauritius (Indian Ocean) – The island of Mauritius is part of the Mascarene archipelago. Its surface is 1865 km^2. The area above 500 m a.s.l. covers only 8% of the island and highest peaks reach to 828 m (Van der Plas *et al.*, 2012). The pollen record from Kanaka Crater was collected at 560 m elevation where montane forest prevails. The surface and elevational profile of this small oceanic island preclude significant altitudinal or latitudinal migration of biomes.

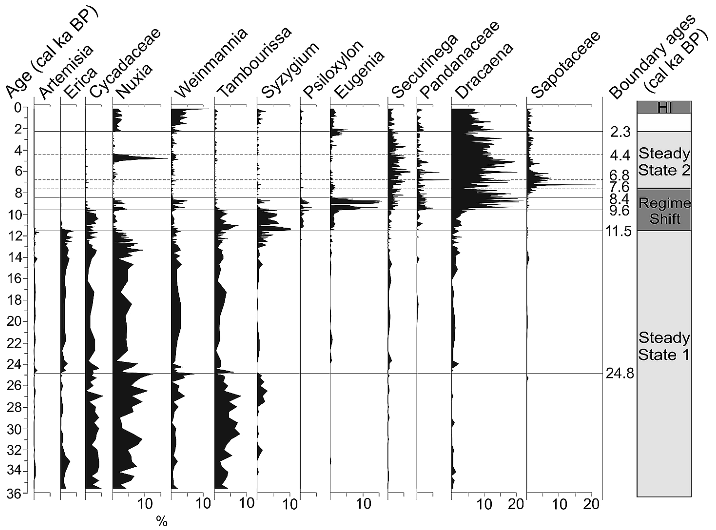

Figure 2. Pollen percentage diagram of Kanaka Crater (560 m elevation) in Mauritius showing selected pollen records documenting the repeated forest re-organisations (after de Boer *et al.*, in review).

The high-resolution pollen record shows a multi-step transition (de Boer *et al.*, 2013a). A stable glacial *Nuxia-Weinamannia*-dominated forest (35.6–11.5 cal. ka interval) changed into a stable Holocene forest (6.8–2.3 cal. ka interval) mainly consisting of *Dracaena*, *Pilea*, *Ficus*, *Cyathea*, Sapotaceae and Euphorbiaceae (Fig. 2). The transition between both «steady states» is of a remarkable complexity. Apparently at ca. 11.5 cal. ka an ecological threshold was crossed propelling the forest biome into a cascade of short-lived forest types. Successively montane forest was for 1900 years characterized by *Syzygium* (11.5–9.6 cal. ka), for 1100 years by *Eugenia* (9.6–8.5 cal. ka), and for 900 years dominated by trees of the Sapotaceae family (7.6–6 cal. ka). *Dracaena*, *Pilea*, *Ficus* and Cyatheaceae tree ferns were a permanent constituent of the forest. Species turnover occurred at a remarkably fast rate (< 150 years) compared to changes during the preceding and following «steady states». The initial change at 11.5 cal. ka, marking the glacial-interglacial transition, was interpreted as climate-driven whereas the suite of short-lived forest types that followed is more likely to reflect internal dynamics of the forest biome and, therefore, interpreted as system-driven (de Boer *et al.*, 2013a). It was hypothesized that wet gallery forest, spatially and temporally stabilized by the drainage system, serves as a reservoir of diversity allowing rapid exchange of species with the surrounding montane forest. In absence of the possibility that a biome keeps balance with changing climatic conditions by migrating to a new location, this pollen record supports the hypothesis that a change of taxonomic composition might be an alternative and equally adequate response for a geographically-locked montane forest.

Southern Italy – From Lago Grande di Monticchio located at 656 m a.s.l. in southern Italy a composite sediment record was collected reflecting the last 15 cal. kyr (Allen *et al.*, 2002). Steppe vegetation dominated by Poaceae, Chenopodiaceae and *Artemisia* dominated up to 14.3 cal. ka. The 1500-years long period from 14.3 to 12.8 cal. ka shows a transitional phase to forest dominated by *Quercus*. During the Holocene repeatedly new taxa enriched the forests, such as *Tilia* (ca. 13.5 cal. ka), *Corylus* (ca. 11.5 cal. ka), *Ostrya* (ca. 10.5 cal. ka), *Alnus* (ca. 10 cal. ka), *Abies* (ca. 9.9 cal. ka and disappeared locally together with *Taxus* ca. 3 cal. ka), *Carpinus* (ca. 9 cal. ka), *Olea* (ca. 2.7 cal. ka), *Castanea* and *Juglans* (ca. 1.5 cal. ka). The record shows a post-glacial taxonomic enrichment of the forest by immigration from glacial source areas possibly located in the condensation zone of the mountains in southern Italy where moist conditions prevailed. When all taxa had arrived in the study area forest composition was relatively stable up to the start of human impact around 3 cal. ka. This record is an example of altitudinally stratified vegetation and migration over a significant distance between glacial and Holocene conditions.

Atlas Mountains, Morocco – In the Moroccan Atlas mountains an informative pollen record comes from Lake Tigalmamine at 1626 m a.s.l. reflecting the last 14 ^{14}C kyr BP (Lamb *et al.*, 1989; Cheddadi *et al.*, 2009). The record shows extensive steppe vegetation (Poaceae, Chenopodiaceae-Amaranthaceae, *Artemisia*) during the last part of the glacial. Around 12 ^{14}C kyr BP steppe decreased rapidly replaced by *Quercus*-dominated forest, at 4 ^{14}C kyr BP *Cedrus* and other Mediterranean trees became also an important constituent of the forest in the western Atlas Mountains. Taxa responsible for the post-glacial vegetation enrichment may have migrated from other areas in the Atlas Mountains where refugial conditions prevailed. The fast and massive expansion of oak forest suggest that oak's glacial residence area was at relatively close distance and isolated from Tigalmamine area by a steep environmental gradient (Cheddadi *et al.*, 1998).

Northwest Saharan Africa – From the western Sahara south of the Atlas Mountains palaeoecological evidence from sedimentary archives is scarce due to dry climatic conditions. The northernmost position of wet forest around 8 ^{14}C kyr BP was documented in several pollen records across the Sahara (Lézine, 1989) of which the multi-proxy record of Lake Yoa from northern Chad is outstanding (Kröpelin *et al.*, 2008; see also Holmes, 2008). Large-scale changes in the latitudinal vegetation distribution in Saharan Africa are also registered in offshore marine cores (e.g. Lézine and Hooghiemstra, 1990; Hooghiemstra *et al.*, 1992). A comparison of modern pollen rain spectra between 13° and 21° N and surface samples from the offshore ocean floor between the same latitudes showed that the ratio between Poaceae pollen (reflecting savanna) and Chenopodiaceae-Amaranthaceae pollen (reflecting desert vegetation) reflects the southern limit of the Sahara (Lézine and Hooghiemstra, 1990). At the northern border of the Sahara the narrow latitudinal width of the *Artemisia*-dominated steppe belt hints to a steep climatic gradient across the Atlas Mountains separating a Mediterranean climate from a steppe and desert climate (Hooghiemstra *et al.*, 1992). The changes in the steepness of the climatic gradient across the Atlas, the changing north-south diameter of the desert, and the abruptness of these changes is remarkable. Increased moisture in northwestern Africa during the last glacial is often related to an enhancement of precipitation from westerly cyclones (Rognon and Coudé-Gaussen, 1996; Van Geel *et al.*, 2000; Suchodoletz *et al.*, 2010). However, there is substantial pollen-based evidence that the trade winds originated in the Western Mediterranean area (Hooghiemstra, 1989) which is not compatible with a more southwards located trajectory of the westerlies. Convincing evidence for climatic moisture in northwest Africa during glacial times is still lacking although Suchodoletz *et al.* (2010) demonstrated enhanced monsoonal activity. In northwest Africa changes in vegetation distribution over hundreds of kilometres are clearly climate-forced.

East African mountains – In the East African mountains the altitudinal vegetation distribution changed significantly at the Lateglacial to Holocene transition (Kiage and Liu, 2006; Wu *et al.*, 2007). The upper forest line, separating the upper montane forests and tropical alpine grasslands, shifted since the LGM over 1000 to maximally 1700 m. Thus, in the East African mountains plant diversity was re-distributed along the slopes and migrated over much shorter (vertical) distances compared to the large (horizontal) distances plants migrated in northwest Africa. Both examples show climate change-forced migration of suites of plant taxa. Apart from changes in taxonomic composition altitudinally constrained plant associations migrated as relatively stable entities.

DISCUSSION

Post-glacial change in land surface of islands

Mauritius and Tenerife – Flat topography in Mauritius caused a 30% surface decrease at last glacial to Holocene transition (Fig. 3) (Rijsdijk *et al.*, this volume). With most of the surface below 500 m, low mountain tops of maximally 828 m, and stable temperatures due to the influence of the permanent Indian Ocean hot water pool, there are little possibilities for an altitudinally developed zonation. In contrast, the surface of Tenerife shrunk only 15% due to the steep sloped 3 km high conical-shaped volcano. Post-glacial contractions of the coastal palm-rich vegetation/coastal shrubland, and lower montane forest/woodland on Mauritius and Tenerife respectively, occurred due to inland migration of the coast line. In addition, the effect of the post-glacial loss of 120 m altitudinal range is much larger in low-profiled Mauritius than in high-profiled Tenerife. On both islands the density of diversity increased with the post-glacial decrease of the island surface potentially giving rise to and increased interspecies competition for space.

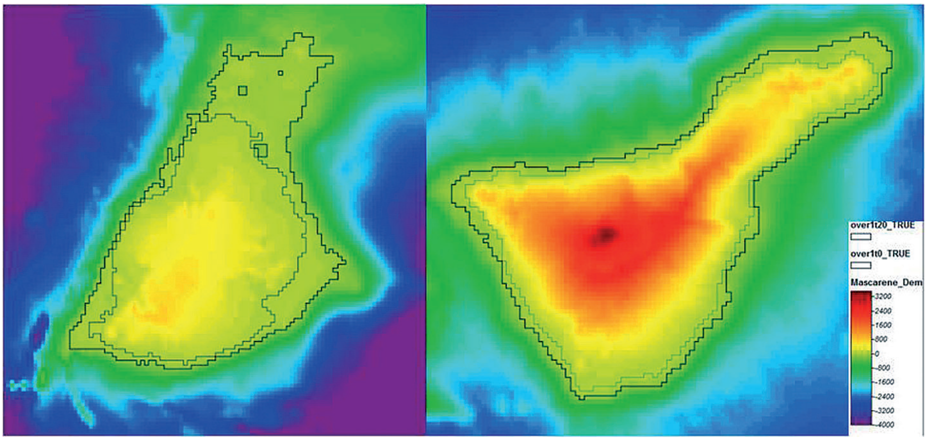

Figure 3. Changes in coastal contours of Mauritius and Tenerife due to sea-level change. Grey inner line represent present-day boundary, black outer line shows the surface during the LGM at 20 ka. Note the significant difference in post-glacial surface reduction: Mauritius 33% and Tenerife 16%. For images generation see Rijsdijk *et al.* this volume.

Cryptic refugia on small oceanic islands

Tenerife – The slopes of Tenerife are cut by fluvially eroded valleys, known as *barrancos*. The *barrancos* do not contain relevant rivers, run with angles ranging between 7° and 17° from the crater rim at ca. 2000 to ca. 2200 m elevation towards the coast, potentially connecting the various zonal montane ecosystems and forming important ecological corridors (Fig. 4A). These *barrancos* can be up to 300 m deep, between ca. 50 m and a few hundred of meters wide and can extent for more than 12 km. Deepest incisions are found in stable slopes that were not affected by large scale landslides (Hurliman *et al.*, 2004). The mid-slope widening of the *barrancos* is caused by sliding and slumping of the unstable steep walls (Menéndez *et al.*, 2008). The *barrancos* have their own microclimate with a higher humidity level and lower mean annual temperature than the surrounding slopes. Also higher lapse rates of the temperature gradient prevail, in particular when *barrancos* are deeper incised than 50 m. Together with the gallery forest along the drainage pattern, higher moisture levels in the *barrancos* may give vascular plant species important shelter during dry episodes.

Mauritius – In Mauritius slopes are cut by steep-sided fluvially incised valleys. In contrast to the dry *barrancos* in Tenerife, these valleys are occupied by active streams. The valleys run from the highest part of the central plateau located in the southwest of the island at ca. 600 m a.s.l. to the coast (Fig. 4B). As soon as these valleys reach the more gentle slopes of the lowlands they narrow

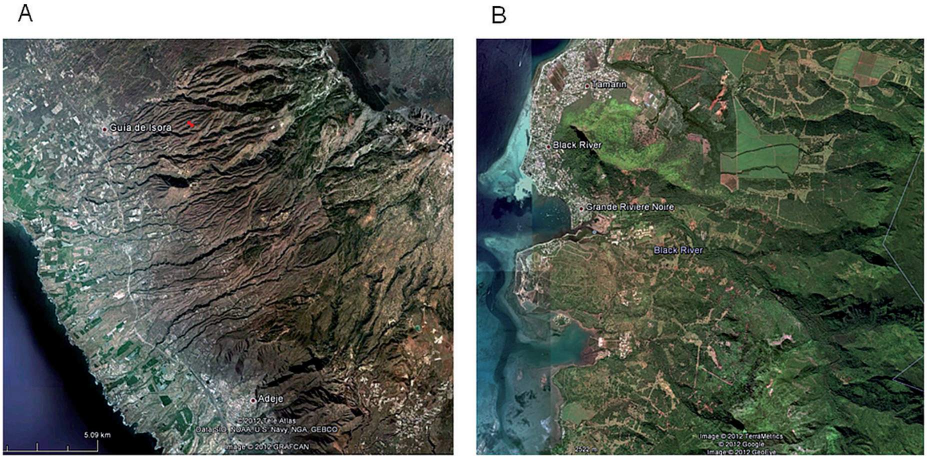

Figure 4. Geomorphological structures relevant for deep-time conservation of diversity. The microclimatic conditions in *barrancos* in southwest Tenerife (left) and deeply incised valleys of the Black River in western Mauritius (right), formed during sea-level lowstands, may have offered refugial conditions for diversity.

down and continue up to some 15 km as narrow (tens of meters) and steep sided (up to 30 m deep) meandering valleys. While the *barrancos* in the steeper slopes of Tenerife run relatively straight forward to the ocean, the more gentle slopes in Mauritius with angles of 3° to 6°, allow the valleys to meander. The valleys are under present-day conditions connected to the drowned valleys in the offshore coral reefs. Although smaller in scale than the *barrancos* in Tenerife, these valleys offer much shade and relatively humid conditions and mean annual temperature is relatively low. In particular during events of drought these valleys potentially offer important shelter to plants at the lower limit of their moisture range.

HOLOCENE VEGETATION DYNAMICS CLIMATE-FORCED OR SYSTEM-DRIVEN?

Terrestrial environments in small oceanic islands are subject to the large buffering capacity of the surrounding ocean. Changes in sea surface temperature (SST) in the (sub)tropics are limited rendering it plausible that small oceanic islands experienced a relatively uniform temperature throughout the Pleistocene. In these small oceanic islands changes in climatic humidity were the most important driver of long-term vegetation change. However, the sensitivity of island floras to changing moisture regimes may vary. For example Madagascar has an old flora that produced a high proportion of endemics (Whittaker and Fernández-Palacios, 2007) of which the ecological range may be expected more tailor-measured to the island habitats. The Mauritian flora includes an intermediate proportion of endemics (Baider *et al.*, 2010) and received elements from source areas as wide as Madagascar, East Africa and the Arabian Peninsula providing the Mauritian flora potentially with a genetic pool wide enough to respond to substantial climate change. The degree to which small island floras of the type of Mauritius are sensitive to environmental and climatic change is questioned and needs further exploration.

During the Pleistocene glacial-interglacial cycles mountains caused restrictions for migration and caused diversity loss. For example, the West European flora was squeezed between the southwards expanding Scandinavian ice sheet and the east-west oriented Alps and Pyrenees leading to a significant impoverishment (Van der Hammen *et al.*, 1971). The steppe vegetation between the northern limit of the Sahara and the Atlas Mountains was also repeatedly squeezed (Hooghiemstra *et al.*, 1992). There, a loss of diversity is not expected as this type of vegetation includes a high proportion of plants with pioneer qualities. In small oceanic islands such latitudinal migration is hardly feasible and concomitant effects are not plausible to have happened.

In mountain areas, biomes migrated altitudinally during the Pleistocene as a response to temperature (Flenley, 1979), atmospheric $p\text{CO}_2$ (Jolly and Haxeltine, 1997; Street-Perrott *et al.*, 1997; 2007; Groot *et al.*, 2011), UV radiation (Flenley, 2011) and moisture. During the LGM in the East African mountains the upper forest line lowered by 1000 to 1700 m (Wu *et al.*, 2007). For comparison, similar values have been reconstructed by Groot *et al.* (2011) in the Andes at 4° N and 2550 m a.s.l., and by González-Carranza *et al.* (2012) in the Andes at 1° N and 2780 m a.s.l. González-Carranza *et al.* (2012) showed events during which cool upper montane forest shifted faster upslope (up to 700 m within 200 years) than the tropical alpine grassland biome was able to migrate in the same direction: a temporary disappearance of these insular tropical alpine grassland areas was documented. The pollen record shows that within few centuries the lost biome returned from source areas that had not been affected by the abrupt vegetation re-organization. A new pollen-based record of vegetation change in the Western Cordillera of the northern Andes shows similar evidence of temporarily lost biomes (Velásquez and Hooghiemstra, 2013). In small oceanic islands consisting of a high single mountain dome, as is the case in Tenerife and in the Azores, diversity is at risk after abrupt climate change and there, differences in moisture between the wet and dry sides of the islands may ensure refugia are around to conserve diversity.

During events when the upper forest line ecotone is shifting through the elevation where the pollen record is collected, the rate of change (RoC) is, as a matter of fact, high. However, this does not necessarily mean that the floral diversity in the migrating biome is at risk. This question can be better assessed when the biome-specific RoC rather than the site-specific RoC is assessed. To do so, a series of pollen records from a number of sites along the slope is required to show how floral diversity of the biome itself is changing. As migration distance along slopes of (sub)tropical mountains is some 1700 m at the maximum there is little reason to expect diversity is lost. Pioneers may migrate faster than late successional taxa giving rise to forest compositions without an analogue to the composition of the previous forest. However, such changes in taxonomic composition may be temporary and fade out when sufficient time is available (González-Carranza *et al.*, 2012).

Small oceanic islands with a low elevational profile, such as Mauritius, offer an interesting test for post-glacial vegetation dynamics as potentially neither altitudinal nor latitudinal re-organisation of the vegetation is expected to be an adequate answer to climate change. In contrast to the pollen records from the small islands of the Azores, Tenerife, and Minorca, in Mauritius each step in vegetation change shows a discrete and short-lived forest phase, i.e. *Syzygium* during 1900 years, followed by *Eugenia* during 1100 years, and subsequently followed by Sapotaceae during 900 years. The taxa *Dracaena*, *Pilea, Ficus* and Cyatheaceae tree ferns were permanently a constituent of the forest. Species turnover between successive forest types occurred in less than ca. 150 years. The initial change at 11.5 cal. ka coincides with the Lateglacial to Holocene transition and we assume that it reflects a climate-forced change. The following steps in the rapid cascade more plausibly reflect intrinsic changes of the forest ecosystem (de Boer *et al.*, 2013a). It was hypothesized that wet gallery forest and deeply incised valleys, spatially and temporally stabilized by the drainage system, serves as a reservoir of diversity allowing rapid exchange of species with the montane forests on the adjacent slopes. This rapidity may have been aided, at least for the many zoochoric species, by a rich fauna of seed disseminators (e.g. Cheke and Hume, 2008; Rijsdijk *et al.* 2009). This cascade of changes in Mauritius contrasts with the records from the other islands where during the Holocene, taxa are successively added to the forest diversity (Fig. 5). Some altitudinal migration due to changing elevations of cloud formation may occur. However, substantial impact of climate-forced migration is hardly expected in these small islands and we rather assume that selected environments with favourable microclimatological conditions, such as gallery forests, *barrancos*, and deeply incised valleys serve as reservoirs of diversity. In continents, individual taxa and consortia of taxa (biomes) may migrate up to distances of over a thousand kilometres. In the latter case long-term conservation of diversity might be more at risk than in small oceanic islands. It is remarkable that after ca. 98% of the original vegetation of Mauritius has been cleared the flora left still belongs to the highly diverse category (Florens *et al.*, 2012). This observation supports the idea that most plant diversity is located in the gallery forest and deeply-incised valleys, areas unsuitable for agricultural activities.

The sequence of mono-taxon dominated montane forest is interpreted as a signal of resilience of these forests to climate change (Rijsdijk *et al.*, 2011): the first step at 11.5 cal. ka is considered as climate-forced and the next steps as system-driven. The sequence of taxa may form a succession driven by variables such as

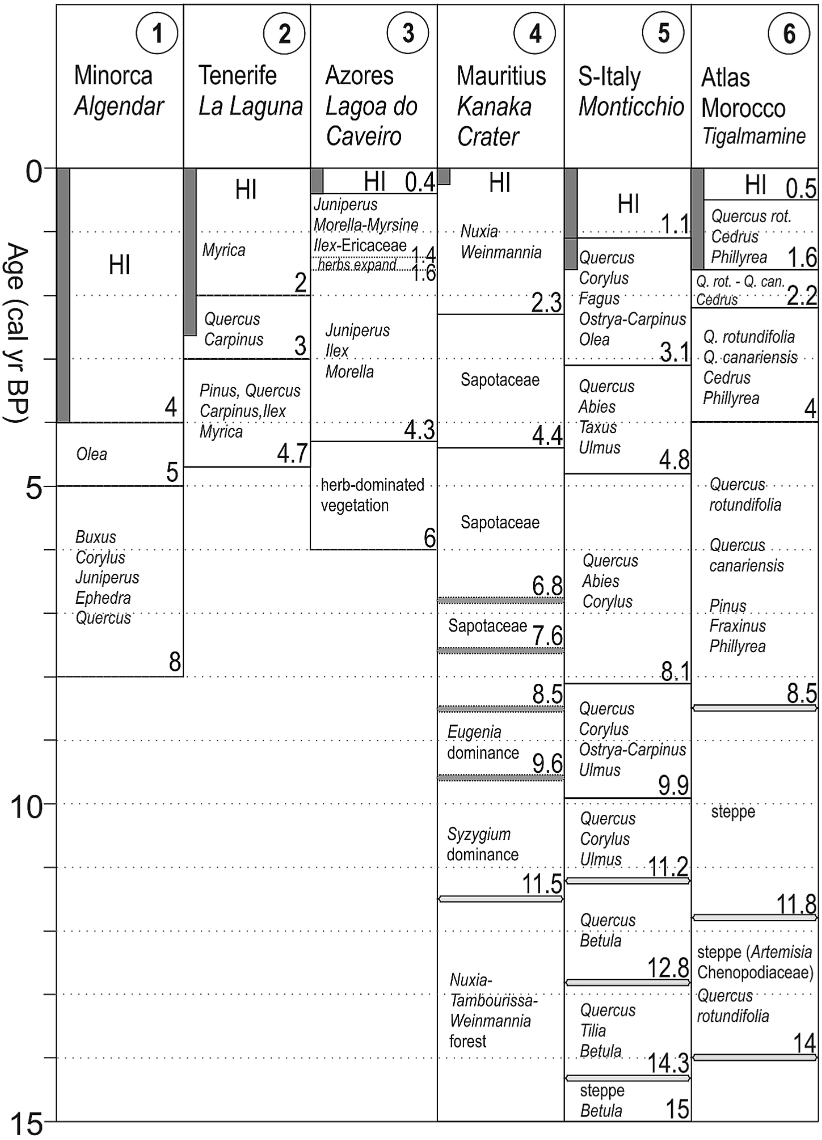

Figure 5. Summary of pollen-based vegetation change in four insular settings (left) and two continental settings (right) plotted on a linear time scale. For site specific information see the text. For each pollen zone dominant taxa of the vegetation are indicated. Transitions between pollen zones show events of change and ages are shown in calibrated years (x 1000) before present (cal. kyr). Open pollen zone boundaries show assumed climate-forced changes; closed pollen zone boundaries show assumed system-driven changes; vertical bars indicate periods with human impact (HI) on the vegetation.

available light (taxa are increasingly shade tolerant), nutrients, and drainage of the soils. The pollen record of Kanaka Crater shows a rare phenomenon and suggests that a change of taxonomic composition might be an adequate response to climate change in a geographically-locked biome.

In the frame of the discussion on Global Change more attention is needed for intrinsic drivers of ecosystem change and climate-driven migration events that occurred so abruptly in the past, and may happen in the future. Whereas ecosystems of intermediate elevations do have more opportunities to persist, marginal ecosystems in highlands and lowlands are more susceptible to disappear either temporarily or permanently. Connectivity between distribution areas is crucial to allow taxa to migrate to areas where populations were lost. The observation that insular biota survived suites of Pleistocene climatic changes implies that island biota are able to respond robustly to environmental change. In small oceanic islands urbanization (fragmentation of connectivity) and degradation of biota possibly are a more serious thread for the future of small island diversity than climate change.

CONCLUSIONS

Post-glacial biome shifts in relatively flat continents are mainly latitudinally driven by precipitation and temperature. Migration may occur over a large distance, from hundreds to up to 1500 km. Migration may lag behind the triggering climate signal as the new areas to be colonized may be temporarily unqualified to receive the new biome. Refugial areas are located at relatively large distance. In mountain areas post-glacial biome shifts are mainly altitudinally over relatively short distances and migration of biomes may be abrupt. Changing temperature and atmospheric CO_2 pressure are the main driving force. Refugial areas are located at maximally ca. 1700 m vertical distance and migration over such short distance includes a low risk for loosing floral diversity.

Plants respond individualistically to climate change. Taxa with pioneer qualities are responding faster than late successional taxa, leading to plant associations that differ from today`s floral composition (non-analogue vegetation) and reaching various levels of community saturation. However, suites of taxa with similar ecological envelopes migrate in concert keeping main altitudinal vegetation associations as a functional entity throughout long-term change. When ecotones are shifting through the elevation of the pollen site, species composition is changing rapidly causing a high site-specific RoC. However, this value is little informative for potential species turnover inside the migrating biome, i.e. biome-specific change. The latter is a relevant proxy to assess the impact of climate change on the vegetation composition.

In small islands with low elevational profiles biomes are «locked» in an environment where ocean waters buffer temperature change and moisture change is the main climatic variable. Pollen records from small oceanic islands mostly show long lasting stable forest associations. The record of Mauritius shows an unprecedented interval of repetitive species turnover at the start of the Holocene. Both examples suggest that small oceanic islands do have reservoirs of plant diversity which serve to provide the necessary species to stock up new forest types after a climate change. In the islands discussed we identified the following areas as potential refugia: 1) gallery forest located along the drainage system (topography constrained), 2) cloud forest located at elevations where cloud formation takes place (sea surface temperature and atmospheric lapse rate constrained), 3) *barrancos* (Tenerife) where relatively humid conditions prevail (geomorphology constrained), and seeds of all elevations are potentially collected in the lowermost part of the valley, and 4) the deeply incised valleys (Mauritius) (geomorphology and sea-level constrained).

ACKNOWLEDGEMENTS

We used the results of many colleagues and we like to express our gratitude to all of them. We thank José María Fernández-Palacios for organizing the workshop in Tenerife leading to valuable discussions; this event was the stimulus to consider palaeoecological evidence in a new perspective to develop thoughts on plant migration. We acknowledge financial support from the Netherlands Foundation for Scientific Research (NWO), the Mauritius Project in particular (project number 819.01.009).

REFERENCES

Allen, J.R.M., Watts, W.A., McGee, E. and Huntley, B. (2002) Holocene environmental variability – the record from Lago Grande di Monticchio, Italy. *Quaternary International*, 88, 69–80.

Baider, C., Florens, F.B.V., Baret, S., Beaver, K., Matatiken, D., Strasberg, D. and Kueffer, C. (2010) Status of plant conservation in oceanic islands of the Western Indian Ocean. Addressing Global Change: a new agenda for botanic gardens. *4th Global Botanic Gardens Congress*, pp. 1–7. National Botanic Gardens of Ireland, Dublin, Ireland.

Bennett, K.D., Bhagwat, S.A. and Willis, K.J. (2012) Neotropical refugia. *The Holocene*, 22, 1207–1214.

Birks, H.J.B. and Birks, H.H. (1980) *Quaternary palaeoecology*. Edward Arnold, London.

Boom, A., Marchant, R., Hooghiemstra, H. and Sinninghe Damsté, J.S., (2002) CO$_2$- and temperature controlled altitudinal shifts of C$_4$- and C$_3$-dominated grasslands allow reconstruction of paleo-atmospheric $p\mathrm{CO}_2$. *Palaeogeography, Paloaeoclimatology, Palaeoecology*, 177, 151–168.

Bouimetarhan, I., Dupont, L., Schefuss, E., Mollenhauer, G., Mulitza, S. and Zonneveld, K., (2009) Palynological evidence for climatic and oceanic variability off NW Africa during the late Holocene. *Quaternary Research*, 72, 188–197.

Bush, M. and de Oliveira, P.E. (2006) The rise and fall of the refugial hypothesis of Amazonian speciation: a paleoecological perspective. *Biota Neotropica*, 6, on-line version available at: http://www.biotaneotropica.org.br/v6n1/pt/abstract?point-of-view+bn00106012006

Cheddadi, R., Lamb, H.F., Guiot, J. and van der Kaars, S. (1998) Holocene climate change in Morocco: a quantitative reconstruction from pollen data. *Climate Dynamics*, 14, 883–890.

Cheddadi, R., Fady, B., Francois, L., Hajar, L., Suc, J.-P., Huang, K., Denarteau, M., Vendramin, G.G. and Ortu, E. (2009) Putative glacial refugia of *Cedrus atlantica* deduced from Quaternary pollen records and modern genetic diversity. *Journal of Biogeography*, 36, 1361–1371.

Cheke, A.S. and Hume, J. (2008) *Lost land of the dodo*. T & AD Poyser, London, United Kingdom.

Coetzee, J.A. (1967) Pollen analytical studies in East and southern Africa. *Palaeoecology of Africa*, 3, 1–146.

CONNOR, S.E., VAN LEEUWEN, J.F.N., RITTENOUR, T.M., VAN DER KNAAP, W.O., AMMANN, B. and BJÖRCK, S. (2012) The ecological impact of oceanic island colonization – a palaeoecological perspective from the Azores. *Journal of Biogeography,* 39, 1007–1023.

DE BOER, E.J., HOOGHIEMSTRA, H., FLORENS, F.B.V., BAIDER, C., ENGELS, S., DAKOS, V., BLAAUW, M. and BENNETT, K.D. (2013a) Rapid succession of plant associations on the small ocean island of Mauritius at the onset of the Holocene. *Quaternary Science Reviews,* 68, 114–125.

DE BOER, E.J., SLAIKOVSKA, M., HOOGHIEMSTRA, H., RIJSDIJK, K.F., VÉLEZ, M.I., PRINS, M., BAIDER, C. and FLORENS, F.B.V. (2013b). Multi-Proxy reconstruction of environmental dynamics and colonization impacts in the Mauritian uplands. *Palaeogeography, Palaeoclimatology, Palaeoecology,* 383–384, 42–51.

DE NASCIMENTO, L., WILLIS, K.J., FERNÁNDEZ-PALACIOS, J.M., CRIADO, C. and WHITTAKER, R.J. (2009) The long-term ecology of the lost forests of La Laguna, Tenerife (Canary Islands). *Journal of Biogeography,* 36, 499–514.

DUPONT, L.M. and HOOGHIEMSTRA, H. (1989) The Sahara-Sahelian boundary during the Brunhes chron. *Acta Botanica Neerlandica,* 38, 405–415.

FLENLEY, J. (1979) *The equatorial rain forest: a geological history.* Butterworths, London-Boston.

FLENLEY, J. (2011) Ultraviolet insolation and the tropical rainforest: altitudinal variations, Quaternary and recent change, extinctions, and the evolution of biodiversity. *Tropical rainforest responses to climate change, 2nd ed.* (ed. by BUSH, M.B., FLENLEY, J. and GOSLING, W.D.), pp. 241–258. Springer, Berlin-Heidelberg.

FLORENS, F.B.V., BAIDER, C., MARTIN, G.M.N. and STRASBERG, D. (2012) Surviving 370 years of human impact: what remains of tree diversity and structure of the lowland wet forests of oceanic island Mauritius? *Biodiversity and Conservation,* 21, 2139–2167.

GIENAPP, P., TEPLITSKY, C., ALHO, J.S., MILLS, J.A. and MERILA, J. (2008) Climate change and evolution: disentangling environmental and genetic responses. *Molecular Ecology,* 17, 167–178.

GONZÁLEZ-CARRANZA, Z., HOOGHIEMSTRA, H. and VÉLEZ, M.I. (2012) Major altitudinal shifts in Andean vegetation on the Amazonian flank show temporary loss of biota in the Holocene. *The Holocene,* 22, 1223–1237.

GROOT, M.H.M., BOGOTÁ, R.G. LOURENS, L.J., HOOGHIEMSTRA, H., VRIEND, M., BERRIO, J.C., TUENTER, E., VAN DER PLICHT, J.H., VAN GEEL, B., ZIEGLER, M., WEBER, S.L. and 14 OTHER FÚQUENE PROJECT MEMBERS (2011) Ultra-high resolution pollen record from the northern Andes reveals rapid shifts in montane climates within the last two glacial cycles. *Climates of the Past,* 7, 299–316.

HOLMES, J.A. (2008) How the Sahara became dry. *Science,* 320, 752–753.

HOOGHIEMSTRA, H. (1989) Variations of the NW African trade wind regime during the last 140,000 years: changes in pollen flux evidenced by marine sediment records. *Paleoclimatology and paleometeorology: modern and past patterns of global atmospheric transport* (ed. by LEINEN, M. and SARNTHEIN, M.), pp. 733–770. Kluwer, Dordrecht, The Netherlands.

Hooghiemstra, H. and Van der Hammen, T. (1998) Neogene and Quaternary development of the neotropical rain forest: the forest refugia hypothesis, and a literature overview. *Earth-Science Reviews*, 44, 147–183.

Hooghiemstra, H. and Van der Hammen, T. (2004) Quaternary ice-age dynamics in the Colombian Andes: developing an understanding of our legacy. *Philosophical Transactions of the Royal Society London B*, 359, 173–181.

Hooghiemstra, H., Stalling, H., Agwu, C.O.C. and Dupont, L.M. (1992) Vegetational and climatic changes at the northern fringe of the Sahara 250,000-5000 years BP: evidence from 4 marine pollen records located between Portugal and the Canary Islands. *Review of Palaeobotany and Palynology*, 74, 1–53.

Hooghiemstra, H., Berrio, J.C., Groot, M.H.M., Bogotá-A, R.G., Moscol-Olivera, M. and González-Carranza, Z. (2012) The dynamic history of the upper forest line ecotone in the northern Andes. *Ecotones between forest and grassland* (ed. by Myster, R.W.). Springer, New York. doi 10.1007/978-1-4614-3797-0_10.

Hoorn, C., Wesselingh, F.P., Ter Steege, H., Bermudez, M.A., Mora, A., Sevink, J., Sanmartín, I., Sanchez-Meseguer, A., Anderson, C.L., Figueiredo, J.P., Jaramillo, C., Riff, D., Negri, F.R., Hooghiemstra, H., Lundberg, J., Stadler, T., Särkinen, T. and Antonelli, A. (2010) Amazonia through time: Andean uplift, climate change, landscape evolution, and biodiversity. *Science*, 330, 927–931.

Hürlimann, M., Martí, J. and Ledesma, A. (2004) Morphological and geological aspects related to large slope failures on oceanic islands. *Geomorphology*, 62, 143–158.

Jolly, D. and Haxeltine, A. (1997) Effect of low glacial atmospheric CO_2 on tropical African montane vegetation. *Science*, 276, 786–787.

Kiage, L.M. and Liu, K.-B.M. (2006) Late Quaternary paleoenvironmental changes in East Africa: a review of multiproxy evidence from palynology, lake sediments, and associated records. *Progress in Physical Geography*, 30, 633–658.

Knapp, R. (1973) *Die Vegetation von Afrika*. Fischer, Stuttgart.

Kröpelin, S., Verschuren, D., Lézine, A.-M., Eggermont, H., Cocquyt, C., Francus, P., Cazet, J.-P., Fagot, M., Rumes, B., Russell, J.M., Darius, F., Conley, D.J., Schuster, M., Suchodoletz, H. von and Engstrom, D.R. (2008) Climate-driven ecosystem succession in the Sahara: the past 6000 years. *Science*, 320, 765–768.

Lamb, H.F., Eicher, U. and Switsur, V.R. (1989) An 18,000-year record of vegetation, lake-level and climatic change from Tigalmamine, Middle Atlas, Morocco. *Journal of Biogeography*, 16, 65–74.

Lézine, A.-M. (1989) Late Quaternary vegetation and climate of the Sahel. *Quaternary Research*, 32, 317–334.

Lézine, A.M. and Hooghiemstra, H. (1990) Land-sea comparisons during the last glacial-interglacial transition: pollen records from west tropical Africa. *Palaeogeography, Palaeoclimatology, Palaeoecology*, 79, 313–331.

Lister, A.M. (2004) The impact of Quaternary ice ages on mammalian evolution. *Philosophical Transactions Royal Society London B*, 359, 221–241.

LOVETT, J.C. and WASSER, S.K. (1993) *Biogeography and ecology of the rain forests of eastern Africa*. Cambridge University Press, Cambridge, UK.

MENÉNDEZ, I., SILVA, P.G., MARTÍN-BETANCOR, M., PÉREZ-TORRADO, F.J., GUILLOU, H. and SCAILLET, S. (2008) Fluvial dissection, isostatic uplift, and geomorphological evolution of volcanic islands (Gran Canaria, Canary Islands, Spain). *Geomorphology*, 102, 189–203.

MILLER, K.G., KOMINZ, M.A., BROWNING, J.V., WRIGHT, J.D., MOUNTAIN, G.S., KATZ, M.E., SUGARMAN, P.J., CRAMER, B.S., CHRISTIE-BLICK, N. and PAKER, S.F. (2005) The Phanerozoic record of global sea-level change. *Science*, 310, 1293–1298.

MISTRY, J. (2000) *World savannas. Ecology and human use*. Pearson Education, Prentice Hall, Harlow, UK.

OSBORNE, P.J. (2012) *Tropical ecosystems and ecological concepts, 2nd ed.* Cambridge University Press, Cambridge, UK.

PAGANI, M., CALDEIRA, K., BERNER, R. and BEERLING, D.J. (2009) The role of terrestrial plants in limiting atmospheric CO_2 decline over the past 24 million years. *Nature*, 460, 85–88.

POREMBSKI, S. and BARTHLOTT, W. (eds.) (2000) *Inselbergs. Biotic diversity of isolated rock outcrops in tropical and temperate regions*. Ecological Studies 146, Springer, Berlin-Heidelberg-New York.

RIJSDIJK, K.F., HUME, J.P., BUNNIK, F., FLORENS, F.B.V., BAIDER, C., SHAPIRO, B., VAN DER PLICHT, J., JANOO, A., GRIFFITHS, O.L., VAN DEN HOEK OSTENDE, L.W., CREMER, H., VERNIMMEN, T., DE LOUW, P.G.B., BHOLAH, A., SAUMTALLY, S., PORCH, N., HAILE, J., BUCKLEY, M., COLLINS, M. and GITTENBERGER, E. (2009) Middle-Holocene concentration-Lagerstatten on oceanic island Mauritius provides a window into the ecosystem of the dodo (*Raphus cucullatus*). *Quaternary Science Reviews*, 28, 14–24.

RIJSDIJK, K.F., ZINKE, J., DE LOUW, G.B., HUME, J.P., VAN DER PLICHT, J., HOOGHIEMSTRA, H., MEIJER, H.J.M., VONHOF, H.B., PORCH, N., FLORENS, F.B.V., BAIDER, C., VAN GEEL, B., BRINKKEMPER, J., VERNIMMEN, T. and JANOO, A. (2011) Mid-Holocene (4200 yr BP) mass mortalities in Mauritius (Mascarenes): insular vertebrates resilient to climatic extremes but vulnerable to human impact. *The Holocene*, 21, 1179–1194.

RIJSDIJK, K.F., HENGL, T., NORDER, S. and FERNÁNDEZ-PALACIOS, J.M. (this volume) Modelling sea level driven change of Macaronesian archipelago configurations since 120 kyr BP. *Climate Change: past, present and future perspectives. A global synthesis from the Atlantic* (ed. by FERNÁNDEZ-PALACIOS, J.M., DE NASCIMENTO, L., HERNÁNDEZ, J.C., CLEMENTE, S., DÍAZ, J.P. and GONZÁLEZ, A.), pp. 127–148. Servicio de Publicaciones, Universidad de La Laguna, (in press).

ROGNON, P. and COUDÉ-GAUSSEN, G. (1996) Paleoclimates off northwest Africa (28-35°N) about 18,000 yr BP based on continental aeolian deposits. *Quaternary Research*, 46, 118–126.

SEXTON, J.P., MCKAY, J.K. and SALA, A. (2002) Plasticity and genetic diversity may allow saltcedar to invade cold climates in North America. *Ecological Applications*, 12, 1652–1660.

SHORROCKS, B. (2007) *The biology of African savannas*. Oxford University Press, Oxford, UK.

Stewart, J.R., Lister, A.M., Barnes, I. and Dalén, L. (2010) Refugia revisited: individualistic responses of species in space and time. *Proceedings Royal Society B*, 277, 661–671.

Street-Perrott, F.A., Huang, Y., Perrott, R.A., Eglinton, G., Barker, P., Ben Khelifa, L., Harkness, D.D. and Olago, D.O. (1997) Impact of lower atmospheric CO_2 on tropical mountain ecosystems. *Science*, 278, 1422–1426.

Street-Perrott, F.A., Barker, P.A., Swain, D.L., Ficken, K.J., Wooller, M.J., Olago, D.O. and Huang, Y. (2007) Late Quaternary changes in ecosystems and carbon cycling on Mt. Kenya, East Africa: a landscape-ecological perspective based on multi-proxy lake-sediment influxes. *Quaternary Science Reviews*, 26, 1838–1860.

Suchodoletz, H. von, Oberhänsli, H., Hambach, U., Zöller, L., Fuchs, M. and Faust, D. (2010) Soil moisture fluctuations recorded in Saharan dust deposits on Lanzarote (Canary Islands) over the last 180 ka. *Quaternary Science Reviews*, 29, 2173–2184.

Taylor, D.M. (1990) Late Quaternary pollen records from two Ugandan mires: evidence for environmental change in the Rukiga Highlands of southwest Uganda. *Palaeogeography, Palaeoclimatology, Palaeoecology*, 80, 283–300.

Thompson, R.S., Anderson, K.H. and Bartlein, P.J. (2000) *Atlas of relations between climatic parameters and distributions of important trees and shrubs in North America (3 volumes).* US Geological Survey Professional Paper 1650A (269 pp.), 1650B (423 pp.), 1650C (386 pp.), Denver, Colorado, USA.

Van der Hammen, T., Wijmstra, T.A. and Zagwijn, W.H. (1971) The floral record of the late Cenozoic of Europe. *Late Cenozoic glacial ages* (ed. by Turekian, K.K.), pp. 391–424. Yale University Press, New Haven-London.

Van der Plas, G.W., De Boer, E.J., Hooghiemstra, H., Florens, F.B.V., Baider, C. and Van der Plicht, J. (2012) Mauritius since the last glacial: environmental and climatic reconstruction of the last 38,000 years from Kanaka Crater. *Journal of Quaternary Science*, 27, 159–168.

Van Geel, B., Heusser, C.J., Renssen, H. and Schuurmans, C.J.E. (2000) Climatic change in Chile at around 2700 BP and global evidence for solar forcing: a hypothesis. *The Holocene*, 10, 659–664.

Van Hengstum, T., Lachmuth, S., Oostermeijer, J.G.B., den Nijs, J.C.M., Meirmans, P.G. and van Tienderen, P.H. (2012) Human-induced hybridization among congeneric endemic plants in Tenerife, Canary Islands. *Plant Systematics and Evolution*, 298, 1119–1131.

Velásquez, C.A. and Hooghiemstra, H. (2013). Pollen-based 17-kyr forest dynamics and climate change from the Western Cordillera of Colombia: no-analogue associations and temporarily lost biomes. *Review of Palaeobotany and Palynology*, 149, 38–49.

Warren, B.H., Strasberg, D., Bruggemann, J.H., Prys-Jones, R.P. and Thébaud, C. (2010) Why does the biota of the Madagascar region have such a strong Asiatic flavour? *Cladistics*, 26, 526–538.

Whittaker, R.J. and Fernández-Palacios, J.M. (2007) *Island biogeography, Ecology, Evolution and Conservation 2nd ed.* Oxford University Press, Oxford.

Willis, K.J. and Van Andel, T.H. (2004) Trees or no trees? The environments of central and eastern Europe during the last glaciation. *Quaternary Science Reviews*, 23, 2369–2387.

Willis, K.J. and Whittaker, R.J. (2000) The refugial debate. *Science*, 287, 1406–1407.

White, F. (1983) *The vegetation of Africa*. UNESCO, Paris.

Wu, H., Guiot, J., Brewer, S., Guo, Z. and Peng, C. (2007) Dominant factors controlling glacial and interglacial variations in the treeline elevation in tropical Africa. *Proceedings National Academy Sciences USA*, 104, 9720–9724.

Yll, E.-I., Perez-Obiol, R., Pantaleon-Cano, J. and Roure, J.M. (1997) Palynological evidence for climatic change and human activity during the Holocene on Minorca (Balearic Islands). *Quaternary Research*, 48, 339–347.

Zazo, C., Dabrio, C.J., Goy, J.L., Lario, J., Cabero, A., Silva, P.G., Bardají, T., Mercier, N., Borja, F. and Riquero, E. (2008) The coastal archives of the last 15 ka in the Atlantic-Mediterranean Spanish linkage area: sea level and climate changes. *Quaternary International*, 181, 72–87.

Zinck, J.A. and Huber, O. (editors) (2011) *Peatlands of the Western Guyana Highlands, Venezuela*. Ecological Studies 217. Springer, Berlin-Heidelberg.

METAPOPULATION REFUGIUM: CEDAR FORESTS IN MOROCCO

Rachid Cheddadi

CLIMATE CHANGE PERSPECTIVES FROM THE ATLANTIC:
PAST, PRESENT AND FUTURE
Jose María Fernández-Palacios, Lea de Nascimento, José Carlos Hernández,
Sabrina Clemente, Albano González & Juan P. Díaz-González (eds.)
Servicio de Publicaciones, Universidad de La Laguna – 2013

ISBN: 978-84-15910-54-1
pp. 75-94

ABSTRACT

The hypothesis proposed here is that Cedars forests in the Middle Atlas, Morocco, have persisted on the long-term as a metapopulation that responded to past climate changes by adapting its altitudinal range. There was probably not a one refugium or multiple local refugia during the last glacial period from which the Middle Atlas mountains have been recolonised but rather a long lasting metapopulation which adapted its composing populations to past climate changes by altitudinal shifts, local recolonisations, extinctions... Thus, during the last glacial period, Cedar forests have migrated at much lower altitudes than today which probably allowed some gene exchanges between closer populations. Conversely, during the early Holocene, when the overall climate became warmer than today, Cedar forests moved at higher altitudes. The resulting effect is the reduction of their range size, which had probably limited potential migration and/or gene flow between local populations. Such hypothesis may be coherent with the genetic data that show that the lowest diversity estimates are found in the Middle Atlas and that there is a weak genetic structure that is related to isolation by distance among populations. The hypothesis here is that Cedar populations had a rather more extended range at lower altitudes during the last glacial period than today in the Middle Atlas and then their range reduced very much during the early warm Holocene because Cedars had to shift towards higher altitudes to compensate the winter temperature increase.

KEYWORDS: *Cedrus atlantica*, glacial refugia, metapopulation, Middle Atlas, Morocco, Quaternary records.

INTRODUCTION

Understanding why and if a forest species may adapt its range size in a mountainous landscape is an important issue in ecology, particularly in the context of rapid future global climate change. *Cedrus atlantica* forests are located nowadays within an altitudinal range that extends between ca. 1400 and 2200 meters above sea level (m a.s.l.). They have a very characteristic landscape form in the Mediterranean area, with great historical, socio-economic and ecological value. Cedar forests' current distribution in Morocco is fragmented in the Rif, the Middle Atlas and the extreme northeastern High Atlas mountains. This fragmentation which was originally natural has become more pronounced with the increasing aridity (Linares *et al.*, 2011a) and human activities which have generally a marked effect on forest ecosystems, probably more important than any other impact during the last centuries (Lamb and Van der Kaars, 1995).

It is important to distinguish between fragmented and natural patchy forests. The latter has rich structures, including trees with different age and height, whereas the artificially fragmented ones may be a simple patch with often the same species and age. In Morocco, the Cedar forests have a patchy distribution and the undergoing pressure (both climate warming and human pressure) generates an additional fragmentation of their habitat.

Nowadays, the forest fragmentation process is a phenomenon that occurs more commonly in tropical forests where human activities can be severe (Laurance *et al.*, 2002) but one can easily observe that it impacts also strongly the Mediterranean forests. The literature on effects of habitat fragmentation on biodiversity is enormous as the process generates several physical and biological changes in the forest ecosystems. Several studies show that there is an increasing chance of loss of biodiversity due to physical changes in the habitat conditions (Hanski, 2005). Although such point of view can be challenged (Fahrig, 2003), the present-day populations of Cedar in the Mediterranean may represent the «last hope» for (their) biodiversity conservation.

The combined effect of climate change and human pressures encourage better conservation management of Cedar forests (Fady *et al.*, 2008). For this it is important to know how these Cedar forests have responded to past climate changes, what were their reactions to adapt, and ultimately have they a chance to cope with the undergoing global climate warming. This obviously could help to develop conservation strategies for a better future management.

Cedars have adjusted their geographical distribution over the glacial and interglacial periods since the Tertiary (Magri, 2012). Past climate changes and related species adaptation are now known to leave their imprints in the genetic structure of the species (Petit *et al.*, 2003). In the case of Cedars, Bou Dagher-Kharrat *et al.* (2007) and Qiao *et al.* (2007) have shown that the Himalayan species, *Cedrus deodara*, diverged first, and then the North African species *Cedrus atlantica* separated from the common ancestor of *Cedrus libani* and *Cedrus brevifolia*. The latter two species are now located in the Eastern Mediterranean region. Qiao *et al.* (2007) used a molecular clock to estimate the timing of the genetic split between *Cedrus atlantica* and the two Eastern Mediterranean species of about 25 Myr ago (Fig. 1). These authors concluded that it is very likely that *Cedrus* migrated into North Africa in the very late Tertiary. Magri (2012) provides a quite detailed reconstruction of the appearance timing of *Cedrus* in the Mediterranean borderlands and, based on a synthesis of long fossil pollen records, the author states that *Cedrus* was present in Morocco throughout the Quaternary which confirms an earlier genetic study on Moroccan Cedars (Terrab *et al.*, 2006).

The question in this book chapter is how did Cedars persist in the Middle Atlas, Morocco, during the last thousand years encompassing the last glacial period and the Holocene? Have they disappeared during the last glacial period, did they

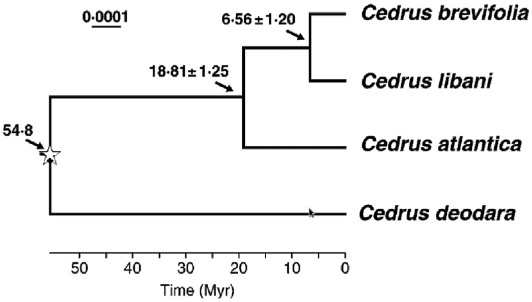

Figure 1. Cedar phylogeny and time scale of evolution (from Qiao *et al.*, 2007).

survive in a few restricted «classical glacial refugia» from which they have recolonized the Middle Atlas or have they had an even more extended range than today?

MATERIALS, METHODS, AND SOME RELATED RESULTS

The approach adopted in this study is based mainly on fossil data available in the Middle Atlas, Morocco.

Unlike in the temperate regions, northern Africa has very few peat bogs, mires or lakes where fossil proxies are well preserved within continuous Quaternary records. Nevertheless, Holocene vegetation changes have been partly documented for the Holocene from several pollen data (Reille, 1977; 1976; Ben Tiba and Reille, 1982; Lamb *et al.*, 1989; 1995; 1999; Salamani, 1991; Benslama *et al.*, 2010). Most of these records are unfortunately quite poorly dated, which does not allow inferring either the potential migration pathways of Cedar or the putative glacial refugia.

In the Middle Atlas, I have selected two well-dated pollen records from Lake Tigalmamine (Lamb *et al.*, 1995) located at 1626 m a.s.l. and Lake Sidi Ali (Lamb *et al.*, 1999) at 2080 m a.s.l. These records cover the Holocene and the last 7000 years BP, respectively. Besides these Holocene sites I have used a record from Lake Ifrah (Cheddadi *et al.*, 2009) collected at 1620 m a.s.l. and a new one from Ras El Ma at 1633 m a.s.l. (Nour El Bait *et al.*, submitted). Both sites are located in the Northern part of the Middle Atlas. The time span covered by the sequence collected in lake Ifrah extends from c. 25 to c. 5 ka and the one from Ras El Ma covers the last 19,000 years continuously. The pollen records of Lake Ifrah and Ras El Ma (Fig. 2) show that Cedar populations were present in the area during the last glacial period. Between 19 and 16 ka, they expanded substantially and then regressed during the early Holocene. The pollen record of Tigalmamine confirms that Cedars were not present between 10 and 7000 years

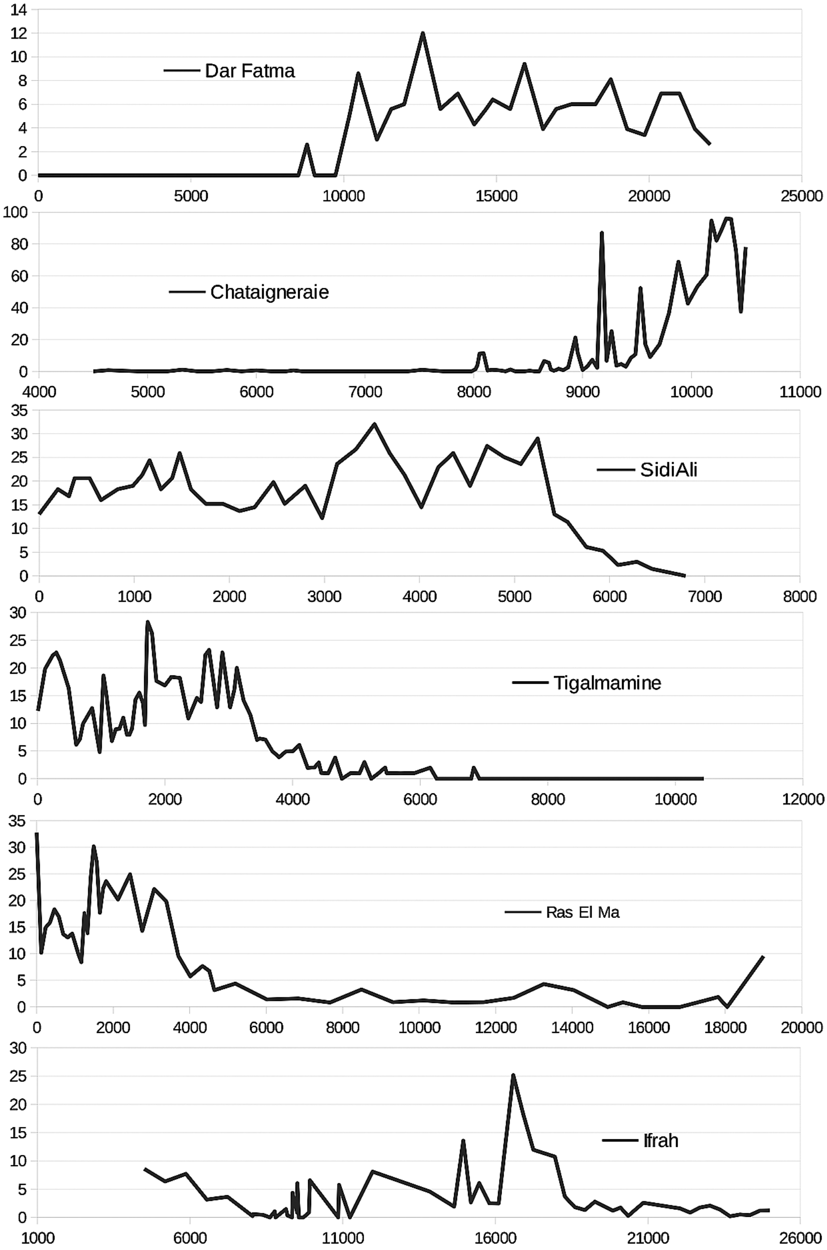

Figure 2. *Cedrus* pollen percentages in the fossil records of Tigalmamine, Ifrah, Sidi Ali and Ras El Ma in Morocco, La Chataigneraie in Algeria and Dar Fatma in Tunisia.

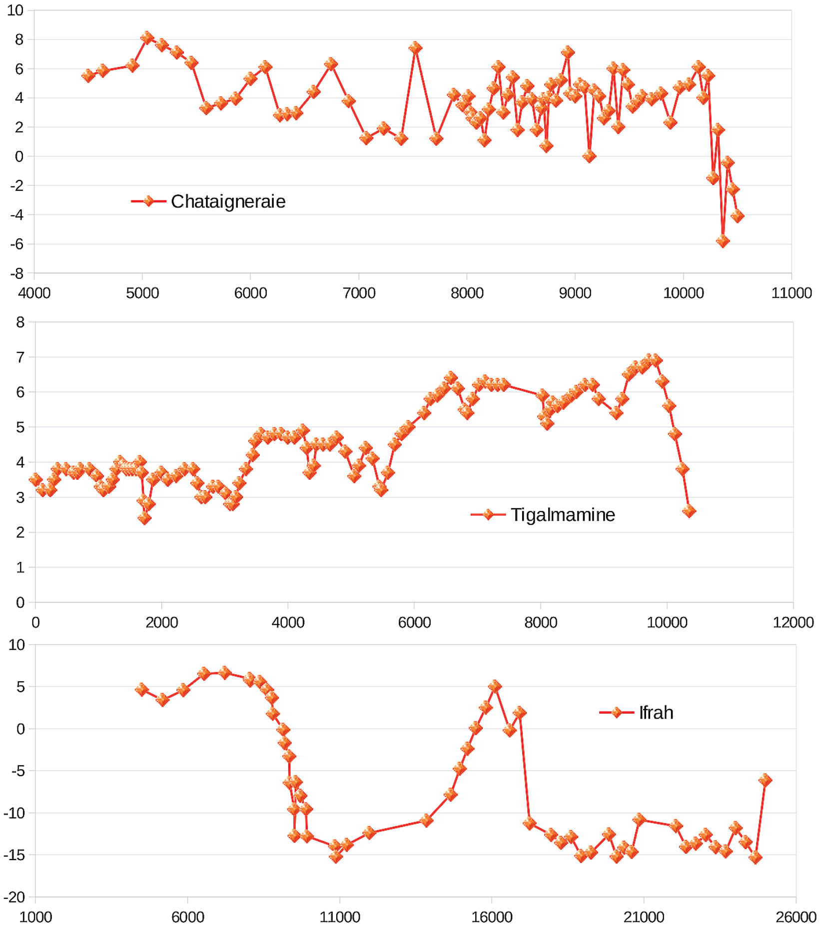

Figure 3. Reconstructed January temperature from Tigalmamine and Ifrah lakes (Morocco) and La Chataigneraie (Algeria).

BP. Then, both Tigalmamine and Sidi Ali records indicate that Cedars expanded only after 7000 years BP.

Although this study concerns only the Middle Atlas in Morocco, it is interesting to fit it into a broader geographical schema and to check if the hypothesis discussed here is reproducible elsewhere. Thus, in Algeria, there are two interesting and detailed pollen records from La Chataigneraie (Salamani, 1991) located at ca. 1225 m a.s.l. which covers approximately the last 11,000 years BP and Garaat-el-ouez (Benslama *et al.*, 2010), at 45 m a.s.l., which encompasses the end of the last glacial period to the Holocene. These Algerian records show that

Cedar populations were present during the end of the last glacial period (Garaat-el-ouez) and the early Holocene until c. 9000 years BP, and then they declined between 9000 and 8000 years BP (La Chataigneraie) (Fig. 2) to the point where they became locally extinct until today.

In Tunisia, despite the presence of sedimentary hiatuses, the pollen records of Dar Fatma (Ben Tiba and Reille, 1982) located at 780 m a.s.l. recorded part of the last glacial period and show that Cedar populations were present in Kroumirie mountains until the early Holocene. Just like in La Chataigneraie (Algeria), Cedars were no longer identified in the pollen record during the late Holocene.

Besides the sites elevations and presence/absence of Cedars in the fossil pollen records I have used the climate reconstructions (Fig. 3) performed on Tigalmamine, Ifrah and La Chataigneraie (Cheddadi *et al.*, 2009). These climate reconstructions were performed using the closest modern analogue technique that is based on the best match between modern and fossil samples using a statistical measure of similarity (Guiot, 1987). In order to be able to discuss the relationship between the reconstructed climate values and *Cedrus* and avoid circular reasoning, Cedar pollen percentages were removed from both the modern and the fossil pollen assemblages.

In order to explore the potential altitudinal range expansion or regression of Cedar forests in the Middle Atlas mountains, I have used a 1 km^2 resolution digital elevation model (DEM) within a GIS (QGIS version 1.8: Quantum GIS Development Team, 2012). Using the fossil pollen data from the seven records in Northern Africa (described above), I have extracted the range of altitudes that may have potentially been available as suitable habitat for Cedar populations during the last glacial period and the early Holocene taking into account their presence/absence in the pollen records, their response to reconstructed past climate changes, and the elevations of the sites where they occur.

DISCUSSION

Identifying the location where a species has persisted during the past is a central issue in palaeoecology where it is designated as «glacial refugium» (Bennett *et al.*, 1991), as «centre of origin» in biogeography (McDowall, 2004), or «hot spot» for phylogeography studies (Petit *et al.*, 2003; 2008).

Genetic studies of several Cedar populations from Rif, Middle Atlas and NE High Atlas (Terrab *et al.*, 2006; Cheddadi *et al.*, 2009) allowed correlating genetic and geographical distances (Mantel test). These genetic data (Fig. 4) show that there is isolation by distance and some low genetic flow between populations. Thus, the question arises about where were Cedar populations during the last glacial period and the Holocene and what was the impact of the past climate changes on their distribution in Morocco and particularly in the Middle Atlas where we observe today the most extended populations?

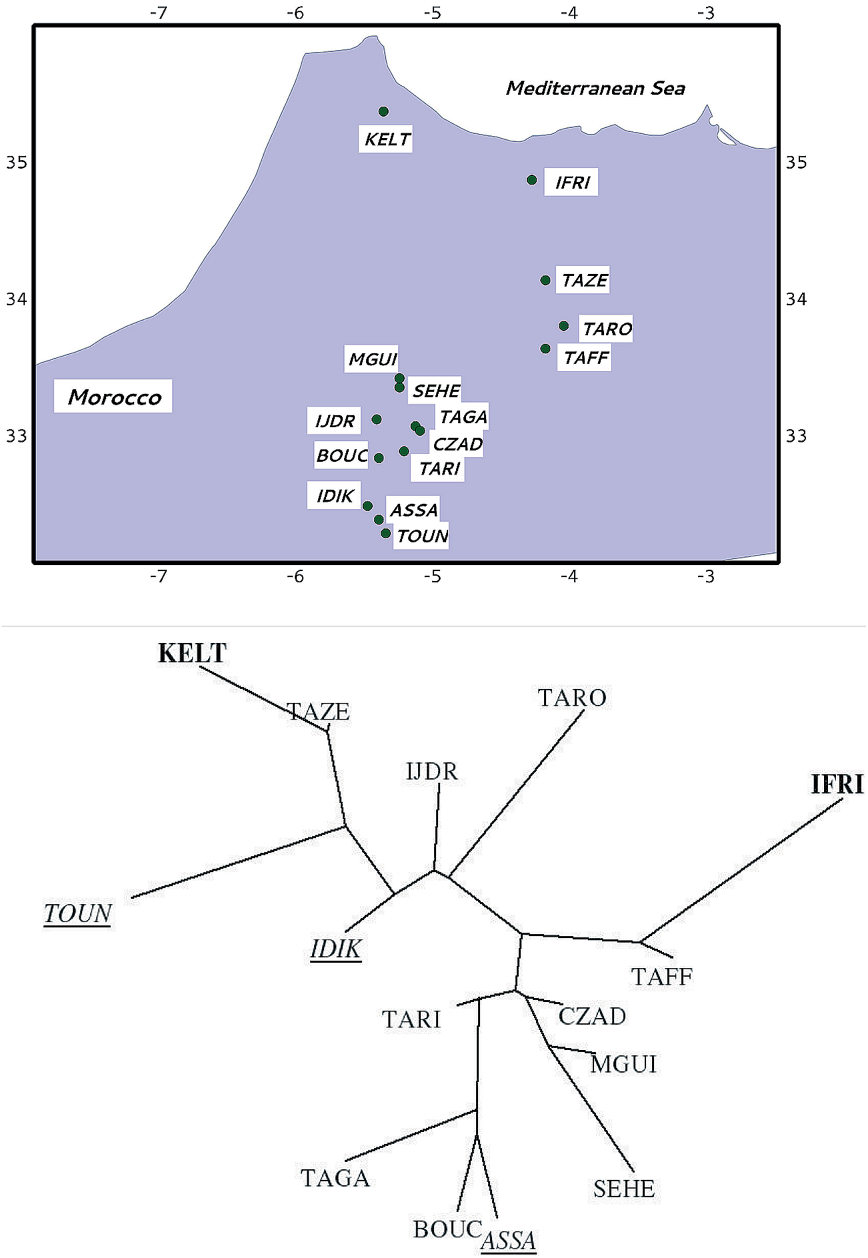

Figure 4. Locations of the Cedar populations and a phylogenetic dendrogram showing the geographical and the genetic distances, respectively (data obtained by B. Fady in Cheddadi *et al.*, 2009).

To address such question, it is essential to know the present-day climate requirements of the species and to examine its behaviour from fossil records that cover both the Holocene and a longer period of time encompassing the last glacial period (even partially).

The present climate requirements of *Cedrus* may be inferred from available climate and its distribution range. A pollen database of modern surface samples allows analyzing the abundance of *Cedrus* pollen grains versus climate variables such as January (Tjan) and July (Tjul) temperatures, and annual precipitation (Pann) (Cheddadi *et al.*, 1998) (Fig. 5). The temperature ranges are between 0 and 5° C for Tjan and between 17 and 26° C for Tjul whilst Pann values are quite wide, roughly between 600 and 1200 mm/year. Plots of these data show that *Cedrus* is geographically more constrained by Tjan variable than by the total amount of annual rainfall or summer temperature. How these climate variables have varied during the past thousand years and how did they impact the Cedar populations in the Middle Atlas?

Reconstructing past climate changes and the Cedars dynamics over the last few millennia may be performed from fossil pollen records. The pollen-based climate reconstruction, excluding *Cedrus atlantica*, from lake Tigalmamine (Cheddadi *et al.*, 1998) shows that throughout the Holocene, Pann was higher than 700 mm/year and Tjul was also within the modern range, between ca. 21 and 24° C. These two climate variables were apparently not limiting factors for the presence of Cedars in the area. Tjan shows more critical values. During the first part of the Holocene (10,000 to 7000 years BP) Tjan was fluctuating between 7 and 5° C which is higher than the values where Cedar populations occur today. During this time period *Cedrus* is not depicted in the pollen record. After 7000 years BP Tjan lowered and remained constantly below 5° C. This is the time period where *Cedrus* seems to have spread in the studied area. These data lead us to suggest that Tjan is potentially controlling the spread of *Cedrus* with a threshold of 5° C above which it does not spread.

The reconstructed Tjan from the lake Ifrah pollen record (Cheddadi *et al.*, 2009) shows that *Cedrus* was present in the area throughout the time period where Tjan was lower than ca. 5° C (Fig. 3) during the last glacial period. The periods with low amount of annual precipitation (around 300 mm/yr) recorded also a limited expansion of Cedars. As observed in Tigalmamine, Cedar populations regressed noticeably during the early Holocene in lake Ifrah. For the new record of Ras El Ma (Nour El Bait *et al.*, submitted), we did not perform a quantitative climate reconstruction but the pollen record confirms both the continuous presence of Cedar populations during the last glacial period in that area of the Middle Atlas and its strong regression during the early Holocene as well. Such widespread regression of Cedars does not necessarily mean an extinction of the species in the Middle Atlas.

In Algeria, the pollen records of La Chataigneraie and Garaat el Ouez both show that Cedar populations were present around 16,000 years BP until about

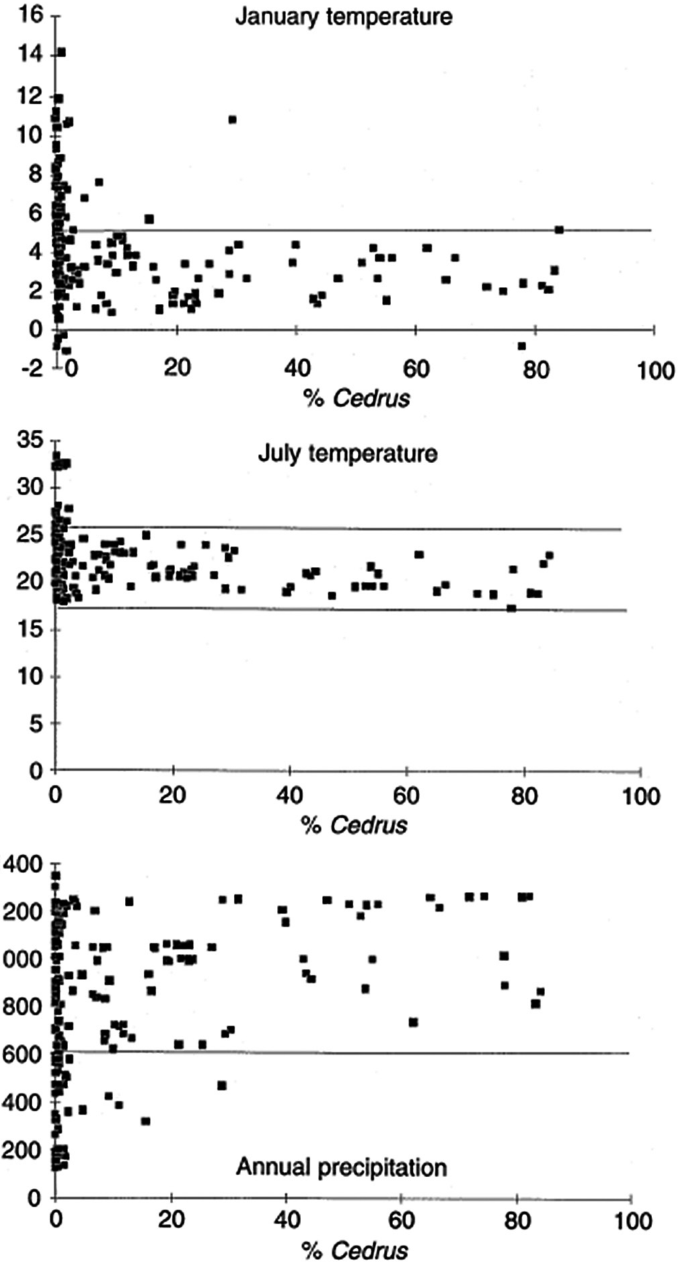

Figure 5. Modern January and July temperatures and annual precipitation versus pollen percentages from modern samples (from Cheddadi *et al.*, 1998).

9000 years BP and then they literally disappeared during the Holocene (Fig. 3). The reconstructed Tjan from La Chataigneraie pollen record (Cheddadi *et al.*, 2009), shows that it was slightly lower than 5° C during the early Holocene and that *Cedrus* was present. After ca. 8 ka and during the remaining part of the Holocene Tjan became higher than that value (Fig. 3) and *Cedrus* was not depicted in the pollen record.

In Tunisia, the pollen record of Dar Fatma indicates that some Cedar populations were present around the site. According to the authors (Ben Tiba and Reille, 1982), the last glacial maximum is partly missing in the record of Dar Fatma. Nevertheless, this record shows clearly that a Cedar population was in Tunisia during the last glacial period until the early Holocene and then, after ca. 8000 years BP, Cedar pollen grains are no longer recorded which translates the absence of the species in the area. Nowadays, there are no Cedar populations in Tunisia.

To sum up, Cedar populations were probably present during the last glacial period at lower altitudes in all Northern African sites cited above. During the Early Holocene when the winter temperatures became higher than the present, Cedar populations had to migrate at higher elevations than 1200 m a.s.l. which may explain their disappearance from the Algerian and Tunisian sites whose elevation is lower than that. After 7000 years BP when Tjan lowered, Cedar populations recolonised areas at lower altitudes. In Morocco this was possible because of the high mountainous range where the studied sites are located but not in the Algerian and Tunisian sites which apparently are located in mountainous areas with a limited elevation range.

Several studies have shown that the treeline altitude is particularly limited by low temperatures (Körner, 1998). Temperature impact on the treeline has also been evaluated at the soil level where a seasonal mean temperature of 7–8° C in the temperate and Mediterranean zones may represent a limiting threshold (Körner and Paulsen, 2004). Taylor (1995) stated that «climate, especially temperature exerts a strong control on tree growth and tree population dynamics» and Hessl and Baker (1997) have came to the conclusion that temperature is the primary factor controlling the treeline. As observed in the fossil pollen records, Tjan had probably a dominant impact on the belt position of *Cedrus atlantica* populations through time. Very low winter temperatures may limit severely tree growth that tree seedlings cannot survive and higher winter temperatures than +5° C may substantially reduce Cedar germination (Takos and Merou, 2001). Although, we know that the causes for treeline changes could be more numerous and particularly more complex than one might expect as they may include carbon cycle, tree phenology, other climate variables, landscape morphology, exposure, competition with other species, soil composition and moisture, etc.

A recent study has shown that the treeline in the European Alps shifted 115 m upwards over the period 1901–2000 (Leonelli *et al.*, 2011). One should stress that this altitudinal shift has been related rather to the increasing role of geomorphological and anthropogenic factors than to winter temperature (Leonelli *et al.*, 2009; 2011). Nevertheless, it is very interesting to have access to these modern observations and quantifications that do show clearly that tree species may migrate in altitude over tens of meters in just one century.

In terms of glacial refugia in Europe, the mountainous areas have played a major role in the long-term survival of trees through the succession of glacials and interglacials because they offered the species the potential for adapting to climate changes probably by shifting their altitudinal range (Bennett *et al.*, 1991). Bennett and Provan (2008) stated about the European glacial refugia that «no direct evidence (such as dated fossils) has been forthcoming to support the notion of survival exactly within the proposed refugial areas». Such statement is partially true since there are several tree taxa such as *Ulmus, Corylus, Carpinus* and *Abies* which have survived over a whole climatic cycle (more than 130,000 years) in the same site (Ioannina, Greece) (Tzedakis *et al.*, 2002).

In North Africa, we do not really know how Cedar forests have responded to the last glacial and the postglacial climates. Were they reduced to a few glacial refugia as in Europe? Have some few populations migrated to areas that were climatically more favourable from which they have recolonised later, or have some populations became locally extinct?

In this work, I suggest that many Cedar populations have formed and continue to form a metapopulation in the Middle Atlas where the fragmented populations composing it may have recorded some local extinctions and/or short migrations between populations. In general, a metapopulation is defined as a network of local populations linked by dispersal where some populations may go extinct or recolonise by migrating to new habitats (Margules and Pressey, 2000; Hanski and Ovaskainen, 2003). A metapopulation of Cedar forests in the Middle Atlas has probably adapted its range size by altitudinal movements in response to past climate changes and during that long-term migrational dynamics there was probably an extinction/recolonisation process that allowed the persistence of the Cedar metapopulation in the Middle Atlas.

The Yoyo effect

I have used a DEM to explore the extent of such potential metapopulation with long-term persisting Cedar populations, which may have adapted their altitudinal range at different time periods (Fig. 6). The upper and lower treeline limits I have used in the DEM are inferred from the presence/absence of Cedar in the pollen records from the seven sites available in Morocco, Algeria and Tunisia (Figs 6 and 7).

Currently, in the Middle Atlas Cedar forests are found between about 1400 and 2200 m a.s.l. (Figs 6A and 7). During the last glacial period, Cedar populations have probably moved at lower elevations to compensate for low winter tem-

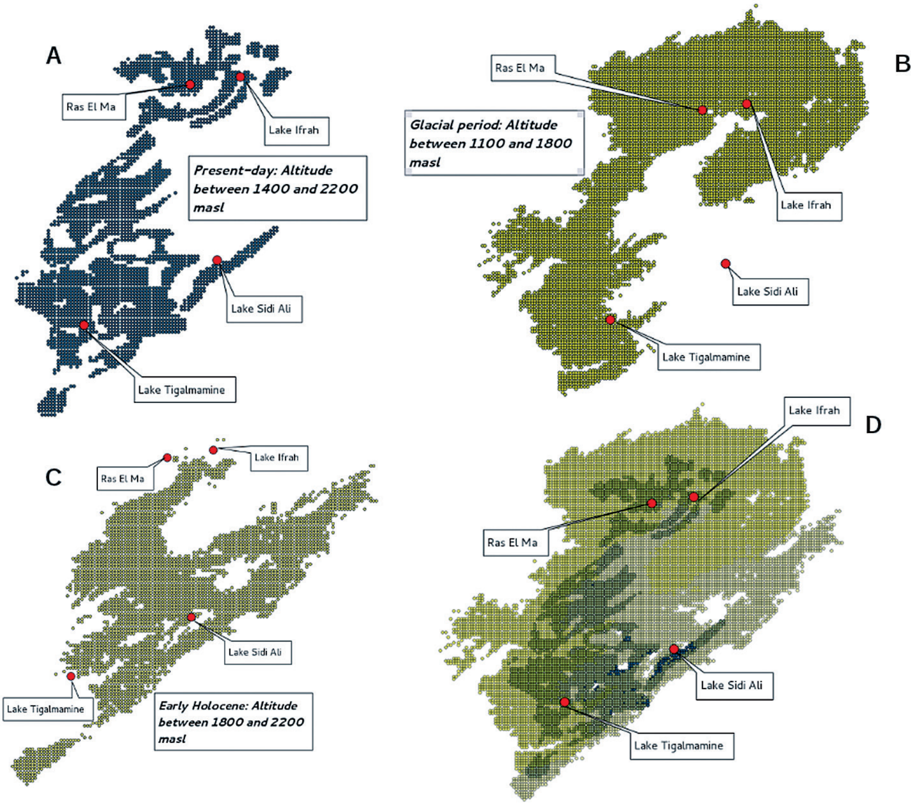

Figure 6. Modern range of *Cedrus atlantica* in the Middle Atlas (A), its potential range within an elevation range of 1100 to 1800 m a.s.l. during the last glacial period (B) and (C) between 1800 to 2200 m a.s.l. during the early Holocene (10,000 to 7000 years BP). Map (D) shows all potential elevation range that can potentially be colonized (including the last glacial period and the Early Holocene ranges).

peratures (Fig. 7). The sites of Lake Ifrah and Ras El Ma (and those in Algeria and Tunisia) still register the Cedar presence (Fig. 6B), which suggests that the upper limit was slightly higher than 1700 m a.s.l. For Sidi Ali that is located at 2000 m a.s.l. the last glacial period is unfortunately not available which does not allow being more accurate concerning the upper limit.

At the beginning of the Holocene, in response to the increasing winter temperature, Cedar populations have migrated to higher altitudes, between ca. 1800 and 2200 m a.s.l. approximately (Figs 6C and 7). The lower limit is based on the elevations of lake Ifrah and Ras El Ma, which are located at slightly higher

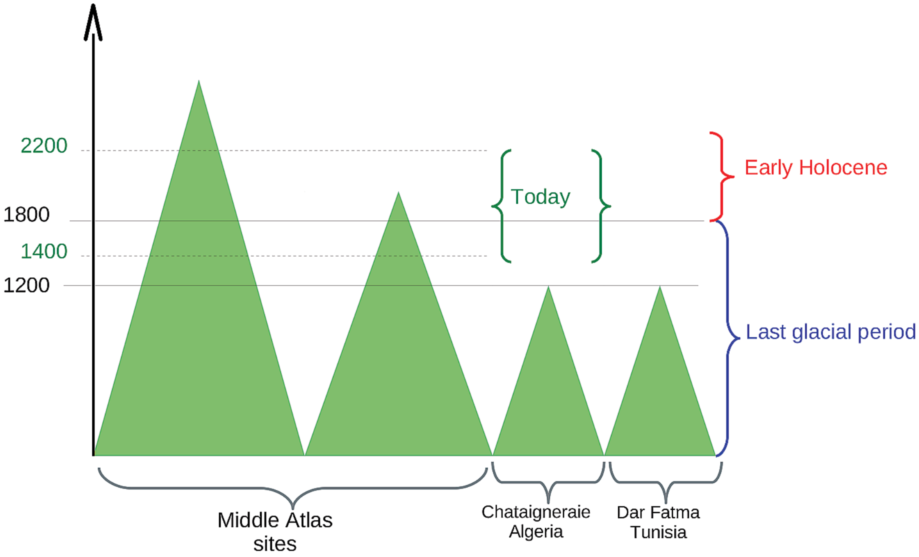

Figure 7. Sketch summarizing the potential shift in altitude during the last glacial period and the early Holocene in the Atlas mountains and in the Algerian and Tunisian sites.

than 1600 m a.s.l. This altitudinal shift corresponds to 700 meters (or more) for the lower limit and 400 meters for the upper limit (Figs 6D and 7). After 7000 years BP the lowering of Tjan, allowed a decrease in the lower limit of at least 400 meters so that Cedar populations may occur at lake Ifrah, Ras El Ma and Tigalmamine.

Leonelli *et al.* (2011) observed a treeline movement of more than 115 m during the last century in the Alps which makes the assumption of an altitudinal shift of Cedar forests up to 700 meters (in more than 700 years) between the last glacial period and the early Holocene quite realistic. However, this response with altitudinal movements of Cedar forests to a change in temperature would only be possible if several biotic and abiotic conditions such as the landscape topography, species physiology, competition with other species, the dispersal and adaptation capacity are met. It is obvious that such an interpretation based on four sedimentary sequences of which only two are covering the last glacial period is preliminary. To highlight this response of Cedar forests to climate change one would require having additional records that meet appropriate spatial-temporal criteria.

Nevertheless, the hypothesis of persistence of Cedar forests as a metapopulation in the Middle Atlas since the last glacial period may explain the genetic survey (Terrab *et al.*, 2006), which suggests that there was no colonization of the whole area from one population located in a glacial refugium. In metapopulations, population extinction is a frequent rather than a unique event (Hanski, 1998) which probably makes the identification of the original glacial population even more complex than in the case of a unique or multiple long lasting isolated glacial refugium in an identified area. The low gene flow between Cedar populations (Terrab *et al.*, 2006) may also be explained/due to some exchanges between local populations during the expansion of their range size when Cedars migrate to lower altitudes. Hanski (1999) stated that «if all local populations have a substantial risk of extinction, long-term survival is possible only at the metapopulation level». Such an assumption or ecological hypothesis, that was initially inferred from the persistence of a present-day butterfly species, may well apply to the Cedar populations in the Middle Atlas at least since the last glacial period if not earlier.

CONCLUSIONS

The hypothesis proposed here consists in considering the persistence of Cedar forests as an extended metapopulation in the Middle Atlas since at least the last glacial period. Such hypothesis requires a minimum number of viable populations which is coherent with the «more than one» long-term isolated populations inferred from the genetic data.

Cedar populations have reacted to past climate changes by adapting their range size in altitude. Their upper and lower limits have varied from 400 to 700 meters (or more) between the last glacial period and the Holocene optimum, respectively. Nevertheless, in order to confirm (or reject) such hypothesis one requires new time series covering the last glacial period and the Holocene that should be collected between 1000 and 2000 meters elevation. Although, one knows that there must very probably be suitable but not colonized areas within the migration range of Cedar. If the altitudinal shift is confirmed by other records then the Early Holocene, which was 2 to 3° C warmer than the present in the Middle Atlas could serve as an analogue for the next century in terms of potential response of Cedar forests to the expected warming.

Finally, if the hypothesis of a «metapopulation refugium» during both the last glacial period and the early Holocene for Cedars in the Middle Atlas proves to be true, then future management strategies should take into account the fact that the minimum viable metapopulation size is directly related to a «minimum number of interacting local populations» which is «necessary for long-term persistence of a metapopulation in a balance between local extinctions and recolonisations» (Hanski *et al.*, 1996). The management strategies should take into account also that if the extinction of local populations is the state toward which the present-day metapopulation is heading (through the increasing human impact) then in order to conserve Cedars one should reverse the process of habitat loss and fragmentation (Hanski *et al.*, 1996).

ACKNOWLEDGMENTS

I would like to thank Bruno Fady and Lara Awad for their valuable comments on this manuscript. I thank also my colleague Ali Rhoujjati for his very efficient and so friendly help on the field. The new record collected from Ras El Ma was analyzed by Majda Nour El Bait who was funded by the project PHC Volubilis: MA/11/251: Egide 24451WG and the field work was funded by CNRS-T, Morocco.

REFERENCES

Ben Tiba, B. and Reille, M. (1982) Recherches pollen analytiques dans les montagnes de Kroumirie (Tunisie septentrionale): premiers résultats. *Ecologia Mediterranea*, 8, 75–86.

Bennett, K.D., Tzedakis, P.C. and Willis, K.J. (1991) Quaternary refugia of north European trees. *Journal of Biogeography*, 18, 103–115.

Bennett, K. and Provan, J. (2008) What do we mean by «refugia»? *Quaternary Science Reviews*, 27, 2449–2455.

Benslama, M., Andrieu-Ponel, V., Guiter, F., Reille, M., De Beaulieu, J.-L., Migliore, J. and Djamali, M. (2010) Pollen analysis from two littoral marshes (Bourdim and Garaat El-Ouez) in the El-Kala wet complex (North-East Algeria). Lateglacial and Holocene history of Algerian vegetation. *Comptes Rendus Biologies*, 333, 744–754.

Bou Dagher-Kharrat, M., Mariette, S., Lefèvre, F., Fady, B., Grenier-de March, G., Plomion, C. and Savouré, A. (2007) Geographical diversity and genetic relationships among *Cedrus* species estimated by AFLP. *Tree Genetics & Genomes*, 3, 275–285.

Cheddadi, R., Lamb, H. F., Guiot, J. and Van der Kaars, S. (1998) Holocene climatic change in Morocco: a quantitative reconstruction from pollen data. *Climate Dynamics*, 14, 883–890.

Cheddadi, R., Fady, B., François, L., Hajar, L., Suc, J.-P., Huang, K., Demarteau, M., Vendramin, G.G. and Ortu, E. (2009) Putative glacial refugia of *Cedrus atlantica* deduced from Quaternary pollen records and modern genetic diversity. *Journal of Biogeography*, 36, 1361–1371.

Fady, B., Lefèvre, F., Vendramin, G.G., Ambert, A., Régnier, C. and Bariteau, M. (2008) Genetic consequences of past climate and human impact on eastern Mediterranean *Cedrus libani* forests. Implications for their conservation. *Conservation Genetics*, 9, 85–95.

Fahrig, L. (2003) Effects of habitat fragmentation on biodiversity. *Annual Review of Ecology and Evolution*, 34, 487–515.

Guiot, J. (1987) Late Quaternary Climatic Change in France Estimated from Multivariate Pollen Time Series. *Quaternary Research*, 28, 100–118.

Hanski, I. (1998) Metapopulation dynamics. *Nature*, 396, 41–49.

Hanski, I. (1999) *Metapopulation Ecology*. Oxford University Press, Oxford, UK.

Hanski, I. (2005) Landscape fragmentation, biodiversity loss and the societal response. *European Molecular Biology Organization*, 6, 388–392.

Hanski, I. and Ovaskainen, O. (2003) Metapopulation theory for fragmented landscapes. *Theoretical Population Biology*, 64, 119–127.

Hanski, I., Moilanen, A. and Gyllenberg, M. (1996) Minimum viable metapopulation size. *The American Naturalist*, 147, 527–541.

Hessl, A.E. and Baker, W.L. (1997) Spruce and fir regeneration and climate in the forest-tundra ecotone of rocky mountain national park, Colorado, U.S.A. *Arctic and Alpine Research*, 29, 173–183.

Körner, C. (1998) A re-assessment of high elevation treeline positions and their explanation. *Oecologia*, 115, 445–459.

Körner, C. and Paulsen, J. (2004) A world-wide study of high altitude treeline temperatures. *Journal of Biogeography*, 31, 713–732.

Lamb, H.F. and Van der Kaars, S. (1995) Vegetational response to Holoene climatic change: pollen and palaeolimnological data from the Middle Atlas, Morocco. *The Holocene*, 5, 400–408.

Lamb, H.F., Eicher, U. and Switsur, V.R. (1989) An 18,000-year record of vegetation, lake-level and climatic change from Tigalmamine, Middle Atlas, Morocco. *Journal of Biogeography*, 16, 65–74.

Lamb, H.F., Gasse, F., Benkaddour, A., El Hamouti, N., Van der Kaars, S., Perkins, W.T., Pearce, N.J. and Roberts, C.N. (1995) Relation between century- scale Holocene arid intervals in tropical and temperate zones. *Nature*, 373, 134–137.

Lamb, H., Roberts, N., Leng, M., Barker, P., Benkaddour, A. and Van der Kaars, S. (1999) Lake evolution in a semi-arid montane environment: responses to catchment change and hydroclimatic variation. *Journal of Paleolimnology*, 21, 325–343.

Laurance, W.F., Lovejoy, T.E., Vasconcelos, H.L., Bruna, E.M., Didham, R.K., Stouffer, P.C., Gascon, C., Bierregaard, R.O., Laurance S.G. and Sampaio, E. (2002) Ecosystem Decay of Amazonian Forest Fragments: a 22-Year Investigation. *Conservation Biology*, 16, 605–618.

Leonelli, G., Pelfini, M. and Di Cella, U.M. (2009) Detecting Climatic Treelines in the Italian Alps: The Influence of Geomorphological Factors and Human Impacts. *Physical Geography*, 30, 338–352.

Leonelli, G., Pelfini, M., Di Cella, U.M. and Garavaglia, V. (2011) Climate Warming and the Recent Treeline Shift in the European Alps: The Role of Geomorphological Factors in High-Altitude Sites. *Ambio*, 40, 264–273.

Linares, J.C., Taïqui, L. and Camarero, J.J. (2011) Increasing Drought Sensitivity and Decline of Atlas Cedar (*Cedrus atlantica*) in the Moroccan Middle Atlas Forests. *Forests*, 2, 777–796.

Magri, D. (2012) Quaternary history of *Cedrus* in southern Europe. *Annali di Botanica*, 2, 57–66.

Margules, C.R. and Pressey, R.L. (2000) Systematic conservation planning. *Nature*, 405, 243–253.

McDowall, R.M. (2004) What biogeography is: a place for process. *Journal of Biogeography*, 31, 345–351.

Petit, R.J., Aguinagalde, I., De Beaulieu, J.-L., Bittkau, C., Brewer, S., Cheddadi, R., Ennos, R., Fineschi, S., Grivet, D., Lascoux, M., Mohanty, A., Müller-Starck, G., Demesure-Musch, B., Palmé, A., Martín, J.P., Rendell, S. and Vendramin, G.G. (2003) Glacial refugia: hotspots but not melting pots of genetic diversity. *Science*, 300, 1563–1565.

Petit, R.J., Hu, F.S. and Dick, C.D. (2008) Forests of the Past: A Window to Future Changes. *Science*, 320, 1450–1452.

Qiao, C.-Y., Ran, J.-H., Li, Y. and Wang, X.-Q. (2007) Phylogeny and Biogeography of *Cedrus* (Pinaceae) Inferred from Sequences of Seven Paternal Chloroplast and Maternal Mitochondrial DNA Regions. *Annals of Botany*, 100, 573–580.

Reille, M. (1976) Analyse pollinique de sédiments postglaciaires dans le Moyer, Atlas et le Haut Atlas marocains: premiers résultats. *Ecologia Mediterranea*, 2, 155–170.

Reille, M. (1977) Contribution pollen analytique a l'histoire holocène de la végétation des montagnes du rif (Maroc septentrional). *Bulletin AFEQ*, 50, 53–76.

Salamani, M. (1991) Premières données palynologiques sur l'histoire Holocène du massif de l'Akfadou (Grande-Kabylie, Algérie). *Ecologia Mediterranea*, 17, 145–159.

Takos, I. and Merou, T. (2001) Effect of Storage Conditions and Seed Treatment on Germination of *Cedrus deodora* Loud. and *C. libani* A. Rich. *Silvae Genetica*, 50, 205–208.

Taylor, A.H. (1995) Forest expansion and climate change in the mountain Hemlock (Tsuga mertensiana) zone, Lassen volcanic park, California, U.S.A. *Arctic and Alpine Research*, 27, 207–216.

Terrab, A., Paun, O., Talavera, S., Tremetsberger, K., Arista, M. and Stuessy, T.F. (2006) Genetic diversity and population structure in natural populations of Moroccan Atlas Cedar (*Cedrus atlantica*; Pinaceae) determined with CPSSR markers. *American Journal of Botany*, 93, 1274–1280.

Tzedakis, P.C., Lawson, I.T., Frogley, M.R., Hewitt, G.M. and Preece, R.C. (2002) Buffered Tree Population Changes in a Quaternary Refugium: Evolutionary Implications. *Science*, 297, 2044–2047.

UNRAVELLING THE PATTERNS AND PROCESSES OF EVOLUTION OF MARINE LIFE IN OCEANIC ISLANDS: A GLOBAL FRAMEWORK

Sérgio P. Ávila

CLIMATE CHANGE PERSPECTIVES FROM THE ATLANTIC:
PAST, PRESENT AND FUTURE
Jose María Fernández-Palacios, Lea de Nascimento, José Carlos Hernández,
Sabrina Clemente, Albano González & Juan P. Díaz-González (eds.)
Servicio de Publicaciones, Universidad de La Laguna – 2013

ISBN: 978-84-15910-54-1 pp. 95-125

Abstract

Whittaker *et al.* (2008) outlined a general dynamic model for the biogeography of oceanic islands that places the MacArthur and Wilson (1967) model into the geological and evolutionary context of oceanic archipelagos. In that paper, they stated that «one of the most important omissions from the framework is the role of Quaternary climate change and the accompanying variation in the configuration of islands». Another important omission is related with the applicability of the model to marine species, rather than terrestrial ones. In this chapter, further evidence is provided in support of Ávila (2006) hypothesis relating modes of larval development, geographical range and bathymetry: nonplanktotrophic species usually living in the intertidal zone or at shallow depths are more prone to be rafted than those from deeper levels and, as a consequence, will have wider geographical ranges. This reasoning is now expanded, relating modes of larval development, geographic range and bathymetry/ecological zonation with evolutionary time. The influence of glaciations and of sea-level oscillations in the shallow marine communities is also discussed in the context of the explanation provided by Ávila *et al.* (2008b) for the life-devoid sandy habitats in oceanic islands. This approach connects a wide range of concepts that usually are not seen as correlated (e.g., time, evolution, speciation, bathymetry, ecological zonation, the geological age of a given species, modes of larval development, dispersal strategies, geographical range, sea-level changes, glacial/interglacial periods, sediment architecture of marine volcanic island shelves, the importance of the marine substrate for species turnover). Moreover, when these concepts are gathered into such a global framework, this explanation incorporates the role of the Late Neogene climate changes into Whittaker's general dynamic model for the biogeography of reefless oceanic islands and is especially designed for marine flora and fauna.

Keywords: evolutionary time, geographic distribution, marine invertebrates, modes of development, oceanic islands, patterns and processes, zonation.

INTRODUCTION

Island biogeography is one of the most exciting topics in present-day marine biology studies. One of the most outstanding contributions in this field was the seminal work of MacArthur and Wilson (1967), «*The theory of island biogeography*», which triggered a flurry of papers and books on this and related subjects: mechanisms of speciation on islands (Rosenzweig, 1995); mechanisms related with the arrival to and posterior morphological change on islands, such as founder effects, genetic drift and bottlenecks (Berry *et al.*, 1992; Carson, 1992); models of species' evolution on islands, such as the taxon cycle (Wilson, 1961) and adaptive and non-adaptive radiation (Grant, 1981; Gittenberger, 1991); species area patterns, species abundance distributions and habitat diversity (Dengler, 2009; Triantis *et al.*, 2012); and island assembly theories (Diamond, 1975; Whittaker *et al.*, 1997). Recent advances on this matter have been leaded by Whittaker and colleagues (Whittaker and Fernández-Palacios, 2007; Whittaker *et al.*, 2008; Fattorini, 2009; Fernández-Palacios *et al.*, 2011) and by Hubble (2001).

Whittaker *et al.* (2008) outlined a general dynamic model for the biogeography of oceanic islands that places the MacArthur and Wilson (1967) model into the geological and evolutionary context of oceanic archipelagos, providing «a general explanation of biodiversity patterns through describing the relationships between fundamental biogeographical processes – speciation, immigration, extinction – through time and in relation to island ontogeny». However, they also explicitly acknowledged that «for those oceanic islands that do conform to the simple ontogenetic model, one of the most important omissions from the framework is the role of Quaternary climate change and the accompanying variation in the configuration of islands». Another important omission is related with its applicability to marine species, rather than terrestrial ones.

Oceanic islands have been associated with the study of evolution since Darwin (1859). Islands represent discrete geographical entities isolated by oceanic barriers that reduce genetic interchanges with continental areas. Islands are further characterized by rapid and dramatic ecological changes resulting from a geological dynamic, associated with historical and contemporary volcanic and erosional activity. Altogether, these factors have promoted fast rates of endemic speciation, making islands ideal natural laboratories for the study of evolution.

The relatively isolated oceanic islands that form the Azores archipelago first appeared in the middle of the northern Atlantic in the Late Miocene (~8 Ma). As volcanic islands, these once empty habitats had to be colonized from elsewhere. The nearest colonizing source is the Madeira archipelago, presently about 900 km southeast, but other plausible sources are the Iberian and West European Atlantic shores, the Mediterranean, the western African shores, the Canary Islands and also the Caribbean region (Fig. 1).

During the latter years, Ávila and co-workers have used the shallow marine molluscs of oceanic islands and seamounts as a model for biogeographical studies (Ávila, 2000; 2005; Ávila and Malaquías, 2003; Ávila *et al.*, 2004; 2008a; 2009b). In the Azores, the main reasons for this choice were: 1) high species diversity and abundance in the recent marine biocoenosis; 2) high number of endemic mollusc species; 3) high species diversity and abundance in the fossil record, and 4) good preservation in the fossil record. Systematic works as well as ecological and populational studies were used as a basis for the first biogeographical accounts on this matter (Ávila, 2000; 2005). The strong Mediterranean component of the marine molluscs of the Azores, known since Mac Andrew's (1854) work, was confirmed

Figure 1. North-Atlantic and geographical location of the Azores islands.

by the aforementioned studies, where the biogeographical relationships of the Azorean marine molluscs were quantified for the first time. Such distributional relationships have been referred to as the «Azorean Biogeographical Paradox» (Ávila, 2000), a concept underlining the evident mismatch between the present sea-surface circulation and the biogeographical relationships of the entire marine fauna of the Azores.

In order to seek explanation for this biogeographical paradox, the fossil record of the Azores Islands was studied and during this research, a most intriguing fact then discovered was the strange disappearance of a group of shallow marine bivalves associated with fine sand. These bivalves – *Ensis minor* (Chenu, 1843), *Lucinella divaricata* (Linnaeus, 1758) and *Laevicardium crassum* (Gmelin, 1791) – were found to be abundant in the Pleistocene fossil record of Santa Maria Island. The explanation provided by Ávila *et al.* (2008b) and here complemented with new data, connects a wide range of concepts that usually are not seen as correlated (e.g., time, evolution, speciation, bathymetry, ecological zonation, the geological age of a given species, modes of larval development, dispersal strategies, geographical range, sea-level changes, glacial/interglacial periods, sediment architecture of marine volcanic island shelves, the importance of the marine substrate for species turnover). Moreover, when these concepts are gathered into such a global framework, this explanation incorporates the role of the Late Neogene climate changes into Whittaker's general dynamic model for the biogeography of reefless oceanic islands and is especially designed for marine flora and fauna.

Stories of success: the patterns and processes of dispersal and the best ways of reaching an oceanic island

One of the most interesting evolutionary and biogeographical problems since Wallace (1880) is the study of how marine species have reached, colonized and (at least some) speciated in oceanic islands. It is a well-known fact that many benthic marine invertebrates disperse by means of pelagic larva. Other plausible means of dispersal are: 1) by foresy, that is, transported by birds attached to their feathers (a common feature in the case of some intertidal molluscs); 2) by rafts of egg-masses, juveniles or adults of small-sized species attached to seaweeds, to carapaces of marine turtles, pumice, logs, and other suitable floating materials (Ávila, 2006).

The duration of the larval phase reflects the dispersal ability of the species and this has evolutionary and biogeographic implications. Since direct observations of larval development are lacking for most species, protoconch inspection is the only way to evaluate the actual duration of the larval phase (Jablonski and Lutz, 1980). Two types of larval development can be considered in marine gastropods: planktotrophic (with a free-swimming feeding stage) and nonplanktotrophic (either lecithotrophic or direct development, both without a free-swimming feeding stage) (Fig. 2). In general, species with a nonplanktotrophic mode of development have reduced dispersal abilities and, as a consequence, a narrower geographical distribution (Scheltema, 1989). However, some species lacking a planktotrophic larval stage may have a wide geographical range, e.g., the brooder bivalve *Lasaea adansoni* (O'Foighil, 1989) or the brooder gastropod *Littorina saxatilis* (Johannesson, 1988).

Species with teleplanic larvae, that is, possessing a pelagic larva with a prolonged free-swimming stage, have no difficulties in reaching faraway islands (Scheltema and Williams, 1983; Scheltema *et al.*, 1996). They may even reach these islands so regularly that speciation is prevented, because of repeated episodes of gene flow between mainland and insular populations. Such species are capable of maintaining populations on both sides of the Atlantic without subsequent allopatric speciation (García-Talavera, 1981).

But, how can we explain the existence in remote islands of benthic shallow water species with a nonplanktotrophic mode of development? A possible explanation would be to postulate a planktotrophic ancestor that later speciated

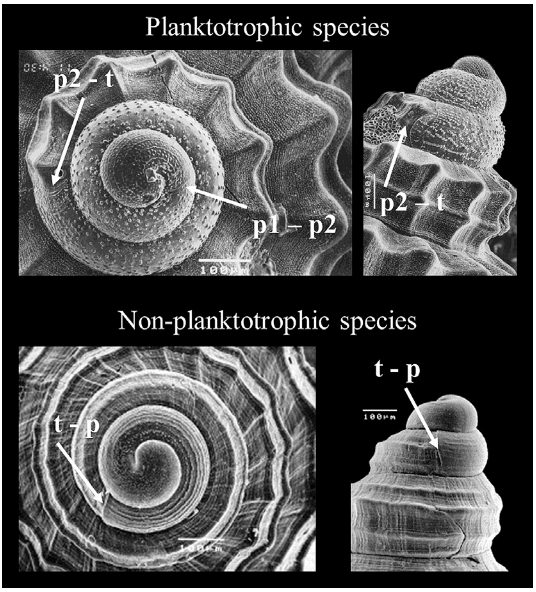

Figure 2. Two types of larval development can be considered in marine gastropods: planktotrophic (with a free-swimming feeding stage and with protoconchs with more than 2 whorls) and nonplanktotrophic (either lecithotrophic or direct development, both without a free-swimming feeding stage and with about 1 to 1.5 whorls in the protoconch). t - teleoconch (shell of the adult); p1 – embrionic shell (intracapsular development); p2 – larval shell; p2-t - transition protoconch/teleoconch.

and acquired a nonplanktotrophic mode of development. Still, how to explain the simultaneous existence of a given species with a nonplanktotrophic mode of development in two nearby archipelagos (e.g. Azores/Madeira, or Selvagens/Canary Islands)? A possible explanation would be that this particular species speciated in one of the archipelagos and later dispersed, reached and successfully established on the other.

It is known that some gastropod species with a nonplanktotrophic mode of development are capable of dispersing by rafting (Johannesson, 1988). A large number of species belonging to the Rissoidae (Mollusca: Gastropoda) have such mode of development (Ávila *et al.*, 2012a). Species of this family possess a posterior pedal gland that secretes threads of mucus, on which they can suspend themselves from the surface film, hence providing them with a plausible means for dispersal, albeit not very effective for large distances. These small-sized species (≤5 mm), usually living amongst algae, probably raft in patches of drifting algae that are pulled out from the littoral by wave action. In oceanic islands, shallow benthic insular species of Rissoidae are located far from other islands or continents, usually separated by deep waters that constitute an effective barrier to adult migration. This is not the case in continents, where the physical continuity of the land mass can provide an effective means for dispersal, by stepwise adult migration of species with nonplanktotrophic mode of development along coastlines, over many generations.

Relating modes of larval development and geographic range with bathymetry/ecological zonation

In contrast to the Atlantic tropical waters, where rafting plays only a secondary role in the dispersal of molluscs (Scheltema, 1995), in temperate Atlantic waters, rafting is an important means of dispersal for shallow water epibenthic molluscs. As dispersion depends on chance events, the more abundant the species, the greater its chance of being rafted. Also, species usually associated with hard substrata or rocky shores covered by algae are, in general, more likely to be rafted, in comparison to infaunal benthic species (Scheltema, 1986). Ávila (2006) showed that admitting rafting as an important method of dispersal for epibenthic intertidal and shallow-sublittoral species with a nonplanktotrophic mode of development leads to the following hypotheses: 1) considering that insular species usually living in the intertidal zone or at shallow depths should be more prone to be rafted than species usually living at deeper levels; 2) then there should be a direct relationship between bathymetry and the geographical range of a given species – that is, intertidal species should generally have a wider geographical range than sublittoral species, and these should generally also have a wider geographical range than deeper ones (Fig. 3); 3) also, if the adults are the rafting stage, then small-sized species would have a wider geographical distribution than medium-sized or large-sized species, because the chances of success would be higher for micro-molluscs.

The above mentioned hypotheses were corroborated by three datasets: 1) the zonation of the most abundant algae-associated molluscan species of the Azores was established from the intertidal down to ~30 m depth (Ávila, 2003; Ávila *et al.*, 2005) and their geographical distribution tabulated. Species were separated according to their bathymetrical zonation: intertidal, shallow sublittoral (down to 5–6 m depth) and deeper littoral species (usually found at depths greater than 10 m). A table containing these species and their mode of development, body size, and geographical range, was compiled (Table 1). 2) the Rissoidae, a family of small-sized gastropods was selected because of their high number of genera and species (many possessing a nonplanktotrophic mode of development), their wide distribution in the Atlantic Ocean, being especially common in the Atlantic islands (Ávila *et al.*, 2012a), and because of their association with algae, therefore potentially able of being rafted.

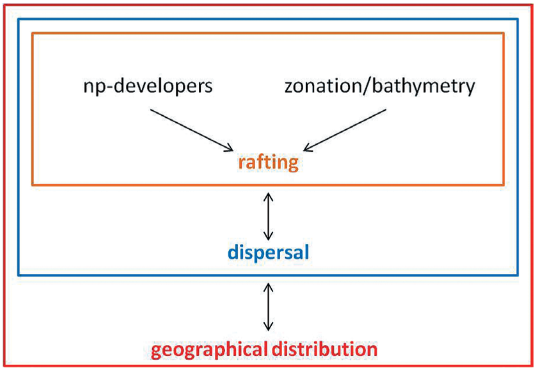

Figure 3. Link between depth occurrence (zonation/bathymetry), where epibenthic, nonplanktotrophic organisms usually live, and rafting as a plausible means for dispersal and their relation with geographical range distribution.

The shallow water rissoid species with nonplanktotrophic mode of development and restricted to two Atlantic archipelagos were selected from the complete database available from Ávila *et al.* (2012a) (Table 2). 3) a checklist of the shallow water marine molluscs of the Azores (down to 50 m depth), containing information about the mode of development of the 155 Caenogastropod species reported in the Azores (Ávila, unpublished data), as well as their geographical range (Table 3).

The first dataset, based on the zonation of the Azorean marine molluscs, showed that four out of the five most abundant intertidal Azorean species are gastropods of small size (up to 2.7 mm), and they all possess a nonplanktotrophic mode of development (Ávila *et al.*, 2005). Notwithstanding, some of them have a wide geographical distribution, ranging from Scandinavia south to the Mediterranean, occurring also in most of the Atlantic archipelagos, e.g., *Omalogyra atomus* (Philippi, 1841) and *Skeneopsis planorbis* (Fabricius, 1780); the latter species has an amphi-Atlantic distribution, occurring also in the Caribbean (Table 1). Analysis of distributions shows that the geographical range of the most abundant Azorean species decreases with depth: shallow water abundant species have a narrower geographical distribution than intertidal species, and *Alvania sleursi*, the only abundant Azorean deeper littoral species, is restricted to the Azores, Madeira and Selvagens Islands (Table 1).

Regarding the second dataset, Ávila *et al.* (2012a) reported 323 shallow water Rissoidae species in the Atlantic and the Mediterranean Sea: 232 have a nonplanktotrophic mode of development, 60 possess a planktotrophic mode of development, and the mode of development of the remaining 31 is unknown; 78 species are endemic to one of the oceanic archipelagos. For this analysis, only a small subset of 13 species (Table 2) is relevant, i.e., the shallow nonplanktotrophic

TABLE 1. Most abundant shallow water species in the Azores. Type of development: np – nonplanktotrophic; p – planktotrophic; br – brooding. AZO – Azores; MAD – Madeira archipelago; SEL – Selvagens; CAN – Canary Islands; CAP – Cape Verde; SCA – Scandinavia; BRI – British Isles; POR – Portugal; MED – Mediterranean Sea; CAR – Caribbean. Species in bold are endemic to the Azores. Data extracted from Ávila (2000, 2005) and Ávila *et al.* (2010, 2012a).

Most abundant species		Type of development	Body size (mm) height x diameter	Geographic range									
				AZO	MAD	SEL	CAN	CAP	SCA	BRI	POR	MED	CAR
Intertidal	*Alvania mediolittoralis* Gofas, 1989	np	2.7 x 1.5	1	1								
	Omalogyra atomus (Philippi, 1841)	np	0.8 x 0.8	1			1	1	1	1	1	1	
	Skeneopsis planorbis (Fabricius O., 1780)	np	1.2 x 1.0	1	1	1	1		1	1	1	1	1
	Pisinna glabrata (Von Mühlfeldt, 1824)	np	1.5 x 0.8	1	1	1	1					1	
	Lasaea adansoni (Gmelin, 1791)	br	3.5 x 3.0	1	1	1	1	1	1	1	1	1	1
Shallow (3-6m)	*Anachis avaroides* Nordsieck, 1975	np	3.5 x 1.5	1	1	1	1						
	Parvicardium vroomi van Aartsen, Menkhorst and Gittenberger, 1984	p	3.5 x 2.6	1	1	1	1					1	
	Alvania angioyi van Aartsen, 1982	np	1.8 x 1.1	1									
	Manzonia unifasciata (Dautzenberg, 1889)	np	2.5 x 1.2	1									
	Rissoa guernei Dautzenberg, 1889	np	2.3 x 1.3	1									
	Gibbula delgadensis Nordsieck, 1982	np	2.0 x 2.0	1									
Deep (10-30m)	*Alvania sleursi* (Amati, 1987)	np	2.5 x 1.6	1	1	1							

species that are simultaneously present in only two archipelagos and absent in continental shores. Of the four Azores/Madeira rissoids (Table 2), one is an abundant intertidal species that may attain densities around 5200 individuals/m^2 (*Alvania mediolittoralis*) and two are shallow water species (the common *Rissoa guernei* and *Crisilla postrema*). The other Azorean rissoid species that also occurs at Selvagens (*Alvania sleursi*) is especially abundant at 20 m depth in the Azorean rocky shores covered by algae, with densities around 500 individuals/m^2 (Ávila, 2003).

Although rafting has been considered a good explanation for the dispersal of benthic species without planktotrophic mode of development, Ávila (2006) was the first to suggest a direct relationship between depth occurrence where epibenthic, nonplanktotrophic organisms usually live, rafting as a plausible mechanism for dispersal of these littoral species, and geographic range distribution. Scheltema (1989) pointed out that the length of the larval phase, determines the dispersal ability of the species, and this is evident for the Azorean gastropods. From a total of 383 benthic shallow water molluscan taxa reported to the Azores, 155 species are Caenogastropods, of which the life history is known for 118 species: 64 are planktotrophic-developers and 54 are nonplanktotrophic species (Ávila, unpublished data). Most of the Azorean species that are amphi-Atlantic have planktotrophic larvae, with the exceptions of the brooding bivalve *Lasaea adansoni* (Gmelin, 1791) and the small gastropods *Skeneopsis planorbis* and *Omalogyra atomus*. In general, the Azorean caenogastropod species with planktotrophic larvae have wider geographical ranges than species with nonplanktotrophic larvae, as shown by other studies (Scheltema, 1989). However, some species without planktotrophic larvae also have wide geographical ranges [e.g. *Ammonicera rota* (Forbes & Hanley, 1850), *Ocenebra erinaceus* (Linnaeus, 1758) and *Haedropleura septangularis* (Montagu, 1803)] (Table 3). Table 3 also shows that four out of the nine Azorean caenogastropod species with widest ranges and possessing a nonplanktotrophic mode of development share common characteristics: all of them are small-sized and are most abundant in the intertidal (*Skeneopsis planorbis* and *Omalogyra atomus*) or in shallow waters (<5 m depths) (*Ammonicera rota* and *Sinezona cingulata*). This supports the hypothesis of a relationship between geographical range and bathymetry: species usually living in the intertidal zone or at shallow depths are more prone to be rafted than those from deeper levels and, as a consequence, will have wider geographical ranges.

Relating modes of larval development, geographic range and bathymetry/ecological zonation with evolutionary time

A corollary of the hypothesis (1) is that, for a given set of congeneric species from nearby archipelagos (e.g., Azores/Madeira) that differ only in their bathymetric range (e.g., one is abundant in the intertidal zone, other abundant around 15–20 m depth), in general, it will be expected that the species living at greater depths speciated longer ago than the shallow one. This means that if both

TABLE 2. Shallow nonplanktotrophic Rissoidae restricted to two Atlantic archipelagos. AZO – Azores; MAD – Madeira; SEL – Selvagens; CAN – Canary Islands. Data extracted from Ávila *et al.* (2012a).

Species	AZO	MAD	SEL	CAN
Alvania mediolittoralis Gofas, 1989	1	1		
Crisilla postrema (Gofas, 1990)	1	1		
Rissoa guernei Dautzenberg, 1889	1	1		
Alvania sleursi (Amati, 1987)	1	1	1	
Alvania aurantiaca (Watson, 1873)		1		1
Alvania euchila (Watson, 1886)		1		1
Alvania macandrewi (Manzoni, 1868)		1		1
Manzonia dionisi Rolán, 1987 = *M. darwini* Moolenbeek & Faber, 1987		1		1
Alvania johannae Moolenbeek & Hoenselaar, 1998			1	1
Alvania subcalathus Dautzenberg & Fischer, 1906			1	1
Manzonia castanea Moolenbeek & Faber, 1987			1	1
Manzonia guitiani Rolán, 1987 = *M. pelorum* Moolenbeek & Faber, 1987			1	1
Setia jansseni (Verduin, 1984)			1	1

species occur in the present times, then it is expected that the sublittoral species be, in a geological sense, longer-lived than the intertidal species, therefore its fossils should be older.

This idea was tested at Santa Maria, the only island of the Azores archipelago where abundant and diversified fossils are found. With an estimated age of ~8 Myr, this is the oldest island of the Azores and it has a complex geological history (Serralheiro and Madeira, 1990; Serralheiro, 2003; Ávila *et al.*, 2012b) that may be summarized as: 1) a first phase of emergent island (Cabrestantes and Porto Formations) during the Mid to Late Miocene; 2) during the Late Miocene, the formation of a lava shield (Anjos Complex); 3) this was followed by a long period during the Late Miocene to Early Pliocene, when erosion predominated and was responsible for the probable total disappearance of the island (the *guyot* stage). Sedimentation of marine and alluvial sediments predominated and submarine volcanism occurred only on the eastern side of the island (Touril Complex); 4) during the Early Pliocene, a new phase of increasingly active volcanism, first exclusively submarine and later subaerial with the formation of lava deltas, caused the resurgence of the island (Facho – Pico Alto Complex); 5) during the Late Pliocene, a new phase, first dominated by erosional processes, was followed by a new period of low volcanic activity, when a series of hydromagmatic and mono-

TABLE 3. Geographic distribution of the Azorean shallow water marine molluscs with widest geographic ranges (Ávila, unpublished data). BIS – Biscay Gulf; MOR – western Morocco; ASC – Ascension Island; STH – Saint Helen Island. Other legends as in Table 1.

Species	Family	Dev	AZO	SCA	BRI	BIS	POR	MED	MOR	MAD	SEL	CAN	CAP	ASC	STH	CAR
Lasaea adansoni (Gmelin, 1791)	Lasaeidae	br	1	1	1	1	1	1	1	1	1	1	1	1	1	1
Lamellaria perspicua (Linnaeus, 1758)	Velutinidae	p	1	1	1	1	1	1		1	1	1	1			1
Fossarus ambiguus (Linnaeus, 1758)	Fossariidae	p	1			1	1	1	1	1	1	1	1	1	1	
Gyroscala lamellosa (Lamarck, 1822)	Epitoniidae	p	1		1	1	1	1	1	1	1	1	1			1
Melarhaphe neritoides (Linnaeus, 1758)	Littorinidae	p	1	1	1	1	1	1	1	1	1	1				
Littorina saxatilis (Olivi, 1792)	Littorinidae	br	1	1	1	1	1	1	1	1	1	1				
Skeneopsis planorbis (Fabricius O., 1780)	Skeneopsidae	np	1	1	1	1	1	1		1	1	1				1
Luria lurida (Linnaeus, 1758)	Cypraeidae	p	1				1	1	1	1	1	1	1	1	1	
Ocenebra erinaceus (Linnaeus, 1758)	Muricidae	np	1	1	1	1	1	1		1	1	1				
Nassarius incrassatus (Ström, 1768)	Nassariidae	p	1	1	1	1	1	1	1	1		1				
Gibbula magus (Linnaeus, 1758)	Trochidae	np	1	1	1	1	1	1		1	1	1				
Ranella olearium (Linnaeus, 1758)	Ranellidae	p	1		1	1	1	1	1	1		1	1			1
Omalogyra atomus (Philippi, 1841)	Omalogyridae	np	1	1	1	1	1	1				1	1	1		
Phalium granulatum (Von Born, 1778)	Tonnidae	p	1				1	1	1	1	1	1	1			1
Cymatium parthenopeum (Von Salis, 1793)	Ranellidae	p	1				1	1	1	1	1	1	1			1
Charonia lampas lampas (Linnaeus, 1758)	Ranellidae	p	1		1	1	1	1	1	1		1	1			
Charonia variegata (Lamarck, 1816)	Ranellidae	p	1					1		1	1	1	1	1	1	1
Tectura virginea (Müller, O.F., 1776)	Lottiidae	np	1	1	1	1	1	1		1	1	1				
Cerithiopsis tubercularis (Montagu, 1803)	Cerithiopsidae	p	1	1	1	1	1	1		1		1	1			
Alvania cancellata (da Costa, 1778)	Rissoidae	p	1		1	1	1	1		1	1	1	1			
Ocinebrina aciculata (Lamarck, 1822)	Muricidae	np	1		1	1	1	1	1	1	1	1				
Raphitoma linearis (Montagu, 1803)	Raphitomidae	p	1	1	1	1	1	1		1		1				
Haedropleura septangularis (Montagu, 1803)	Horaiclavidae	np	1	1	1	1	1	1		1		1				
Ammonicera rota (Forbes & Hanley, 1850)	Omalogyridae	np	1	1	1	1	1	1				1				
Sinezona cingulata (Costa O. G., 1861)	Scissurellidae	np	1					1		1	1	1	1			

genetic magmatic cones was produced (Feteiras Formation); 6) from the Late Pliocene to the present no more eruptions occurred at Santa Maria and erosion of the edifice was the dominant process. Adding to this complex geological history, the island has been subjected to an uplift of, at least, 180–200 m since the end of the last active volcanic phase (Feteiras Formation).

During the *guyot* stage, a large package of sediments, very rich in fossiliferous content was deposited (Touril Complex). These fossils are Late Miocene to Early Pliocene and most of the species are presently extinct (Janssen *et al.*, 2008; Winkelmann *et al.*, 2010; Madeira *et al.*, 2011; Ávila *et al.*, 2012b; Meireles *et al.*, 2012) or have locally disappeared from the waters of the Azores (Kroh *et al.*, 2008) due to the Middle Pliocene and Pleistocene climatic deterioration (Landau *et al.*, 2007; Monegatti and Raffi, 2007). There are also Late Pleistocene fossils that are preserved in scattered outcrops around the island and that were dated as Eemian (corresponding to the last interglacial, ~120–130 ka) (Ávila *et al.*, 2008a). Molluscs (bivalves and gastropods) are the most common of the fossil invertebrates that are present in both Mio–Pliocene and Late Pleistocene outcrops (Ávila *et al.*, 2002; 2010).

The fossil Rissoidae collected in the outcrops of Santa Maria Island were used to test the idea that the aforesaid sublittoral species are, in a geological sense, longer-lived than the intertidal species, and that, as a consequence, we expect its fossils to be older. Pleistocene (Ávila *et al.*, 2002; 2009b; 2010) as well as Mio–Pliocene specimens (work in progress) were found and the latter are here reported for the first time. Mio–Pliocene rissoids are only abundant and well preserved at Ponta do Castelo outcrop but Late Pleistocene (Eemian) rissoids are very abundant and well preserved at several outcrops, namely Lagoinhas, on the north, and Prainha/Praia do Calhau, Vinha Velha and Pedra-que-pica, all on the south shores of the island (Fig. 4).

The Pleistocene outcrops yielded a total of 17 rissoid species (Ávila *et al.*, 2002; 2010), all of them still living on the recent Azorean shores (Ávila, 2000; 2005) with the sole exception of the thermophilic *Zebina vitrea* that locally disappeared during the last glaciation. Of these 17 rissoids, one species (*Alvania mediolittoralis*) is particularly abundant, reaching densities over 600 individuals/kg. From a total of 10 kg of fossiliferous sands collected and sorted from Lagoinhas outcrop, *A. mediolittoralis* comprised 21.8% of all specimens collected (Ávila *et al.*, 2009a). In the present times, this is a common species that lives in the intertidal algal turf of the Azores, reaching densities of 54,400 individuals/m^2 (Ávila *et al.*, 2005) and it lives in the Azores, being also reported in Madeira (see Table 2). *Alvania sleursi* was also found at Lagoinhas outcrop reaching densities over 250 individuals/kg. It is much rarer than *A. mediolittoralis*, comprising 6.9% of all specimens collected (Ávila *et al.*, 2009a). Presently, this species is especially abundant around 15–25 m depth and may reach maximum densities of about 470 individuals/m^2 (Ávila, 2003). It is reported from the Azores, Madeira and Selvagens (Table 2).

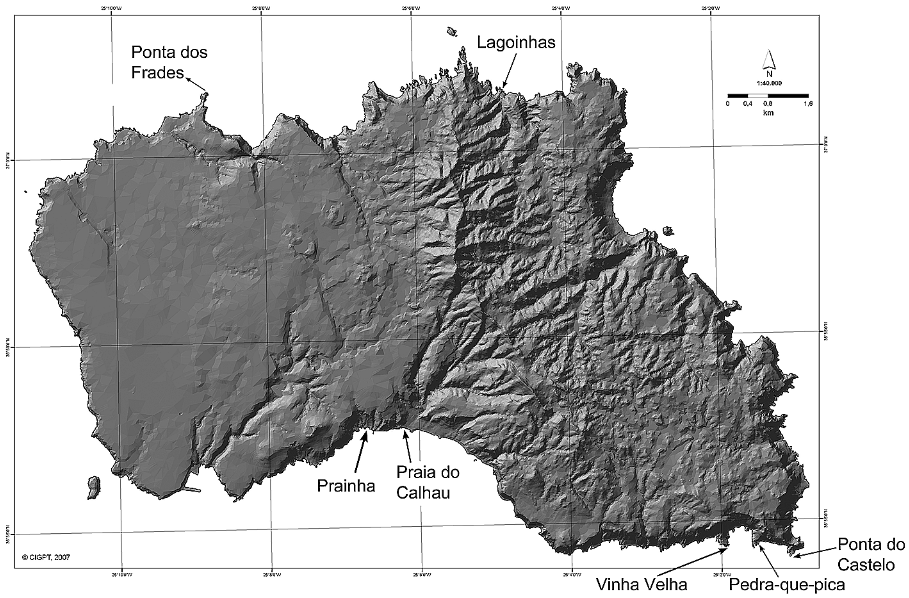

Figure 4. Pleistocene (Eemian, ~120–130 ka) outcrops (Lagoinhas, Prainha, Praia do Calhau and Pedra-que-pica) and Late Miocene–Early Pliocene outcrops (Pedreira dos Frades and Ponta do Castelo) where Rissoidae (Mollusca: Gastropoda) were collected, at Santa Maria Island (Azores).

Most of the abundant material collected from the Late Miocene–Early Pliocene outcrops of Santa Maria is still under study. Bivalves dominate these taphocoenoses and microgastropods are rarely preserved, the best specimens being from Ponta do Castelo and Ponta dos Frades outcrops. Among several new species waiting to be described, a specimen of *Alvania sleursi* was found at Ponta do Castelo (Fig. 5).

The finding of Mio–Pilocene fossils of *Alvania sleursi* and its occurrence at Pleistocene (Eemian) and recent, is evidence that this species speciated long ago in the Azores and later reached Madeira and Selvagens (it was not found in the Eemian deposits of these latter archipelagos). It also corroborates the corollary that correlates a nonplanktotrophic mode of larval development with geographic range, bathymetry/ecological zonation and evolutionary time. In this case, and comparing the two *Alvania* species (the intertidal *A. mediolittoralis* with the sublittoral *A. sleursi*) we predict that a phylogenetic analysis of this family will produce a tree similar to the one presented in Fig. 6, where *A. sleursi* will be in a basal position in relation to *A. mediolittoralis*.

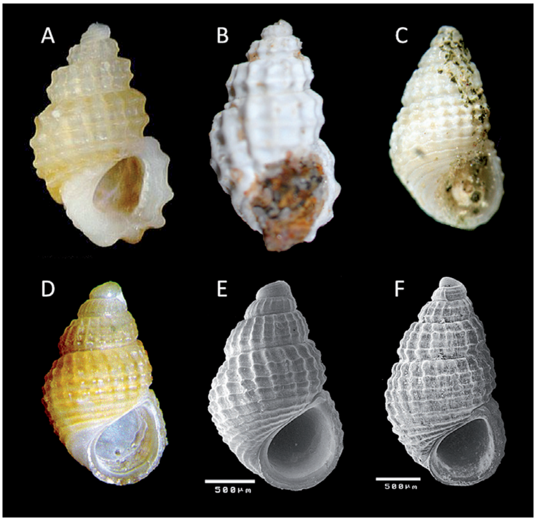

Figure 5. Fossil and Recent rissoid species collected at Santa Maria Island. A – *Alvania sleursi* (Recent, NMR 38832, ©Natural History Museum Rotterdam); B – *A. sleursi* (Late Miocene – Early Pliocene, Ponta do Castelo: DBUA-F 1058-2); C – *A. mediolittoralis* (Pleistocene, Eemian, Prainha: DBUA-F 125/143-4); D – *A. mediolittoralis* (Recent, Lajes do Pico: DBUA 663/90-1); E – *A. mediolittoralis* (SEM photography of the shell; Recent, Lajes do Pico: DBUA 663/90-1); F – *A. mediolittoralis* (SEM photography of the shell; Pleistocene, Lagoinhas: DBUA-F 138/155-3).

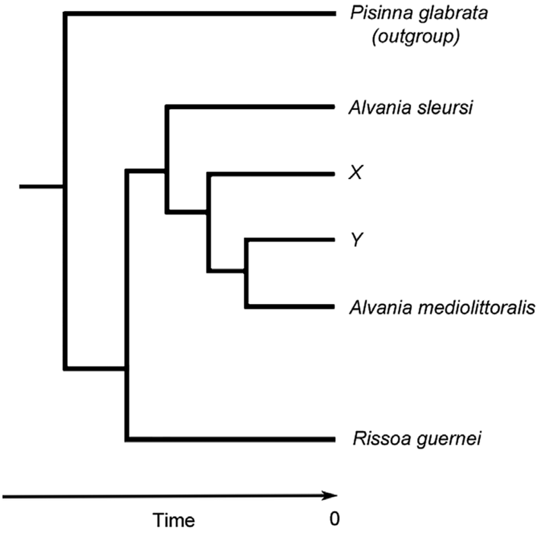

Figure 6. Hypothetical phylogenetic tree of the Azorean Rissoidae with the expected relative positions of *Alvania mediolittoralis* (intertidal) and *Alvania sleursi* (subtidal) species. «X» and «Y» are other *Alvania* species presently reported in the Azores.

Time, evolution and speciation in oceanic islands: why are reefless oceanic island sandy beaches almost devoid of life?

A continental marine biologist not acquainted with insular marine life will certainly be surprised when walking along a sandy beach of a reefless oceanic island. In fact, and in contrast with his experience of similar habitats in continental margins, where life strives and many marine invertebrates or their remains and traces are common, in oceanic islands, these sandy beaches are notoriously devoid of life!

Morton *et al.* (1998) explored in detail the intertidal zone of the few sandy beaches that, in the present-times, have some expression in the Azores and concluded that they are almost devoid of animal life in the intertidal zone, with the notable exceptions of the sandhopper amphipod *Talitrus saltator* (Montagu, 1808) and the beachflea amphipod *Orchestia gammarellus* (Pallas, 1766). Those authors postulated that this pattern was probably due to the isolation of the Azores archipelago or to the oligotrophic nature of the islands, as most of the species living in beaches are dependent on the allochthonous supply of nutrients from the sea (Morton *et al.*, 1998). Bamber and Robbins (2009) also studied the littoral and sublittoral soft-sediment benthos at São Miguel Island (Azores) and found that the sedimentary infauna was particularly sparse. They attributed the «impoverished sedimentary infauna (...) to sediment instability». But, are these really the main reasons?

Volcanic oceanic islands arise at the boundaries between tectonic plates by accretion from convection of magma in the earth's mantle. Such islands do not possess the geotectonic characteristics of a continent and were never in connection with a continental land mass. When compared to continents, oceanic islands are usually characterized by a depauperate and disharmonic fauna and flora, in the sense that common species in continents are not present in the insular habitats. For instance, in the Atlantic shores of Cohasset (Massachusetts, USA), located at a similar latitude of the Azores, marine intertidal species such as the barnacle *Semibalanus balanoides* and the bivalve *Mytilus edulis* are both preyed by the gastropod *Nucella lapillus*; at the same latitude but 5000 km to the east, on the European Atlantic shores of Cascais (Portugal), the pulmonate limpet *Siphonaria pectinata* feeds on algae while the extremely abundant bivalve *Mytilus galloprovincialis* covers almost all available space. Similarly to the American shores of Massachusetts, also in this part of Europe the carnivore gastropod *Nucella lapillus* preys on barnacles and on the mytilid bivalves (Morton *et al.*, 1998). With the exception of the pulmonate *Siphonaria pectinata*, none of the above mentioned common species are present in the Azores, Madeira, Selvagens or Cape Verde islands. The non-existence of *Mytilus* spp. in these archipelagos might well be related with the reasons outlined by Morton *et al.* (1998) – the isolation and the oligotrophic nature of the islands. However, and as will be shown below, the explanation for the life-devoid sandy habitats is historical, rather than ecological, so what we need here is a new dimension: geological time.

The influence of glaciations on the shallow marine communities living in reefless oceanic islands

Although glaciations have been a common feature of our planet, they have increased in both duration and intensity since the beginning of the Early Pleistocene Gelasian, 2.588 Myr (Gradstein *et al.*, 2004). During the last one million years, sea-level was higher or very similar to that of the present for (at least) six times (Fig. 7) (Miller *et al.*, 2005). The marine record of the last interglacial, known as the Marine Isotopic Stage 5e (MIS 5e) is one of the best studied interglacials. It begun at the middle of Termination 2, the transition from MIS 6 to MIS 5e (see Fig. 8) at 135±2 ka (Henderson and Slowey, 2000) and it ended at ~115 ka. During the climatic optimum that lasted from 132 to 125 ka, sea-level was relatively stable at +2.5 m and the North Atlantic experienced a milder climate of at least 2º C higher sea surface temperatures (SST) (Rasmussen *et al.*, 2003). This highstand was followed by a minor regression and then sea-level rose to +3 to +4 m. Circa 120 to 118 ka, by the end of the MIS 5e, global sea-level abruptly peaked at least 6.6 m higher than today (Kopp *et al.*, 2009) and formed notches and narrow benches as high as +9 m (Hearty *et al.*, 2007). After this, sea-level rapidly fell into the glacial lower sea-levels of MIS 4. The transition in sea-level from MIS 4 to MIS 3 occurred around 59 ka. During MIS 3 (59 to 25 ka) sea-level rose from -70 m to approximately -50 m (early period of MIS 3) and subsequently dropped to -80 m (late period of MIS 3). At least four sea-level fluctuations with 20 to 30 m magnitude occurred during MIS 3 (Siddal *et al.*, 2008). Sea-level then fell to MIS 2 lowest sea-levels of the last glacial episode (-120 to -130 m), between 23–18 ka. Transition 1 marks the change from the peak of the last glaciation (MIS 2) to the present interglacial (MIS 1). The last glacial stage (MIS 2) ended at 18,000 years BP (Before Present; by «Present» meaning 1950), when temperatures increased, causing a very rapid deglaciation at a global scale (Wilson *et al.*, 2000). The pace of rising of the sea-level was fast and in just 5000 years, sea-level rose from -100 m (around 14,500 years BP) to -10 m (9000 years BP), reaching present sea-level at about 7000 years BP (Fig 8).

The Pleistocene glacial/interglacial episodes and the associated sea-level oscillations affected differently the continental and the insular shallow marine communities, mainly due to: 1) the insular shelf being narrower and steeper than continental shelves, so accommodation space for deposition and residence time of sediments is smaller in islands; 2) in continents, the base level falls below the shelf break at depths around -200 m, whereas in islands the shelf breaks usually at depths from -60/-80 to -100 m (Ávila *et al.*, 2008b).

The shelves of reefless volcanic islands are unique among the offshore islands as they are wave-cut features superimposed on the volcanic slopes; moreover, sediment supply to the shelf is mostly from marine erosion during sea-level highstands and volcanic-related processes (Quartau, 2007; Quartau *et al.*, 2012). In contrast, around continental margins, stratigraphy develops from a complex

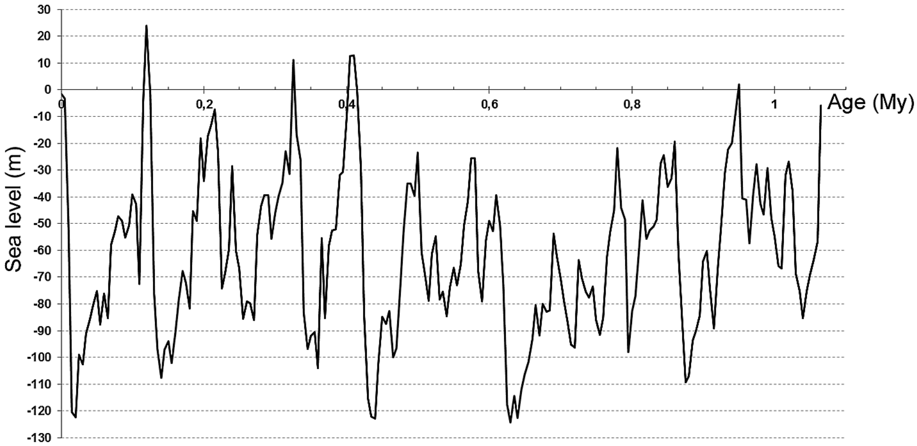

Figure 7. Sea-level curve during the last one million years (Miller *et al.*, 2005).

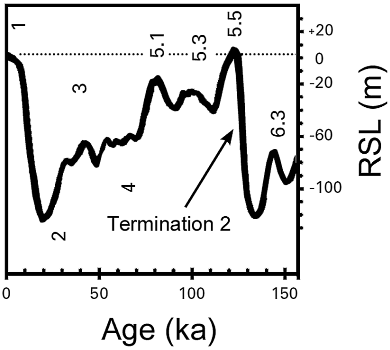

Figure 8. Sea-level curve for the last 150,000 years (adapted from Waelbroeck *et al.*, 2002). RSL – Relative sea-level (in relation to the present sea-level).

interplay of sediment supplied from the continent, transport by currents, shoreline processes and erosion during lowered sea-level (Johnson and Baldwin, 1986). As it will be demonstrated below, these different processes as well as the differences in the shelf break depths of continents versus oceanic islands are crucial items for explaining the repeated phenomena of local disappearances in islands of the shallow species associated to fine sand.

Ávila (2005) called the attention for a group of bivalves that were extremely common in the Pleistocene (MIS 5e) outcrops of Santa Maria Island and provided a plausible explanation for the local disappearance of these species from the Azorean shores during the course of the last glaciation. These species (the jackknife *Ensis minor*, the small *Lucinella divaricata* and the large *Laevicardium crassum*) share similar features: with the exception of *L. crassum* that is reported from 0–195 m depth, they were shallow species that lived associated to sandy or muddy habitats (*L. crassum* is also reported in gravel bottoms and, although it has never been collected in the Azores in samples from 0–300 m depth, it is possible that *L. crassum* still lives in the Azores, but at greater depths). None of these species lives nowadays in the shallow waters of the Azores.

The processes and mechanisms responsible for the vanishing of these species were further explained (Ávila *et al.*, 2008b) and a palaeoecological interpretation of the impact on the shallow marine communities was produced (Ávila *et al.*, 2010). Basically, in reefless oceanic islands, when the sea drops below the level of the present highstand, sediment supply becomes sparse due to lack of major river systems, reduced precipitation in glacial periods and low subaerial erosion of the palaeomarine cliffs left behind (Ávila *et al.*, 2008b). Consequently, during sea-level falls, the lack of sediment supply prevents the formation of large lowstand deposits. On the other hand, when the base level falls below the shelf break the preservation potential of the falling stage strata that accumulates on the shelf is very slow, making the Low Stand System Tract very reduced or non-existent. Furthermore, the presence of a narrow and steeper insular margin may enable faster transport of sediment offshore, with regressive ravinements sweeping away the highstand sediments from the shelf, leaving the shelf devoid of sediments (Ávila *et al.*, 2008b; 2010).

For a better understanding of the ecological implications described above, a complete glacial/interglacial/glacial sequence (MIS 6–MIS 5 to MIS 2) will be used as an example and a well-studied outcrop (Prainha, Santa Maria Island) will serve as a proxy for what has happened in similar oceanic islands and outcrops worldwide.

Prainha outcrop is located in the southern shores of Santa Maria Island (Fig. 9). It is located at 2–4 m above present sea-level and the majority of the fossils found in the area are molluscs (gastropods and bivalves), with echinoderms, bryozoans, ostracods and foraminifera as accessory fauna (Ávila *et al.*, 2010). These fossils were dated as MIS 5e (Ávila *et al.*, 2008a). Ávila *et al.* (2009a) described the sections studied at Prainha as «exposures of unconsolidated shallow water deposits overlying a basement formed by basaltic lavas (...) associated with wave-cut platforms formed during a Pleistocene transgression». The base of this marine sequence overlays an irregular wave-cut platform on top of ankaramitic basalts. Directly overlaying this unconformity, there is a strongly cemented basalt conglomerate (Fig. 10, subunit A1) that passes laterally and upward into a calcareous algal framework (biostromic crust) (Fig. 10, subunit A2); the sediments of subunits A1 and A2 correspond to a beach shoreface facies. Fossiliferous sands (Fig. 10, subunit B1) correspond to beach foreshore (interstadial) facies and are very similar in both grain size and composition to the recent beach sands

Figure 9. Aerial view of Praia Formosa (Santa Maria Island, Azores) with the Late Pleistocene (MIS 5e) outcrop of Prainha (Praia do Calhau).

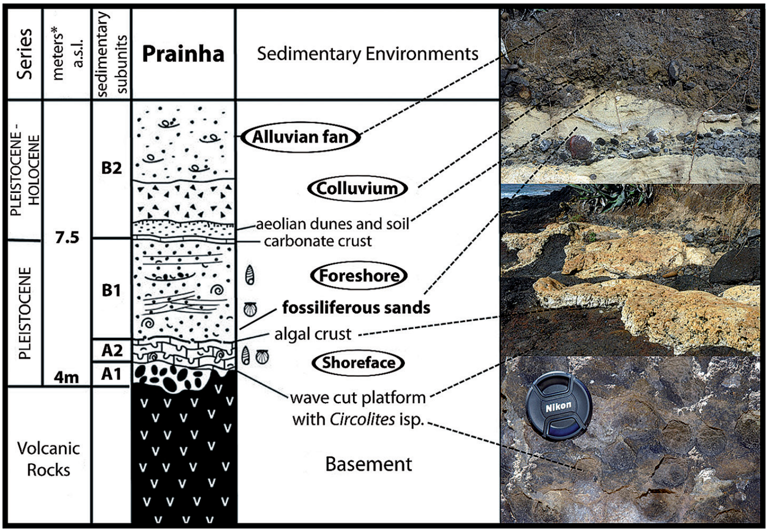

Figure 10. Stratigraphic section of Prainha. * Maximum altitude above sea-level (a.s.l.), measured at low tide; mean annual tidal range around 1.5 m. Modified after Ávila *et al.* (2002; 2009a). The beds A1, A2 and B1 are MIS 5e (Ávila *et al.*, 2008b).

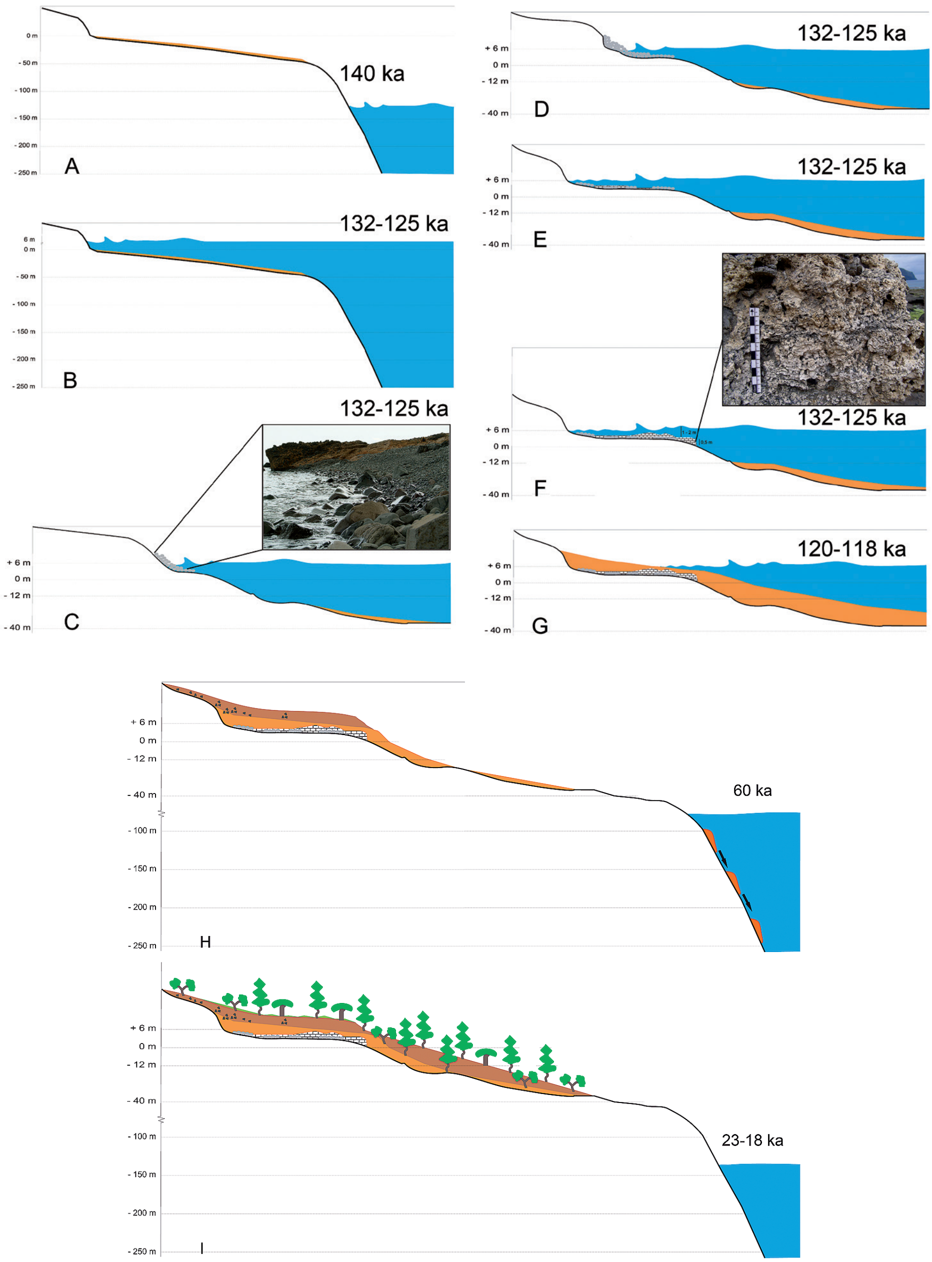

Figure 11 (A–I). Influence of the sea-level fluctuations on the marine life associated to fine sandy habitats and on the bottom topography of the shores south of Prainha outcrop (adapted from Ávila *et al.*, 2010).

collected at Prainha (Ávila *et al.*, 2009a). The sand layer is capped by dunes and colluvial-alluvial fan deposits that protect the marine Pleistocene strata from weathering (Fig. 10, subunit B2).

About 140 ka, sea-level was about -130 m in relation to the present sea-level (Fig. 11A) and at Prainha, the shoreline would be about 2.5 km south in relation to the present coastline. With the rapid deglaciation (Termination 2) that marks the ending of MIS 6, the sea-level rose very fast (~130 m in 5000–6000 years) (Fig. 11B). As explained before, during the 132–125 ka period sea-level still stand around +2.5 m. During this period, marine erosion produced by the constant impact of waves and by the high shock pressures of the waves breaking on the shore, resulted on the accumulation of boulders at the base of cliffs (Fig. 11C). Progressively, a wave-cut platform was carved inland (Fig. 11D) and the shallow shelf got wider (Fig. 11E). The sediments produced by subaerial erosion inland and that were discharged by rivulets on the shore, together with those that were produced on the intertidal zone, mainly from the abrasion of boulders, were swept away and deposited further offshore (Fig. 11F). At this time, the calcareous algae crust was growing upwards and laterally, promoting also the stabilization of the boulders of the beaches. Meanwhile, sand grains were increasing in numbers and sandy beaches increased in size. With the final rising of the sea-level between 120–118 ka, intertidal zone migrated inland and sands covered (thus killing) the coralline algal crusts (Fig. 11G). With the beginning of MIS 5d, sea-level lowered. Throughout the last glaciation, with sea-level progressively lowering, all animals living in the intertidal or in the first 30 m of water and associated with a sandy or muddy habitat, were forced to follow the retreat of the sea. The present-day offshore of Prainha has an average slope of 2–4% in the shallow areas (between intertidal and -60 to -80 m) and 36–48% (from -60 to -80 m down to -300 m) (Ávila *et al.*, 2008b). As long as the slope was smooth (2–4%), those littoral sandy species basically retreated along the coastal slope until the insular shelf break was reached. At Prainha, depending on the bottom topography, this critical point of the shelf varies between -60 to -80 m. From that depth on, slope changes abruptly to 36–48% and species faced a major problem!

As in other places, in the Azores and in the present times, winter storms usually remove the sand from the littoral strip of Santa Maria, leaving sand-stripped beaches. These beaches are again refurbished with sand during the next summer (Borges, 2003). However, when sea-level reached the shelf break below 60–80 m depth it became physically impossible to keep the sand in the littoral of Prainha. While winter storms continued to remove sand, a fair-weather regime could no longer restore it because it had been lost to the island slopes (Fig. 11H) (Ávila *et al.*, 2008b). As a result of this tendency, sand beaches became progressively poorer and depleted of sand and this heavily affected the shallow species associated to sandy and muddy habitats that locally disappeared due to the loss of proper habitat. Other species with similar environmental requirements, namely some echinoderms and amphipods, probably also suffered severely from the lack of sand. For instance, species such as the irregular sea urchin *Brissus unicolor* (Leske, 1778) or the heart-urchin *Echinocardium cordatum* (Pennant, 1777), presently living in the Azores in fine sandy beaches between 10 and 30 m depth, must have either locally disappeared from these islands or, at least, became very rare, passing through a drastic reduction of the population size (bottleneck effect) (Ávila *et al.*, 2008b).

THE INFLUENCE OF GLACIATIONS ON THE TERRESTRIAL COMMUNITIES LIVING IN REEFLESS OCEANIC ISLANDS

Finally, a small note about the consequences of a glacial episode on the terrestrial flora and fauna. The drop of the sea-level until the 120–130 m depth in relation to the present sea-level was a global phenomenon. Worldwide, all reefless oceanic islands were affected in a similar way to Santa Maria in the Azores. Depending on the topography of the island, the terrestrial area of the island increased, as more and more of the shelf of the island was progressively available for colonization by terrestrial plants that, with some time-lag, were followed by terrestrial animals (Fig. 11I). In Santa Maria, a volcanic island with no volcanic eruptions for the last 2 Myr, the subaerial area would be very similar to the present bathymetric contour of the island at -130 m (Fig. 12). This would mean that during the last glacial maximum (MIS 2) the terrestrial area of this island (estimated as 206 km^2 at the -100 m isobathymetric line) would more than double the current area (97 km^2)! We can only imagine the number of local disappearances and extinctions that rising sea-levels caused on terrestrial life...

CONCLUSIONS

Ávila (2008b) explained why shallow endobenthonic bivalves associated with sand and present in the Azores during the MIS 5e have locally disappeared from these islands during the last glaciation. This also explains the very low biodiversity of the present sandy beaches of the Azores, which is linked with the lack of suitable habitat (sand) due to the sea-level drop during the last glaciation. It is expected that other species living in the MIS 5e beaches of Santa Maria Island (a warmer interglacial than the present one) must also have been affected. More importantly, this process must have been very widespread and it certainly occurred in previous glacial/interglacial cycles (e.g. MIS 7, 9 and 11), thus the life-devoid sandy habitats in oceanic islands explanation rely on historical rather than on ecological reasons. Another very important corollary is that this model also explains the lack of endemic shallow species associated to sandy habitats in oceanic islands. Lastly, this model also predicts that the genetic variability of the extant insular populations of these shallow-water species living in fine sand should be

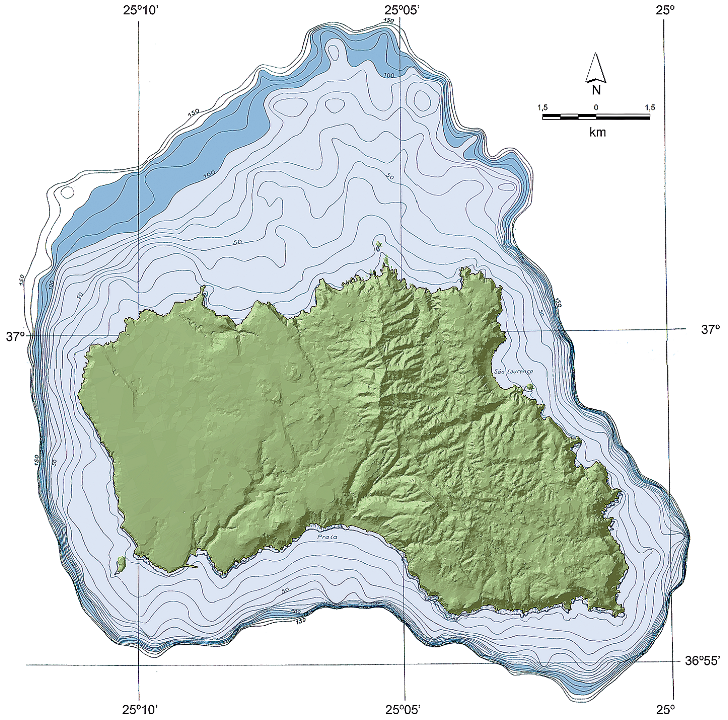

Figure 12. Subaerial area of Santa Maria Island in the present times (green) and during MIS 2, the peak of the last glaciation (total area = green + light blue + dark blue areas). Light blue corresponds to the -100 m isobathymetric; dark blue to the -130 m isobathymetric. Isobathymetric lines are represented each 10 m depth.

lower than continental European ones, either due to the bottlenecking process or to a recent colonization event, and this hypothesis may be tested.

This study illustrates the effect of glaciations on the littoral marine species of the Azores. Temperate oceanic islands such as the Azores have been repeatedly colonized (most probably during Terminations – see Ávila *et al.*, 2009b) by warm-water fauna that lives during interglacials and that locally disappears from the islands during the course of glacial episodes. Species associated to sandy habitats will also disappear from such islands if and when sea-level drops below the insular shelf edge. Species associated to hard substrata (e.g., rocky shores covered by algae) and that are able to cope with the drop of sea-temperatures will surpass glaciations without major problems. Interestingly, Ávila *et al.* (2008c) discovered that the endemic Azorean Rissoidae *Alvania mediolittoralis*, a very common species in sheltered places and particularly abundant among the algal turf covering the lower half of the intertidal and upper subtidal rocky shores, is able to reproduce throughout the year, with two spawning peaks, one during early spring and the other in late autumn. Evidently, this will be an enormous ecological competitive advantage in times of lower sea-surface temperatures as those occurring during glaciations, and it may be a plausible explanation for the survival of these species to glacial episodes.

Finally, the proposed relationship between modes of larval development, geographic range and bathymetry/ecological zonation with evolutionary time, was supported by the fossil record of the Azorean rissoids.

ACKNOWLEDGEMENTS

I thank Dr. André Levy (Centro de Biociências/ISPA-IU, Lisbon), Prof. Frias Martins and Ricardo Cordeiro (both from CIBIO-Açores/INBIO Laboratório Associado, University of the Azores) for revising the manuscript and for their constructive critics. I am also in debt to Carlos Melo (Fig. 10) and António Monteiro (Fig. 12) (both, University of the Azores).

REFERENCES

Ávila, S.P. (2000) Shallow-water marine molluscs of the Azores: biogeographical relationships. *Arquipélago*, 2, 99–131.

Ávila, S.P. (2003) The littoral molluscs (Gastropoda, Bivalvia and Polyplacophora) of São Vicente, Capelas (São Miguel Island, Azores): ecology and biological associations to algae. *Iberus*, 21, 1–23.

Ávila, S.P. (2005) *Processos e Padrões de Dispersão e Colonização nos Rissoidae (Mollusca: Gastropoda) dos Açores*. PhD Thesis, Universidade dos Açores, Ponta Delgada.

Ávila, S.P. (2006) Oceanic islands, rafting, geographical range and bathymetry: a neglected relationship? *Proceedings of the 5th international symposium on the fauna and flora of Atlantic Islands* (ed. by Hayden, T.J., D.A. Murray and J.P. O'connor), pp. 22–39. Irish Biogeographical Society, Dublin.

Ávila S.P. and Malaquías, M.A. (2003) Biogeographical relationships of the molluscan fauna of the Ormonde seamount (Gorringe bank, Northeast-Atlantic Ocean). *Journal of Molluscan Studies*, 69, 145–150.

Ávila, S.P., Amen, R., Azevedo, J.M.N., Cachão, M. and García-Talavera, F. (2002) Checklist of the Pleistocene marine molluscs of Prainha and Lagoinhas (Santa Maria Island, Azores). *Açoreana*, 9, 343–370.

Ávila, S.P., Cardigos, F. and Santos, R.S. (2004) D. João de Castro bank, a shallow-water hydrothermal-vent in the Azores: checklist of the marine mollusks. *Arquipélago*. 21A, 75–80.

Ávila, S.P., Santos, A.C. Penteado, A.M., Rodrigues, A.M., Quintino, I. and Machado, M.I. (2005) The molluscs of the intertidal algal turf in the Azores. *Iberus*, 23, 67–76.

Ávila, S.P., Madeira, P., Mendes, N., Rebelo, A., Medeiros, A., Gomes, C., García-Talavera, F., Silva, C.M., Cachão, M., Hillaire-Marcel, C. and Martins, A.M.F. (2008a) Mass extinctions in the Azores during the last glaciation: fact or myth? *Journal of Biogeography*, 35, 1123–1129.

Ávila, S.P., Madeira, P. Silva, C.M., Cachão, M., Landau, B., Quartau, R. and Martins, A.M.F. (2008b) Local disappearance of bivalves in the Azores during the last glaciation. *Journal of Quaternary Science*, 23, 777–785.

Ávila, S.P., Madeira, P., Zazo, C., Kroh, A., Kirby, M., Silva, C.M., Cachão, M. and Martins, A.M.F. (2009a) Palaeocology of the Pleistocene (MIS 5.5) outcrops of Santa Maria

Island (Azores) in a complex oceanic tectonic setting. *Palaeogeography, Palaeoclimatology, Palaeoecology*, 274, 18–31.

Ávila, S.P., Silva, C.M., Schiebel, R., Cecca, F., Backeljau, T. and Martins, A.M.F. (2009b) How did they get here? Palaeobiogeography of the Pleistocene marine molluscs of the Azores. *Bulletin of the Geological Society of France*, 180, 295–307.

Ávila, S.P., Rebelo, A., Medeiros, A., Melo, C., Gomes, C., Bagaço, L., Madeira, P., Borges, P.A., Monteiro, P., Cordeiro, R., Meireles, R. and Ramalho, R. (2010) *Os fósseis de Santa Maria (Açores). 1. A jazida da Prainha.* OVGA, Lagoa.

Ávila, S.P., Borges, J.P. and Martins, A.M.F. (2011) The littoral Trochoidea (Mollusca: Gastropoda) of the Azores. *Journal of Conchology*, 40, 408–427.

Ávila, S.P., Goud, J. and Martins, A.M.F. (2012a) Patterns of diversity of the Rissoidae (Mollusca: Gastropoda) in the Atlantic and the Mediterranean Region. *The Scientific World Journal*, Article ID-164890, 1–30.

Ávila, S.P., Ramalho, R. and Vullo, R. (2012b) Systematics, palaeoecology and palaeobiogeography of the Neogene fossil sharks from the Azores (Northeast Atlantic). *Annales de Paléontologie*, 98, 167–189.

Bamber, R.N. and Robbins, R. (2009). The soft-sediment infauna off São Miguel, Azores, and a comparison with other Azorean invertebrate habitats. *Açoreana*, 6, 201–210.

Berry, R.J., Berry, A.J., Anderson, T.C.J. and Scriven, P. (1992) The house mice of Faray, Orkney. *Journal of Zoology (London)*, 228, 233–246.

Borges, P.A. (2003) *Ambientes litorais nos Grupos Central e Oriental do Arquipélago dos Açores. Conteúdos e Dinâmica de Microescala.* PhD thesis, Universidade dos Açores, Ponta Delgada.

Carson, H.L. (1992) Genetic change after colonization. *Geojournal*, 28, 297–302.

Darwin, C.R. (1859) *On the Origin of Species by Means of Natural Selection, or the Preservation of Favoured Races in the Struggle for Life.* John Murray, London.

Dengler, J. (2009) Which function describes the species–area relationship best? A review and empirical evaluation. *Journal of Biogeography*, 36, 728–744.

Diamond, J.M. (1975). Assembly of species communities. *Ecology and evolution of communities* (ed. by Cody, M.L. and Diamond, J.M.), pp. 342–444. Harvard University Press, Cambridge.

Fattorini, S. (2009) On the general dynamic model of oceanic island biogeography. *Journal of Biogeography*, 36, 1100–1110.

Fernández-Palacios, J.M., de Nascimento, L., Otto, R., Delgado, J.D., García-del-Rey, E., Arévalo, J.R. and Whittaker, R.J. (2011) A reconstruction of Palaeo-Macaronesia, with particular reference to the long-term biogeography of the Atlantic island laurel forests. *Journal of Biogeography*, 38, 226–246.

García-Talavera, F. (1981) Los moluscos gasterópodos antiatlánticos (estudio paleo y biogeográfico de las especies bentónicas litorales). *Universidad de la Laguna, Colección Monografías*, 10, 1–352.

Gittenberger, E. (1991) What about non-adaptive radiation? *Biological Journal of the Linnean Society*, 43, 263–272.

Gradstein, F., Ogg, J, and Smith, A. (2004) *A Geologic Time Scale.* Cambridge University Press, Cambridge.

Grant, P.R. (1981) Speciation and the adaptive radiation of Darwin's finches. *American Scientist*, 69, 653–663.

Hearty, P.J., Hollin, J.T., Neumann, A.C., O'leary, M.J. and Mcculloch, M. (2007) Global sea-level fluctuations during the Last Interglaciation (MIS 5e). *Quaternary Science Reviews*, 26, 2090–2112.

Henderson, G.M. and Slowey, N.C. (2000) Evidence from U–Th dating against Northern Hemisphere forcing of the penultimate deglaciation. *Nature*, 404, 61–66.

Hubble, S.P. (2001) *The unified neutral theory of biodiversity and biogeography.* Princeton University Press, New Jersey.

Jablonski, D. and Lutz, R.A. (1980) Molluscan larval shell morphology: ecological and paleontological applications. *Skeletal Growth of Aquatic Organisms* (ed. by Rhoads, D.C. and Lutz, R.A.), pp. 323–377. Plenum, New York.

Janssen, A.W., Kroh, A. and Ávila, S.P. (2008) Early Pliocene heteropods and pteropods (Mollusca, Gastropoda) from Santa Maria Island (Azores, Portugal): systematics and biostratigraphic implications. *Acta Geologica Polonica*, 58, 355–369.

Johannesson, K. (1988) The paradox of Rockall: Why is a brooding gastropod (*Littorina saxatilis*) more widespread than one having a planktonic larval dispersal stage (*L. littorea*)? *Marine Biology*, 99, 507–513.

Johnson, H.D. and Baldwin, C.T. (1986) Shallow siliclastic seas. *Sedimentary Environments and Facies*, 2nd (ed. by Reading, H.G.), pp. 229–282. Blackwell Scientific, Oxford.

Kopp, R.E., Simons, F.J., Mitrovica, J.X., Maloof, A.C. and Oppenheimer, M. (2009) Probabilistic assessment of sea level during the last interglacial stage. *Nature*, 462, 863–868.

Kroh, A., Bitner, M.A. and Ávila, S.P. (2008) *Novocrania turbinata* (Brachiopoda) from the Early Pliocene of the Azores (Portugal). *Acta Geologica Polonica*, 58, 473–478.

Landau, B., Capelo, J.C. and Silva, C.M. (2007) Patterns of extinction and local disappearance of tropical marine gastropods; contrasting examples from across the North Atlantic. *Açoreana*, 5, 50–58.

Mac Andrew, R. (1854) *On the geographical distribution of testaceous Mollusca in the North Atlantic and neighbouring seas.* H. Greenwood, Liverpool.

MacArthur, R.H. and Wilson, E.O. (1967) The theory of island biogeography. Princeton University Press, New Jersey.

Madeira, P., Kroh, A., Cordeiro, R., Meireles, R. and Ávila, S.P. (2011) The fossil echinoids of Santa Maria Island, Azores (Northern Atlantic Ocean). *Acta Geologica Polonica*, 61, 243–264.

MEIRELES, R.P., FARANDA, C., GLIOZZI, E., PIMENTEL, A., ZANON, V. and ÁVILA, S.P. (2012) Late Miocene marine ostracods from Santa Maria Island, Azores (NE Atlantic): Systematics, palaeoecology and palaeobiogeography. *Révue de Micropaléontologie,* 55, 133–148.

MILLER, K.G., KOMINZ, M.A., BROWNING, J.V., WRIGHT, J.D., MOUNTAIN, G.S., KATZ, M.E., SUGARMAN, P.J., CRAMER, B.S., CHRISTIE-BLICK, N. and PEKAR, S.F. (2005) The Phanerozoic Record of Global Sea-Level Change. *Science,* 310, 1293–1298.

MONEGATTI, P. and RAFFI, S. (2007) Mediterranean-middle eastern Atlantic façade: molluscan biogeography and ecobiostratigraphy throughout the Late Neogene. *Açoreana,* 5, 126–139.

MORTON, B., BRITTON, J.C. and MARTINS, A.M.F. (1998) *Ecologia Costeira dos Açores.* Sociedade Afonso Chaves, Ponta Delgada.

O'FOIGHIL, D. (1989) Planktotrophic larval development is associated with a restricted geographic range in *Lasaea,* a genus of brooding, hermaphroditic bivalves. *Marine Biology,* 103, 349–358.

QUARTAU, R. (2007) *The insular shelf of Faial: Morphological and sedimentary evolution.* PhD Thesis, Universidade de Aveiro, Aveiro.

QUARTAU, R., TEMPERA, F., MITCHELL, N.C., PINHEIRO, L.M., DUARTE, H., BRITO, P.O., BATES, C.R. and MONTEIRO, J.H. (2012) Morphology of the Faial Island shelf (Azores): the interplay between volcanic, erosional, depositional, tectonic and mass-wasting processes. *Geochemistry, Geophysics, Geosystems,* 13, DOI: 10.1029/2011GC003987.

RASMUSSEN, T.L., THOMSEN, E., KUIJPERS A. and WASTEGARD, S. (2003) Late warming and early cooling of the sea surface in the Nordic seas during MIS 5e (Eemian Interglacial). *Quaternary Science Reviews,* 22, 809–821.

RICKLEFS, R.E. and COX, G.W. (1972) Taxon cycles in the West Indian avifauna. *The American Naturalist,* 106, 195–219.

RICKLEFS, R.E. and COX, G.W. (1978) Stage of taxon cycle, habitat distribution, and population density in the avifauna of the West Indies. *The American Naturalist,* 112, 875–895.

ROSENZWEIG, M.L. (1995) *Species diversity in space and time.* Cambridge University Press, Cambridge.

SCHELTEMA, R.S. (1986) On dispersal and planktonic larvae of benthic invertebrates: an eclectic overview and summary of problems. *Bulletin of Marine Science,* 39, 290–322.

SCHELTEMA, R.S. (1989) Planktonic and non-planktonic development among prosobranch gastropods and its relationship to the geographic range of species. *Reproduction, Genetics and Distribution of Marine Organisms* (ed. by RYLAND, J.S. and TYLER, P.A.), pp. 183–188. Olsen & Olsen, International Symposium Series.

SCHELTEMA, R.S. (1995) The relevance of passive dispersal for the biogeography of Caribbean mollusks. *American Malacological Bulletin,* 11, 99–115.

SCHELTEMA, R.S. and WILLIAMS, I.P. (1983) Long-distance dispersal of planktonic larvae and the biogeography and evolution of some Polynesian and western Pacific mollusks. *Bulletin of Marine Science,* 33, 545–565.

SCHELTEMA, R.S., WILLIAMS, I.P. and LOBEL, P.S. (1996) Retention around and long-distance dispersal between oceanic islands by planktonic larvae of benthic gastropod mollusca. *American Malacological Bulletin,* 12, 67–75.

SERRALHEIRO, A. (2003) A geologia da ilha de Santa Maria, Açores. *Açoreana*, 10, 141–192.

SERRALHEIRO, A. and MADEIRA, P. (1990) *Stratigraphy and geochronology of Santa Maria island (Azores).* Livro de Homenagem ao Prof. Carlos Romariz, Departamento de Geologia da Faculdade de Ciências da Universidade de Lisboa, Lisboa.

SIDDAL, M., ROHLING, E.J., THOMPSON, W.G. and WAELBROECK, C. (2008) Marine Isotope Stage 3 sea level fluctuations: data synthesis and new outlook. *Reviews of Geophysics,* 46, doi: 10.1029/2007RG000226.

STRATHMANN, R.R. (1974) The spread of sibling larvae of sedentary marine invertebrates. *American Naturalist,* 108, 29–44.

TRIANTIS, K.A., GUILHAUMON, F. and WHITTAKER, R.J. (2012) The island species–area relationship: biology and statistics. *Journal of Biogeography,* 39, 215–231.

WAELBROECK, C., LABEYRIE, L., MICHEL, E., DUPLESSY, J.C., MCMANUS, J.F., LAMBECK, K., BALBON, E. and LABRACHERIE, M. (2002) Sea-level and deep water temperature changes derived from benthic foraminifera isotopic records. *Quaternary Science Reviews,* 21, 295–305.

WALLACE, A.R. (1880) *Island Life: Or, The Phenomena and Causes of Insular Faunas and Floras, Including a Revision and Attempted Solution of the Problem of Geological Climates.* Macmillan & Co., London.

WHITTAKER, R.J. and FERNÁNDEZ-PALACIOS, J.M. (2007) *Island Biogeography. Ecology, Evolution, and Conservation,* 2nd Ed. Oxford University Press, Oxford.

WHITTAKER, R.J., JONES, S.H. and PARTOMIHARDJO, T. (1997) The re–building of an isolated rain forest assemblage: how disharmonic is the flora of Krakatau? *Biodiversity and Conservation*, 6, 1671–1696.

WHITTAKER, R.J., TRIANTIS, K.A. and LADLE, R.J. (2008) A general dynamic theory of oceanic island biogeography. *Journal of Biogeography,* 35, 977–994.

WILSON, E.O. (1961) The nature of the taxon cycle in the Melanesian ant fauna. *The American Naturalist*, 95, 169–193.

WILSON, R.C.L, DURY, S.A. and CHAPMAN, J.L. (2000) *The Great Ice Age: Climate Change and Life.* Routledge, London.

WINKELMANN, K., BUCKERIDGE, J.S., COSTA, A.C., DIONÍSIO, M.A.M., MEDEIROS, A., CACHÃO, M. and ÁVILA, S.P. (2010) *Zullobalanus santamariaensis* sp. nov. a new late Miocene barnacle species of the family Archeobalanidae (Cirripedia: Thoracica), from the Azores. *Zootaxa,* 2680, 33–44.

MODELLING SEA LEVEL DRIVEN CHANGE OF MACARONESIAN ARCHIPELAGOS CONFIGURATIONS SINCE 120 KYR BP

Kenneth F. Rijsdijk, Tom Hengl, Sietze Norder, Sérgio P. Ávila,
José María Fernández-Palacios

CLIMATE CHANGE PERSPECTIVES FROM THE ATLANTIC:
PAST, PRESENT AND FUTURE

Jose María Fernández-Palacios, Lea de Nascimento, José Carlos Hernández,
Sabrina Clemente, Albano González & Juan P. Díaz-González (eds.)
Servicio de Publicaciones, Universidad de La Laguna – 2013

ISBN: 978-84-15910-54-1
pp. 127-148

ABSTRACT

The MacArthur and Wilson island biogeography theory relates species diversity on islands as the result of equilibrium between extinctions and colonization events which rates depend on island size and isolation. Although island size and isolation can be considered static on ecological timescales (<100 years) they are not static on longer time scales. Since the last million years sea levels fluctuate with a period of ca. 120 kyr between -120 m and up to +10 m MSL (Mean Sea Level). Due to these sea level changes islands have changed in size and ultimately may have drowned or emerged. The rate and degree of their drowning depends on island morphometry and the shape of the sea level change curve. We explore the effects of global sea level cycles on the configuration of archipelagos and volcanic islands of Macaronesia. The results indicate that the islands changed shape considerably during the last 120 kyr. Notably the period between 80 kyr and 15 kyr ago sea levels were at least 80 m lower than present and several islands now isolated were merged or were much larger than present. Recent shrinking of islands due to the sea level rise since the last glacial maximum period (20 kyr BP) led to more than 50% reductions in island size, significant loss of coastal habitat and a significant increase in isolation by the increase of distances between islands and island and continents. Island size reduction must have induced pressures especially on terrestrial insular ecosystems, inducing upward migrations and interspecies competitions, and probable extinctions. The splitting of merged islands must have led to separations of populations leading to gene flow losses for some biota. Present day islands are not representative for the mean island configurations during the last Myr but rather represent an anomaly. Islands at present are smallest and most isolated and this configuration makes the insular biota even more vulnerable to human impact.

KEYWORDS: island biogeography, last glacial cycle, Palaeo-Macaronesia, sea level change.

INTRODUCTION

Since its introduction by MacArthur and Wilson (1963; 1967), the Dynamic Equilibrium Model has been the ruling paradigm in island biogeography and nature conservation. It models species abundances (S) on an island of given size (A) as a dynamic equilibrium between numbers of species immigrating to the islands and number of species that become extinct. It predicts that as soon as the carrying capacity (K) of a given island is reached, some species inhabiting the islands begin to undergo extinction processes. Furthermore, it becomes harder for species to settle and survive. A dynamic equilibrium between immigration and extinction

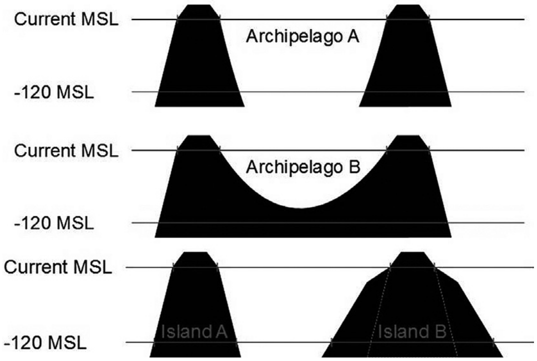

Figure 1. Basic principles of island morphology affecting size changes during sea level falls or rises. When volcanic islands are steep cones (Island A), surface change is minimal. When islands are relatively flat surface (Island B) change is large. A land bridge may emerge during sea level fall between islands of Archipelago B.

numbers is reached, resulting in an island equilibrium number of species (S*). S* has a log linear relationship between area (A) and distance to continents (D). Size is in this model approximates the carrying capacity (K) of islands, with larger islands holding more species. The dynamic equilibrium model assumes however that island and archipelagos are static through time, i.e. they remain static in size and configuration. Although island size and isolation can be considered static on ecological timescales (<100 years) they are not static on longer time scales (>1 kyr). Following the calls by Heaney (2000; 2007) and Brown and Lomolino (2000) to develop a comprehensive theory for oceanic island biogeography that unifies ecological and evolutionary biogeography, Whittaker, Fernández-Palacios and coauthors (2001; 2007; 2008) evaluated the role of island ontogeny on explaining biodiversity. They pointed out that volcanic islands are dynamic on evolutionary time scales (>100 kyr). On these longer time scales evolutionary processes, migration and extinction rates are affected by island ontogeny and plate tectonics. Here size and thus K is modified by island ontogeny which changes during a complete cycle of the islands emergence (youth), erosion (maturity) and final submergence (old age) as volcanism ceased (Fig. 1). K therefore follows a hump-shaped trend, increasing during island youth and finally decreasing during islands senescence. Based on this, Whittaker *et al.* (2007; 2008) postulated their General Dynamic Model (GDM) whereby terrestrial single-island endemic species (SIE) on evolutionary time scales show a parabolic relationship with Time (T):

$$\text{Number SIE} = \log A + aT + aT^2$$

For a number of islands and taxa they demonstrated that the abundance of SIEs is significantly correlated in the GDM (Whittaker *et al.*, 2008). These findings strongly suggest that SIEs abundances are to a large degree controlled by island age.

Towards a model that includes sea level dynamics

At «sub-evolutionary» time scales, between 1 kyr and 100 kyr, island sizes (A) and archipelago configurations are not static either. Due to the rise and fall of sea levels islands may shrink or expand dramatically, resulting in a dynamically changing of A and K and thus affecting biota on islands and biota migrating between islands (Warren *et al.*, 2010; Fernández-Palacios *et al,*. 2011). Furthermore, currently drowned seamounts may emerge and submerge due to sea level fluctuations, opening or closing specific dispersal routes within or among archipelagos as well as among archipelagos and the closest continents (García-Talavera, 1999; Ávila, 2000; Ávila and Malaquías, 2003). Natural sea level change results by long term climatic change, driven by astronomical cycles. The Serbian civil engineer and mathematician Milutin Milanković(1879–1958), suggested in the 1940s that climatic cycles were driven by the cumulative effects of the shape of the earth's orbit around the sun (eccentricity), and changes in the inclination of the earth axis towards the sun (precession and obliquity). As a result of the interplay between these astronomic variables the net radiation the Earth receives varies leading to natural climate change cycles. While Milankovićtheory of climate change was not accepted until decades after his demise, the theory has been proven correctly to explain the periodicity and intensity of climatic change cycles (Hays *et al.*, 1976; Imbrie and Imbrie, 1980). With the emergence of radiometric dating methods and their application in sea level dynamic research since the 1960s it has been found that major cycles of sea level rise follow those of climatic change. Oxygen isotopic analyses on marine microfossils in marine cores have provided continuous records of global sea level cycles from 5 Myr ago until present (Lisiecki and Raymo, 2005). Spectral analysis of these cycles confirmed that they are superimposed astronomical cycles. Due to the superimposition of the precession, eccentricity and obliquity cycles the amplitude and duration of sea level fluctuations changes through time. During the Pliocene (before 2.6 Ma) climatic change cycles were dominated by the precession cycles (22 kyr) leading to low magnitude short duration cycles of climate change (Lisiecki and Raymo, 2005). With the onset of the Quaternary 2.6 Myr ago climatic cycles were driven by obliquity with amplitudes of global temperatures and periodicity increasing to 41 kyr. Climatic change has become most extreme since 0.9 Myr ago when they became eccentricity forced with 100 kyr cycles (Ruddiman, 2003). As a result, ice ages lasting 100 kyr alternate with interglacials lasting ca. 10 kyr coinciding with low and high sea level stands respectively. During the glacial maxima when ice sheets reached their largest

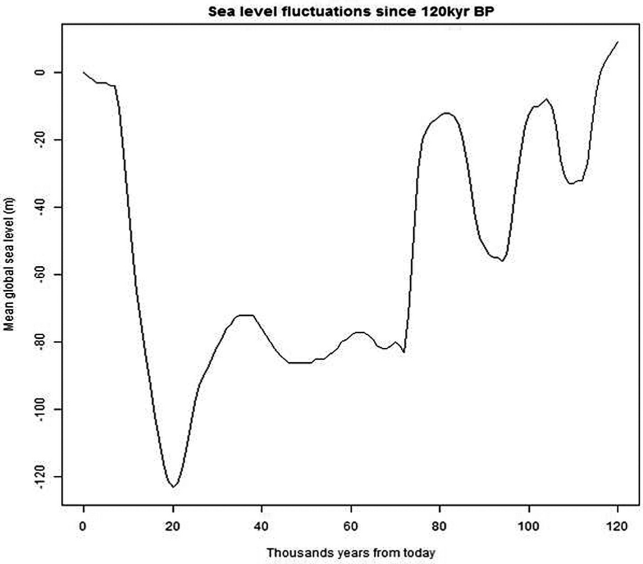

Figure 2. Sea level change reconstruction since 120 ka BP based on Camoin *et al.* (2004). Regions that are uncertain in Camoin *et al.* (2004) are here linearly interpolated.

extent, sea levels fell -120 to -130 m below present Mean Sea Level (MSL). Highest sea levels were reached during interglacials of up to +10 m MSL during the last interglacial. Based on radiometric dating of stalagmites in caves and corals that drowned and emerged during the last sea level cycle global sea level fluctuation since 120 kyr BP and especially since 10 kyr ago are reconstructed in detail (Fig. 2) (Cutler *et al.*, 2003; Zinke *et al.*, 2003; Camoin *et al.*, 2004). The last sea level cycle (Fig. 2) commenced 120 kyr ago with a relative short high stand during the pre–last interglacial lasting 10 kyr. During the subsequent glacial (120 to 70 kyr BP) sea levels fell and fluctuated between -20 and -60 m MSL. This period was followed by an extreme rapid fall of 10.6 (m/kyr) to -80 m MSL lasting 40 kyr followed by a further fall to -120 m MSL during the glacial maximum (40 to 16 kyr BP) (Cutler *et al.*, 2003). From ca. 19 kyr ago sea levels started to rise initially very rapidly 7 m/kyr until 7 kyr ago, when sea level rise decelerated to ca. 1 m/kyr. Global sea level stabilized and reached present levels ca. 2500 years ago (Zinke *et al.*, 2003; Camoin *et al.*, 2004). The last very rapid phase of sea level rise must have had major repercussions for terrestrial species on drowning islands. It is intriguing and biogeographically relevant to realize that current interglacial sea level at 0 m MSL is anomalously high for the Quaternary, and that ca. -60 m MSL is the mean for the last glacial interglacial cycle.

The rate and degree of surface change, drowning or emerging of islands depends on island morphometry and the shape of the sea level change curve. Depending on the morphometry of the drowned part of the islands the effect of sea level rise in size reduction and isolation can be more or less profound (Fig. 1, see below). Hence the effect of sea level change on volcanic islands differs among islands. In addition, for terrestrial species the connectivity between islands (and between island and mainland) decreases as a consequence of submerged topographical variability. Also seamounts currently submerged, when within a depth of 120 m were islands during the glacial forming important additional stepping stones (e.g. Warren *et al.*, 2010). Thus, both the marine and terrestrial biota of islands and archipelagos must have been affected by these changes (e.g. Ávila *et al.*, 2008; Fernández-Palacios *et al.*, 2011; Ávila, this volume).

In order to assess the effect of sea level induced change of islands on biota and biodiversity, and add the sea level history as an explaining variable to the GDM, we constructed a GIS (Geographical Information System) based algorithm that is able to reconstruct palaeo island sizes and island configurations and to derive quantitative metrics that can be used to investigate the role of sea level change on biota configurations (Rijsdijk *et al.*, submitted). Using merged digital elevation models of topography and bathymetry, volcanic island configuration change driven by sea level change is modelled over the last sea level cycle (120 kyr – present). We present here the sea-level driven change of island areas and archipelagos configuration during the last glaciation cycle for the Macaronesian biogeographic region (the North-East Atlantic volcanic archipelagos of Azores, Madeira, the Canaries and Cape Verde). We discuss some important biogeographical implications of those sea level changes and the potential to implement the model to extend the GDM.

MATERIAL AND METHODS

We developed a novel way of modelling palaeo island change and deriving geomorphometrical metrics using the Free and Open Source software for statistical computing R in combination with the OSGeo software FWTools and GIS (Rijsdijk *et al.*, submitted). The link between GIS and R operations is established via various R libraries (RSAGA, RODBC, rgdal) (Bivand *et al.*, 2008). SAGA GIS has been used for manipulation and calculations within spatial grids, while R is the central programming environment which stands on-top of the external GIS applications (Hengl, 2009). In the resulting model island size and archipelago configuration change are driven by one sea level cycle (from 120 kyr to present). In the following sections, it will be described how island metrics are calculated and which palaeo-island configuration maps are created with the algorithm.

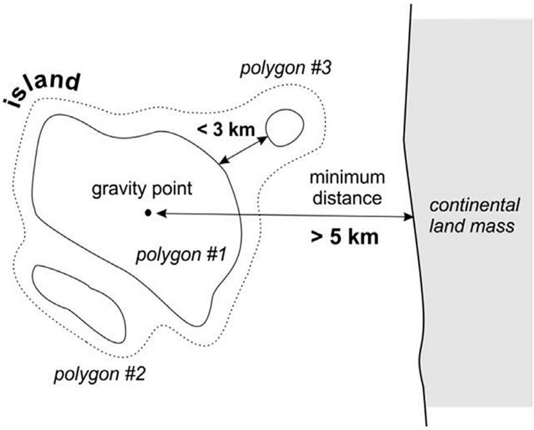

Figure 3. In order to model surface changes of islands it is crucial to employ a morphometric definition of an island that can be used in an algorithm. Here an island is considered a separate entity when (at current MSL) the area of its bounding box is larger than 3 km^2, and the distance of its gravity point to a continent is larger than 5 km and its minimum boundary distance to another island or continent is larger than 3 km (see Table 1 for a complete description of island classification).

TABLE 1. Criteria for defining polygons as separate islands (area and distance are measured at current MSL).

Classification	Area (km2) of polygon bounding box		Distance (km) to edge of other polygon		Species data
One polygon classified as separate island:	> 3	AND	>3 km	AND	Species data is gathered for separate polygon
Several polygons classified as largest island			< 3km (including 'stepping stones')	AND	Species data is gathered for polygons
Polygons are omitted	< 3	AND	> 3 km	OR	Species data is not available for polygon

Island definitions

The island administrative boundaries from the global administrative areas database (GADM, courtesy of Robert Hijmans and colleagues) were used to obtain present day island boundary polygons and derive present island surface areas for Macaronesian islands. Missing island boundaries were digitized manually from the high-resolution Ikonos images of Google Earth. In GIS terms, an island is defined as a collection of closed polygons representing land mass. To reduce computer calculation time, the minimum size for polygons to be included in the analysis as separate island was set to 3 km^2 (see Fig. 3 and Table 1 for the island classification rules). Reconstructed sizes are based on raster calculations with a cell size of 1 km^2. The resulting generalization error increases with island size decreasing, therefore areas of small islands (<10 km^2) are significantly overestimated, with the most extreme case representing an island of 1 km^2 of which the boundaries overlap with four grid cells.

Modelling palaeo-island extents

In order to derive the distances from oceanic islands to the nearest continents, we used the World Vector Shoreline dataset at scale 1:250,000 to construct a grid of closest distances from points (oceanic islands) to continents (Fig. 4, www.worldgrids.org). Distance to closest island as a grid was derived iteratively for each island using buffer distance operations in a Geographic Information System (GIS) software (SAGA GIS, System for Automated Geoscientific Analyses, http://www.saga-gis.org). In order to obtain the required metrics from palaeo-extents of islands we merged a terrestrial digital elevation model (DEM), based mainly on data from the Shuttle Radar Topography Mission (SRTM) with a detailed bathymetric model (Becker *et al.*, 2009), both on a 1 km^2 resolution. This merged topographic and bathymetric DEM model is used to calculate the palaeo-island extents at various sea level heights through R-algorithms and SAGA GIS (Bivand *et al.*, 2008; Hengl, 2009) (Fig. 5). The palaeo-BioIslands GIS (pBIG) model we developed produces maps of the palaeo-extent of islands and palaeo-configurations for selected time windows of the four archipelagos of Macaronesia. For all palaeo-configurations maps area created with buffer distances from each island to the nearest other islands and emerged seamounts within the same archipelago. Surfaces and configurations are calculated for each of the 120 time steps with intervals of 1 kyr. The resulting area and distance maps are used to construct island indices that reflect the change in island size and archipelago configuration. The pBIG model does not take into account the changes in shape of islands that may result by landslides or volcanic activity.

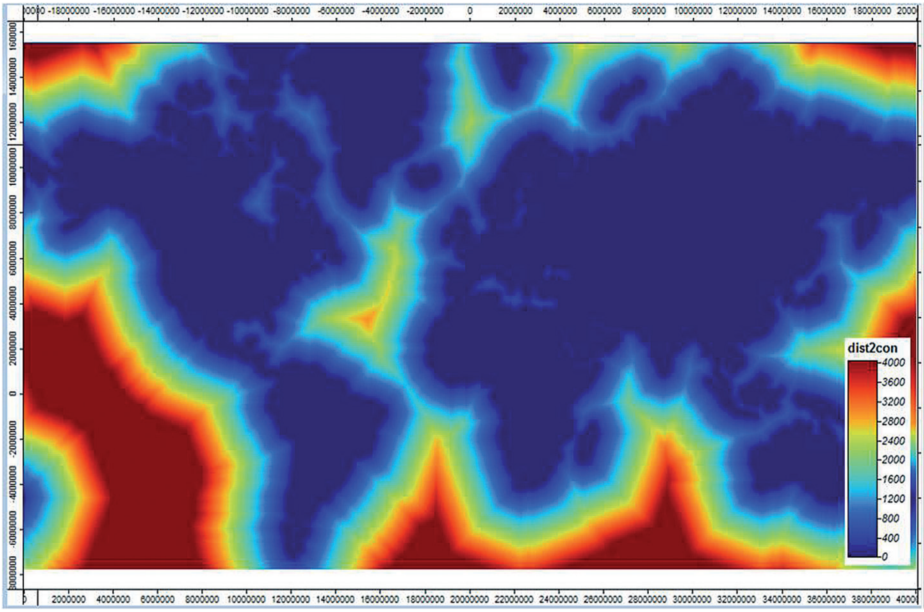

Figure 4. Distance to continents buffer grid (source: www.worldgrids.org).

In order to obtain the required metrics from palaeo-extents of islands we merged a terrestrial digital elevation model (DEM), based mainly on data from the Shuttle Radar Topography Mission (SRTM) with a detailed bathymetric model, both on a 1 km^2 resolution.

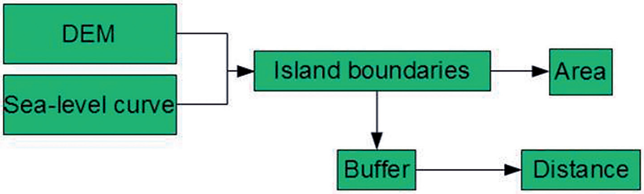

Figure 5. Flow diagram with processing steps for calculating distance and area. These steps are carried out for each island per 1 kyr during 120 kyr. In turn, the resulting area and distance maps are used to calculate island indices.

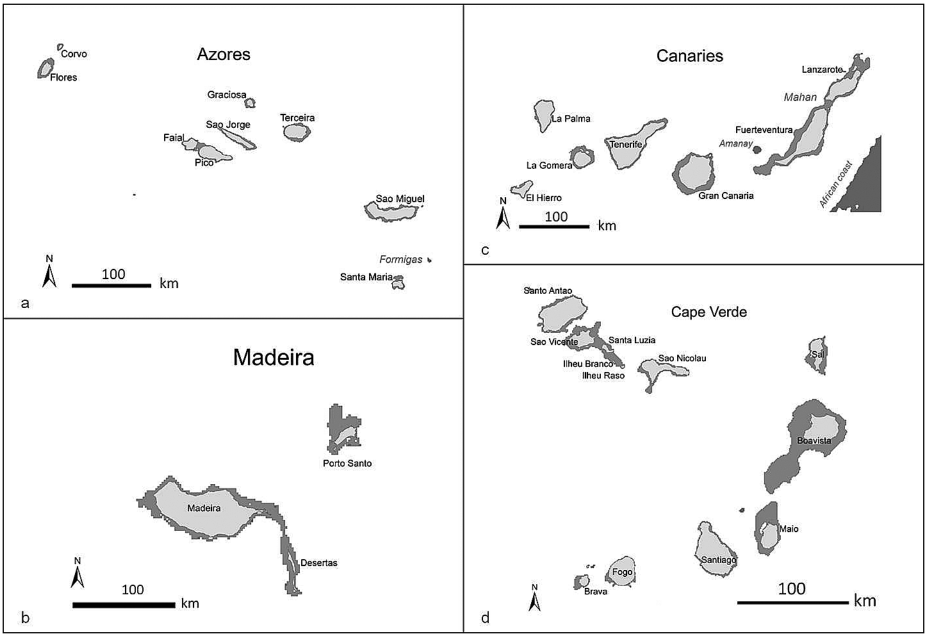

Figure 6. Surface change maps of a) Azores, b) Madeira, c) Canaries, and d) Cape Verde (Rijsdijk *et al.*, submitted). The light grey area represent the current island area, the dark grey shaded area reflects the maximum extensions of the islands during the glacial extreme low MSL stand 21 ka BP (-120 m below current level). Grey letters are names of palaeo-islands that emerged or were merged during the last glacial period. a) Azores, b) Madeira, c) Canaries, d) Cape Verde.

RESULTS

Morphometric results

Within these reconstructions we focus upon the effects on island geometry for the last 80 kyr and the Holocene sea level rise (see Fig. 2), because from this period onward islands expanded and shrunk in sizes maximally. From 80 kyr ago sea level dropped with the highest rates recorded of 10.6 m/ kyr to -80 m MSL. Then it remained stable for 40 kyr after it dropped another 40 m to -120 m MSL during the last glacial maximum (Cutler *et al.*, 2003). Then it rose very fast from 10 kyr ago at a rate of ca. 6 m/kyr to reach its present level at 0 m MSL ca. 2.5 kyr ago (Camoin *et al.*, 2004). The fast sea level rise from ca. 19 kyr ago led to abrupt separations of merged islands within several millennia and maximum shrinkage of areas.

Since the LGM most islands of the Azores shrunk between 20 and 50% during the Holocene sea level rise (Figs 6a and 7a). The islands of Faial (173 km^2)

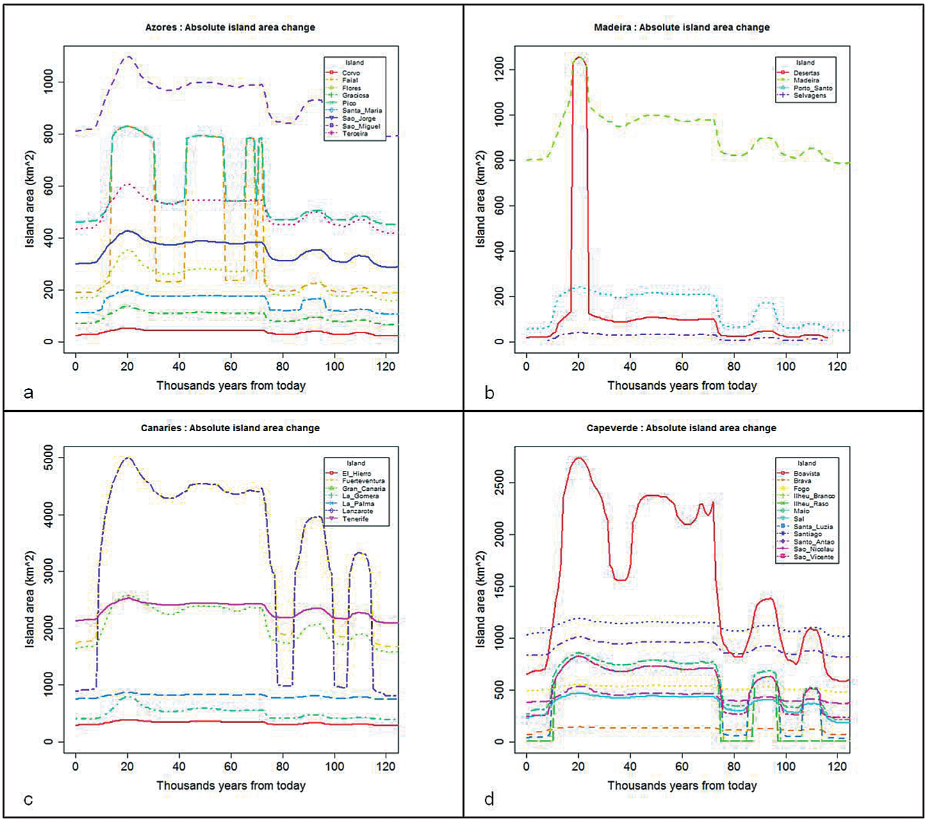

Figure 7. Absolute island area changes for Macaronesian islands since 120 kyr ago (Rijsdijk *et al.*, submitted).

and Pico (444 km^2) were merged for a period of ca. 16 kyr between 30 and 14 kyr ago to form Laurinsula (the name derives from Laurel forests which at that time covered the land), an island of circa 800 km^2. Also between 57 and 43 ka BP and 72 and 66 ka BP these islands were connected (except for a short interval around 70 ka BP). In addition the present-day Formigas islets, with a maximum height of only 14 m and an area of just 0.01 km^2, were during the LGM much larger (~40 km^2) and higher (130–140m) (Ávila, 2005).

Madeira (742 km^2) increased for more than 50% in size during the LGM reaching 1256 km^2 (Figs 6b and 7b). The main event here is the connection of Desertas (Ilheu de Chão, Deserta Grande and Bugio, comprising together 14 km^2) to Madeira during the LGM between 23 kyr and 18 kyr ago. However, within a single millennium, Desertas abruptly became separated from Madeira again, some 18 kyr ago. Between 72 and 13 ka BP, Porto Santo (today 43 km^2) was ca. five times larger than present (reaching 240 km^2 during the LGM).

The most significant event in the Canary Islands (Figs 6c and 7c), which happened between 77 and 9 ka BP during the LGM, was the merging of Fuerteventura (1677 km^2) and Lanzarote (850 km^2), as well the islets located North of Lanzarote (Alegranza, Montaña Clara and La Graciosa) or North of Fuerteventura (Isla de Lobos), into a single larger island, called today Mahan (García-Talavera, 1999), that was larger than 5000 km^2. North to the western tip of Mahan, some 15 km from its coast, a present-day seamount called Amanay was emerged during glaciation times, achieving in the LGM an area of ca. 200 km^2 and an altitude of ca. 100 m. The distance between Fuerteventura and Gran Canaria increased from 55 km during the LGM to 87 km at present. The distance from the African coast to Mahan was only 56 km during the LGM versus today's 96 km separating Fuerteventura and the Saharan coast. Finally, also noteworthy for this archipelago is that during the LGM, the island of La Gomera (373 km^2) was nearly twice its current size, whereas Gran Canaria (1574 km^2) was over 1.5 times larger than today.

Finally, the Cape Verde experienced the most radical size and configuration changes in the last glaciation cycle among the Macaronesian archipelagos (Figs 6d and 7d). Four windward islands (São Vicente, Santa Luzia, Ilhéu Branco and Ilhéu Raso) were merged to form a large island between 74 kyr and 13 kyr ago of up to 830 km^2 during the LGM. These merged islands approached Santo Antão for less than 5 km (currently 12 km). Most significantly the distance between island São Nicolau and Santo Antão, currently ca. 75 km, was in this period through the merged islands less than 5 km. The island Boa Vista (632 km^2) was on average 3.5 times larger than today between 72 and 14 kyr ago (maximum of ca. 2750 km^2 during LGM). During this period the island Maio (today 273 km^2) was more than 850 km^2, and the distance from Maio to Boa Vista was reduced to less than 7.5 km, compared to its present 77 km isolation.

DISCUSSION

Sea level curves and local variation

Due to various geological factors volcanic islands may sink or rise independent of global sea level change inducing a regional relative sea level rise or fall. It is therefore important to assess in how far these factors affected Macaronesian islands. When oceanic volcanoes become inactive they load the lithosphere which as a result may flex downward, leading to the sinking of the volcano (Whittaker *et al.*, 2008). On the other hand the loading of the lithosphere by newly formed volcanoes may induce uplift of older volcanoes that are situated on the same tectonic moat (Menéndez *et al.*, 2008). Other factors inducing uplift include for instance lithosphere flexure as a result of tectonic plate collision (Menéndez *et al.*, 2008), reheating of the lithosphere above hotspots (Crough, 1978), lithospheric flexing and bulging around the point of loading (Grig and Jones, 1997), and upwelling mantle plume dynamics (Davies, 1988; Morgan *et al.*, 1995; Ribe and Christensen, 1999). Recently Ramalho *et al.* (2010) relate the uplift of Cape Verdean islands to expanding laccoliths that formed underneath marine sediments and volcanic edifice. Menéndez *et al.* (2008) mention erosive removal of terrestrial sediments (large-scale landslides) may lead to a decrease in loading and result in vertical uplift of the lithosphere. Empirical data for Macaronesian archipelagos suggests these factors all have less than 10% effect on the last sea level cycle from 120 kyr to present. In the Canarias, raised Pliocene sea level markers such as pillow lavas indicate maximum mean uplift rates between 0.022 and 0.024 m/kyr (Meco *et al.*, 2002; Zazo *et al.*, 2003; Menéndez *et al.*, 2008). These local uplift rates are not significantly modifying the eustatic sea level rise curves for the last 120 kyr. Zazo *et al.* (2003) derive mean uplift rates from Marine Isotope Stage 5e highstands in the Canaries and Baleares ranging between +0.046 and -0.007 m/kyr, these rates amount at maximum to ca. 5 m height differences over 120 kyr and can be considered insignificant in affecting the palaeo insular shape change patterns presented here. A sequence of Middle Pleistocene (330 ka BP) to Holocene marine terraces on Sal island in the Cape Verdean archipelago ranges between +50 and +2 m MSL indicate a maximum uplift rate of 0.14 m/kyr, or 14 m/100 kyr (Zazo *et al.*, 2007; Ramalho *et al.*, 2010). If correctly dated and interpreted this may be significant affecting island shapes given the «sensitivity» to sea level change of the relatively low Cape Verdean islands (see Figs 6d and 7d). Other factors that lead to regional deviations of the global sea level curve is the global redistribution of melt water in the oceans leading to ocean water loading effects of the lithosphere and differential crustal flexing (Lambeck and Chappel, 2001; Milne and Mitrovica, 2008; see Gehrels and Long, 2008 for a review). The precise effects and amounts of vertical movement vary across the globe as a function of crustal rigidity, mantle rheology and water distribution. However effects that are recorded within the (sub-)tropical zone are generally in order of several meters during the last maximum sea level rise of 120 m suggesting the total contribution of this component is minor. A final effect is that melt water is not evenly distributed across the globe, but as a function of the dynamic interplay between the gravity pull of ice sheets and the ocean water mass. As the volume of water in the oceans increases due to polar ice sheet melting at the same time, the strength of the gravity pull from the ice sheet decreases. The overall effect is a regionally different response but overall resulting in faster sea-level rise in areas distal from the melting source (Milne and Mitrovica, 2008). While the archipelagos nearby the African continents seem rather insensitive to this effect, the Azores are located in the middle of the Atlantic Ocean, representing an area that was sensitive to these effects (>15 m differences during LGM) and consequently sea level reconstructions must be interpreted carefully. Although the individual effects of local factors modifying island shape-change may be limited during one sea level cycle (120 kyr), their combined effects may complicate sea level based reconstructions of palaeo-islands and hence local assessment of these combined effects on the global eustatic sea level curve is crucial for precise reconstructions of island area and archipelago configurations.

Biogeographic implications

The present island area, and related features, such as shape, altitude, isolation or geographic configuration of archipelagos represent transitory stages that result by two long-term dynamic processes, 1) the ontogenetic history of the volcanic islands themselves, lasting millions of years (Whittaker *et al.*, 2007; 2008), and 2) the incidence of the Pleistocene Glaciation cycles, lasting hundreds of millennia (Warren *et al.*, 2010; Fernández-Palacios *et al.*, 2011; Ávila, this volume; Rijsdijk *et al.*, submitted). It is therefore indispensable to take these processes into account for a correct interpretation of the biogeographical, ecological and evolutionary processes shaping present-day insular biotic assemblages, as well as their constituting species distributions and geographical affinities. As these processes progressively transform islands and archipelagos, these dynamically changing geographical conditions will create spatiotemporal dynamic biogeographical contexts, to which the species and ecosystems will have to adapt. The degree of emergence and submergence of volcanic islands due to sea level fluctuations will depend on their age or «ontogenic stage» (cf. Whittaker *et al.*, 2007; 2008). The older (>4 Myr) islands of archipelagos, which are in the mature or senile stages, are more sensitive to sea level changes than the younger and steeper islands. The older islands have generally more extensive submarine topography and marine platforms due to post volcanic subsidence, and longer periods of subaerial and marine erosion and reef building. Examples include Santa Maria in the Azores, Porto Santo in Madeira, Fuerteventura or Lanzarote in the Canaries, or Maio and Boa Vista in the Cape Verde. In contrast, the younger immature islands of the archipelagos are minimally affected by the sea level changes due to their steep submarine topography, for example, Corvo in Azores, El Hierro and La Palma in the Canaries or Fogo in Cape Verde.

As demonstrated, the volcanic archipelagos comprising Macaronesia constitute an outstanding example that illustrates how Quaternary sea level rise and retreat cycles can significantly alter the islands geographic characteristics that are controlling colonization processes, for instance, by decreasing significantly the inter-insular and island-mainland isolations in the Last Glaciation Maximum, or by merging different islands (Faial with Pico, Madeira with Desertas, Lanzarote with Fuerteventura and related islets or São Vicente, Santa Lucia, Branco and Raso) (Figs 6 and 7). Furthermore, the emergence and submergence of shallow seamounts with summits less than 120 m below present sea-level (e.g., Ormonde seamount, Gorringe Bank, Seine seamount, Dacia seamount, etc.), by acting as biological stepping stones must have repeatedly opened or locked dispersal routes within archipelagos, between archipelagos and between archipelagos and the mainland (Ávila and Malaquías, 2003; Fernández-Palacios *et al.*, 2011; Warren *et al.*, 2010).

Of course, sea level driven changes of islands and archipelagos were adjoined by significant changes in climate (temperature, precipitation, wind and marine currents regimes) on the islands (see Hooghiemstra *et al.*, this volume). As temperature increased during interglacial periods, islands contracted in size and previously merged islands became separated leading to inland and upward (to the cooler summits) migration of terrestrial species and ecosystems (see Hooghiemstra *et al.*, this volume). During glacials species migrated back towards the expanded coasts. Both climate change and sea level induced change led to a continuous biotic rearrangement of insular communities on the islands. In contrast to continents insular biota could not migrate to extensive hinterlands and were forced to endure these changes. This may have resulted into extinctions of single island endemics, local extirpations of species on some islands, or increase in resilience of insular species (Rijsdijk *et al.*, 2009; Hooghiemstra *et al.*, this volume). Furthermore, the expansion of the islands, doubling in sizes (Santa Maria, Azores or La Gomera, Canaries), by three times increases (Fuerteventura and Lanzarote, Canaries) or even more than three times increases (Formigas, Azores; Porto Santo, Madeira or Boa Vista, Cape Verde), must have created new opportunities for colonizers, but on the other hand also increased significantly the competition for space when the island shrunk during interglacials. Sea level driven island and archipelago changes did affect islands globally, consequently interpreting present insular species composition or population genetic traits in terms of present-day islands' or archipelagos' geographical features, i.e. considering area, carrying capacity, and isolation as static variables, may lead to erroneous interpretations. New island biogeographical theories must include the whole spectrum of spatiotemporal changes in area, carrying capacity and isolation and assess to what degree this affected biota in the past and how it will affect them in the future.

Further work

Further work will use a modified version of pBIG to assess with generalized linear models (GLM's) what role palaeo-island size/configurations may play in explaining biodiversity patterns on islands. pBIG will be modified with R algorithms that automatically analyses species data sets in relation to various abiotic explanatory variables including indices that are derived from palaeo-extents of islands and archipelagos. For this purpose data sets of insular species that have comparative dispersal traits should be collected. However, biodiversity data from volcanic islands covering most islands of an archipelago are scarce, or are at least poorly disclosed. A BioIslands.org data portal has been set-up to collect species data of islands supplied by experts. This allows building up data sets of various islands that allow for statistical assessments. A further objective is to network researchers and research organizations actively involved in insular biodiversity research and gather enough world data to develop more accurate (global) models of island biodiversity. We call upon colleagues to join this initiative and supply insular species data of volcanic island archipelagos (www.BioIslands.org, see below).

CONCLUSIONS

We have outlined a PalaeoGIS based methodology to reconstruct past island size changes and archipelago changes driven by sea level fluctuations. The method is successfully applied for four Macaronesian archipelagos (Azores, Madeira, the Canaries and Cape Verde) (Fig. 6) (Rijsdijk *et al.*, submitted). The results indicate that islands changed shape considerably during the last 120 kyr. Notably in the period between 80 kyr and 15 kyr ago, several islands now isolated were merged or were much larger than present. Ecologically and biogeographically the recent shrinking of islands due to the sea level rise since the last glacial maximum period (20 kyr) led in some cases to more than 50% reductions in island size, significant loss of coastal habitat and a significant increase in isolation by the increase of distances between islands and island continents. Every island and archipelago has its own specific morphometric change history as a function of its shape and the local sea level fluctuations. For instance, young volcanic islands characterized by steep conical submarine slopes (such as El Hierro or La Palma in The Canaries) have smaller area or shape changes compared to relatively flat old islands (such as Boa Vista in Cape Verde) that changed significantly their areas. In addition, the presence of submerged topography during sea level fall induced merging of isolated islands in a larger one, such as Lanzarote merged with Fuerteventura in the Canaries. The island size reduction must have induced pressures on the insular ecosystems, inducing upward migration and interspecies competition. The split of merged island must have led to separations of populations leading to gene flow losses for some biota. Critically the present day configurations, island sizes and isolation is not representative for the mean island configurations during the last Myr but rather represents an anomaly that only represents ca. 10% of the past Myr. Islands at present are smallest and most isolated and this configuration makes the insular biota even more vulnerable to human impact. The pBIG sea level algorithm we present here can be used to include past MSL as an explanatory variable for current biodiversity patterns on oceanic islands. We set up the BioIsland.org initiative to collect abundance data from insular species to statistically and qualitatively assess in what respect past sea level configurations must have affected biota, ecosystems and biodiversity.

ACKNOWLEDGEMENTS

We acknowledge valuable discussions with Robert Whittaker, Benn Warren, Henry Hooghiemstra, Kostas Triantis, Jens Zinke, Emiel van Loon and Christophe Thébaud. We thank DodoAlive for the funding of our Sea Level workshop held in 2010 in Oxford.

REFERENCES

Ávila, S.P. (2000) Shallow-water marine molluscs of the Azores: biogeographical relationships. Arquipélago. *Life and Marine Sciences*, Supplement 2 (Part A), 99–131.

Ávila, S.P. (2005) Processos e Padrões de Dispersão e Colonização nos Rissoidae (Mollusca: Gastropoda) dos Açores. PhD Thesis, Universidade dos Açores, Ponta Delgada.

Ávila, S.P. (this volume). Unravelling the patterns and processes of evolution of marine life in oceanic islands: a global framework. *Climate Change: past, present and future perspectives. A global synthesis from the Atlantic* (ed. by Fernández-Palacios, J.M., de Nascimento, L., Hernández, J.C., Clemente, S., Díaz, J.P. and González, A.), pp. 95–126. Servicio de Publicaciones, Universidad de La Laguna, (in press).

Ávila, S.P. and Malaquías, M.A.E. (2003) Biogeographical relationships of the molluscan fauna of the Ormonde seamount (Gorringe bank, Northeast-Atlantic Ocean). *Journal of Molluscan Studies*, 69, 145–150.

Ávila, S.P., Madeira, P., Marques da Silva, C., Cachão, M., Landau, B., Quartau, R. and de Frias Martins, A.M. (2008). Local disappearance of bivalves in the Azores during the last glaciation. *Journal of Quaternary Science*, 23, 777–785.

Becker, J.J., Sandwell, D.T., Smith, W.H.F., Braud, J., Binder, B., Depner, J., Fabre, D., Factor, J., Ingalls, S., Kim, S.-H., Ladner, R., Marks, K., Nelson, S., Pharaoh, A., Trimmer, R., Von Rosenberg, J., Wallace, G. and Weatherall, P. (2009) Global Bathymetry and Elevation Data at 30 Arc Seconds Resolution: SRTM30_PLUS, *Marine Geodesy*, 32, 355–371.

Bivand, R., Pebesma, E. and Rubio, V. (2008) *Applied Spatial Data Analysis with R*. Springer, Heidelberg.

Brown, J.H. and Lomolino, M.V. (2000) Concluding remarks: historical perspective and the future of island biogeography theory. *Global Ecology and Biogeography*, 9, 87–92.

Camoin, G., Montaggioni, L. and Braithwaite, C. (2004) Late glacial to post glacial sea levels in the Western Indian Ocean. *Marine Geology*, 206, 119–146.

Crough, S.T. (1978) Thermal origin of mid-plate hot-spot swells. *Geophysical Journal of the Royal Astronomical Society*, 55, 451–469.

Cutler, K.B., Edwards, R.L., Taylor, F.W., Cheng, H., Adkins, J., Gallup, C.D., Cutler, P.M., Burr, G.S. and Blomm, A.L. (2003) Rapid sea-level fall and deep-ocean temperature change since the last interglacial period. *Earth and Planetary Science Letters*, 206, 253–271.

DAVIES, G.F. (1988) Ocean bathymetry and mantle convection 1. Large-scale flow and hotspots. *Journal of Geophysical Research*, 93, 10467–10480.

FERNÁNDEZ-PALACIOS, J.M., DE NASCIMENTO, L., OTTO, R., DELGADO, J.D., GARCÍA-DEL-REY, E., ARÉVALO, J.R. and WHITTAKER, R.J. (2011) A reconstruction of Palaeo-Macaronesia, with particular reference to the long-term biogeography of the Atlantic island laurel forests. *Journal of Biogeography*, 38, 226–246.

GARCÍA-TALAVERA, F. (1999) Consideraciones geológicas, biogeográficas y paleoecológicas. *Ecología y cultura en Canarias* (ed. by Fernández-Palacios, J.M., Bacallado, J.J. and Belmonte, J.A.), pp. 39–63. Museo de la Ciencia y el Cosmos, Cabildo Insular de Tenerife, Santa Cruz de Tenerife.

GEHRELS, R. and LONG, A. (2008) Sea level is not level, *Geography*, 93, 11–16.

GRIGG, R. and JONES, A. (1997) Uplift caused by lithospheric flexure in the Hawaiian Archipelago as revealed by elevated coral deposits. *Marine Geology*, 141, 11–25.

HAYS, J.D., IMBRIE, J. and SHACKLETON, N.J. (1976) Variations in the Earth's Orbit: Pacemaker of the Ice Ages. *Science*, 194, 1121–1132.

HEANEY, L.R. (2000) Dynamic disequilibrium: a long-term, large-scale perspective on the equilibrium model of island biogeography. *Global Ecology and Biogeography*, 9, 59–74.

HEANEY, L.R. (2007) Is a new paradigm emerging for oceanic island biogeography? *Journal of Biogeography*, 34, 753–757.

HENGL, T. (2009) *A Practical Guide to Geostatistical Mapping*. University of Amsterdam, Amsterdam.

HOOGHIEMSTRA, H., RIJSDIJK, K., DE BOER, E., DE NASCIMENTO, L., FLORENS, F.B.V. and BAIDER, C. (this volume). Insular environmental change; climate-forced and system-driven. *Climate Change: past, present and future perspectives. A global synthesis from the Atlantic* (ed. by FERNÁNDEZ-PALACIOS, J.M., DE NASCIMENTO, L., HERNÁNDEZ, J.C., CLEMENTE, S., DÍAZ, J.P. and GONZÁLEZ, A.), pp. 51–74. Servicio de Publicaciones, Universidad de La Laguna, (in press).

IMBRIE, J. and IMBRIE, J.Z. (1980) Modeling the Climatic Response to Orbital Variations. *Science*, 207, 943–953.

LAMBECK, K. and CHAPPELL, J. (2001) Sea level change through the last glacial cycle. *Science*, 292, 679–686.

LISIECKI, L.E. and RAYMO, M.E. (2005) A Pliocene-Pleistocene stack of 57 globally distributed benthic $\delta^{18}O$ records. *Paleoceanography*, 20, 1–17.

MACARTHUR, R.H. and WILSON, E.O. (1963) An equilibrium theory of insular zoogeography. *Evolution*, 17, 373–387.

MACARTHUR, R.H. and WILSON, E.O. (1967) *The theory of island biogeography*. Princeton University Press, Princeton.

Meco, J., Guillou, H., Carracedo, J.-C., Lomoschitz, A., Ramos, A.-J.G. and Rodríguez-Yánez, J.-J. (2002) The maximum warmings of the Pleistocene world climate recorded in the Canary Islands. *Palaeogeography, Palaeoclimatology, Palaeoecology*, 185, 197–210.

Menéndez, I., Silva, P.G., Martín-Betancor, M., Pérez-Torrado, F.J., Guillou, H. and Scaillet, S. (2008) Fluvial dissection, isostatic uplift, and geomorphological evolution of volcanic islands (Gran Canaria, Canary Islands, Spain). *Geomorphology*, 102, 189–203.

Milne, G.A. and Mitrovica, J.X. (2008) Searching for eustasy in deglacial sea-level histories. *Quaternary Science Reviews*, 27, 2292–2302.

Morgan, J.P., Morgan, W.J. and Price, E. (1995) Hotspot melting generates both hotspot volcanism and a hotspot swell? *Journal of Geophysical Research*, 100, 8045–8062.

R Core Team (2012) *R: A Language and Environment for Statistical Computing*. R Foundation for Statistical Computing, Vienna, Austria.

Ramalho, R., Helffrich, G., Cosca, M., Vance, D., Hoffmann, D. and Schmidt, D.N. (2010) Episodic swell growth inferred from variable uplift of the Cape Verde hot spot islands. *Nature Geoscience*, 3, 774–777.

Ribe, N.M. and Christensen, U.R. (1999) The dynamical origin of Hawaiian volcanism. *Earth and Planetary Science Letters*, 171, 517–531.

Rijsdijk, K.F., Hume, J.P., Bunnik, F., Florens, F.B.V., Baider, C., Shapiro, B., van der Plicht, J., Janoo, A., Griffiths, O., van den Hoek Ostende, L.W., Cremer, H., Vernimmen, T., De Louw, P.G.B., Bholah, A., Saumtally, S., Porch, N., Haile, J., Buckley, M., Collins, M. and Gittenberger, E. (2009) Mid-Holocene vertebrate bone Concentration-Lagerstätte on oceanic island Mauritius provides a window into the ecosystem of the dodo (*Raphus cucullatus*), *Quaternary Science Reviews*, 28, 14–24.

Rijsdijk, K.F., Hengl, T., Nouda, S., Otto, R., Emerson, B.C., Ávila, S.P., López, H., van Loon, E.E., Tjørve, E. and Fernández-Palacios, J.M. (submitted) Quantifying surface area changes of volcanic islands driven by Pleistocene sea level cycles: Biogeographic implications for Macaronesian archipelagos, Atlantic Ocean. *Journal of Biogeography*.

Ruddiman, W.F. (2003) Orbital insolation, ice volume, and greenhouse gases. *Quaternary Science Reviews*, 22, 1597–1629.

Warren, B.H., Strasberg, D., Bruggemann, J.H., Prys-jones, RP. and Thébaud, C. (2010) Why does the biota of the Madagascar region have such a strong Asiatic flavor? *Cladistics*, 26, 526–538.

Whittaker, R.J., Willis, K.J. and Ladle, R.F. (2001) Scale and species richness: towards a general, hierarchical theory of species diversity. *Journal of Biogeography*, 28, 453–470.

Whittaker, R.J., Ladle, R.J., Araújo, M.B., Fernández-Palacios, J.M., Delgado, J.D. and Arévalo, J.R. (2007) The island immaturity speciation pulse model of island evolution: an alternative to the «diversity begets diversity» model. *Ecography*, 30, 321–327.

Whittaker, R.J., Triantis, K. and Ladle, R.J. (2008) A general dynamic theory of oceanic island biogeography. *Journal of Biogeography*, 35, 977–994.

Zazo, C., Goy, J.L., Dabrio, C.J., Bardají, T., Hillaire-Marcel, C., Ghaleb, B., González-Delgado, J.A. and Soler, V. (2003) Pleistocene raised marine terraces of the Spanish Mediterranean and Atlantic coasts: records of coastal uplift, sea-level highstands and climate changes. *Marine Geology*, 194, 103–133.

Zazo, C., Goy, J.L., Dabrio, C.J., Soler, V., Hillaire-Marcel, C., Ghaleb, B., González-Delgado, J.A., Bardají, T. and Cabero, A. (2007) Quaternary marine terraces on Sal Island (Cape Verde archipelago). *Quaternary Science Reviews*, 26, 876–893.

Zinke, J., Reijmer, J.J.G., Thomassin, B.A. and Dullo, W. (2003) Postglacial flooding history of Mayotte Lagoon (Comoro Archipelago, southwest Indian Ocean). *Marine Geology*, 194, 181–196.

HOLOCENE PALAEOCLIMATE AND PALAEOVEGETATION ON THE ISLANDS OF FLORES AND PICO

Simon E. Connor, Willem O. van der Knaap,
Jacqueline F.N. van Leeuwen, Petr Kuneš

CLIMATE CHANGE PERSPECTIVES FROM THE ATLANTIC:
PAST, PRESENT AND FUTURE
Jose María Fernández-Palacios, Lea de Nascimento, José Carlos Hernández,
Sabrina Clemente, Albano González & Juan P. Díaz-González (eds.)
Servicio de Publicaciones, Universidad de La Laguna – 2013

ISBN: 978-84-15910-54-1
pp. 149-162

ABSTRACT

Palaeoclimatic stability is regarded as an important factor in explaining patterns of endemism in the Azorean flora. However, modelling simulations and quantitative reconstructions for the last 6000 years suggest considerable palaeoclimatic variability. Here we explore the link between Holocene palaeoclimate and palaeovegetation on the islands of Flores and Pico. Modern pollen assemblages indicate that most major plant communities can be detected using pollen analysis and that, in some cases, the pre-colonisation vegetation was quite similar to present-day relict vegetation. A 200–500-year pollen record from Alagoinha, a low-elevation mire in western Flores, shows that *Juniperus brevifolia*-dominated communities were widespread at lower elevations prior to large-scale deforestation. Today these communities are generally restricted to higher elevations. While our results are preliminary, there appears to be a weak link between palaeovegetation (which was primarily influenced by volcanism, soil formation and human impact) and palaeoclimatic changes detected through geochemical proxies. Even if the Azorean palaeoclimate varied substantially, its impact on the pristine vegetation, at least in terms of pollen production, was relatively small.

KEYWORDS: Azores, Holocene, Macaronesia, palaeoclimate, palaeovegetation, Portugal.

INTRODUCTION

Globally, most archipelagos harbour a large number of single-island endemic species relative to the number of all-island endemics, but on the Azores the pattern for vascular plants seems quite different (Carine and Schaefer, 2010). Several theories have been developed to explain why Azorean endemic plants are few and widespread – a climatic stability hypothesis, which states that long-term stability in the climate of the Azores has limited diversification (Carine and Schaefer, 2010); a geographical hypothesis, which links low rates of single-island endemism to the youth, size and homogeneity of the Azores (Triantis *et al.*, 2011); and a cryptic diversity hypothesis, which proposes that the apparent lack of endemism is only «skin deep» and does not reflect real genetic diversity (Schaefer *et al.*, 2012).

Climatic modelling simulations suggest that the Azores were less climatically stable during the Holocene and Last Glacial Maximum than the Canary Islands and Madeira, archipelagos which harbour many single-island endemic plants (Triantis *et al.*, 2011). Palaeoclimatic reconstructions from geochemical proxies on the Azorean island of Pico provide a clear North Atlantic Oscillation (NAO) signal (Björck *et al.*, 2006). However, this NAO signal is not clearly detected in palynological data from the same sediment records and complementary pollen data from the island of Flores point to remarkable palaeovegetational stability (Carine *et al.*, 2012; Connor *et al.*, 2012b). There may be a weak link between climatic changes and vegetation changes on these islands, which could be one factor contributing to the lack of morphological diversification amongst Azorean endemic plants.

According to Dias (1996), historical reports from the Azores suggest that there was no vegetation zonation with respect to altitude. If this is true, there are two important implications: firstly, the lack of elevational zones means that Azorean native plant communities may not exhibit a clear response to changes in temperature, both now and in the past; and secondly, the current distribution of native plants in relation to altitude may be a consequence of human activities since European colonisation, rather than a reflection of bioclimatic factors. We gathered pollen data on the present and past vegetation of the Ilha das Flores to explore these issues.

MATERIALS AND METHODS

Surface samples were collected from 16 locations on the island of Flores to better interpret previous palaeoecological records from the highlands of Flores (Lagoa Rasa, 530 m above sea level) and Pico (Lagoa do Caveiro, 903 m a.s.l., and Pico Bog, 873 m a.s.l.; Björck *et al.*, 2006; Connor *et al.*, 2012b). Each sample was an agglomeration of moss subsamples gathered from a 1 m^2 area. Plant cover-abundance was measured in five 5 × 5 m quadrats, one at the sampling site and four others spaced 15 m in each direction from the sample.

To complement previous palaeoecological records from the highland sites, a sediment core was obtained from a low-elevation mire on the western side of Flores, Alagoinha (39°25'37"N, 31°14'30"W, approx. 270 m a.s.l.). The site is a *Cladium mariscus*-dominated mire at the base of a 200-m-high cliff, 1.3 km ESE of Fajãzinha township. *Persicaria hydropiperoides, Carex pendula* and *Equisetum telmateia* are prevalent around the margins. The mire is fed by cascades and surrounded by forests of the introduced Australian tree, *Pittosporum undulatum,* along with *Acacia melanoxylon, Cryptomeria japonica,* a few relict patches of Laurisilva (*Laurus azorica*-dominated forest) and *Festuca* communities on the cliffs. The invasive *Hedychium gardneranum* dominates the understory. The slopes below the site are abandoned agricultural terraces that have been overgrown by *Pittosporum.*

The sediment core was collected from the centre of the mire in June 2012 using a square-rod piston corer (Wright, 1967). Cores were extruded, sectioned, wrapped in plastic film and stored in a refrigerator. Sediment samples of 1 cm^3 and bulk samples of surface moss were treated with 10% HCl, 10% KOH, 48% HF and acetolysis to isolate the pollen and spores (Moore *et al.*, 1991) and mounted in glycerol for identification at 400× magnification. A minimum of 200 (average

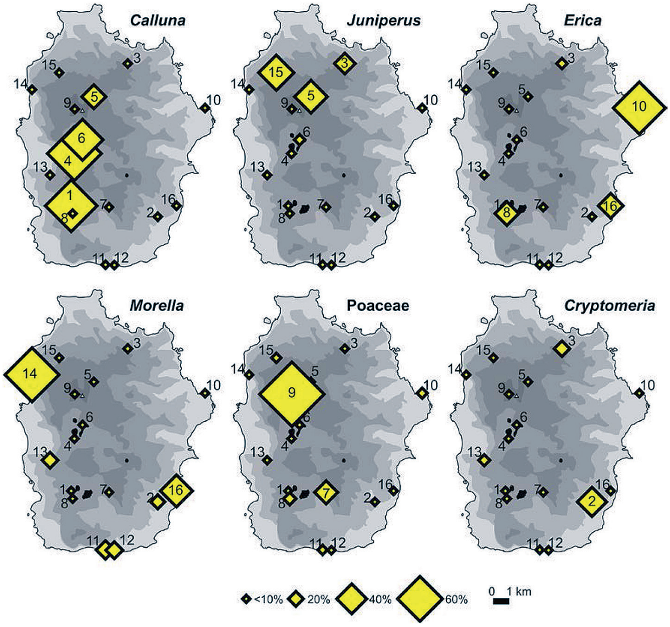

Figure 1. Locations of surface sediment samples on the island of Flores, Azores, with symbols scaled to represent the quantity of major pollen types in each sample.

1100) terrestrial pollen and spores were identified in each sample. Taxonomy follows Silva *et al.* (2010) and Connor *et al.* (2012b).

The new pollen data were combined with earlier data from Flores and Pico (Connor *et al.*, 2012b) and analysed using Detrended Correspondence Analysis and hierarchical clustering (Ward's method) with PC-Ord software (McCune and Mefford, 1999).

A single radiocarbon date was obtained from the sediment core at a depth of 493–497 cm. Age determination was made on plant macrofossils, which were isolated from the sediment by filtering over a tea strainer and then hand sorted using a dissecting microscope. Several *Erica* seeds, two *Juniperus* scales, an unidentified flower and some twigs were dated using Accelerator Mass Spectrometry (AMS).

RESULTS

Modern pollen assemblages on the island of Flores clearly reflect the local vegetation at each of the sampling points (Fig. 1). Samples from the extensive peatbogs of the central plateau have a prevalence of *Calluna vulgaris* pollen; areas

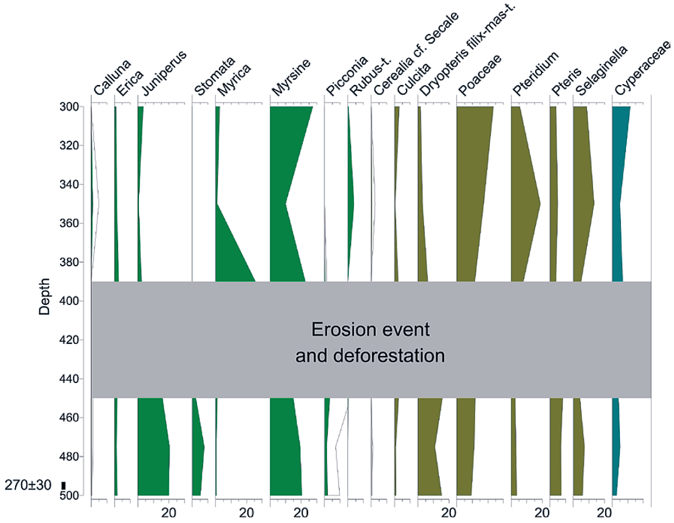

Figure 2. Preliminary pollen diagram from Alagoinha, Flores.

of relict *Juniperus brevifolia* forest have high *Juniperus* values; *Erica azorica* pollen is dominant in some coastal and heavily grazed areas; *Morella* is most abundant at low elevations; Poaceae prevails in the higher elevation grasslands; *Cryptomeria* pollen reflects proximity to plantations; and *Picconia* and *Pittosporum* exhibit high percentages where the trees are dominant in the surrounding vegetation. *Calluna, Erica* and *Juniperus* are well represented palynologically, whereas *Morella* tends to be over-represented and *Ilex* tends to be under-represented in pollen assemblages compared to the surrounding vegetation (Connor *et al.*, 2012a).

Coring at Alagoinha penetrated to a depth of 5 m. The uppermost 3 m of sediment was unconsolidated organic material and was not recovered. From 3–4 m, the sediment consisted of clayey gyttja mixed with varying quantities of volcanic sand and gravel. A layer of eroded material (mostly scoria) was encountered between 4–4.5 m. From 4.5–5 m, the sediment consisted of organic gyttja with black sand and abundant diatoms. The core terminated in impenetrable gravel at 5 m. The single AMS date from 493–497 cm (Beta-330609) yielded a radiocarbon age of 270±30 before 1950 AD (BP). This corresponds to calendar years between 1515–1598 AD (44% probability at 2σ), 1617–1678 (49%) and 1782–1797 (6%), thus post-dating the Flemish colonisation of Flores in 1472 AD.

Results of preliminary pollen analysis of the Alagoinha core are shown in Fig. 2. Pollen assemblages in the lower section of the core, prior to the erosion event, are dominated by *Juniperus* and *Myrsine*. Poaceae and *Dryopteris* *filix-mas*-type are also relatively abundant. The presence of *Datura* pollen confirms that *D. stramonium* was an early introduction to the flora (Schaefer, 2003). Following the erosion event, *Morella (Myrica)* exhibits a large peak and *Juniperus* declines. *Pteridium* is more abundant after the erosion event, whereas *Picconia* and *Solidago*-type are less frequent. These preliminary observations suggest that *Juniperus brevifolia*-dominated vegetation prevailed around Alagoinha during the 14th–15th centuries, prior to more recent deforestation. A moss sample (AZ13) collected from the margins of the mire contained large amounts of *Pittosporum* (51%), *Morella* (21%) and *Cryptomeria* (15%) pollen, reflecting the present-day vegetation of the area, with the notable exception of *Laurus azorica*. Two moss samples from under a large *Laurus azorica* tree near Alagoinha were processed with and without acetolysis, showing that *Laurus azorica* pollen does not survive this treatment (as in most Lauraceae: van der Merwe *et al.*, 1990). Even when acetolysis is avoided, *Laurus azorica* appears to be a poor pollen producer, assemblages under this tree having less than 10% *Laurus azorica* pollen and much greater amounts of *Morella* (~40%), *Pittosporum* (~20%) and *Cryptomeria* (~15%).

The DCA result is very similar to the previous result for Pico Bog, Lagoa do Caveiro and Lagoa Rasa (Connor *et al.*, 2012b), with the first axis interpreted as a moisture-availability gradient and the second axis as a forest-cover gradient (Fig. 3). Pollen taxa most correlated with the ordination axes are given in Table 1. Surface samples from the most intact forest stands (e.g. AZ04, AZ05 and AZ06) are found in the top right of the ordination plot near the pre-colonisation samples from Lagoa Rasa. Samples from partly deforested, but still intact, areas in the northern part of the island (i.e. AZ03 and AZ15) have similar pollen composition to early post-colonisation samples from Lagoa Rasa and Alagoinha. Samples from forest areas in the dry SE part of Flores (AZ02 and AZ12) appear to be similar to post-colonisation samples from the island of Pico. However, the majority of the surface samples cluster in the lower right of the ordination plot with the most recent samples from Pico Bog and Alagoinha. The Alagoinha record exhibits the same temporal trend seen in all pollen records from Pico and Flores – toward higher moisture availability and lower forest cover (see Connor *et al.*, 2012b). These trends have no clear relationship to palaeoclimatic oscillations reconstructed using other proxies (Fig. 4).

Ward's minimum-variance clustering produced comparable results to the DCA, clearly displaying the affinity of modern *Juniperus brevifolia* forests with the pre-colonisation vegetation surrounding Lagoa Rasa and Lagoa do Caveiro (group B, Fig. 3). The three *Calluna*-dominated samples are separated from the remaining samples (group F, Fig. 3). Lagoa do Caveiro samples associated with volcanic eruptions form a distinct group (E), as do pre-colonisation samples from Pico Bog (D) and post-colonisation samples from Lagoa Rasa (A). The remaining samples, including those from Alagoinha, form a large group (C), indicative of the post-colonisation vegetation.

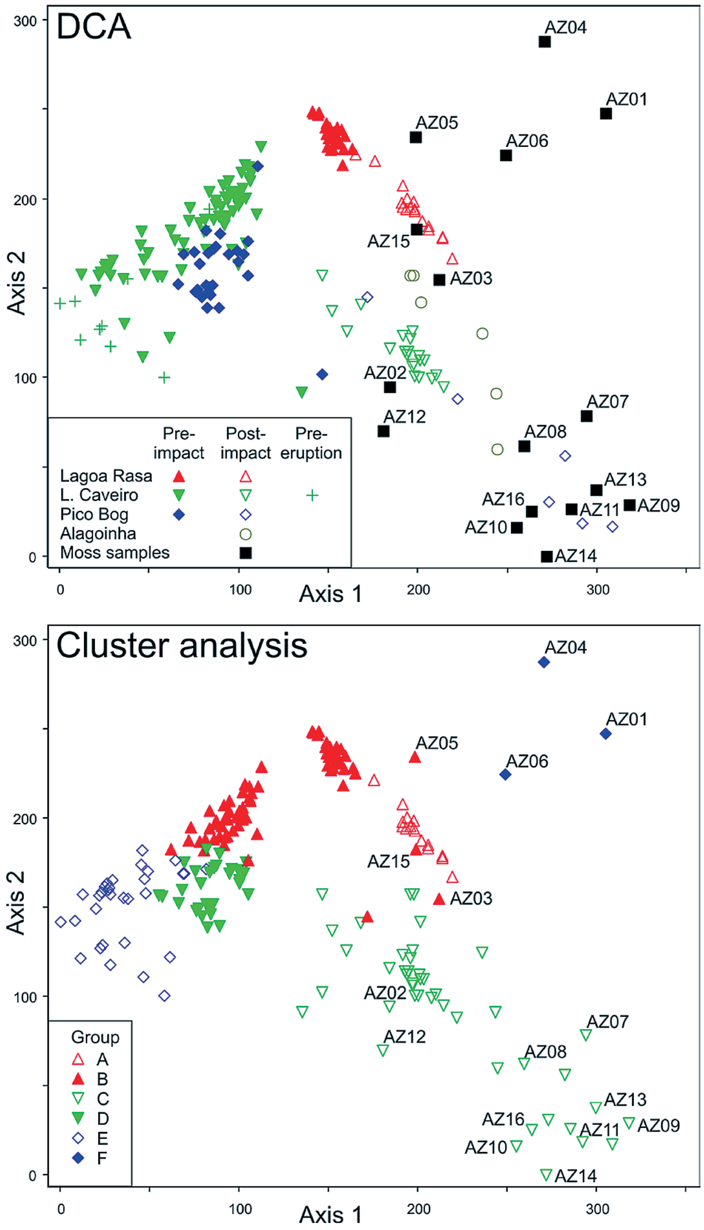

Figure 3. Detrended Correspondence Analysis (DCA) result for the surface samples and pollen records from Alagoinha, Lagoa Rasa (Flores), Lagoa do Caveiro and Pico Bog (Pico). Cluster analysis results are shown below in the same ordination space. Taxa most correlated with the ordination axes are given in Table 1.

TABLE 1. Pollen taxa most correlated with the first two DCA axes and their correlation coefficients (*r*). The first axis explains 39% of variance and the second 25%. Abbreviations: *O. azoric.* – *Ophioglossum azoricum; O. lusitan.* – *Ophioglossum lusitanicum; P. coronop.* – *Plantago coronopus; P. lanceol.* – *Plantago lanceolata*-type; *R. cortusif.* – *Ranunculus cortusifolius*-type.

DCA axis 1				DCA axis 2			
Positive	r	Negative	r	Positive	r	Negative	r
Poaceae	0.63	*Angelica*	-0.78	*Juniperus*	0.78	*Morella*	-0.60
Pteridium	0.53	Cichorioideae	-0.72	*Osmunda*	0.44	*Pteridium*	-0.59
Morella	0.45	*R. cortusif.*	-0.65	*O. lusitan.*	0.41	Poaceae	-0.56
Myrsine	0.41	*Ilex*	-0.61	*Viburnum*	0.38	*Hydrocotyle*	-0.47
Potentilla	0.39	*Bellis*	-0.53	*Myrsine*	0.37	*Erica*	-0.47
Hydrocotyle	0.39	*Euphorbia*	-0.51	*Umbillicus*	0.35	*P. coronop.*	-0.41
P. coronop.	0.37	*Huperzia*	-0.40	*Frangula*	0.33	*Lysimachia*	-0.33
Viburnum	0.34	Apiaceae	-0.39	*O. azoric.*	0.30	*Pinus*	-0.29
P. lanceol.	0.33	*Selaginella*	-0.33	*Culcita*	0.26	*P. lanceol.*	-0.28
Trichomanes	0.31	*Culcita*	-0.29	*Betula*	0.24	*Selaginella*	-0.27

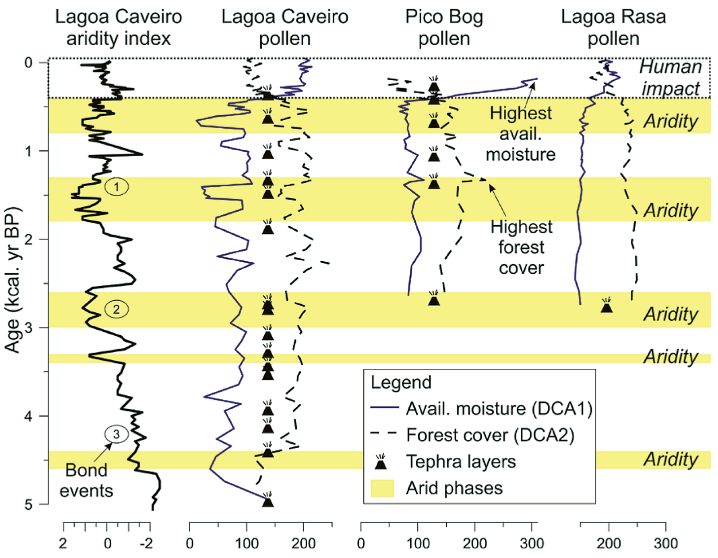

Figure 4. Comparison of ordination results from Azorean pollen records (Fig. 3) with the palaeoclimatic aridity index from Lagoa do Caveiro, Pico Island (from Björck *et al.*, 2006).

DISCUSSION

Modern pollen assemblages are a useful tools for interpreting past vegetation changes recorded in fossil pollen. On the island of Flores, our data suggest that the vegetation around Lagoa Rasa prior to European colonisation was very similar to today's extensive *Juniperus brevifolia* forests to the N and NW of Morro Alto, the highest mountain on Flores. This area therefore appears to preserve a truly relict vegetation type and its protection status should be carefully maintained.

Colonisation of the islands in the 15th century led to changes in vegetation structure and composition, particularly clearance of juniper forests and the spread of *Sphagnum* mosses (Connor *et al.*, 2012b). The Alagoinha record indicates that *Juniperus brevifolia*-dominated communities extended to relatively low elevations on Flores in the early period of colonisation. There is a possibility that the streams that flow into Alagoinha carried some pollen down from higher altitudes, though the presence of well preserved macrofossils and stomata suggest that *Juniperus brevifolia* trees were present locally (see Birks and Birks, 2000). Indigenous trees that are widespread in lowland and coastal areas today, such as *Morella faya* and *Picconia azorica*, are also poorly represented in the early part of the Alagoinha pollen record. This leads us to the conclusion that *Juniperus brevifolia* forests, which today are mainly preserved in the highest parts of Flores, were the prevailing vegetation type over a much larger area of the island in the past, possibly extending down to the coast in some places (compare Fig. 41a in Schaefer, 2003). Human activities since colonisation, such as deforestation and grazing, have led to the expansion of *Morella faya*, which was historically less favoured for timber than *Juniperus* and can survive on degraded soils because of its nitrogen-fixing capacity. It must be emphasised that juniper's wide elevational amplitude in the past may only apply to the island of Flores, which is the wettest island of the Azores Archipelago.

The mild, wet climate of the Azores is thought to have been an important factor in limiting both endemism and altitudinal zonation (Carine and Schaefer, 2010; Schirone *et al.*, 2010). Most endemic plants occur over the entire elevational range of the archipelago, with few endemic or native species occupying particular altitudinal zones (Schaefer, 2003). The lack of altitudinal zonation in Azorean indigenous vegetation means that past changes in temperature are unlikely to leave a strong signal in pollen records. Precipitation changes may register in palaeoecological records from the Azores, although in some records it is difficult to distinguish real palaeovegetation changes from taphonomic alterations caused by lake-level changes and volcanism (e.g. Lagoa do Caveiro: Connor *et al.*, 2012b).

Triantis *et al.* (2011) used palaeoclimatic modelling results to challenge Carine and Schaefer's (2010) assertion that the Late Quaternary climate of the Azores was far more stable than on the Canary Islands. A recent pollen study from a high elevation crater on La Gomera, Canary Islands, demonstrates that mid-Holocene precipitation changes had a significant impact on the palaeovegetation, causing a steep decline in hygrophilous taxa (Nogué *et al.*, 2013). The change coincides with the end of the African Humid Period (deMenocal *et al.*, 2000) and a phase of dune instability and aridification in the eastern Canary Islands around 5500 cal. years BP (Ortiz *et al.*, 2006). In the midlands of Tenerife, however, the palaeovegetation appears to have remained quite stable from approx. 5000 years ago until the arrival of humans (de Nascimento *et al.*, 2009). Hence vegetation response to climatic changes on the Canaries may be altitude-dependent. On the Azores, palaeovegetation stability is also observed in the Lagoa Rasa pollen record from Flores prior to human arrival (Connor *et al.*, 2012b). Holocene pollen records from high elevations on Pico are more changeable, largely due to the frequent occurrence of volcanic eruptions and lake-level changes on this island (Björck *et al.*, 2006). As yet there is no clear evidence for climate-induced palaeovegetation change from the Azores during the Holocene; volcanic eruptions, soil formation and human impacts being the most important factors (Connor *et al.*, 2012b).

The available pollen data lend support to the Azorean climatic stability hypothesis put forward by several authors (Avila *et al.*, 2008; Carine and Schaefer, 2010; Schirone *et al.*, 2010; Carine *et al.*, 2012). Even if the Azorean palaeoclimate was generally more variable than that of the Canary Islands (Triantis *et al.*, 2011), its impact on the vegetation, as gauged through pollen production, was minor. We wonder if high levels of cryptic endemism in the Azorean flora (Schaefer *et al.*, 2011) are related to the broad altitudinal range of most endemic plants. The combination of low morphological diversity and high molecular diversity amongst endemic plants could stem from adaptation to non-climatic factors, such as competition, periodic disturbances, soil texture, geological age and nutrient availability.

Pollen analysis is unlikely to shed much light on this question due to taxonomic constraints at the species level (Birks and Birks, 2000). However, it can reconstruct distribution patterns for many Azorean plant species before human colonisation and thereby determine the original altitudinal range of Azorean plants. More detailed studies, from a variety of islands and altitudes, are required to fully explore the link between Azorean palaeoclimate and palaeovegetation.

CONCLUSIONS

Modern pollen data from the Azores show that the major vegetation types are clearly represented in pollen assemblages, the exception being vegetation dominated by *Laurus azorica*. Fossil data from Alagoinha show that forests of *Juniperus brevifolia*, which today occur mainly at higher elevations on Flores, extended to much lower elevations in the early period of colonisation. Our results add support to the idea that Azorean vegetation was not arranged in strict altitudinal zones prior to human arrival. The implication of this is that Holocene vegetation changes on Flores are likely to be predominantly a reflection of non-climatic factors. More data from various islands and settings are required to confirm this hypothesis for the Azores generally.

ACKNOWLEDGEMENTS

Thanks to João Araújo (University of the Algarve) for preparing samples from Alagoinha.

REFERENCES

Ávila, S.P.A., Madeira, P., Mendes, N., Rebelo, A., Medeiros, A., Gomes, C., García-Talavera, F., Silva, C.M., Cachão, M., Hilaire-Marcel, C. and Martins, A.M.F. (2008) Mass extinctions in the Azores during the last glaciation: fact or myth? *Journal of Biogeography*, 35, 1123–1129.

Birks, H.H. and Birks, H.J.B. (2000) Future uses of pollen analysis must include plant macrofossils. *Journal of Biogeography*, 27, 31–35.

Björck, S., Rittenour, T., Rosén, P., França, Z., Möller, P., Snowball, I., Wastegård, S., Bennike, O. and Kromer, B. (2006) A Holocene lacustrine record in the central North Atlantic: proxies for volcanic activity, short-term NAO mode variability, and long-term precipitation changes. *Quaternary Science Reviews*, 25, 9–32.

Carine, M.A. and Schaefer, H. (2010) The Azores diversity enigma: why are there so few Azorean endemic flowering plants and why are they so widespread? *Journal of Biogeography*, 37, 77–89.

Carine, M.A., Jones, K., Moura, M., Maciel, M.G.B., Rumsey, F.J. and Schaefer, H. (2012) Putting biogeography's cart back behind taxonomy's horse: a response to Triantis *et al. Journal of Biogeography*, 39, 1184–1187.

Connor, S.E., van der Knaap, W.O. and van Leeuwen, J.F.N. (2012a) A pollen's-eye view of Azorean vegetation – some insights from Flores. *FloraMac2012 Scientific Program, Abstract Book and Excursion Guide* (ed. by Menezes de Sequeira, M.), p. 93. Grafimadeira, Funchal.

Connor, S.E., van Leeuwen, J.F.N., Rittenour, T.M., van der Knaap, W.O., Ammann, B. and Björck, S. (2012b) The ecological impact of oceanic island colonisation – a palaeoecological perspective from the Azores. *Journal of Biogeography*, 39, 1007–1023.

deMenocal, P.B., Ortiz, J., Guilderson, T., Adkins, J., Sarnthein, M., Baker, L. and Yarusinski, M. (2000) Abrupt onset and termination of the African Humid Period: rapid climate response to gradual insolation forcing. *Quaternary Science Reviews*, 19, 347–361.

de Nascimento, L., Willis, K.J., Fernández-Palacios, J.M., Criado, C. and Whittaker, R.J. (2009) The long-term ecology of the lost forests of La Laguna, Tenerife (Canary Islands). *Journal of Biogeography*, 36, 499–514.

Dias, E. (1996) *Vegetação natural dos Açores: ecologia e sintaxonomia das florestas naturais.* Unpublished PhD Thesis, Universidade dos Açores, Angra de Heroismo.

McCune, B. and Mefford, M.J. (1999) *PC-ORD: Multivariate Analysis of Ecological Data*. MjM Software Design, Gleneden Beach, Oregon.

Moore, P.D., Webb, J.A., and Collinson, M.E. (1991) *Pollen Analysis.* Blackwell Science Publishers, Oxford.

Nogué, S., de Nascimento, L., Fernández-Palacios, J.M., Whittaker, R.J. and Willis, K.J. (2013) The ancient relict forests of La Gomera, Canary Islands, and their sensitivity to human and climate change. *Journal of Ecology*, 101, 368–377.

Ortiz, J.E., Torres, T., Yanes, Y., Castillo, C., de la Nuez, J., Ibáñez, M. and Alonso, M.R. (2006) Climatic cycles inferred from the aminostratigraphy and aminochronology of Quaternary dunes and palaeosols from the eastern islands of the Canary archipleago. *Journal of Quaternary Science*, 21, 287–306.

Schaefer, H. (2003) Chorology and diversity of the Azorean flora. *Dissertationes Botanicae*, 374, 1–130.

Schaefer, H., Moura, M., Maciel, M.G.B., Silva, L., Rumsey, F.J. and Carine, M. (2011) The Linnean shortfall in oceanic island biogeography: a case study in the Azores. *Journal of Biogeography*, 38, 1345–1355.

Schirone, B., Ferreira, R.C., Vessela, F., Schirone, A., Piredda, R. and Simeone, M.C. (2010) Taxus baccata in the Azores: a relict form at risk of imminent extinction. *Biodiversity and Conservation*, 19, 1547–1565.

Silva, L., Moura, M., Schaefer, H., Rumsey, F. and Dias, E.F. (2010) Vascular plants (Tracheobionta). *A list of the terrestrial and marine biota from the Azores* (ed. by Borges, P.A.V., Costa, A., Cunha, R., Gabriel, R., Gonçalves, V., Martins, A.F., Melo, I., Parente, M., Raposeiro, P., Rodrigues, P., Santos, R.S., Silva, L., Vieira, P. and Vieira, V.), pp. 117–146. Princípia, Cascais.

Triantis, K.A., Hortal, J., Amorim, I., Cardoso, P., Santos, A.M.C., Gabriel, R. and Borges, P.A.V. (2011) Resolving the Azorean knot: a response to Carine and Schaefer (2010). *Journal of Biogeography*, 39, 1179–1184.

Van der Merwe, J.J.M., van Wyk, A.E. and Kok, P.D.F. (1990) Pollen types in the Lauraceae. *Grana*, 29, 185–196.

Wright, H.E. (1967) A square-rod piston sampler for lake sediments. *Journal of Sedimentary Petrology*, 37, 975–976.

THE ROLE OF CAPE VERDE AND THE CANARY ISLANDS IN THE ATLANTIC-MEDITERRANEAN MOLLUSCAN MIGRATIONS (INTERGLACIAL STAGES)

Ana Cabero, Caridad Zazo, José Á. González-Delgado,
José L. Goy, Cristino J. Dabrio, Javier Lario, Teresa Bardají,
Claude Hillaire-Marcel, Bassam Ghaleb

CLIMATE CHANGE PERSPECTIVES FROM THE ATLANTIC:
PAST, PRESENT AND FUTURE
Jose María Fernández-Palacios, Lea de Nascimento, José Carlos Hernández,
Sabrina Clemente, Albano González & Juan P. Díaz-González (eds.)
Servicio de Publicaciones, Universidad de La Laguna – 2013

ISBN: 978-84-15910-54-1
pp. 163-189

ABSTRACT

A comparative study of the climatic signals recorded in the Last Interglacial (~135–117 ka) coastal deposits from Sal Island (Cape Verde Archipelago), the Canary Islands and S-SE Iberian Peninsula is presented in this work, with particular attention paid to the fossil mollusc content. Palaeontological analyses are supported by previous geomorphological, stratigraphical and petrographical field data, including detailed mapping of marine and terrestrial deposits. Data are compared with previous works to reconstruct the coastal environments and climatic conditions during this time-period. Modern species distribution is compared with the fossil content in order to: 1) define those species that could be considered as warm-water proxies in the past; 2) describe the distribution of these species during the Last Interglacial in the Atlantic-Mediterranean linkage area; 3) interpret the oceanographic conditions that controlled the distribution and expansion of these molluscs during this time-period. A checklist of 52 warm-water species for the Canary and Mediterranean area is presented. In the Cape Verde archipelago and NW African coasts, more data related to the last and previous interglacial stages are necessary to confirm the palaeoclimatic and oceanographic interpretations.

KEYWORDS: climatic changes, Pleistocene, Last Interglacial, Senegalese fauna.

INTRODUCTION

The geomorphological and palaeontological analyses of coastal zones provide much data about past sea level and climatic changes, as well as about tectonic and coastal environmental evolution during the Quaternary. The evaluation of the consequences of temperature rise and sea level variations must be supported by data from different geographical settings, where repeated changes have been recorded. Climatic conditions during the Last Interglacial (MIS 5 – Marine Isotopic Stage 5 –, ~135–75 ka) were characterized both by higher temperatures and a higher sea level than today. Preservation of MIS 5 deposits above the present sea level has allowed their analyses and study in numerous locations around the world. However, the sea level (height, duration, timing and number of highstands) as well as the climatic and oceanographic coastal conditions during this time-span, is still being debated. This discussion extends beyond the peak of the Last Interglacial (substage 5e) to the remaining substages (MIS 5c and 5a). Data from the Mediterranean realm suggest that this area is more sensitive to climatic and sea level variability than the Spanish Atlantic coast, particularly in the case of rapid and abrupt changes (Martrat *et al.*, 2004; Zazo *et al.*, 2013). The characteristics of the Mediterranean basin may favour the amplification and recording of small-scale sea level and climate variations. In order to discern the global and regional components of sea level and climatic changes in the Mediterranean, an approximately N-S transect analyses is needed. Therefore, studies carried out in the Canary and Cape Verde Islands play an important role in distinguishing natural regional changes from those established by global models on sea-level, climate and faunal changes occurred during Quaternary interglacials.

The Last Interglacial coastal deposits in the Mediterranean-Atlantic linkage area are characterized by the presence of warm-water molluscs. The most characteristic species of this warm fauna (so called Senegalese fauna) is *Strombus latus* (Gmelin, 1791), with its fossil specimens being commonly cited as *Strombus bubonius* (Lamarck, 1822). This species has also been cited as *Lentigo latus* (Galili *et al.*, 2007) and *Persististrombus latus* (De Torres *et al.*, 2010) taking into account recent taxonomic revisions (Galili *et al.*, 2007; De Torres *et al.*, 2010 see references herein). *S. latus* and other warm species entered the Mediterranean during different Quaternary interglacial periods (at least during MIS 7 and MIS 5, Zazo *et al.*, 2003; De Torres *et al.*, 2010). Some of these warm species also appeared in the Macaronesian islands during the Last Interglacial (Lecointre, 1965; García-Talavera *et al.,* 1978; Avila *et al.*, 2002; Zazo *et al.*, 2003; 2007; 2010; Meco *et al.*, 2006; among others), whereas most of them were absent along the north-western African coast of Morocco, Sahara Occidental and Mauritania (Lecointre, 1965; Brébion, 1979; Weisrock *et al.*, 1999; among others). Assuming that the Cape Verde Archipelago and Gulf of Guinea coasts acted as source areas for the Senegalese fauna during MIS 5, its presence or absence along the transect from Cape Verde to western Mediterranean may yield information about the oceanographic conditions that controlled these migrations and the expansion into the Mediterranean during recent interglacial periods. Present day sea surface temperature (SST) and salinity (SSS) of the Cape Verde and West African tropical waters, along with the ecology of some characteristic species, provide useful information for the reconstruction of the palaeoenvironment and regional climatic and oceanographic variations.

PHYSIOGRAPHICAL AND GEOLOGICAL SETTING

The surface currents of the North Atlantic Subtropical Gyre (Fig. 1), the position of the Azores High Pressure Centre and the Intertropical Convergence Zone (ITCZ) control the climate of the Mediterranean-Atlantic linkage area. The Azores High and the ITCZ present a seasonal behaviour marked by a northerly position during spring-summer and southerly one during autumn-winter. Moreover, the Canary Islands, Cape Verde Archipelago and the whole northwestern coast of Africa are highly influenced by trade winds. Permanent and seasonal upwelling

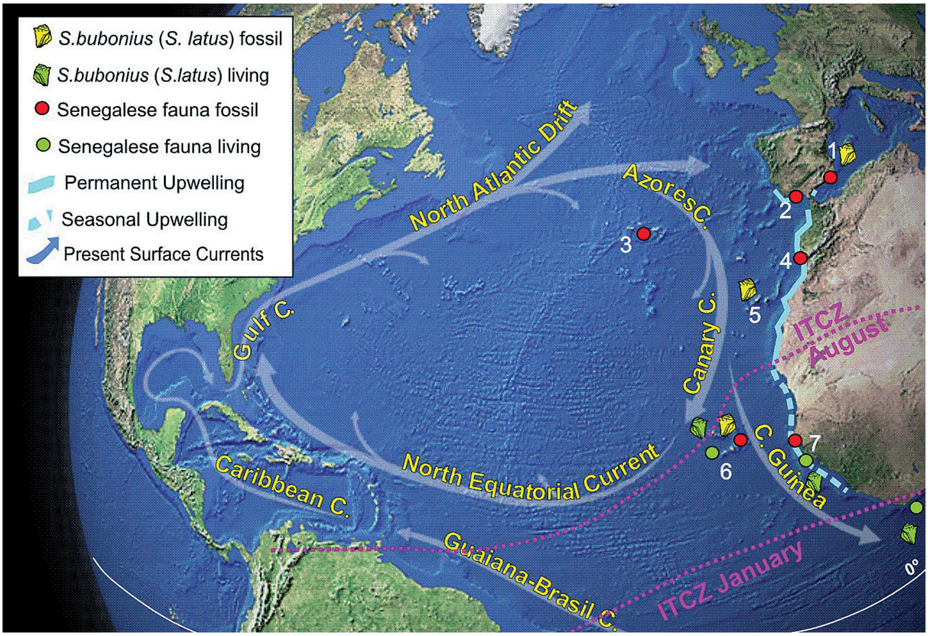

Figure 1. Present pattern of the main superficial currents forming the North Atlantic Subtropical Gyre and distribution (present and fossil) of the warm-water Senegalese fauna with indication of the presence/absence of *Persististrombus latus* (Syn: *Strombus bubonius*). Numbers: study sites cited on this work, (1) Western Mediterranean area, (2) Gulf of Cadiz, (3) Azores, (4) Morocco, (5) Canary Islands, (6) Cape Verde (Sal Island), (7) Dakar (Senegal).

along northwest African and southern Portuguese coasts extends to the South (African coast) and East (Iberian coasts) during winter under the influence of increased trade and westerly winds, respectively (Figs. 1 and 2).

The geological framework is dominated by the northward movement of the African plate in the case of the Iberian coasts, and by the volcanic and tectonic activity (hot-spot volcanism) in the case of the Canary and Cape Verde Islands.

METHODOLOGY: REVISION OF THE SENEGALESE FAUNA

This study presents a comparison of the palaeontological content and the sea-level changes recorded along the S-SE Iberian peninsular coasts, in the Canary Islands and Cape Verde Archipelago during the Last Interglacial. Comparison of climatic and sea level events in different areas is based on previous

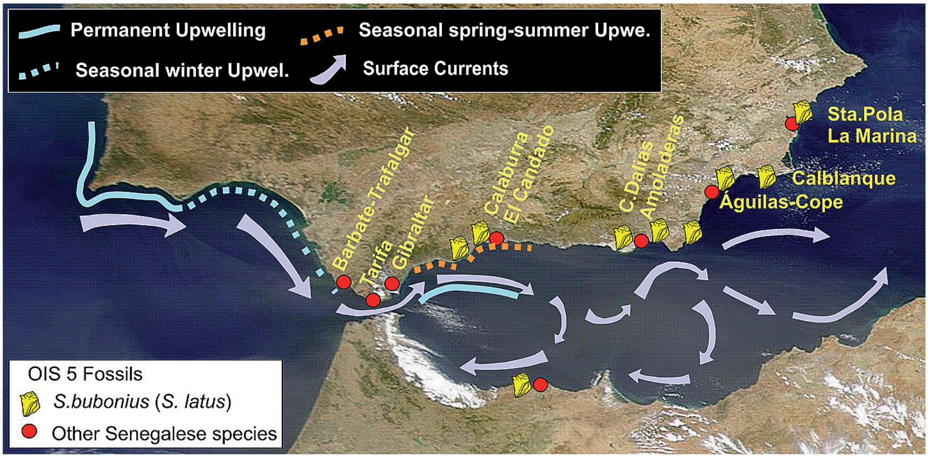

Figure 2. Present pattern of the main superficial currents at the Atlantic-Mediterranean linkage area, and distribution of *Strombus bubonius* (*S. latus*) and other Senegalese species.

chronological, geomorphological and tectonic analyses of the coastal record. All these previous studies have selected the best preserved and complete coastal sequences to be compared. Consequently, the paleontological comparison and climatic discussions in this work have been possible due to the numerous previous studies already carried out on the S-SE Iberian coasts (Goy *et al.*, 1993; 2006; Hillaire-Marcel *et al.*, 1996; Zazo *et al.*, 2003; 2005; 2008b; Bardají *et al.*, 2009; Cabero, 2009; among others), Canary Islands (Zazo *et al.*, 2002; 2008a; Meco *et al.*, 2006, among others), and Sal Island in Cape Verde Archipelago (Zazo *et al.*, 2007; 2010). In this study, we present new paleontological data (Cabero, 2009) from the western Mediterranean (Alicante, SE Spain), Fuerteventura (Canary Islands) and Sal Island (Cape Verde Archipelago) to compare with the MIS 5 faunal content described by other authors in deposits from the western Mediterranean, north-western Africa, Azores, Canary Islands and Cape Verde Archipelagos (Lecointre, 1965; Cuerda, 1987; Avila *et al.*, 2002; Zazo *et al.*, 2003; 2007; 2010; Meco *et al.*, 2006). The objective of this paleontological review is to define in each area the species that could be considered as tropical warm-water proxies in the past (Senegalese fauna *sensu stricto* – *s.s.*). The analyzed coastal deposits correspond to shoreface, foreshore and backshore environments, so the fossil record of these Last Interglacial beach deposits may provide information about coastal changes that occurred within the first few meters of the water column.

The first references of the Senegalese fauna in the Mediterranean are from Gignoux (1911) and Issel (1914), and since then this term has been used to refer to the presence of *S. latus* and a variety of species associated with it, particularly

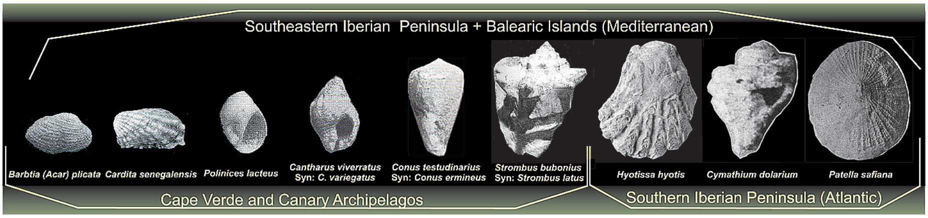

Figure 3. Common thermophilic species (Senegalese species *s.l.*) present in the S-SE Iberian Peninsula, Balearic Islands, Canary Islands and Cape Verde.

in the western Mediterranean (Fig. 3). Nevertheless, the consideration of some of these species as warm-water proxies changes when you move to the Macaronesian region, where some of these species currently inhabit. In addition, some of these warm-water species have appeared repeatedly in different Mediterranean areas since Plio–Pleistocene, having a different biogeographical and palaeoenvironmental significance depending on the author (Cuerda, 1987; Bellomo, 1998; Garilli, 2011). Some of these Senegalese species have been considered thermophilic species of different nature and significance, thus a review of the real, tropical warm water species is required. Selection of the Senegalese species *s.s.* has been made taking into account that: 1) they currently inhabit the Gulf of Guinea and/or the Cape Verde Archipelago, and 2) they are not present today on the coasts where they flourished during the Late Pleistocene. The results of this palaeontological review are presented in Table 1, where a total of 52 Senegalese taxa *s.s.* (38 gastropods and 14 bivalves) were identified. The current distribution and nomenclature of the species from the Gulf of Guinea and Cape Verde Archipelago was studied taking into account the Mollusc databases CLEMAN (Check List of European Marine Mollusca), WoRMS (World Register of Marine Species), and ERMS (European Register of Marine Species, Costello *et al.*, 2008), the West African Mollusc collection of the Muséum National d'Histoire Naturelle (Paris) along with Poppe and Goto (1991; 2000); Abbot and Dance (2000) and Rolán (2005). Some of the Plio–Pleistocene species cited in Italy (Bellomo, 1998) are extinct, with no current similar species, so they have not been included in these check-list, however they could be included in the future (see Discussion).

THE LAST INTERGLACIAL ALONG S-SE IBERIAN COASTS: CHARACTERISTICS AND PALEONTOLOGICAL UPDATE

Marine deposits of the Last Interglacial are well preserved along the S-SE peninsular Spanish coasts, with a higher topographic position around the Gibraltar Strait due to the tectonic uplift of the area (Zazo *et al.*, 1999; 2003). On the SE

TABLE 1. Species selected as Senegalese fauna s.s.
Abbreviations and symbols*

Species	Also cited as	Fossil presence during OIS 5 (Ref.)
Gastropoda		
Acteocina knockeri (E.A. Smith 1871)		Alicante (11,12), Italy (16)
Acteon bovetensis (Sequenza)		Italy (16)
Angiola lineata (Da Costa 1778)	*Planaxis lineatus* (Da Costa) *Planaxis herrmanseni* Dunker 1853	Canary I. (GC,T, LZ, FV) (1,5,27), Cape Verde (23,27)
Bursa pustulosa Reeve 1844	*Bursa corrugata pustulosa* Reeve *Bursa corrugata*	Italy (16), Morocco (19), Senegal (21), Cape Verde (23)
Cantharus viverratus (Kiener 1834)	*Cantharus variegatus* Gray *Pisania variegata* (Gray)	Canary I. (GC, T, FV) (1,4,7), Balearic I. (10), Alicante (11,12), Málaga (13), Italy (16), Sardinia (17,18), Morocco (19, 20), Senegal (21), Cape Verde (22,25,26*,27), Azores (SM) (28,29,31)
Cerithium atratum (Born 1778)		Canary I. (GC, LZ) (1,5), Mauritania, Cape Verde (23,25,26*)
Clavatula rubrifasciata (Reeve 1845)		Morocco (20,9)
Clavatula sacerdos (Reeve 1845)		Canary I. (GC) (1)
Conus ambiguus Reeve 1844	*Conus tabidus* (4)	Italy (16), Cape Verde (23), Azores (SM) (31)
Conus cf. miruchae Röckel, Rolán & Monteiro, 1980		Azores (SM) (31)
Conus cf. roeckeli Rolán 1980		Azores (SM) (28,31)
Conus ermineus Born 1778	*Conus testudinarius* Martini 1773	Canary I. (GC, T, LZ, FV) (1,2, 5,7,27), Balearic I. (10), Alicante (11), Italy (16), Sardinia (17,18), Senegal (21), Sahara, Cape Verde (23,25,26*), Azores (SM) (28,29,31)
Conus venulatus Hwass in Bruguière 1792		Azores (SM) (28,31), Cape Verde* (26*)
Cymatium trigonum (Gmelin 1791)	*Cymatium ficoides* (Reeve) *Triton ficoides*	Canary I. (GC, T, FV) (1,4,7), Alicante (11), Italy (16), Cape Verde (25,26*,27)
Favartia burnayi Houart 1981	*Favartia celullosa* (Conrad 1846)	Canary I. (T) (5)
Harpa doris Röding 1798	*Harpa rosea* Lamarck 1816	Canary I. (GC, LZ, FV) (1,2), Senegal (21), Cape Verde (22,25,26*,27)
Hexaplex rosarium (Röding 1798)	*Murex saxatilis* Linné 1758 (36,33)	Italy (16), Canary I. (GC) (1)
Hipponix antiquatus (Linné 1767)		Canary I. (LZ) (5), Cape Verde (25,26*,27)
Imbricaria carbonacea (Hinds 1844)	*Mitra carbonacea* Hinds 1844 (33)	Italy (16)
Kleinella gruveli (Dautzenberg 1910)		Canary I. (GC) (1)
Marginella cincta Kiener 1834		Canary I. (GC) (5)
Mitra nigra (Gmelin 1791)		Canary I. (GC, FV) (1,7), Cape Verde (25), Salvagem I. (32)
Mitra scrobiculata Brocchi	*Cancilla scrobiculata?*	Italy (16)
Morula nodulosa (C.B. Adams 1845)	*Trachypollia nodulosa* *Drupa nodulosa*	Canary I. (T, FV) (5,7), Senegal (21), Cape Verde* (23,26*), Azores (SM) (28,31)
Nassarius wolffi (Knudsen 1956)	*Nassa wolffi* Knudsen 1956	Italy (16)
Natica acynonyx Marche-Marchad 1957		Italy (16)
Natica turtoni E.A. Smith 1890	*Naticarius turtoni*	Balearic I. (10), Italy (16)
Polinices lacteus (Guilding 1834)	*Naticina lactea* Guilding 1834 *Natica lactea*	Canary I. (GC, T) (1,2,4,5), Balearic I. (10), Alicante (11), Italy (16), Sardinia (17,18), Senegal (21), Cape Verde (25), Azores (SM) (28,29,31)

Pusionella nifat (Brugière 1789)	*Buccinum nifat* Brugière 1789 *Clavatula nifat*	Italy (16)
Sinum concavum (Lamarck 1822)		Italy (16)
Strombus Latus Gmelin 1791	*Strombus bubonius* Lamarck 1822 *Lentigo latus* Gmelin 1791 (38) *Persististrombus latus* Gmelin 1791 (40)	Canary I. (GC, T, FV, LZ) (1,2,3,4,6,8), Balearic I. (10), Alicante (11), Málaga (13, 15), Italy (16), Sardinia (17,18), (and other Mediterranean zones, 14), Cape Verde (22,23,25,24,26*,27)
Terebra corrugata Lamarck 1822	*Terebra acuminata* Borson (16)	Italy (16), Cape Verde* (26*)
Thais nodosa (Linné 1758)	*Thais coronata* Lamarck 1816 *Purpura neritoides*	Canary I. (LZ) (5), Senegal (21), Cape Verde (22,23,25,26* 27)
Trachypollia suga (Gmelin)	*Ocinebrina suga?*	Canary I. (T) (5)
Trachypollia turricula (Von Maltzan 1884)		Italy (16)
Zonaria petitiana (Crasse)		Italy (16)
Zonaria picta (Gray 1824)	*Cypraea picta* Gray 1824	Azores (SM) (28,31), Cape Verde (23,25,26*)
Zonaria zonata (Chemnitz 1788)	Zonaria zonaria Gmelin 1791 Cypraea zonaria Gmelin 1791	Canary I. (GC) (1), Senegal (21), Cape Verde* (26*)
BIVALVIA		
Anadara geissei (Dunker 1891)		Balearic I. (10), Alicante (11,12), Italy (16)
Arcopsis afra (Gmelin 1791)	*Arca afra* Gmelin (16) *Striarca afra* (16)	Italy (16), Canary I. (T)(4), Cape Verde (25)
Atactodea glabrata (Philippi 1791)	*Mactra glabrata* (Philippi 1791) *M. largillierti* (16)	Italy (16)
Barbatia (Acar) plicata (Chemnitz 1870)	*Barbatia (Acar) plicata* (Dillwyn, 1817)	Canary I. (GC, FV) (1,27), Balearic I.(10), Alicante (11), Sardinia (17,18), Cape Verde* (26*,27)
Basterotia clancula Von Cosel 1995		Italy (16), Azores (SM) (31)
Brachidontes senegalensis (Lamarck 1819)	*Mytilus senegalensis* *Brachyodontes puniceus* (Gmelin 1788)	Canary I. (GC, T, FV) (1,4,7), Balearic I. (10), Alicante (11), Italy (16), Sardinia (17,18), Senegal (21), Cape Verde (25,27)
Cardita senegalensis Reeve 1843	*Cardita calyculata senegalensis* (Reeve, 1843)	Canary I. (GC) (1), Balearic I. (10), Italy (16), Sardinia (17,18), Senegal (21), Cape Verde* (26*)
Corbula revoluta Brocchi	*Corbula cadenati* (16)	Italy (16)
Chama crenulata Lamarck 1819		Canary I. (GC) (1)
Hyotissa hyotis (Linné 1758)	*Lopha hyotis* (Linné 1767) *Hyotissa mcgintyi* (16)	Canary I.(GC) (1), Balearic I. (10), Alicante (11), Italy (16), Sardinia (17,18), Cape Verde* (26*,27)
Lutraria senegalensis Gray 1837		Italy (16)
Megaxinus appendiculatus (Locard 1898)	*Loripes smithii* (16) *Megaxinus smithii* (Sequenza)	Italy (16)
Tugonia anatina (Gmelin 1791)		Italy (16)
Venerupis dura (Gmelin 1791)	*Tapes dura* (Gmelin) *Paphia dura* (16)	Italy (16)

[*] Canary Islands: LZ: Lanzarote; GC: Gran Canaria; FV: Fuerteventura; T: Tenerife; (*): fossil presence cited without age specifications. References: (1)- Meco *et al.* (2006) ;(2)- Meco *et al.* (2003); (3)- Meco (1977); (4)- García-Talavera *et al.* (1978); (5)- García-Talavera (1983); (6)- García-Talavera (1990a); (7)- Gacía-Talavera *et al.*- Carta paleontológica de Fuerteventura; (8)- Zazo *et al.* (2002); (9)- Brébion *et al.* (1986); (10)-Cuerda (1987); (11)-Cuerda and Sanjaume (1978); (12)- Cuerda (1995); (13)- Zazo *et al.* (1999); (14)- Zazo *et al.* (2003); (15)- Vera-Peláez *et al.* (2004); (16)- Bellomo (1998); (17)- Spano (1980); (18)- Spano *et al.* (2005); (19)- Brébion (1979); (20)- Weisrock *et al.* (1999); (21)- Lecointre (1965); (22)- Lecointre (1962); (23) -García-Talavera and Bacallado (1981); (24)- Zazo *et al.* (2007); (25)- García-Talavera (1999); (26*)-Mitchell-Thomé (1976); (27)- This work (28)- García-Talavera (1990b); (29)- Callapez and Ferreira Soares (2000); (30)- Poppe and Goto (1991, 2000); (31)- Avila *et al.* (2008); (32)- García-Talavera and Sánchez-Pinto (2002); (33)- Rolan (2005); (34)- Kendrick *et al.* (1991); (35)- Segers (2002); (36)- Abbott and Dance (2000); (37)- von Cosel (2006); (38)- Galili *et al.* (2007); (39) – Meco *et al.* (2008). (40) De Torres *et al.* 2010

Spanish coasts, three different highstands have been described for MIS 5e (Zazo *et al.*, 2003; Bardají *et al.*, 2009) the second of which, being worldwide, is considered the most stable one (~130–120 ka). Millennial, century and decade-long patterns of sea-level oscillations have also been found in the second highstand, suggesting a contribution of relatively rapid ice sheet melting and subsequent slower ice build-up (Dabrio *et al.*, 2011).

The Senegalese fauna *s.s.* is mainly present on the SE peninsular coasts and Balearic Islands, but species linked to warm conditions are also present along the southern Mediterranean coasts (Figs. 2 and 3, Table 1). Another important characteristic of the Mediterranean MIS 5 deposits is the development of oolitic beaches and dunes at the beginning (first highstand) of MIS 5e (Goy *et al.*, 1993; Zazo *et al.*, 2003; Bardají *et al.*, 2009) (Fig. 4). The presence of oolites (small spherical grains of calcium carbonate, formed by concentric lamellae) is related to shallow environments with persistent tidal or wind movement of the water, carbonate supply to the coast, and high evaporation (warm temperatures) that promote $CaCO_3$ water saturation and, hence, oolite precipitation (Bardají *et al.*, 2009 and references therein). The final part of MIS 5e and the subsequent substages (MIS 5c and 5a) are characterized by a sudden change in sedimentary style, related to the global climatic deterioration that followed the peak of the Last Interglacial. On Spain's Peninsular Mediterranean coasts, oolitic dune–beach systems are replaced either by siliciclastic dune beach systems or by reddish clayey conglomerates (Fig. 4). Senegalese species are still present in these facies (although with less diversity and abundance) (Cuerda, 1987; Bardají *et al.*, 2009). These reddish facies suggest an important meteorological change marked firstly by an increase in runoff that removed former red soils, and secondly by an increase in storminess that eroded and rounded the boulders embedded in the red matrix (Zazo *et al.*, 2003; Bardají *et al.*, 2009). The main characteristics of the MIS 5e deposits, facies, and paleontological content are presented in the Fig. 5.

This review of the Last Interglacial paleontological content on this area, including other Western Mediterranean references (see sites and references in Table 1) allowed us to define at least 39 Senegalese species *s.s.* (14 bivalves and 25 gastropods). Most of these species also appear in the Last Interglacial deposits of the Canary, Azores, and Sal (Cape Verde) Islands; however six species should not be considered as Senegalese *s.s.* in the Canary or Azores Islands because they currently inhabit there (see Table 2). These species are: the gastropods *Bursa pustulosa*, *Cantharus viverratus*, *Natica turtoni* and *Polinices lacteus*, and the bivalve *Megaxinus appendiculatus* for the Canary Islands; and the bivalve *Basterotia clancula* for the Azores.

The absence from the list of some gastropod species cited previously as thermophilic and/or Senegalese (*Bursa scrobiculator*, *Cabestana dolaria*, *Patella ferruginea*, and *Vermetus semisurrectus*, see Cabero, 2009 for more details) is because they have currently been found living in the Mediterranean, despite being scarce and appearing on deeper sea bottoms than during Last Interglacial. Given this dis-

Figure 4. Examples of Senegalese species bearing present and Last Interglacial beaches. 1) Detail of *S. bubonius* (*S. latus*) bearing oolitic beach facies (La Marina, Alicante; from Goy *et al.*, 2006); 2) detail of the reddish facies from the final part of OIS 5e with *S. bubonius* (*S. latus*) (Aguilas, Murcia) from Bardají *et al.*, 2009; 3) detail of *S. bubonius* (*S. latus*)-bearing beach facies (Matas Blancas, Fuerteventura); 4) present day beach with *S. bubonius* (*S. latus*) at Sal Island (Cape Verde).

tribution, some authors consider them as species with high palaeoenvironmental interest and thermophilic meaning (Spano, 1980; Cuerda, 1987, among others).

THE LAST INTERGLACIAL IN THE CANARY ISLANDS AND CAPE VERDE ARCHIPELAGO: CHARACTERISTICS AND PALAEONTOLOGICAL UPDATE

Quaternary deposits in both archipelagos are influenced by the tecto-volcanic activity over time. The age and distribution of the islands are controlled by the hot-spot activity and the African plate movement that lead to the presence of older islands to the east (Fuerteventura, Lanzarote and Gran Canaria in the case

TABLE 2: Senegalese species selected for the Canary Islands and Western Mediterranean Areas[*].

Class	Species	Canary I.	W. Medit.
Bivalvia	*Basterotia clancula* Von Cosel 1995		*
Gastropoda	*Bursa pustulosa* Reeve 1844		*
Gastropoda	*Cantharus viverratus* (Kiener 1834)	*	*
Bivalvia	*Megaxinus appendiculatus* (Locard 1898)		*
Gastropoda	*Natica turtoni* E.A. Smith 1890		*
Gastropoda	*Polinices lacteus* (Guilding 1834)	*	*
Gastropoda	*Acteocina knockeri* (E.A. Smith 1871)		*
Gastropoda	*Acteon bovetensis* (Sequenza)		*
Bivalvia	*Anadara geissei* (Dunker 1891)		*
Bivalvia	*Arcopsis afra* (Gmelin 1791)	*	*
Bivalvia	*Atactodea glabrata* (Philippi 1791)		*
Bivalvia	*Barbatia (Acar) plicata* (Chemnitz 1870)	*	*
Bivalvia	*Brachidontes senegalensis (*Lamarck 1819)	*	*
Bivalvia	*Cardita senegalensis* Reeve 1843	*	*
Gastropoda	*Clavatula rubrifasciata* (Reeve 1845)		*
Gastropoda	*Conus ambiguus* Reeve 1844		*
Gastropoda	*Conus cf. miruchae* Röckel, Rolán & Monteiro, 1980		*
Gastropoda	*Conus cf. roeckeli* Rolán 1980		*
Gastropoda	*Conus ermineus* Born 1778	*	*
Gastropoda	*Conus venulatus* Hwass in Bruguière 1792		*
Bivalvia	*Corbula revoluta* Brocchi		*
Gastropoda	*Cymatium trigonum* (Gmelin 1791)	*	*
Gastropoda	*Hexaplex rosarium* (Röding 1798)	*	*
Bivalvia	*Hyotissa hyotis* (Linné 1758)	*	*
Gastropoda	*Imbricaria carbonacea* (Hinds 1844)		*
Bivalvia	*Lutraria senegalensis* Gray 1837		*
Gastropoda	*Mitra scrobiculata* Brocchi		*
Gastropoda	*Nassarius wolffi* (Knudsen 1956)		*
Gastropoda	*Natica acynonyx* Marche-Marchad 1957		*
Gastropoda	*Pusionella nifat* (Brugière 1789)		*
Gastropoda	*Sinum concavum* (Lamarck 1822)		*
Gastropoda	*Strombus Latus* Gmelin 1791	*	*
Gastropoda	*Terebra corrugata* Lamarck 1822		*
Gastropoda	*Trachypollia turricula* (Von Maltzan 1884)		*
Bivalvia	*Tugonia anatina* (Gmelin 1791)		*
Bivalvia	*Venerupis dura* (Gmelin 1791)		*
Gastropoda	*Zonaria petitiana* (Crasse)		*
Gastropoda	*Zonaria picta* (Gray 1824)		*

Gastropoda	*Angiola lineata* (Da Costa 1778)	*
Gastropoda	*Cerithium atratum* (Born 1778)	*
Bivalvia	*Chama crenulata* Lamarck 1819	*
Gastropoda	*Clavatula sacerdos* (Reeve 1845)	*
Gastropoda	*Favartia burnayi* Houart 1981	*
Gastropoda	*Harpa doris* Röding 1798	*
Gastropoda	*Hipponix antiquatus* (Linné 1767)	*
Gastropoda	*Kleinella gruveli* (Dautzenberg 1910)	*
Gastropoda	*Marginella cincta* Kiener 1834	*
Gastropoda	*Mitra nigra* (Gmelin 1791)	*
Gastropoda	*Morula nodulosa* (C.B. Adams 1845)	*
Gastropoda	*Thais nodosa* (Linné 1758)	*
Gastropoda	*Trachypollia suga* (Gmelin)	*
Gastropoda	*Zonaria zonata* (Chemnitz 1788)	*

* presence in Last Interglacial deposits (see sites and references in Table 1). Colours: yellow: species that should not be considered as Senegalese *s.s.* in Canary Islands or Azores because inhabit there nowadays, white: Senegalese species *s.s.* for both areas (Canary I. and W. Mediterranean), grey: Senegalese species in the Canary Islands (absent in the Mediterranean deposits).

of Canary Islands; Sal, Boavista an Maio in the case of Cape Verde Archipelago) and younger, more active islands to the west (e.g. El Hierro at Canary Islands; and Fogo at Cape Verde). The Quaternary record is therefore wider and better preserved in the eastern islands. Our previous studies in the Canary Islands were centred on Lanzarote and Fuerteventura (Zazo *et al.*, 2002), and on Sal Island in the Cape Verde Archipelago (Zazo *et al.*, 2007; 2010). The number of quaternary marine terraces and their geomorphological arrangement is very similar in the studied islands from both archipelagos (Fig. 6). Likewise, the Last Interglacial deposits have similar elevations above present sea level (lower than on the Iberian coasts, between +2.5 m and +0.5 m), and are discontinuous and less well-preserved on the northern coasts. Two highstands for MIS 5e have also been distinguished in both archipelagos, with Senegalese species and high coralline algae content (Fig. 4) (Zazo *et al.*, 2002; 2007; 2010; Cabero, 2009). For the Canary Islands, the former characteristics are indicative of warmer conditions during MIS 5e.

The review of the Last Interglacial palaeontological content on the Canary Islands, including other Macaronesian references (see sites and references in Table 1) led to the identification of at least 23 Senegalese species *s.s.* (six bivalves and 17 gastropods). Some of these species are also cited in the Mediterranean, but 14 species are only present in the Canary Islands (see Table 2): the bivalve *Chama crenulata*, and the gastropods *Angiola lineata*, *Cerithium atratum*, *Clavatula sacer-*

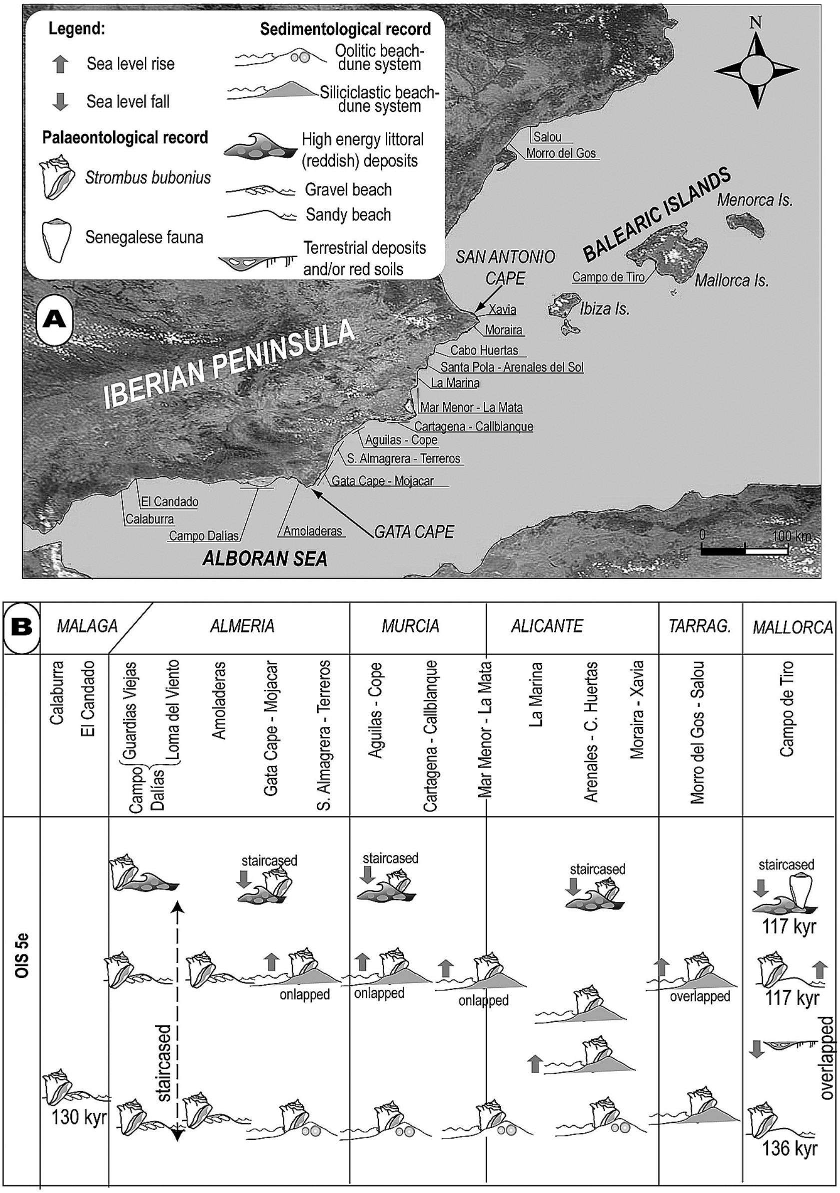

Figure 5. A: Location of OIS 5e (MIS 5e) sites along the Mediterranean coasts of Iberian Peninsula; B: Main palaeontological, geomorphological and sedimentological features of OIS 5e deposits according to Bardají *et al.*, 2009 (see references herein). The symbol *Strombus bubonius* represents the presence of *S. latus* and other Senegalese species. In the latest deposits of MIS 5e of Mallorca, *S. latus* is absent.

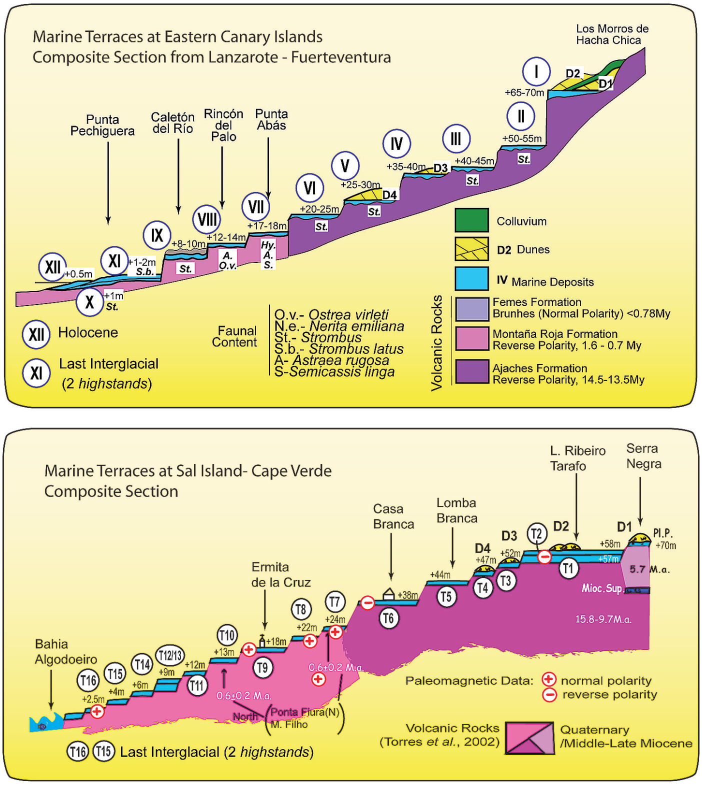

Figure 6. Marine terraces at Lanzarote-Fuerteventura (Composite Section) according to Zazo *et al.*, 2002. Marine terraces at Sal Island (Composite Section) according to Zazo *et al.* 2007.

dos, Favartia burnayi, Harpa doris, Hipponix antiquatus, Kleinella gruveli, Marginella cincta, Mitra nigra, Morula nodulosa, Thais nodosa, Trachypollia suga, Zonaria zonata.

As occurred in the Mediterranean area, in the Canary Islands, there are some species cited as thermophilic and/or Senegalese that are not present in our list because of their current (but scarce) presence on the islands: *Ctena eburnea, Cheila equestris*. We can also include in this group the species mentioned above as no Senegalese for the Mediterranean area but which do appear in the Last Interglacial Canarian deposits (*Bursa scrobiculator, Cabestana dolaria, Patella ferruginea*, and *Vermetus semisurrectus*).

In Cape Verde, we have less palaeontological data (many fossil samples are still being analyzed), and some of the palaeontological references have no chronological information, so it is difficult to assign them to the Last Interglacial.

However, our first fossil data of Last Interglacial species from Sal Island point to very similar content to the present day species, so the coastal conditions could have been similar to the present day ones (Zazo *et al.*, 2007; 2010; Cabero, 2009).

DISCUSSION

Palaeoenvironmental conditions for Senegalese species

The present day sea surface temperatures (SST) and salinity (SSS) of Cape Verde and West African tropical waters provide data about the mean annual SST and SSS values required by Senegalese species, as well as their tolerance to seasonal temperature changes (Fig. 7). All the West African tropical regions show a lower degree of seasonality in comparison with the Mediterranean and Canary Islands (Fig. 7). Generally speaking, a mean annual SST between 23–25º C, a seasonal gradient lower than 6º–8º C and a mean SSS around 34–35 PSU are assumed to be the optimum conditions for the survival of the *S. latus* and other Senegalese species (Meco *et al.*, 2006; Bardají *et al.*, 2009; Zazo *et al.*, 2010). The sea surface temperatures related to this fauna agree with other sea-surface palaeotemperature indicators around the Iberian Peninsula (Martrat *et al.*, 2004; Pérez Folgado *et al.*, 2004). However, taking into account the non-homogeneous distribution of the bulk of the Senegalese fauna *s.s.* mentioned above, we can distinguish between the 14 Senegalese species cited only for the Canary Islands and the rest of species that reached the Western Mediterranean. The first group may have probably required different environmental conditions, with lower seasonal SST variations, higher mean annual SST and/or lower salinity than the species that colonized the Mediterranean.

Regarding the ecology of these species, many authors have focused on the *S. latus* due to its abundance in some Last Interglacial deposits (Fig. 4) and its significance as Late Pleistocene warm-water species. Nowadays *S. latus* occurs around the Gulf of Guinea, in an area limited by the Canary Current to the north and the Benguela Current to the south. The Cape Verde Islands represent its northern border (Kreipl and Poppe, 1999). *S. latus* is a detritivorous, vegetarian species (Morri *et al.*, 2000; Mendes Lopes, 2002). It has been described as inhabiting sandy to gravelly bottoms in moderately exposed coasts between 4 and 40 m deep (Morri *et al.*, 2000), and sandy-muddy bottoms and seagrass meadows related to beach, lagoon and river mouths environments (Meco, 1967, among others). This species tolerates a SST range from 15º to 30º C and lower salinity environments (Meco, 1967; 1977). The palaeoenvironments for most of the MIS 5 coastal deposits with *S. latus* are similar to those where it lives today (soft to gravelly bottoms related to sand beaches, lagoons and estuaries). The ecological characteristics of this species, with high tolerance of temperature and salinity variations, along with an ample tolerance ranging from gravelly to muddy bot-

Locality	Lat./Long.	SST (ºC)*	SST * annual	SSS ** (psu)	Ref. * **
1. W Mediterranean (Spanish Coast)	41º-35º N 5º W-15º E	12 (winter) 24 (summer)	**18**	**37**	(1) (1)
2. Gulf of Cadiz (Spanish Coast)	37º-36º N 9º -5º W	16,5 (winter) 22,5 (summer)	**19, 6**	**35, 5**	(3) (1)
3. Azores	40º-37º N 31º-25º W	17 (Dec-Jan) 25 (Aug-Sept)	**21**	**36**	(1) (1)
4. Morocco (Atlantic Coast)	34º-30º N 7º- 9º W	17 (winter) 22 (summer)	**19, 5**	**~36**	(1) (1)
5. Canary I. (Lanzarote and Fuerteventura)	27º-30º N 18º-13º W	19 (winter) 23 (summer)	**21**	**36, 6**	(1) (2)
6. Cape Verde (Sal)	15º-17º N 26º-22º W	21-22(Jan-May) 25-26 (Sep-Dec)	**23, 5**	**35**	(1) (1)
7. Senegal (Dakar)	14º 30' N 17º 30' W	19-21 (winter) 27-28 (summ.)	**24**	**34**	(1) (4)

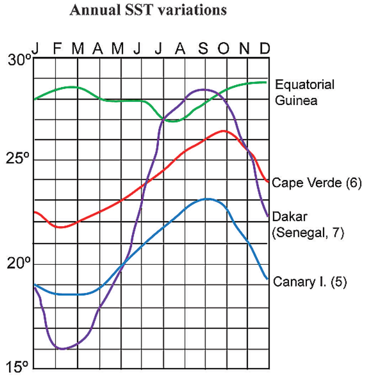

Figure 7. Sea Surface Temperatures (SST) and Sea Surface Salinity (SSS) in the Mediterranean-Atlantic linkage area. Data (note asterisks after): (1) NOAA-WOA, 2001; (2) Pelegri *et al.*, 2005; (3) Vargas *et al.*, 2003; (4) Le Loeuff and Von Cosel, 1998. Curves of SST variation throughout the year according to Bellomo (1998).

toms may have favoured its adaptation and colonization of Mediterranean coasts during the Last Interglacial.

Other climate scenarios during the Last Interglacial

Climatic models based on orbital configuration (Montoya *et al.*, 1998; Montoya, 2007) estimated some global characteristics for the Last Interglacial: higher temperatures in the Northern Hemisphere (related to slightly greater obliquity), a higher seasonal gradient (because of greater eccentricity of the Earth's orbit) and different seasonality, with warmer and shorter summers, and milder and longer winters in the Northern Hemisphere (because the Perihelion took place in northern summer).

Displacements to higher latitudes of warm-water molluscs during MIS 5 have also been described in other areas. In general these migrations occur from the Tropics of Cancer and Capricorn, to the north and south respectively (Matsuura, 1985; Kendrick *et al.*, 1991; Ortlieb *et al.*, 1994; Muhs *et al.*, 2002; Murray-Wallace, 2002; Rivadeneira and Carmona, 2008). The presence of this fauna is linked to higher temperatures at these latitudes, whereas in the subtropical-equatorial zones these faunal and temperature changes have not occurred. Our first results from the Cape Verde Archipelago also point to this behaviour.

The northwards Senegalese fauna distribution during the Last Interglacial agrees with these other migrations, but one difference should be considered: the highest diversity and abundance are present in the Atlantic islands instead of the African continental coasts (Fig. 1, Table 1). *S. latus* and other Senegalese species are absent along the Atlantic coasts of Azores, Morocco, Western Sahara, Mauritania, and Senegal. These absences are also recorded along the Spanish peninsular coasts, where *S. latus* appears in the Mediterranean MIS 5 deposits, but not in the Atlantic realms (Fig. 2) (Zazo *et al.*, 2003; Bardají *et al.*, 2009). In the Canary Islands the *Strombus* genus appears in deposits from Early Pleistocene to Late Pleistocene (Zazo *et al.*, 2002; 2003). The absence of *S. latus* and other Senegalese species along the Atlantic coasts of the Iberian Peninsula and the northwest of Africa could be related to two main factors: a) unsuitable coastal scenarios (different bottom and littoral dynamics during the Last Interglacial) and/or different fossil preservation, b) differences in SST/SSS.

With regard to SST differences, the activity of the permanent and seasonal upwelling occurring in northwest Africa and southern Portugal could have played an important role in the faunal distribution. The upwelling along the northern coasts of Africa extends to the south during winter, under the influence of increased trade winds (Fig.1). The southern Portuguese upwelling extends to the east also during winter, influenced by intense westerly winds (Fig. 2) (Le Loeuff and Von Cosel, 1998; Vargas *et al.*, 2003). Winter SSTs in Senegal can be 3–6º C lower than in the Cape Verde archipelago because of the upwelling (Fig. 7).

Orbital forcing during MIS 5 induced an increased insolation in the Northern Hemisphere, but also longer winters and shorter summers, with higher seasonal variations than today (Montoya *et al.*, 1998). This situation could explain the absence of some Senegalese taxa on these coasts: longer and more intense upwelling activity, together with shorter summers, may have favoured lower mean SST as compared with other areas (Cabero, 2009). Changes in the upwelling intensity related to increased trade winds have also been cited in deep-core marine records to the north of Canary Islands (Moreno *et al.*, 2001). Winds and upwelling activity increased during Terminations of glacial periods, and also during stadials phases of the MIS 5 and MIS 7 (Moreno *et al.*, 2001). During these intervals, the subtropical anticyclonic circulation may have intensified (Moreno *et al.*, 2001; Paillier and Bard, 2002). Changes in the trajectory and/or strength of surface oceanic currents have certainly played a major role in carrying the larvae of theses species to the Mediterranean. The variations on the latitudinal position and strength of these currents at the beginning of the MIS 5 and during stadials events (Calvo, *et al.*, 2001; Paillier and Bard, 2002) may have forced the Islands' colonization and favoured entrance into the Mediterranean. In this sense, the Atlantic archipelagos may have an important role in the migration of these species, allowing disperse colonization, avoiding the «oceanographic-barrier» of the African upwelling (Cabero, 2009).

The seasonality changes could have intensified at the end of the Last Interglacial, promoting the final disappearance of the Senegalese species in the Mediterranean. The changes in seasonality (related to orbital precession variations) have been reflected in some deep-core marine records as the driving-mechanisms of changes in some atmospheric (for example winds) and oceanographic features during Last Glacial cycle in the Mediterranean-Atlantic linkage area (Moreno, 2002 and references herein). Although seasonality changes are difficult to estimate in coastal sediments, in SE Spain and in the Canary Islands, climate deterioration and increase in runoff and storms at the end of Last Interglacial have been described (Zazo *et al.*, 2003; Bardají *et al.*, 2009; Cabero, 2009). The changes in seasonality (linked to changes in insolation in Northern Hemisphere) were probably the driving-mechanisms for the climate changes and faunal disappearance at the end of MIS 5.

In addition to the upwelling and seasonality gradients, other ecological and biological factors should be taken into account, such as the local coastal environments and ecology for each species, their larval characteristics and processes of dispersion, etc.

Detailed ecological and palaeontological analyses focusing on selected species are required to evaluate all the environmental and biological factors. Regarding the Canary Islands and the Macaronesian biogeography, a more in-depth ecological analysis of the Senegalese species *s.s.* that did not reach the Mediterranean area is necessary. The ecology, temperature and salinity required for the survival of these species, could provide new data about the palaeoceanography, coastal conditions and latitudinal temperature gradients during Last Interglacial and other quaternary interglacials.

The variation of the species throughout the Quaternary must also be taken into account in the reconstruction of the migration processes. Some of the Senegalese fossil species *sensu lato* (*s.l.*) cited in the Mediterranean have been considered as «repetitive immigrants» given their punctuated presence during the Plio–Pleistocene. This group of «repetitive-immigrant» species appear mainly in the central and Eastern Mediterranean, and their warm-water significance and evolution during Quaternary has recently been analyzed (Garilli, 2011). The Plio–Pleistocene coastal outcrops on the Spanish coasts are less preserved and studied from a palaeontological point of view, a review and new studies of the Plio-Pleistocene molluscs is therefore required in order to complete the list of Western Mediterranean thermophilic species, and to compare it with the central and Eastern Mediterranean records. This analysis should also be extrapolated to the Canary Islands, Cape Verde and Northwest African coasts, with the aim of estimating the biogeographical distribution of these species during Quaternary and the climate events and variations related to the migrations of these species.

CONCLUSIONS

A list of 52 Senegalese species *s.s.* linked to tropical warm-waters has been selected from the review of the paleontological data. Those species that appear in the Canary Islands but do not reach the Mediterranean, must be highlighted as potential indicators of latitudinal differences in SST/SSS during MIS 5. *S. latus* lives today in environments characterized by warm waters presenting a high tolerance to temperature and salinity variations. In order to use the Senegalese species as an accurate proxy for palaeo SST and SSS during MIS 5, more research on the ecological features for each selected species is required.

Changes in the seasons length and also the seasonal temperature variations that occurred during Last Interglacial (linked to changes in insolation) could have played an important role in the location of adequate coastal environments for these species. More analyses and research on previous interglacials are required in order to evaluate more precisely the global factors that promoted sea level and climatic changes during Quaternary.

ACKNOWLEDGEMENTS

This work has been supported by funds of the following research projects: CGL2012/33430, CGL-2008-4000/BTE, CGL-2008-3998/BTE, Consolider-GRACCIE (CSD-2007-00067) IGCP 588, INQUA CMP Commission, GEOTOP Lab. Contrib., UCM R.G. 910198.

REFERENCES

Abbott, R.T. and Dance, S.P. (2000) *Compendium of Seashells.* Odyssey Publishing, USA.

Ávila, S.P., Amen, R., Azevedo, J.M.N., García-Talavera, F. and Cachão, M. (2002) Checklist of the Pleistocene marine molluscs of Praínha and Lagoínhas (Santa María island, Azores). *Açoreana*, 9/4, 343–370.

Ávila, S.P., Madeira, P., Mendes, N., Rebelo, A., Medeiros, A., Gomes, C., García-Talavera, F., Marques da Silva, C., Cachão, M., Hillaire-Marcel, C. and de Frías Martins, A.M. (2008) Mass extinctions in the Azores during the last glaciation: fact or myth? *Journal of Biogeography*, 35, 1123–1129.

Ávila, S.P., Marques da Silva, C., Schiebel, R., Cecca, F., Backeljau, T. and de Frías Martins, A.M. (2009) How did they get here? The biogeography of the marine molluscs of the Azores. *Bulletin de la Societe Geologique de France,* 180, 295–307.

Bardají, T., Goy, J.L., Zazo, C., Hillaire Marcel, C., Dabrio, C.J., Cabero, A., Ghaleb, B., Silva, P.G. and Lario, J. (2009) Sea-level and climate changes during OIS 5 in western Mediterranean (Spain). *Geomorphology*, 104, 22–37.

Bellomo, E. (1998) *Le Tyrrhenien d'Italie Meridionale: Paleoenvironmements de depots et evolution tectonique dans le cadre biogeographique de la Mediterrannée.* Ph.D. Thesis, Université Paris vi.

Brébion, P. (1979) Iconographie critique des Gastéropodes marins du Pliocéne supérieur et du Quaternaire marocains atlantiques. *Bulletin du Muséum d'Histoire Naturelle,* 4, 137–149.

Brébion, P., Raynal, J.P., Texier, J.P. and Alouane, M. (1986) Nouvelles données sur le Quaternaire littoral du Maroc atlantique à Casablanca et Cap Achakar. *Comptes rendus de l'Académie des sciences. Série 2, Sciences de la Terre,* 302, 901–904.

Cabero, A. (2009) *Registro costero de los cambios eustáticos y climáticos durante los interglaciares recientes cuaternarios: S y SE Peninsular, Islas Baleares, Canarias y Cabo Verde.* Ph.D. Thesis, Universidad de Salamanca.

Callapez, P. and Ferreira Soares, A. (2000) Late Quaternary warm marine molluscs from Santa Maria (Azores) paleoecologic and palaeobiogeographic considerations. *Ciências da Terra (UNL)*, 14, 313–322.

Calvo, E., Villanueva, J., Grimalt, J.O., Boelaert, A. and Labeyrie, L. (2001) New insights into the glacial latitudinal temperature gradients in the North Atlantic. Results from U^{k}_{37} sea surface temperatures and terrigenous inputs. *Earth and Planetary Science Letters*, 188, 509–519.

CLEMAN (Check List of European Marine Mollusca). Available at: http://www.somali.asso.fr/clemam/index.clemam.html

Cosel, R. von (2006) Taxonomy of tropical West African bivalves. vi. Remarks on Lucinidae (Mollusca, Bivalvia), with description of six new genera and eight new species. *Zoosystema*, 28, 805–851.

Costello, M.J., Bouchet, P., Boxshall, G., Arvantidis, C. and Appeltans, W. (2008) European Register of Marine Species. Available at: http://www.marbef.org/data/erms.php

Cuerda Barceló, J. (1987) *Moluscos marinos y salobres del Pleistoceno Balear.* Caja de Baleares «Sa Nostra», Palma de Mallorca.

Cuerda Barceló, J. (1995) Significación climática y cronológica de algunos yacimientos del Pleistoceno Superior de Alicante. *El Cuaternario del País Valenciano*, pp. 251–259. Universitat de Valéncia, Asociación para el Estudio del Cuaternario, Valencia.

Cuerda, J. and Sanjaume, E. (1978) Datos paleontológicos y sedimentológicos del litoral Pleistoceno de Santa Pola. *Cuadernos de Geografía (Universidad de Valencia)*, 23, 19–62.

Dabrio, C.J., Zazo, C., Cabero, A., Goy, J.L., Bardají, T., Hillaire-Marcel, C., González-Delgado, J.A., Lario, J., Silva, P.G., Borja, F. and García-Blázquez, A.M. (2011) Millennial/submillennial-scale sea-level fluctuations in western Mediterranean during the second highstand of MIS 5e. *Quaternary Science Reviews*, 30, 335–346.

De Torres, T., Ortiz, J.E., Arribas, I., Delgado, A., Julià, R. and Martín-Rubí, J.A. (2010) Geochemistry of *Persististrombus latus* Gmelin from the Pleistocene Iberian Mediterranean realm. *Lethaia*, 43, 149–163.

Galili, E., Zviely, D., Ronen, A. and Mienis, H.K. (2007) Beach deposits of MIS 5e high sea stand as indicators for tectonic stability of the Carmel coastal plain, Israel. *Quaternary Science Reviews*, 26, 2544–2557.

García-Talavera, F. (1983) *Los moluscos gasterópodos anfiatlánticos: estudio paleo y biogeográfico de las especies bentónicas litorales.* Ph.D. Thesis, Universidad de La Laguna, Sta. Cruz de Tenerife.

García-Talavera, F. (1990a) Sobre la presencia de *Strombus latus* GMEL. (*Mollusca, Mesogastropoda*) en el Cuaternario marino de Tenerife. *Homenaje al profesor Dr. Telesforo Bravo*, Tomo i, pp. 375–382. Universidad de la Laguna, Tenerife.

García-Talavera, F. (1990b) Fauna Tropical en el Neotirreniense de Santa María (I. Azores). *Lavori S.I.M.*, 23, 439–443.

García-Talavera, F. (1999) Fauna malacológica del cuaternario marino de Cabo Verde. *Revista Academia Canaria de las Ciencias*, XI, 9–25.

García-Talavera, F. and Bacallado, J.J. (1981). Nuevas aportaciones a la fauna de gasterópodos marinos *(Mollusca, Gastropoda)* de las islas de Cabo Verde. *Boletín del Instituto Español de Oceanografía*, Tomo VI/328, 201–208.

García-Talavera, F. and Sánchez-Pinto, L. (2002) Moluscos marinos fósiles de Selvagem Pequenha e Ilheu de Fora (Islas Salvajes). Descripción de una nueva especie de neogasterópdo. *Revista de la Academia Canaria de Ciencias*, 13, 9–21.

García-Talavera, F., Kardas, S.J.Jr. and Richards, H.G. (1978) Quaternary marine mollusks from Tenerife, Canary Islands. *The Nautilus*, 92, 97–102.

García-Talavera, F., Sánchez-Pinto, L., López-Rondón, J. and Martín Oval, M. (2007) Carta paleontológica de Fuerteventura. Convenio de colaboración. Organismo Autónomo de Museos y Centros del Cabildo de Tenerife - Cabildo de Fuerteventura, Santa Cruz de Tenerife.

Garilli, V. (2011) Mediterranean Quaternary interglacial molluscan assemblages: Palaeobiogeographical and palaeoceanographical responses to climate change. *Palaeogeography, Palaeoclimatology, Palaeoecology,* 312, 98–114.

Gignoux, M. (1911) Les couches à Strombus bubonius (Lmk.) dans la Méditerranée occidentale. *Compte Rendus des Séances de l'Académie des Sciences*, 1991, 1–3.

Goy, J.L., Zazo, C., Bardají, T., Somoza, L., Causse, Ch. and Hillaire-Marcel, C. (1993) Eléments d'une chronostratigraphie du Tyrrhénien des régions d'Alicante-Murcie, Sud-Est de l'Espagne. *Geodinamica Acta,* 6, 103–119.

Goy, J.L., Hillaire-Marcel, C., Zazo, C., Ghaleb, B., Dabrio, C.J., González-Delgado, J.A., Bardají, T., Civis, J., Preda, M., Yébenes, A. and Forte, A.M. (2006) Further evidence for a relatively high sea level during the penultimate interglacial: open system U-series ages from La Marina (Alicante, East Spain). *Geodinamica Acta*, 19/6, 409–426.

Hillaire-Marcel, C., Gariepy, C., Ghaleb, B., Goy, J.L., Zazo, C. and Cuerda, J. (1996) U-series measurements in Tyrrhenian deposits from Mallorca. Further evidente for two Last- Interglacial high sea-levels in the Balearic Islands. *Quaternary Science Reviews,* 15, 53–62.

Issel, A. (1914) Lembi fossiliferi quaternari e resentí nella Sardegna meridionale. *Accademia Nazionale dei Lincei*, Serie 5–23, 759–770.

Kendrick, G.W., Wyrwoll, K.-H. and Szabo, B.J. (1991) Pliocene- Pleistocene coastal events and history along the western margin of Australia. *Quaternary Science Reviews*, 10, 419–439.

Kreipl, K. and Poppe, G. (1999) *The Family Strombidae. A Conchological Iconography.* ConchBooks, Hackenheim.

Lecointre, G. (1962) Le Quaternaire de l'île de Sal (archipel du Cap-Vert). *Compte Rendue Sommaire des Séances Société Géologique de France*, 3–92.

Lecointre, G. (1965) Le Quaternaire marin de l'Afrique du nord-ouest. *Quaternaria,* vii, 9–28.

Le Loeuff, P. and Von Cosel, R. (1998) Biodiversity patterns of the marine benthic fauna on the Atlantic coast of tropical Africa in relation to hydroclimatic conditions and paleogeographic events. *Acta Oecologica,* 19, 309–321.

Matsuura, N. (1985) Successive changes of the marine molluscan faunas from Pliocene to Holocene in Hokuriku region, central Japan. *Bulletin of the Mizunami Fossil Museum,* 12, 71–158.

Martrat, B., Grimalt, J.O., López-Martínez, C., Cacho, I., Sierro, F.J., Flores, J.A., Zahn, R., Canals, M., Curtis, J.H. and Hodell, D.A. (2004) Abrupt Temperature Changes in the Western Mediterranean over the Past 250.000 years. *Science*, 306, 1762–1765.

Meco, J. (1967) Donées actuelles pour l'étude paléontologique du *Strombus bubonius* Lamarck. *Congrès Panafricain de Préhistoire, Dakar,* 391–394.

Meco, J. (1977) Los *Strombus* neógenos y cuaternarios del Atlántico euroafricano (taxonomía, biostratigrafía y paleoecología). *Paleontología de Canarias, Tomo i.* Cabildo Insular de Gran Canaria. Las Palmas-Madrid.

Meco, J., Ballester, J., Perera, M.A., Marrero, R., Ginés, G. and Pallarés, A. (2003) *Paleoclimatología de Lanzarote y La Graciosa (yacimientos paleontológicos).* Servicio de Patrimonio Histórico del Cabildo de Lanzarote, Universidad de Las Palmas de Gran Canaria, Las Palmas de Gran Canaria.

Meco, J., Ballester, J., Betancort, J.F., Cilleros, A., Scaillet, S., Guillou, H., Carracedo, J.C., Lomoschitz, A., Petit-Maire, N., Ramos, A.J.G., Perera, N. and Meco, J.M. (2006) *Paleoclimatología del Neógeno en las Islas Canarias. Geliense, Pleistoceno y Holoceno.* Ministerio de Medio Ambiente, Universidad de Las Palmas de Gran Canaria, Las Palmas.

Meco, J., Betancort, J.F., Ballester, J., Fontugne, M., Guillou, H., Scaillet, F., Lomostchiz, A., Cilleros, A., Carracedo, J.C., Petit-Maire, N., González, A.J., Perera, M.A., Soler-Onís, E., Medina, P., Montesinos, M. and Meco, J.M. (2008) *Historia geológica del clima en Canarias.* Las Palmas de Gran Canaria.

Mendes Lopes, R.C. (2002) *Caracterização da Pesca de Búzio-cabra (Strombus latus Gmelin, 1791) na ilha de São Vicente, Cabo Verde.* Ph.D. thesis, Universidade do Algarve, Faro.

Mitchell-Thomé, R.C. (1976) *Geology of the middle Atlantic Islands. Beiträge zur Regionalen Geologie der Erde.* Gebrüder Borntraeger, Berlin.

Montoya, M. (2007) The Last Interglacial. *Encyclopaedia of Quaternary Science Paleoclimate Modeling* (ed. by Elías, S.A.), pp. 1916–1926. Elsevier.

Montoya, M., Crowley, T.J. and Von Storch, H. (1998) Temperatures at the last interglacial simulated by a coupled ocean-atmosphere climate model. *Paleoceanography,* 13, 170–177.

Moreno Caballud, A. (2002) *Registro del aporte de polvo de origen sahariano y de la productividad oceánica en la Cuenca del Norte de Canarias y en el Mar de Alborán. Respuesta a los últimos 250.000 años de cambio climático.* Ph.D. thesis, Universidad de Barcelona, Barcelona.

Moreno, A., Targarona, J., Henderiks, J., Canals, M., Freudenthal, T. and Meggers, H. (2001) Orbital forcing of dust supply to the North Canary Basin over the last 250 kyrs. *Quaternary Science Reviews,* 20, 1327–1339.

Morri, C.R., Cattaeno-Vietti, G., Sartoni, G. and Banchi, N. (2000) Shallow epibenthic communities of Ilha do Sal (Cape Verde Archipelago, eastern Atlantic). *Arquipélago. Life and Marine Sciences,* Supplement 2 (Part A), 157–165.

Muhs, D.R., Simmons, K.R. and Steinke, B. (2002) Timing and warmth of the last interglacial period: New U-series evidence from Hawaii and Bermuda and a new fossil compilation for North America. *Quaternary Science Reviews,* 21, 1355–1383.

Murray-Wallace, C. (2002) Pleistocene coastal stratigraphy, sea-level highstands and neotectonism of the southern Australian passive continental margin – a review. *Journal of Quaternary Science,* 17, 469–489.

NOAA-WOA (2001) Available at: http://iridl.ldeo.columbia.edu/SOURCES/.NOAA/.NODC/ .WOA01

Ortlieb, L., Guzmán, N. and Candia, M. (1994) Moluscos litorales del Pleistoceno superior en el área de Antofagasta, Chile: primeras determinaciones e indicaciones paleoceanográficas. *Estudios Oceanológicos*, 13, 57–63.

Paillier, D. and Bard, E. (2002) High frequency palaeoceanographic changes during the past 140 000 yr recorded by the organic matter in sediments of the Iberian Margin. *Palaeogeography, Palaeoclimatology, Palaeoecology*, 181, 431–452.

Pelegrí, J.L., Arístegui, J., Cana, L., González-Dávila, M., Hernández-Guerra, A., Hernández-León, S., Marrero-Díaz, A., Montero, M.F., Sangrà, P. and Santana-Casiano, M. (2005) Coupling between the open ocean and the coastal upwelling region off northwest Africa: water recirculation and offshore pumping of organic matter. *Journal of Marine Systems*, 54, 3–37.

Pérez-Folgado, M., Sierro, F.J., Flores, J.A., Grimalt, J.O. and Zahn, R. (2004) Paleoclimatic variations in foraminifer assemblages from the Alboran Sea (Western Mediterranean) during the last 150 ka in ODP Site 977. *Marine Geology*, 212, 113–131.

Poppe, G.T. and Goto, Y. (1991) *European Seashells, Vol. I. Polyplacophora, Caudofoveata, Solenogastra, Gastropoda*. Verlag Christa Hemmen, Germany.

Poppe, G.T. and Goto, Y. (2000) *European seashells, Vol. II. Scaphopoda, Bivalvia, Cephalopoda*. ConchBooks, Hackenheim.

Rivadeneira, M.M. and Carmona, E.R. (2008) A Late Pleistocene macrobenthic assemblage in Caleta Patillos, northern Chile: paleoecological and paleobiogeographical interpretations. *Revista Geológica de Chile*, 35, 163–173.

Rolán, E. (2005) *Malacological Fauna from the Cape Verde Archipelago, Part 1*. ConchBooks, Hackenheim.

Segers, W. (2002) On some shallow-water marine molluscs of the Azores. *Gloria Maris*, 41, 84–104.

Spano, C. (1980) Fauna del Tirreniano-Tipo di Is Mesas-Calamosca (Sardegna meridionale). *Comptes-Rendus Excursion-Table Ronde Tyrrhenien de Sardaigne, INQUA*, 65-101.

Spano, C., Belluomini, G., Carboni, S., Congiu, A.C., Murgia, D., Tomassi, A.V. and Vesica, P. (2005). A Synthesis of the Tyrrhenian in Sardinia (Italy). Correlations, Biocenotic-Bathymetric and Palaeoenvironmental aspects. Pleistocene deposits in the Cagliari coastal area (Sardinia, Italy), with particular attention to the «Piano Tirreno» fossiliferous deposits of Issel (1914). *Cuaternario Mediterráneo y poblamiento de Homínidos, VI Reunión del Cuaternario Ibérico* (ed. by Rodríguez Vidal, J., Finlayson, J.C. and Giles Pacheco, F.), pp. 50–55. Gibraltar Museum, AEQUA, Gibraltar.

Torres, C.P., Silva, L.C., Serralheiro, A., Mendes, M.H., Macedo, J.R. and Gomes, A.M. (2002) Geología da Ilha do Sal. *Comunicações do Instituto de Investigação Científica Tropical, Série de Ciências da Terra*, 10.

Vargas, J.M., García-Lafuente, J., Delgado, J. and Criado, F. (2003) Seasonal wind-induced variability of Sea Surface Temperature patterns in the Gulf of Cádiz. *Journal of Marine Systems*, 38, 205–219.

Vera-Peláez, J.L., Lozano-Francisco, M.C., Ramos Fernández, J. and Cortés Sánchez, M. (2004) Moluscos del Tirreniense (Pleistoceno Superior) de la playa La Araća-Cala del Moral (Málaga). *Revista Española de Paleontología*, 19, 251–259.

Weisrock, A., Occhietti, S., Hoang, C.T., Lauriat-Rage, A., Brébion, Ph. and Pichet, P. (1999) Les séquences littorales pléistocćnes de l'Atlas atlantique entre Cap Rhir et Agadir, Maroc. *Quaternaire*, 10, 227–224.

WoRMS (World Register of Marine Species). Available at: http://www.marinespecies.org/index.php.

Zazo, C., Silva, P.G., Goy, J.L., Hillaire-Marcel, C., Ghaleb, B., Lario, J., Bardají, T. and González, A. (1999) Coastal uplift in continental collision plate boundaries: data from the Last Interglacial marine terraces of the Gibraltar Strait area (south Spain). *Tectonophysics*, 301, 95–109.

Zazo, C., Goy, J.L., Hillaire-Marcel, C., Gillot, P.Y., Soler, V., González, J.A., Dabrio, C.J. and Ghaleb, B. (2002) Raised marine sequences of Lanzarote and Fuerteventura revisited - a reappraisal of relative sea-level changes and vertical movements in the eastern Canary Island during the Quaternary. *Quaternary Science Reviews*, 21, 2019–2046.

Zazo, C., Goy, J.L., Dabrio, C.J., Bardají, T., Hillaire-Marcel, C., Ghaleb, B., González-Delagdo, J.A. and Soler, V. (2003) Pleistocene raised marine terraces of the Spanish Mediterranean and Atlantic coasts: records of coastal uplift, sea-level highstands and climate changes. *Marine Geology*, 194, 103–133.

Zazo, C., Mercier, N., Silva, P., Dabrio, C.J., Goy, J.L., Roquero, E., Soler, V., Borja, F., Lario, J., Polo, M.D. and Luque, L. (2005) Landscape evolution and geodynamic controls in the Gulf of Cádiz (Huelva Coast, SW Spain) during the Late Quaternary. *Geomorphology*, 68, 269–290.

Zazo, C., Goy, J.L., Dabrio, C.J., Soler, V., Hillaire-Marcel, C., Ghaleb, B., González-Delgado, J.A., Bardají, T. and Cabero, A. (2007) Quaternary marine terraces on Sal Island (Cape Verde archipelago). *Quaternary Science Reviews*, 26, 876–893.

Zazo, C., Hansen, A., Goy, J.L., Criado, C., González-Delgado, J.A., Dabrio, D.J., Hillaire-Marcel, C., Bardají, T., Silva, P.G., Cabero, A., Civis, J., Soler, V. and Ghaleb, B. (2008a) Geomorfología volcánica y variaciones del nivel del mar en Lanzarote y Fuerteventura (Plio-Cuaternario). Excursión Post-Congreso 5. *Itinerarios Geológicos por las Islas Canarias: Fuerteventura, Lanzarote, Tenerife, La Gomera y El Hierro. Geo-Guias 6.* (ed. by Perez Torrado, F.J. and Cabrera, M.C.), pp. 143–172. SGE, Las Palmas de Gran Canaria.

Zazo, C., Mercier, N., Lario, J., Roquero, E., Goy, J.L., Silva, P., Cabero, A., Borja, F., Dabrio, C.J., Bardají, T., Soler, V., García-Blázquez, A. and Luque, L. (2008b) Palaeoenvironmental evolution of the Barbate-Trafalgar coast (Cádiz) during the last ~140 ka: tectonics, climate and sea-level interactions. *Geomorphology*, 100, 212–222.

Zazo, C., Goy, J.L., Hillaire-Marcel, C., Dabrio, C.J., González Delgado, J.A., Cabero, A., Bardají, T., Ghaleb, B. and Soler, V. (2010) Sea Level Changes During the Last and Present Interglacials in Sal Island (Cape Verde Archipelago). *Global and Planetary Change*, 72, 302–317.

Zazo, C., Goy, J.L., Dabrio, C.J., Lario, J., González-Delgado, J.A., Bardají, T., Hillaire-Marcel, C., Cabero, A., Ghaleb, B., Borja, F., Silva, P.G., Roquero, E. and Soler, V. (2013) Retracing the Quaternary history of sea-level changes in the Spanish Mediterranean-Atlantic coasts: geomorphological and sedimentological approach. *Geomorphology*, 196, 36–49.

QUATERNARY LAND SNAIL ASSEMBLAGES FROM THE EASTERN CANARY ISLANDS: AN OVERVIEW

Yurena Yanes, María R. Alonso, Miguel Ibáñez

CLIMATE CHANGE PERSPECTIVES FROM THE ATLANTIC:
PAST, PRESENT AND FUTURE
Jose María Fernández-Palacios, Lea de Nascimento, José Carlos Hernández,
Sabrina Clemente, Albano González & Juan P. Díaz-González (eds.)
Servicio de Publicaciones, Universidad de La Laguna – 2013

ISBN: 978-84-15910-54-1 pp. 191-223

Abstract

The Canary Islands presently exhibit a relatively rich terrestrial malacofauna. Numerous land snail shells are also well-preserved in Quaternary eolian deposits, which are particularly abundant in the easternmost islands of the archipelago. This fossil material has been investigated over the years to: 1) examine the quality and fidelity of the fossil record (do fossil snails reflect the biological signature of the once living communities?), 2) estimate glacial and interglacial palaeoenvironmental conditions (has the climate fluctuated throughout the Quaternary?), 3) evaluate potential changes in the taxonomic composition through time (has snail diversity remained steady in deep time?), and 4) identify potential factors that may shape snail communities (what factors cause temporal variations in snail abundance, distribution, diversity and body size?). The main results from this research suggest that: 1) shelly assemblages preserved in carbonate-rich areas exhibit high ecological fidelity; 2) C_4 plants were more abundant during some glacial intervals than today; 3) relative humidity has fluctuated but declined overall to present values; 4) snail diversity and body size varied but generally decreased from the last-glacial to the Holocene; 5) the geographical distribution of some species is smaller today than in the past; and finally, 6) snail communities are shaped by both ecological (e.g., interspecific competition) and environmental (e.g., relative humidity and island area) factors combined. Here we review the potential and limits of fossil land snail assemblages in palaeoenvironmental studies and outline pending work. This study may serve as a brief guideline for future studies in other Macaronesian islands rich in Quaternary land snail shelly accumulations.

Keywords: Canary Islands, land snails, palaeoecology, palaeoclimate, Quaternary, taphonomy.

INTRODUCTION

The Canary Islands (latitude: 27–29° N) are a volcanic and oceanic archipelago situated ~100 km off the Moroccan coast (Fig. 1). The region is affected recurrently by oceanic (e.g., Canarian cool current, coastal upwelling) and atmospheric (e.g., Saharan dust storms, trade winds) circulation systems. The archipelago is formed by seven main islands and multiple small islets, with a total area of ~7447 km^2, a maximum altitude of 3718 m above sea level (a.s.l.), and a maximum subaerial age of ~20.5 Myr (Fernández-Palacios and Whittaker,

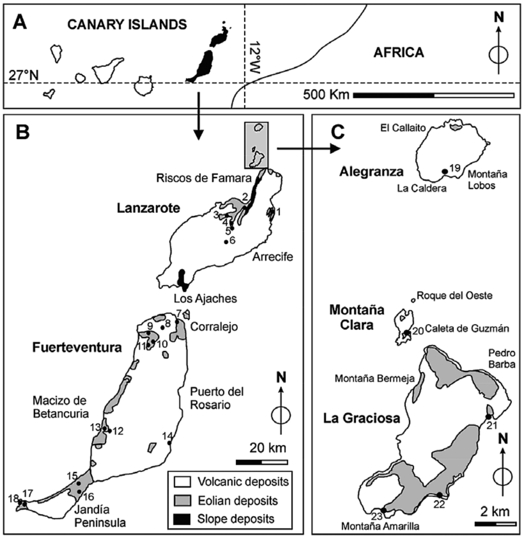

Figure 1. Geographical location of some studied Quaternary eolian deposits (adapted from Yanes *et al.*, 2011b). A. The Canary Islands. B. Lanzarote and Fuerteventura. C. The islets to the north of Lanzarote Island. (1) Mala, (2) Las Casitas, (3) Muñique, (4) Tao, (5) Loma de San Andrés, (6) Montaña Guatisea, (7) Corralejo, (8) El Quemado, (9) Montaña Costilla, (10) Barranco de la Cal, (11) Barranco de los Encantados, (12) Barranco del Tabaibejo, (13) Jable de Vigocho, (14) Pozo Negro, (15) Atalayeja Grande, (16) Barranco del Pecenescal, (17) Montaña Azufra, (18) Degollada de Agua Cabras, (19) Montaña Lobos, (20) Caleta de Guzmán, (21) Morros Negros, (22) Caleta del Sebo, (23) La Cocina.

2008). These islands exhibit a remarkable diversity of habitats, ranging from subdesertic coastal scrubs to humid evergreen forests and subalpine landscapes (e.g., Yanes *et al.*, 2009).

The easternmost islands, Fuerteventura and Lanzarote, are the oldest islands (~20.5–15.5 Myr) closest to Africa (~95–125 km) with the lowest altitude (~807–670 m a.s.l.) out of the archipelago. The climate in the eastern islands is semiarid, with less than ~100–250 mm of annual precipitation and annual average air temperatures of ~20° C. Despite minimal precipitation, the oceanic influence permits the islands to retain an annual relative humidity of ~70%, on average (Dorta, 2005). The vegetation cover is open, principally formed by xerophytic grasses and shrubs. Around 678 plant species have been catalogued in the eastern islands, most of them following a C_3 photosynthetic pathway. Around 67 species are classified as C_4 plants (e.g., Scholz, 2005).

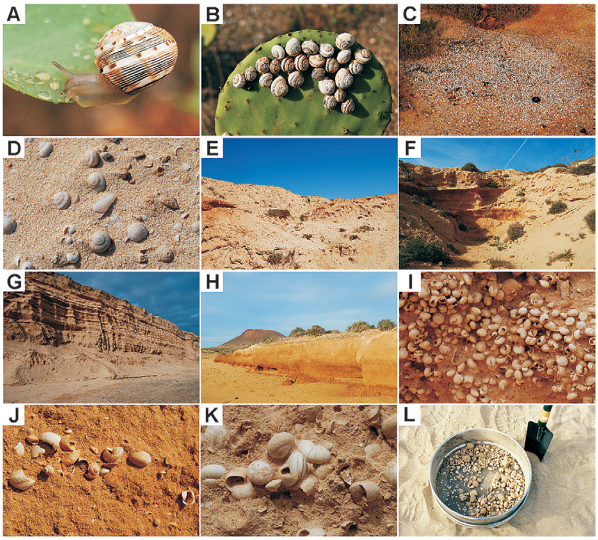

Figure 2. Photographs of land snails and Quaternary eolian deposits from the eastern Canary Islands. A. Living *Theba geminata* from La Graciosa. B. Living *Theba geminata* attached to a CAM plant in Lanzarote. C. Shelly accumulation on the soil surface in La Graciosa. D. Shelly accumulation on the soil surface in Corralejo, Fuerteventura. E. Quaternary eolian deposit of Barranco de los Encantados, Fuerteventura. F. Quaternary eolian deposit of Mala, Lanzarote. G. Quaternary eolian deposit of Cantera de Melián, Fuerteventura. H. Paleosol of Caleta del Sebo, La Graciosa. I. Quaternary shell assemblage of Cantera de Melián, Fuerteventura. J. Quaternary shell assemblage of Mala, Lanzarote. K. Detailed view of a Quaternary shell assemblage of Cantera de Melián, Fuerteventura. L. Sample replicate gathered with a 1-mm mess diameter sieve. (Photographs taken by Y. Yanes, 2010–2012).

The easternmost islands have been longer under sedimentation and erosion processes due to their older age with respect to central and western islands. These islands and nearby islets contain fairly thick sequences of Quaternary eolian deposits (Fig. 2E–K). The eolian successions consist of bioclastic dunes which are capped by ~20–60 cm thick palaeosols. Eolianites are rich in carbonates (~50–90% by weight) and contain a mixture of marine and continental carbonate minerals (calcite, magnesium calcite, and aragonite) (Damnati *et al.*, 1996). Also, clay minerals such as authigenic smectite and Saharan-derived illite-kaolinite, quartz grains from the Sahara, and basaltic clasts from weathering of local rocks are present (Damnati *et al.*, 1996; Williamson *et al.*, 2004). These eolianites are relatively rich in fossil land snail shells, nests of solitary bees, coleopterans and locusts, and occasionally, vertebrates (e.g., Yanes *et al.*, 2008b; 2011a; Meco *et al.*, 2011). Fossil land snails are surprisingly abundant and well-preserved in these eolianites. They offer an excellent opportunity to attempt to reconstruct the Quaternary terrestrial ecosystems of the westernmost Sahara zone. This material has been studied using multiple techniques and combining disparate data to address a broad variety of questions (e.g., Yanes, 2003; 2005; Yanes *et al.*, 2007; 2008a; 2008b; 2011a; 2011c; Huntley *et al.*, 2008). Taphonomic and palaeoecological data provide information of the shell burial processes and the ecological fidelity of the fossil record. Diversity, geographical distribution and body size data may be used to evaluate organism-environment integrations. Carbon and oxygen stable isotope composition of the shell provides palaeovegetation and palaeoatmospheric information during the shell calcification process. In this study we present a synthesis of the main findings derived from our published and some unpublished data, summarize the potential and caveats of snail assemblages as palaeoenvironmental proxies, and outline pending work on fossil land snail research investigations.

MATERIAL AND METHODS

Sampling strategy

Eolian successions were studied directly in the field by Yanes (2003; 2005), Ortiz *et al.* (2006) and Yanes *et al.* (2007) to identify differing stratigraphic horizons based on colour, texture, and mineralogical composition features in chronological order. Levels from the bottom of the section depict the oldest material whereas horizons from the top of the section depict the youngest intervals. Fossil shells were collected in each stratigraphic horizon by dry-sieving using 1-mm mesh size. Four to six sample replicates, spaced laterally ~0.5 m, were taken from each bed when possible. Each sample represents ~5 kg of sediment before sieving. This sampling approach assured to acquire representative bulk samples of land snail shells per horizon (Yanes, 2005).

Taphonomy and time-averaging

X-ray diffraction analyses were performed for numerous fossil shells (Yanes *et al.*, 2007; 2008b; 2011a; 2011c) in the Instituto Andaluz de Ciencias de la Tierra, CSIC-UGR (Spain), the Southern Methodist University (USA), the Savannah River Ecology Laboratory, University of Georgia (USA), and the Instituto Universitario de Bio-orgánica Antonio González (Spain), to evaluate the mineralogical composition of fossil shells.

Shell material was studied by Yanes *et al.* (2008b; 2011a) in the laboratory under a binocular microscope for macroscopic taphonomic features. Seven palaeoecological and taphonomic variables were studied: 1) minimum number of individuals (MIN), 2) fragmentation, 3) pedogenic carbonate coating, 4) roundness of fragments, 5) colour preservation, 6) proportion of juveniles and adults, and 7) mineralogical composition of the shell. Minimum number of individuals considered only specimens that preserve the embryonic shell. Fragmentation is measured as the number of fragments divided by the sum of fragments and entire specimens. Shell fragments represent any piece of gastropod shells that have lost more than the 10% of the shell. Colour preservation was quantified as the proportion of shells with some original colour preserved. Carbonate coating was quantified as the proportion of shells with carbonate coating. Roundness refers to the degree of smoothing of the edges of the shell fragments.

Quantitative estimates of the scale of time-averaging (= age-mixing of non-contemporaneous shells within a single shell bed) were carried out by Yanes *et al.* (2007). Multiple shells from the same stratigraphic horizon were individually dated by aminoacid racemisation calibrated against radiocarbon (see methodology in Ortiz *et al.*, 2006; Yanes *et al.*, 2007). The age dispersion within a shell bed was contrasted with the error that could be generated by dating imprecision alone. If the range of ages obtained from individually-dating different shells preserved together in the same shell bed exceeded the error expected from the dating technique, then real time-averaging occurred (see details in Yanes *et al.*, 2007).

STABLE ISOTOPE ANALYSES

Carbon and oxygen stable isotope analyses of numerous modern and fossil land snail shells and carbonate-rich sediments were carried out by Yanes *et al.* (2008a; 2011c) using the stable isotope facilities of the University of Kentucky (USA), the Instituto Andaluz de Ciencias de la Tierra, CSIC-UGR (Spain), the Southern Methodist University (USA), and the Savannah River Ecology Laboratory, University of Georgia (USA). Pre-cleaned and finely ground entire shells were treated with 3% NaOCl (reagent grade) overnight at room temperature (~22° C) to remove organic contaminants. About 150 µg of carbonate was placed in a 6 ml Exetainer^{TM} vial which was subsequently flushed with helium to replace the headspace. The carbonate was converted to CO_2 by adding 0.1 ml of 100% H_3PO_4 at 25°C. The resulting CO_2 was analyzed after 24 hours using the GasBench II connected to the Finnigan Delta^{PLUS} XP continuous flow isotope ratio mass spectrometer. Stable isotope results are reported in δ notation relative to Pee Dee Belemnite (PDB). The δ values are defined as:

$$\delta^{13}C \text{ or } \delta^{18}O = [(R_{sample} / R_{standard}) - 1] \times 1000\ (‰)$$

where R= $^{13}C/^{12}C$ or $^{18}O/^{16}O$. Analytical uncertainty was ± 0.1‰ based on the repeated measurements of in-house and international standards throughout a run. Isotopic data were quantitatively evaluated using two-source simple mass balance equations (see Yanes *et al.*, 2008a) and the evaporative steady-state flux balance mixing model by Balakrishnan and Yapp (2004).

PALAEOGEOGRAPHY, PALAEOECOLOGY, MORPHOMETRICS

Presence/absence data of living land snail species were taken by Ibáñez and Alonso (unpublished data) over decades. Species geographical distribution data of some fossil species was obtained by Yanes (2003; 2005) and by Ibáñez and Alonso (unpublished data). From these databases associated with geographical coordinates, maps showing present and past geographical distribution of some species were achieved (personal unpublished data).

Relative species abundance data was obtained by Yanes (2003; 2005). A total of 8366 land snail individuals were collected by dry sieves (1 mm mesh) to minimize bias by-hand collecting. The same sampling effort was applied to each stratigraphic horizon to make samples statistically comparable. Shells were water-cleaned, sonicated and analyzed in the laboratory under a binocular microscope. All individuals were identified to species level based on shell features alone except slugs, which were identified to genus level. The number of individuals of each species was counted.

Morphometric data was acquired by Yanes (2003) and Huntley *et al.* (2008). Six bidimensional measurements (length, width, height of the two last spires, height of the last spire, aperture height and aperture width) were taken following Kerney and Cameron (1979) methodology. Geometric mean of log-transformed shell length and width was computed as a proxy of body size. The area of shells was estimated by studying shell photographs in the J software.

STATISTICAL ANALYSES

Non-parametric univariate and multivariate analyses were performed using PAST 2.13 and SAS software, considering statistical significance at $\alpha = 0.05$. Spearman's correlation analyses were used to explore the potential rank-based relationship between variables. The Mann-Whitney *U* test and Kruskal-Wallis test were used to compare the median distribution among samples. Cluster analysis based on the Manhattan distance and group-average linkage method was used to identify taphofacies. Taxonomic mismatches among groups were examined by non-metric multidimensional scaling (nMDS) ordination of the proportional species abundance using the Bray-Curtis similarity index. The proportions of species abundances were previously square-root transformed to reduce the effect of the dominant species.

The raw number of species was sample-size standardized via rarefaction. Margalef's richness index estimates the number of species divided by the log of the sample size. The simplest-dominant index (Berger-Parker dominance) was calculated as the number of individuals of the dominant taxon divided by sample size. Shannon diversity was computed as the proportion of each species relative to the total number of species, multiplied by the natural logarithm of this proportion.

RESULTS AND DISCUSSION

Present terrestrial malacofauna

The great variety of microclimates in the Canary Islands, together with the isolated condition, has favoured land snail speciation and radiation processes. As a result, the current native terrestrial malacofauna is relatively rich, with 28 families, 51 genera and ~270 species, of which ~88% are endemic to the archipelago (Núñez and Núñez, 2010). The number of species of land snails in the Canary Islands is over twice than that of native vertebrates.

Land snails from the Canary Archipelago originate in the Tertiary from two main sources, North Africa and South Europe (e.g., Greve *et al.*, 2010; 2012; Holyoak *et al.*, 2011). Thus, land snails from the Canary Islands, in particular from the eastern islands, exhibit high taxonomic affinities with those from northwestern Africa (Greve *et al.*, 2010; 2012). Snails colonized the islands during various waves via several dispersal agents. The variety of colonization processes may have occurred by chance and/or by differing ecological and climatic tolerances among species. Although land snails display poor active dispersal abilities, they successfully colonize islands from mainland sources using passive dispersal methods, e.g., by birds, driftwood, and wind (e.g., Aubry *et al.*, 2006). Passive dispersal by anthropogenic activities has occurred during the last 600 years since the archipelago was conquered by Castilians. Possibly, most cosmopolitan species living today in the region were introduced during the past several centuries. However, such type of passive dispersal has not been quantified in the Canary Islands.

The current most species rich genera of the Canary Islands include the endemic *Napaeus* Albers, 1850 (Enidae) with ~67 known species (Yanes *et al.*, 2011b), *Hemicycla* Swainson, 1840 (Helicidae) with ~50 known species (Neiber *et al.*, 2011) and *Canariella* Hesse, 1918 (Hygromiidae) with ~27 known species (Núñez and Núñez, 2010). Other genera also relatively rich in species are *Insulivitrina* Hesse, 1923 (Vitrinidae) with ~14 known species, *Monilearia* Mousson, 1872 (Cochlicellidae) with ~14 known species, and *Canaridiscus* Alonso & Ibáñez, 2011 (Discidae) with ~12 known species. These genera have experienced a remarkable speciation in the islands and have been able to occupy almost all habitat types across the archipelago. Non-native land snail species recently introduced by human activities are also present in the islands, like the helicids *Otala lactea* (O. F. Müller, 1774), *Cornu aspersum* (O. F. Müller, 1774) or *Theba pisana* (O. F. Müller, 1774) (and many other species). However, research on invasive land snail species in the Canary Archipelago and their potential threat to native species is pending

TABLE 1. Modern land snail species (n=50) presently living in Lanzarote and Fuerteventura Islands (data adopted from Núñez and Núñez, 2010).

Species	Distribution
Pomatias lanzarotensis (Wollaston, 1878) *	L
Granopupa granum (Draparnaud, 1801)	T C F L
Monilearia granostriata (Mousson, 1857) *	F
Monilearia loweana (Wollaston, 1878) *	L
Monilearia monilifera (Webb & Berthelot, 1833) *	F L
Monilearia multipunctata (Mousson, 1872) *	F
Monilearia persimilis (Shuttleworth, 1852) *	H P G T C F L
Monilearia tubaeformis Alonso & Groh, 2006 *	F
Obelus discogranulatus Alonso & Groh, 2003 *	F
Obelus moderatus (Mousson, 1857) *	F
Obelus moratus (Mousson, 1872) *	F
Obelus pumilio (Dillwyn, 1817)	C F
Napaeus huttereri Henríquez, 1991 *	L
Napaeus lichenicola Alonso & Ibáñez, 2007 *	F
Napaeus rufobrunneus (Wollaston, 1878) *	L
Ferussacia attenuata (Mousson, 1872) *	L
Ferussacia fritschi (Mousson, 1872) *	L
Ferussacia lanzarotensis (Mousson, 1872) *	L
Ferussacia submajor (Wollaston, 1878) *	F
Ferussacia valida (Mousson, 1872) *	F
Ferussacia vitrea (Webb & Berthelot, 1833) *	F L
Sculptiferussacia clausiliaeformis Alonso & Ibáñez, 1992 *	F
Hemicycla desculpta (Mousson, 1872) *	F
Hemicycla flavistoma Ibáñez & Alonso, 1991 *	L
Hemicycla paeteliana (L. Pfeiffer, 1859) *	F
Hemicycla sarcostoma (Webb & Berthelot, 1833) *	F L
Otala lactea (Müller, 1774)	H G T C F L
Theba clausoinflata (Mousson, 1857) *	F
Theba geminata (Mousson, 1857) *	H P G T C F L
Theba impugnata (Mousson, 1857) *	F L
Canariella eutropis (Shuttleworth, 1861) *	F
Canariella jandiaensis Ibáñez & Ponte- Lira, 2006 *	F

Canariella orzolae Gittenberger & Ripken, 1985 *	L
Canariella plutonia (R.T Lowe, 1861) *	F L
Candidula ultima (Mousson, 1872) *	F
Caracollina lenticula (Michaud, 1831)	H P G T C F L
Cernuella virgata (Da Costa, 1778)	T C F L
Xerotricha lancerottensis (Webb & Berthelot, 1833) *	F L
Lauria cylindracea (Da Costa, 1778)	H P T C F
Oxychilus draparnaudi (H. Beck, 1837)	H P T C L
Cryptella alegranzae Hutterer & Groh, 1991 *	L
Cryptella auriculata (Mousson, 1872) *	F
Cryptella canariensis Webb & Berthelot, 1833 *	F L
Cryptella famarae Hutterer & Groh, 1991 *	L
Cryptella susannae (Hutterer, 1990) *	F
Gibbulinella dealbata (Webb & Berthelot, 1833) *	P G T C F?
Rumina decollata (Linnaeus, 1758)	H P G T C F L
Vitrea contracta (Westerlund, 1871)	H P G T C F L
Paralaoma servilis (Shuttleworth, 1852)	H P T L
Truncatellina purpuraria Hutterer & Groh, 1993 *	F L

* Denotes endemic species to the Canary Islands.

to be examined in a quantitative manner. Ibáñez and Alonso (2001) pointed out that the majority of extinctions of endemic land snails from Tenerife and Gran Canaria islands were the consequence of urbanization and habitat destruction. Thus, historical and recent anthropogenic activities have clearly disturbed the native terrestrial malacofauna of the islands. Rigorous studies on biodiversity and conservation of modern lands snails from the region remain to be assessed. Some species display a highly restricted distribution area within one single island or even on a single mountain, and may require protection measures, such as *Canariella pontelirae* Hutterer, 1994 in Teno (Tenerife) (Ibáñez *et al.*, 2006) or the species that inhabit the Zarza peak in the south of Fuerteventura, including *Sculptiferussacia clausiliaeformis* Alonso & Ibáñez, 1992, *Canariella jandiaensis* Ibáñez & Ponte-Lira in: Alonso *et al.*, 2006 and *Napaeus lichenicola* Alonso & Ibáñez in: Ibáñez *et al.*, 2007 (Alonso *et al.*, 1992; 2006; Ibáñez *et al.*, 2007).

The oldest and easternmost islands of the archipelago are poorer in land snail species than central and western islands. This is due to their lower altitude (less than 807 m a.s.l.) and as a result, poorer diversity in microhabitats, despite their relatively large area. Consequently, only 50 species (out of 270) live today in Lanzarote and Fuerteventura (Table 1). The dominant genus in the easternmost islands is *Theba* Risso, 1826 (Helicidae), with three known extant species (Table 1), two extinct Quaternary species (Table 2) and one extinct Pliocene species. Recent studies suggest that the number of *Theba* species in the Canary Islands is higher, and new *Theba* species are pending to be described (Greve *et al.*, 2010; 2012).

Snails that inhabit the eastern islands are generally adapted to semiarid conditions. Land snails are capable of surviving under such dry scenario (less than 100–200 mm of annual precipitation) because of the relatively high water content in the air, especially at night. Thus, most species become active at night, when relative humidity is the highest (~90–91%, Yanes *et al.*, 2013). Most species are short-lived generalized herbivorous (Speiser, 2001), so they appear to consume all plant types in the landscape indiscriminately, in relation to their abundance and availability. The dominant *Theba geminata* from the eastern Canary Islands and islets consumes living and decayed C_3, C_4 and CAM plants arbitrarily in natural conditions and does not show a preference for a specific plant type (Yanes *et al.*, 2008a). Accordingly, they are promising palaeovegetation proxies.

Shell preservation, taphonomy and time-averaging

X-ray diffraction analyses (XRD) reveal that all living land snails from the eastern Canary Islands contain shells formed by pure aragonite. In contrast, the internal shells of living slugs of the endemic genus *Cryptella* (Parmacellidae) are formed by calcite. Similarly, XRD analyses of numerous Quaternary shells collected from multiple eolian deposits of the eastern Canary Islands demonstrate that the fossil shelly material retained their original aragonitic (or calcitic in the case of slugs) composition, with minor replacements by calcite in a negligible number of specimens (Yanes *et al.*, 2007; 2008b; 2011a). Furthermore, scanning electronic microscope (SEM) photographs show that Quaternary shells (Fig. 3C–D) exhibit a shell microstructure equivalent to that of living specimens (Fig. 3A–B). This reinforces that secondary overgrowth or recrystallisation processes are not perceptible among Quaternary shells. As a comparison, the shell microstructure of diagenetically-modified shells from Pliocene deposits of Fuerteventura show, however, a clear recrystallisation of shell layers (Fig. 3E–F). Overall, the XRD and microscopic results demonstrate that Quaternary shells are very well preserved and they are suitable for further geochemical analyses (Yanes *et al.*, 2008b; 2011a), as opposed to Pliocene shells.

Quaternary land snail shells were affected by various taphonomic features, including fragmentation, corrosion, colour loss and carbonate coating (Fig. 4). Shell fragments, however, did not show signs of rounding, bioerosion or encrustation (Fig. 4D). Shell scar repairs were neither observed in the studied Quaternary shelly material (Yanes *et al.*, 2008b; 2011a). Shells of juveniles and adults differed notably in the taphonomic condition. Adults were generally more fragmented and showed higher colour loss than juveniles. Taphonomic conditions and shell

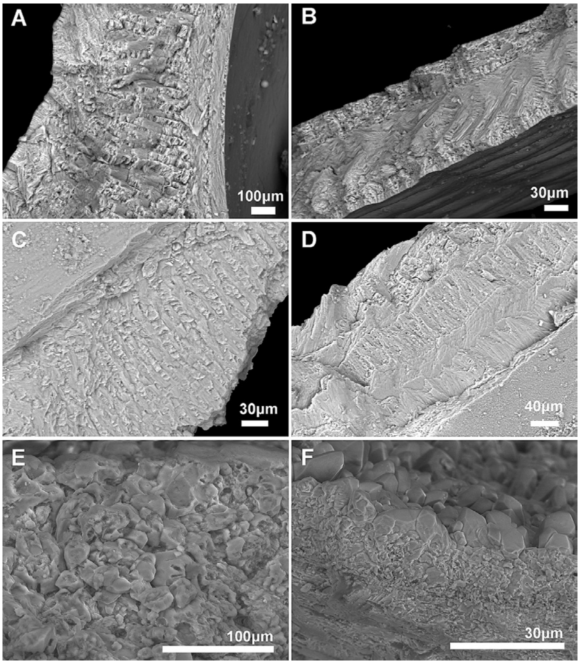

Figure 3. Scanning electronic microscope (SEM) micrographs of shell fragments from Fuerteventura (adapted after Yanes *et al.*, 2011a; 2011b). A–B. Live collected *Theba geminata* shell fragment. C–D. Well-preserved Pleistocene *Theba geminata* shell fragment. E–F. Badly preserved Pliocene *Leonia sp.* shell fragment.

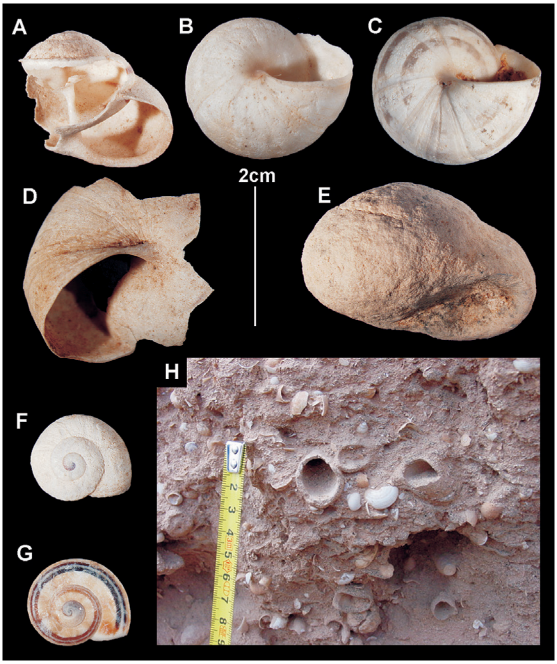

Figure 4. Taphonomic features studied in the Quaternary land snail assemblages from the eastern Canary Islands (adopted from Yanes, 2005). A. Fragmented shell. B. Shell with signs of corrosion. C. Shell without sings of corrosion. D. Fragment edge-rounding. E. Carbonate coating. F. Shell with colour loss. G. Shell with colour preserved. H. Bioturbation by arthropods.

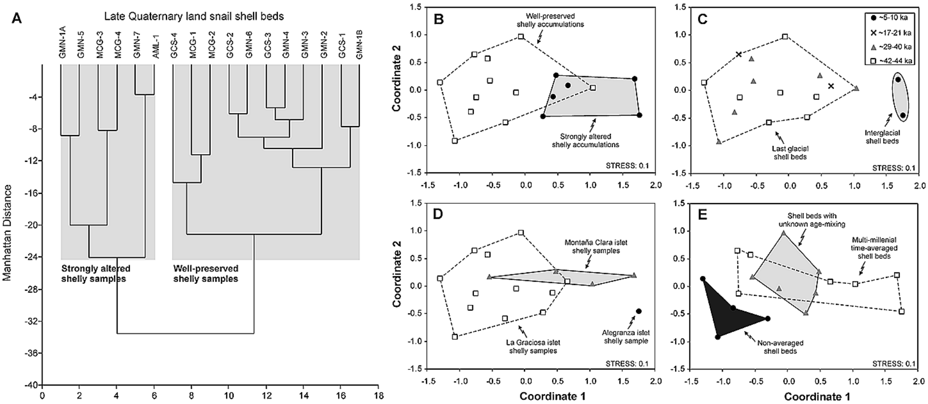

Figure 5. Quantitative taphonomic results of Quaternary land snail assemblages from the islets to the north of Lanzarote (adopted from Yanes *et al.*, 2011a). A. Cluster analysis of shelly assemblages based on taphonomic data using Manhattan distance and group linkage method. B–E. Non-metric multidimensional scaling (nMDS) ordination of the taxonomic composition of Quaternary shelly samples using Bray-Curtis similarity, grouped by taphonomic condition (B), geological age (C), locality (D) and scale of timeaveraging (E).

abundance were also different between dunes and palaeosols (Yanes *et al.*, 2008b). Shells were loosely packed (Fig. 2I–K) in both dune and palaeosol layers, and exhibited random orientation and weak-sorting (Yanes *et al.*, 2008b).

Cluster analysis (Fig. 5A) based on taphonomic features grouped samples in two taphofacies (=assemblages with comparable taphonomic condition): strongly and weakly altered taphofacies (Yanes *et al.*, 2008b; 2011a). Shelly assemblages with different preservation status are expected to differ in species abundances due to differential post-mortem sorting, destruction, and between-habitat mixing of species. Accordingly, the taxonomic composition of highly altered samples can differ from that of weakly altered samples (e.g., Tomašových, 2006). Comparisons of the relative species abundance using NMDS ordination revealed that shelly assemblages from Mala section (northeastern Lanzarote) were not biased notably by post-mortem processes because both taphofacies showed statistically-equivalent taxonomic composition (Yanes *et al.*, 2008b). In contrast, Quaternary shelly samples from the islets to the north of Lanzarote with different taphonomic condition also differed significantly in species abundances (Fig. 5B). However, because different taphofacies did not differ in shell durability, taphonomic bias could not be demonstrated (Yanes *et al.*, 2011a). Furthermore, other factors besides taphonomic condition, such as geological age (Fig. 5C), locality (Fig. 5D), or the scale of time-averaging (Fig. 5E) clearly accounted to some extent for the observed patterns (Yanes *et al.*, 2011a). Conclusively, published taphonomic studies suggest that snail palaeocommunities were not notably biased by post-mortem and burial process, which implies that Quaternary land snail assemblages preserved in carbonate-rich sites exhibit a high preservation potential and fidelity (see also Yanes, 2012a).

Time-averaging, known as the age-distance from the time of death of the oldest to the youngest individual in the assemblage (Kidwell and Flessa, 1996), was evaluated quantitatively by Yanes *et al.* (2007) for Quaternary shells of the eastern Canary Islands. Between 5 to 10 shells were aminoacid dated combined with computer-intensive statistical approaches (= Monte Carlo simulation). The results of Yanes *et al.* (2007) reflected that 11 out of 44 studied shell beds exhibited a scale of age-mixing of hundreds to thousands of years. The average magnitude of age-mixing per shell bed was ~2900 years, ranging from ~7200 years to ~510 years (Yanes *et al.*, 2007). The results agreed with previous time-averaging studies of marine shelly-rich accumulations (e.g., Kowalewski and Bambach, 2003) and terrestrial vertebrate remains (e.g., Behrensmeyer *et al.*, 2000). The main findings by Yanes *et al.* (2007) suggested that the scale of time-averaging uncorrelated with the geological age. Thus, older palaeosols did not display larger degree of age-mixing. Such apparently steady scale of time-averaging in the Quaternary shell beds of the eastern Canary Islands suggested that the dynamics of shell accumulation were similar across age-intervals. Also, the documented multimillennial age-mixing of Quaternary shells were likely associated with the time span of soil genesis rather than reworking of shells (Yanes *et al.*, 2007). The multimillennial scale of age-mixing observed among Quaternary shelly assemblages also indicates that the studied material was not buried rapidly. Although snail shells resided in the taphonomic active zone for hundreds to thousands of years, shell destruction rates were considerably low, possibly associated with carbonate coating (Yanes *et al.*, 2008b).

PALAEOCLIMATIC INFERENCES

The carbon stable isotope composition ($\delta^{13}C$) of land snail shells primarily reflects the isotopic signature of the consumed vegetation (Stott, 2002). Thus, shell $\delta^{13}C$ values of fossil specimens may be used as a proxy for palaeovegetation. Higher shell $\delta^{13}C$ values are linked to higher consumption of C_4 plants whereas lower values reflect higher ingestion of C_3 plants (Goodfriend and Ellis, 2000; 2002). Quaternary land snails from the eastern Canary Islands exhibited a substantial scatter of shell $\delta^{13}C$ values (from -8.9‰ to +3.8‰) across age intervals, reflecting the simultaneous presence of C_3/C_4 plants through time. Yanes *et al.* (2008a) observed that shell $\delta^{13}C$ values of living snails from the eastern Canary Islands were affected by the $\delta^{13}C$ values of both plants and carbonate-rich sediments. Simple mass balance equations indicate that snails assimilated ~20–40%

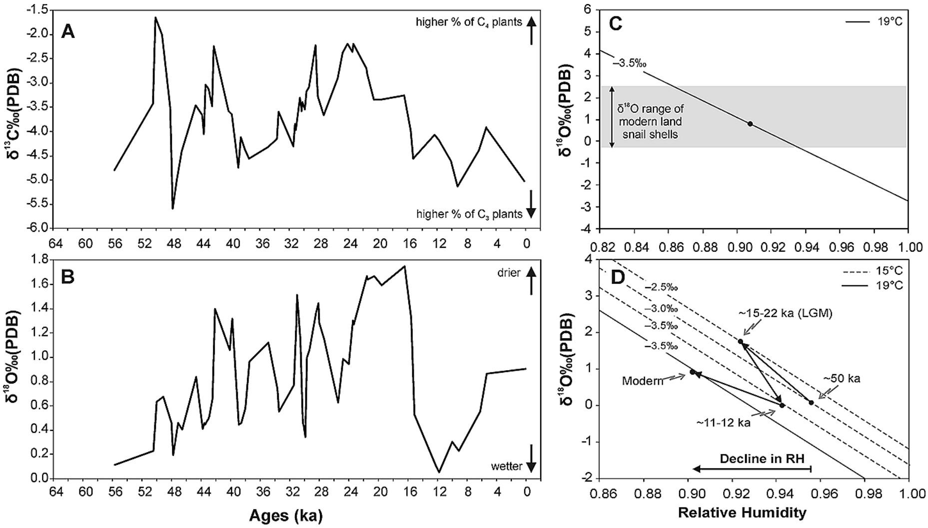

Figure 6. Stable isotope results of Quaternary land snails from the eastern Canary Islands (adapted after Yanes *et al.*, 2011b). A–B. 3-point running average of the average carbon (A) and oxygen (B) isotope values over the last glacial–Holocene period. C–D. Calculated oxygen isotope values as a function of relative humidity using the model by Balakrishnan and Yapp (2004) for modern individuals (C) and for fossil shells (D).

of carbonates in the shell. Even though shell δ^{13}C values may be shifted by a few per mil due to carbonate ingestion, the shell δ^{13}C provides rough estimates of changes in the snail diet (Yanes *et al.*, 2011c). The results indicate that modern specimens ingested higher proportion of C_3 plants than individuals from some of the previous glacial intervals (Fig. 6A). This may reflect somewhat drier conditions and/or lower atmospheric CO_2 concentrations during the last glacial than today (e.g., Koch *et al.*, 2004). These findings agreed with the dominance of C_4 plants in Africa during glacial periods (e.g., Gasse, 2000; Gasse *et al.*, 2008).

The oxygen stable isotope composition (δ^{18}O) of land snail shells is a function of relative humidity, δ^{18}O values of the rainfall and water vapour, and air temperature during calcification (Balakrishnan and Yapp, 2004). Thus, shell δ^{18}O values of fossil specimens may be used as a palaeoatmospheric proxy. Higher shell δ^{18}O values are often linked to somewhat drier and/or hotter conditions whereas lower values often reflect wetter and/or cooler settings (Balakrishnan and Yapp, 2004). The shell δ^{18}O values (from -1.9‰ to +4.5‰) of Quaternary shells from the eastern Canary Islands exhibited a large scatter across age intervals, which reflected the large environmental variability at the microhabitat scale. Shell δ^{18}O values showed the following overall pattern (Fig. 6B): 1) an overall increase from

+0.1‰ at ~50 ka to +1.6-1.8‰ during the LGM (~15–22 ka); 2) an abrupt decline in post-LGM; and 3) an overall increase of shell $\delta^{18}O$ values to modern values of +0.9‰ (Fig. 6B). Calculations of the snail flux balance model by Balakrishnan and Yapp (2004) combined with independent proxy data suggest that living snails in the eastern islands deposit shell at times when relative humidity is ~90–91%, on average (Fig. 6C). Such predicted relative humidity value by the model agrees with the measured values in the field, at night, in the soil-air interface (Yanes *et al.*, 2013). The model, constrained with published estimates of temperature and rainfall $\delta^{18}O$ values, was consecutively used to calculate palaeohumidity changes in the Canary Islands over the Quaternary. The main findings of Yanes *et al.* (2011c) suggest that conditions during the last glacial in the eastern Canary Islands were notably wetter than at present (Fig. 6D). Relative humidity appears to have shifted but declined overall through the Quaternary, reaching the current semiarid values that today characterize the easternmost islands of the archipelago. This finding is consistent with published local studies that used other proxy data (Suchodoletz *et al.*, 2010) and with the observed aridification trend in the nearby Sahara (Gasse, 2000; Gasse *et al.*, 2008). According to Yanes *et al.* (2011c), relative humidity and the $\delta^{18}O$ values of the rainfall are the most important factors that influence the shell $\delta^{18}O$ values of land snails from the Canary Islands. The environmental information recorded in the carbon and oxygen stable isotope composition of land snail shells can be better understood by the use of simple mass balance equations and flux balance mixing models (Balakrishnan and Yapp, 2004).

Quaternary palaeoecology

A total of 25 species of land snails (Table 2; Fig. 7) have been identified so far in the Quaternary eolian deposits of Lanzarote and Fuerteventura (Yanes, 2003; 2005). All species are extant, apart from the extinct species *Cochlicella* sp., *Theba costillae*, and *Cryptella parvula* (Table 2). *Theba arinagae* disappeared from the easternmost islands and lives today in Gran Canaria island only. Twenty-one species are endemic to the Canary Islands whereas only four (*Rumina decollata*, *Obelus pumilio*, *Caracollina lenticula* and *Granopupa granum*) are non-endemic, showing wider geographical distributions. Because human first arrived to the islands about 2500 years ago (Navarro-Mederos, 1983), snail species should have colonized the archipelago by natural causes without human influence. *Theba geminata* and *T. arinagae* numerically dominate the Quaternary eolian successions of the eastern islands, with a relative abundance exceeding 70% in most samples.

Geographical distributions of some species were different in the past with respect to the present. For example, personal unpublished data suggest that a couple of species (*Monilearia granostriata* and *Canariella eutropis*) in southern Fuerteventura exhibited a wider distribution in the late Pleistocene, reaching coastal sites, whereas today, living specimens are only found in a more constrained

TABLE 2. Fossil land snail species (n=25) found so far in Quaternary eolian deposits from Lanzarote and Fuerteventura Islands (data adapted from Yanes, 2005).

Species	Extinct in the easternmost islands	Extinct in the entire archipelago
Pomatias lanzarotensis (Mousson, 1872) *		
Granopupa granum (Draparnaud, 1801)		
Ferussacia fritschi (Mousson, 1872) *		
Ferussacia valida (Mousson, 1872) *		
Hemicycla flavistoma Ibáñez & Alonso, 1991 *		
Hemicycla sarcostoma (Webb & Berthelot, 1833) *		
Theba arinagae Gittenberger & Ripken, 1987 *	†	
Theba costillae Hutterer, 1990 *		†
Theba geminata (Mousson, 1857) *		
Theba impugnata (Mousson, 1857) *		
Canariella eutropis (Shuttleworth, 1860) *		
Canariella plutonia Lowe, 1861 *		
Candidula ultima (Mousson, 1872) *		
Caracollina lenticula (Michaud, 1831)		
Cochlicella sp. *		†
Monilearia granostriata (Mousson, 1857) *		
Monilearia monilifera (Webb & Berthelot, 1833) *		
Obelus pumilio (Dillwyn, 1817)		
Cryptella alegranzae Hutterer & Groh, 1991 *		
Cryptella auriculata (Mousson, 1872) *		
Cryptella canariensis Webb & Berthelot, 1833 *		
Cryptella famarae Hutterer y Groh, 1991 *		
Cryptella parvula (Hutterer, 1990) *		†
Cryptella susannae (Hutterer, 1990) *		
Rumina decollata (Linnaeus, 1758)		

* Denotes endemic species to the Canary Islands.

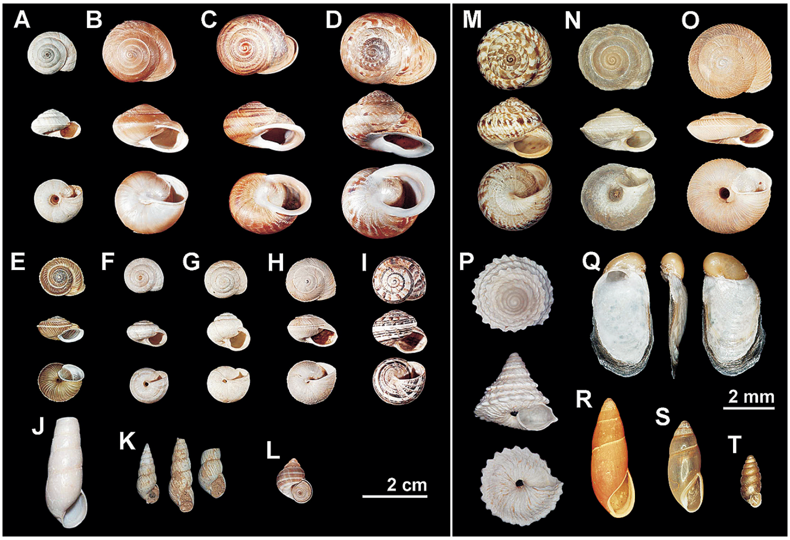

Figure 7. Photographs of land snail species found preserved in Quaternary eolian deposits of the eastern Canary Islands (adopted from Yanes, 2005). A. *Candidula ultima.* B. *Canariella plutonia.* C. *Hemicycla flavistoma.* D. *Hemicycla sarcostoma.* E. *Canariella eutropis.* F. *Theba costillae.* G. *Theba arinagae.* H. *Theba impugnata.* I. *Theba geminata.* J. *Rumina decollata.* K. *Cochlicella* sp. L. *Pomatias lanzarotensis.* M. *Monilearia monilifera.* N. *Monilearia granostriata.* O. *Caracollina lenticula.* P. *Obelus pumilio.* Q. *Cryptella canariensis.* R. *Ferussacia valida.* S. *Ferussacia fritschi.* T. *Granopupa granum.*

area, at higher elevation (Fig. 8). Such variation of distribution of species points to differing environmental and/or ecological conditions in the past than today. Isotopic data by Yanes *et al.* (2011c) suggested that conditions were notably wetter during the last glacial than presently. Thus, it is plausible that a wetter scenario during the late Quaternary allowed wider distributions of species. In addition, island area changes may have in part played a role on the observed patterns. The easternmost Canary Islands were unified forming a one unique wider island, so-called Mahan island, during the last glacial when sea levels were lower (Fernández-Palacios and Whittaker, 2008). As sea level rose during the Holocene, the eastern islands became narrower and were segregated (Fig. 9). Such changes in island area may also account to some degree for changes in the geographical distribution of some species. Personal field surveys over decades suggest that the geographical distribution of most modern species (apart from a few dominant and highly abundant species) is considerably patchy and discontinuous in each eastern island. This is also evident in the fossil record. A species may be dominant

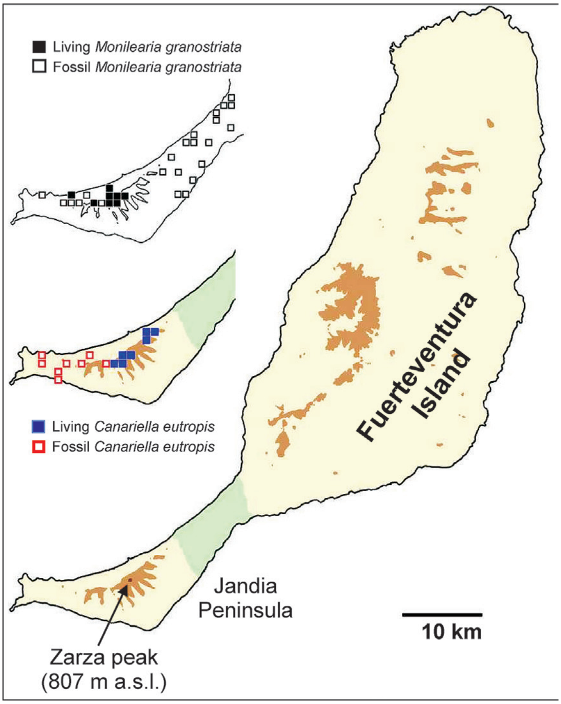

Figure 8. Present and ancient geographical distribution of *Monilearia granostriata* (black and white symbols) and *Canariella eutropis* (coloured symbols) in southern Fuerteventura.

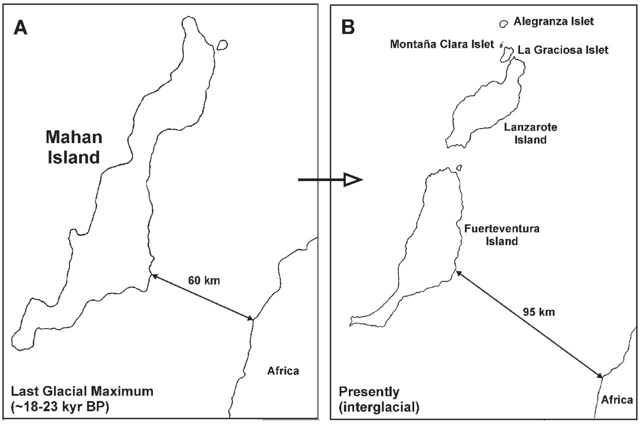

Figure 9. Changes of island area in the eastern Canary Archipelago during the last glacial (A) and the present interglacial (B) as a consequence of sea level shifts (adapted after García-Talavera, 1999).

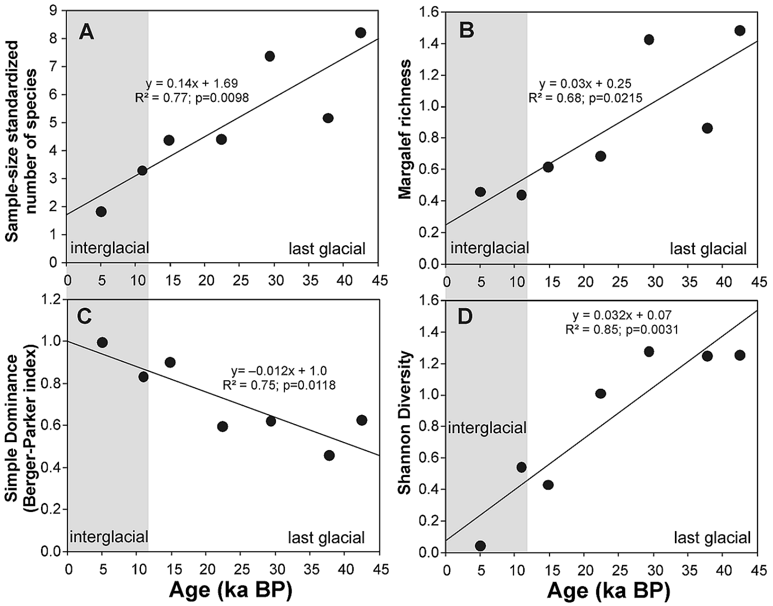

Figure 10. Several measures of richness and diversity of Quaternary land snails from the islets to the north of Lanzarote Island. A. Sample-size standardized snail richness. B. Margalef's richness. C. Simple dominance. D. Shannon-diversity index.

in one part of the stratigraphic horizon but could disappear in the same level from another locale (personal field data, 2010–2012).

Several measures of diversity of Quaternary land snail assemblages from the islets to the north of Lanzarote Island (Fig. 10) reveal that snail palaeocommunities were taxonomically richer during the last glacial than during the Holocene (personal unpublished data). Land snail diversity is affected by the interaction of multiple environmental and biological factors (Cowie, 1992). Certain climatic variables like temperature and humidity (or rainfall) may constrain land snail physiology and life cycle (Moine and Rousseau, 2002; Moine *et al.*, 2002; Chiba, 2007), which ultimately drive snail diversity. In addition to climate, island area changes and/or land fractionation could also have been responsible for shifts on land snail diversity (Cowie, 1995; Marui *et al.*, 2004). Therefore, it is plausible that the apparent decline in land snail diversity (Fig. 10) was caused by both, the decline in humidity and the decrease in island area (Fig. 9).

Huntley *et al.* (2008) observed that the two dominant *Theba* species (*T. geminata* and *T. arinagae*) from the islets to the north of Lanzarote have experienced an overall decrease in shell size while both species coexisted (Fig. 11A–B). Multiple environmental and ecological factors control shell size, but humidity appears to

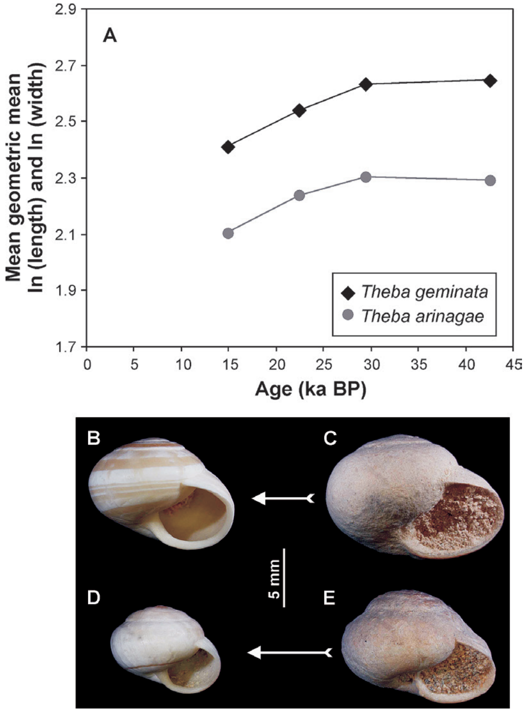

Figure 11. Body size (=mean geometric mean of ln of length and width) of two sympatric *Theba* species preserved in Quaternary eolian deposits from the islets to the north of Lanzarote (adapted after Huntley *et al.*, 2008). A. Gradual decline in body size of both species over the last glacial cycle. B–C. ~15 kyr old (B) and ~43 kyr old (C) *Theba geminata* shells. D–E. ~15 kyr old (D) and ~43 kyr old (E) *Theba arinagae*.

be one of the most important (e.g., Goodfriend, 1986). The documented decline in relative humidity in the study area (Yanes *et al.*, 2011c) possibly accounted, at least partially, for the observed patterns. Under wetter conditions, snails are active and feed longer, aestivate less, and experience overall higher growth rates. Thus, snail size is often larger under wetter conditions, but smaller at drier times. However, the published literature shows controversial results (Hausdorf, 2006) and therefore, the magnitude and direction to which shell size responds to climate may vary across locales and taxa (e.g., Yanes *et al.*, 2012). The fact that shells from the islets to the north of Lanzarote have decreased in size (Fig. 11A–B), a trend parallel to the inferred decline in relative humidity (Yanes *et al.*, 2011c), suggests that body size of *Theba* was in part influenced by humidity. Interestingly, both *Theba* species did not only decline in size throughout time, but maintained a constant morphometric distance from one other at various last glacial age-intervals (Fig. 11A). This finding also reflects that interspecific competition occurred through the Quaternary between these two species (Huntley *et al.*, 2008).

Huntley *et al.* (2008) tested if limiting similarity was an ecological process preserved in deep time through the evaluation of: 1) ecological character displacement (= similar species differ in size to reduce competition in sympatry while differences are minimal in allopatry) and 2) community wide character displacement (= over-dispersion of size between competitors in an assemblage). The morphometric results suggested that limiting similarity could not be fully demonstrated at all age-intervals and accordingly, Huntley *et al.* (2008) concluded that limiting similarity seems to be a temporary ecological phenomenon rather than a long-term evolutionary process. Moreover, personal unpublished data indicate that *Theba* density (i.e., the number of shells per volume of sediment) in Quaternary eolian deposits from northern Fuerteventura generally correlated negatively with body size at three different ontogenetic stages examined (Fig. 12A–B). This negative relationship suggests that shell size of *Theba* was also partially driven by intra-specific competition during the Quaternary, as observed in many animal groups, including land snails (Perry and Arthur, 1991).

Caveats and future directions in fossil land snail investigations

Published records reveal that aminoacid racemisation is a valuable method to estimate the age of Quaternary land snail shells (e.g., Goodfriend, 1992; Hearty, 2003; Hearty and Kaufman, 2009). However, careful attention should be taken when choosing the appropriate radiometric technique to calibrate the method, and if possible, multiple dating techniques may be used jointly and compared (e.g., Mylroie, 2008). Several studies have attempted to estimate the age of the Quaternary eolian deposits of the eastern Canary Islands by dating land snail shells. For example, Hillaire-Marcel *et al.*, (1995) dated shells from an eolian succession in Lanzarote using the U-series method combined with aminoacid racemisation and radiocarbon dating. Their findings revealed that fossil land snails ranged in age from ~41 kyr in the bottom of the section to ~27 kyr in the top of the deposit. Thereafter, Ortiz *et al.* (2006) analyzed a large number of fossil shells using aminoacid racemisation calibrated against radiocarbon. Their results suggested that Quaternary land snails from the easternmost islands ranged in age from ~55.7 kyr to ~4.6 kyr. The geochronological context of these Quaternary eolian deposits is however controversial because recent studies suggest that the eolian deposits in which shells are preserved are considerably older based on TL, ESR and OSL dating (Meco *et al.*, 2006; 2011; Suchodoletz *et al.*, 2008; 2012). Thus, it is likely that some Quaternary land snail shells from the eastern Canary Islands are older than those estimated by Hillaire-Marcel *et al.* (1995) and Ortiz

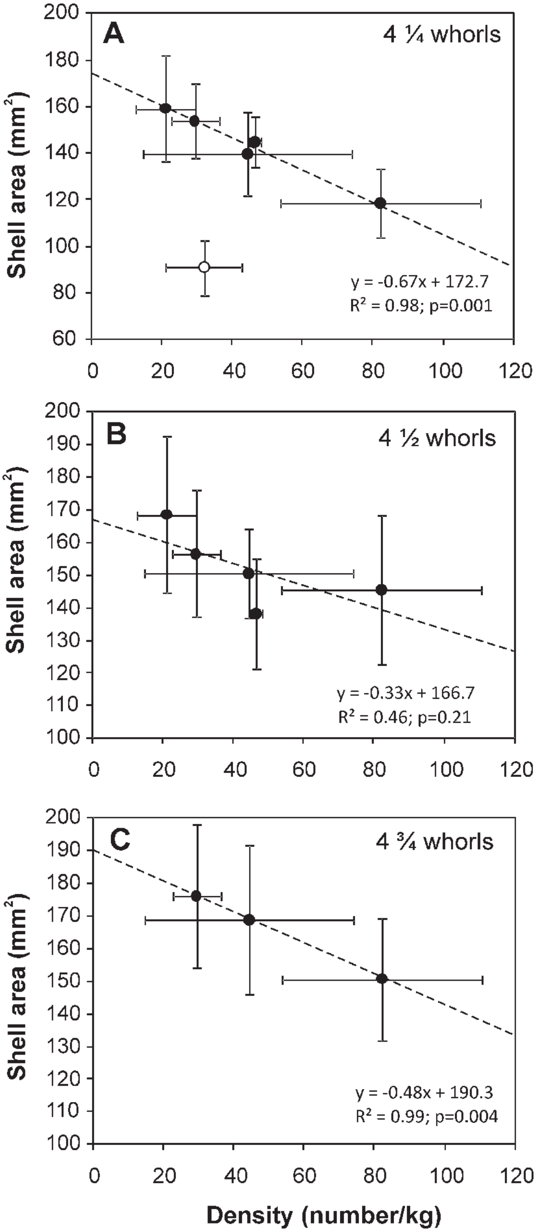

Figure 12. Body size (=area of the dorsal view of the shell) of Quaternary *Theba geminata* shells from northern Fuerteventura plotted against density of *Theba* specimens (number of shells/kg). A. Shells with 4 1/4 whorls spires. B. Shells with 4 1/2 whorl spires. C. Shells with 4 3/4 whorl spires.

et al. (2006). The controversial results suggest that 1) multiple age-dating techniques should probably be combined to estimate the age of the fossil assemblage; 2) radiocarbon dating is only adequate for younger (latest glacial-Holocene) shell assemblages and should not be employed to date all fossil shell beds of the eastern Canary Islands; and 3) in future studies, aminoacid racemisation data from the eastern Canary Islands may be calibrated with other methods besides radiocarbon dating, like OSL method. Hence, it is advisable to revise and improve the geochronological context of Quaternary eolianites from the eastern Canary Islands using different methods in addition to radiocarbon dating.

Personal field observations over years in the eastern Canary Islands suggest that, apart from a few dominant and highly abundant taxa, most land snail species exhibit patchy distributions associated with specific microclimates. This is also reflected in the Quaternary fossil record. We have observed that a single taxon may change its degree of abundance or even disappear within the same stratigraphic horizon or age-interval at other locales. Accordingly, palaeoenvironmental and/or geochronological inferences derived from the presence/absence of species alone may not be adequate and requires careful assessments. In addition, multiple laterally-separate sample replicates from the same shell bed should be collected when possible to gather representative data of the target fossil assemblage.

Comparative taphonomy studies on Quaternary land snails from the Canary Islands revealed that buried shell assemblages were not strongly biased by post-mortem processes (Yanes *et al.*, 2008b; 2011a). Nevertheless, live-dead fidelity studies (=taxonomic comparisons of living and death assemblages) on land snails from the Canary Islands and other Macaronesian archipelagos have not been achieved. This type of study is ideal because the death assemblage, which has already experienced some post-mortem processes, can be directly compared taxonomically with the living community (Rundell and Cowie, 2003; Yanes, 2012a, 2012b).

Land snail diversity, abundance, geographical distribution and shell size of Quaternary land snails from the eastern Canary Islands seem to have been affected by humidity, island area and intra- and interspecific competition (Yanes, 2003; 2005; Huntley *et al.*, 2008; Yanes *et al.*, 2011a; 2011c). However, other factors not studied here (e.g., soil carbonate content, soil chemical properties, predation pressure, diseases, anthropogenic disturbances, etc.) may also account for some of the observed patterns and remain to be evaluated in present and ancient ecosystems of the archipelago. Studies of living snail assemblages from the Canary Islands along environmental, ecological and urban to rural gradients are uncommon in the published literature (but see Yanes *et al.*, 2009). Apart from Madeira (e.g., Cook *et al.*, 1993; Goodfriend *et al.*, 1994; 1996; Cameron and Cook, 1999; Cameron *et al.*, 2006), these kinds of studies on snail assemblages are also rare in other Macaronesian archipelagos. Besides paleontological sites, archaeological sites may contain ancient land snail shells. In particular, late Holocene shell middens from the Canary Islands often comprise land snail shells preserved jointly with sea shells, bones, and/or other archaeological artefacts. Such archaeological material remains to be studied as well.

Many published studies have manifestly demonstrated over decades that the carbon and oxygen stable isotope composition of fossil land snail shells are complex although valuable retrospective environmental archives (e.g., Balakrishnan and Yapp, 2004). But besides light stable isotopes, other geochemical approaches have not been tested in a rigorous manner in land snails. For example, nitrogen stable isotopes of shell organic matrix, clumped isotopes, heavy stable isotopes, and minor and trace elements (including heavy metals). Hence, the environmental significance of other, less commonly studied, geochemical proxies remain to be evaluated meticulously in modern and fossil land snails.

CONCLUSIONS

Shelly assemblages buried in carbonate-rich semiarid sites from the eastern Canary Islands exhibit a good preservation degree and high ecological fidelity despite variable scales of taphonomic alteration and centennial to multimillennial time-averaging. Carbon stable isotope values of fossil land snail shells reflect that the proportion of C_4 plants increased during various glacial intervals associated with lower atmospheric CO_2 levels. Oxygen stable isotope values of the shell suggest that the last glacial climate was noticeably wetter and cooler while conditions became gradually drier and warmer throughout the Holocene, culminating in the current semiarid conditions. Land snail abundance, diversity and body size of some species seem to have declined from ~42.5 ka to ~5.1 ka in the islets to the north of Lanzarote Island. The geographical distribution of some species was noticeably wider and occupied coastal sites whereas today, they are restricted to the highest and wettest parts of the islands. Two-congeneric species maintained a constant morphometric distance from each other across age-intervals, which points to maintained inter-specific competition through time. The decrease in land snail diversity, body size and geographical distribution may have been caused, at least partially, by a parallel gradual increase in aridity and a decrease in island area from the last glacial to the present.

Some important caveats and recommendations that may be considered when studying fossil land snails include: 1) multiple age dating techniques should probably be combined to determine accurate ages of shelly assemblages; 2) presence/absence of snail species may not be adequate to infer palaeoenvironmental conditions and the geochronological context alone; 3) multiple bulk sample replicates from the same shell bed should be collected when possible; 4) snail body size fluctuations through time appear to be caused by multiple ecological and environmental factors operating jointly rather than one; 5) modern analogues of the study locale are essential to better comprehend local fossil assemblages; and

6) carbon and oxygen stable isotope values of land snails are better understood if explored using simple mass balance equations and flux balance models.

The Macaronesian archipelagos are relatively rich in terrestrial malacofaunas and many islands also contain rich accumulations of fossil shells preserved in diverse paleontological and archaeological sites. These fossil shelly assemblages are yet poorly studied and may help to reconstruct Quaternary terrestrial ecosystems of the Macaronesian region. In this study we illustrated that fossil land snail assemblages preserved in oceanic islands are valuable retrospective proxies of ancient terrestrial ecosystems, especially when studied in a multidisciplinary manner combining disparate data from different techniques.

ACKNOWLEDGEMENTS

The Spanish Ministry of Economía y Competitividad grant CGL2011-29898/BTE to Y.Y. funded this study. Special thanks go to many scientists who have collaborated (or collaborate) on the described research line here, including (in no particular order) Dominik Faust (University of Dresden), Crayton J. Yapp (Southern Methodist University), Christopher S. Romanek (University of Kentucky), Michał Kowalewski (University of Florida and Florida Museum of Natural History), John W. Huntley (University of Missouri), Antonio Delgado (CSIC), Julio Aguirre (Universidad de Granada), Adam Tomašových (Slovak Academy of Sciences), and José Eugenio Ortiz and Trinidad de Torres (ETSIM-UPM). Additional thanks go to John W. Huntley who kindly reviewed this manuscript and provided thoughtful comments.

REFERENCES

Alonso, M.R., Groh, K. and Ibáñez, M. (1992) *Sculptiferussacia clausiliaeformis* n. sp. (Gastropoda Pulmonata: Ferussaciidae) de Fuerteventura (Islas Canarias). *Bollettino Malacologico*, 22, 35–46.

Alonso, M.R., Ponte-Lira, C.E., Castillo, C., Yanes, Y., Groh, K. and Ibáñez, M. (2006) A new *Canariella* species (Gastropoda: Helicoidea: Hygromiidae) of the new subgenus *Majorata*, both endemic to the Jandía peninsula (Fuerteventura, Canary Islands). *Zootaxa*, 1316, 45–56.

Aubry, S., Labaune, C., Magnin, F., Roche, P. and Kiss, L. (2006) Active and passive dispersal of an invading land snail in Mediterranean France. *Journal of Animal Ecology*, 75, 802–813.

Balakrishnan, M. and Yapp, C.J. (2004) Flux balance model for the oxygen and carbon isotope compositions of land snail shells. *Geochimica Cosmochimica Acta*, 68, 2007–2024.

Behrensmeyer, A.K., Kidwell, S.M. and Gastaldo, R.A. (2000) Taphonomy and paleobiology, *Paleobiology*, 26, 103–147.

Cameron, R.A.D. and Cook, L.M. (1999) Land snail faunas of the Deserta Islands, Madeiran Archipelago, past and present. *Journal of Conchology*, 36, 1–15.

Cameron, R.A.D., Cook, L.M., Goodfriend, G.A. and Seddon, M.B. (2006) Fossil land snail faunas of Porto Santo, Madeiran Archipelago: Change and stasis in Pleistocene to recent times. *Malacologia*, 49, 25–59.

Chiba, S. (2007) Species richness patterns along environmental gradients in island land molluscan fauna. *Ecology*, 88, 1738–1746.

Cook, M.L., Goodfriend, G.A. and Cameron, R.A.D. (1993) Changes in the land snail fauna of Eastern Madeira during the Quaternary. *Philosophical Transactions: Biological Sciences*, 339, 83–103.

Cowie, R.H. (1992) Evolution and extinction in Partulidae, endemic Pacific island land snails. *Philosophical Transactions: Biological Sciences*, 335, 167–191.

Cowie, R.H. (1995) Variation in species diversity and shell shape in Hawaiian land snails: In situ speciation and ecological relationships. *Evolution*, 49, 1191–1202.

Damnati, B., Petit-Maire, N., Fontugne, M., Meco, J. and Williamson, D. (1996) Quaternary paleoclimates in the eastern Canary Islands. *Quaternary International*, 31, 37–46.

DORTA, P. (2005) El clima. *Patrimonio natural de la isla de Fuerteventura* (ed. by RODRÍGUEZ-DELGADO, O.), pp. 81–89. Cabildo de Fuerteventura, Gobierno de Canarias, Centro de la Cultura Popular Canaria, Islas Canarias.

GARCÍA-TALAVERA, F. (1999) La Macaronesia. Consideraciones geológicas, biogeográficas y paleoecológicas. Ecología y Cultura en Canarias (ed. by J.M. FERNÁNDEZ-PALACIOS, J.J. BACALLADO and J.A. BELMONTE), pp. 39–63. Organismo Autónomo de Museos y Centros. Cabildo Insular de Tenerife, Santa Cruz de Tenerife.

GASSE, F. (2000) Hydrological changes in the African tropics since the Last Glacial Maximum, *Quaternary Science Reviews*, 19, 189–211.

GASSE, F., CHALIE, F., VINCENS, A., WILLIAMS, M.A.J. and WILLIAMSON, D. (2008) Climatic patterns in equatorial and southern Africa from 30,000 to 10,000 years ago reconstructed from terrestrial and near-shore proxy data. *Quaternary Science Reviews*, 27, 2316–2340.

GOODFRIEND, G.A. (1986) Variation in land snail shell form and size and its causes: a review. *Systematic Zoology*, 35, 204–223.

GOODFRIEND, G.A. (1992) Rapid racemization of aspartic acid in mollusk shells and potential for dating over recent centuries. *Nature*, 357, 399–401.

GOODFRIEND, G.A. and ELLIS, G.L. (2000) Stable carbon isotope record of middle to late Holocene climate changes from land snail shells at Hinds Cave. Texas. *Quaternary International*, 67, 47–60.

GOODFRIEND, G.A. and ELLIS, G.L. (2002) Stable carbon and oxygen isotope variations in modern *Rabdotus* land snail shells in the southern Great Plains, USA, and their relation to environment. *Geochimica Cosmochimica Acta*, 66, 1987–2002.

GOODFRIEND, G.A., CAMERON, R.A.D. and COOK, L.M. (1994) Fossil evidence of recent human impact on the land snail fauna of Madeira. *Journal of Biogeography*, 21, 309–320.

GOODFRIEND, G.A., CAMERON, R.A.D., COOK, L.M., COURTY, M.A., FEDOROFF, N., LIVETT, E. and TALLIS, J. (1996) The Quaternary eolian sequence of Madeira: stratigraphy, chronology, and paleoenvironmental interpretation. *Palaeogeography, Palaeoclimatology, Palaeoecology*, 120, 195–234.

GREVE, C., HUTTERER, R., GROH, K., HAASE, M. and MISOF, B. (2010) Evolutionary diversification of the genus *Theba* (Gastropoda: Helicidae) in space and time: A land snail conquering islands and continents. *Molecular Phylogenetics and Evolution*, 57, 572–584.

GREVE, C., GIMNICH, F., HUTTERER, R., MISOF, B. and HAASE, M. (2012) Radiating on oceanic islands: Patterns and processes of speciation in the land snail genus *Theba* (Risso 1826). *PLoS ONE*, 7, e34339. DOI:10.1371/journal.pone.0034339.

HAUSDORF, B. (2006) Is the interspecific variation of body size of land snails correlated with rainfall in Israel and Palestine? *Acta Oecologica*, 30, 374–379.

HEARTY, P.J. (2003) Stratigraphy and timing of eolianite deposition on Rottnest Island, Western Australia. *Quaternary Research*, 60, 211–222.

HEARTY, P.J. and KAUFMAN, D.S. (2009) A *Cerion*-based chronostratigraphy and age model from the central Bahama Islands: Amino acid racemization and ^{14}C in land snails and sediments. *Quaternary Geochronology*, 4, 148–159.

Hillaire-Marcel, C., Ghaleb, B., Gariépy, C., Zazo, C., Hoyos, M. and Goy, J.L. (1995) U-series dating by the TIMS technique of land snails from paleosols in the Canary Islands. *Quaternary Research,* 44, 276–282.

Holyoak, G.A., Holyoak, D.T., Yanes, Y., Alonso, M.R. and Ibáñez, M. (2011) Taxonomic revision, habitats and biogeography of the land snail family Discidae (Gastropoda: Pulmonata) in the Canary Islands. *Journal of Conchology*, 40, 583–603.

Huntley, J.W., Yanes, Y., Kowalewski, M., Castillo, C., Delgado-Huertas, A., Ibáñez, M., Alonso, M.R., Ortiz, J.E. and Torres, T. (2008) Testing limiting similarity in Quaternary terrestrial gastropods. *Paleobiology*, 34, 378–388.

Ibáñez, M. and Alonso, M.R. (2001) La extinción reciente de la malacofauna endémica en Tenerife y Gran Canaria. *Estudios Canarios (Anuario del Instituto de Estudios Canarios)*, 45, 9–22.

Ibáñez, M., Siverio, F., Alonso, M.R. and Ponte-Lira, C.E. (2006) Two *Canariella* species (Gastropoda: Helicodea: Hygromiidae) endemic to the Northwest Tenerife (Canary Islands). *Zootaxa,* 1258, 33–45.

Ibáñez, M., Alonso, M.R., Yanes, Y., Castillo, C. and Groh, K. (2007) Presence of the genus *Napaeus* (Gastropoda: Pulmonata: Enidae) living in all the islands of the Canarian archipelago: *Napaeus lichenicola* sp. nov. from Fuerteventura island. *Journal of Conchology,* 39, 381–389.

Kerney, M.P. and Cameron, R.A.D. (1979) *A field guide to the land snails of Britain and North-West Europe.* Collins, London.

Kidwell, S.M. and Flessa, K.W. (1996) The Quality of the fossil record: Populations, species, and communities. *Annual Reviews in Earth and Planetary Sciences*, 24, 433–464.

Koch, P.L., Diffenbaugh, N.S. and Hoppe, K.A. (2004) The effects of late Quaternary climate and pCO_2 change on C_4 plant abundance in the south-central United States. *Palaeogeography, Palaeoclimatology, Palaeoecology*, 207, 331–357.

Kowalewski, M. and Bambach, R.K. (2003) The limits of paleontological resolution. *High resolution approaches in stratigraphic paleontology: Topic in geobiology series* /ed. by Harries, P.J.) pp. 1-48. Plenum Press/Kluwer, New York.

Marui, Y., Chiba, S., Okuno, J. and Yamasaki, K. (2004) Species-area curve for land snails on Kikai Island in geological time. *Paleobiology*, 30, 222–230.

Meco, J., Ballester, J., Betancort, J.F., Scaillet, S., Guillou, H., Carracedo, J.C., Lomoschitz, A., Petit-Maire, N., Ramos, A.J.G., Perera, N. and Meco, J.M. (2006) *Paleoclimatología del Neógeno en las Islas Canarias. Geliense, Pleistoceno y Holoceno.* Ministerio de Medio Ambiente, Universidad de Las Palmas de Gran Canaria.

Meco, J., Muhs, D.R., Fontugne, M., Ramos, A.J.G., Lomoschitz, A. and Patterson, D. (2011) Late Pliocene and Quaternary Eurasian locust infestations in the Canary Archipelago. *Lethaia*, 44, 440–454.

Moine, O. and Rousseau, D.D. (2002) Mollusques terrestres et temperatures: une nouvelle function de transfert quantitative. *Comptes Rendus Palevol,* 1, 145–151.

Moine, O., Rousseau, D.D., Jolly, D. and Vianey-Liaud, M. (2002) Paleoclimatic reconstruction using mutual climatic range on terrestrial mollusks. *Quaternary Research,* 57, 162–172.

Mylroie, J.E. (2008) Late Quaternary sea-level position: Evidence from Bahamian carbonate deposition and dissolution cycles. *Quaternary International,* 183, 61–75.

Navarro-Mederos, J.F. (1983) El poblamiento humano de Canarias. *Canarias, origen y poblamiento* (ed. by Báez, M., Bravo, T. and Navarro-Mederos, J.F.), pp 85–96. Círculo de Estudios Sociales de Canarias, Madrid.

Neiber, M.T., Vega-Luz, R. and Koenemann, S. (2011) *Hemicycla* (*Adiverticula*) *diegoi* (Gastropoda: Pulmonata: Helicidae), a new species from Tenerife, Canary Islands, with a phylogenetic analysis of conchologically similar species in the genus *Hemicycla* Swainson, 1840. *Zootaxa,* 2757, 29–46.

Núñez, L. and Núñez, J. (2010) Mollusca. *Lista de especies silvestres de Canarias. Hongos, plantas y animales terrestres* (ed. by Arechavaleta, M., Rodríguez, S., Zurita, N. and García, A.), pp 182–189. Gobierno de Canarias, Santa Cruz de Tenerife.

Ortiz, J.E., Torres, T., Yanes, Y., Castillo, C., De la Nuez, J., Ibáñez, M. and Alonso, M.R. (2006) Climatic cycles inferred from the aminostratigraphy and aminochronology of Quaternary dunes and palaeosols from the eastern islands of the Canary Archipelago. *Journal of Quaternary Science,* 21, 287-306.

Perry, R. and Arthur, W. (1991) Shell size and population density in large helicid land snails. *The Journal of Animal Ecology,* 60, 409–421.

Rundell, R.J. and Cowie, R.H. (2003) Preservation on species diversity and abundances in Pacific Island land snail death assemblages. *Journal of Conchology,* 38, 155–169.

Scholz, S. (2005) Las plantas vasculares. Catálogo Florístico. *Patrimonio natural de la isla de Fuerteventura* (ed. by Rodríguez-Delgado, O.), pp. 241-280. Cabildo de Fuerteventura, Gobierno de Canarias, Centro de la Cultura Popular Canaria, Islas Canarias.

Speiser, B. (2001) Food and Feeding Behavior. *The biology of terrestrial mollusk* (ed. by Barker, G.M.), pp 259–288. CABI publishing, UK.

Stott, L.D. (2002) The influence of diet on the δ^{13}C of shell carbon in the pulmonate snail *Helix aspersa. Earth and Planetary Science Letters,* 195, 249–259.

Suchodoletz, H. von, Fuchs, M. and Zöller, L. (2008) Dating Saharan dust deposits on Lanzarote (Canary Islands) by luminescence dating techniques and their implication for palaeoclimate reconstruction of NW Africa. *Geochemistry, Geophysics, and Geosystems,* 9, doi: 10.1029/2007GC001658.

Suchodoletz, H. von, Oberhänsli, H., Hambach, U., Zöller, L., Fuchs, M. and Faust, D. (2010) Soil moisture fluctuations in Saharan dust deposits on Lanzarote (Canary Islands) during the last 180 ka controlled by high latitude processes – the effects of precipitation variability versus temperature fluctuations. *Quaternary Science Reviews,* 29, 2173–2184.

Suchodoletz, H. von, Blanchard, H., Hilgers, A., Radtked, U., Fuchs, M., Dietze, M. and Zöller, L. (2012) TL and ESR dating of Middle Pleistocene lava flows on Lanzarote island, Canary Islands (Spain). *Quaternary Geochronology,* 9, 54–64.

TOMAŠOVÝCH, A. (2006) Linking taphonomy to community-level abundance: Insights into compositional fidelity of the Upper Triassic shell concentrations (Eastern Alps). *Paleogeography, Palaeoclimatology, Palaeoecology*, 235, 355–381.

WILLIAMSON, D., JACKSON, M., BANERJEE, S.K. and PETIT-MAIRE, N. (2004) The magnetism of a glacial aeolianite sequence from Lanzarote (Canary Islands): coupling between luvic calcisol formation and Saharan dust trapping processes during wet deposition events off northwestern Sahara. *Geophysical Journal International*, 157, 1090–1104.

YANES, Y. (2003) Estudio paleobiológico de las asociaciones de gasterópodos terrestres de los Islotes al norte de Lanzarote. M.S. Thesis, Universidad de La Laguna, La Laguna.

YANES, Y. (2005) Estudio paleobiológico de las asociaciones de gasterópodos terrestres de las islas orientales del Archipiélago Canario. Ph.D. Thesis, Universidad de La Laguna, La Laguna.

YANES, Y. (2012a) Shell taphonomy and fidelity of living, dead, Holocene and Pleistocene land snail assemblages. *Palaios*, 27, 127–136.

YANES, Y. (2012b) Anthropogenic effect recorded in the live-dead compositional fidelity of land snails from San Salvador Island (Bahamas). *Biodiversity and Conservation*, 21, 3445-3466.

YANES, Y., KOWALEWSKI, M., ORTIZ, J.E., CASTILLO, C., TORRES, T. and NUEZ, J. (2007) Scale and structure of time-averaging (age mixing) in terrestrial gastropod assemblages from Quaternary eolian deposits of the eastern Canary Islands. *Palaeogeography, Palaeoclimatology, Palaeoecology*, 251, 283–299.

YANES, Y., DELGADO, A., CASTILLO, C., ALONSO, M.R., IBÁÑEZ, M., DE LA NUEZ, J. and KOWALEWSKI, M. (2008a) Stable isotope (δ^{18}O, δ^{13}C, and δD) signatures of recent terrestrial communities from a low-latitude, oceanic setting: endemic land snails, plants, rain, and carbonate sediments from the eastern Canary Islands. *Chemical Geology*, 249, 377–392.

YANES, Y., TOMAŠOVÝCH, A., KOWALEWSKI, M., CASTILLO, C., AGUIRRE, J., ALONSO, M.R. and IBÁÑEZ, M. (2008b) Taphonomy and compositional fidelity of Quaternary fossil assemblages of terrestrial gastropods from carbonate-rich environments of the Canary Islands. *Lethaia*, 41, 235–256.

YANES, Y., ROMANEK, C.S., DELGADO, A., BRANT, H.A., NOAKES, J.E., ALONSO, M.R. and IBÁÑEZ, M. (2009) Oxygen and carbon stable isotopes of modern land snail shells as environmental indicators from a low-latitude oceanic island. *Geochimica et Cosmochimica Acta*, 73, 4077–4099.

YANES, Y., AGUIRRE, J., ALONSO, M.R., IBÁÑEZ, M. and DELGADO, A. (2011a) Ecological fidelity of Pleistocene-Holocene land snail shell assemblages preserved in carbonate-rich paleosols. *Palaios*, 26, 406–419.

YANES, Y., SANTANA, J., ARTILES, M., DENIZ, F., MARTÍN, J., ALONSO, M.R. and IBÁÑEZ M. (2011b) Five new *Napaeus* species (Gastropoda: Pulmonata: Enidae) from Gran Canaria and El Hierro (Canary Islands). *Zootaxa*, 2901, 35–51.

Yanes, Y., Yapp, C.J., Ibáñez, M., Alonso, M.R., De la Nuez, J., Quesada, M.L., Castillo, C. and Delgado, A. (2011c) Pleistocene-Holocene environmental change in the Canary Archipelago as inferred from stable isotopes of land snail shells. *Quaternary Research*, 65, 658–669.

Yanes, Y., Gutiérrez-Zugasti, I. and Delgado, A. (2012) Late glacial-Holocene transition in northern Spain deduced from terrestrial gastropod shelly accumulations. *Quaternary Research*, 78, 373–385.

Yanes, Y., García-Alix, A., Asta, M.P., Ibáñez, M., Alonso, M.R. and Delgado, A. (2013) Late Pleistocene-Holocene environmental conditions in Lanzarote (Canary Islands) inferred from calcitic and aragonitic land snail shells and bird bones. *Palaeogeography, Palaeoclimatology, Palaeoecology*, 378, 91–102.

PAST VEGETATION DYNAMICS TO INFER HOLOCENE CLIMATE CHANGES IN TENERIFE AND LA GOMERA, CANARY ISLANDS

Sandra Nogué, Lea de Nascimento, José María Fernández-Palacios,
Kathy J. Willis

CLIMATE CHANGE PERSPECTIVES FROM THE ATLANTIC:
PAST, PRESENT AND FUTURE

Jose María Fernández-Palacios, Lea de Nascimento, José Carlos Hernández,
Sabrina Clemente, Albano González & Juan P. Díaz-González (eds.)
Servicio de Publicaciones, Universidad de La Laguna – 2013

ISBN: 978-84-15910-54-1 pp. 235-241

ABSTRACT

Oceanic islands in the low latitudes, such as the Canary Islands, are generally considered to have been well buffered from the climate change of the Quaternary period. However, questions remain about whether past climatic changes on Atlantic islands are synchronous with those occurring in Africa and the Mediterranean coast or if the climate remained stable during the Holocene. Here we used fossil pollen and charcoal time series on Tenerife and La Gomera in order to: 1) provide the first inter-island picture of vegetation dynamics through the last 9600 years of this important biodiverse region of Europe; 2) detect the vegetation sensitivity, mainly tree communities, to past climatic changes; and, 3) provide evidence for human-induced changes at this potentially highly informative point. Preliminary analyses suggest very little climatic change during the period 4000 years to present, but this requires confirmation by reference to additional coring sites. In La Gomera, we found strong evidence of a shift towards drier conditions at around 5500 years ago. The general vegetation pattern observed was a decrease in hygrophilous trees (Canarian palm and willow) and an expansion of *Morella-Erica* woody heath. Our results provide the first evidence to suggest that the general Northern Africa and Mediterranean shift towards drier conditions may be traced in the Canary Islands.

KEYWORDS: fire, island ecology, key species, palaeoecology, palaeoclimate, pollen fossil.

INTRODUCTION

Currently, a high number of environmental assessments (e.g. Millennium Ecosystem Assessment, 2003; IPCC report, 2007) have been highlighting the importance of understanding the sensitivity of vegetation to changes in the environment. In this context, oceanic islands are of particular interest as some of them (mainly small islands) have been identified as vulnerable to the adverse impacts of climate change (e.g. Pacific Islands) (Mimura *et al.*, 2007).

In general, islands offer an opportunity to detect major past climatic changes, without influence from anthropogenic impacts as they are considered to be among the latest regions to be colonized by humans. For instance, according to palaeoclimatic results, high-latitude islands (e.g. Arctic islands) have been the most affected by climatic oscillations while low-latitude oceanic islands (e.g. Eastern Island, Galápagos) have been considered well buffered from past climate changes. This is being challenged by fossil pollen time series in tropical and subtropical islands which have shown evidence of the effects of past global climate changes upon the local (isolated) vegetation (Whittaker and Fernández-Palacios, 2007).

The Macaronesian archipelagos (Azores, Madeira, Selvagens, Canary Islands, and Cape Verde) stand out as an interesting biogeographical region to study the climatic history and vegetation sensitivity to the changing environment. In the Canary Islands, palaeoecological reconstructions based on pollen fossil are scarce (but see de Nascimento *et al.*, 2009; Nogué *et al.*, 2013) in comparison to the nearby continental regions (Carrión *et al.*, 2010 and references therein). This is because of the limited availability of sites, mainly due to the volcanic nature of the sediments and the lack of permanent water bodies. Moreover, eastern islands (Lanzarote, Fuerteventura, and Gran Canaria) have been more frequently studied than the western islands (Tenerife, La Gomera, La Palma, and El Hierro) thanks to the existence of Quaternary deposits with good profiles for fossil and sediment analysis (Damnati, 1996; Lomoschitz *et al.*, 2002; Meco *et al.*, 2010; Suchodoletz *et al.*, 2010; Yanes *et al.*, 2011).

Main plant communities in the Canaries are distributed along an altitudinal gradient associated with different climatic zones (Fernández-Palacios and de Nicolás, 1995; del Arco *et al.*, 2010). Vegetation units from coast to peak are: coastal shrubland, thermophilous woodland, evergreen laurel forest, pine forest and summit scrub. Depending on the island's elevation and aspect (windward and leeward) some communities might be absent. The incidence of trade winds, on those windward slopes which are high enough for cloud banks formation (usually around 800–1500 m above sea level – a.s.l.), is considered to be a key element for the existence of the evergreen laurel forest (Höllermann, 1981; Ritter *et al.*, 2009). Therefore, changes in distribution and intensity of the cloud belt due to future changes in climate may compromise the future of the laurel forest (Sperling *et al.*, 2004; Martín *et al.*, 2012).

In this study we reviewed the fossil pollen and microscopic charcoal of two sites in La Gomera and Tenerife, to determine the long-term vegetation and fire history of the western Canary Islands. We also analysed the sensitivity of four key taxa from different Canarian forests: hygrophilous species (*Phoenix canariensis* and *Salix canariensis*), *Carpinus*, *Quercus*, and the *Morella-Erica* heath (*Morella faya* and *Erica sp.*). We aim to provide the first inter-island review of the past vegetation dynamics and climatic history of this important biodiverse region of Europe and to detect the vegetation sensitivity, mainly that of tree communities, to past climatic changes.

MATERIAL AND METHODS

Two former lagoons in the Canary Islands

In this chapter, we describe the results of two former lakes in the Islands of Tenerife and La Gomera (Table 1).

TABLE 1. Information of the main characteristics of the studied sites.

	La Laguna	Laguna Grande
Island	Tenerife	La Gomera
Coordinates	28˚ 29´ N, 16˚ 19´ W	28° 07´ N, 17° 15´ W
Height (m a.s.l.)	560	1250
Mean annual precipitation (mm)	550	650
Mean annual temperature (ºC)	16	13.5
Main vegetation type	Cultivated lands	*Morella-Erica* woody heath with *Ilex canariensis*
Maximum age (cal. years BP)	4700	9600
Number of zones (zonation method)	3	2
Significant vegetation transitions (cal. years BP)	2900; 2000	5500
Reference	de Nascimento *et al.*, 2009	Nogué *et al.*, 2013

The former lagoon of La Laguna (Fig. 1), in Tenerife (28˚ 29' N, 16˚ 19' W; 560 m a.s.l.) was mapped by Torriani in the XVI century and was calculated to cover a surface area of 27 ha (Criado, 2002). The mean annual precipitation is about 550 mm and the mean annual temperature is 16˚ C. Due to intensive land-use over the last centuries the vegetation of the basin is largely agricultural with the monteverde from the Anaga massif, at 3 km to the northeast, forming the closest natural forest. This forest is mainly composed by *Morella-Erica* woody heath; although some well-preserved stands of laurel forest are also present (del Arco *et al.*, 2006).

Laguna Grande (28° 07' N, 17° 15' W; 1250 m a.s.l.), located in the National Park of Garajonay in La Gomera (Fig. 1), originated in the basin of an old crater with a total surface area of 3 ha (Rodríguez-Rodríguez *et al.*, 2009). Mean annual precipitation is 625 mm, although it can be doubled by water condensation, and mean annual temperature is 13.5° C (Marzol and Sánchez, 2009). Its position in the upper boundary of the sea cloud belt determines the presence of different forest types around the basin. Above 1300 m a.s.l. the forest is dominated by *Morella faya* typically found in cooler summits and surpassing towards southern slopes where the effect of trade winds stops during the summer. Below this altitude on windward humid slopes is located the laurel forest where the most common trees are from the Lauraceae family (del Arco *et al.*, 2006). Laguna Grande was used in the past as a crossroads and there is no evidence of agricultural uses in the area (Navarro, 2009).

Both lagoons are nowadays subjected to temporal flooding during the rainy season, although La Laguna was artificially channelled 240 years ago (Table 1).

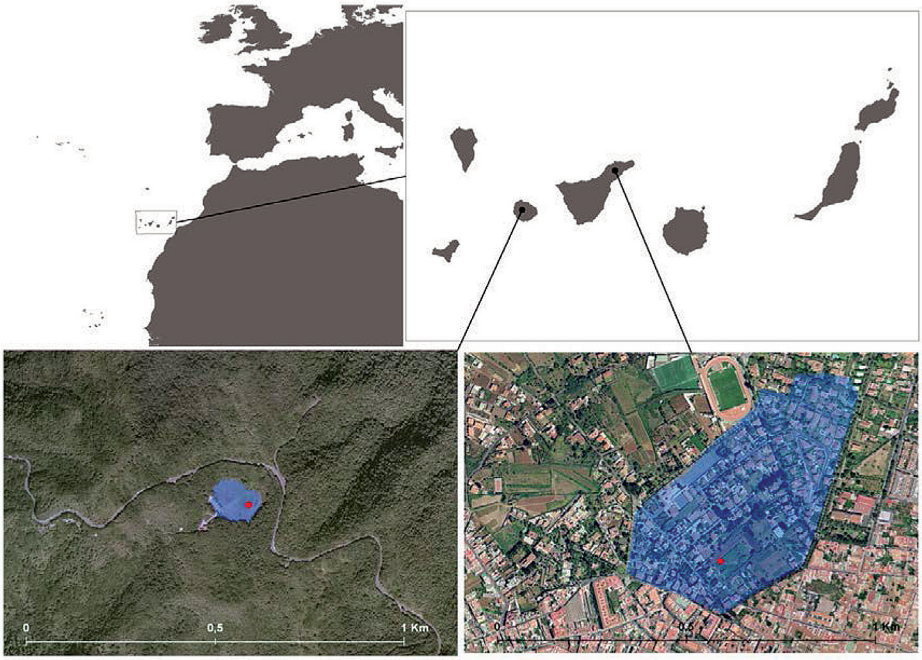

Figure 1. Study sites

Palaeoecological methods

The sedimentary sequences were taken using a modified Livingstone piston corer and wireline drilling technology and transported and stored at the Long-term Ecology Laboratory at the University of Oxford (UK), and the «Instituto Universitario de Enfermedades Tropicales y Salud Pública de Canarias» at the University of La Laguna (Spain). To reconstruct the vegetation dynamics of both sequences we followed the standard procedure, involving sub-sampling and processing the samples (Bennett and Willis, 2001). We then, identified pollen and spores using Reille (1992; 1995; 1998) and the reference collection of the Long-term Ecology Laboratory. We also reconstructed regional fire through the measurement of micro-charcoal (<150 µm; cm^2/cm^3) following standard procedures (Clark, 1982; Whitlock and Larsen, 2001). Three and six samples from La Laguna and Laguna Grande respectively, were dated using ^{14}C Accelerator Mass Spectrometry carried out at different laboratories.

In this chapter we summarized the pollen time-series for four key taxa: hygrophilous species (*Phoenix canariensis* and *Salix canariensis*), *Carpinus*, *Quercus*, and the *Morella-Erica* heath (*Morella faya* and *Erica sp.*). Details of other vegetation types and the depth-age model can be found in de Nascimento *et al.* (2009), and Nogué *et al.* (2013).

MULTIVARIATE ECOLOGICAL METHODS

Results from the pollen percentage data and zonation analyses, through numerical zonation of the pollen data using optimal splitting based on information content (Bennett *et al.,* 1996), were described by de Nascimento *et al.* (2009) and Nogué *et al.* (2013). In this chapter we used these zones (Phase 1, 2, 3, and 4) and the significant vegetation transitions (I, II, III) for further analyses (Table 1, Fig. 2). We followed the methodology applied by Nogué *et al.* (2013) in La Gomera, for the Tenerife pollen data. Thus, we interpolated pollen data from La Laguna sequence at a constant time-step of 20 years and opened a time window of 200 years before and after the previously identified vegetation transition (II, III) (de Nascimento *et al.*, 2009). A window of this size should be large enough to detect any significant response to changes in climate and fire events. Significant changes in vegetation composition and abundance of taxa in this time-window were quantified using one-way permutational ANOVA (Anderson *et al.*, 2008) obtaining a *Pseudo-F* from Bray-Curtis distances and a *P*-value from a Monte Carlo test using 9999 permutations. Similarity percentages procedure (SIMPER) was used to determine the dissimilarity before and after each vegetation transition and to identify those taxa that contributed to the dissimilarity. PRIMER 6 with PERMANOVA+ software was used to perform both analyses. For more details see Nogué *et al.* (2013).

RESULTS

WHAT THE FOSSIL POLLEN DATA EXPLAIN: VEGETATION CHANGES OVER THE LAST 9600 YEARS

The long-term vegetation data presented here representes the pollen data from La Laguna Grande (La Gomera, 9600 years BP) and from La Laguna (Tenerife, 4700 years BP). Thus, the results of the first 4900 cal. years BP (9600 to 4700) are inferred from the La Gomera data alone.

In Phase 1 (9600 to 5500) hygrophilous taxa dominated (*Phoenix canariensis* and *Salix canariensis*) although decreasing towards the end of the zone. On the contrary, low values for *Morella-Erica* heath can be observed at the beginning of the sequence, followed by an increasing trend at the end of the zone (Fig. 2a). Thus, a shift from evergreen forest with presence of hygrophilous trees to an evergreen forest with *Morella faya* and *Erica sp.* occurred around 5500 years ago. During this phase there was no evidence of intense fire occurring in Garajonay (Fig. 2c). The period from 5500 to 2900 cal. years BP (Phase 2) was a flourish-

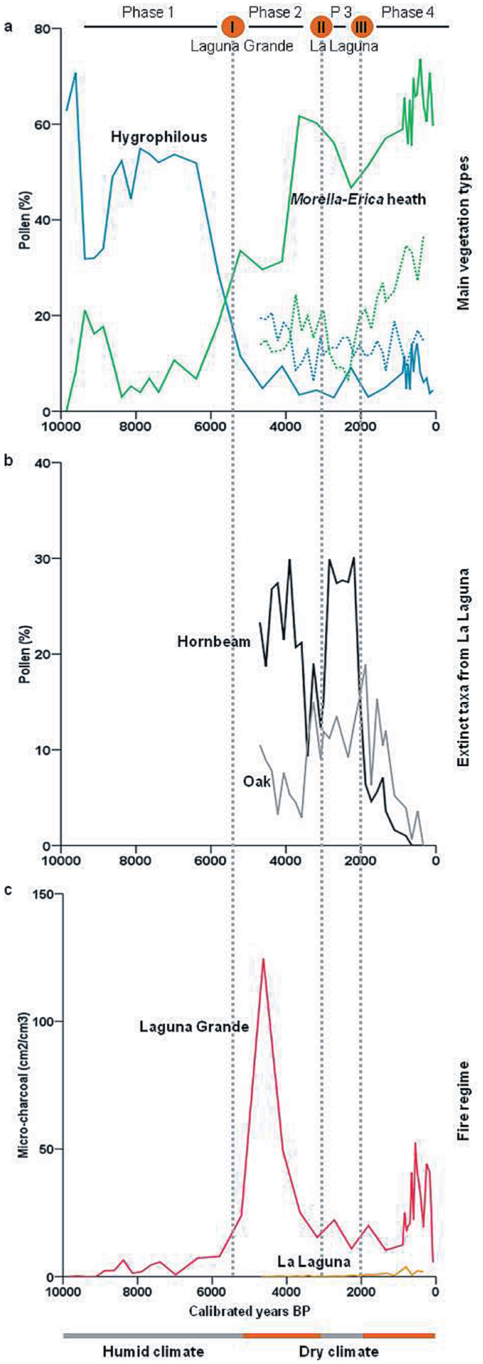

Figure 2. Pollen percentages for selected vegetation types for Laguna Grande (La Gomera) and La Laguna (Tenerife). a) *Morella-Erica* heath (green lines) and hygrophilous taxa (blue lines) for Laguna Grande (solid lines) and La Laguna (dotted lines); b) *Carpinus* (black line) and *Quercus* (grey line) for La Laguna; c) Micro-charcoal concentration (cm^2/cm^3) for Laguna Grande (red line) and La Laguna (orange line). Vertical dotted lines indicate vegetation transitions I, II, and III.

ing stage for the *Morella-Erica* heath in both sites although displaying different abundances. While in Laguna Grande (La Gomera) *Erica* sp. is very abundant, in La Laguna, the most abundant taxa are *Quercus* and *Carpinus* (taxa absent in Laguna Grande). Moreover, *Carpinus* experienced a decrease at the end of the zone and *Quercus* an increase (Fig. 2b). At the same time, hygrophilous taxa showed the minimum abundance of the entire sequence in both sites (Fig. 2a). There was a low micro-charcoal concentration for both islands with the exception of a peak in La Gomera, at 4800 cal. years BP (Fig. 2c). The next phase (Phase 3; 2900–2000 cal. years BP) is a transition zone where the *Morella-Erica* heath decreased while hygrophilous vegetation experienced a small increase (Fig. 2a). In La Laguna, *Carpinus* increased and *Quercus* remained constant (Fig. 2b). Microfossil charcoal remained low throughout all this phase (Fig. 2c). Finally, the last phase (Phase 4; 2000 cal. years BP to present) was characterized by a steep decrease of *Carpinus* and *Quercus* and an increase in *Morella-Erica* heath (Fig. 2a, 2b).

VEGETATION TRANSITIONS AND VEGETATION SENSITIVITY

In previous publications (de Nascimento *et al.*, 2009; Nogué *et al.*, 2013), three significant vegetation transition boundaries were identified. One in Laguna Grande (La Gomera) at 5500 cal. years BP (I), and two in La Laguna (Tenerife) at 2900 (II) and 2000 (III) cal. years BP, respectively (Table 1).

In La Laguna, the average dissimilarity for the vegetation transition II (2900 cal. years BP), is 15% (*Pseudo-F* = 18, *P* (MC) < 0.01). The vegetation differentiation was driven primarily by an increase of *Carpinus* (21.11%), *Quercus* (2.25%), and *Salix canariensis* (6.13%) and a decrease of *Morella faya* (8.73%) and *Phoenix canariensis* (5.73%) (Table 2). The average dissimilarity for the vegetation transition III (2000 cal. years BP) for La Laguna showed a significant average dissimilarity for +/- 200 years of 21% (*Pseudo-F* = 42, *P* (MC) < 0.01). Vegetation differentiation either side of the boundary was driven mainly by a decrease in *Carpinus* (24.19%) and an increase of *Quercus* (5.98%) and *Morella faya* (9.20%) (Table 2). See Nogué *et al.* (2013) and Table 2 for SIMPER results for La Gomera.

DISCUSSION

INTER-ISLAND VEGETATION DYNAMICS THROUGH THE LAST 9600 YEARS: TRACKING CLIMATE AND HUMAN CHANGES

Although traditionally, the oceanic islands have been considered well-buffered from past climatic changes (Whittaker and Fernández-Palacios, 2007), recent data from the Canary Islands indicates a synchronicity with the palaeoclimate of

TABLE 2. Simper results (percentage of contribution) for a time window of +/- 200 years either site of the vegetation transition (5500, 2900 and 2000 cal. yeas BP) for six taxa. Permanova *Pseudo-F* values, significance and percentage of dissimilarity are given. Arrows show the direction of change from the simper analysis. *data from Nogué *et al.* (2013), **$P\ (MC) < 0.01$.

Taxa	I Laguna Grande*		II La Laguna		III La Laguna	
Carpinus	-	-	21.00	↑	21.19	↓
Erica	11.30	↑	-	-	-	-
Morella faya	5.57	↑	8.73	↓	9.20	↑
Phoenix canariensis	20.98	↓	5.73	↓	1.41	↑
Quercus	-	-	2.25	↑	5.98	↓
Salix canariensis	-	-	6.13	↑	-	-
	(*Pseudo F*=75.2)** 15%		(*Pseudo F*=18.0)** 15%		(*Pseudo F*=42.2)** 21%	

North Africa (Meco *et al.*, 2002; Ortiz *et al.*, 2006; Meco *et al.*, 2010; Suchodoletz *et al.*, 2010; Yanes *et al.*, 2011). These results suggest a more complex climatic past frame, where not only the position of the islands (close to the African continent), but also the topographic complexity may have played an important role. For instance, within Macaronesia, the Canary Islands display a significant elevation gradient which encompasses high ecosystem diversity (Fernández-Palacios and de Nicolás, 1995; Whittaker *et al.*, 2008).

For example, in the eastern islands it has been described frequent and abrupt transitions between humid and arid conditions during the last glacial-interglacial cycle. These humid/arid phases are thought to reflect changes in the strength of palaeomonsoon activity in North Africa, the enhancement in westerly cyclonic activity, and/or variations in sea surface and air temperatures (Ortiz *et al.*, 2006; Suchodoletz *et al.*, 2010). In a smaller time frame, our results also suggest a climatic-induced shift towards drier conditions in La Gomera (Nogué *et al.*, 2013). Starting 9600 years ago, the landscape around Laguna Grande (1250 m a.s.l.) was dominated by monteverde forest complemented with high abundances of *Salix canariensis* and *Phoenix canariensis.* The latter is, considered a hygrophilous species, indicative of wet conditions or permanently flooded lakes. This landscape dramatically changed with a sharp vegetation transition 5500 years ago where the hygrophilous species displayed a decreasing trend and the *Morella-Erica* heath expanded. Another indication of a climatic shift is the increase in regional burning (micro-charcoal) 4800 years ago.

These results indicate that the climate could have been very similar to that observed in Northern Africa (Hooghiemstra *et al.*, 1992; deMenocal *et al.*, 2000;

Kröpelin *et al.*, 2008) where it was suggested a shift ocurred from a more humid to a drier climate (e.g. the end of the African Humid Period). For instance, pollen records and variation in water levels from different lakes covering the African Humid Period in Northern Africa, have shown a progressive desiccation of the region during the Holocene (Damnati, 2000; deMenocal *et al.*, 2000; Kröpelin *et al.*, 2008). Thus, at the beginning of the African Humid Period, the Sahara was vegetated with a combination of trees and shrubs and tropical species adapted to humid conditions with no current modern analogue (Watrin *et al.*, 2009). Towards the end of the period (between 7000–5000 years BP) a «desert» state covered the area. Our pollen data clearly showed a climatic signal in both islands, although in La Laguna, the vegetation shift occurs later in time (approximately 2900 years BP). We interpret this potential delay, as resulting from the influence of different environmental conditions, including climate, local vegetation composition, and topography (Table 1). Moreover, in La Laguna, during the period 2900 to 2000 cal. years ago, there is an increase of hygrophilous taxa which suggests a deviation from the general climatic trend (drier climate) described in many Mediterranean and Northern African regions.

According to archaeological studies, the first human settlement occurred approximately 3000–2500 years ago by pastoralists of full Neolithic culture, who brought with them goats, sheep and pigs (Rando *et al.*, 1999), and triggered the extinction of several animal species (Bocherens *et al.*, 2006; Rando and Alcover, 2008). It is unclear how many influxes occurred after initial settlement and prior to the Hispanic contact in the 15th Century. Thus, from approximately 2500 cal. year BP to present, potential climatic changes cannot be interpreted from the pollen record without taking into account the role of human impacts.

What was still unknown until de Nascimento *et al.* (2009) and Nogué *et al.* (2013) was the extent of human impact on vegetation. While in Garajonay forests, we have not found strong human impacts, in La Laguna, there are several sources of evidences for such. First, the total disappearance of two taxa, *Quercus* and *Carpinus* by 700 cal. years BP, which likely formed a dominant part of the lost woodland zone. Second, a substantial increase in charcoal 2000 years ago which approximately coincides with the first wave of human colonization. From a climatic perspective, the relevance of the presence of *Quercus* and *Carpinus* is difficult to interpret.

VEGETATION SENSITIVITY TO PAST CLIMATIC CHANGES

Understanding the feedbacks associated with the climatic transition is an active area of research and the SIMPER analysis may provide an insight into how different species might respond to climatic changes.

There is not a definitive future climatic prediction for the Canaries (but see Sperling *et al.*, 2004; Martín *et al.* 2012), but what is recognized is a climate-related zonation of vegetation types. Thus, if climate changes, vegetation responses are likely to follow. One of the main contributions of this analysis is identifying which species are more sensitive to changes in climate. Our results show that the decline in humidity (e.g. 5500 cal. years ago) was followed by a decrease in *Phoenix canariensis*, and an increase in *Morella-Erica* heath. On the other hand, a potential increase in water availability (e.g. 2900 cal. years BP) was followed by a decrease in *Morella-Erica* heath and an increase in pollen grains of *Carpinus*, *Quercus,* and *Salix canariensis*. *Phoenix canariensis* is a hygrophilous species but also a thermophilous element, thus a decrease in this species under humid conditions, as occurred in the transition II in La Laguna, suggests some temperature cooling. For the last vegetation transition occurring 2000 cal. years BP, the role of human impact on the vegetation prevents us from attributing any change solely to natural forcing.

Based on this, it is clear that future changes in climate are likely to affect the species compositions. In general, there are two possible scenarios associated with the expected increase in temperature (IPCC, 2007): 1) increase in humidity, and 2) a drying trend. If humid conditions prevail, taxa sensitive to moisture-balance variability would be expected to have a rapid response. If this is the case, our results suggest that *Phoenix canariensis* and *Salix canariensis* will expand. On the other hand, if drier conditions become established our results indicate that an increase in the *Morella-Erica* heath may be expected.

CONCLUSIONS

These two long-term vegetation (Holocene) sequences have provided the first opportunity to compare and describe a general climatic pattern for the western Canary Islands. Although the sites are located at different elevations and surrounded by different vegetation types, we conclude that:

1) There is no strong evidence of human impact in Garajonay forests. On the contrary, the La Laguna study revealed the extent to which prehistoric human impact has altered the natural vegetation of Tenerife (de Nascimento *et al.*, 2009). Thus, we suggest that high elevation forests may be the last areas settled by humans (Nogué *et al.*, 2013) owing to their preference for certain habitats, climatic conditions, and vegetation structures.
2) The absence of a signal of human impact in La Gomera, allows us to suggest that global climate changes (e.g. the end of the African Humid period) may be traced in the Canaries (Nogué *et al.*, 2013). Moreover, there is a general trend in both islands: an increase in *Morella-Erica* heath and a decrease in hygrophilous species, suggesting the establishment of drier conditions at approximately 5500 cal. years BP (Fig. 2a).
3) One of the main contributions of this analysis is the identification of taxa sensitive to changes in climate. *Phoenix canariensis* and *Salix canariensis* stand

out as the most sensitive taxa to a drier climate while *Erica* and *Morella* are favoured by these climatic conditions.

4) A practical conclusion is that high elevation areas, such as Laguna Grande (1250 m a.s.l.) in La Gomera, form some of the best palaeoecological sites to detect the effect of major global climatic events on oceanic islands. On the other hand, the consequences of past climatic changes at lower elevations might be hidden by the buffering effect of the Ocean.

This chapter provides an example of how palaeoecological results in the Canary Islands offer a wonderful opportunity to study past climatic changes, vegetation transitions, and extinctions. Future work will focus on new sites in order to better understand the vegetation changes in this archipelago.

ACKNOWLEDGEMENTS

The results of this research have been obtained from different research projects funded by the Spanish Ministry of Science and Innovation (project CGL 2009-10939), the Royal Society of London, the Spanish Ministry of the Environment and Rural and Marine Environs, Autonomous Organisation of National Parks (project 003/2008), and the Canarian Agency for Research, Innovation and Information for Society and the European Regional Development Fund (project SolSubC200801000053). Sandra Nogué participated through a postdoctoral fellowship from the Spanish Ministry of Education (EX2009-0669).

REFERENCES

Anderson, M.J., Gorley, R.N. and Clarke, K.R. (2008) *PERMANOVA+ for PRIMER: Guide to software and statistical methods.* PRIMER-E: Plymouth, United Kingdom.

Arnay de la Rosa, M., González-Reimers, E., Yanes, Y., Velasco-Vázquez, J., Romanek, C.S. and Noakese, J.E. (2010) Paleodietary analysis of the prehistoric population of the Canary Islands inferred from stable isotopes (carbon, nitrogen and hydrogen) in bone collagen. *Journal of Archaeological Science,* 37, 1490–1501.

Bennett, K.D. (1996) Determination of the number of zones in a biostratigraphical sequence. *New Phytologist,* 132, 155–170.

Bennett, K.D. and Willis, K.J. (2001) Pollen. *Tracking Environmental Change Using Lake Sediments, Volume 3: Terrestrial, Algal, and Siliceous Indicators* (ed. by Smol, J.P., Birks, H.J.B. and Last, W.M.), pp. 5–32. Kluwer Academic Publishers, Dordrecht, the Netherlands.

Bocherens, H., Michaux, J., García-Talavera, F. and Van der Plicht, J. (2006) Extinction of endemic vertebrates on islands: the case of the giant rat *Canariomys bravoi* (Mammalia, Rodentia) on Tenerife (Canary Islands, Spain). *Comptes Rendus Palevol,* 5, 885–891.

Carrión, J.S., Fernández, S., González-Sampériz, P., Gil-Romera, G., Badal, E., Carrión-Marco, Y., López-Merino, L., López-Saéz, A., Fierro, E. and Burjachs, F. (2010) Expected trends and surprises in the Lateglacial and Holocene vegetation history of the Iberian Peninsula and Balearic Islands. *Review of Palaeobotany and Palynology,* 162, 458–475.

Clark, R.L. (1982) Point count estimation of charcoal in pollen preparations and thin sections of sediments. *Pollen et Spores,* 24, 523–535.

Criado, C. (2002) *Breve e incompleta historia del antiguo lago de la ciudad de San Cristóbal de La Laguna.* Concejalía de Cultura y Patrimonio Histórico Artístico, San Cristóbal de La Laguna.

Damnati, B. (2000) Holocene lake records in the Northern Hemisphere of Africa. *Journal of African Earth Sciences,* 31, 253–262.

Damnati, B., Petit-Maire, N., Fontugne, M., Meco, J. and Williamson, D. (1996) Quaternary paleoclimates in the eastern Canary Islands. *Quaternary International,* 31, 37–46.

del Arco, M.J., Wildpret, W., Pérez de Paz, P.L., Rodríguez, O., Acebes, J.R., García, A., Martín, V.E., Reyes, A., Salas, M., Díaz, M.A., Bermejo, J.A., González, R., Cabrera, M.V. and García, S. (2006) *Mapa de la vegetación de Canarias.* GRAFCAN, Santa Cruz de Tenerife.

del Arco, M.J., González-González, R., Garzón-Machado, V. and Pizarro-Hernández, B. (2010) Actual and potential natural vegetation on the Canary Islands and its conservation status. *Biodiversity Conservation*, 19, 3089–3140.

deMenocal, P.B., Ortiz, J., Guilderson, T., Adkins, J., Sarnthein, M., Baker, L. and Yarusinski, M. (2000) Abrupt onset and termination of the African Humid Period: Rapid climate response to gradual insolation forcing. *Quaternary Science Review*, 19, 347–361.

de Nascimento, L., Willis, K.J., Fernández-Palacios, J.M., Criado, C. and Whittaker, R.J. (2009) The long-term ecology of the lost forests of La Laguna, Tenerife (Canary Islands). *Journal of Biogeography*, 36, 499–514.

Fernández-Palacios, J.M. and de Nicolás, J.P. (1995) Altitudinal Pattern of Vegetation Variation on Tenerife. *Journal of Vegetation Science*, 6, 183–190.

Höllermann, P. (1981) Microenvironmental studies in the laurel forest of the Canary Islands. *Mountain Research and Development*, 3, 193–207.

Hooghiemstra, H., Stalling, H., Agwu, C.O.C. and Dupont, L.M. (1992) Vegetational and climatic changes at the northern fringe of the Sahara 250000–5000 years BP: evidence from 4 marine pollen records located between Portugal and Canary Islands. *Review of Palaeobotany and Palynology*, 74, 1–53.

IPCC (2007) *Climate Change 2007: The Physical Science Basis. Contribution of Working Group I to the Fourth Assessment Report of the Intergovernmental Panel on Climate Change* (ed. by Solomon, S., Qin, D., Manning, M., Chen, Z., Marquis, M., Averyt, K.B., Tignor, M. and Miller, H.L.). Cambridge University Press, Cambridge, United Kingdom and New York, NY, USA.

Kröpelin, S., Verschuren, D., Lézine, A.M., Eggermont, H., Cocquyt, C., Francus, P., Cazet, J.P., Fagot, M., Rumes, B., Russell, J.P., Darius, F., Conley, D.J., Schuster, M., Suchodoletz, H. von and Engstrom, D.R. (2008) Climate-driven ecosystem succession in the Sahara: the past 6000 years. *Science*, 320, 765–768.

Lomoschitz, A., Meco, J. and Corominas, J. (2002) The Barranco de Tirajana basin, Gran Canaria (Spain). A major erosive landform caused by large landslides. *Geomorphology*, 42, 117–130.

Martín, J.L., Bethencourt, J. and Cuevas-Agulló, E. (2012) Assessment of global warming on the island of Tenerife, Canary Islands (Spain). Trends in minimum, maximum and mean temperatures since 1944. *Climatic Change*, 114, 343–355.

Marzol, M.V. and Sánchez, J.L. (2009) El clima del Garajonay en el contexto insular. *Parque Nacional de Garajonay Patrimonio Mundial* (ed. by Fernández, A.B.), pp. 93–115. Publicaciones Turquesa S.L., Santa Cruz de Tenerife.

Meco, J., Guillou, H., Carracedo, J.C., Losmoschitz, A., Ramos A.J.G. and Rodríguez-Yanez, J.J. (2002). The maximum warmings of the Pleistocene world climate recorded in the Canary Islands. *Palaeogeography, Palaeoclimatology, Palaeoecology*, 185, 197–210.

Meco, J., Petit-Maire, N., Ballester, J., Betancort, J.F. and Ramos, A.J.G. (2010) The Acridian plagues, a new Holocene and Pleistocene palaeoclimatic indicator. *Global and Planetary Change*, 72, 318–320.

Millennium Ecosystem Assessment (Program) (2003) *Ecosystems and human well-being: a framework for assessment.* Island Press, Washington, D.C.

Mimura, N., Nurse, L., McLean, R.F., Agard, J., Briguglio, L., Lefale, P., Payet, R. and Sem, G. (2007) Small islands. *Climate Change 2007: Impacts, Adaptation and Vulnerability. Contribution of Working Group II to the Fourth Assessment Report of the Intergovernmental Panel on Climate Change* (ed. by Parry, M.L., Canziani, O.F., Palutikof, J.P., van der Linden, P.J. and Hanson, C.E.), pp. 687–716. Cambridge University Press, Cambridge, UK.

Navarro, J.F. (2009) Los antiguos gomeros y Garajonay. *Parque Nacional de Garajonay Patrimonio Mundial* (ed. by Fernández, A.B.), pp. 549–561. Publicaciones Turquesa S.L., Santa Cruz de Tenerife.

Nogué, S., de Nascimento, L., Fernández-Palacios, J.M., Whittaker, R.J. and Willis, K.J. (2013) The ancient relict forests of La Gomera, Canary Islands, and their sensitivity to environmental change. *Journal of Ecology*

Ortiz, J.E., Torres, T., Yanes, Y., Castillo, C., de la Nuez, J., Ibáñez, M. and Alonso, M.R. (2006) Climatic cycles inferred from the aminostratigraphy and aminochronology of Quaternary dunes and palaeosols from the eastern islands of the Canary Archipelago. *Journal of Quaternary Science*, 21, 287–306.

Rando, J.C. and Alcover, J.A. (2008) Evidence for a second western Palaearctic seabird extinction during the last Millennium: the Lava Shearwater Puffinus olsoni. *Ibis*, 150, 188–192.

Rando, J.C., Cabrera, V.M., Larruga, J.M., Hernández, M., González, A.M., Pinto, F. and Bandelt, H.J. (1999) Phylogeographic patterns of mtDNA reflecting the colonization of the Canary Islands. *Annals of Human Genetics*, 63, 413–428.

Reille, M. (1992) *Pollen et spores d'Europe et d'Afrique du Nord.* Laboratoire de Botanique historique et Palynologie, Marseille.

Reille, M. (1995) *Pollen et spores d'Europe et d'Afrique du Nord. Supplément 1.* Laboratoire de Botanique historique et Palynologie, Marseille.

Reille, M. (1998) *Pollen et spores d'Europe et d'Afrique du Nord. Supplément 2.* Laboratoire de Botanique historique et Palynologie, Marseille.

Ritter, A., Regalado, C.M. and Aschan, G. (2009) Fog reduces transpiration in tree species of the Canarian relict heath-laurel cloud forest (Garajonay National Park, Spain). *Tree Physiology*, 29, 517–528.

Rodríguez-Rodríguez, A., Arbelo, C.D., Notario, J.S., Mora, J.L., Guerra, J.A. and Armas, M.C. (2009) Los suelos del Parque Nacional de Garajonay. *Parque Nacional de Garajonay Patrimonio Mundial* (ed. by Fernández, A.B.), pp. 63–91. Publicaciones Turquesa S.L., Santa Cruz de Tenerife.

Sperling, F.N., Washington, R. and Whittaker, R.J. (2004) Future climate change of the subtropical North Atlantic: implications for the cloud forests of Tenerife. *Climatic Change*, 65, 103–123.

Stockmarr, J. (1971) Tablets with spores used in absolute pollen analysis. *Pollen et Spores*, 13, 615–620.

Suchodoletz, H. von, Oberhänsli, H., Hambach, U., Zöller, L., Fuchs, M. and Faust, D. (2010) Soil moisture fluctuations recorded in Saharan dust deposits on Lanzarote (Canary Islands) over the last 180 ka. *Quaternary Science Reviews*, 29, 2173–2184.

Watrin, J., Lézine, A.M., Hély, C. and contributors (2009) Plant migration and plant communities at the time of the «green Sahara». *Comptes Rendus Geoscience*, 341, 656–670.

Whitlock, C. and Larsen, C. (2001) Charcoal as a fire proxy. *Tracking environmental change using lake sediments. Vol. 3: Terrestrial, algal, and siliceous indicators* (ed. by Smol, J.P., Birks, H.J.B. and Last, W.M.), pp. 75–97. Kluwer Academic Publishers, Dordrecht, the Netherlands.

Whittaker, R.J. and Fernández-Palacios, J.M. (2007) *Island biogeography: ecology, evolution and conservation,* 2nd edn. Oxford University Press, Oxford.

Whittaker, R.J., Triantis, K.A. and Ladle, R.J. (2008) A general dynamic theory of oceanic island biogeography. *Journal of Biogeography*, 35, 977–994.

Yanes, Y., Yapp, C.J., Ibáñez, M., Alonso, M.R., De-la-Nuez, J., Quesada, M.L., Castillo, C. and Delgado, A. (2011) Pleistocene–Holocene environmental change in the Canary Archipelago as inferred from the stable isotope composition of land snail shells. *Quaternary Research*, 75, 658–669.

LATE HOLOCENE WOOD REMAINS FROM ALLUVIAL/COLLUVIAL DEPOSITS IN THE CALDERA DE TABURIENTE NATIONAL PARK (LA PALMA, CANARY ISLANDS)

Juan Manuel Rubiales, Andrés Díez-Herrero, Mar Génova,
Juan Antonio Ballesteros-Cánovas,
Lea de Nascimento, José María Fernández-Palacios

CLIMATE CHANGE PERSPECTIVES FROM THE ATLANTIC:
PAST, PRESENT AND FUTURE
Jose María Fernández-Palacios, Lea de Nascimento, José Carlos Hernández,
Sabrina Clemente, Albano González & Juan P. Díaz-González (eds.)
Servicio de Publicaciones, Universidad de La Laguna – 2013

ISBN: 978-84-15910-54-1 pp. 243-257

ABSTRACT

The geomorphological dynamics of the Barranco de Taburiente gorge, in La Palma (Canary Islands), has exposed sub-fossil organic layers in its riverbanks and margins, in which a large number of woody remains have been recovered. Samples have been located along ~3 km of the river and are clustered in three sites. Radiocarbon dating of the remains indicates that the recovered samples date from the late Holocene and have been identified as *Pinus canariensis*, a pine species that may have long been dominant and stable in the landscapes of the Caldera de Taburiente. The deposition of the remains could be explained by a single geomorphic event related to a humid (and probably torrential) episode. The factors that would explain the persistence of these pinewoods are discussed.

KEYWORDS: Caldera de Taburiente, geomorphic events, Holocene, *Pinus canariensis*, sub-fossil wood.

INTRODUCTION

La Palma, the most north-westerly of the Canary Islands, is also one of the youngest islands of the archipelago. Recent volcanic activity is very important on this island and has made it a key place of interest for scientists during the last decades. Since the latest subaerial volcanic eruption in Spain (emergence of the Teneguía volcano) during 1971, this island has been the subject of many, diverse geological studies, including ones on sedimentological features, gravitational collapses or eruptions (e.g. Day *et al.*, 1999; Vegas *et al.*, 1999; Klügel *et al.*, 2000; Ward and Day, 2001).

However, little is known about the Quaternary history of vegetation on the island. The vegetal remains found at the archaeological site of the cave of El Tendal (San Andrés y Sauces), at 150 m a.s.l. on the northeast of the island, is to date, the only one that has been investigated using carpological and anthracological studies (Machado, 1995; Morales Mateos *et al.*, 2004). At this site, charcoals from layers corresponding to ~2200 cal. years BP and ~1000 cal. years BP show the dominance of laurel forests during this period. On other islands of the Canarian archipelago, studies on macrofossils have been developed mainly from charcoal recovered from archaeological sites. On the nearby island of El

Hierro, the archaeobotanical evidence from the site of Guinea (80 m above sea level – a.s.l.) records the existence of *Pinus* and *Juniperus*, as well as other species of laurel forests and the *fayal-brezal* (Machado, 2002). Late-Holocene anthracological records have also been studied in Tenerife, La Gomera, Gran Canaria and Fuerteventura (e.g. Machado, 1996; Machado *et al.*, 1997; Machado and Galván, 1998; Navarro *et al.*, 2000; Navarro, 2003; Mireles *et al.*, 2005). However, non-archaeological sites with plant macrofossils are rare in the Canary Islands, and only Miocene–Pliocene sites have been studied (García-Talavera *et al.*, 1995; Vegas *et al.*, 1999; Anderson *et al.*, 2009 and references therein). In the Caldera de Taburiente, pollen and megafossil assemblages corresponding to the Upper Miocene–Middle Pleistocene show the existence of helophytes and point to the presence of marshes in that period (Vegas *et al.*, 1998; Álvarez Ramis *et al.*, 2000). Recent findings in these deposits suggest the existence of a former lake in the basin of La Caldera and evidenced the presence of Lauraceae trees in the site ca. 200,000 years ago (see news in http://www.diariodeavisos.com/caldera-taburiente-fue-gran-lago-hace-200-000-anos/).

Geomorphological processes have been used as indicators of palaeoclimatic events in the Canary Islands. The work of Lomoschitz *et al.* (2002) on Gran Canaria suggests that the timing of landslide events corresponds to the wet episodes of the interglacials, and such relationships can be also found in debris-avalanches and erosive episodes (Lomoschitz *et al.*, 2008). More recent events have also been investigated, such as the cold period of the Little Ice Age that has been linked with the occurrence of periglacial landforms in the Teide volcano on Tenerife (Martínez de Pisón and Quirantes, 1994; Marín Moreno, 2010).

The aim of this work is to interpret the presence of woody macrofossils that were detected during the geomorphological mapping of the eroded river banks of the Barranco de Taburiente, in an area of great biological interest: the Caldera de Taburiente National Park. Despite the fact that macro- and megafossil assemblages found at this type of site rarely provide sequential records, this material is interesting because precise taxonomic identifications are frequently achieved and the dispersion of the remains is much more restricted when compared to pollen analysis. Until the finding described in this work, no palaeobotanical studies had been published on the area's Holocene woody macrofossil remains from natural contexts and in the interior of the island of La Palma.

MATERIAL AND METHODS

Study area

The Caldera de Taburiente is a massive depression located in the central part of La Palma Island. It is approximately 8.5 km wide and was declared a National Park in 1954. It is surrounded by a semicircular ridge that reaches 2426 m a.s.l.

at the highest point of the island, the Roque de los Muchachos. The altitudinal range is wide, as erosion has intensely modelled the depression and slopes are steep. The lower altitude of the National Park, at the bottom of the Barranco de Las Angustias is 430 m a.s.l.

Geologically, this landform is not strictly a volcanic caldera (which is a subsidence near the crater following a large and explosive eruption) but a majestic volcano derived from several overlaying volcanoes that were shaped by giant landslides and intense erosion. Lithology is mainly composed of basalt and volcanoclastic rocks (Carracedo *et al.*, 1999; Vegas *et al.*, 1999).

Sub-fossils were found in a stretch of approximately three kilometres in the Barranco de Taburiente, whose northern part is called Playa de Taburiente (800 m a.s.l.). This part is an alluvial braided bar plain with large boulders, cobbles and gravels where two (sometimes three) shallow streams flow through the bottom terrace, with a high riverbank of ~2.3 m on average. To the south, the stream is narrowly entrenched and meanders among boulders and cobbles.

The climate is Mediterranean with little to moderate annual precipitations (~900 mm) and intense summer drought. The influence of the Atlantic currents makes seasonal variations in temperature relatively small, with mean annual temperatures of approximately 15 °C. However the big difference in altitudes make climatic parameters (precipitations and temperatures) vary greatly on the island. Moist trade winds that often generate cloud banks at mid to high altitudes on the northeastern side of the island do not affect the Caldera (Mestre Barceló and Filipe Nunes, 2012).

The vegetation is dominated by forests of *Pinus canariensis* often accompanied by shrubs, such as *Cistus symphytifolius* and *Lotus hillebrandii*, and *Erica arborea* at humid locations. At high altitudes (higher than ~1800 m a.s.l.), *Adenocarpus viscosus* occurs and dominates the landscape in the summit areas. At lower altitudes (under ~1000 m a.s.l.) other shrubs are present such as *Spartocytisus filipes* or *Cistus monspeliensis* (Fuertes Díaz, 1995; Arco *et al.*, 2006). At the Playa de Taburiente, near the sites studied in this work, stands of *Salix canariensis* dominate locally along the riverbanks. This buffer forest of willows is of natural origin but most of its current area is the result of recent afforestations.

MATERIALS AND METHODS

The detailed search for woody samples was conducted by a careful screening of the exposed profiles of the Barranco de Taburiente. Subfossils were located at three different sites, separated by approximately 1 km along the stream (Figs. 1 and 2). In all, 39 woody samples were recovered, one of them from a large tree that was found buried and laying horizontally in the bank sediments as represented in Fig. 3 (site 2, Fig. 2b).

Woody remains were prepared for wood anatomical (thin sections) or anthracological observation (manual fracture) depending of on their preservation

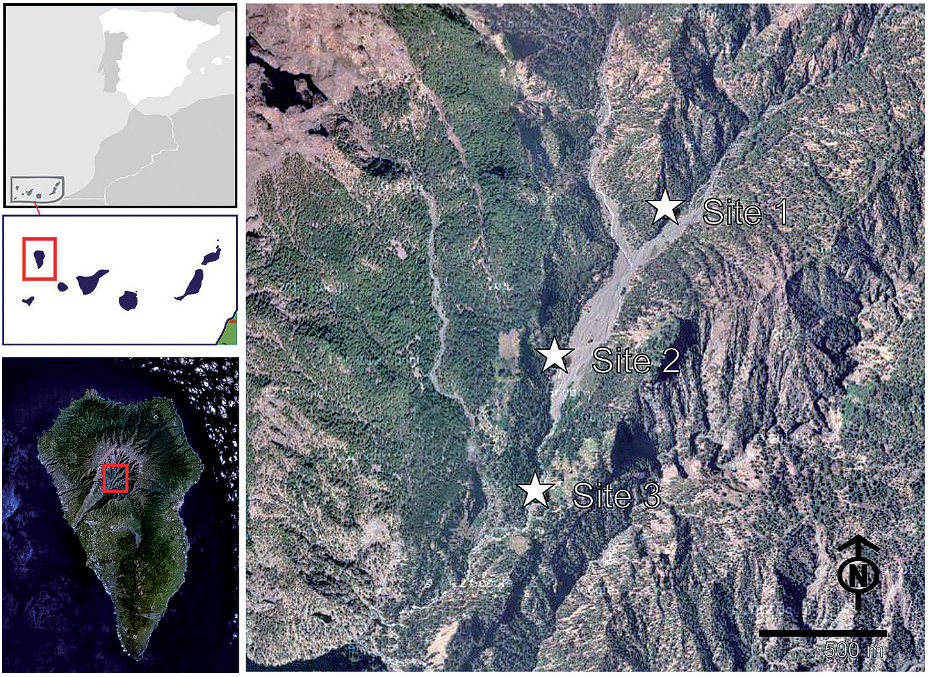

Figure 1. Location of the sites in Caldera de Taburiente. Map sources: Wikimedia commons, Ginkgo maps and Google Maps.

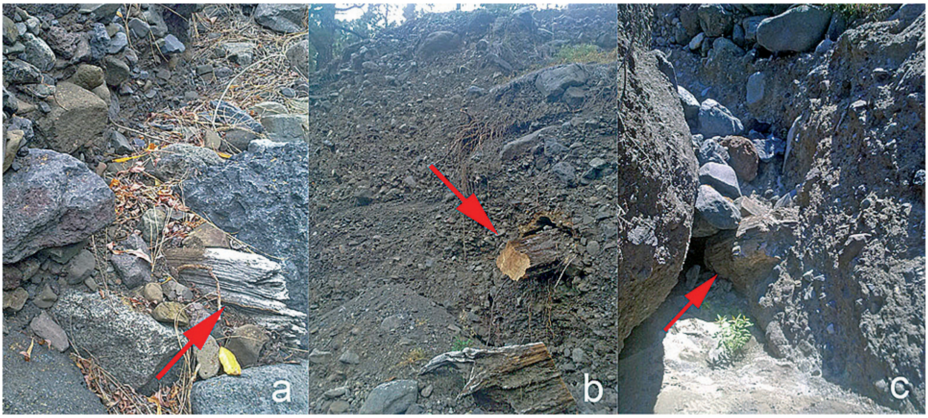

Figure 2. Pictures of the sites where woody remains were recovered, a: site 1, b: site 2, c: site 3.

Fig 3. Sedimentological sketch of the vertical section revealed at site 2. Legend: 1) Coarse gravels, grain supported in discontinuous layers with cobbles; 2) Medium gravels, matrix-supported in sandy clay dark brown matrix, presenting interlensing with gray matrix; 3) Decreasing grain-size sequence of coarse gravels, sand and clay; 4) Alternation of layers of coarse gravel–grain supported gravel with layers of fine gravel matrix-supported with a dark clay matrix; 5) Layer of grain supported cobbles with a palaeochannel in a lateral, intercalated with finer gravels with dark matrix. The log was found into a lag or bar; 6) Alternation of grain supported cobbles and coarse gravel layers with more matrix.

state. Thin sections (approximately 15 to 20 µm thick) of non carbonised specimens were obtained using a sliding microtome. Slices were stained with safranin and dehydrated with alcohol and *Histoclear*. Radial and tangential sections were successfully obtained but no appropriate cross sections were obtained due to poor preservation. Sections were then mounted, coverslipped with a hardening epoxy (*Eukit*) and dried. Furthermore, charcoals and carbonised wood were fractured manually to obtain transversally, radially and tangentially aligned surfaces, and then examined under reflected-light microscopy at different magnifications (50x, 100x and 200x). Wood identification was achieved using keys to wood anatomy, including those of Peraza and López de Roma (1967), García Esteban and Guindeo (1988), and Vernet *et al.* (2001).

Three samples (one from each site) were selected for AMS radiocarbon dating that was carried out at the ^{14}Chrono Centre (Queens University Belfast, UK) and the Centro Nacional de Aceleradores (Seville, Spain). Date calibration was conducted with the *CALIB 6.0.1* software (Stuiver and Reimer, 1993) with the

TABLE 1. Site location and radiocarbon dates for selected samples of each site.

Site	Lat. (degrees N)	Long. (degrees W)	Altitude (m a.s.l.)	Sample ID	Radiocarbon age (yr BP)	2 sigma (cal. yr BP)
Site 1	28.7315	-17.8706	850	UBA 18436	3256 ± 24	3405–3559
Site 2	28.7257	-17.8761	770	CNA 1368	3550 ± 35	3720–3961
Site 3	28.7189	-17.8798	700	UBA 18435	3086 ± 42	3170–3390

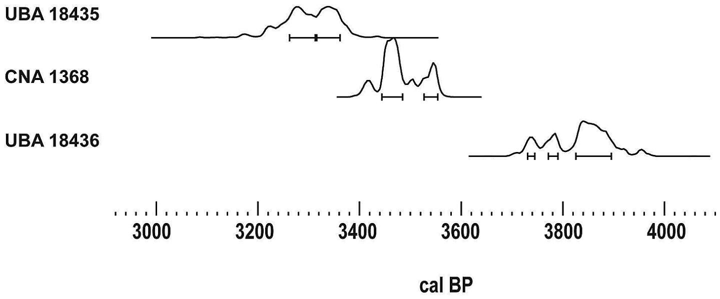

Figure 4. Probability distributions of the calibrated radiocarbon dates.

last dataset available (INTCAL 09, Reimer *et al.*, 2009). The dates were expressed as 2 sigma calibrated years BP (Table 1, Fig. 4).

RESULTS

Wood anatomical analysis allowed the identification of all the samples. The 39 woody remains correspond to *Pinus canariensis* and present the following features, previously reported for this species in Peraza and López de Roma (1967), García Esteban and Guindeo (1988), García Esteban *et al.*, (2005): In the cross section, growth rings are clearly defined with tracheids of irregular to square shape that often present intercellular spaces in the earlywood. Resin ducts are frequent, with an average size of ~200 microns of diameter; epithelial cells are thin-walled and are surrounded by parenchyma cells. In the radial section, tracheids show uniseriate rows of areolate pits and cross fields pits (area of contact between radial parenchyma–axial tracheid) are of pinoide type, generally with one or two per field. Ray tracheids are located in a marginal position or in the interior of the ray and have irregular thickenings, without extensive marked dentations. However, some dentations are present in the latewood of some ring growths. In the tangential section, two types of rays appear: uniseriate rays, of about 10 to 15 cells and multiseriate, with horizontal resin ducts.

The deposits of sites 1 and 2 are coarse gravel layers in the river banks and lower terraces, showing different depositional events corresponding to flooding events of different magnitudes in layers higher up to that where the subfossils were retrieved (Figs. 2a and 2b; Fig. 3). The deposit at site 3 is a chaotic matrix-supported conglomerate (Fig. 2c).

Three AMS radiocarbon dates were obtained yielding an age of 3960 to 3170 cal. years BP for the samples (Table 1, Fig. 3).

DISCUSSION

The fact that the sedimentary context is similar for the three sites may indicate that all the specimens could have been deposited at the same period. The differences in radiocarbon dates could be explained by an *old wood effect*, as the method does not date the moment at which the sample dies (or it is deposited), but the moment when the tissue was created. So, although it could be possible that three (or two) different events may have occurred during this period, or that relocated subfossils may have been deposited by a single event, what seems more reasonable is that the differences correspond to differences in longevity between specimens. While at site 1 rings that were dated may have been created more than 350 years before the moment when the tree died and was drowned by the flood, at sites 2 and 3, the trees died at a younger date. Age estimates for the specimen dated at site 2 (Fig. 2b, the biggest specimen retrieved) are over ~290 years, but longevity of pines on the island may exceed 800 years, as reported for the species by Génova and Santana (2006). Thus, all the specimens may have been deposited at the same time (somewhere around 3200 cal. years BP).

This event could correspond to a large lateral landslide or debris-flow (site 3) probably triggered by a wet episode. The landslide may have been followed by a river blockage which provoked a progressive alluvial filling of the valley bottom upstream (sites 2 and 1). After this event, several minor but more frequent flooding episodes were needed to open the drainage. These kinds of large landslides and debris-flows have been described in the literature (see Vegas *et al.*, 1999), and can be still observed nowadays together with flash flood events, albeit with lower magnitudes (see Díez Herrero *et al.*, 2012). To date there is no evidence that the floods have significantly affected the shape of the Barranco bed due to the incised valley morphology. However, these lacustrine deposits at Playa de Taburiente have been recently discovered (July 2013) and they are currently under study.

The Barranco de Taburiente is to date, the only site in La Palma at which Holocene megafossils have been found. *Pinus canariensis* subfossil data suggest the persistence of the species in this area throughout the end of the Holocene. Nowadays, La Palma is the island that hosts the best conserved forests of Canarian pine and, relative to its surface area, is the island with the largest part of its territory covered by forests of this species (Arévalo and Fernández-Palacios, 2009). In the Canary Islands, *Pinus canariensis* appeared during the Miocene, around 13 Myr ago (García Talavera *et al.*, 1995) in the site of Macizo de Inagua, Gran Canaria. Palaeoecological and genetic evidence from other sites from the archipelago indicate that the distribution area of *Pinus canariensis* responds, over the Quaternary, to processes of expansion and extinction related to volcanism (Navascués *et al.*, 2006). Shifts of pine demise are recorded in the second half of the Holocene (de Nascimento *et al.*, 2009), which could be linked to climatic variation. The pollen records from La Gomera and Tenerife, however, show a continuous signal of *Pinus* throughout the Holocene (de Nascimento *et al.*, 2009; Nogué *et al.*, 2013) even though forest cover of Canarian pine have suffered a severe reduction over the last millennium primarily due to the intensification of human activities on the islands (e.g. Machado, 1996; Machado and Galván, 1998). Thus, pine may be a key species sensitive to environmental changes over time, such as volcanism, climate or human activity.

Evidence of recent extinctions of *Pinus canariensis* is found in some marginal populations. In Fuerteventura, anthracological data indicate intense deforestation as a consequence of both the use of wood as fuel, and land clearing for agriculture and pastoralism. Archaeological charcoals document the extinction of pines on the island between 1400 and 900 cal. years BP (Machado, 1996). This pattern is repeated on La Gomera (Navarro *et al.*, 2000; Navarro, 2003; Morales Mateos *et al.*, 2007), although, natural pines still persist on this island. The signal of *Pinus* in the Laguna Grande is relatively small but continuous from ~9600 cal. years BP, although it is higher during the mid Holocene (~6000 to ~3000 cal. years BP). From 3000 cal. years BP onwards, *Pinus* percentages have decreased, while *Cistus* (characteristic of the pine forest understory and disturbed sites) has increased progressively since 5500 cal. years BP (Nogué *et al.*, 2013). In Gran Canaria, the genetic and demographic study of the marginal population of Arguineguín, below the standard elevational range of the pine belt, also shows the severe recent contraction of this pine population (López de Heredia *et al.*, 2010).

Several factors may account for the long-term presence of pinewoods in the Caldera de Taburiente. First, the geographical configuration of the Caldera, with unstable slopes and numerous ridges, makes access very difficult compared to the other regions of the island. This would have discouraged humans from using this space for wood extraction or intense pastoralism, which would have drastically transformed the vegetation (e.g. Garzón-Machado *et al.*, 2010). Despite the fact that goats were introduced by the *benahoritas*(La Palma aborigines) about 2500 cal. years BP and have grazed in the park since then (Pais, 1995), this space has remained protected from intense management. Instead of livestock or wood resources, water has been the main source of incomes for the owners of this area, at least since the Hispanic stage (Palomares, 2005). Second, extremely steep slopes also influence negatively the processes of soil formation in the interior of the Caldera, and when heavy torrential rains occur, soil denudation stops the process of soil development. If erosion is not dramatic, pine recruitment is however possible in poor soils (López de Heredia, 2010) and may benefit from a great advantage over other potential tree competitors under different climate conditions. Finally, disturbances such as fire or other geomorphic events (i.e. landslides, flows) may serve to rejuvenate the system, which can be also favourable for *Pinus canariensis*, allowing recolonisation or controlling the establishment of other woody species.

ACKNOWLEDGEMENTS

The projects IDEA-GesPPNN-163/2010 (Organismo Autónomo de Parques Nacionales, Ministerio de Agricultura, Alimentación y Medio Ambiente) and DINECOFOR-CGL2011-27229 (Ministerio de Ciencia e Innovación) provided financial support. We would like to thank Ángel Palomares as well as the guides and staff of the National Park. Thanks also to Pablo Mayer, Luis Fernández, Luis Barca and Alberto Carrera for their field assistance.

REFERENCES

Anderson, C.L., Channing, A. and Zamuner, A.B. (2009) Life, death and fossilization on Gran Canaria – implications for Macaronesian biogeography and molecular dating. *Journal of Biogeography*, 36, 2189–2201.

Álvarez-Ramis, M.C., Laamarti, N. and Vegas J. (2000) A preliminary palynological study of epiclastic deposits from «Caldera de Taburiente». La Palma Island, Canary Archipelago, Spain. *Plant Cell Biology and Development*, 11, 50–57.

Arco, M.J., Wildpret, W., Pérez de Paz, P.L., Rodríguez, O., Acebes, J.R., García, A., Martín, V.E., Reyes, A., Salas, M., Díaz, M.A., Bermejo, J.A., González, R., Cabrera, M.V. and García, S. (2006) *Mapa de la vegetación de Canarias*. GRAFCAN, Santa Cruz de Tenerife.

Arévalo, J.R. and Fernández-Palacios, J.M. (2009). 9550 Pinares endémicos canarios, *Bases ecológicas preliminares para la conservación de los tipos de hábitat de interés comunitario en España*. Madrid, Dirección General de Medio Natural y Política Forestal, Ministerio de Medio Ambiente, y Medio Rural y Marino.

Carracedo, J.C., Day, S.J., Guillou, H. and Pérez Torrado, F.J. (1999) Giant quaternary landslides in the evolution of La Palma and El Hierro, Canary Islands. *Journal of Volcanology and Geothermal Research*, 94, 169–190.

Day, S., Carracedo, J., Guillou, H. and Gravestock, P. (1999) Recent structural evolution of the Cumbre Vieja volcano, La Palma, Canary Islands: volcanic rift zone reconfiguration as a precursor to volcano flank instability? *Journal of Volcanology and Geothermal Research*, 94, 135–167.

de Nascimento, L., Willis, K.J., Fernández-Palacios, J.M., Criado, C. and Whittaker, R.J. (2009) The long-term ecology of the lost forests of La Laguna, Tenerife (Canary Islands). *Journal of Biogeography*, 36, 499–514.

Díez Herrero, A., Génova, M., Mayer, P., Ballesteros, J.A., Becerril, L., Rubiales, J.M., Hernández, M., Saz, M.A., Bodoque, J.M. and Ruiz, V. (2012) Investigaciones dendrogeomorfológicas aplicadas al estudio de la peligrosidad por avenidas e inundaciones en el parque nacional de la Caldera de Taburiente (La Palma, Islas Canarias). *Avances de la Geomorfología de España* (ed. by González Díez, A.), pp. 159–162. Actas de la xii Reunión Nacional de Geomorfología, Santander.

Fuertes Díaz, J. (1995) Vegetación. *Mapa Forestal de España, Hoja 9–10/11 Santa Cruz de la Palma* (ed. by Ruiz de la Torre, J.), pp. 9–11. Dirección General de Conservación de la Naturaleza, Madrid.

García Esteban, L. and Guindeo, A. (1988) *Anatomía e identificación de las maderas de coníferas españolas.* AITIM, Madrid.

García Esteban, L., Gasson, P., Climent, J.M., de Palacios, P. and Guindeo, A. (2005) The wood of *Pinus canariensis* and its resinous heartwood. *IAWA Journal,* 26, 69–77.

García-Talavera, F., Sánchez-Pinto, L. and Socorro, S. (1995) Vegetales fósiles en el complejo traquítico-sienítico de Gran Canaria. *Revista de la Academia Canaria de Ciencias,* VII, 77–91.

Garzón-Machado, V., González-Mancebo, J.M., Palomares-Martínez, A., Acevedo-Rodríguez, A., Fernández-Palacios, J.M., Del Arco, M.J. and Pérez-de-Paz, P.L. (2010) Strong negative effect of alien herbivores on endemic legumes of the Canary pine forest. *Biological Conservation,* 143, 2685–2694.

Génova, M. and Santana, C. (2006) Crecimiento y longevidad en el pino canario (*Pinus canariensis* Smith.). *Investigacion agraria. Sistemas y Recursos forestales,* 15, 296–307.

Klügel, A., Hoernle, K.A., Schmincke, H.U. and White, J.D.L. (2000) The chemically zoned 1949 eruption on La Palma (Canary Islands): Petrologic evolution and magma supply dynamics of a rift zone eruption. *Journal of Geophysical Research,* 105, 5997–6016.

Lomoschitz, A., Meco, J. and Corominas, J. (2002) The Barranco de Tirajana basin, Gran Canaria (Spain). A major erosive landform caused by large landslides. *Geomorphology,* 42, 117–130.

Lomoschitz, A., Hervás, J., Yepes, J. and Meco, J. (2008) Characterisation of a Pleistocene debris-avalanche deposit in the Tenteniguada Basin, Gran Canaria Island, Spain. *Landslides,* 5, 227–234.

López de Heredia, U., Venturas, M., López, R.A. and Gil, L. (2010) High biogeographical and evolutionary value of Canary Island pine populations out of the elevational pine belt: the case of a relict coastal population. *Journal of Biogeography,* 37, 2371–2383.

Machado, C. (1995) Approche paléoécologique et ethnobotanique du site archéologique ‘El Tendal’ (NE de l’Ile de La Palma, Archipel des Canaries). *L’Homme Préhistorique et la Mer,* 120, 179–186.

Machado, C. (1996) Reconstrucción paleoecológica y etnoarqueológica por medio del análisis antracológico. La cueva de Villaverde, Fuerteventura. *Biogeografía Plesitocena-Holocena de la Península Ibérica* (ed. by Ramil-Rego, P., Fernández, C. and Rodríguez, M.), pp. 261–274. Universidad de Santiago de Compostela, Santiago de Compostela.

Machado, C. (2002) El yacimiento de Guinea (El Hierro), aportaciones antracológicas. *xiv Coloquio de Historia Canario-Americana,* 361–369.

Machado, C. and Galván, B. (1998) La vegetación en el valle de Chafarí (Las Cañadas del Teide, Tenerife), antes de la conquista castellana. *Cuaternario y Geomorfología,* 12, 117–25.

Machado, C., Arco, M.C., Vernet, J.L. and Ourcival, J.M. (1997) Man and vegetation in northern Tenerife (Canary Islands, Spain), during the prehispanic period based on charcoal analyses. *Vegetation History and Archaeobotany,* 6, 187–95.

Martínez de Pisón, E. and Quirantes, F. (1994) El modelado periglaciar de Canarias. *Periglaciarismo en la Península Ibérica, Canarias y Baleares: estudios significativos* (ed. by Simón, M., Salvador, F. and Gómez, O.), pp. 203–216. Universidad de Granada, Servicio de Publicaciones, Granada.

Martín Moreno, R. (2010) La Pequeña Edad de Hielo en el Alto Teide (Tenerife, Islas Canarias). Menciones históricas y morfogénesis periglaciar. *Ería*, 83, 331–342.

Mestre Barceló, A. and Filipe Nunes, L. (2012) *Atlas climático de los archipiélagos de Canarias, Madeira y Azores. Temperatura del aire y precipitación (1971-2000)*. Agencia Estatal de Meteorología, Ministerio de Agricultura y Alimentación y Medio Ambiente, Instituto de Meteorologia de Portugal, Spain.

Mireles, F., Olmo, S. and Rodríguez, A. (2005) El poblado prehispánico costero de playa de El Burrero y su entorno arqueológico (Ingenio, Gran Canaria). *El Museo Canario*, 60, 31–92.

Morales Mateos, J., Marrero Rodríguez, A. and Rodríguez Rodríguez, A.C. (2004) La socialización de nuevos espacios: transformación del medio y explotación de los productos vegetales en el yacimiento de El Tendal, La Palma (Islas Canarias). *El Museo Canario*, 59, 19–42.

Morales Mateos, J., Rodríguez Rodríguez, A., Alberto Barroso, V., Machado Yanes, M.C. and Criado Hernández, C. (2007) El impacto de las actividades humanas sobre el medioambiente de las Islas Canarias durante la prehistoria. *El Indiferente*, 19, 73–79.

Navarro, J.F. (2003) Arqueología en el Parque Nacional de Garajonay. *Ambienta*, 26, 18–22.

Navarro, J.F., Hernández, C.M., Alberto, V., Borges, E., Barro, A. and Hernández, J.C. (2000) Aras de sacrificio y grabados rupestres en el Lomo del Piquillo (isla de La Gomera). *Anuario del Instituto de Estudios Canarios*, 45, 317–340.

Navascués, M., Vaxevanidou, Z., González-Martínez, Climent, J., Gil, L. and Emerson, B.C. (2006) Chloroplast microsatellites reveal colonization and metapopulation dynamics in the Canary Island pine. *Molecular Ecology*, 15, 2691–2698.

Nogué, S., de Nascimento, L., Fernández-Palacios, J.M., Whittaker, R.J. and Willis, K.J. (2013) The ancient forests of La Gomera, Canary Islands, and their sensitivity to environmental change. *Journal of Ecology*, 101, 368–377.

Pais, F.J. (1995) Los asentamientos de los benahoaritas en La Caldera de Taburiente (Isla de La Palma). *El Museo Canario*, 50, 45–78.

Palomares, A. (2005) *Parque Nacional de la Caldera de Taburiente: Guía de Visita*. Organismo Autónomo de Parques Nacionales, Madrid.

Peraza Oramas, C. and López de Roma, A. (1967) *Estudio de las principales maderas de Canarias*. Ministerio de Agricultura, Madrid.

Reimer, P.J., Baillie, M.G.L., Bard, E., Bayliss, A., Beck, J.W., Blackwell, P.G., Bronk Ramsey, C., Buck, C.E., Burr, G.S., Edwards, R.L., Friedrich, M., Grootes, P.M., Guilderson, T.P., Hajdas, I., Heaton, T.J., Hogg, A.G., Hughen, K.A., Kaiser, K.F., Kromer, B., McCormac, F.G., Manning, S.W., Reimer, R.W., Richards, D.A., Southon, J.R., Talamo, S., Turney, C.S.M., van der Plicht, J. and Weyhenmeyer, C.E. (2009) INTCAL09 and MARINE09 radiocarbon age calibration curves, 0-50,000 years cal BP. *Radiocarbon*, 51, 1111–1150.

Stuiver, M. and Reimer, P.J. (1993) Extended 14C database and revised CALIB radiocarbon calibration program. *Radiocarbon*, 35, 215–230.

Vegas, J., Álvarez-Ramis, C. and Laamarti, N. (1998) Reconstrucción de los megarrestos vegetales fósiles encontrados en los sedimentos epiclásticos de La Caldera de Taburiente. La Palma (Islas Canarias). *Actas de las XIV Jornadas de Paleontología*, 187–189.

Vegas, J., Marfil, R. and Hernández Pacheco, A. (1999) Los depósitos volcanoclásticos de la Isla de la Palma (Canarias): su relación con la evolución de las Calderas de Taburiente y Cumbre Nueva. *Boletín Geológico y Minero*, 110, 15–38.

Vernet, J.L., Ogererau, P., Figueiral, I., Machado Yanes, C. and Uzquiano, P. (2001) *Guide d'identification des charbons de bois préhistoriques et récents. Sud-Ouest de l'Europe: France, Péninsule ibérique et Iles Canaries.* CNRS editions, Paris

Ward, S.N. and Day, S. (2001) Cumbre Vieja volcano—potential collapse and tsunami at La Palma, Canary Islands. *Geophysical Research Letters*, 28, 3397–3400.

VEGAS AND DUNE-PALAEOSOIL-SEQUENCES – TWO DIFFERENT PALAEOENVIRONMENTAL ARCHIVES ON THE EASTERN CANARY ISLANDS

Hans von Suchodoletz, Ludwig Zöller, Alexandra Hilgers,
Ulrich Radtke, Dominik Faust

CLIMATE CHANGE PERSPECTIVES FROM THE ATLANTIC:
PAST, PRESENT AND FUTURE
Jose María Fernández-Palacios, Lea de Nascimento, José Carlos Hernández,
Sabrina Clemente, Albano González & Juan P. Díaz-González (eds.)
Servicio de Publicaciones, Universidad de La Laguna – 2013

ISBN: 978-84-15910-54-1
pp. 259-274

ABSTRACT

The eastern Canary Islands (Lanzarote and Fuerteventura) are located at the transition between the Mediterranean and the Saharan climate region off NW-Africa. Thus, they are a key area for the investigation of palaeoenvironmental changes. During the last years we investigated two different kinds of palaeoenvironmental archives there: 1) *vega* sediments, i.e. a mixture of hardly weathered Saharan dust, soil material from the surrounding slopes and local volcanic material trapped in volcanically dammed valleys, and 2) dune-palaeosol sequences, where dunes mostly consisting of marine shell detritus originally blown out from the insular shelf are intercalated with several palaeosol horizons with slightly higher clay and silt content. Unlike the dune-sands, the soils indicate more stable landscape conditions with trapping of Saharan dust. We investigated both kinds of palaeoenvironmental archives at the eastern Canary Islands, together covering a time-range from the Middle Pleistocene till the Holocene. Here, we compare these two different kinds of archives with respect to their different geomorphologic mechanisms when recording environmental signals, and thus the different significations of palaeoenvironmental information derived from them.

KEYWORDS: Canary Islands, dune-palaeosol sequences, geomorphology, palaeoenvironmental archives, Quaternary, *vegas*.

INTRODUCTION

In view of the predicted global change during the coming decades (e.g. IPCC, 2007) it is necessary to understand driving mechanisms and feedbacks of the climate system, in order to anticipate future climate changes more realistically. In this context, specifically critical are naturally instable and vulnerable environments like those of semi-arid and arid regions (e.g. desert margins), as e.g. found in northwest Africa (Mountney, 2003; Lioubimtseva, 2004). An understanding of the complex relationships in the climate and environmental system can be obtained when looking into past periods with other boundary conditions, what can be achieved using palaeoenvironmental archives. The investigation of terrestrial palaeoenvironmental archives can give information on processes directly active on the land surface, as e.g. precipitation or landscape activity and stability. However, such archives are not very widespread in the semi-arid to semi-humid region of northwestern Africa,

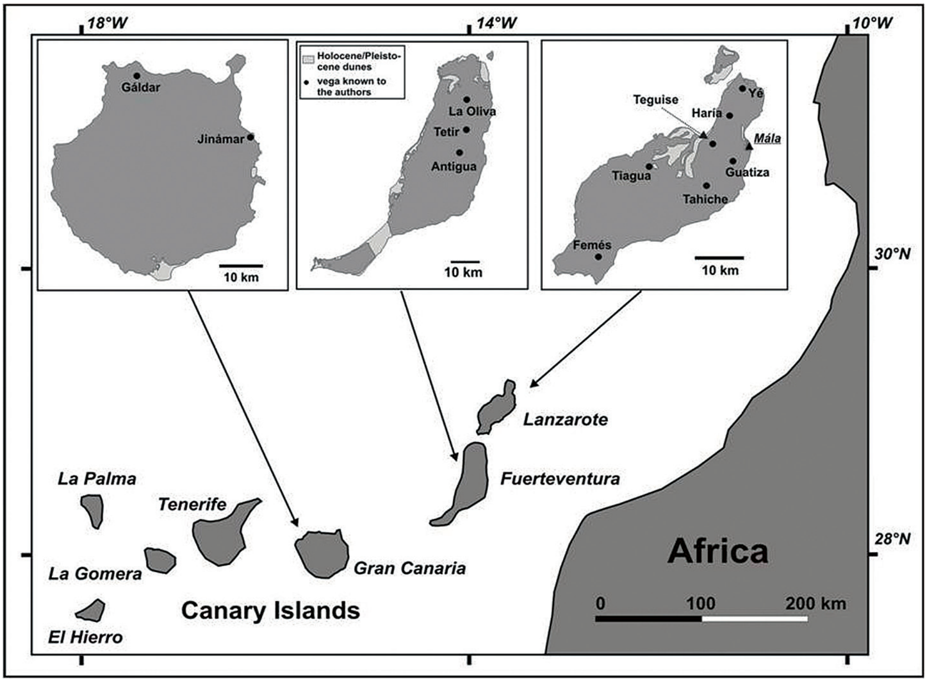

Figure 1. Overview of the Canary Islands. The insets show the locations of *vegas* (for Lanzarote and Fuerteventura own observations; for Gran Canaria after Menéndez *et al.*, 2009a) as well as Pleistocene/Holocene dune-fields (after Rothe, 1996) on the eastern Canary Islands. The location of the Mala dune-palaeosol sequence on Lanzarote, a main focus of this study, is indicated by a triangle.

and often face the problem that they are discontinuous and/or cover only some parts of the Holocene or latest Pleistocene (e.g. Gasse *et al.*, 1987; Cheddadi *et al.*, 1998; Lancaster *et al.*, 2002; Linstädter and Zielhofer, 2010). In difference, a large number of marine drillings were carried out along the northwest-African margin during the last years, but it is often difficult to derive direct information on the processes active on the land surface from these archives (e.g. Moreno *et al.*, 2001; Freudenthal *et al.*, 2002; Kuhlmann *et al.*, 2004; Meyer *et al.*, 2010).

The Canary Islands off northwest Africa are located at the transition between the Mediterranean and the Saharan climate (Fig. 1). Thus, they are a key area for the investigation of palaeoenvironmental changes in this region. However, one has to differentiate between different islands of the Canarian archipelago: Due to their mostly quite young age and thus a relatively fresh and steep volcanic relief (Carracedo *et al.*, 1998) there are only some dispersed and clearly discontinuous loess-like layers mainly derived from Saharan dust found on the western islands (La Palma, El Hierro, La Gomera, Tenerife), containing some relicts of palaeosols that hold some information about former climates (e.g. Menéndez *et al.*, 2009b). These discontinuous archives are complemented by a desiccated lake in the north of Tenerife from where a vegetation record of the middle and late Holocene was obtained (de Nascimento *et al.*, 2009). Unlike from the western islands, we have much more palaeoenvironmental information from the generally older and thus more eroded eastern Canary Islands (Lanzarote, Fuerteventura, Gran Canaria) (Carracedo *et al.*, 1998). There, two main types of palaeoenvironmental archives are found (Fig. 1): 1) *Vega* sediments, i.e. a mixture of hardly weathered Saharan dust, soil material from the surrounding slopes and local volcanic material trapped in volcanically dammed valleys (e.g. Zöller *et al.*, 2003; Menéndez *et al.*, 2009a; Suchodoletz *et al.*, 2010b). 2) Dune-palaeosol sequences, where dunes mostly consisting of marine shell detritus originally blown out from the insular shelf are intercalated with several palaeosol horizons with slightly higher clay and silt content. Unlike the dune-sands, the palaeosols indicate more stable landscape conditions with trapping of Saharan dust (e.g. Petit-Maire *et al.*, 1986; Ortiz *et al.*, 2006; Suchodoletz *et al.*, 2012).

Both kinds of palaeoenvironmental archives on the eastern Canary Islands follow different geomorphologic mechanisms and cover different time slices. This article gives an overview over the geomorphologic processes active in these two types of archives and compares their palaeoenvironmental significance.

PALAEOCLIMATE ARCHIVES ON THE EASTERN CANARY ISLANDS

Vega sediments

Due to long peneplanation processes that took place especially on Lanzarote and Fuerteventura, the oldest subaerial volcanic complexes of Tertiary and Early Pleistocene age were strongly eroded (cf. Höllermann, 2006) and thus show generally smoothed and concave slopes. Following, these old volcanic complexes were dissected by numerous U-shaped valleys and smaller gullies (*barrancos*), whereas some larger valleys were dammed by volcanic material (lava flows, pyroclastica) during the Lower and Middle Pleistocene. Subsequently, these dammed valleys (locally called *vegas*) served as sediment traps for Saharan dust and local volcanic material with changing proportions throughout different times.

Generally, the slopes of the dammed valleys are either covered with only a thin layer of dust-borne or volcanic material or are even bare of any loose material. In difference, the sediments deposited in the *vega*-bottoms show thicknesses of up to several decametres and are horizontally layered, intercalating between yellowish/silty loess-like and reddish/clayey soil-like material (Fig. 2). Thus, not only in-situ aeolian and volcanic material is found in the valley bottoms, but also material that

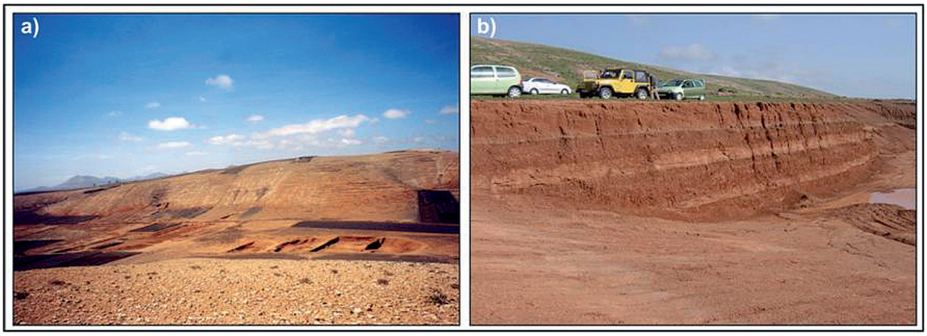

Figure 2. The *vega* of Teguise in the north of Lanzarote (location see Fig. 1): a) Overview of the *vega*. The steep slopes are almost bare of fine sediments, whereas the valley-bottom is filled with horizontally layered sediments that are outcropped by the local population for agricultural use and thus accessible for investigations. b) *Vega* sediments from Teguise in detail: the yellowish/silty loess-like layers are much lighter than the reddish/clayey ones that were derived from pedogenetic processes (photo: M. Zech).

was transported as colluvium into the *vega*-bottoms after its original deposition on the slopes. Consequently, the material filling the *vega*-bottoms consists of a mixture of in-situ aeolian and volcanic fallout as well as of colluvially reworked material from the slopes. However, apart from one exception around 20 ka, luminescence dating results from three *vegas* on Lanzarote do not show large hiatuses in the record until ca. 180 ka (Suchodoletz *et al.*, 2008). Furthermore, there are no fine sedimentary sub-layers recognizable in the large reddish or yellowish sediment packages, demonstrating that the transport from the slopes into the valley bottoms occurred with high-frequency and low magnitude, rather than with low frequency and high magnitude.

Thus, *vega*-bottom sediments constitute quasi-continuous palaeoenvironmental sediment archives, only showing temporal biases of maximal some thousand years due to sediment storage on the slopes and subsequent mixing with in-situ aeolian and volcanic material after its colluvial transport into the *vega*-bottoms (Suchodoletz *et al.*, 2009). Using different palaeoenvironmental proxies (grain size combined with XRD-analyses, bulk and frequency dependent magnetic susceptibility) it could be shown that the quartz-rich fine sand fraction of these sediments records changes of the properties of Saharan dust during the past. This is due to the fact that quartz is not autochthonously crystallized from the basaltic volcanism of the eastern Canary Islands and was thus exclusively transported to the islands by aeolian processes (Suchodoletz *et al.*, 2010a). Furthermore, it could be demonstrated that the reddish and clay-rich layers in the sequences are the product of pedogenetic processes at the slopes and in the *vega*-bottoms that were caused by higher soil moisture. Such phases of higher soil moisture occurred during cold

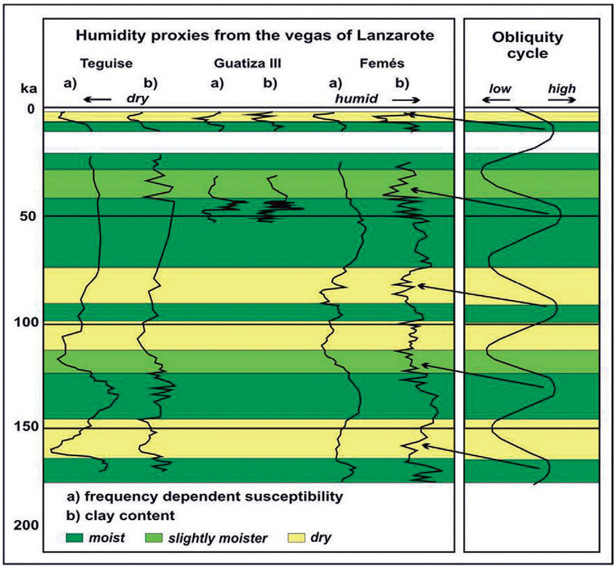

Figure 3. Proxies of soil moisture from three investigated *vegas* on Lanzarote (adapted from Suchodoletz *et al.*, 2010a; locations see Fig. 1). The obliquity-cycle was taken from Zachos *et al.* (2001).

phases of the Pleistocene during at least the last 180 kyr, thereby following a 41 kyr-cyclicity as the obliquity pattern of the Milankovich-cycles (Suchodoletz *et al.*, 2010b) (Fig. 3). Thus, the *vega*-sediments of the eastern Canary Islands constitute the only quasi-continuous terrestrial sediment-archives in the northwest-African region that extend beyond the last glacial-interglacial cycle.

Dune-palaeosol sequences

Loose carbonate sands are found at several coasts of the eastern Canary Islands where they form active dune-fields today (e.g. Höllermann, 1991). Additionally, at the coast and also at some places in the inland palaeodunes of Pleistocene and Holocene age occur (e.g. Rognon *et al.*, 1989; Criado *et al.*, 2004; Meco, 2008; see Fig. 1). Furthermore, locally dunes of even Tertiary age are found (Miocene and Pliocene; Rothe, 1996; Meco, 2008; Alcántara-Carrió *et al.*, 2010). The generally whitish dune-sands partly consist of fragments of volcanic material, whereas the largest part is composed of broken marine shells that had lived on the shelves around the islands and were blown out during glacial periods when global sea level was lower than today (Skene *et al.*, 1998). These dunes

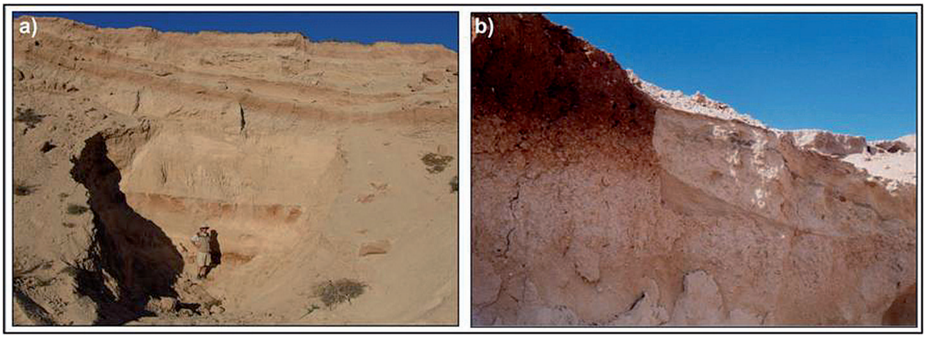

Figure 4. Examples of dune-palaeosol sequences on the eastern Canary Islands: a) The succession of dune-sands and palaeosol horizons in the Mala-dune in the north of Lanzarote (location see Fig. 1). b) In the dune-field of the Barranco de los Enamorados in the north of Fuerteventura a layer of dune-sand and an overlying palaeosol horizon were cut by a ravine that was refilled with younger dune-sand, demonstrating the discontinuity of this kind of palaeoenvironmental archive.

are often intercalated with layers of volcanic material (lava flows, pyroclastica), as well as with reddish-yellowish palaeosols containing a certain amount of clay and silt (Fig. 4a). At some places, periods of pedogenesis are also indicated by the presence of calcrete horizons in the dune-sands, demonstrating the former activity of percolating water. The occurrence of allochthonous quartz with sandy and silty grain sizes in the palaeosols indicates that similar to the *vega*-sediments at least a part of the fine material was derived from Saharan dust. However, the frequent incision of dune-layers and palaeosol horizons and the fact that they are discordantly overlain by new generations of dunes and palaeosols demonstrates that sedimentation of the dune-sequences was not continuous (Fig. 4b). Consequently, these sequences constitute discontinuous palaeoenvironmental archives.

Generally, palaeosols indicate phases of landscape stability (Rohdenburg, 1970), when the surface of the dunes was stabilized by a vegetation cover that stopped migration of the dune-sands and allowed pedogenesis with trapping of Saharan dust. However, the question remains which palaeoenvironmental conditions were the cause of periods of landscape stability in the areas covered with loose sand, when dune-migration stopped and pedogenesis became active. Several authors suggest a regional climatic trigger, where humidity is proposed to be the main player (e.g. Petit-Maire *et al.*, 1986; Ortiz *et al.*, 2006). Accordingly, in this case palaeosols should have formed during more humid periods at the eastern Canary Islands. However, stability could also be triggered by the availability of sand. In this case low sand-availability stopped the delivery of material so that no dunes could form and the land-surface was stabilized allowing the development of a vegetation cover. So it is known that dune-development exclusively controlled by sand-availability could be

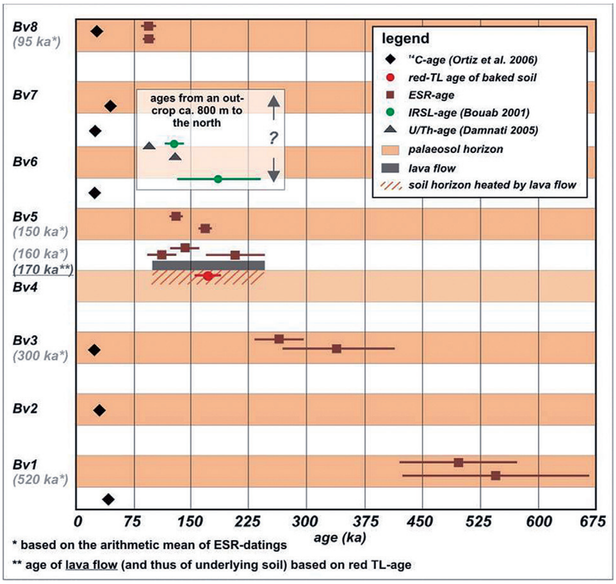

Figure 5. Schematic sketch of the Mala dune-palaeosol sequence in the north of Lanzarote with dune-accumulations (white), palaeosols (red), a lava flow (grey) and different numerical dating results with error bars (horizontal lines).

caused by anthropogenic activity (e.g. Tolksdorf and Kaiser, 2012). However, in the case of the eastern Canary Islands periods of low sand-availability should be caused by a high global sea-level during warm periods, when insular shelves were flooded so that they could not serve as sources for marine shell detritus. According to this model, palaeosols should have formed during periods of high global sea level.

Unlike the *vega*-sediments where luminescence dating worked quite well for at least the last 100 kyr (Suchodoletz *et al.*, 2008), there are large problems when establishing chronostratigraphies for the dune-palaeosol sequences. During the last decades, most authors based their chronologies and thus their palaeoenvironmental interpretations on ^{14}C dating that was regarded to yield reliable ages (e.g. Petit-Maire *et al.*, 1986; Rognon *et al.*, 1989; Ortiz *et al.*, 2006). However, in the case of the Mala dune-sequence (Fig. 4a) in the north of Lanzarote (Fig. 1) different dating methods were applied during the last years that showed large discrepancies between each other. Whereas a combination of ^{14}C- and amino acid dating of land snail shells yielded ages between 28 and 43 ka for the investigated outcrop (Ortiz *et al.*, 2006), ESR-dating of the same kind of material delivered ages between 95 and 500 ka (Suchodoletz *et al.*, 2012 and unpublished data) (Fig. 5). For instance, three singular ESR-datings from one dune-layer showed a rather large uncertainty but yielded an average age of ca. 158 ka. This average age is supported by a red thermoluminescence (TL) age of 172 ka obtained from quartz grains extracted from the palaeosol horizon underlying the dune-layer that was heated by a lava flow (Suchodoletz *et al.*, 2012) (Fig. 5). Moreover, U/Th-datings from the upper part of a parallel outcrop in the same dune-complex ca. 800 m north of the investigated site yielded two individual ages of 95 and 138 ka (Damnati, 2005). These U/Th-datings are confirmed by a parallel infrared-stimulated luminescence (IRSL)-age of ca. 130 ka, whereas an IRSL-dating from the upper part of the underlying sedimentary unit yielded 191 ka (Bouab, 2001). Altogether, this strongly pleads for a Late to Middle Pleistocene age of the whole Mala dune-palaeosol-sequence rather than for a Late Pleistocene age as suggested by Ortiz *et al.* (2006) (Fig. 5). General problems with ^{14}C-dating are also known from other arid regions as reported by Singhvi and Krbetschek (1996). Accordingly, a general lack of reliability of ^{14}C-ages from the eastern Canary Islands beyond the Holocene period was also stated by Meco (2008). Consequently, we built the chronostratigraphy of the Mala dune-palaeosol-sequence on (mainly unpublished) ESR-datings and the red TL age (Suchodoletz *et al.*, 2012). This sedimentary archive should serve here as an exemplary site to understand the gemomorphologic behaviour of dune-palaeosol sequences on the eastern Canary Islands, and thus their palaeoenvironmental significance. As shown below, the latter can only be achieved by a comparison with other archives and proxies.

In the whitish box in the upper part of the stratigraphy IRSL and U/Th-ages from a parallel outcrop in the same dune-sequence ca. 800 m to the north are shown. Although their exact stratigraphical correlation to the investigated outcrop is not known yet (indicated by a question mark), these ages are clearly in the same Late/Middle Pleistocene age range of our ESR ages and red TL age.

COMPARISON BETWEEN VEGA-SEDIMENTS AND DUNE-PALAEOSOL SEQUENCES

Since the investigated Mala dune palaeosol sequence in the north of Lanzarote should serve as an example for other dune-palaeosol sequences on the eastern Canary Islands, we compared this archive with palaeo-soil moisture derived from *vega*-sediments on Lanzarote (Suchodoletz *et al.*, 2010b) as well as with global sea level (Skene *et al.*, 1998) (Fig. 6).

This comparison should concentrate on palaeosols Bv8, Bv5 and Bv4 since numerical dating has the lowest uncertainty here (cf. Fig. 5). From figure 6 it seems that palaeosols Bv5 and Bv4 developed during periods of low global sea level, i.e. during periods when the shelves of the Canary Islands were exposed to the atmosphere so that marine shell detritus could be blown out. To a lower degree this holds also true for palaeosol Bv8 that developed when global sea level

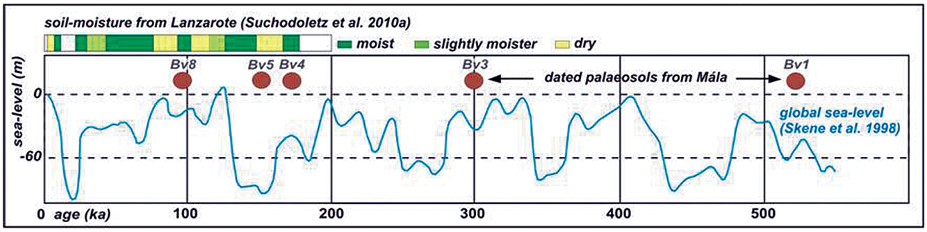

Figure 6. Comparison between soil-moisture derived from *vega*-sediments on Lanzarote (Suchodoletz *et al.*, 2010b), global sea level (Skene *et al.*, 1998) and the occurrence of palaeosols in the Mala-dune-palaeosol sequence (own data).

was lowered by about 10 m, exposing the upper part of the shelf and thus showing a somewhat enhanced sand-availability than e.g. during the Holocene. On the other hand, palaeosols Bv8 and Bv4 seem to have developed during periods when enhanced soil moisture was recorded in the *vega*-sediments, indicating more humid periods on the island during that time. In difference, palaeosoil Bv5 obviously developed during a dry period. However, it has to be kept in mind that small-scale humidity fluctuations can not be resolved by the *vega*-bottom sediments due to the mixture of in-situ and slope-derived material, producing a temporal bias of some kyr. Consequently, it seems that for the development of palaeosols in the dune-sequences geomorphic stability triggered by humidity can be assumed as the main cause. Thus, in agreement with former studies (e.g. Petit-Maire *et al.*, 1986; Ortiz *et al.*, 2006; Meco, 2008), the occurrence of palaeosols in dune-palaeosol sequences on the eastern Canary Islands can obviously be regarded an indicator of more humid conditions, causing the formation of a vegetation cover that hinders the mobility of sand and allows pedogenesis with the trapping of Saharan dust. However, palaeosols Bv4 and Bv5 originating from a period with very low global sea level are rather weakly developed compared with palaeosols Bv8, Bv7 and Bv6 that (probably) all developed during a generally higher sea level during marine isotope stage (MIS) 5 (Bv7 and Bv6 developed before Bv8 and after Bv5, but are separated from the latter by a strong hiatus so that a temporal proximity with Bv8 is likely). Thus, it can not be excluded that also sand availability controlled by global sea level played a certain role for development/intensity of the palaeosols. We believe that this effect could possibly also explain the hiatus in the Mala-dune above Bv8 (after ca. 95 ka). After that date, global sea level strongly fell and rose up significantly only in the beginning of the Holocene about 10 kyr ago (Fig. 6). Consequently, all palaeosols that had formed after Bv8 must have been only weakly developed and only palaeosol(s) that developed during the Holocene should have had shown stronger intensities. Since anthropogenic activity strongly altered the land-surface of Lanzarote during the last 2 kyr as is known from geoarchaeological studies (e.g. Santana-Santana, 2003; Criado and Atoche, 2004), Holocene palaeosol(s) as well as loose Late Pleistocene dune-material including weakly developed palaeosols were probably eroded during that period, and only the relatively hard surface of Bv8 impeded this erosional process to go deeper. However, these assumptions are very speculative yet and have to be tested during further investigations. Nevertheless, it became clear that due to the failure of ^{14}C-dating in such calcareous sequences as clearly demonstrated for the case of Mala, palaeoclimate studies based on that dating method must be re-evaluated with respect to geochronology. Thus, palaeoclimatic models stating regular humidity cycles of some kyr as a cause of palaeosol formation as e.g. proposed by Ortiz *et al.* (2006) can not be sustained any more and have to be revised.

CONCLUSIONS

In this article we could show that there are two different kinds of palaeoenvironmental archives on the eastern Canary Islands that are complementary to each other. On the one hand, *vega*-sediments continuously record the intensity of pedogenesis caused by changes of palaeo-soil moisture that were controlled by humidity fluctuations during the past. On the other hand, dune-palaeosol sequences are discontinuous archives that directly record phases of landscape activity and stability on the eastern Canary Islands connected with more humid and arid phases, possibly overlain by the effects of sand availability triggered by global sea level. Furthermore, whereas due to the limited depth of existing outcrops investigations of *vega*-sediments are limited to the last ca. 200 kyr yet, outcropped dune-palaeosol sequences cover a much larger time frame. The latter is demonstrated by two facts: 1) Tertiary sequences are already described in the geologic literature (e.g. Rothe, 1996; Meco 2008) 2) amino acid racemisations measured on different dune-palaeosol sequences from the eastern Canary Islands (Ortiz *et al.*, 2006) show that the Mala-sequence covering the time-slice from about 95–>520 ka only comprises aminozones 3 and 4. Thus, sequences comprising aminozones 1 and 2 must be older than ca. 520 ka, and those comprising zones 5 till 8 must be younger than 95 ka. Consequently, these sequences have to be re-investigated using other numerical dating methods than ^{14}C, in order to obtain a comprehensive picture of phases of landscape activity and stability on the eastern Canary Islands.

REFERENCES

Alcántara-Carrió, J., Fernández-Bastero, S. and Alonso, I. (2010) Source area determination of aeolian sediments at Jandia Isthmus (Fuerteventura, Canary Islands). *Journal of Marine Systems*, 80, 219–234.

Bouab, N. (2001) *Application des méthodes de datation par luminescence optique à'l évolution des environnements désertiques - Sahara occidental (Maroc) et Iles Canaries (Espagne)*. PhD-thesis, Université de Québec à Montréal, Montréal.

Carracedo, J.C., Day, S., Guillou, H., Rodríguez-Badiola, E., Canas, J.A. and Pérez-Torrado, F.J. (1998) Hotspot volcanism close to a passive continental margin: the Canary Islands. *Geological Magazine*, 135, 591–604.

Cheddadi, R., Lamb, H.F., Guiot, J. and van der Kaars, S. (1998) Holocene climate change in Morocco: A quantitative reconstruction from pollen data. *Climate Dynamics*, 14, 883–890.

Criado, C. and Atoche, P. (2004) ¿Influyó la ganadería de los mahos en el deteriorio paleoambiental de la isla de Lanzarote? *Revista Tenique*, 6, 139–157.

Criado, C., Guillou, H., Hansen, A., Hansen, C., Lillo, P., Torres, J.M. and Naranjo, A. (2004) Geomorphological evolution of parque natural de Las Dunas de Corralejo (Fuerteventura, Canary Islands). *Contribuciones recientes sobre geomorfología* (ed. by Benito, G. and Díez-Herrero, A.), pp. 291–297. SEG and CSIC, Madrid, Spain.

Damnati, B. (2005) Sedimentologie et minéralogie de la séquence sedimentaire «Mala» située à Lanzarote (Iles Canaries, Espagne): Les significations paléoclimatiques. *Revista de la Sociedad Geológica de España*, 18, 179–185.

de Nascimento, L., Willis, K.J., Fernández-Palacios, J.M., Criado, C. and Whittaker, R.J. (2009) The long-term ecology of the lost forests of La Laguna, Tenerife (Canary Islands). *Journal of Biogeography*, 36, 499–514.

Freudenthal, T., Meggers, H., Henderiks, J., Kuhlmann, H., Moreno, A. and Wefer, G. (2002) Upwelling intensity and filament activity off Morocco during the last 250.000 years. *Deep-Sea Research II*, 49, 3655–3674.

Gasse, F., Fontes, J.C., Plaziat, J.C., Carbonel, P., Kaczmarska, I., de Deckker, P., Soulié-Marsche, I., Callot, Y. and Dupeuble, P.A. (1987) Biological remains, geochemistry and stable isotopes for the reconstruction of environmental and hydrological changes in the Holocene lakes from North Sahara. *Palaeogeography, Palaeoclimatology, Palaeoecology*, 60, 1–46.

Höllermann, P. (1991) *Untersuchungen zur äolischen Morphodynamik im Driftsandgürtel von Lanzarote (Kanarische Inseln).* Studien zur Physischen Geographie und zum Landnutzungspotential der östlichen Kanarischen Inseln, Erdwissenschaftliche Forschung, Band xxv, Mainz.

Höllermann, P. (2006) Zur geomorphologischen Wasserwirkung in den arid-semiariden Subtropen – Fallstudie Fuerteventura (Kanarische Inseln, Spanien). *Bayreuther Geographische Arbeiten*, 27, 55–103.

Intergovernmental Panel on Climate Change (2007) *Climate Change 2007, the Fourth Assessment Report.* IPCC, Geneva, Switzerland.

Kuhlmann, J., Freudenthal, T., Helmke, P. and Meggers, H. (2004) Reconstruction of palaeoceanography off NW Africa during the last 40,000 years: influence of local and regional factors on sediment accumulation. *Marine Geology*, 207, 209–224.

Lancaster, N., Kocurek, G., Singhvi, A., Pandey, V., Deynoux, M., Ghienne, J.F. and Lo, K. (2002) Late Pleistocene and Holocene dune activity and wind regimes in the western Sahara desert of Mauritania. *Geology*, 30, 991–994.

Linstädter, A. and Zielhofer, C. (2010) Regional fire history shows abrupt responses of Mediterranean ecosystems to centennial-scale climate change (*Olea-Pistacia* woodlands, NE Morocco). *Journal of Arid Environments*, 74, 101–110.

Lioubimtseva, E. (2004) Climate change in arid environments: revisiting the past to understand the future. *Progress in Physical Geography*, 28, 1–29.

Meco, J. (2008) *Historia Geológica del Clima en Canarias.* Las Palmas de Gran Canaria.

Menéndez, I., Cabrera, L., Sánchez-Pérez, I., Mangas, J. and Alonso, I. (2009a) Characterisation of two fluvio-lacustrine loessoid deposits on the island of Gran Canaria, Canary Islands. *Quaternary International*, 196, 36–43.

Menéndez, I., Derbyshire, E., Engelbrecht, J., Suchodoletz, H. von, Zöller, L., Dorta, P., Carillo, T. and Rodríguez de Castro, F. (2009b) Saharan dust and the aerosols on the Canary Islands: past and present. *Airborne particulates* (ed. by Cheng, M. and Liu, W.), pp. 39–80. Novapublishers, Hauppauge NY, USA.

Meyer, I., Davis, G. and Stuut J.B.W. (2010) Grain size control on Sr-Nd-isotope provenance studies and impact on paleoclimate reconstructions: an example from deep sea sediments offshore NW-Africa. *Geochemistry, Geophysics, and Geosystems*, 12, doi: 10.1029/2010GC003355.

Moreno, A., Taragona, J., Henderiks, J., Canals, M., Freudenthal, T. and Meggers, H. (2001) Orbital forcing of dust supply to the North Canary Basin over the last 250 kyr. *Quaternary Science Reviews*, 20, 1327–1339.

Mountney, N.P. (2003) Modelling the Response of aeolian Desert Systems to Climate Change. *British Sedimentological Research Group Annual General Meeting* (ed. by Bass, J.H.). University of Leeds, Leeds, United Kingdom.

Ortiz, J.E., Torres, T., Yanes, Y., Castillo, C., de la Nuez, J., Ibañez, M. and Alonso, M.R. (2006) Climatic cycles inferred from the aminostratigraphy and aminochronology of Quaternary dunes and palaeosols from the eastern islands of the Canary Archipelago. *Journal of Quaternary Science*, 21, 287–306.

Petit-Maire, N., Delibrias, G., Meco, J., Pomel, S. and Rosso, J.C. (1986) Paléoclimatologie des Canaries orientales (Fuerteventura). *Comptes Rendues de l´Académie des Sciences*, 303, 1241–1246.

Rognon, P., Coudé-Gaussen, G., Le Coustumer, M.-N., Balouet, J.C. and Occhietti, S. (1989) Le massif dunaire de Jandía (Fuerteventura, Canaries): Évolution des paléoenvironnements de 20.000 BP à l´actuel. *Bulletin de l´Association francaise pour l´étude du Quaternaire*, 1989, 31–37.

Rohdenburg, H. (1970) Morphodynamische Aktivitäts- und Stabilitätszeiten statt Pluvial- und Interpluvialzeiten. *Eiszeitalter und Gegenwart*, 21, 81–96.

Rothe, P. (1996) *Kanarische Inseln*. Sammlung Geologischer Führer, Gebrüder Bornträger Berlin, Stuttgart.

Santana-Santana, A. (2003) Consideraciones en torno al medio natural canario anterior a la conquista. *Eres (Arqueología/Antropología)* 11, 61–75.

Singhvi, A.K. and Krbetschek, M.R. (1996) Luminescence dating: a review and a perspective for arid zone sediments. *Annals of the Arid Zone*, 35, 249–279.

Skene, K.I., Piper, D.J.W., Aksu, A.E. and Syvitsky, J.P.M. (1998) Evaluation of the global oxygen isotope curve as a proxy for Quaternary sea level by modeling of delta progradation. *Journal of Sedimentary Research*, 68, 1077–1092.

Suchodoletz, H. von, Fuchs, M. and Zöller, L. (2008) Dating Saharan dust deposits at Lanzarote (Canary Islands) by luminescence dating techniques and their implication for paleoclimate reconstruction of NW Africa. *Geochemistry, Geophysics, and Geosystems*, 9, doi: 10.1029/2007GC001658.

Suchodoletz, H. von, Faust, D. and Zöller, L. (2009) Geomorphological investigations of sediment traps on Lanzarote (Canary Islands) as a key for the interpretation of a palaeoclimate archive off NW Africa. *Quaternary International*, 196, 44–56.

Suchodoletz, H. von, Oberhänsli, H., Faust, D., Fuchs, M., Blanchet, C., Goldhammer, T. and Zöller, L. (2010a) The evolution of Saharan dust input on Lanzarote (Canary Islands) – influenced by human activity in the Northwest Sahara during the Early Holocene? *The Holocene*, 20, 1–11.

Suchodoletz, H. von, Oberhänsli, H., Hambach, U., Zöller, L., Fuchs, M. and Faust, D. (2010b) Soil moisture fluctuations recorded in Saharan dust deposits on Lanzarote (Canary Islands) over the last 180 ka. *Quaternary Science Reviews*, 29, 2173–2184.

Suchodoletz, H. von, Blanchard, H., Hilgers, A., Radtke, U., Fuchs, M., Dietze, M. and Zöller, L. (2012) TL and ESR-dating of Middle Pleistocene lava flows on Lanzarote island, Canary Islands (Spain). *Quaternary Geochronology*, 9, 54–64.

Tolksdorf, J.F. and Kaiser, K. (2012) Holocene aeolian dynamics in the European sandbelt as indicated by geochronological data. *Boreas*, 41, 408–421.

Zachos, J., Pagani, M., Sloan, L., Thomas, E. and Billups, K. (2001) Trends, rhythms, and aberrations in global climate 65 Ma to present. *Science*, 292, 686–693.

Zöller, L., Suchodoletz, H. von and Küster, N. (2003) Geoarchaeological and chronometrical evidence of early human occupation on Lanzarote (Canary Islands). *Quaternary Science Reviews*, 22, 1299–1307.

EVIDENCE OF HISTORICAL EXTREME HEAVY RAINS ON LANZAROTE (CANARY ISLANDS, SPAIN)

Constantino Criado, Pedro Dorta, José Bethencourt,
Juan F. Navarro, Carmen Romero

CLIMATE CHANGE PERSPECTIVES FROM THE ATLANTIC:
PAST, PRESENT AND FUTURE

Jose María Fernández-Palacios, Lea de Nascimento, José Carlos Hernández,
Sabrina Clemente, Albano González & Juan P. Díaz-González (eds.)
Servicio de Publicaciones, Universidad de La Laguna – 2013

ISBN: 978-84-15910-54-1

pp. 275-298

ABSTRACT

The Timanfaya eruption (1730–1736) has been the most important volcanic event on the Canary Islands during historical times (after the 15th Century AD). It produced lava flows and pyroclastic layers burying around 23% of Lanzarote's surface. Throughout the island, artificial cross-sections such as soil quarries and road trenches reveal an ash layer, covering palaeosoils (Argids) or interbedded with alluvial sediment that infill the bottom of U-shaped valleys. Sedimentological analyses including Munsell colour, textures, carbonates, grain-size study of the sand fraction, mineralogy using X-ray diffraction, and geochemistry (total oxides and trace elements), have been carried out on five cross-sections located in different parts of the island (Puerto Calero, Femés, Tiagua, Guatiza and Valle de San José). This data, along with radiocarbon ages, archaeological remains (pottery) and historical documents, allow the ash layer to be identified as part of the Timanfaya eruption. The alluvial sediment covering this layer could have been produced by runoff from heavy rain events, probably the famous *Huracán de 1826*, also known as *Tormenta de San Florencio.*

KEYWORDS: Canary Islands, *Huracán de 1826*, Lanzarote, Paleargids, soil erosion, Timanfaya eruption.

INTRODUCTION

Lanzarote, the north-easternmost island of the Canary Archipelago, is only 862 km^2 and has little altitude, barely reaching 700 m above sea level (m a.s.l.) (Fig. 1). Eruption activity started during the Miocene, producing two areas with significant volcanic emissions: the Femés massif (the highest point in Atalaya de Femés, 606 m a.s.l.), located in the southern part of the island, and the Famara massif (the highest point in Peñas del Chache, 686 m a.s.l.), in the north. Between both structures, boreholes made during the seventies provided evidence of Miocene rocks, but the volcanic activity has obviously been weaker in the central area than in the northern and southern massifs; these minor volcanic emissions produced lowlands (Hansen and Moreno, 2000; Romero, 2003). After a long period of erosion, volcanic activity restarted during the Pliocene, but the most important volcanic event occurred during the Quaternary, covering the majority of the island's lowlands with lava fields and cinder cones. On these sectors of the island we can differentiate cinder cones, isolated or aligned, with Matuyama

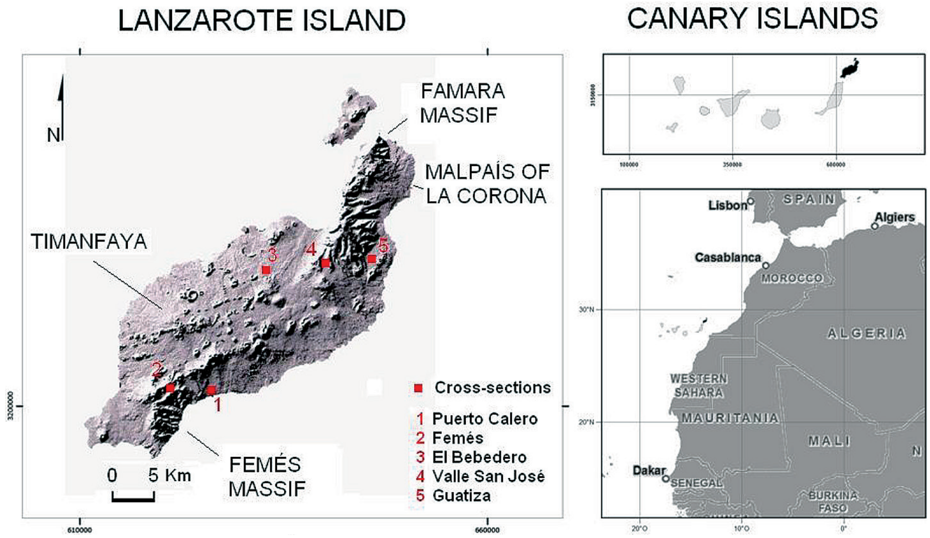

Figure 1. Location of cross-sections in Lanzarote island.

reverse polarity or Brunhes normal polarity (Fúster and Carracedo, 1979; Coello *et al.*, 1992), and absolutes ages ranging from 1.20 Ma to 0.034 Ma (Carracedo *et al.*, 1991; 1992; Coello *et al.*, 1992; IGME, 2005). More recently (91 and 20.7 kyr BP), the Los Helechos and La Corona eruptions produced several conspicuous cinder cones and a big lava field (Carracedo *et al.*, 2003). The massive Timanfaya eruption occurred in the historical era (1730–1736) and, a little later the small event of Nuevo del Fuego, Tao and Tinguatón in 1824 (Carracedo *et al.*, 1990; Romero, 1991; 1997; 2003).

The island has an arid climate, receiving just 109 mm year^{-1} of rain (Guacimeta Airport) and an ETP (Thornwaithe method) estimated at 984 mm year^{-1}. Therefore, the UNEP index is 0.11 inside the arid type (Thomas, 1997). The humidity is usually high, except when Saharan continental air reaches the island. It receives 2944 hours of sunlight per year. However, the wind is moderate (57% blowing between 6–28 km h^{-1}), mostly from the NW, N and NE (72% a year and 92% in July).

METHODS

We studied five detailed cross-sections in different parts of the island (Puerto Calero, Femés valley, Tiagua (El Bebedero archaeological site), Valle de San José and the Guatiza soil quarry; we found volcanic ash layers in all of them, presumably

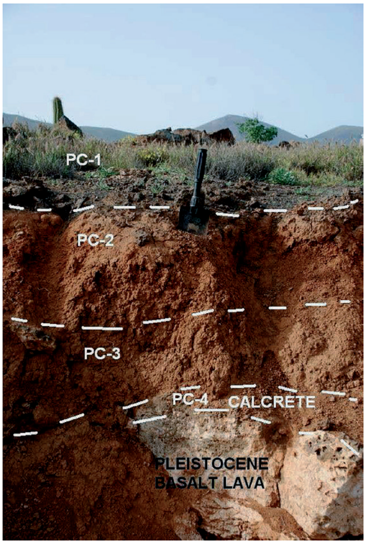

Figure 2. Puerto Calero cross-section.

produced by the Timanfaya eruption (1730–1736 AD). We determined the exact locations of each cross-section using UTM coordinates from a Garmin GPS. In all the sequences we carried out textural analyses (Bouyoucos method) and determined the Munsell colour and percentage of carbonates (Bernard method). Furthermore, the volcanic ash layers were studied under microscope, and sieving – removing carbonates using acetic acid – was employed to obtain grain-size parameters (using GRADISTAT). The mineralogical composition of the crystalline fraction was obtained by XRD (SIDIX, University of La Laguna), while the geochemistry (total oxides and trace elements) was determined in the Jaume Almera Earth Sciences Institute (CSIC, Barcelona). The chronology of cross-sections was established using tephrochronology, archaeology (pottery remains), and three radiocarbon ages, two of which we published in previous papers (Criado and Atoche, 2003; 2004). Finally we also used several written records found in historical archives of the Canary Islands.

RESULTS

Puerto Calero cross-section

This small cross-section is located on a road going from Puerto Calero to Puerto del Carmen. It provided evidence of the landscape of this island before the historical eruptions (Fig. 2). It also helped to understand the evolution of the flat

TABLE 1. Sedimentological features of Puerto Calero cross-section.

Layer	% > 2 mm	% < 2 mm	Munsell Colour	Sand (%)	Silt (%)	Clay (%)	Texture	Carbonates (%)
1	13.65	86.35	7.5 YR 5/6	75.47	19.46	5.06	Loamy sand	3.80
2	1.58	98.41	7.5 YR 5/8	11.91	50.67	37.43	Silty clay loam	15.25
3	0.86	99.14	7.5 YR 5/6	10.60	47.27	42.13	Silty clay	22.03
4	Calcrete		7.5 YR 8/3					38.98
5	Basalt Serie III							

areas far away from the steep slopes (Table 1). The textural analysis, the colour and the existence of a Ca horizon indicate the presence of Paleargid soil, overlapped by a layer of tephra probably produced by the Timanfaya volcano group (Fig. 3). Due to the lack of conspicuous landforms in this area, no recent sediments produced by historical soil erosion and carried out by runoff processes have covered the tephra. The XRD analysis of the lapilli and ash layers shows an important amount of olivine; in addition, the grain-size parameters indicate a coarse size and poorly sorted sample, which can be explained by proximity to the volcanic vents, located to the south of the cross-section. The airborne trajectory of coarse volcanic materials is easy to understand due to the short distance from the vent and the presence of wind blowing from the NW, N and NE at speeds of up to 63 km h^{-1}.

Femés valley cross-section

This cross-section is found within an asymmetrical, U-shaped valley located in the Miocene massif of Femés (Fig. 4). The altitudinal gradient from the ridges to the base is over 100 meters. The former valley has been dammed by two volcanoes whose activity occurred during the Lower Pleistocene (Caldera Gritana and Caldera Riscada, 1.13 Ma; IGME, 2005). In the bottom of this valley several areas have been used as soil quarries (Table 2); in them we can see an interesting palaeosoil sequence (Hernández *et al.*, 1991), which also has been explained as the result of soil processes that occurred on peridesert *loess* depots (Zoller *et al.*, 2003; Suchodoletz *et al.*, 2009). The lowest layers (four) are Paleargids soils with calcretes. Layers four and five are a sedimentary depot with loam texture and very clear sedimentary structures, providing solid evidence of runoff. We can also see the remains of terrestrial fauna living in open air (terrestrial snails and

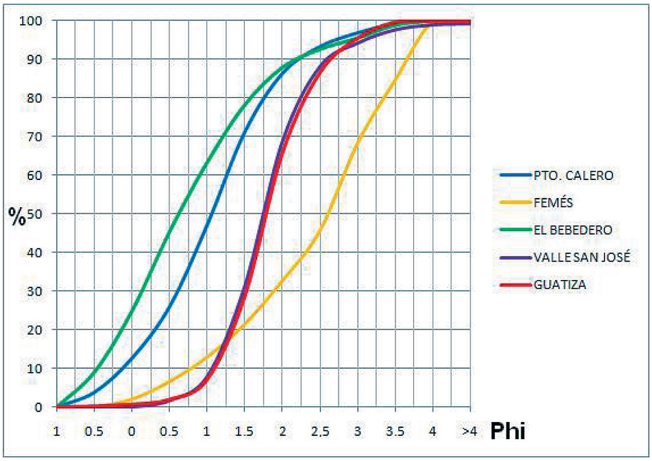

Figure 3. Grain-size curves of tephra layers obtained in the cross-sections.

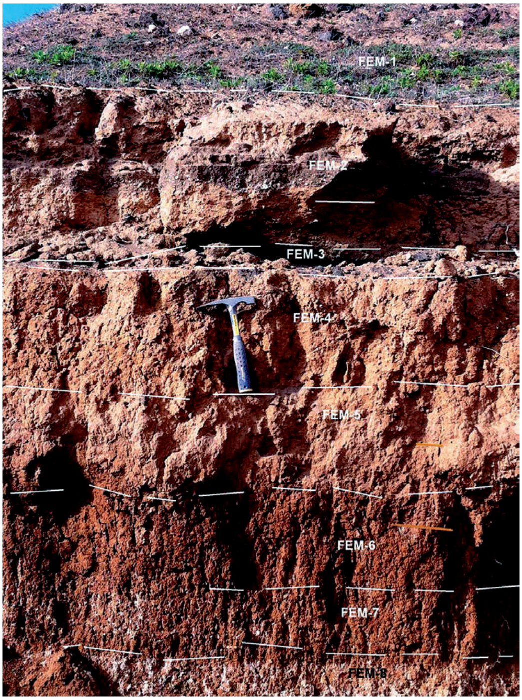

Figure 4. Femés valley cross-section.

TABLE 2. Sedimentological features of Femés valley cross-section.

Layer	% > 2 mm	% < 2 mm	Munsell Colour	Sand (%)	Silt (%)	Clay (%)	Texture	Carbonates (%)
1	6.1	93.9	7.5 YR 5/2	85.62	3.92	10.44	Sandy loam	4.08
2	5.8	94.2	7.5 YR 5/6	58.06	29.27	12.66	Loam sand	10.40
3	7.0	93.0	7.5 YR 5/3	82.00	6.95	11.05	Sandy loam	3.67
4	11.9	88.1	7.5 YR 5/4	13.21	47.57	39.22	Silt clay loam	8.10
5	5.7	94.3	7.5 YR 4/6	13.14	53.30	33.56	Silt clay loam	6.90
6	0.0	100.0	5 YR 4/6	0.00	37.93	62.07	Clay	1.63
7	17.3	82.7	5 YR 4/4	0.00	35.58	64.52	Clay	3.06
8	13.8	86.2	7.5 YR 5/4	1.21	42.48	56.31	Silt clay	12.4
9	9.2	90.8	7.5 YR 4/4	13.22	68.25	18.53	Silt loam	13.4

insect nests). A sample of terrestrial snails taken from Stratum 4 gave an age of 1890±40 years BP (Beta-172350). We have found a volcanic ash layer over Stratum 4 that is very rich in olivine (XRD) and finer and better sorted than the Puerto Calero sample (Fig. 3). The position of this layer, overlapping others dated by radiocarbon, could have resulted from the primary deposition of airborne ashes from the Timanfaya volcanoes spread by the usual wind blowing on this island. Over it we can see a thin layer very rich in pyroclastic rocks, with typical runoff structures. In our opinion it was produced by an unusual runoff event which eroded the ridges and upper slopes of the Femés valley, where today calcretes appear, former Ca horizons of eroded Paleargids. The surface layer is clearly anthropogenic and can be explained as an *enarenado*, a traditional agricultural system used to get productive crops without irrigation systems.

El Bebedero archaeological site cross-section

This cross-section is found near Tiagua, located inside an old volcanic crater (Pleistocene). It was discovered when a sedimentary depot was used as a soil quarry. The archaeological profile shows five different layers (Fig. 5) (Table 3). B-3 is the most recent from an archaeological point of view (Atoche *et al.*, 1995;

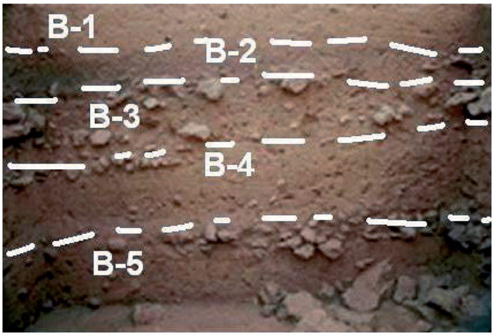

Figure 5. El Bebedero cross-section.

TABLE 3. Sedimentological features of El Bebedero archaeological site.

Layer	% > 2 mm	% < 2 mm	Munsell Colour	Sand (%)	Silt (%)	Clay (%)	Texture	Carbonates (%)
1	8.4	91.6	7.5 YR 5/6	34.1	51.2	14.7	Silt loam	3.7
2	17.1	82.9	10 YR 5/4	82.4	14.0	3.6	Sand	2.5
3	21.5	78.5	10 YR 5/4	30.0	54.5	15.5	Silt loam	5.8
4	26.1	73.9	10 YR 5/4	35.3	49.9	14.8	Silt loam	13.4
5	0.6	99.4	7.5 YR 5/6	28.6	62.9	8.5	Silt loam	3.3

Criado and Atoche, 2003), dated by radiocarbon at 635 ± 50 years BP (GrA-2463). It is overlapped by a tephra layer (B-2), very rich in olivine (XRD) presumably carried airborne by the wind from the eastern vent of the Timanfaya eruption (Fig. 3). The B-1 layer is sedimentary material, including historical pottery remains, produced by the runoff of intense heavy rains.

Valle de San José cross-section

The U-shaped Valle de San José is located in the Miocene massif of Famara. It has gentle slopes with rounded ridges, reaching an altitude of less than 50 m from the base. The former valley drained to the South but it was dammed by the Guanapay eruption (1.20 Ma, Coello *et al.*, 1992). The deposition of ashes was

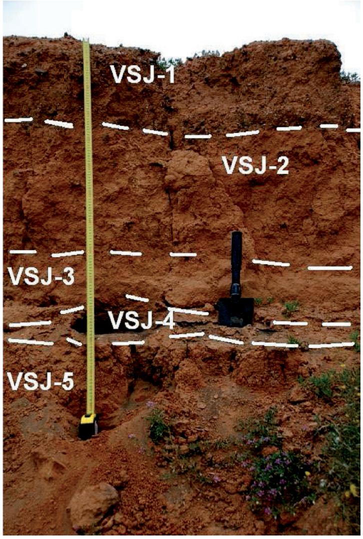

Figure 6. Valle de San José cross-section.

TABLE 4. Sedimentological features of Valle de San José cross-section.

Layer	% > 2 mm	% < 2 mm	Munsell Colour	Sand (%)	Silt (%)	Clay (%)	Texture	Carbonates (%)
1	15.88	84.12	7.5 YR 5/6	53.82	33.06	13.12	Loam	20.30
2	1.42	98.58	7.5 YR 5/8	43.12	43.30	11.57	Loam	16.94
3	0.66	99.34	7.5 YR 5/6	58.49	34.33	7.17	Sandy loam	28.81
4	0.34	99.66	7.5 YR 4/1	96.05	0.88	3.06	Sand	11.86
5	0.35	99.65	7.5 YR 5/6	4.22	71.63	24.15	Silty clay loam	8.47

followed by weathering in wet palaeoclimates, producing Paleargids which today are badlands on the slopes of the volcano.

The Valle de San José cross-section contains a heavy contrast between the Paleargid at the bottom (VSJ-5) and the upper layers (Fig. 6) (Table 4). The lowest palaeosoil shows weak carbonatation, while the increase of this feature seen in the upper layers (VSJ-1, VSJ-2 and VSJ-3) can be explained by the arrival

Figure 7. Surface calcretes on the ridges from Valle de San José.

of sediment richer in carbonates, occasionally gravels or stones produced by the erosion of calcretes today exposed at the surface of ridges and upper slopes of this valley (Fig. 7).

The tephra layer (VSJ-4) contains a significant amount of olivine (XRD), and the grain-size is very well sorted (Fig. 3). In the VSJ-2 layer we have found several fragments of traditional pottery, some of which were made with a wheel and have a glazed honey colour. These characteristics date them to somewhere between the 15th and 20th centuries AD; also, there is a fragment of handmade Mojón pottery, a very common style during the historical era. So, the pottery is evidence that the upper layers of this cross-section are recent. In addition, a goat bone was found in this layer, identified as the right pelvis of a young female *Capra hircus*. After identification, the bone was sent to Beta Labs (USA) and found to have a radiocarbon age of 160 ± 40 years BP (Beta-264367). Therefore, in our opinion the tephra layer is the result of pyroclastic material spread aerially by wind blowing from SW or W during the Timanfaya eruption.

GUATIZA CROSS-SECTION

This cross-section is located inside a soil quarry near the village of Guatiza (Fig. 8). The place is an endorheic basin generated by the volcanic activity during the Pleistocene (Second Cycle). Sediments carried from the eastern slope of the

Figure 8. Guatiza cross-section.

TABLE 5. Sedimentological features of Guatiza cross-section.

Layer	% > 2 mm	% < 2 mm	Munsell Colour	Sand (%)	Silt (%)	Clay (%)	Texture	Carbonates (%)
1	0.12	99.88	7.5 YR5/6	78.42	18.12	3.46	Loamy sand	23.72
2	0.23	99.77	7.5 YR5/6	44.21	48.24	7.55	Sandy loam	35.89
3	59.13	40.17	7.5 YR5/6	97.19	1.09	1.72	Sand	23.70
4	0.86	99.14	7.5 YR5/3	90.81	8.60	0.59	Sand	11.86
5	0.18	99.82	7.5 YR5/6	29.16	49.92	20.92	Silt loam	23.72

Famara massif by torrential activity produced the infilling of the primal topographical depression. We do not know the exact depth of the sediment infilling but we cannot see the rocky substratum. The sedimentary layers do not look like peridesert *loess*, as they are mainly formed by coarse sediments (Fig. 8) (Table 5). The GUAT-3 layer has a pocket of gravel and coarse sands. In addition, there are typical sedimentary structures providing solid evidence of fluvial processes. Below it, the GUAT-4 tephra layer is well sorted (Fig. 3). Our field and laboratory data indicate that the GUAT-4 is an ash layer produced by the aerial deposition of fine tephra from the Timanfaya eruption. One map and texts coetaneous of the eruption provide evidence about Timanfaya tephra reaching Guatiza, far away from the volcanic vents.

DISCUSSION

THE DISPERSAL OF HISTORICAL TEPHRA

The geological history of Lanzarote is well known. The early contributions to the volcanostratigraphy of the island (Hernández-Pacheco, 1909; Hausen, 1959; Fúster *et al.*, 1968) have recently been improved through palaeomagnetic mapping and absolute chronology (Fúster and Carracedo, 1979; Abdel-Monen *et al.*, 1971; Ibarrola *et al.*, 1988; Coello *et al.*, 1992; Carracedo *et al.*, 2003; IGME, 2005; von Suchodoletz *et al.*, 2012). Today we have a reasonable understanding of the volcanic activity from the Upper Pleistocene until present.

The first studies presumed a Holocene age for the La Corona Volcano group, because of its very good morphological preservation and the existence of a Holocene raised beach over its lava flows. All authors agree that this is a polygenetic volcanic area. The stratigraphic relationships provide a volcanic sequence: the older ones are La Quemada de Órzola, Los Helechos and La Cerca, and the younger one is La Corona Volcano, with its extensive lava field. However, there is no agreement about the age of this group. Zazo *et al.*, (1997) describe one raised beach dated at 5.8 ka using U/Th and ^{14}C dating; for them the raised beach is below the La Corona Volcano lava flows. In contrast, Carracedo *et al.*, (2003), believe the raised beach (+0.5 m over sea level) is over these lava flows. They based their opinion on two new absolutes ages: Los Helechos was dated at 91.2 ka and La Corona at 20.7 ka; these dates are in accord with the Last Glacial Maximum, when the sea level was at -120 m. This is in agreement with the development of Los Verdes cave, whose Atlantida Tunnel is now under sea level, at around 1600 m from the coast and 80 m deep (Carracedo *et al.*, 2003). The absolute dating of these volcanoes is very important for our purposes. The tephra spread by these eruptions would arrive very early to the Guatiza and San José *vegas*, and, obviously, they could not be near the surface but should be buried by a thick pocket of different kinds of material, including fluvial sediments and recent volcanic tephra.

The Holocene age has been proposed for the Calderetas de Guatiza and Montaña La Guenia (IGME, 2005) volcanic group. However recent dating proposes an age of 170 ka for this group (Suchodoletz *et al.*, 2012). The first one is well preserved, but the lava flows have been cut off by the Holocene sea level, including raised beaches in the southern village of Arrieta (IGME, 2005).

Regarding the Timanfaya group, Carracedo *et al.* (1991) believed that some of these volcanoes were older than historical ones. However, their palaeomagnetic study of 114 samples in 44 different places, found differences of declination of about 20° between Group II (cinder cones that lack evidence to be attributed to the Timanfaya eruption) and Group III (Timanfaya eruption) and greater than 10° in inclination between Group III and Group I (cinder cones that were clearly edified before Timanfaya eruption). These authors believe that the similarity in inclination between Groups I and III (apparently belonging to a different secular derive curve) reduces the confidence of this method, with no solid evidence to separate two different eruptive phases (Late Holocene and Historical).

In conclusion, today it is generally accepted that the only volcanic activity that occurred on Lanzarote during the Holocene are the giant Timanfaya eruption (1730–1736 AD), and the minor Volcán Nuevo, Tao and Tinguatón eruptions (1824), the majority of which occurred over the landscape created by the previous Timanfaya eruption, except for the Tao Volcano, which was outside of the area occupied by Timanfaya material, and whose tephra did not spread far from its crater (Romero, 1997): *«...and also a very important amount of sand, which fell on the Tao area»*.

Between 1730 and 1736, for 2053 days Lanzarote experienced one of world's largest basaltic eruptions in historical times. As a result, extensive areas of the island were covered by lava flows and pyroclastic layers (Romero, 1997). Many eruptive events, occurring between 1 September, 1730 and 6 April, 1736, edified at least 30 cinder cones and an even greater number of secondary cones and *hornitos*. All the volcanic edifices are on a 14 kilometre long tectovolcanic fissure. The new materials covered an area of 200 km^2, with a calculated volume of between 3 to 5 km^3 (Carracedo *et al.*, 1990). Due to its magnitude, the eruption was visible from Gran Canaria, more than 200 km away.

The volcanic material covered 23.2% of the island's surface and had a devastating effect on the economy (agriculture and livestock) and inhabitants. A recent doctoral thesis has identified the exact location of the goods destroyed by the volcano (De León, 2009). Historical records permit the sectors covered by ash during the first months of activity to be mapped (Romero, 1991; 1997). The places affected were: Vegueta, Yuco, Tiagua, Tao, Cercado, San Bartolomé, Calderetas, Montañablanca, Mosaga, Lomo de San Andrés, Conil, Masdache, Asomada, Guaguaro, Testenia, Nazaret, Tahiche, Sonsamas, Geria, Manchablanca Chiquita, Ynaguaden, Fiquinineo, Peñalomas, Jarretas (mostly destroyed by the lava flows) and a portion of Tingata.

Some months later the list of places damaged by the tephra deposition included: Uga, El Tablero, Temuime, some areas of Femés, and Fenanso valley, Yaiza, La Vega de Machín, Guerma, Montaña Blanca de Perdomos, Tenesar, Chimadatagaste, Tingafa and Tinajo. In fact, there is a map, drawn only three months after the eruption started, showing the area covered by lava flows and tephra. This information has been transposed on to a current map of the island (Fig. 9). Ashes reached the Haría valley, in northern Lanzarote, but the layer was very shallow and did not destroy the fields; ashes even reached Fuerteventura, falling in places located 90 km away from the vents.

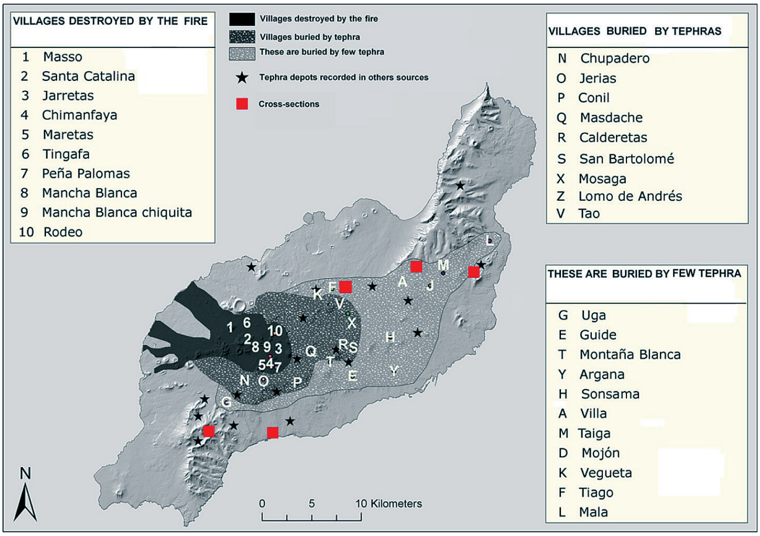

Figure 9. Reconstruction of damaged areas by tephra and lava during the eruption of Timanfaya (1730–1736).

The mineralogical data obtained from XRD show olivine (mainly as forsterite) and augite as the primary minerals found in all tephra layers present in the cross-sections; data from the Timanfaya eruption confirm that a majority of the minerals in the lava flow composition were issued during this event, classified as olivine-augite basalts (Carracedo *et al.*, 1990).

More evidence is provided by geochemistry analysis. We obtained the total oxides and trace elements from the Jaume Almera Earth Sciences Institute (CSIC, Barcelona, Spain). We studied the geochemical composition of five different tephra layers (Puerto Calero, Femés, El Bebedero, Valle de San José and Guatiza) and we compared the results with previous data obtained by Carracedo *et al.* (1990). Using the TAS diagram (Le Bas *et al.*, 1986), we classified the tephra samples from our five cross-sections as basalt that is very similar to samples from Phase I, IV and V of the Timanfaya eruption. However, the diagram of variations between Ce *versus* Ce/Zr (Fig. 10) provides solid evidence that the tephra layers of the cross-sections were issued from the Timanfaya eruption, with values similar to those of Pico Partido (Guatiza, Femés and El Bebedero), Caldera de Santa Catalina (Valle de San José) and Caldera de Los Cuervos (Puerto Calero). All these vents belong to Phase I of activity. The eruption of Caldera de Los Cuervos occurred between 10 and 19 September, 1730, under a regime of wind from the first quadrant and it is quite probable that the tephra produced by this event raised the Puerto Calero area; the date provided by Carracedo *et al.* (1990)

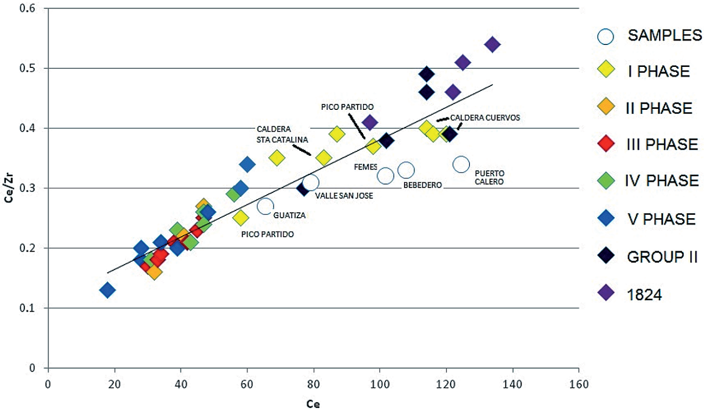

Figure 10. Relations Ce *vs* Ce/Zr from tephra of studied cross-sections and samples from Timanfaya analyzed by Carracedo and Rodríguez-Badiola (1990).

and Carracedo and Rodríguez-Badiola (1991) for the activity in Pico Partido and Caldera de Santa Catalina is between 10 October and the end of February, during the season when wind can blow from the third quadrant. Marzol (1984) indicated that the depressions raising the Canary Islands, with winds from the SW, arrived normally from late November until the middle of April. This helps to explain how the Timanfaya tephra reached the Valle de San José, El Bebedero and Guatiza, while with normal wind – blowing from the first quadrant –, the tephra could reach the Femés valley. We were unable to find a significant correlation between the mean grain size of the tephra and distance from the vents, probably because there are also other variables determining the particle size of the tephra, such as the force of the explosion in the vent and the speed of the wind at the moment material was ejected. Both variables are very difficult to evaluate 290 years after the eruption.

Finally, our ^{14}C ages confirm that tephra was distributed between the 14th Century AD (B-3 strata of the El Bebedero archaeological site) and 19th Century AD (VSJ-2 strata in Valle de San José cross-section) (Table 6) (Fig. 11).

In conclusion, by evaluating data from different fields we can presume that the tephra layer of the Timanfaya eruption affected the entire island, thereby providing a tephrocronology control (Dugmore and Newton, 2009).

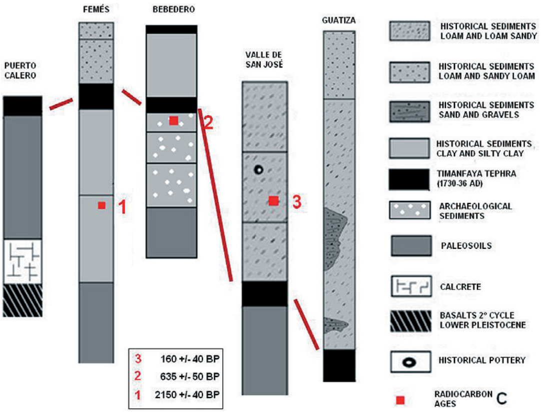

Figure 11. Correlations between the five cross-sections based in tephrocronological, archaeological, geochronological, sedimentological and soil criteria.

TABLE 6. Radiocarbon ages.

Place	Ref. sample	Method	Age ^{14}C	Cal. (2σ)
Femés (FEM-4)	Beta-172350	AMS	1890 ± 40 BP	28 - 230 AD
El Bebedero (B-3)	Gr-2463	Radiometric	635 ± 50 BP	1280 - 1406 AD
Valle San José (VSJ-4)	Beta-246367	AMS	160 ± 40 BP	1663 - 1953 AD

SEDIMENT INFILLING THE U-SHAPE VALLEYS

The features of the sedimentary layers placed over the ash strata, presumably issued from the Timanfaya eruption, indicate an alluvial origin. In Femés and Valle de San José, they present a coarser texture than the Paleargid soils present in the base of these cross-sections. The percentage of clay in the FEM-6 and FEM-7 samples is in the same order of magnitude as VSJ-5 and probably is evidence for palaeosoils developed inside both *vegas* by intense weathering of the volcanic ashes issued from Atalaya de Femés (Brunhes normal polarity < 0.78 Ma) and Volcán de Guanapay (Matuyama reversed polarity, 1.20 Ma, Coello *et al.*, 1992) in wetter climates than today. In agreement with other authors, evidence was found of the influence of Saharan dust on their geochemical and mineralogical composition (Zöller *et al.*, 2003; Suchodoletz *et al.*, 2009a; 2009b; 2010).

In all cross-sections the layers located above the ash layer had a coarse texture, ranging from sandy loam to loam. There is a clear increase in gravels (particles > 2 mm Ø) in all these layers; even in Guatiza there are some layers formed by a gravelly lens (sand texture), with sedimentary structures consistent with high energy fluvial processes.

The upper layers of the Guatiza cross-sections (GUAT-1, GUAT-2 and GUAT-3) are made up of between 23.7% and 35.9% carbonates, with sand particles and gravels produced by the erosion of calcrete outcrops and carried by fluvial processes. Similar features (percentage of carbonate between 17–28% in VSJ-1, VSJ-2 and VSJ-3) appear in the Valle de San José. In our opinion, these characteristics prove that a great deal of soil degradation has occurred on the slopes and ridges of Famara massif.

Environmental degradation after the 18th Century

The impact of the Timanfaya eruption on the local inhabitants was traumatic, causing at least 2395 people to starve. Extensive areas, used mainly as grazing areas for a large number of goats, sheep, camels and donkeys, disappeared. This led to a migration of the herds to areas where the lava flows did not arrived and the tephra covering was very shallow. There are historical records talking about increase of population in Haría valley, where the number of parcels cultivated grew (Romero, 1997). Indeed, during the first few years of the 19th Century AD, several unusual wind storms produced a movement of sand in the Jable sector (Tejedor *et al.*, 1995); as a result, some villages were abandoned, and grazing pastures in this part of the island were dramatically reduced.

In conclusion, we believe that throughout the majority of the 18th Century AD and the first quarter of 19th Century the island suffered significant environmental degradation due to overgrazing, agricultural needs and the demand for fuel resources. The Statistics of the Canary Islands, 1793–1806 recorded by Francisco Escolar (Hernández, 1983), provides information on the livestock in Lanzarote between the end of the 18th Century and the start of the 19th Century. There were a large number of domestic animals, including 9039 sheep, 7135 goats, 5655 cattle, 2713 donkeys, 1747 camels, 1659 pigs, 144 horses and 5 mules, in total 28,097 domestic animals. Thus, the highest areas, including ridges and slopes, and the valleys were stripped of natural vegetation making them highly vulnerable to soil erosion.

Historical evidence of the San Florencio Storm in Lanzarote

The most extreme wind and heavy rain event on the Canary Islands occurred in November, 1826. The first scientific description about it was provided by Sabin Berthelot, a French naturalist living in Tenerife at the time. The impor-

TABLE 7. List of floods happened in Lanzarote since last years of XVII (Modified from Romero *et al.*, 1994).

Year	Place	Region	Remarks
1694			Before Timanfaya eruption
1768			
1798			
1813	Valle de Fena	Femés Massif	Very important
1826	Los Valles	Famara Massif	The most important
1933			
1955			No evidences in the landscape
1956			No evidences in the landscape
1966			No evidences in the landscape

tance of this event has been increasing recently and new information about it (Bethencourt and Dorta, 2010) confirms that it was tropical storm and probably a tropical cyclone. The effect has been studied in Tenerife where it produced 294 casualties and very significant damage to the forests, goods, infrastructures and agriculture; in addition several sailing ships in the area were sunk.

Recently we have found an interesting document, confirming that this extreme storm passed through Lanzarote. The following document reports the effects of this storm around the Famara massif, close to Teguise village, at the time the capital of the island: «*The weather was variable until eight o'clock in the morning when the wind became stable, blowing from the SW; at the same time the rains started, with winds increasing at two in the afternoon and heavy rains continuing until half past five in the afternoon. Ravines formed even in flat areas, and gullies going down the mountains, meeting in several places and washing away everything in their path, destroying solid stone walls, which had been built as horizontal steeps to catch rain water in order to improve the productivity of the fields and allow some crops to be grown*». «*Indeed some livestock has been lost...*».

Very few floods have occurred on Lanzarote in historical times. A list of them was compiled by Romero *et al.* (unpublished report, 1994) (Table 7), and the most significant occurred in the Valle de Fena (close to Femés) in 1813 and specially the storm of 1826. Both are consistent with the radiocarbon date obtained on a goat bone in Valle de San José (Table 6) (Fig. 11).

CONCLUSIONS

The microscopic examination of all the tephra layers included in the five cross-sections studied in this work, identify them as volcanic ash. They preserve the typical morphology of recent ash, with no evidence of intense weathering, although they have been mixed with silty particles and, in some areas, with coarse particles produced by the erosion of Pleistocene calcretes. In addition, mineralogical analyses reveal the presence of olivine in all the samples, a mineral that was very common in the Timanfaya eruption. Olivine is easily weathered, so the fact that it is well preserved, even in an arid climate, can be seen as evidence of a young geological age.

The relationship between trace elements (Ce *versus* Ce/Zr) obtained from tephra samples from our five cross-sections coincides with data obtained by previous authors on samples from different places of the Timanfaya eruption. Using these relationships allows correlations to be found between tephra layers in Guatiza, Femés and the El Bebedero archaeological site linking them to the Pico Partido eruption, while the tephra found in Valle de San José can be related to the Santa Catalina Caldera eruption. On the other hand, the tephra layer overlapping the Paleargids in Puerto Calero could have been issued from Caldera de Los Cuervos.

Furthermore the radiocarbon data from Femés and El Bebedero, obtained from samples below the tephra layer, gave ages earlier than the 18th Century AD, while the bone dated in the Valle de San José, obtained from a layer over the tephra, gave an age around the first half of 19th Century AD. We believe that the tephra layer present in all the sequences studied in this paper is the same and that it was produced by the Timanfaya eruption. Therefore, the tephra layer can be used as a tephrochronological layer.

The sedimentary infilling of the *vegas* overlapping these tephra layers obviously must be younger than 1730–1736 AD. The presence of shards of traditional pottery and the ^{14}C age for the bone sampled in the Valle de San José provide solid evidence to date the runoff processes responsible for the deposition of upper sedimentary layers in the *vegas* at some time between the Timanfaya eruption and the end of the 19th Century. The structures and sedimentological features of the layers located over the tephra layers in sediments infilling the *vegas* are typical of fluvial processes under high energy conditions, produced by intense heavy rains working on a degraded landscape at extreme risk of soil erosion due to overgrazing and fuel needs, where calcretes appear on the surface. Finally, the historical document allows us to conclude that the main part of these sedimentary layers was probably produced during a historical flood which occurred on Lanzarote after the Timanfaya eruption, possibly the 1813 Valle de Fena flood and even more likely the San Florencio Storm in 1826, the most extreme weather event that occurred in Canary Islands in the last six centuries.

ACKNOWLEDGEMENTS

The description of the goat bone found in the Valle de San José cross-section was provided by Dr J.C. Rando (ULL). Dr F. Pérez-Torrado (ULPGC) helped us in the discussion of geochemistry data. The geochemistry data was obtained from the Jaume Almera Earth Sciences Institute (CSIC, Barcelona); we are very grateful to Dr Marta Rejas and Dr José Luis Fernández-Turiel, members of the staff of this institution. The XRD was carried out in SIDIX at the University of La Laguna. We used GRADISTAT software to get particle size parameters, and OXCAL software to calibrate our radiocarbon dates. We send our grateful thanks to these people and institutions.

REFERENCES

Abdel-Monem, A., Watkins, N.D. and Gast, P.W. (1971) Potassium-Argon ages, volcanic stratigraphy, and geomagnetic polarity history of the Canary Islands: Lanzarote, Fuerteventura, Gran Canaria, and La Gomera. *American Science*, 271, 490–521.

Atoche, P., Paz, J.A., Ramírez, A. and Ortiz, M.E. (1995) *Evidencias arqueológicas del mundo romano en Lanzarote (Islas Canarias)*. Servicio de Publicaciones del Excmo. Cabildo Insular de Lanzarote, Colección Rubicón, Lanzarote.

Bethencourt, J. and Dorta, P. (2010) The Storm of November 1826 in the Canary Islands: possibly a tropical cyclone? *Geografiska Annaler*, 92, 329–337.

Carracedo, J.C. and Rodríguez-Badiola, E. (1991) *La erupción volcánica de 1730. Estudio volcanológico de una de las erupciones basálticas fisurales de mayor duración y magnitud de la historia*. Cabildo Insular, Servicio de Publicaciones, Lanzarote.

Carracedo, J.C., Rodríguez-Badiola, E. and Soler, V. (1990) Aspectos volcanológicos y estructurales, evolución petrológica e implicaciones en riesgo volcánico de La erupción de 1730 en Lanzarote, Islas Canarias. *Estudios Geológicos*, 46, 25–55.

Carracedo, J.C., Rodríguez-Badiola, E. and Soler, V. (1992) The 1730-1736 eruption of Lanzarote, Canary Islands: a long high magnitude basaltic fissure eruption. *Journal of Volcanology and Geothermal Research*, 53, 239–250.

Carracedo, J.C., Singer, B., Jicha, B., Guillou. H., Rodríguez-Badiola, E., Meco, J., Pérez-Torrado, F., Gimeno, D., Socorro, S. and Laínez, A. (2003) La erupción y el tubo volcánico del Volcán de La Corona (Lanzarote, Islas Canarias). *Estudios Geológicos,* 59, 227–302.

Coello, J.J., Cantagrel, J.M., Hernán, F., Fúster, J.M., Ibarrola, E., Ancochea, E., Casquet, C., Jamond, C., Díaz de Terán, J.R. and Cendrero, A. (1992) Evolution of the eastern volcanic ridge of the Canary Islands based on new K-Ar data. *Journal of Volcanology and Geothermal Research*, 53, 251–274.

Criado, C. and Atoche, P. (2003) Estudio geoarqueológico del yacimiento de El Bebedero (Lanzarote, Islas Canarias). *Cuaternario y Geomorfología,* 17, 91–104.

Criado, C. and Atoche, P. (2004) ¿Influyó la ganadería de los *Mahos* en el deterioro paleoambiental de la isla de Lanzarote? *Tenique*, 6, 138–157.

De León, J. (2009) *Lanzarote bajo el volcán. Los pueblos y el patrimonio edificado sepultados por las erupciones del S. xviii.* Casa de Los Volcanes, Lanzarote.

DUGMORE, A.J. and NEWTON, A. (2009) Tephrocronoloy. *Encyclopedia of Paleoclimatology and Ancient Environment* (ed. by GORNITZ, V.), pp. 937–938. Springer Verlag, Düsseldorf.

FÚSTER, J.M. and CARRACEDO, J.C. (1979) Magnetic polarity mapping of Quaternary volcanic activity of Fuerteventura and Lanzarote (Canary Islands). *Estudios Geológicos*, 35, 59–65.

FÚSTER, J.M., FERNÁNDEZ SANTÍS, S. and SAGREDO, J. (1968) *Geología y Vulcanología de las Islas Canarias. Lanzarote.* Instituto Lucas Mallada, CSIC, Madrid.

HANSEN, A. and MORENO, C. (2003) *Lanzarote. Guía del Relieve.* Geomorphological chart 1:100.000 scale. Cabildo de Lanzarote, Lanzarote.

HAUSEN, H. (1959) On the Geology of Lanzarote, Graciosa and the Isletas (Canarian archipelago). *Societas Scientiarum Fennica, Commentationes Physico-Mathematicae*, 23, 1–117.

HERNÁNDEZ, G. (1983) *Estadística de las Islas Canarias de Francisco Escolar y Serrano 1793-1806.* CIES, Las Palmas.

HERNÁNDEZ, L., GONZÁLEZ, M.C., JIMÉNEZ, C.M., ORTEGA, J., PADRÓN, P., RODRÍGUEZ, A., TORRES, J.M. and VARGAS, G.E. (1991) Suelos de la isla de Lanzarote. Características generales. *XVIII Reunión Nacional de Suelos*, (ed. by Departamento de Edafología y Geología, Universidad de La Laguna), pp 311–330. Universidad de La Laguna. Servicio de Publicaciones, Santa Cruz de Tenerife.

HERNÁNDEZ-PACHECO, E. (1909) Estudio geológico de Lanzarote y de las Isletas Canarias. *Mememorias de la Real Sociedad Española de Historia Natural*, 6, 107–342.

IBARROLA, E., CANTAGREL, J.M., FÚSTER, J.M., COELLO, J. and JAMOND, C. (1988) Geocronología de las series volcánicas neógenas de Lanzarote (Islas Canarias). *II Congreso Geológico de España, SGE*, pp. 345–348. Universidad de Granada, Granada.

IGME (2005) *Mapa Geológico de España a escala 1:100.000. Lanzarote.* IGME, Madrid.

LE BAS, M.J., LE MAITRE, R.W., STRECKEISEN, A. and ZANETTIN, B. (1986) A chemical classification of volcanic rocks based on total alkali-silica diagram. *Journal of Petrology*, 27, 745–750.

MARZOL, V. (1984) *El Clima. Geografía de Canarias.* Interinsular Canaria, Santa Cruz de Tenerife.

QUIRANTES, F., FERNÁNDEZ-PELLO, L., ROMERO, C. and YANES, A. (1993) Los aluviones históricos en Canarias. *XIII Congreso Nacional de Geografía*, pp. 611–615. Universidad de Sevilla, Sevilla.

ROMERO, C. (1991) *La erupción de Timanfaya (Lanzarote, 1730-36).* Secretariado de Publicaciones, Universidad de La Laguna, La Laguna.

ROMERO, C. (1997) *Crónicas documentales sobre las erupciones de Lanzarote.* Fundación Cesar Manrique, Lanzarote.

ROMERO, C. (2003) *El relieve de Lanzarote.* Cabildo de Lanzarote, Colección Rubicón, Lanzarote.

ROMERO, C., QUIRANTES, F., FERNÁNDEZ-PELLO, L. and YANES, A. (1994) *Los aluviones históricos de las islas Canarias.* Unpublished report.

Suchodoletz, H. von and Zöller, L. (2009) Past Records of Saharan Dust on the Canary Islands. *Airborne Particulates* (ed. by Cheng. M. and Liu, E.), pp. 48–57. Nova Science, New York.

Suchodoletz, H. von, Faust, D. and Zöller, L. (2009) Geomorphological investigation of sediment traps on Lanzarote (Canary Islands) as a key for the interpretation of a palaeoclimate archive off NW Africa. *Quaternary International*, 196, 44–56.

Suchodoletz, H. von, Oberhänsli, H., Hambach, U., Zöller, L., Fuchs, M. and Faust, D. (2010). Soil moisture fluctuations recorded in Saharan dust deposits on Lanzarote (Canary Islands) over the last 180 ka. *Quaternary Science Reviews*, 29, 2173–2184.

Suchodoletz, H. von, Blanchard H., Hilgers, A., Radtke, U., Fuchs, M., Dietze, M., and Zöller, L. (2012) TL and ESR-dating of Middle Pleistocene lava flows on Lanzarote island, Canary Islands (Spain). *Quaternary Geochronology*, 9, 54–64.

Tejedor, M.L., Hernández, L.A. and Ortega, M.J. (1995) Fieldtrip in Lanzarote. Guide Book. *Meeting on «The soils as strategic resource: degradation processes and conservation measures (Canary Islands, Spain).*

Thomas, D.S.G. (1997) *Arid Zone Geomorphology: Process, Form and Change in Drylands.* Wiley and Sons, Ltd., Chichester.

Zazo, C., Hillaire-Marcel, C., Goy, J.L., Ghaleb, B., Lario, J., Bardají, T. and González, A. (1997) Cambios de nivel del mar en los últimos 250 ka (Canarias Orientales). *Boletín Geológico y Minero*, 108, 159–169.

Zöller, L., von Suchodoletz, H. and Küster, N. (2003) Geoarchaeological and chronometrical evidence of early human occupation on Lanzarote (Canary Islands). *Quaternary Science Reviews*, 22, 1299–1307.

WHAT DO WE KNOW AND WHAT DO WE NEED TO KNOW ABOUT THE MACARONESIAN PALAEOCLIMATE? ANSWERING WITH PARTICIPATORY APPRAISAL METHODS

Lea de Nascimento, Silvia Fernández-Lugo, Luis A. Bermejo,
José María Fernández-Palacios

CLIMATE CHANGE PERSPECTIVES FROM THE ATLANTIC:
PAST, PRESENT AND FUTURE

Jose María Fernández-Palacios, Lea de Nascimento, José Carlos Hernández,
Sabrina Clemente, Albano González & Juan P. Díaz-González (eds.)
Servicio de Publicaciones, Universidad de La Laguna – 2013

ISBN: 978-84-15910-54-1
pp. 299-330

Abstract

Participatory appraisal (PA) is an approach or research procedure that seeks to incorporate the knowledge and opinions of a community with the aim of improving an area of concern. PA has several advantages over scientific discussions, as it can be used to share, analyse and evaluate diverse issues, and because it enhances creativity and group participation, regardless of participants' backgrounds. PA is based on flexible, innovative, and highly visual tools that allow the generation of large amounts of information in short time. In this case, our aim was to define the state of knowledge about palaeoclimate of Macaronesia. To do this, we tried to address the following questions: What do we know? How sure are we? Do we agree? What are the key events and their consequences? Then, we established a research agenda by asking: What should we study next? Results indicated the best known regions (Azores-Canaries) and periods (Holocene to LGM), and highlighted a certain degree of uncertainty about our knowledge of climate history in the region. Key climatic events were mainly related to four environmental variables (temperature, humidity, wind regime and sea level oscillation), which were also considered as decisive variables for future research. Researchers agreed that most of the topics requiring future research should be addressed urgently.

Keywords: brainstorm, last glacial cycle, palaeoclimatic variables, Macaronesian archipelagos, participatory tools, scientific discussion.

INTRODUCTION

The Macaronesian archipelagos, including Azores, Madeira, Savage Islands, Canary Islands and Cape Verde, constitute an important biogeographical region listed as a biodiversity hotspot by Conservation International since 2005 (Whittaker and Fernández-Palacios, 2007). Understanding the present configuration of species and communities on these islands requires knowledge from the past in relation to their geological, climatic and human colonization history. In the last decades many authors from different disciplines (Biogeography, Geoarchaeology, Geochemistry, Geology, Geomorphology, Palaeoecology, Palaeoceanography, Palaeontology, etc.) have studied the evolution of climate in this region by means of various palaeoenvironmental variables (e.g., Hoghiemstra *et al.*, 1992; Damnati, 1996; Meco *et al.*, 2002; Björck *et al.*, 2006; Ávila *et al.*, 2008; Suchodoletz *et al.*, 2010; Zazo *et al.*, 2010; Yanes *et al.*, 2011). Despite all the knowledge obtained, there are still significant gaps, so that for example, specific time periods or regions remain almost unknown. Some inconsistencies may also be found when reviewing specific literature. In order to obtain a general picture of palaeoclimate in Macaronesian archipelagos, we need to identify these gaps as well as to discard uncertain information, and reach some consensus on the most reliable evidence.

Using participatory appraisal (PA) methods, we tried to evaluate the knowledge that we, as a group of experts from different disciplines, have generated in relation to palaeoclimate of the Macaronesian archipelagos spanning the last glacial cycle. PA is a family of methods that enable communities (e.g., scientific communities) to share, develop and analyse their own knowledge (Chambers, 1994). These methods use visual and flexible tools that ensure the participation of everyone regardless of their different fields of expertise. PA also enables the group to identify their priorities and to make decisions about the future, as for example in the organization of a research agenda.

METHODS

A total of 23 scientists took part in the discussion sessions at the First Macaronesian Palaeoclimate Workshop (PALAEOCLIMAC 2012) (Fig. 1). Participants attending belonged to 13 different institutions from several countries (France, Germany, Portugal, Spain, the Netherlands and United Kingdom). Fields of expertise among participants covered various disciplines: Biogeography, Botany, Geography, Geology, Palaeoceanography, Palaeoecology, and Palaeontology, and with research being carried out in the Macaronesian region, North Africa and/or the Iberian Peninsula.

A list of questions was raised dealing with two main issues: 1) analysis of the state of knowledge and 2) the creation of a research agenda in relation to the palaeoclimate of the Macaronesian region. Three types of participatory tools were applied in order to answer the list of questions and organize the information: result shower, matrixes and flowcharts (Chambers, 2002; 2007). As a first step a brainstorming session provided a list of results in answer to the question *what do we know?* (Fig. 2). The results where then organized in matrixes using the ranking tool according to the level of certainty and agreement, as decided by participants, to answer the question *how sure are we?* (Fig. 3). Results with best scores in the ranking were classified as key events. A simplified flowchart was used to indicate the consequences of the previously selected key events, responding to *what are the key events and their consequences?* (Fig. 4). The results that obtained lowest scores in the ranking were classified as topics requiring additional research to determine *what should we study next?* Finally, these topics were ranked according to their priority for future research, as decided by participants.

Figure 1. Participants at the First Macaronesian Palaeoclimate Workshop (PALAEOCLIMAC 2012).

Figure 2. Result showers obtained for different regions and periods.

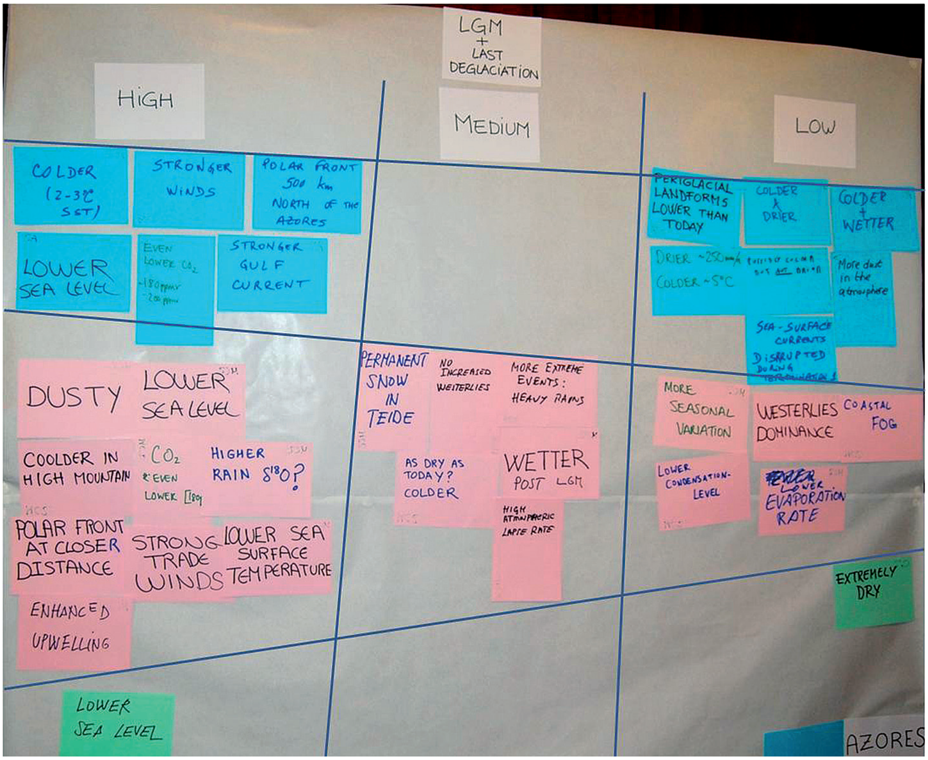

Figure 3. Matrix of certainty showing results ranked by high, medium and low levels of certainty.

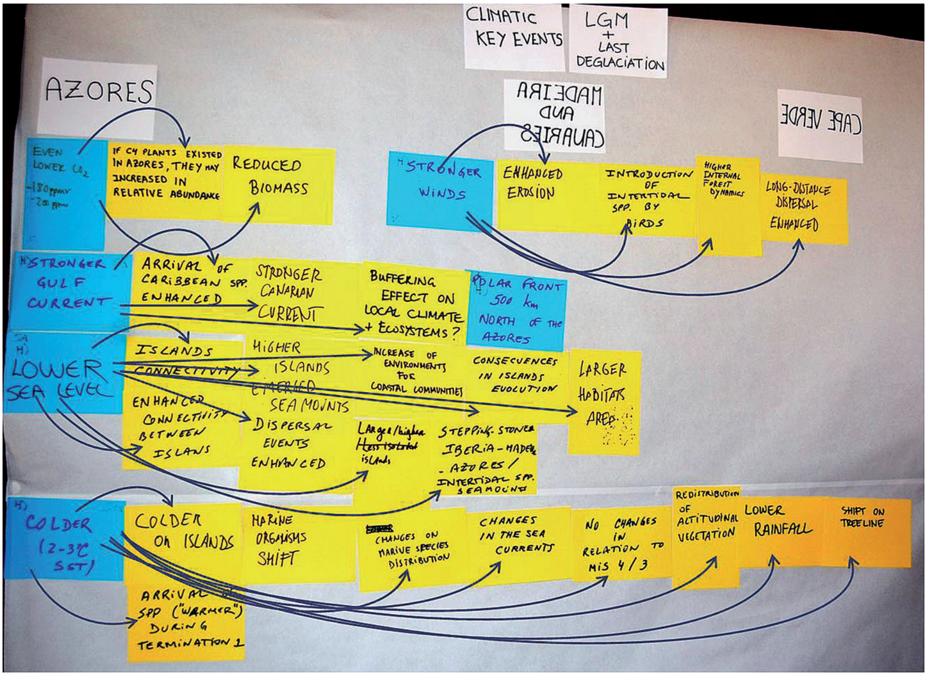

Figure 4. Flowchart with arrows indicating the consequences of key events.

Questions were arranged by region and time period, so that all main questions were repeated for every region and period. The Macaronesian region was subdivided into: Azores, Canaries-Madeira (including Savage Islands), and Cape Verde. North Africa and the south of the Iberian Peninsula were also considered in the result shower. Time was separated in the following periods: last interglacial (Eemian), last glaciation (Weichselian), Last Glacial Maximum (LGM)–last deglaciation, and the present interglacial (Holocene). Questions were formulated in relation to the present moment, defined as the last 60 years (1950–2012).

As part of the participatory methodology, some questions were slightly modified during the discussion. In order to check if the questions, defined a priori for the discussion, coincided with the interests of participants, we asked them to formulate their own key questions on the discussion theme.

All results were written by participants on coloured cards with capital letters and fixed on adhesive paper and hung on the wall so that information could be visible and handy, allowing for flexibility in the addition or removal of cards.

Two facilitators worked with the group in the process of discussion (Figs 5 and 6).

Figure 5. Group of researchers and facilitator during the participatory appraisal.

Figure 6. Participants during the discussion of results.

RESULTS

What do we know?

From a total of 190 results, 13 palaeoenvironmental variables were mentioned in the result shower (Table 1). Results were mainly related to humidity (35%), temperature (25%), wind regime (14%) and sea level oscillation (7%),

TABLE 1. Result shower by region (Azores, Canaries-Madeira, Cape Verde, Iberian Peninsula and North Africa) and period (Holocene, LGM–last deglaciation, last glaciation, Eemian). Climatic variables were assigned to each result. Letters indicate the level of certainty (H = high, M = medium, L = low) given to the results from Azores, Canaries-Madeira and Cape Verde.

Region	Variable	Certainty
Azores		
Holocene		
Lower CO_2 approx. 280 ppmv (current 390 ppmv)	CO_2 concentration	H
Phases of aridity	humidity	H
Phases of humidity	humidity	H
Larger islands (Early Holocene)	sea level oscillation	H
Do not know	--	H
More hurricanes	wind regime	M
Wet islands wetter, dry islands drier	humidity	L
Microclimates in some islands	humidity/temperature	L
Larger variations in climate within islands	humidity/temperature	L
Shifts in sea levels	sea level oscillation	L
Temperature stability	temperature	L
LGM–last deglaciation		
Even lower CO_2 approx. 180–200 ppmv	CO_2 concentration	H
Stronger Gulf current	marine circulation	H
Lower sea level	sea level oscillation	H
Colder SST 2–3°C	SST	H
Stronger winds	wind regime	H
Polar front at 500 km north from the Azores	wind regime/temperature	H
More dust in the atmosphere	dust input	L

Drier approx. 250 mm/y	humidity	L
Periglacial landforms lower than today	summit glaciers	L
Colder approx. 5°C	temperature	L
Possibly colder but not drier	temperature/humidity	L
Colder and wetter	temperature/humidity	L
Last glaciation		
Lower sea level	sea level oscillation	H
Stronger winds	wind regime	H
Polar front at varying distance	wind regime/temperature	H
More dust in the atmosphere (40–10 ka)	dust input	M
Lower evaporation	temperature	L
Ice free	temperature	L
Possibly colder but with some variations among islands	temperature	L
Stable climate (80–30 ky BP)	temperature/humidity	L
Colder an drier	temperature/humidity	L
Eemian		
Sea level +4/+6 m (132–125 ka) +8/+9 (120–118 ka)	sea level oscillation	H
2–3°C higher SST	SST	H
Wetter	humidity	L
Higher condensation level	temperature/humidity/ sea of clouds	L
Canaries-Madeira		
Holocene		
Lower CO_2	CO_2 concentration	H
More Saharan dust (8–3 ka)	dust input	H
High humidity (Early Holocene)	humidity	H
Summer insolation decreases after 9 ka	insolation	H
Lower sea level (Early Holocene)	sea level oscillation	H
Colder SST (ca. 8 ka)	SST	H
Prevalence of trade winds	wind regime	H
Dryer (4–2 ka)	humidity	M
Wetter (2–0.5 ka)	humidity	M
Dryer (0.5–0 ka)	humidity	M

High energy littoral dynamic (4.5, 3.5 and 3 ky BP)	marine circulation	M
Existence of Saharan winds	wind regime	M
Monsoon front at position of Canary Islands (Early Holocene)	wind regime	M
Same as present	humidity/temperature	L
Microclimates same as present	humidity/temperature	L
LGM–last deglaciation		
Even lower CO_2 180 ppmv	CO_2 concentration	H
Dusty	dust input	H
Higher rain ($\delta^{18}O$)	humidity	H
Enhanced upwelling	marine circulation	H
Lower sea level	sea level oscillation	H
Lower SST	SST	H
Colder in high mountains	temperature	H
Strong trade winds	wind regime	H
Polar front at closer distance	wind regime/temperature	H
As dry as today	humidity	M
Wetter (post LGM)	humidity	M
More extreme events, heavy rains	humidity	M
Permanent snow in El Teide	summit glaciers	M
Colder	temperature	M
High atmosphere lapse rate	temperature/humidity	M
No increased westerlies	wind regime	M
Lower evaporation rate	temperature	L
More seasonal variation	temperature/humidity	L
Lower condensation level	temperature/humidity/ sea of clouds	L
Coastal fog	temperature/humidity/ sea of clouds	L
Westerlies dominance	wind regime	L
Last glaciation		
More aeolian sand dunes	dunes formation	H
Less effective moisture in MIS3 than MIS4, but more than today	humidity	H

Wetter	humidity	H
Colder	temperature	H
Lots of environmental changes (MIS 3–MIS 4)	temperature/humidity	H
Stronger winds in lower atmosphere	wind regime	H
Higher rain ($\delta^{18}O$)	humidity	M
Weaker African easterly jet	wind regime	L
Eemian		
Higher sea level	sea level oscillation	H
Warmer SST	SST	H
Low trade wind intensity	wind regime	H
Soil development on eastern Canary Islands	humidity	M
African summer monsoon at the Canaries	wind regime	M
More humid than present	humidity	L
Same sea-surface currents as today	marine circulation	L
Changes on seasonality (larger winters shorter summers)	seasonality	L
Higher evaporation	temperature	L
Similar temperature and humidity	temperature/humidity	L
Cape Verde		
Holocene		
Less Saharan dust until ca. 5 ka	dust input	M
More monsoon rains (Early Holocene)	humidity	L
Reinforcement of African easterly jet (5–0 ka)	wind regime	L
LGM–last deglaciation		
Lower sea level	sea level oscillation	H
Extremely dry	humidity	L
Climate variability	temperature/humidity	L
Last glaciation		
Displacement of the trade winds 5–8°C south	wind regime	M
Eemian		
Higher sea level	sea level oscillation	H
Similar SST	SST	M
Wetter than today	humidity	L

Iberian Peninsula	
Holocene	
Less dust (Early Holocene)	dust input
North wet as today	humidity
South wetter (8–4 ka)	humidity
South drier (3 ka)	humidity
Wetter (Early Holocene)	humidity
Increasing aridity (Late Holocene)	humidity
Strong fluvial activity (Little Ice Age)	humidity
Changes in rainfall seasonality?	humidity/seasonality
Climatic shifts sunspot-driven (4–0.3 ka)	temperature
High temperature contrast N-S	temperature
Up to 5C° warmer	temperature
Low contrast in winter-summer temperature	temperature
Warmer winters and cooler summers (Early Holocene)	temperature
Periods of variability (Late Holocene) Iberian Roman Humid Period, Medieval Climate Anomaly, Little Ice Age	temperature
LGM–last deglaciation	
Sand-dunes in inner mainland	dunes formation
Enhanced dust input during LGM	dust input
Drier	humidity
Drier during LGM	humidity
Increasing humidity during deglaciation	humidity
Dry and cold (12 ka)	humidity/temperature
High summer insolation	insolation
Stronger deep water circulation during LGM	marine circulation
No significant area increase	sea level oscillation
Glaciers in the main ranges	summit glaciers
Less cold in south and stable in inland Spain	temperature
High temperature contrast E-W	temperature
Polar front at north border of Portugal	temperature
Colder and wetter winters	temperature/humidity
Intense trade winds	wind regime

Westerlies influence	wind regime
Last glaciation	
More dust transport	dust input
Drier in central Spain	humidity
Drier	humidity
Dry-wet-dry (MIS 3)	humidity
Well constrained SST stability	SST
Milder in the south	temperature
More wind	wind regime
Eemian	
Wetter	humidity
Wet and warm	humidity/temperature
Similar to the Holocene with Mediterranean and Atlantic phases	humidity/temperature
Subtropical waters offshore	marine circulation
Higher sea-level	sea level oscillation
Sea level oscillations (MIS 5e)	sea level oscillation
Warmer SST	SST
North Africa	
Holocene	
Increasing dust input (Late Holocene)	dust input
Little dust in atmosphere	dust input
Wetter (African Humid Period)	humidity
Drier at high altitude (10–6 ka)	humidity
increasing aridity (along the Holocene)	humidity
Sahel wetter (Early Holocene)	humidity
Drier 100 mm/yr (10–6 ka)	humidity
2–4°C warmer (10–6 ka)	temperature
Similar temperature	temperature
Strong climate gradient across Atlas Mountains	temperature/humidity
Warmer and wetter (8–5 ka)	temperature/humidity
Similar to present	temperature/humidity
Weak trades	wind regime

Frequent Saharan winds	wind regime
Shift in ITCZ to north (Early Holocene)	wind regime/humidity
LGM–last deglaciation	
Lower CO_2	CO_2 concentration
Strong dune formation	dunes formation
Much dust in atmosphere	dust input
As dry as today	humidity
Drier	humidity
Drier in some areas	humidity
About 300 mm/y drier	humidity
More humid, maybe colder	humidity/temperature
Strong climate gradient across Atlas Mountains	humidity/temperature
Wetter and windy	humidity/wind regime
Maximum extension of Sahara N-S	humidity
Enhanced Canary current and upwelling	marine circulation
Extension of coastline ± 40–50 km	sea level oscillation
Cooler	temperature
About 15°C colder	temperature
Affected by westerlies	wind regime
Intensive trade winds	wind regime
African easterly jet did not vary in strength	wind regime
Last glaciation	
Wet phases (24 and 22 ka)	humidity
Large lakes	humidity
Sahara diameter varied N-S	humidity
High Atlas glaciers	summit glaciers
Warmer (29–24 ka)	temperature
Enhanced trade winds	wind regime
Maximum intensity of trade winds (40–10 ka)	wind regime
Eemian	
Moist Sahara	humidity
Large and deep lakes	humidity

Upwelling less intense	marine circulation
Weak trade winds	wind regime
Higher influence of monsoon	wind regime/humidity
West African summer monsoon	wind regime/humidity

the other 19% referred to dust input, sea surface temperature (SST), marine circulation, CO_2 concentration, summit glaciers, dunes formation, sea of clouds, insolation and seasonality (Fig. 7). The importance of these palaeoenvironmental variables changed depending on the region. Considering just those variables accounting for more than 10% of results, temperature and humidity stood out in the Iberian Peninsula and Azores; sea level oscillation was also significant for the Azores (Fig. 8). In Canaries-Madeira and North Africa, wind regime played also an important role together with humidity and temperature (Fig. 8), whereas humidity, wind regime and sea level oscillation were the most frequent variables in Cape Verde.

How much do we know?

Results showed that the best known region is the group formed by Canaries-Madeira (29%), followed by North Africa (24%), the Iberian Peninsula (23%) and Azores (19%) with similar percentages, in contrast, Cape Verde (5%) is the least known (Fig. 9A). In general, our knowledge by period is higher for the LGM–last deglaciation (36%) and the Holocene (31%) and lower for the last glaciation (17%) and the Eemian (16%) (Fig. 9B). Exploring the knowledge by time period for each region (Fig. 10), we can observe a similar trend, the LGM–last deglaciation and the Holocene are the best documented periods, except for Cape Verde where the Eemian is as well known as the Holocene.

How sure are we?

From the initial shower of 190 results, we selected only those from the archipelagos, then, the group decided if the level of certainty for each of the 99 remaining statements was high, medium or low. Overall, high certainty statements did not account for more than 43% of the total. By region, we found differences in the degree of certainty (Fig. 11A). In Azores, results were equally distributed between low (50%) and high (44%) certainty. For the Canaries-Madeira, there was high (46%) or medium (30%) certainty about most of the results, with this region showing the least results of low certainty (24%). Cape Verde was the re-

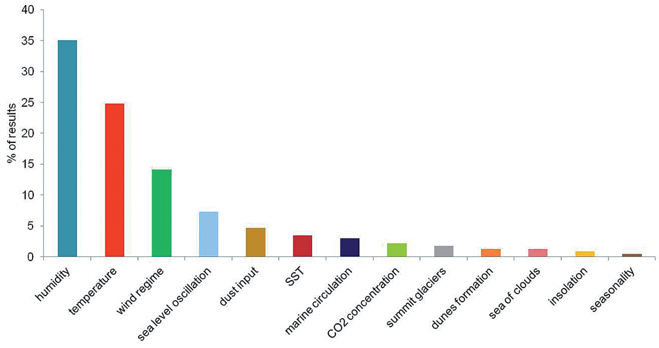

Figure 7. Percentage of results grouped by corresponding palaeoenvironmental variable.

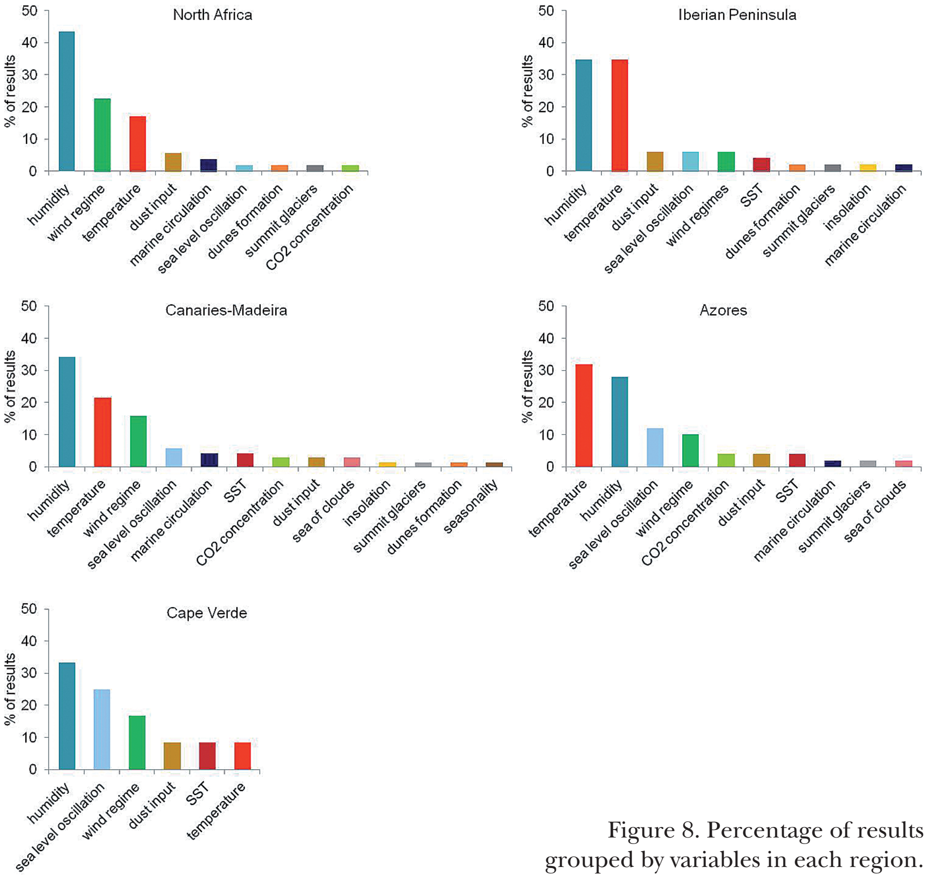

Figure 8. Percentage of results grouped by variables in each region.

gion with most uncertainty, results were grouped in either low (44%) or medium certainty (33%), and only 22% were highly certain. Considering the time period (Fig. 11B), the last glaciation represents the period of highest certainty, 50% of high certainty results, whereas the Eemian was the most uncertain period: 47% were low certainty results.

Which are the key events and their consequences?

Based on their level of agreement and certainty, the 43 best scored results were classified as key events. These key events were related to 10 environmental variables (Fig. 12A). We tried to identify critical nodes according to the number of consequences arising from each key climatic event. Sea level oscillation appeared to be an important critical node, which was given up to 70 consequences (40% of the total) (Fig. 12A). Other critical variables were wind regime, SST, humidity and temperature, each responsible for 10–15% of the effects (Fig. 12A). By period, the LGM–last deglaciation was the most critical, with more than 40% of the effects caused by key climatic events occurring at that time (Fig. 12B). Examining the raw number of consequences by region and time, we noticed some differences. Canaries-Madeira grouped more key climatic events (26); then came the Azores (15), and Cape Verde only had two, representing the same variable in different periods (Fig. 13). Sea level oscillation was the most critical variable in almost all periods and all regions: in Cape Verde it was the only climatic variable rated as key event. Humidity was the other critical node during the Holocene in Azores and Canaries-Madeira, with wind regime also being crucial for the latter region. SST affected the LGM–last deglaciation in both regions, whereas temperature, in general, was significant for the Canaries-Madeira. During the last glaciation, wind regime and temperature also had considerable effects. The Eemian was the only period when SST (Azores and Canaries-Madeira) and wind regime (only in Canaries-Madeira) had greater implications than sea level oscillation (Fig. 13).

What should we study next?

We obtained 56 results, defined as topics requiring future research (Table 2). The level of urgency needed to address these topics was considered high, 72% of the topics were evaluated as highly urgent (Fig. 14A). A high percentage of the topics were related to humidity (32%), temperature (27%) and wind regime (17%) (Fig. 15). Other variables considered were sea level oscillation, dust input, marine circulation, seasonality, SST, summit glaciers and sea of clouds. Among the regions, Cape Verde was the one that required the most urgent study (100% of the topics) (Fig. 14A). Azores and Canaries-Madeira were in a similar situation; over 60% of the topics were highly urgent, however, this urgency changed

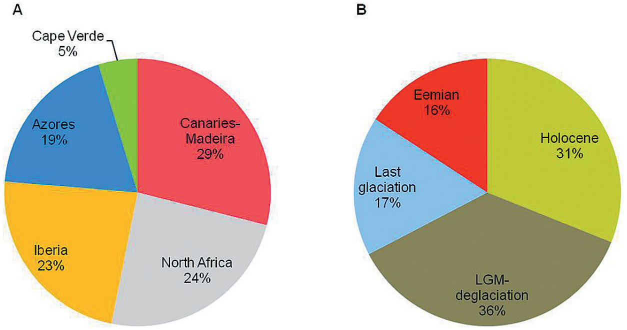

Figure 9. Percentage of results obtained by region (A) and time period (B).

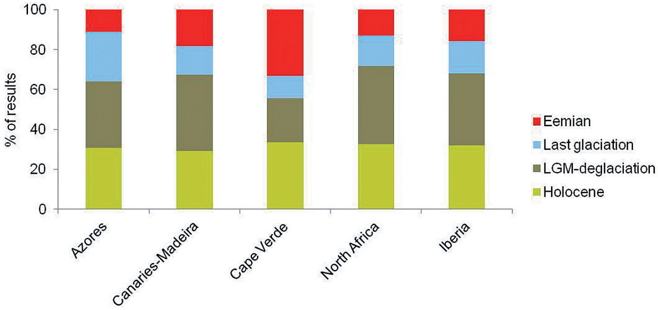

Figure 10. Percentage of results contribution by time period in each region.

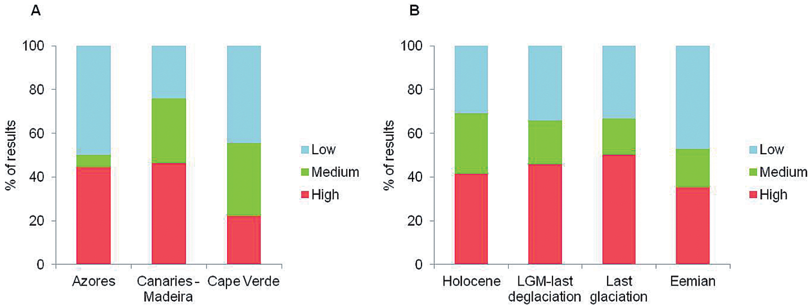

Figure 11. Percentage of results classified as high, medium or low certainty by region (A) and time period (B).

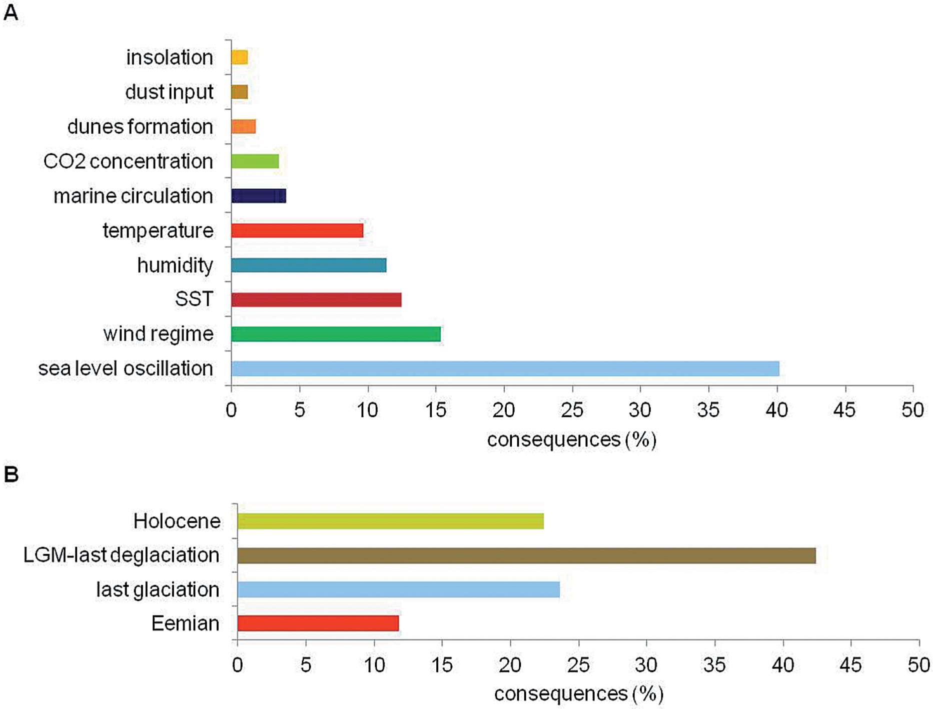

Figure 12. Percentage of consequences from key events arranged by variables (A) and time period (B).

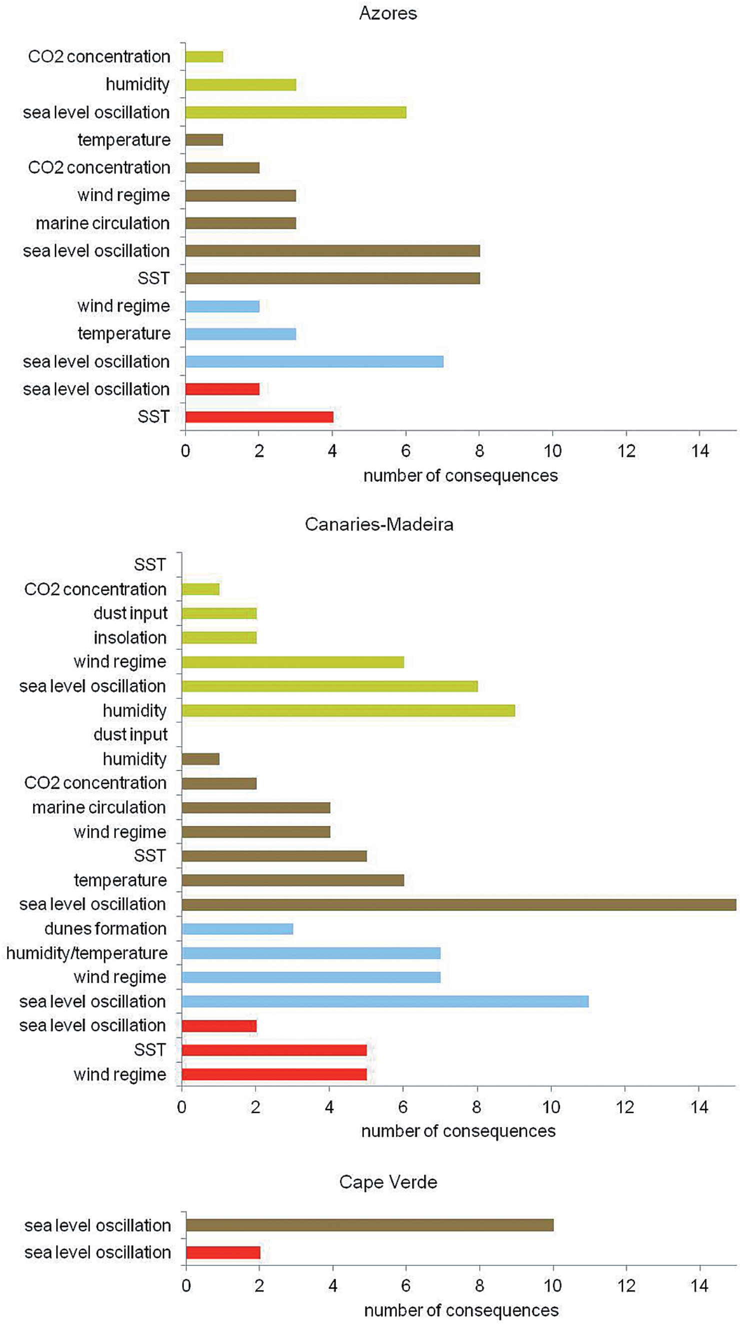

Figure 13. Number of consequences from key events by region and time period.

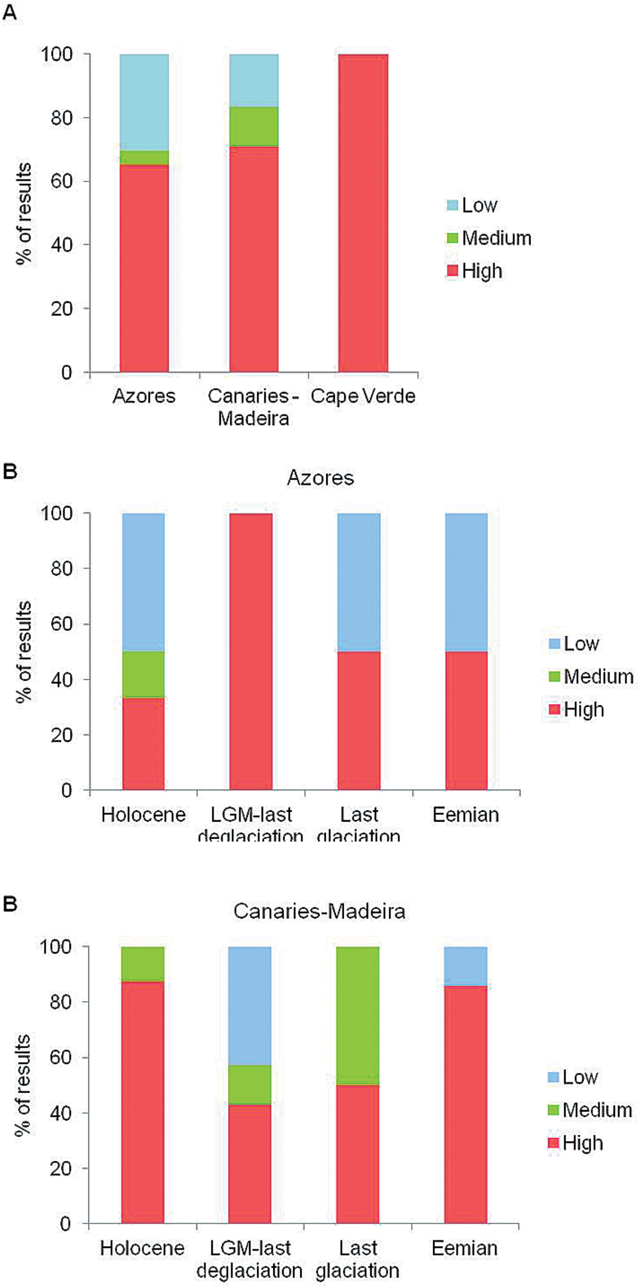

Figure 14. Percentage of results requiring high, medium or low urgency in future research by region (A) and time period (B).

TABLE 2. List of topics requiring future research by region and period. Letters indicate the level of urgency given to each topic (H = high, M = medium, L = low).

Azores		Canaries-Madeira		Cape Verde	
Holocene		**Holocene**		**Holocene**	
Temperature stability	H	Climate variability (Late Holocene)	H	Less Saharan dust until ca. 5 ka	H
More hurricanes	H	dryer (4–2 ka)	H	More monsoon rains (Early Holocene)	H
Wet islands wetter, dry islands drier	M	wetter (2–0.5 ka)	H	Reinforcement of African easterly jet (5–0 ka)	H
Microclimates in some islands	L	dryer (0.5–0 ka)	H		
Larger variations in climate within islands	L	same as present	H		
Shifts in sea levels	L	microclimates same as present	H		
		Existence of Saharan winds	H		
		Monsoon front at position of Canary Islands (Early Holocene)	H		
		High energy littoral dynamic (4.5, 3.5 and 3 ky BP)	M		
LGM–last deglaciation		**LGM–last deglaciation**		**LGM–last deglaciation**	
Variability in climate history	H	Climate variability	H	Climate variability	H
drier aprox. 250 mm/y	H	as dry as today	H	extremely dry	H

colder aprox. 5°C	H	wetter (post LGM)	H	High resolution bottom topography down to 150 m around islands	H
possibly colder but not drier	H	colder	H		
colder and wetter	H	more seasonal variation	H		
More dust in the atmosphere	H	more extreme events, heavy rains	H		
Sea surface currents disrupted	H	lower condensation level	H		
Periglaciar landforms lower than today	H	No increased westerlies	H		
High resolution bottom topography down to 150 m around islands	H	High resolution bottom topography down to 150 m around islands	H		
		High atmosphere lapse rate	M		
		Permanent snow in El Teide	L		
		Lower evaporation rate	L		
		Coastal fog	L		
		Westerlies dominance	L		
Last glaciation		**Last glaciation**		**Last glaciation**	
Variability in climate history	H	Higher rain ($\delta^{18}O$)	H	Displacement of the trade winds 5–8°C south	H
colder an drier	H	Weaker African easterly jet	M		

possibly colder but with some variations among islands	H				
stable climate (80–30 ky BP)	H				
More dust in the atmosphere (40–10 ka)	L				
Lower evaporation	L				
Ice free	L				
Eemian		**Eemian**		**Eemian**	
Wetter	H	Climate variability	H	Wetter than today	H
Higher condensation level	L	changes on seasonality (larger winters shorter summers)	H	Similar SST	H
		more humid than present	H		
		similar temperature and humidity	H		
		higher evaporation	H		
		Same sea-surface currents as today	H		
		African summer monsoon at the Canaries	H		
		Soil development on eastern Canary Islands	L		

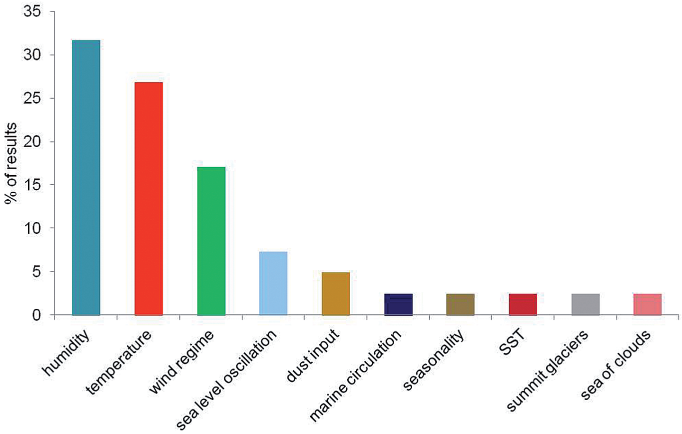

Figure 15. Percentage of results requiring future research arranged by variable.

depending on the period. In Azores, priority was given to the LGM–last deglaciation (Fig. 14B), whereas in Canaries-Madeira over 80% of the climatic events occurring in the two interglacials (Holocene and Eemian) need to be studied urgently (Fig. 14B).

WHAT WERE THE INTERESTS OF PARTICIPANTS?

Experts participating formulated a total of 38 questions related to 21 different topics (Table 3). Participants coincided in several topics that were repeated at least three times, showing their main interests: factors controlling biogeographical distribution and diversity, time and type of response to climate changes, climate variability in different time periods, latitudinal migration in time of African monsoon, and marine and wind patterns. Most of them were dealt during the discussion session, except for some questions related to methodological aspects, such as the need for unification of dating methods, the possibilities of finding new potential palaeorecords and the application and communication of our knowledge to support biodiversity conservation.

DISCUSSION

Although a great amount of information was initially collected, more than half of the results were uncertain. Researchers were unsure of many of the ideas and could not validate them, either because they had no evidence to support

TABLE 3. Summary of topics related to key questions raised by participants about the palaeoclimate of the Macaronesian region. Number in brackets indicates the number of times that a theme has appeared.

Topics
Biodiversity
Palaeoclimatic factors controlling biogeographical distribution/biodiversity (4)
Time and type of response to climate changes of vegetation/soils/fauna/landscapes (4)
Effects of sea level change on endemicity/species number/species traits (2)
Palaeoclimatic evidences derived of terrestrial fossils (2)
Role of historical processes on biodiversity (1)
Climatic refugia and species turnover (1)
Climatic variability
Latitudinal migration in time of African monsoon (3)
Climate variability in the Holocene/LGM/Eemian (3)
Different effects of climate fluctuation depending on island height and size (2)
Natural vs. cultural climate change (2)
Oceanic islands stability: fact or fiction (1)
Correspondence of climate oscillation and responses between islands and continents (1)
Marine and wind patterns
Current circulation, marine and wind patterns (3)
Role of westerlies (1)
Consequences of terminations in sea surface currents (1)
Mechanisms reversing Canary current (1)
Effects of climate change on thermohaline circulations (1)
Correlations between marine and terrestrial records and dating (1)
Methodologies
Use of general palaeoclimate models instead of fragmentary and uncertain knowledge (1)
Unification of dating methods (1)
Location of new potential palaeorecords (1)
Application and communication of knowledge to support biodiversity conservation (1)

them or because they were controversial. Even so, the validated results confirmed that the farther back in time and the farther south, the less we know, so that Cape Verde stands out as being almost unknown compared to the better known Canaries-Madeira and Azores. Little is known in Cape Verde and there is little precision about what is known, in contrast, researchers are more confident about their knowledge of the other archipelagos. It seems that the last 25,000 years are in general the best studied, however, there is more certainty about events that occurred during the last glaciation.

The knowledge about Macaronesian palaeoclimate is mainly related to four environmental parameters: humidity, temperature, wind regime and sea level oscillation. Wind regime in particular seems to have been very relevant in the studies of the central-southern archipelagos and North Africa, whereas the implications of sea level oscillation have been the focus of research in the peripheral archipelagos (Azores and Cape Verde). In general, variation of sea level was identified as a key event responsible for many effects, involving the geographical transformation of islands (size, height, isolation) and the associated consequences for biodiversity (colonization, speciation, extinction, migration). In this respect, the LGM–last deglaciation was highlighted as the period of greatest impact on the islands and this is very likely connected to the effects of sea level rise.

Other climatic variables were considered to have significant effects on the Azores and Canaries-Madeira, although these were more or less important depending on the time period. Thus, we conclude that humidity had considerable effects mainly in the Holocene while wind regime, SST and temperature were crucial at all other times.

From the number of key events and consequences, we could deduce that the Canaries-Madeira is the region subjected to most climatic variability, although this may have to do with the fact that it is also the best known region.

Participants agreed that most of the topics requiring further research had to be addressed urgently, emphasising the pressing need for more studies in Cape Verde. In all archipelagos, humidity and temperature were crucial variables to be studied and were finally grouped under the heading «climatic variability». Researchers not only commented on the importance of studying the Holocene prior to human occupation and distinguishing between human impact and natural climate changes, especially in the Canaries, but also of understanding the responses of terrestrial ecosystems on the different islands. To better understand climatic variability during the LGM–last deglaciation transition researchers consider interesting to detect shifts of altitudinal climatic and ecological zonation and they also believe that it would be useful to incorporate palaeo-data into climate models. The confirmation of extreme events with heavy rains during this period in the Canaries would help to clarify the resilience of geomorphic and biotic systems to this kind of events.

With respect to wind regime and atmospheric circulation systems, the behaviour of westerlies is considered a hot topic for research in combination with trade winds shifts to the south or changes in their intensity. This west-wind circulation could be confirmed by an increase in the arrival of hurricanes to the islands in the past, but it will be difficult to find appropriate archives to prove this. On the other hand, periods of high energy littoral dynamics in the Canary Islands might serve as an indicator of variations in trade wind intensity. Another key question was the position of the monsoonal front during interglacials, since it will have important implications in the event of a warmer future climate. It is also of interest in connection with climatic variability in Cape Verde and the Canary Islands. The influence of Saharan winds on various archipelagos during the Holocene is also questioned and researchers pointed out the importance of dust for tracing atmospheric processes, such as the reinforcement of the African easterly jet in the Holocene or its weakening during the last glaciation, which might have consequences for the fertilization of more distant regions.

High resolution bottom topography down to 150 m around all islands was requested by the group to better understand the processes related to the LGM–last deglaciation transition. Determining the similarity of sea surface currents and SST between both interglacials is important for climate modelling and to establish a possible analogy to the future climate in the region. By answering the question of whether sea surface currents were disrupted during the LGM–last deglaciation or not, we could explain the biogeographical paradox of the Azores causing a «revolution» in palaeoceanography.

Participants formulated highly original questions and interests. Although most themes arose from the questions posed by participatory tools, some were partly or not covered during this workshop and should be considered for future discussions in similar meetings.

CONCLUSIONS

The work presented here is the result of three days of analysis and discussion on the main issues related to past climate dynamics in Macaronesia and nearby regions. By means of participatory tools, researchers from different disciplines have shared their knowledge, highlighted the weaknesses of the subject, and decided urgent topics for future research. The following is a summary of the main conclusions:

1) More than half of the results describing palaeoclimate in Macaronesia are uncertain, either because there is no supporting evidence or because the results are controversial.
2) The farther back in time (Eemian) and the farther southward in direction (Cape Verde), the less is known. Canaries-Madeira and Azores are palaeoclimatically better known. By period, LGM to present is in general the best studied; however, events occurring during the last glaciation are the most certain.

3) Knowledge about the Macaronesian palaeoclimate is mainly related to four environmental variables: humidity, temperature, wind regime and sea level oscillation. These vary in importance depending on the region.
4) LGM–last deglaciation was highlighted as the period of greatest impact on the islands very likely due to the effects of sea level rise.
5) Participants agreed that most of the topics requiring further research should be addressed urgently. In all archipelagos, humidity and temperature were crucial variables. The behaviour of westerlies in combination with trade winds shifts and changes in its intensity are considered a hot topic. Another key question was the position of the monsoonal front during interglacials. High resolution bottom topography around all islands was considered to be necessary.

ACKNOWLEDGEMENTS

The organization of this workshop has been funded through the «Campus de Excelencia Atlántico Tricontinental ULL-ULPGC». We would like to warmly thank all participants for their active involvement during the discussion sessions. Hans von Suchodoletz helped specially by taking notes on the arguments on priority research issues. We are greatly in debt with the Vice Rector for Internationalization and Excellence Rodrigo Trujillo and Lidia Carrillo for all the logistic support.

REFERENCES

Ávila, S.P., Madeira, P., Mendes, N., Rebelo, A., Medeiros, A., Gomes, C., García-Talavera, F., Marques Da Silva, C., Cachão, M., Hillaire-Marcel, C. and De Frias Martins, A.M. (2008) Mass extinctions in the Azores during the last glaciation: fact or myth? *Journal of Biogeography*, 35, 1123–1129.

Björck, S., Rittenour, T., Rosén, P., França, Z., Möller, P., Snowball, I., Wastegård, S., Bennike, O. and Kromer, B. (2006) A Holocene lacustrine record in the central North Atlantic: proxies for volcanic activity, short-term NAO mode variability, and long-term precipitation changes. *Quaternary Science Reviews*, 25, 9–32.

Chambers, R. (1994) The origins and practice of participatory rural appraisal. *World Development*, 22, 953–969.

Chambers, R. (2002) *Relaxed and Participatory Appraisal: notes on practical approaches and methods for participants in PRA/PLA-related familiarisation workshops.* Institute of Development Studies, Brighton.

Chambers, R. (2007) From PRA to PLA and Pluralism: Practice and Theory. *IDS Working Paper*, 286, 1–39.

Damnati, B., Petit-Maire, N., Fontugne, M., Meco, J. and Williamson, D. (1996) Quaternary paleoclimates in the eastern Canary Islands. *Quaternary International*, 31, 37–46.

Hooghiemstra, H., Stalling, H., Agwu, C.O.C. and Dupont, L.M. (1992) Vegetational and climatic changes at the northern fringe of the Sahara 250000–5000 years BP: evidence from 4 marine pollen records located between Portugal and Canary Islands. *Review of Palaeobotany and Palynology*, 74, 1–53.

Meco, J., Guillou, H., Carracedo, J.C., Losmoschitz, A., Ramos A.J.G. and Rodríguez-Yanez, J.J. (2002). The maximum warmings of the Pleistocene world climate recorded in the Canary Islands. *Palaeogeography, Palaeoclimatology, Palaeoecology*, 185, 197–210.

Suchodoletz, H. von, Oberhänsli, H., Hambach, U., Zöller, L., Fuchs, M. and Faust, D. (2010) Soil moisture fluctuations recorded in Saharan dust deposits on Lanzarote (Canary Islands) over the last 180 ka. *Quaternary Science Reviews*, 29, 2173–2184.

Whittaker, R.J. and Fernández-Palacios, J.M. (2007) *Island biogeography: ecology, evolution, and conservation*, 2^{nd} edn. Oxford University Press, Oxford.

Yanes, Y., Yapp, C.J., Ibáñez, M., Alonso, M.R., De-la-Nuez, J., Quesada, M.L., Castillo, C. and Delgado, A. (2011) Pleistocene–Holocene environmental change in the Canary

Archipelago as inferred from the stable isotope composition of land snail shells. *Quaternary Research*, 75, 658–669.

Zazo, C., Goy, J.L., Hillaire-Marcel, C., Dabrio, C.J., González-Delgado, J.A., Cabero, A., Bardají, T., Ghaleb, B. and Solerf, V. (2010) Sea level changes during the last and present interglacials in Sal Island (Cape Verde archipelago). *Global and Planetary Change*, 72, 302–317.

PRESENT: RESPONSES OF KEY SEA URCHIN POPULATIONS TO CLIMATE CHANGE PROCESSES: FROM LARVAE TO ECOSYSTEMS

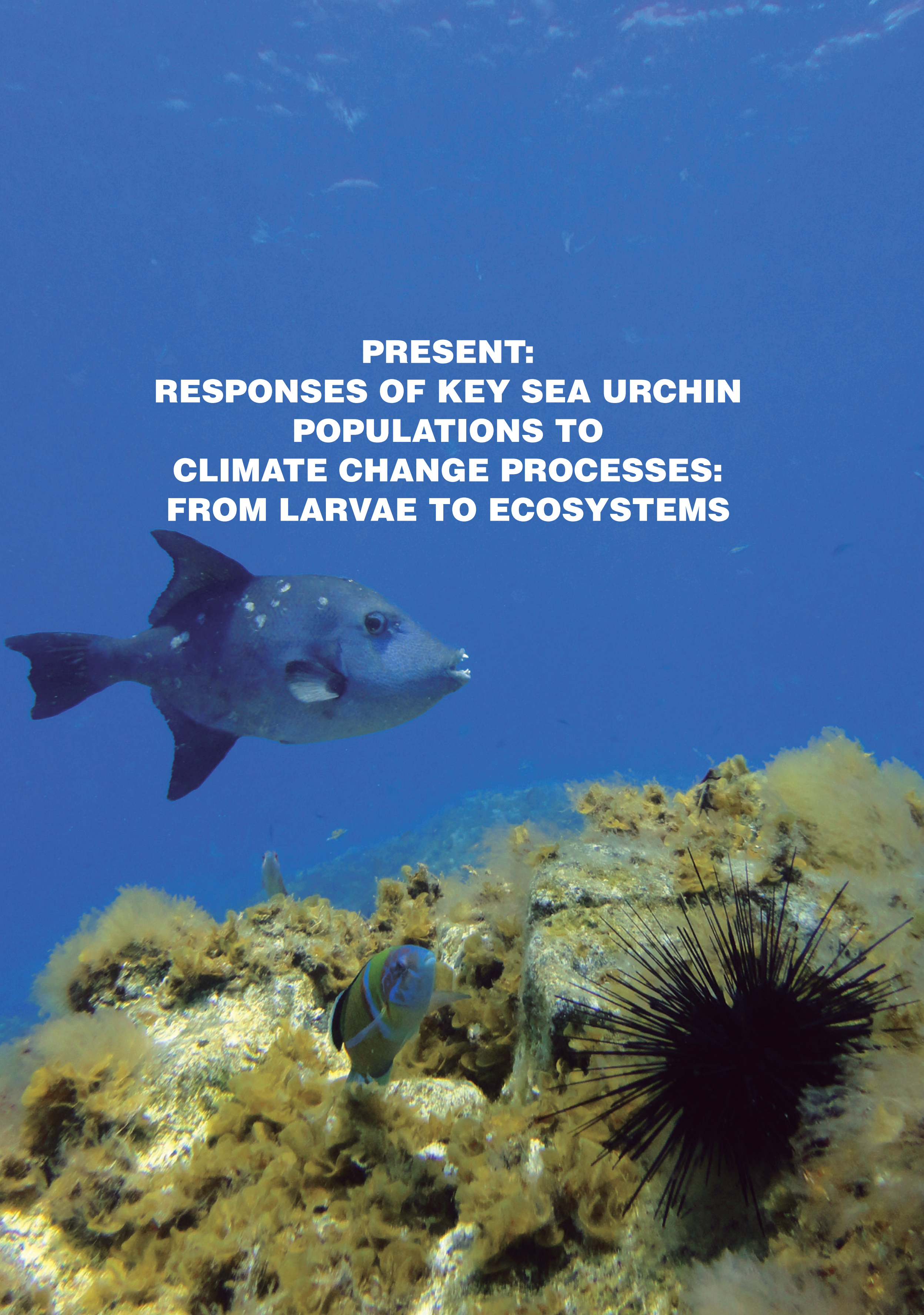

LIST OF AUTHORS

JUAN M. BARRIO
Viceconsejería de Medioambiente. Gobierno de Canarias. Las Palmas de Gran Canaria, Spain.

SÉFORA BETANCOR
Centro de Biodiversidad y Conservación (BIOGES) Departamento de Biología, Universidad de Las Palmas de Gran Canaria. Las Palmas de Gran Canaria, Spain.

HARTVIG C CHRISTIE
Norwegian Institute for Water Research (NIVA), Gaustadalléen, Oslo, Norway.

SABRINA CLEMENTE
Biodiversidad, Ecología Marina y Conservación. Universidad de La Laguna, Departamento de Biología Animal (Ciencias Marinas). La Laguna, Tenerife, Islas Canarias.
E-mail: msclemen@ull.es

MISHAL COHEN-RENGIFO
Biodiversidad, Ecología Marina y Conservación. Universidad de La Laguna, Departamento de Biología Animal (Ciencias Marinas). La Laguna, Tenerife, Islas Canarias.
Université Littoral Côte d'Opale. 1 Place d'Yser – BP 1022 59375 Dunkerque Cedex, France.
E-mail : mishal.cohen.r@gmail.com

DAVID DIAZ
Centre Oceanogràfic de Balears, Instituto Español de Oceanografía, Palma de Mallorca, Spain.

SAM T. DUPONT
Department of Biological and Environmental Sciences, The Sven Lovén Centre for Marine Sciences, University of Gothenburg, Kristineberg, Fiskebäckskil, 45178 Gothenburg, Sweden.
E-mail: sam.dupont@bioenv.gu.se

THOMAS A. EBERT
Department of Zoology, Oregon State University, Corvallis, OR 87331 USA.
E-mail: ebertt@science.oregonstate.edu

CAMILLA W. FAGERLI
Norwegian Institute for Water Research (NIVA), Gaustadalléen, Oslo, Norway.
E-mail: cwf@niva.no

COLETTE J. FEEHAN
Biology Department, Dalhousie University, Halifax, Nova Scotia B3H 4J1, Canada.
Stein Fredriksen.
Department of Biology, University of Oslo, Oslo, Norway.

DAISUKE FUJITA
Tokyo University of Marine Science and Technology, Tokio, Japan.
E-mail: d-fujita@kaiyodai.ac.jp

ELISEBA GARCÍA
Biodiversidad, Ecología Marina y Conservación. Universidad de La Laguna, Departamento de Biología Animal (Ciencias Marinas). La Laguna, Tenerife, Islas Canarias.
E-mail: egpadron@ull.es

SARA GARCÍA-SANZ
Centro de Biodiversidad y Conservación (BIOGES) Departamento de Biología, Universidad de Las Palmas de Gran Canaria. Las Palmas de Gran Canaria, Spain.

JOAQUIM GARRABOU
Institut de Ciències del Mar, Consejo Superior de Investigacions Cientificas, Barcelona, Spain.

TEBA GIL DÍAZ
Centro de Biodiversidad y Conservación (BIOGES) Departamento de Biología, Universidad de Las Palmas de Gran Canaria. Las Palmas de Gran Canaria, Spain.

RICARDO HAROUN
Centro de Biodiversidad y Conservación (BIOGES) Departamento de Biología, Universidad de Las Palmas de Gran Canaria. Las Palmas de Gran Canaria, Spain.
E-mail: rharoun@dbio.ulpgc.es

BERNAT HEREU
Departament d'Ecologia, Universitat de Barcelona, Barcelona, Spain.
E-mail: hereu@ub.edu

CELSO A. HERNÁNDEZ
Biodiversidad, Ecología Marina y Conservación. Universidad de La Laguna, Departamento de Biología Animal (Ciencias Marinas). La Laguna, Tenerife, Islas Canarias.
E-mail: cahernan@ull.es

JOSÉ CARLOS HERNÁNDEZ
Biodiversidad, Ecología Marina y Conservación. Universidad de La Laguna, Departamento de Biología Animal (Ciencias Marinas). La Laguna, Tenerife, Islas Canarias.
E-mail: jocarher@ull.es

JEAN-SÉBASTIEN LAUZON-GUAY
Fisheries and Oceans Canada, Institut Maurice-Lamontagne, Mont-Joli, Quebec G5H 3Z4, Canada.

HARILAOS A. LESSIOS
Smithsonian Tropical Research Institute, Balboa, Panama.
E-mail: Lessiosh@post.harvard.edu

CRISTINA LINARES
Departament d'Ecologia, Universitat de Barcelona, Barcelona, Spain.

SCOTT D. LING
Institute for Marine & Antarctic Studies, University of Tasmania, Hobart. Tas. 7001, Australia.
E-mail: Scott.Ling@utas.edu.au

JOSÉ CARLOS MENDOZA DURÁN
Biodiversidad, Ecología Marina y Conservación. Universidad de La Laguna, Departamento de Biología Animal (Ciencias Marinas). La Laguna, Tenerife, Islas Canarias.
E-mail: jcmendoza85@gmail.com

JACOB LORENZO-MORALES
University Institute of Tropical Diseases and Public Health of The Canary Islands, University of La Laguna, Avenida Astrofísico Francisco Sánchez SN, 38203 La Laguna, Tenerife, Canary Islands, Spain.
E-mail: jmlorenz@ull.es

PABLO G. NAVARRO
Viceconsejería de Medioambiente. Gobierno de Canarias. Las Palmas de Gran Canaria, Spain.
Centro de Biodiversidad y Conservación (BIOGES) Departamento de Biología, Universidad de Las Palmas de Gran Canaria. Las Palmas de Gran Canaria, Spain.
E-mail: pgonnav@gmail.com

KJELL M. NORDERHAUG
Norwegian Institute for Water Research (NIVA), Gaustadalléen, Oslo, Norway.
Department of Biology, University of Oslo, Oslo, Norway.
E-mail: Kjell.Norderhaug@niva.no

CREU PALACÍN
Department of Animal Biology, Universitat de Barcelona, Barcelona, Spain.
E-mail: cpalacin@ub.edu

MORTEN F. PEDERSEN
Department of Environmental, Social & Spatial Change (ENSPAC), Roskilde University, Roskilde, Denmark.

RUBÉN RÁMIREZ
Centro de Biodiversidad y Conservación (BIOGES) Departamento de Biología, Universidad de Las Palmas de Gran Canaria. Las Palmas de Gran Canaria, Spain.

ENRIC SALA
National Geographic Society, Washington, D.C., United States of America.
Centre d'Estudis Avançats de Blanes, Consejo Superior de Investigacions Cientificas, Blanes, Spain.

CARLOS SANGIL
Biodiversidad, Ecología Marina y Conservación. Universidad de La Laguna, Departamento de Biología Animal (Ciencias Marinas). La Laguna, Tenerife, Islas Canarias.
E-mail: casangil@ull.es

ROBERT E. SCHEIBLING
Biology Department, Dalhousie University, Halifax, Nova Scotia B3H 4J1, Canada.
E-mail: rescheib@dal.ca

MIKE S. THORNDYKE
Department of Biological and Environmental Sciences, The Sven Lovén Centre for Marine Sciences, University of Gothenburg, Kristineberg, Fiskebäckskil, 45178 Gothenburg, Sweden.

The Royal Swedish Academy of Sciences, The Sven Lovén Centre for Marine Sciences, Kristineberg, Fiskebäckskil, 45178 Gothenburg, Sweden.
E-mail: mike.thorndyke@bioenv.gu.se

XAVIER TURON
Center for Advanced Studies of Blanes (CEAB-CSIC), Spain.

FERNANDO TUYA
Centro de Biodiversidad y Conservación (BIOGES) Departamento de Biología, Universidad de Las Palmas de Gran Canaria. Las Palmas de Gran Canaria, Spain.
E-mail: ftuya@yahoo.es

OWEN S. WANGENSTEEN
Department of Animal Biology, Universitat de Barcelona, Barcelona, Spain.

MIKEL ZABALA
Departament d'Ecologia, Universitat de Barcelona, Barcelona, Spain.

FOREWORD

This conference addresses the question of responses of sea urchin populations to climatic changes. It is an important question because sea urchins are major components of shallow-water habitats and could be greatly impacted by climatic changes.

The importance of long-term studies on populations is addressed. These field studies establish what is occurring in the field and provide clues to the factors responsible. As several contributions point out, multiple changes in the habitat can result from a change in temperature and pH and that placing the sea urchin into the context of its community is essential. Changes in temperature affect not only the sea urchin but its foods and predators.

We lack basic information about the temperature tolerance of most sea urchin species. Information is needed on the effect of sub-lethal temperatures. The effect of temperature on development of larvae has been done for several species. Similar studies on feeding, growth and reproduction of post-metamorphic individuals are needed to establish temperature tolerances. How closely do the temperatures at which populations occur and development completed correspond to the temperatures at which populations are found in the field? How do these tolerances predict the potential for expansion or retraction of the present distribution of sea urchin species in response to predicted temperature changes?

If both temperature and pH affect sea urchins and their larvae, it is necessary to have factorial experiments in which multiple levels of each are used in combination. It allows establishing the effect of each factor and interaction between factors on the response variable. This has been done with larvae but not with post-metamorphic individuals.

Sea urchins have different life-history strategies. Some species are tolerant to stress; others are not. Knowledge of life-history strategies will be an important tool in predicting how species will respond to changes in temperature and pH.

The contributions to this conference show that sea urchins are an excellent model to study the effects of climatic change on marine invertebrates. They make an important contribution to the field. An impressive amount of information is available for use in future studies.

By John M. Lawrence
Department of Integrative Biology
University of South Florida, Tampa, Florida, USA

«NATURAL» POPULATION DENSITY FLUCTUATIONS OF ECHINOIDS. DO THEY HELP PREDICT THE FUTURE?

Harilaos A. Lessios

CLIMATE CHANGE PERSPECTIVES FROM THE ATLANTIC:
PAST, PRESENT AND FUTURE
Jose María Fernández-Palacios, Lea de Nascimento, José Carlos Hernández,
Sabrina Clemente, Albano González & Juan P. Díaz-González (eds.)
Servicio de Publicaciones, Universidad de La Laguna – 2013
ISBN: 978-84-15910-54-1
pp. 341-359

Abstract

In order to determine whether future changes in population density of sea urchins are caused by anthropogenic increases in temperature, acidity, or sea level it is necessary to have baseline data of how populations change in response to natural causes. I review cases of species with relatively stable populations over a decade, of species in which populations are known to have expanded and denuded the benthos of algae, and of species in which populations have crashed. Such documented cases are rare, because there is a dearth of information regarding long-term changes in population parameters for most echinoid species. An alternative method of deciphering past population fluctuations on the basis of genetic diversity of populations is used to show that *Diadema antillarum* became abundant long before human colonization of the Caribbean. The mass mortality suffered by this species in 1983-1984 was thus not due to abnormal population density due to the removal of its predators and competitors by humans. The existing data do not permit firm predictions regarding the future of echinoid populations under global change, but they do establish that some species are subject to boom-bust fluctuations accentuated by disproportional effects of adult population changes upon recruitment and juvenile survivorship.

Keywords: sea urchins, population fluctuations, *Diadema*

INTRODUCTION

The impending global changes due to the accumulation of carbon dioxide has worried scientists during the last two decades. Concern about marine ecosystems has understandably focused on the future of coral reefs in light of increased ocean temperatures and in sea water acidity (e.g., Kleypas *et al.* 1999; Hoegh-Guldberg *et al.* 2007; Knowlton and Jackson 2008; Kiessling and Simpson 2011; Pandolfi *et al.* 2011). A number of models have attempted to forecast changes in these ecosystems (e.g., Halpern *et al.*, 2008; Anthony *et al.*, 2011). Curiously, these models do not explicitly consider the effects of higher temperature and decreased pH on echinoids, even though echinoids are known to be important in coral reef ecosystems as herbivores that keep corals from being overgrown by algae (Carpenter, 1986; Hughes, 1994; McClanahan *et al.*, 1996) and as agents of bioerosion (Hunter, 1977; Scoffin *et al.*, 1980; Bak, 1990, 1994). The present compendium thus fills a need in that it focuses attention on a subject well-worth discussing. As oceans change, what will happen to sea urchin populations, and how will such changes affect ecosystems in which sea urchins play a role?

Although some attempts have been made to predict the future of certain sea urchin species under impending changes in temperature (Francour *et al.*, 1994; Guidetti and Dulcic, 2007; Gianguzza *et al.*, 2011; Privitera *et al.*, 2011) or acidity (Catarino *et al.*, 2012; Doo *et al.*, 2012), the straight-forward answer to the question of future changes in echinoid populations is that we do not know what will happen. This is, of course, true for all organisms; however, for those that have a good fossil record, such as corals, informed guesses can be made on the basis of past changes in their abundance that have resulted from environmental change, as documented from proxies of temperature and carbon dioxide concentration (e.g., Kiessling, 2009). Such efforts could not possibly succeed with echinoids, because the echinoid fossil record is not extensive enough for this purpose (Kier, 1977). Attempts to determine past echinoid abundance from fossils have been made, but they have produced results that can only be described as mixed (Simenstad *et al.*, 1978; Greenstein, 1989; Donovan, 2005). Information about population fluctuations of echinoids in times that precede global change is, thus, sorely needed. We would like to have such information for two reasons: (1) in the absence of information on past fluctuations, it will be difficult to determine whether any future ones are due to «natural» or to anthropogenetic causes; (2) the ecological effects observed in past changes of echinoid abundance can guide the predictions of what may happen when they occur in response to global change. It is, therefore, useful to look at changes in echinoid populations documented in the literature in order to establish a baseline of what can happen before ocean temperatures rise and pH falls.

The available data can be placed in two general categories: direct observations of population fluctuations, and reconstructions of recent or more distant past demographic history by indirect means. Neither set of data is perfect for our purposes. Published direct observations have only been possible in the «anthropocene», the period of time in which humans have already started affecting marine environments. There will, thus, always be doubts as to whether their causes are natural, or have resulted from overfishing, pollution, or some other effect caused by humans. Indirect reconstructions, such as the ones, derived from old documents (Jackson, 1997), museum specimens (Levitan, 1992), or genetic markers (Lessios *et al.*, 2001a), suffer from biases (different in each case). They are also not suitable for determining the cascade of effects that changes in population density of sea urchins have had on the ecosystem. Nevertheless, it is worth putting all this information together and attempt to use it in speculating about the future.

POPULATION FLUCTUATIONS

Uthicke *et al.*, (2009) called echinoderms a «boom-bust» phylum because of large population fluctuations undergone by some of its species. They reviewed evidence of population crashes or break-outs of 28 echinoderm species, eight of them belonging to the Echinoidea: *Arbacia lixula, Diadema antillarum, Echinometra mathaei, Echinocardium cordatum, Paracentrotus lividus, Strongylocentrotus droebachiensis, S. purpuratus, and S. franciscanus.* To these, one should add the range expansion of *Centrostephanus rodgersii* into Tasmanian waters (Ling, 2008; Ling and Johnson, 2009) and the frequent population increases and unusual population fluctuations of the Caribbean and western Atlantic *Lytechinus variegatus* (Beddingfield and McClintock, 1994; Macia and Lirman, 1999; Rose *et al.*, 1999). Lawrence (1996) has reviewed mass mortalities of echinoderms due to abiotic factors. Mortalities due to such physical factors are generally localized, ephemeral, and infrequent, so they may not hold any lessons regarding the possible effects of global change. This chapter is intentionally unbalanced: contributions by other authors to the same compendium cover the population fluctuations of *Strongylocentrotus droebachiensis* on the East coast of North America (Scheibling, this volume), *Paracentrotus lividus* and *Arbacia lixula* in the Mediterranean (Hereu, this volume), *Centrostephanus rodgersii* in Tasmania (Ling, this volume) and *Diadema africanum* (Hernández, this volume). The present chapter will, therefore, concentrate on species that are not the main focus of other contributions. Additional imbalance comes from the variable amount of published information regarding each of these case studies. Finally, documentation of such population fluctuations is not independent of the geographical distribution of research centers in Europe, North America, Australia, and the Caribbean.

Stable population densities

Densities of every natural population go up or down through time. To determine what constitutes boom-bust population fluctuations, one first needs to decide what changes occur under «normal» circumstances. Unfortunately, data on long-term population monitoring of echinoid populations are scarce (Uthicke *et al.*, 2009), so one has to generalize from a few examples. Pearse and Hines (1987) studied populations of *Strongylocentrotus franciscanus* and of *S. purpuratus,* at irregular intervals ranging from 1 to 8 months, in a reserve on the coast of California from 1972 to 1981. During the nine years of this study, population densities of *Strongylocentrotus franciscanus* stayed uniformly low. *S. purpuratus*, on the other hand, experienced a single event of high recruitment that temporarily increased its density from 0.2 to 5 individuals per m^2. Most of these recruits had disappeared a year later. This species, like its congener *S. droebachiensis* on the East coast of North America, is involved in «urchin barrens», where kelp is almost entirely removed (Dayton *et al.*, 1992). Hereu *et al.* (2012) monitored populations of *Paracentrotus lividus* from 1991 to 2010 and of *Arbacia lixula* from 1995 to 2010 in annual censuses in North-West Mediterranean. They found that annual density differences in *P. lividus* living in boulders could be as high as eightfold, whereas densities of the same species living in vertical walls were not significantly different between years. Similar inter-annual variation was seen in *A. lixula*. Increases were due to pulses of recruitment, but the overall densities were smoothed within a year by mortality. Wing (2009) monitored populations of *Evechinus chloroticus* in the Fiordland of the South Island of New Zealand from 1998 to 2007 at intervals ranging from one to three years. Fjords in this area are characterized by dense kelp growth at the entrances, replaced by broken blades and debris in the innermost areas, and by fresh water lenses overlaying layers of normal salinity. Sea urchin populations at the fjord entrances were composed of large individuals and a stable size structure, indicating steady recruitment, whereas at the inner areas there was evidence of high turnover, caused by severe mortality followed by high recruitment.

In summary, the few available sets of data from long-term monitoring, all of them from species in the temperate zone, suggest that fluctuations in population density of sea urchins do occur, but there are also stabilizing mechanisms of recruitment followed by mortality, and of mortality followed by recruitment that, in a decadal scale, tend to maintain fairly steady levels. Ability of sea urchin species to recolonize areas in which physical factors have caused localized mortalities (e.g., Andrew, 1991; Lawrence, 1996; Junqueira *et al.*, 1997; Beddingfield and McClintock, 2000; Lawrence and Agatsuma, 2007) also suggest that if sufficient numbers of individuals of a species survive in areas close enough for larvae to reach and reseed bare patches, overall populations will remain relatively stable.

There is, of course, some circularity in designating as «normal» situations that appear to be stable, but the object here is to provide a baseline with which to compare phenomena of instability. Large echinoid population fluctuations, appearing to drive marine ecosystems into alternate stable states have also been noted. Such deviations from «normal» fluctuations in echinoid population density have generally been noticed and studied after they have occurred. Population expansions as a rule manifest themselves as sea urchin barrens due to overgrazing. Population constrictions are sometimes obvious from the accumulation of dead tests. In either case, interpretation of causes and quantification of the magnitude of the event are hampered by the lack of data as to the state of the populations before the change occurred.

Population expansions

Unusual increases in population densities of particular species of echinoids have been documented in several parts of the world. As a rule, they have dramatic consequences on the benthic communities by removing algae and leaving bare substrate in their path.

One of the earliest reported major positive changes in sea urchin abundance was the increases of *Strongylocentrotus purpuratus* and *S. franciscanus* off the coast of southern California (North and Pearse, 1970). The increase has been ascribed to the removal of predators, such as sea otters (Estes *et al.*, 1989) and lobsters (Lafferty, 2004), and of competitors, such as abalone (Dayton *et al.*, 1998). The ecological effect was devastation of kelp forests during sea urchin population increases, followed by recovery when sea urchins were removed by disease or overfishing (Dayton *et al.*, 1992).

The best documented case of the ecological effects of sea urchin population density increases is that of *Strongylocentrotus droebachiensis* off the coast of Nova Scotia, studied over the last thirty years by Robert Scheibling and colleagues. As this topic is covered in another chapter (Scheibling, this volume), there is little that needs to be added here. The same species also caused barrens in laminarian kelp forests in northern Norway in the early 1980s (Hagen, 1983).

The case of echinoid population expansion most likely to be the product of global change is that of *Centrostephanus rodgersii* in Tasmania, first observed in 1978 (Andrew and Byrne, 2001; Johnson *et al.*, 2005; Ling, 2008). This case is also covered in another chapter (Ling, this volume), so it will only be briefly mentioned here. *C. rodgersii* off New South Wales has increased its populations in recent times to a density that has created sea urchin barrens. The increase is attributed to the reduction of its predators through overfishing (Andrew and Byrne, 2001). Although it was originally absent from Tasmania, *C. rodgersii* recently invaded this island with the same ecological impact as in its historic range. This range expansion, reflected by a number of other species (Poloczanska *et al.* 2007), was most likely the result of pole-ward intrusions by the East Australian Current (Johnson *et al.* 2005). To the extent that echinoid species ranges are controlled by temperature, such spreading of species towards lower latitudes are expected as the planet warms and ocean current circulation patterns are altered.

Although the expansion has not been documented for lack of previous data, there appears to have been an increase of population density of *Diadema africanum* (Rodríguez *et al.* 2013) in the Canaries due to overfishing of its predators (Tuya *et al.,* 2004). This increase has manifested itself in the formation of barrens devoid of macroalgae. Hernández *et al.* (2008) monitored populations of *Diadema* at multiple islands in the Canaries in irregular intervals between 2001 and 2006. As a rule, the population densities fluctuated by a factor of two, but there was an outbreak in 2006. By December 2006 populations in three islands appeared to be on their way to returning to their previous levels.

Echinometra mathaei in heavily exploited reefs off the coast of Kenya showed a ten-fold increase in population density between 1970 and 1985 (McClanahan and Muthiga, 1988). Large differences between protected and unprotected areas indicated that the increased abundance of *Echinometra* was due to the removal of its predators (McClanahan and Shafir, 1990).

An extreme case of local echinoid population density increase was documented in the Outer Bay of Florida (Macia and Lirman, 1999; Rose *et al.*, 1999).

Between 1996 and 1997 average density of *Lytechinus variegatus* in the Outer Florida Bay was 0.2 individuals per m^2. In September 1997 a large aggregation of this species reached densities of 364 sea urchins per m^2. It formed a large 2-3 km grazing front that denuded approximately 0.81 km^2 of the *Syringodium filiforme* sea grass bed. By the time of the last observations in April 1998, densities had dropped to approximately 18.5 sea urchins per m^2. Such a grazing front by *L. variegatus* in the northeast Gulf of Mexico had also been reported previously (Camp *et al.*, 1973), though without data of population densities in normal times.

Thus, echinoids appear capable of expanding their populations when predators are removed, or when conditions become favorable for recruitment. Interestingly, population regulation does not appear to be exercised through food limitation. Even after they have created barrens, sea urchins were able to maintain high population densities until another factor, such as disease caused drastic reductions (Lang and Mann, 1976; Andrew, 1991; Dayton *et al.*, 1992; Lauzon-Guay and Scheibling, 2007).

Population crashes

Whereas populations of *Centrostephanus rodgersii* in Tasmania appear to remain stable or still increase, population expansions of *Strongylocentrotus* in three parts of the world are checked by mass mortalities, so that kelp ecosystems fluctuate in alternate stable states. At both coasts of North America, as well as in Scandinavia, barren-causing sea urchin populations are confronted by pathogens or parasites, sometimes in combination with other factors, such as storms. In California one population of *S. purpuratus* was decimated by disease, allowing kelp to recruit to the site (Dayton *et al.*, 1992). At Norway populations of *S. droebachiensis* that had overgrazed algae were infested by *Echinomermella matsi*, a nematode parasite of sea urchins, which is presumed to have reduced their density, so that kelp could recover (Hagen, 1987, 1992, 1995). The only case in which the pathogen was unambiguously identified and studied in detail was that of *S. droebachiensis* off the coast of Nova Scotia. The causative agent, proven by Koch's postulates, is an amoebozoan, *Paramoeba invadiens* (Jones *et al.*, 1985; Jones and Scheibling, 1985). Infection by *Paramoeba* only flares up when sea water temperatures exceed 10° C, so that high mortality occurs seasonally in the summer and early fall, and is also correlated with hurricane activity (Feehan *et al.*, 2012). At the Canaries, moribund *Diadema africanum* were found to contain trophozoites of *Neoparamoeba branchiphila*, a close relative of *Paramoeba invadiens* (Dykova *et al.*, 2011). Thus, events of unusual population increases may, in some cases, be followed by events of unusual mortality. To some, this may indicate the resilience of an ecosystem to perturbations, whereas to others it is an indication of alternate stable states (Simenstad *et al.*, 1978; Scheibling, 1984).

Two cases in which population crashes do not appear to be due to self-correction are the fairly gradual decline of *Paracentrotus lividus* populations at Lough Hyne in Ireland and the mass mortality of *Diadema antillarum* in the Caribbean and the western Atlantic. *Paracentrotus lividus* population fluctuations due to recurrent recruitment and mortality in the North Western Mediterranean have been mentioned in this chapter as an example of a stable population. This has not been the case at the oldest marine reserve in Europe, Lough Hyne, a semi-enclosed lagoon. *P. lividus* at Lough Hyne was present at high densities from 1964 to 1984 but has undergone a steady decline between 1984 and 2000 (Barnes *et al.*, 2001; Barnes and Crook, 2001) eventually completely disappearing in 2002 (Barnes *et al.*, 2002). The actual causes of the decline remain unclear. Given the apparent stability of the Irish populations over twenty years and their eventual demise over the next twenty, one could argue that the Mediterranean populations of the same species, followed by Hereu *et al.*, (2012) for ten years, might meet the same fate if one were to monitor their density long enough. If so, my having designated them as stable is premature. Only time will address this point.

The *Diadema antillarum* die off in the Caribbean and the American Atlantic coast is the most severe and most extensive case of mass mortality in a marine organism documented to date. It was first noticed on the coast of Panama in January 1983. In a little more than a year it had spread to the entire Caribbean, Florida and Bermuda (Lessios *et al.*, 1984a). The mass mortality did not reach the eastern Atlantic (Hernández *et al.*, 2008) either because currents did not carry the pathogen across, or because *Diadema africanum* is actually a different species (Lessios, 2001; Lessios *et al.*, 2001b; Rodríguez *et al.* 2013). Pre-mortality population density data were available in eight areas in the Caribbean. The average population reduction at these sites ranged between 87 and 100 % (Lessios, 1988a). The cause of the mortality was never identified, but indirect evidence points to a species-specific pathogen (Lessios *et al.*, 1984a,b; Lessios, 1988a). The immediate result of the removal of *Diadema* from the reefs was increase by macroalgal cover, which, in time, prevented recruitment of corals and even overtopped adult colonies (de Ruyter van Steveninck and Bak, 1986; Hughes *et al.*, 1987; Hughes, 1994). Populations of other echinoids on the reefs were not affected either negatively by the pathogen, or positively by possible release from competition (Lessios, 1988b). Herbivorous fishes, on the other hand, did benefit. By 1990, populations of the surgeon fishes *Acanthurus coeruleus* and *A. chirurgus* in the San Blas area of Panama had increased their population density by more than 160%, whereas those of *A. bahianus*, which feeds in areas where *Diadema* was never present, remained constant (Robertson, 1991). Genetic diversity of *D. antillarum*, measured by isozymes before and after the mass mortality, did not change (Lessios, 1985). This species also maintained much higher molecular diversity in mitochondrial DNA in the Caribbean than *D. africanum* did in the eastern Atlantic and *D. mexicanum* in the eastern Pacific (Lessios *et al.* 2001a).

Despite some early signs that population recovery of *Diadema antillarum* would commence soon after mass mortality (Lessios *et al.*, 1984b; Hunte and Younglao, 1988), it proved to be very slow. A number of studies started monitoring populations after the mass mortality and found some increases, but at locations without pre-mortality data it is not possible to determine the extent of recovery. Subjective impressions of the species being plentiful once again can be misleading, because *Diadema* tends to aggregate in shallow areas, so that patches with high spot densities can be misjudged as indications of high overall abundance. The only objective determinations can come from locations in which there were pre-mortality data. Twenty years after mass mortality, population density in Panama was at 6.5% of their pre-1983 values (Lessios, 2005a). Eighteen years after January 1984, when mass mortality reached the US Virgin Islands, populations at St. Croix were at 5.2% of pre-mortality levels (Miller *et al.*, 2003). Nineteen years after die offs in Curacao, populations of *D. antillarum* on the leeward side of the island were at 1.9-9.6 % of what the used to be (Debrot and Nagelkerken, 2006), and continued to be low three years later despite evidence of renewed recruitment (Vermeij *et al.*, 2010). In Discovery Bay, Jamaica, increases in population density of *Diadema* were accompanied by higher incidence of coral recruits (Edmunds and Carpenter, 2001). A correlation between *Diadema* and coral recruit abundance was also found in six other sites of the Caribbean (Carpenter and Edmunds, 2006).

Was the mass mortality of *Diadema antillarum* a natural correction in a species that had overpopulated its environment due to anthropogenic causes? Hay (1984), through comparisons between areas in the Caribbean with different fishing pressures, had suggested that the removal of fish predators and competitors of the sea urchin had been responsible for high pre-mortality densities. Levitan (1992), in a study of the relative size of test and jaw dimensions of museum specimens in space and time (a proxy for food limitation), concluded that fishing had an effect on *Diadema* population density, but that this effect was minor. Jackson (1997), on the basis of anecdotal accounts in 16th century Spanish manuscripts, argued that *Diadema* was abundant in the Caribbean before fishing pressure increased. Donovan (2005), on the basis of a very patchy and fragmentary fossil record of *D. antillarum* ossicles in sediments, concluded that the species had been abundant long before prehistoric times.

One way to answer the question of population size in past ages is the study of DNA. Diversity of selectively neutral genetic markers depends only on the rate of substitution of the marker in question and on effective population size. Thus, if the former is known, the latter can be modeled. Lessios *et al.* (2001a) sequenced two genes of mitochondrial DNA in 110 individuals of *D. antillarum* from seven localities around the Caribbean. They estimated rate of substitution from divergence between *D. antillarum* and *D. mexicanum*, separated 2-3 million years ago by the rise of the Isthmus of Panama. They were thus able to estimate the trajectory of female effective population expansion through time, and found that it began between 400 and 100 millennia ago. The conclusion is that human activity may have had some effect upon *Diadema* population densities, but the large increase of the population occurred too far back in time to have been caused by humans.

In summary, sea urchin populations appear to remain stable for undetermined periods of time, but some species at certain times may undergo break out increases that alter the ecosystem through their grazing, and some species experience die offs from which they can recover rapidly if the mortality is localized, but take decades to be repaired if the majority of individuals throughout the species range have died.

WHY SHOULD THE ECHINOIDEA SHOW BOOM-BUST FLUCTUATIONS?

Uthicke *et al.* (2009), in examining severe population fluctuations in 28 species of echinoderms, concluded that anthropogenic disturbance, including climate change and disease outbreaks, were the most common causes. They also suggested that boom-bust cycles are linked to two life history traits, common among all the examples mentioned above: broadcast spawning and planktotrophic larvae. External fertilization depends on the proximity of sperm and eggs during spawning, the probability of which decreases rapidly with increased distance of individuals of the two sexes (Pennington, 1985; Levitan, 1991; Lauzon-Guay and Scheibling, 2007). This leads to an Allee effect, a feedback loop of disproportional effects of adult population rarity upon the abundance of juveniles in the next generation. According to Uthicke *et al.* (2009), planktotrophic larvae decouple factors that regulate resources for the early life stages from adult resources, so that rate of recruitment is dependent on the rate of larval production and on the vagaries of survival in the plankton, rather than being limited by adult densities. An additional mechanism that forms self-reinforcing loops and would accentuate the magnitude of positive and negative fluctuations has been documented for several species of sea urchins. This is the positive feedback resulting from the negative correlation between algal abundance and sea urchin recruitment. Adult sea urchins, by grazing algae, provide suitable substrate (possibly due to the absence of micropredators) for the settlement of larvae. This may well be the case in *Centrostephanus rodgersii* (Ling and Johnson, 2009), *Strongylocentrotus droebachiensis* (Lang and Mann, 1976), *S. purpuratus, S. franciscanus* (Tegner and Dayton, 1981) and *Diadema antillarum* (Bak, 1985). A yet additional feedback mechanism in some of the same species is the protection afforded to juveniles by adult spine canopies, as it happens in *S. purpuratus* (review in Rogers-Bennett, 2007), and apparently also in *Diadema antillarum* (Miller *et al.*, 2007). Thus, increases in adult echinoid population densities in each generation lead to new disproportional increases in the next; decreases in adults lead to disproportional reductions in recruitment and survivorship of juveniles.

DO DATA FROM THE PAST HELP PREDICT THE FUTURE?

Predictions based on scant data are always dangerous, but certain points can be made on the basis of cases I have summarized. If echinoids are, in fact, subject to boom-bust trends, global warming may affect their populations disproportionally relative to those of other organisms. Guessing which species will be affected and to what degree is not possible by the present data, but some may succumb to disease, whereas others may experience large population increases that would wreck havoc with the ecosystems they occupy. Given the association of outbreaks of *Paramoeba invadiens* in *Strongylocentrotus droebachiensis* with higher temperatures and hurricanes, it seems very likely that mass mortalities in this species will continue or, more likely, increase with global warming. Similarly, the coincidence between bald sea urchin disease in *Paracentrotus lividus* with high temperatures at the Canaries (Girard *et al.*, 2012) does not auger well for the prospects of temperate sea urchins as the seas become warmer. Temperature, however, is not always the trigger for echinoid disease. Even though the *Diadema* mortality occurred in an El Niño year, the initiation of its outbreak in Panama preceded the increase of temperatures in the Caribbean by several months (Lessios *et al.* 1984b).

To the extent that higher temperatures may not always cause disease, echinoids (other than species living close to the poles, which have no escape towards lower latitudes) may be affected much more severely by overfishing and pollution than by global warming and ocean acidification. Sea urchins in the tropical eastern Pacific survive well, despite the low pH values in this ocean (Manzello *et al.*, 2008). They also survive with no apparent ill effects high temperatures during El Nino events that cause extensive coral bleaching and mortality (Lessios, 2005b). If anything, species like *Diadema mexicanum* and *Eucidaris thouarsi* benefit from coral mortality, because it opens new areas for algal colonization. This, by no means, indicates that echinoids will be immune to global change. They might, however, become even more prominent components of benthic ecosystems.

REFERENCES

ANDREW, N.L. (1991) Changes in subtidal habitat following mass mortality of sea urchins in Botany-Bay, New South Wales. *Australian Journal of Ecology*, 16, 353–362.

ANDREW, N.L. and BYRNE, M. (2001) The ecology of *Centrostephanus rodgersii*.. *Edible sea urchins: biology and ecology* (ed. by Lawrence, J.M.), pp. 149–160. Elsevier, Amsterdam.

ANTHONY, K.R.N., MAYNARD, J.A., DIAZ-PULIDO, G., MUMBY, P.J., MARSHALL, P.A., CAO, L. and HOEGH-GULDBERG, O. (2011) Ocean acidification and warming will lower coral reef resilience. *Global Change Biology* 17, 1798–1808.

BAK, R.P.M. (1985) Recruitment patterns and mass mortalities in the sea urchin *Diadema antillarum. Proceedings of the 5th Inernational Coral Reef Congress,* 5, 267–272.

BAK, R.P.M. (1990) Patterns of echinoid bioerosion in two Pacific coral reef lagoons. *Marine Ecology Progress Series*, 66, 267–272.

BAK, R.P.M. (1994) Sea urchin bioerosion on coral reefs: place in the carbonate budget and relevant variables. *Coral Reefs*, 13, 99–103.

BARNES, D.K.A. and CROOK, A.C. (2001) Implications of temporal and spatial variability in *Paracentrotus lividus* populations to the associated commercial coastal fishery. *Hydrobiologia*, 465, 95–102.

BARNES, D.K.A., CROOK, A., O'MAHONEY, M., STEELE, S. and MAGUIRE, D. (2001) Sea temperature variability and *Paracentrotus lividus* (Echinoidea) population fluctuations. *Journal of the Marine Biological Association of the United Kingdom*, 81, 359–360.

BARNES, D.K.A., VERLING, E., CROOK, A., DAVIDSON, I. and O'MAHONEY, M. (2002) Local population disappearance follows (20 yr after) cycle collapse in a pivotal ecological species. *Marine Ecology-Progress Series*, 226, 311–313.

BEDDINGFIELD, S.D. and MCCLINTOCK, J.B. (1994) Environmentally induced catastrophic mortality of the sea urchin *Lytechinus variegatus* in shallow seagrass habitats of Saint Josephs Bay, Florida. *Bulletin of Marine Science*, 55, 235–240.

BEDDINGFIELD, S.D. and MCCLINTOCK, J.B. (2000) Demographic characteristics of *Lytechinus variegatus* (Echinoidea: Echinodermata) from three habitats in a North Florida Bay, Gulf of Mexico. *Marine Ecology - Pubblicazioni Della Stazione Zoologica di Napoli,* 21, 17–40.

CAMP, D.K., COBB, S.P. and van BREEDVELD, J.F. (1973) Overgrazing of seagrasses by a regular urchin, *Lytechinus variegatus. Bioscience*, 23, 37–38.

Carpenter, R.C. (1986) Partitioning herbivory and its effects on coral-reef algal communities. *Ecological Monographs*, 56, 345–363.

Carpenter, R.C. and Edmunds, P.J. (2006) Local and regional scale recovery of *Diadema* promotes recruitment of scleractinian corals. *Ecology Letters*, 9, 268–277.

Catarino, A.I., De Ridder, C., Gonzalez, M., Gallardo, P. and Dubois, P. (2012) Sea urchin *Arbacia dufresnei* (Blainville 1825) larvae response to ocean acidification. *Polar Biology*, 35, 455–461.

Dayton, P.K., Tegner, M.J., Parnell, P.E. and Edwards, P.B. (1992) Temporal and spatial patterns of disturbance and recovery in a kelp forest community. *Ecological Monographs*, 62, 421–445.

Dayton, P.K., Tegner, M.J., Edwards, P.B. and Riser, K.L. (1998) Sliding baselines, ghosts, and reduced expectations in kelp forest communities. *Ecological Applications*, 8, 309–322.

de Ruyter van Steveninck, E.D. and Bak, R.P.M. (1986) Changes in abundance of cora reef bottom components related to mass mortality of the sea urchin *Diadema antillarum. Marine Ecology Progress Series*, 34, 87–94.

Debrot, A.O. and Nagelkerken, I. (2006) Recovery of the long-spined sea urchin *Diadema antillarum* in Curacao (Netherlands Antilles) linked to lagoonal and wave sheltered shallow rocky habitats. *Bulletin of Marine Science*, 79, 415–424.

Donovan, S.K. (2005) The fossil record of *Diadema* in the Caribbean. *Coral Reefs*, 24, 603–605.

Doo, S.S., Dworjanyn, S.A., Foo, S.A., Soars, N.A. and Byrne, M. (2012) Impacts of ocean acidification on development of the meroplanktonic larval stage of the sea urchin *Centrostephanus rodgersii. ICES Journal of Marine Science*, 69, 460–464.

Dykova, I., Lorenzo-Morales, J., Kostka, M., Valladares, B. and Peckova, H. (2011) *Neoparamoeba branchiphila* infections in moribund sea urchins *Diadema* aff. *antillarum* in Tenerife, Canary Islands, Spain. *Diseases of Aquatic Organisms*, 95, 225 –231.

Edmunds, P.J. and Carpenter, R.C. (2001) Recovery of *Diadema antillarum* reduces macroalgal cover and increases abundance of juvenile corals on a Caribbean reef. *Proceedings of the National Academy of Sciences of the United States of America*, 98, 5067–5071.

Estes, J.A., Duggins, D.O. and Rathbun, G.B. (1989) The ecology of extinctions in kelp forest communities. *Conservation Biology*, 3, 252 –264.

Feehan, C., Scheibling, R.E. and Lauzon-Guay, J.S. (2012) An outbreak of sea urchin disease associated with a recent hurricane: Support for the «killer storm hypothesis» on a local scale. *Journal of Experimental Marine Biology and Ecology*, 413, 159–168.

Francour, P., Boudouresque, C.F., Harmelin, J.G., Harmelinvivien, M.L. and Quignard, J.P. (1994) Are the Mediterranean waters becoming warmer? Information from biological indicators. *Marine Pollution Bulletin*, 28, 523–526.

Gianguzza, P., Agnetta, D., Bonaviri, C., Di Trapani, F., Visconti, G., Gianguzza, F. and Riggio, S. (2011) The rise of thermophilic sea urchins and the expansion of barren grounds in the Mediterranean Sea. *Chemistry and Ecology*, 27, 129–134.

GIRARD, D., CLEMENTE, S., TOLEDO-GUEDES, K., BRITO, A. and HERNANDEZ, J.C. (2012) A mass mortality of subtropical intertidal populations of the sea urchin *Paracentrotus lividus*: analysis of potential links with environmental conditions. *Marine Ecology-an Evolutionary Perspective*, 33, 377–385.

GREENSTEIN, B.J. (1989) Mass mortality of the West-Indian echinoid *Diadema antillarum* (Echinodermata: Echinoidea): A natural experiment in taphonomy. *Palaios*, 4, 487–492.

GUIDETTI, P. and DULČIĆ, J. (2007) Relationships among predatory fish, sea urchins and barrens in Mediterranean rocky reefs across a latitudinal gradient. *Marine Environmental Research*, 63, 168–184.

HAGEN, N.T. (1983) Destructive grazing of kelp beds by sea urchins in Vestfjorden, northern Norway. *Sarsia*, 68, 177–190.

HAGEN, N.T. (1987) Sea urchin outbreaks and nematode epizootics in Vestfjorden, northern Norway. *Sarsia*, 72, 213–229.

HAGEN, N.T. (1992) Macroparasitic epizootic disease: a potential mechanism for the termination of sea urchin outbreaks in northern Norway. *Marine Biology*, 114, 469–478.

HAGEN, N.T. (1995) Recurrent destructive grazing of successionally immature kelp forests by green sea urchins in Vestfjorden, northern Norway. *Marine Ecology Progress Series*, 123, 95–106.

HALPERN, B.S., WALBRIDGE, S., SELKOE, K.A., KAPPEL, C.V., MICHELI, F., D'AGROSA, C., BRUNO, J.F., CASEY, K.S., EBERT, C., FOX, H.E., FUJITA, R., HEINEMANN, D., LENIHAN, H.S., MADIN, E.M.P., PERRY, M.T., SELIG, E.R., SPALDING, M., STENECK, R. and WATSON, R. (2008) A global map of human impact on marine ecosystems. *Science*, 319, 948–952.

HAY, M.E. (1984) Patterns of fish and urchin grazing on Caribbean coral reefs: are previous results typical? *Ecology*, 65, 446–454.

HEREU, B., LINARES, C., SALA, E., GARRABOU, J., GARCIA-RUBIES, A., DIAZ, D. and ZABALA, M. (2012) Multiple processes regulate long-term population dynamics of sea urchins on Mediterranean rocky reefs. *PLoS ONE*, 7, e36901.

HERNÁNDEZ, J.C., CLEMENTE, S., SANGIL, C. and BRITO, A. (2008) The key role of the sea urchin *Diadema* aff. *antillarum* in controlling macroalgae assemblages throughout the Canary Islands (eastern subtropical Atlantic): A spatio-temporal approach. *Marine Environmental Research*, 66, 259–270.

HOEGH-GULDBERG, O., MUMBY, P.J., HOOTEN, A.J., STENECK, R.S., GREENFIELD, P., GOMEZ, E., HARVELL, C.D., SALE, P.F., EDWARDS, A.J., CALDEIRA, K., KNOWLTON, N., EAKIN, C.M., IGLESIAS-PRIETO, R., MUTHIGA, N., BRADBURY, R.H., DUBI, A. and HATZIOLOS, M.E. (2007) Coral reefs under rapid climate change and ocean acidification. *Science*, 318, 1737–1742.

HUGHES, T.P. (1994) Catastrophes, phase shifts, and large-scale degradation of a Caribbean coral reef. *Science*, 265, 1547–1551.

HUGHES, T.P., REED, D.C. and BOYLE, M.J. (1987) Herbivory on coral reefs: community structure following mass mortalities of sea urchins. *Journal of Experimental Marine Biology and Ecology*, 113, 39–59.

Hunte, W. and Younglao, D. (1988) Recruitment and population recovery of *Diadema antillarum* (Echinodermata, Echinoidea) in Barbados. *Marine Ecology Progress Series*, 45, 109–119.

Hunter, I.G. (1977) Sediment production by *Diadema antillarum* on a Barbados fringing reef. *Proceedings of the 3rd Inernational Coral Reef Symposium*, 2, 111–119.

Jackson, J.B.C. (1997) Reefs since Columbus. *Proceedings of the 8th International Coral Reef Symposium* (ed. by Lessios, H.A. and Macintyre I.G.), pp. 97–106. Smithsonian Tropical Research Institute, Panama.

Johnson, C.R., Ling, S.D., Ross, J., Shepherd, S. and Miller K. (2005) *Establishment of the long-spined sea urchin (Centrostephanus rodgersii) in Tasmania: first assessment of potential threats to fisheries.* Fisheries Research and Development Corporation, Deakin West, ACT, Australia.

Jones, G.M. and Scheibling, R.E. (1985) *Paramoeba* sp. (Amebida, Paramoebidae) as the possible causative agent of sea-urchin mass mortality in Nova-Scotia. *Journal of Parasitology*, 71, N5, 559–565.

Jones, G.M., Hebda, A.J., Scheibling, R.E. and Miller, R.J. (1985) Histopathology of the disease causing mass mortality of sea urchins (*Strongylocentrotus droebachiensis*) in Nova Scotia. *Journal of Invertebrate Pathology*, 45, 260–271.

Junqueira, A.D.R., Ventura, C.R.R., Decarvalho, A.L.P.S. and Schmidt, A.J. (1997) Population recovery of the sea urchin *Lytechinus variegatus* in a seagrass flat (Araruama lagoon, Brazil): the role of recruitment in a disturbed environment. *Invertebrate Reproduction & Developmentk,* 31, 143–150.

Kier, P.M. (1977) The poor fossil record of the regular echinoid. *Paleobiology*, 3, 168–174.

Kiessling, W. (2009) Geologic and biologic controls on the evolution of reefs. *Annual Review of Ecology Evolution and Systematics*, 40, 173–192.

Kiessling, W. and Simpson, C. (2011) On the potential for ocean acidification to be a general cause of ancient reef crises. *Global Change Biology*, 17, 56–67.

Kleypas, J.A., Buddemeier, R.W., Archer, D., Gattuso, J.P., Langdon, C. and Opdyke, B.N. (1999) Geochemical consequences of increased atmospheric carbon dioxide on coral reefs. *Science*, 284, 118–120.

Knowlton, N. and Jackson, J.B.C. (2008) Shifting baselines, local impacts, and global change on coral reefs. *PLoS Biology*, 6, 215–220.

Lafferty, K.D. (2004) Fishing for lobsters indirectly increases epidemics in sea urchins. *Ecological Applications*, 14, 1566 –1573.

Lang, C. and Mann, K.H. (1976) Changes in sea urchin populations after the destruction of kelp beds. *Marine Biology*, 36, 321–326.

Lauzon-Guay, J.S. and Scheibling, R.E. (2007) Importance of spatial population characteristics on the fertilization rates of sea urchins. *Biological Bulletin*, 212, 19 –205.

Lawrence, J.M. (1996) Mass mortality of echinoderms from abiotic factors. *Echinoderm studies* (ed. by Jangoux, M. and Lawrence, J.M.), pp. 103–137. Balkema, Rotterdam.

Lawrence, J.M. and Agatsuma, Y. (2007) Ecology of *Tripneustes. Edible Sea Urchins: Biology and Ecology* (ed. by Lawrence, J.M.), pp. 449–520. Elsevier, Amsterdam.

Lessios, H.A. (1985) Genetic consequences of mass mortality in the Caribbean sea urchin *Diadema antillarum. Proceedings of the 5th Inernational Coral Reef Congress*, 4, 119–126.

Lessios, H.A. (1988a) Mass mortality of *Diadema antillarum* in the Caribbean: what have we learned? *Annual Review of Ecology and Systematics*, 19, 371–393.

Lessios, H.A. (1988b) Population dynamics of *Diadema antillarum* (Echinodermata: Echinoidea) following mass mortality in Panama. *Marine Biology*, 99, 515–526.

Lessios, H.A. (2001) Molecular phylogeny of *Diadema*: Systematic implications. *Echinoderms 2000. Proceedings of the 10th International Echinoderm Conference* (ed. by Barker, M.), pp. 487– 95. Swets and Zeitinger, Lisse.

Lessios, H.A. (2005a) *Diadema antillarum* populations in Panama twenty years following mass mortality. *Coral Reefs*, 24, 125–127.

Lessios, H.A. (2005b) Echinoids of the Pacific Waters of Panama: Status of knowledge and new records. *Revista de Biologia Tropical*, 53, 147–170.

Lessios, H.A., Robertson, D.R. and Cubit, J.D. (1984a) Spread of *Diadema* mass mortality through the Caribbean. *Science*, 226, 335–337.

Lessios, H.A., Cubit, J.D., Robertson, D.R., Shulman, M.J., Parker, M.R., Garrity, S.D. and Levings, S.C. (1984b) Mass mortality of *Diadema antillarum* on the Caribbean coast of Panama. *Coral Reefs*, 3, 173–182.

Lessios, H.A., Garrido, M.J. and Kessing, B.D. (2001a) Demographic history of *Diadema antillarum*, a keystone herbivore on Caribbean reefs. *Proceedings of the Royal Society B-Biological Sciences*, 268, 2347–2353.

Lessios, H.A., Kessing, B.D. and Pearse, J.S. (2001b) Population structure and speciation in tropical seas: global phylogeography of the sea urchin *Diadema. Evolution*, 55, 955–975.

Levitan, D.R. (1991) Influence of body size and population density on fertilization success and reproductive output in a free-spawning invertebrate. *Biological Bulletin*, 181, 261–268.

Levitan, D.R. (1992) Community structure in times past:influence of human fishing pressure on algal urchin interactions. *Ecology*, 73, 1597–1605.

Ling, S. (2008) Range expansion of a habitat-modifying species leads to loss of taxonomic diversity: a new and impoverished reef state. *Oecologia*, 156, 883–894.

Ling, S.D. and Johnson, C.R. (2009) Population dynamics of an ecologically important range-extender: kelp beds versus sea urchin barrens. *Marine Ecology Progress Series*, 374, 113–125.

Macia, S. and Lirman, D. (1999) Destruction of Florida Bay seagrasses by a grazing front of sea urchins. *Bulletin of Marine Science*, 65, 593–601.

Manzello, D.P., Kleypas, J.A., Budd, D.A., Eakin, C.M., Glynn, P.W. and Langdon, C. (2008) Poorly cemented coral reefs of the eastern tropical Pacific: Possible insights into reef development in a high-CO_2 world. *Proceedings of the National Academy of Sciences of the United States of America*, 105, 10450–10455.

McClanahan, T.R. and Muthiga, N.A. (1988) Changes in Kenyan coral reef community structure and fundtion due to exploitation. *Hydrobiologia*, 166, 269–276.

McClanahan, T.R. and Shafir, S.H. (1990) Causes and consequences of sea urchin abundance and diversity in Kenyan Coral reef lagoons. *Oecologia*, 83, 362–370.

McClanahan, T.R., Kamukuru, A.T., Muthiga, N.A., Yebio, M.G. and Obura, D. (1996) Effect of sea urchin reductions on algae, coral, and fish populations. *Conservation* Biology, 10, 136–154.

Miller, R.J., Adams, A.J., Ebersole, J.P. and Ruiz, E. (2007) Evidence for positive density-dependent effects in recovering *Diadema antillarum* populations. *Journal of Experimental Marine Biology and Ecology*, 349, 215–222.

Miller, R.J., Adams, A.J., Ogden, N.B., Ogden, J.C. and Ebersole, J.P. (2003) *Diadema antillarum* 17 years after mass mortality: is recovery beginning on St. Croix? *Coral Reefs*, 22, 181–187.

North, W.J. and Pearse, J.S. (1970) Sea urchin population explosion in southern California soastal waters. *Science*, 167, 209

Pandolfi, J.M., Connolly, S.R., Marshall, D.J. and Cohen, A.L. (2011) Projecting coral reef futures under global warming and ocean acidification. *Science*, 333, 418–422.

Pearse, J.S. and Hines, A.H. (1987) Long-Term Population-Dynamics of Sea-Urchins in a Central California Kelp Forest - Rare Recruitment and Rapid Decline. *Marine Ecology Progress Series*, 39, 275–283.

Pennington, J.T. (1985) The ecology of fertilization of echinoid eggs: the consequences of sperm dilution, adult aggregation, and synchronous spawning. *Biological Bulletin*, 169, 417–430.

Poloczanska, E.S., Babcock, R.C., Butler, A., Hobday, A., Hoegh-Guldberg, O., Kunz, T.J., Matear, R., Milton, D.A., Okey, T.A. and Richardson, A.J. (2007) Climate change and Australian marine life. *Oceanography and Marine Biology, Vol 45* (ed. by. Gibson, R.N., Atkinson, R.J.A. and Gordon, J.D.M.), pp. 407–478. Crc Press-Taylor & Francis Group, Boca Raton.

Privitera, D., Noli, M., Falugi, C. and Chiantore, M. (2011) Benthic assemblages and temperature effects on *Paracentrotus lividus* and *Arbacia lixula* larvae and settlement. *Journal of Experimental Marine Biology and Ecology*, 407, 6-11.

Robertson, D.R. (1991) Increases in surgeonfish populations after mass mortality of the sea urchin *Diadema antillarum* in Panama indicate food limitation. *Marine Biology*, 111, 437–444.

Rodríguez, A., Hernández, J.C., Clemente, S. and Coppard, S. (2013) A new species of *Diadema* (Echinodermata: Echinoidea: Diadematidae) from the eastern Atlantic Ocean and a neotype designation of *Diadema antillarum* (Philippi, 1845). Zootaxa 3636(1): 144–170.

ROGERS-BENNETT, L. (2007) The ecology of *Strongylocentrotus franciscanus* and *Strongylocentrotus purpuratus. Edible sea urchins: biology and ecology* (ed. by LAWRENCE, J.M.), pp. 393–425. Elsevier, Amsterdam.

ROSE, C.D., SHARP, W.C., KENWORTHY, W.J., HUNT, J.H., LYONS, W.G., PRAGER, E.J., VALENTINE, J.F., HALL, M.O., WHITFIELD, P.E. and FOURQUREAN, J.W. (1999) Overgrazing of a large seagrass bed by the sea urchin *Lytechinus variegatus* in Outer Florida Bay. *Marine Ecology Progress Series*, 190, 211–222.

SCHEIBLING, R.E. (1984) Echinoids, epizootics and ecological stability in the rocky subtidal off Nova Scotia, Canada. *Helgolander Meeresuntersuchungen*, 37, 233–242.

SCOFFIN, T.P., STEARN, C.W., BOUCHER, D., FRYDL, P., HAWKINS, C.M., HUNTER, I.G. and MACGEACHY, J.K. (1980) Calcium carbonate budget of a fringing reef on the west coast of Barbados. Part II. Erosion, sediments and internal structure. *Bulletin of Marine Science*, 30, 475–508.

SIMENSTAD, C.A., ESTES, J.A. and KENYON, K.W. (1978) Aleuts, sea otters, and alternate stable-state communities. *Science*, 200, 403–411.

TEGNER, M.J. and DAYTON, P.K. (1981) Population structure, recruitment and mortality of two sea urchins (*Strongylocentrotus franciscanus* and *S. purpuratus*) in a kelp forest. *Marine Ecology Progress Series*, 5, 255–268.

TUYA, F., BOYRA, A., SANCHEZ JEREZ, P., BARBERA, C. and HAROUN, R.J. (2004) Relationships between rocky-reef fish assemblages, the sea urchin *Diadema antillarum* and macroalgae throughout the Canarian Archipelago. *Marine Ecology Progress Series*, 278, 157–169.

UTHICKE, S., SCHAFFELKE, B. and BYRNE, M. (2009) A boom-bust phylum? Ecological and evolutionary consequences of density variations in echinoderms. *Ecological Monographs*, 79, 3–24.

VERMEIJ, M.J.A., DEBROT, A.O., VAN DER HAL, N., BAKKER, J. and BAK, R.P.M. (2010) Increased recruitment rates indicate recovering populations of the sea urchin *Diadema antillarum* in Curaçao. *Bulletin of Marine Science*, 86, 719–725.

WING, S.R. (2009) Decadal-scale dynamics of sea urchin population networks in Fiordland, New Zealand are driven by juxtaposition of larval transport against benthic productivity gradients. *Marine Ecology Progress Series*, 378, 125–134.

CLIMATE CHANGE, DISEASE AND THE DYNAMICS OF A KELP-BED ECOSYSTEM IN NOVA SCOTIA

Robert E. Scheibling, Colette J. Feehan, Jean-Sébastien Lauzon-Guay

CLIMATE CHANGE PERSPECTIVES FROM THE ATLANTIC:
PAST, PRESENT AND FUTURE
Jose María Fernández-Palacios, Lea de Nascimento, José Carlos Hernández,
Sabrina Clemente, Albano González & Juan P. Díaz-González (eds.)
Servicio de Publicaciones, Universidad de La Laguna – 2013
ISBN: 978-84-15910-54-1
pp. 361-387

Abstract

Along the Atlantic coast of Nova Scotia, cyclical alternations between kelp beds and sea urchin barrens are driven by sporadic introductions of a pathogenic amoeba *Paramoeba invadens* that causes mass mortality of green sea urchins *Strongylocentrotus droebachiensis*, thereby enabling kelps to recolonize the rocky seabed. Sea urchins gradually repopulate disease-affected areas and destructively graze the emergent kelp beds, returning the system to the barrens state. Using a logistic regression model, we showed that the probability of mass mortality of sea urchins is related to the intensity and proximity of tropical storms and hurricanes, hypothesized to deliver the pathogenic agent, and post-storm ocean temperature above a threshold (12°C) for a disease outbreak. We also showed that the likelihood of deadly storms for sea urchins increased over a 30-year period (1980–2009), a trend expected to accelerate with future ocean warming and increased hurricane intensity. We currently are testing the validity of this model in a field experiment designed to compare predicted and observed disease outbreaks and extend our trend analysis over 5 more years. The experiment also provides insight into spatial and temporal patterns of disease outbreaks in relation to coastal warming and a changing hydrodynamic and biotic regime. If observed trends continue, the resilience of the kelp bed state will be enhanced, and the sea urchin fishery doomed, in areas potentially affected by disease.

Keywords: kelp bed, sea urchin, disease, mass mortality, climate change, ecosystem dynamics, predictive modeling.

INTRODUCTION

The notion that communities of interacting species can exist in alternative organizational states, dominated by different groups of organisms at different times, is well entrenched in ecology and currently is an area of active research and synthesis (May, 1977; Beisner *et al.*, 2003; Petraitis and Hoffman, 2010). Numerous theoretical studies indicate the potential for alternative states in community models, and alternative states have been documented in various terrestrial (forests, grassland), freshwater (wetlands, lakes), and marine (rocky intertidal and subtidal communities, soft-bottom assemblages, coral reefs) systems (Scheffer *et al.*, 2001; Folke *et al.*, 2004; Knowlton, 2004). Understanding mechanisms that determine the stability of a given community state or drive transitions (or phase shifts) between states is crucial to assessing the consequences of anthropogenic stressors and climate change on the structure and dynamics of ecosystems, and the services that they provide to people. Disease has been identified as an important driver of shifts in community state in marine systems (Harvell *et al.*, 1999). The incidence of disease in various marine organisms has increased in recent decades, a trend that has been linked to ocean warming (Harvell *et al.*, 2002). Widespread mass mortality due to disease has been observed in sea grasses, corals, molluscs, crustaceans, echinoderms and marine mammals (Lafferty *et al.*, 2004; Ward and Lafferty, 2004). Disease outbreaks that affect key producers or consumers can lead to profound alterations in marine food webs and community structure (Lessios, 1988; Muelhstein, 1989).

Along the Atlantic coast of Nova Scotia, Canada cyclical alternations between kelp beds and sea urchin barrens are driven by recurrent outbreaks of an amoebic disease (paramoebiasis) that causes mass mortality of the green sea urchin *Strongylocentrotus droebachiensis*, the dominant herbivore (Scheibling, 1984a; Lauzon-Guay *et al.*, 2009). This release from grazing pressure enables kelps and other macroalgae to colonize the rocky seabed. Sea urchins gradually repopulate disease-affected areas through larval recruitment or adult migration from refuge populations in deeper waters. As sea urchins increase in density, they form feeding aggregations (or fronts) that destructively graze the emergent kelp beds, returning the system to the barrens state.

Here, we briefly review the literature on the etiology and epizoology of paramoebiasis in *Strongylocentrotus droebachiensis* and the ecological consequences of this disease for alternative-state dynamics of the rocky subtidal ecosystem off Nova Scotia. We examine evidence that increases in ocean surface temperature and storm frequency and intensity may influence the frequency and severity of epizootics resulting in sea urchin mass mortality, and present results of ongoing empirical studies to test a statistical model relating mortality events to these oceanographic/meteorologic factors. We also consider potential effects of local hydrodynamic features, sea urchin population density and distribution, and the physiological ecology of the pathogenic agent, on the introduction, spread and persistence of disease. Finally, we apply trend analysis and simulation models to project the frequency of disease events along this coast over the next three decades, and discuss the implications of these projections for alternative-state dynamics of the shallow subtidal ecosystem.

OUTBREAKS OF SEA URCHIN DISEASE IN NOVA SCOTIA

Recurrent outbreaks of disease causing mass mortalities of shallow (<20 m depth) populations of *Strongylocentrotus droebachiensis* were first recorded along the Atlantic coast of Nova Scotia between 1980 and 1983 (Miller and Colodey, 1983; Scheibling, 1984a, 1986; Miller, 1985), and then sporadically over the next 3 decades (Scheibling and Hennigar, 1997; Miller and Nolan, 2000, 2008; Scheib-

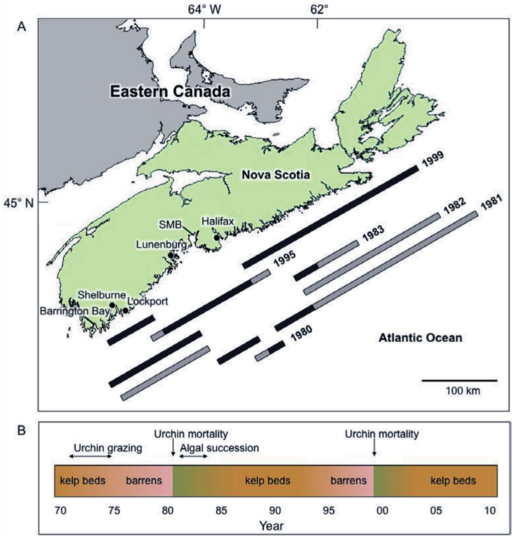

Figure 1. A) Range of mass mortalities of *Strongylocentrotus droebachiensis* during widespread outbreaks of disease in the shallow subtidal zone along the Atlantic coast of Nova Scotia, in the early 1980s (Source: Miller, 1985; Scheibllng, 1986) and the mid to late 1990s (Source: Scheibling and Hennigar, 1997; Miller and Nolan, 2000): black bars, near-complete mortality; grey bars, partial mortality. Also shown are St. Margarets Bay (SMB) and other locations mentioned in the text. B) Schematic of transitions between alternative community states (kelp beds and barrens) following mass mortality of sea urchins and destructive grazing of kelp.

ling *et al.*, 2010; Feehan *et al.*, 2012a) (Fig. 1A). Anecdotal evidence suggests mass mortalities have occurred in previous decades (Miller, 1985). Estimated annual mortalities of sea urchins in the early 1980s ranged from 80 to 260 Kt fresh weight in areas of complete die-off (Miller and Colodey, 1983; Miller, 1985b; Scheibling, 1986). Mortalities in the 1990s were of similar magnitude (Miller and Nolan, 2000), while those in the 2000s were more localized, as sea urchin populations were depleted or eliminated along large tracts of coast (Scheibling *et al.*, 2010; Feehan *et al.*, 2012a).

The disease in *Strongylocentrotus droebachiensis* is characterized by progressive deterioration of muscle tissue of the body wall and water-vascular system, resulting in loss of function of the tube feet, spines and mouthparts (Jones *et al.*, 1985). In early stages of infection, sea urchins cease feeding and movement, and are unable to attach to the substratum. Many succumb to predators or are washed ashore (Miller and Colodey, 1983; Scheibling 1984b; Feehan *et al.*, 2012a); moribund sea urchins and tests accumulate on the seabed and on beaches (Fig. 2A, B). Spine loss and epidermal necrosis occur as the disease progresses (Scheibling

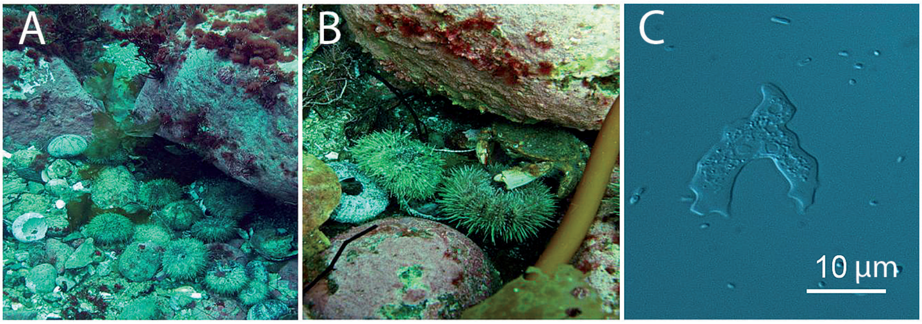

Figure 2. A) Moribund and dead *Strongylocentrotus droebachiensis* accumulating on the sea bed, and B) a Jonah crab (*Cancer borealis*) scavenging a moribund sea urchin, during a disease outbreak in St. Margarets Bay in 2009 (photographs by R. E. Scheibling). C) *Paramoeba invadens* isolated from a moribund sea urchin (photograph by J. Johnson-MacKinnon).

and Stephenson, 1984; Roberts-Regan *et al.*, 1988). At peak water temperatures (see below), the disease terminates in death within weeks (Scheibling and Stephenson, 1984).

A previously undescribed marine amoeba, *Paramoeba invadens*, isolated from tissues of diseased sea urchins was identified as the causal agent of mass mortality of *S. droebachiensis* (Jones, 1985; Jones and Scheibling, 1985; reviewed by Scheibling, 1988) (Fig. 2C). Recent genetic analysis of amoebae similarly isolated from infected sea urchins during an epizootic in 2011 confirm the identity of *P. invadens* as a unique species, most closely related to *Neoparamoeba branchiphila*, a parasite of other sea urchins and salmonid fish in aquaculture (Feehan *et al.*, 2013). Amoebae of the genera *Paramoeba* and *Neoparamoeba* are associated with disease in sea urchins, decapod crustaceans, and fish worldwide. These infections typically exhibit strong temperature-dependence with threshold dynamics. *Paramoeba invadens* is waterborne and can be cultured on marine bacteria, indicating a free-living existence and facultative parasitism (Jones and Scheibling, 1985). The inability of *P. invadens* to survive in culture at temperatures (2 °C) above the typical winter minimum (~ 0 °C) in coastal waters of Nova Scotia suggests it is periodically introduced from warmer regions (Jellett and Scheibling, 1988; Scheibling and Hennigar, 1997). These epizootics are highly specific to *S. droebachiensis* (Scheibling and Stephenson, 1984; Jellett *et al.*, 1988) and sea urchin density-dependent (Scheibling, 1984a, 1988).

Temperature is a key factor regulating the transmission and progression of paramoebiasis in *S. droebachiensis* (Scheibling and Stephenson, 1984; Jellett and Scheibling, 1988). Epizootics occur during the peak in sea temperature in late summer or early fall, often in unusually warm years, and the rate and extent of mortality is directly related to the magnitude and duration of peak tempera-

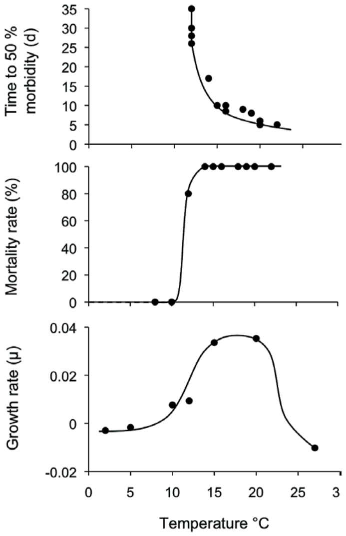

Figure 3. Median time to ≥ 50% morbidity and percent mortality of *Strongylocentrotus droebachiensis* exposed to diseased conspecifics in water-borne transmission experiments in the laboratory (from Scheibling, 1984a), and specific growth rate of *Paramoeba invadens* in monoxenic culture (from Jellett and Scheibling, 1988).

tures (Miller and Colodey, 1983; Scheibling and Stephenson, 1984; Miller, 1985; Scheibling, 1986; Scheibling and Hennigar, 1997; Brady and Scheibling, 2005; Feehan *et al.*, 2012a). In the laboratory, the disease progresses exponentially between 12 and 20°C and is arrested at 10 to 12°C (Scheibling and Stephenson, 1984) (Fig. 3). The time to morbidity and mortality of sea urchins infected at different temperatures is consistent with the temperature-dependent growth rate of *Paramoeba invadens* in monoexnic culture, which is zero at 5°C and greatest at 15–20°C (Jellett and Scheibling, 1988) (Fig. 3). Infected individuals recover within 30 days by lowering temperature to at least 8°C. In nature, disease outbreaks are terminated by declining temperatures in the late fall and surviving sea urchins recover over winter (Scheibling and Stephenson, 1984; Scheibling and Hennigar, 1997). Sea urchins in deeper, colder waters below the seasonal thermocline have a refuge from disease (Brady and Scheibling, 2005; Scheibling *et al.*, 2010; Feehan *et al.,* 2012a). Nutritional condition does not affect the rate of mortality from paramoebiasis, and both juveniles and adults of *S. droebachiensis* are susceptible (Scheibling and Stephenson, 1984). Extensive mortalities of *S. droebachiensis,* on the scale of those recorded in Nova Scotia, have not been observed elsewhere in the Northwest Atlantic, although there are reports of disease and localized die-offs of sea urchins in Newfoundland (Hooper, 1980) and in the St. Lawrence Estuary and Gulf of St. Lawrence (Himmelman *et al.*, 1983; Dumont *et al.*, 2004). These mortalities were associated with colder waters, and not likely due to paramoebiasis. In the Gulf of Maine however, sea urchin mortalities in fall 1999 coincided with an outbreak of disease in lobsters that was caused by *Neoparamoeba pemaquidensis* (Mullen *et al.*, 2004; 2005) and Caraguel *et al.* (2007) isolated *N. pemaquidensis* from moribund sea urchins in fall 2002.

SPATIAL AND TEMPORAL VARIATION IN DISEASE OUTBREAKS AND TRANSITIONS BETWEEN COMMUNITY STATES

Ocean currents and local hydrodynamic features presumably influence the introduction and spread of the water-borne pathogenic agent along the coast of Nova Scotia (Scheibling and Hennigar, 1997). Free-living *Paramoeba*, morphologically indistinct from laboratory cultures of *P. invadens*, were detected in the seawater and sediment samples near the outfall of Dalhousie University's seawater facility, which released untreated effluent from flow-through tanks containing infected sea urchins at the time (Jellett *et al.*, 1989). However, there has been no attempt to sample amoebae in the water-column or sediments along the Atlantic coast of Nova Scotia. Although the residual surface current flows southwestward, outbreaks of disease and mass mortality of sea urchins appear to have spread both southwest and northeast along this coast in the early 1980s (Scheibling and Stephenson, 1984; Miller, 1985; Scheibling, 1986) and mid to late 1990s (Scheibling and Hennigar, 1997; Brady and Scheibling, 2005) (Fig. 1A). Detailed records of the temporal sequence of mortalities are lacking and it is possible that the disease spread from various foci rather than from a single origin (Scheibling, 1988). River outflow may have limited the spread of disease in 1981, resulting in a discrete boundary to the mass mortality along the southwestern coast of Nova Scotia (Miller and Colodey, 1983; Scheibling and Stephenson, 1984).

The population density of *Strongylocentrotus droebachiensis* affects the rate of propagation and transmission of paramoebiasis and the range of epizootics along the coast (Scheibling and Stephenson, 1984). In areas and years of partial die-offs of sea urchins, morbidity and mortality were highest at shallow depths (< 5 m) where sea urchins were most dense (Scheibling and Stephenson, 1984; Scheibling, 1988; Miller, 1985). Extreme densities of sea urchins, particularly along grazing fronts, likely accelerate the propagation of the disease (Scheibling and Hennigar, 1997). Prior to the first documented outbreak of disease in Halifax Harbour in 1980 (Miller and Colodey, 1983), sea urchin barrens extended along the entire Atlantic coast of Nova Scotia (Wharton and Mann, 1981), providing an extensive host population for recurrent epizootics, which spread along ~ 600 km (linear distance) of coast between 1981 and 1983 (Miller, 1985; Scheibling, 1986) (Fig. 1A).

The depth range of sea urchin mass mortality is limited by the thermal threshold (10–12°C) for transmission and propagation of paramoebiasis (Scheibling and Stephenson, 1984). This threshold usually occurs at 20 to 25 m depth and varies with changes in thermal structure of the water column due to wave-driven vertical mixing (upwelling and downwelling) during summer and fall (Scheibling, 1984a; Brady and Scheibling, 2005). The depth range of mass mortality also is limited by the extent of rocky habitat in areas where the substratum grades to sand at depths above the thermal threshold, such as in large embayments (Filbee-Dexter and Scheibling, 2012). Sea urchins surviving below the threshold depth form the source population for recolonization of areas affected by disease. Where sea urchins occur immediately below the zone of mortality, random foraging movements extend the population to shallower depths, as kelps and other macroalgae begin to recolonize the former barrens (Lauzon-Guay *et al.*, 2008, 2009).

Coastal bathymetry and substratum type will determine the resilience of sea urchin barrens after a mass mortality event, and hence the potential for the kelp-bed state to establish and persist. On steeply sloping shores, where the offshore (along-bottom) extent of urchin mortality (which defines the potential transition zone for alternative community states) may be only 10s of meters, foraging sea urchins can repopulate the barrens habitat within 1 to 2 years, preempting the establishment of kelp beds and maintaining a barrens state (Brady and Scheibling, 2005). Where the seabed slopes more gradually to the threshold depth, the zone of mass mortality may extend 100s of meters to more than a kilometer offshore (Moore and Miller, 1983). A prolonged release from sea urchin grazing enables kelps and other macroalgae to colonize these extensive barrens via propagules dispersing from shallow fringe populations, in a wave-mediated refuge from sea urchin grazing, leading to the establishment of luxuriant algal beds within 2 to 3 years (Miller, 1985; Scheibling, 1986; Johnson and Mann, 1988). Sea urchins grazing along the offshore extent of these developing beds form aggregations (or fronts) that gradually advance onshore to reestablish the barrens state. Deep-dwelling sea urchins on rock or sedimentary bottoms also contribute to a larval pool that provides recruits to the expanding barrens (Brady and Scheibling, 2005). Recruitment to established kelp beds also may enable sea urchins to increase in abundance within beds to the point at which they form destructive grazing aggregations (Hart and Scheibling, 1988), although direct evidence for this is lacking (Lauzon-Guay and Scheibling, 2010; Feehan *et al.*, 2012b). In areas where sea urchins are eliminated throughout the rocky subtidal zone (i.e., where the lower boundary is above the threshold depth for the spread of paramoebiasis), kelp beds reestablish and can persist for more than a decade before migrating sea urchins in offshore sandy habitats encounter the beds and form grazing fronts along their deep edge (Scheibling *et al.*, 1999; Filbee-Dexter and Scheibling, 2012).

Disease drives the alternative-state system in the rocky subtidal zone off Nova Scotia (Fig. 1B). Epizootics terminate the barrens phase in the transitional zone and subsequent alternation between the kelp-bed and barrens state is dependent upon the distance to physically-mediated spatial refuges for the dominant species of each state: wave-swept shallows for kelp, colder deeper waters for sea urchins. As kelps colonize offshore areas after release from grazing pressure, sea urchin fronts gradually migrate onshore to consume them. The introduction of *P. invadens* to the shallow subtidal zone, and hence the potential for an epizootic that causes a shift to the kelp-bed state, may be largely determined by stochastic processes associated with broad-scale meteorological and hydrodynamic conditions that are poorly understood (Scheibling and Hennigar, 1997). On the other hand, the reverse shift to the barrens state occurs through a series of deterministic processes (e.g., algal succession, sea urchin foraging behaviour, kelp and sea urchin population dynamics) that are well documented (Johnson and Mann, 1988). Mathematical models that describe the alternation between states following a disease event demonstrate a high degree of concordance between predicted and observed dynamics (Lauzon-Guay *et al.*, 2008, 2009).

The timing of introduction of *P. invadens* to the coast of Nova Scotia, in relation to the prevailing ocean temperature and state of the ecosystem, determines the likelihood of an epizootic and the extent of sea urchin mass mortality. If the pathogen were introduced when the system is in the kelp-bed state, sea urchin density likely would be too low to trigger an epizootic (even when temperatures are conducive to the spread of disease) and the kelp-bed state would be maintained. On the other hand, when the pathogen is introduced in the barrens state and ocean temperatures are around the seasonal maximum (16–20 °C), the disease propagates rapidly leading to widespread mass mortality and a shift to the kelp-bed state (Scheibling and Hennigar, 1997; Brady and Scheibling, 2005). However, when the introduction occurs later in the year, as falling temperatures approach the threshold level, the disease is arrested before extensive mortality can occur and the barrens state is maintained (Scheibling and Stephenson, 1984). Recurrent introductions of *P. invadens*, depending on the frequency, can result in reversals in the transition between states. For example, an epizootic that eliminates sea urchins and enables kelps to expand their offshore range can be followed by a gradual return to the barren state as a sea urchin front forms along the deep margin of the bed and advances shoreward; a subsequent epizootic can arrest this transition and once again return the system to the kelp-bed state (Scheibling *et al.*, 1999). Thus, frequent introductions of *P. invadens* stabilize the kelp bed state, whereas rare introductions enable the persistence of barrens.

KILLER STORMS: HURRICANES AND OUTBREAKS OF PARAMOEBIASIS

Using a logistic regression model (see below), Scheibling and Lauzon-Guay (2010) showed that the probability of mass mortality of sea urchins can be predicted by the intensity and proximity of tropical storms and hurricanes, hypothesized to deliver *P. invadens* to the coast, and post-storm ocean temperature above a threshold (12°C) for a disease outbreak. They showed that the likelihood of deadly storms for sea urchins increased over a 30-year period (1980–2009), a trend expected to accelerate in the near future with ocean warming and increased hurricane intensity (Bender *et al.*, 2010). These storm events could transport *P. invadens* to coastal areas by horizontal advection from distant source populations or vertically mix amoebae residing locally in deep basins (Scheibling and Hennigar, 1997; Scheibling *et al.,* 2010).

We currently are testing the validity of this model in a field experiment designed to compare predicted and observed disease outbreaks over a 4- to 6-year period. Beginning in 2010, we have transplanted *S. droebachiensis* in July or early August (before the start of the hurricane season off Nova Scotia) from a headland (Splitnose Point) near Halifax, Nova Scotia, where sea urchin populations have persisted in the shallow subtidal zone for at least a decade, into cages in kelp beds at 8 m depth in and around St. Margarets Bay, where localized outbreaks of disease were observed following hurricanes in recent years (Scheibling *et al.*, 2010; Feehan *et al.*, 2012a). Throughout the hurricane season (August to November), we measured sea urchin morbidity and mortality in these cages at weekly to biweekly intervals, while monitoring sea temperature and hurricane activity. For site descriptions and details of the experimental design and sampling procedures in 2010, see Feehan *et al.* (2012a). In 2011–2012, 3 of the 6 sites within the bay in 2010 were retained and 2 new sites were added, one at the headland on each side of the bay; the number of replicate cages at each site was 2 in 2010 and 4 in 2011 and 2012. At one site, we also placed sea urchins in cages at 18 m depth, below the seasonal thermocline where temperatures generally were below the threshold for paramoebiasis.

In September of 2010 and 2011, we observed morbidity of caged sea urchins at 8 m depth following the passage of a hurricane with a high probability of association with an urchin mass mortality (P_m), according to the model: Hurricane Earl, $P_m = 43\%$, and Hurricane Katia, $P_m = 70\%$ (Fig. 4). Moribund sea urchins displayed overt signs of paramoebiasis and transmitted the disease via a water-borne route to healthy conspecifics in the laboratory (Feehan *et al.*, 2012a, Feehan *et al.*, 2013). *Paramoeba invadens* was isolated from tissues of field-collected moribund sea urchins and cross-infected individuals in controlled laboratory experiments, satisfying Koch's postulates. In each year, the P_m of the hurricane was not significantly different (*t*-test) from the mean P_m of "candidate storms" in 1980–2009 (57 ± 28% SD, n = 12), based on the model (Hurricane Earl: $p = 0.11$; Hurricane Katia: $p = 0.14$). For each storm, we predicted the time to ≥ 50% morbidity of sea urchins with paramoebiasis (t_{50}, d) using a relationship based on water-borne disease transmission experiments in the laboratory:

$$t_{50} = 23492T^{-2.7476}$$

where T (°C) is water temperature during the period of infection (Scheibling *et al.*, 2010). We estimated t_{50} following a hurricane from temperature records at 8 m depth in St. Margarets Bay during the field experiment. In 2010 and 2011,

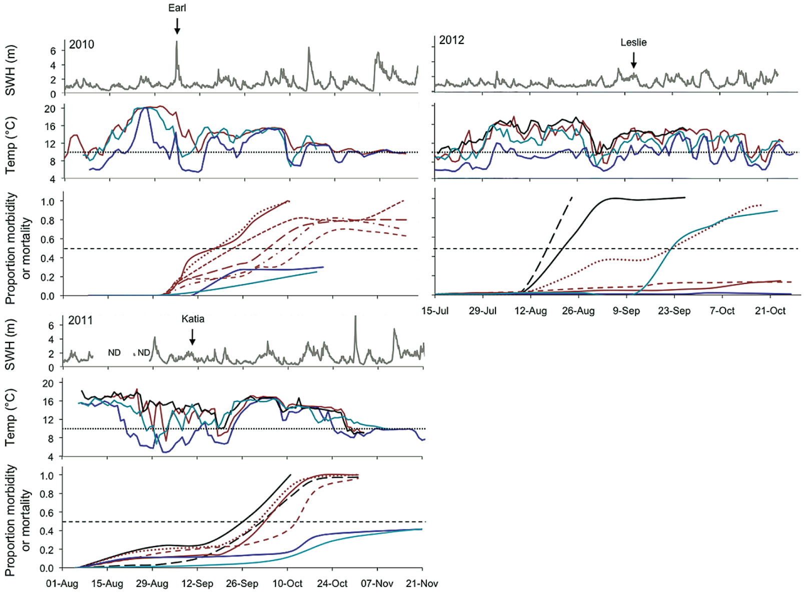

Figure 4. Significant wave height (SWH) at Halifax Harbour, and temperature and the proportion of dead or moribund *Strongylocentrotus droebachiensis* in experimental cages at 8-m depth at 3 (2011–2012) or 6 (2010) sites within St. Margarets Bay (red lines), at 2 sites (2011–2012) at the headlands on either side of the bay (black lines), at 1 site (Splitnose Point) where sea urchins were collected for all cages (procedural control; green lines), and at 18-m depth at 1 site within the bay (blue lines), before and after a hurricane or tropical storm that preceded an outbreak of paramoebiasis in sea urchins. Dotted horizontal line is the lower temperature threshold (10°C) at which sea urchins do not exhibit signs of morbidity due to paramoebiasis. Dashed horizontal line is the time to 50 % morbidity (t_{50}) of sea urchins. Arrows indicate the date at which each storm passed closest to the study area. ND: No data.

the observed t_{50} of sea urchins in cages at 8 m, pooled across all sites, closely approximated the predicted t_{50} based on water temperature following the hurricane: the difference between observed and predicted values ranged from 2 to 3 days.

Although a strong tropical cyclone did not pass close to the coast of Nova Scotia during the 2012 hurricane season, a mass mortality of *S. droebachiensis* due to paramoebiasis occurred in August/September. Following a report of large numbers of dead and dying sea urchins washing onshore in Halifax Harbour on 12 August, we conducted diving and towed-video surveys in this area over the next 2 weeks. *Paramoeba invadens* was isolated from tissues of diseased sea urchins, and we estimated that > 65% of the population on cobble and boulder barrens up to 700 m offshore, and across a depth range from 2 to 10 m, was moribund or dead at this time. The mass mortality in Halifax Harbour was preceded by a sharp peak in significant wave height (2.7 m) on 1 August, followed by a 4-week period of unusually warm sea surface temperatures (mean ± SD: 20 ± 1 °C). The high incidence of morbidity/mortality by mid-August is consistent with an introduction of *P. invadens* around the time of the wave event, given a t_{50} of 11.5 days based on an estimated mean bottom temperature of 16 °C during the intervening 2-week period (estimate based on mean temperature at 2 – 10 m depth in Halifax Harbour). Interestingly, a similar peak in significant wave height (2.9 m) occurred on 27 June, followed by a 10-day period of similarly warm sea surface temperatures (19 ± 1 °C), but there was no report of unusual mortality of sea urchins in July. These wave events were due to local weather disturbances and not associated with passing tropical storms. Such wave events during summer are infrequent along the coast of Nova Scotia. For example, a significant wave height > 2.6 m in August was only observed in 5 out of 34 years (1976–2009) in the Halifax region.

On 24 August 2012, 60 and 100 % of caged sea urchins were dead or dying at our two sites on the headlands on either side of St. Margarets Bay, compared to 20 % at one site on the eastern shore of the bay (Luke Island) and none at the remaining two sites along the western shore (Fig. 4). Mortality due to disease gradually increased at Luke Island, exceeding 50 % by 26 September and reaching 90 % by 19 October. No further mortality was observed over the next 18 days, while bottom temperatures remained around the 10 – 12 °C threshold for paramoebiasis. Sea urchins at the other two sites remained asymptomatic throughout the experimental period with minimal mortality by 6 November. At Splitnose Point, the control site and source of experimental animals, morbidity and mortality first was observed in cages (and on the surrounding seabed at 8 m) on 24 September (~ 40 days after the mass mortality in Halifax Harbour), accounting for 55 % of the caged sea urchins (Fig. 4). At this time scattered pockets of diseased and dying sea urchins and their tests also were evident at shallower depths (3 – 4 m). Disease was not present at this site or at two nearby sites (Duncan's Cove and Bear Cove) 4 km N and 7 km NNW (linear distance) from Splitnose Point, during towed-video surveys on 27 August. By 23 October, mortality of caged urchins at Splitnose Point had reached 90 %.

In each year, rates of morbidity and mortality were much lower for sea urchins in cages at 18 m at a site (The Lodge) on the western shore of St. Margarets Bay, in accordance with lower water temperatures at this depth (rarely above 12 °C) compared to 8 m (Fig. 4). However, when surviving asymptomatic sea urchins were collected at the end of the experiment in 2010 and maintained at 16 °C in the laboratory, they succumbed to paramoebiasis and transferred the disease to healthy conspecifics through a waterborne route (Feehan *et al.*, 2012a). This suggests that sea urchins in deeper, colder waters can harbor the pathogen for some period after a disease outbreak in shallower water. A similar effect of depth on the propagation of disease was observed in Halifax Harbour in August 2012. The rate of morbidity and mortality decreased linearly with depth from 2 to 10 m, where temperature dropped from

20 to 13 °C respectively; moribund sea urchins or tests were not observed below 10 m, where temperature continued to decrease to 11 °C at 18 m depth, 1 km offshore.

Thus far, the results from our field experiment provide equivocal support for the "killer storm" hypothesis and the efficacy of the statistical model of Scheibling and Lauzon-Guay (2010) to predict disease outbreaks in sea urchins based on hurricane or tropical storm activity and post-storm seawater temperature. The occurrence of a mass mortality in 2012, without a prior storm that passed near to the coast of Nova Scotia (only tropical storm Chris with $P_m = 0.1$ % on 19 June was within the spatial range considered in the model prior to the disease outbreak), indicates that other advective mechanisms may account for the introduction of *P. invadens* to shallow coastal areas. This is not inconsistent with previous records off Nova Scotia. A widespread mass mortality of *S. droebachiensis* occurred in 1983, also a year without significant tropical storm or hurricane activity (Scheibling and Hennigar, 1997). In fact, this was the only year (out of 13) in which a mass mortality event was not preceded by a tropical cyclone in the 30-year record used in the statistical model (Scheibling and Lauzon-Guay, 2010). Scheibling and Lauzon-Guay (2010) suggest that experiments that incidentally or deliberately released laboratory-cultured *P. invadens* along the coast may have caused the mortality event in 1983. This is unlikely to have been the cause of the 2012 event because infected sea urchins were maintained in flow-through aquaria in a quarantine facility at Dalhousie University, in which all effluent seawater was treated with strong bleach before being released into the ocean.

Our experiment and observations of sea urchin mortality in surrounding areas provide insight into spatial and temporal patterns of disease outbreaks along the coast of Nova Scotia. In 2010, the time to morbidity or mortality of transplanted sea urchins varied widely among sites and 20 – 40 % survived at 3 of the 6 sites within the bay, once water temperatures fell below the 12 °C threshold in November (Fig. 4). Importantly, there was no evidence of paramoebiasis prior to Hurricane Earl, although temperatures at 8 m depth averaged 19 °C for a 15-day period in August. The predicted t_{50} at this temperature is 7 days, indicating sea urchins likely were not infected before the storm. We did not observe diseased sea urchins or unusual mortality among our source population at Splitnose Point or along headlands adjacent to Halifax Harbour (~ 40 km linear distance from St. Margarets Bay) in 2010, suggesting the disease outbreak was a localized event. *Paramoeba invadens* may have been locally introduced, perhaps by vertical mixing within the bay, or more broadly distributed along the coast but disease may not have propagated outside of the bay. Large semi-protected embayments such as St. Margarets Bay may serve as "incubation" sites for *P. invadens*, with warmer surface temperatures and longer water residence times (Heath, 1973), compared to the outer coast. In 2011, variation among sites in the rate of morbidity was much lower following Hurricane Katia and mortality was complete at all experimental sites within the bay and at adjacent headlands (Fig. 4). There also was a partial die-off of sea urchins at Splitnose Point in late October and sea urchin fishers

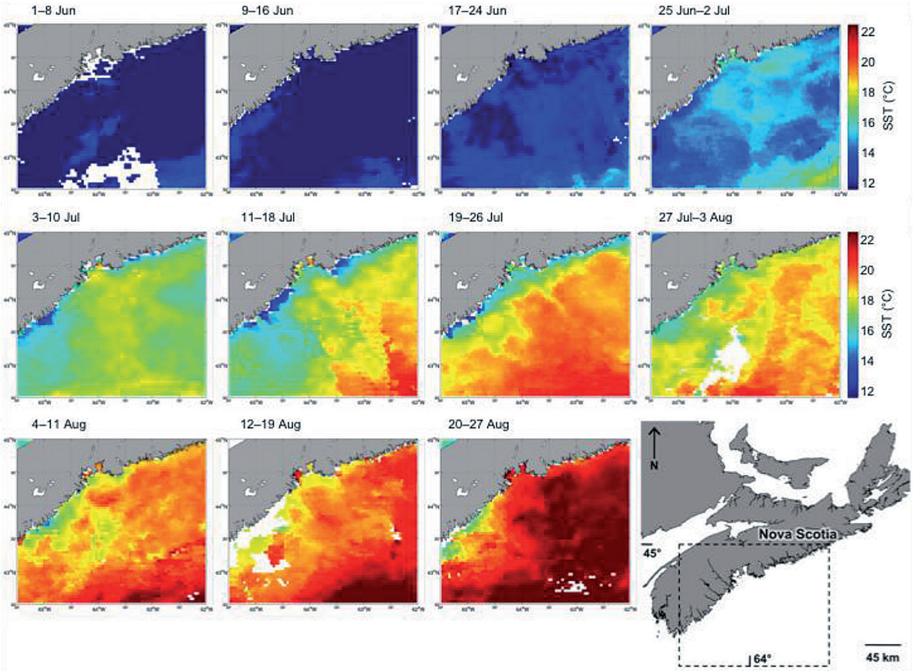

Figure 5. Sea surface temperature (SST) along the Atlantic coast of Nova Scotia (see inset map to locate measurement grid) averaged over 8-day intervals from 1 June to 27 August 2012. These images were generated from global Level-3 standard mapped images (SMIs) of 4 x 4 km spatial resolution MODIS/Aqua 11 µm daytime SST. The SMIs were obtained from the NASA Goddard Space Flight Center Ocean Color Web (Feldman and McClain, 2012).

observed mass mortalities around this time at sites along the southwestern shore (Lockport and Shelburne) and southern tip of Nova Scotia (Barrington Bay), spanning 40 km (linear distance) of coast (C. Hopkins, sea urchin harvester, Shelburne, Nova Scotia, personal communication).

In 2012, the initial observation of paramoebiasis in Halifax Harbour in early August, followed by subsequent outbreaks of disease at our experimental sites around the mouth of St. Margarets Bay, suggests a southwesterly spread of disease, consistent with the residual current direction. Alternatively, there may have been separate introductions in these two areas separated by several weeks. In the absence of a major storm event, the introduction of *P. invadens* may have been associated with warm water intrusions from across the shelf. Satellite imagery shows a broad band of warm (18 – 19 °C) surface water impinging on the central part of the mainland coast near Halifax in late July and early August (Fig. 5), which preceded the disease outbreak in Halifax Harbour around mid-August. A second intrusion of even warmer water (20 – 21 °C) moved into this area and along shore to the northeast in mid to late August, which may have contributed to a secondary outbreak of disease at the mouth of St. Margarets Bay. Entrainment of large volumes of slope and shelf water by mesoscale cyclonic eddies (warm-core rings), emanating from the Gulf Stream, results in mixing and advective transport of planktonic organisms, such as fish larvae (Flierl and Wroeblewski, 1985; Myers and Drinkwater, 1989), across the shelf. Scheibling and Hennigar (1997) suggest that these warm water intrusions also may contribute to the transport of *P. invadens* to coastal areas.

The widespread mass mortality of sea urchins in 1983 also was associated with unusually warm sea surface temperatures along the coast in a year without a major tropical cyclone (Scheibling and Lauzon-Guay, 2010). These sporadic occurrences indicate that large storm events, such as hurricanes, do not necessarily precede mass mortalities of sea urchins and therefore are not the only mechanism of introduction of *P. invadens* to coastal areas. This does not preclude the possibility of a synergistic interaction between severe storms and warm-water intrusions that may accelerate advection and mixing of surface waters (Craddock *et al.*, 1992) and the transport of the planktonic pathogen. In 2012, we first observed paramoebiasis at Splitnose Point 14 days after tropical storm Leslie (P_m = 0.325) had passed close to the coast of Nova Scotia on 10 September. The temperature at 8 m depth at this site over the 2-week period following Leslie was ~ 13 °C. This gives a t_{50} of 20 days, which exceeds the observed time to > 50 % morbidity by almost a week. However, a peak in significant wave height, possibly associated with Leslie, occurred on 5 September, 21 days before we observed > 50 % morbidity, which is consistent with the predicted t_{50}. Mixing due to this relatively weak tropical storm may have locally introduced the pathogen to this area after the outbreaks of disease in Halifax and St. Margarets Bay. It did not appear sufficient, however, to spread *P. invadens* throughout St. Margarets Bay, as evidenced by the survival of asymptomatic sea urchins at our two sites along the western shore during the experimental period in 2012.

The occurrence of subtropical and tropical fish species in coastal waters of Nova Scotia in late summer and fall is further evidence of cross-shelf advection that could transport a planktonic pathogen. In 1995, there were reports of tropical fish and sea turtles in the shallow nearshore waters immediately preceding a sea urchin epizootic (Scheibling and Hennigar, 1997). We observed grey triggerfish (*Balistes capriscus*) actively swimming near the mouth of St. Margarets Bay on 22 July and 22 August 2012, during the warm-water events that coincided with outbreaks of paramoebiasis in the region. The local media also reported triggerfish and other subtropical and tropical species, including flying fish and seahorses, in the region around this time (http://www.cbc.ca/player/News/Canada/NS/ID/2270769998/). These observations of exotic species in coastal waters provide circumstantial evidence for a mechanistic link between outbreaks of sea urchin disease and meteorologic and oceanographic features (Scheibling and Hennigar, 1997).

Interestingly, the disease outbreaks that we observed in transplanted sea urchins between 2010 and 2012, and during another experiment in St. Margarets Bay in 2009 (Feehan *et al.*, 2012b), occurred among artificially generated aggregations of sea urchins in cages or experimental plots, at sites where naturally occurring adults were rare. This may reflect previous situations when *P. invadens* was introduced to coastal areas in a kelp-bed state, but the disease passed unnoticed because of a low density of adult sea urchins in kelp beds.

CLIMATE CHANGE AND ECOSYSTEM EFFECTS OF DISEASE IN SEA URCHIN POPULATIONS

Scheibling and Lauzon-Guay (2010) found that the strongest storms passing along the coast of Nova Scotia tended to increase in intensity and proximity to the coast over a 30-year period (1980–2009). Sea temperatures during the hurricane season also increased during this period. These trends were associated with an increase in the frequency of hurricanes and tropical storms with the greatest potential for sea urchin mortality. If these trends continue due to a changing ocean climate, this could limit the resilience of sea urchin populations and maintain the ecosystem in the kelp-bed state.

To explore the possible effects of climate change, we used quantile regression to conduct a trend analysis of storm characteristics (wind speed, distance from the coast) and ocean temperature that affect the probability of sea urchin mass mortality (P_m), using procedures described by Scheibling and Lauzon-Guay (2010). We first performed a separate regression for every 5th quantile from the 5th to the 95th quantile for each of these factors over a 30-year period (1980–2009). To predict the distribution of each factor over a 100-year period, we then extended the regression equation for each quantile backwards to 1940 and forwards to 2040. For each year from 1940 to 2040, we randomly picked a number of storms (n) from the empirical distribution of the number of storms observed annually between 1980 and 2009. For each of the n storms in a given year, we obtained a maximum sustained wind speed (W, km h^{-1}) when the hurricane was closest to the coast (within our study grid between 35°N and the coast of Nova Scotia, and between 55°W and 70°W) by randomly selecting one of the 19 wind-speed quantiles for that year, and followed the same procedure for distance of a storm from the coast (D, 100s km) and water temperature (T), a dummy variable for the temperature threshold based on the mean temperature (T_m) at 0–10 m depth in the 2-week period following each storm ($T = 1$ if $T_m > 12.2$ °C, $T = 0$ if $T_m < 12.2$ °C). Based on these environmental factors, we calculated P_m for each of the n storms in a year using the logistic regression model of Scheibling and Lauzon-Guay (2010):

$$P_m = 1/(1 + e^{-z})$$
$$z = -14.352 + 0.082W - 0.069D^2 + 4.966T$$

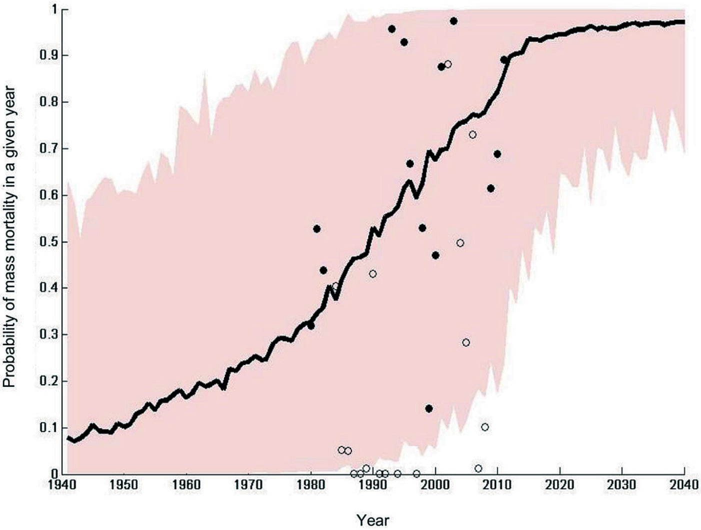

Figure 6. Results of simulations to predict the cumulative probability of mass mortality (cP_m) of *Strongylocentrotus droebachiensis* due to paramoebiasis associated with passing hurricanes or tropical storms along the Atlantic coast of Nova Scotia from 1940 to 2040, based on trends in storm characteristics (wind speed, distance from the coast) and post-storm water temperature measured from 1980 to 2009. Data are mean cP_m and 95% CI for each year over the 100-year period. Circles are the predicted cP_m each year from 1980 to 2011 based on actual storm and temperature data for these years (Scheibling and Lauzon-Guay, 2010). Solid circles are years when mass mortalities of sea urchins were recorded in the shallow subtidal zone to 25 m depth; open circles are years when mass mortalities were not reported (Scheibling and Lauzon-Guay, 2010; this study).

We then calculated the cumulative probability of having a mass mortality (cP_m) in that year based on the P_m for each storm:

$$cP_m = 1 - ((1 - P_{m1}) \bullet (1 - P_{m2}) \bullet \ldots \bullet (1 - P_{mn}))$$

We repeated this procedure 1000 times and calculated the mean cP_m and 95% CI of these iterations for each year. For comparison with predicted values of cP_m, we calculated the observed cP_m for each year from 1980 to 2011 using P_m values based on the actual storms occurring in those years.

Our simulations yield a sigmoidal trajectory of mean cP_m over a 100-year period from 1940 to 2040 (Fig. 6). The mean cumulative probability of a mass mortality event was low (< 30%) prior to the 1980s, when the first outbreaks of sea urchin disease were documented (Miller and Colodey, 1983), and steadily

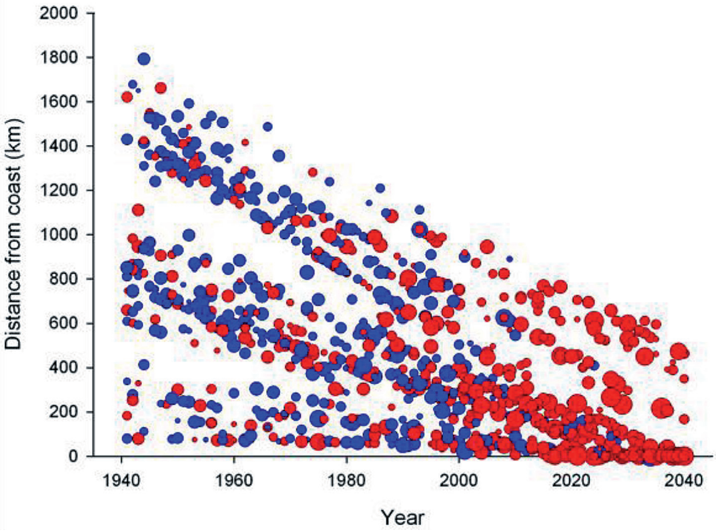

Figure 7. Results of simulations based on trend analysis of hurricane or tropical storm characteristics and post-storm water temperature measured from 1980 to 2011 (Scheibling and Lauzon-Guay, 2010; this study), showing: 1) a decline in the upper limit of the distance of a storm from the coast, 2) an increase in maximum sustained wind speed when the storm was closest to the coast (relative size of bubbles), and 3) an increase in post-storm temperatures above the threshold (12°C) for an outbreak of paramoebiasis in *Strongylocentrotus droebachiensis* (blue bubbles, below threshold; red bubbles, above threshold), over the 100-year period from 1940 to 2040.

increased over the next 3 decades to 90% by 2012. The projected cP_m reaches a plateau at ~ 98% by 2030. The observed cP_m each year from 1980 to 2011 fell within the 95% CI of the predicted mean cP_m (Fig. 6). During this period, there is a significant correlation (r = 0.46, P = 0.015, n = 31) between the predicted mean cP_m each year based on our simulations and the cP_m predicted using the storm and temperature data given in Scheibling and Lauzon-Guay (2010) (Fig. 6).

Using the quantile regression procedures described above to estimate cP_m, we predicted hurricane and tropical storm characteristics and post-storm temperatures for 10 random storms per year between 1940 and 2040. Our trend analysis over the 100-year period shows: 1) a clear decline in the upper limit of the distance of a storm from the coast, 2) an increase in maximum sustained wind speed when the storm was closest to the coast, and 3) an increase in post-storm temperatures above the threshold for an epizootic (Fig. 7). The results of these simulations are consistent with the increase in cP_m over this period, based on an independent simulation model.

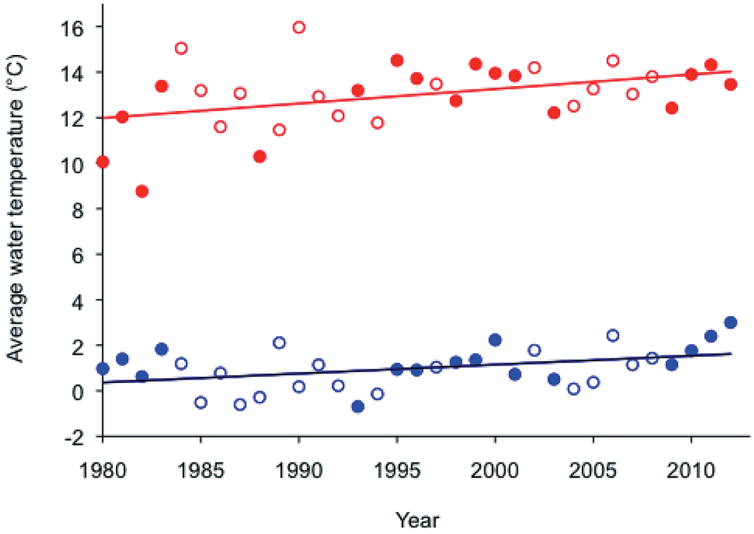

Figure 8. Average daily water temperature along the Atlantic coast of Nova Scotia during the annual summer/fall peak (August, September and October; red circles) and the winter trough (February and March; blue circles) over a 33-year period (1980 – 2012). Data for 1980–2009 are based on records at 0–10-m depth over 70 km (linear distance) of coast (from Halifax to Lunenburg) and 5 km offshore (for data source, see Scheibling and Lauzon-Guay, 2010). To extend these records to 2012, we used average daily temperature based on our temperature records at 8-m depth along the western shore of St. Margarets Bay for each period (August – October, February – March). Lines represent the linear regression of average temperature in each year at the peak (T_{peak}) or trough (T_{trough}) of the annual cycle against year (Y) based on the 33-year record ($T_{peak} = 0.064Y - 114.4$, $r^2 = 0.175$, $p = 0.015$); $T_{trough} = 0.039Y - 77.2$, $r^2 = 0.170$, $p = 0.017$)

A changing ocean climate also may influence the spatial range of *Paramoeba invadens* and the frequency of epizootics as the winter minimum in water temperature begins to exceed 2 °C, the predicted lower tolerance limit of the amoeba (Jellett and Scheibling, 1988). On the Atlantic coast of Nova Scotia, water temperature typically drops below 2 °C in February and March, the two coldest months. Regression analysis of a 33-year temperature record (0 – 10-m depth) along the central region of this coast shows a significant warming trend in February/March (Fig. 8). During our experiment, winter temperature at 8-m depth in St. Margarets Bay rarely dropped below the 2 °C tolerance limit for *P. invadens* in 2011 (4 days) and 2012 (1 day), indicating that the pathogen may be capable of overwintering in the shallow subtidal zone as temperature continues to rise. Given the observed rate of warming over the past three decades (0.039 °C y^{-1}), the predicted average winter temperature will reach 2.0 °C by 2020 and 2.7 °C by

2040. The rate of warming for the summer/fall peak in the annual temperature cycle is even greater (0.064 °C y^{-1}), with predicted average peak temperatures of 14.5 °C by 2020 and 15.8 °C by 2040.

An increase in the frequency of sea urchin epizootics associated with increasing hurricane intensity and increasing ocean surface temperatures off Nova Scotia is expected to shift the rocky subtidal ecosystem to a kelp-bed state that would remain stable for the foreseeable future (Scheibling and Lauzon-Guay, 2010). This could benefit lobster and finfish fisheries that rely on kelp beds as nursery habitat and a major source of primary production for benthic food webs (Wharton and Mann, 1981; Steneck *et al.*, 2002). On the other hand, recurrent mass mortality of *Strongylocentrotus droebachiensis* has caused the collapse of the sea urchin fishery in Nova Scotia (Miller and Nolan, 2000, 2008), and there is little prospect for recovery on a coastal scale. Changes in the shallow subtidal ecosystem resulting from an increased frequency of sea urchin epizootics also are likely to have profound effects on the structure and functioning of adjacent communities that utilize kelp detritus and sea urchin feces as a food resource (Sauchyn *et al.*, 2011; Krumhansl and Scheibling, 2012a). This connectivity in the flux of organic matter and energy between kelp beds and offshore benthic assemblages across a depth gradient remains largely unexplored (Krumhansl and Scheibling, 2012b).

CONCLUSIONS AND PERSPECTIVES FOR FUTURE RESEARCH

The origin of infective populations of *Paramoeba invadens* and mechanisms of dispersal, propagation and survival of amoebae in nature remain unresolved, despite three decades of observation along the Atlantic coast of Nova Scotia (Scheibling and Lauzon-Guay, 2010) and recently renewed research efforts (Feehan *et al.*, 2012a). Reports by sea urchin harvesters in the 1990s (Miller and Nolan, 2000) and our recent field studies (Scheibling *et al.*, 2010; Feehan *et al.*, 2012a, b) suggest that outbreaks of paramoebiasis can be patchy along this coast. More extensive monitoring of disease outbreaks across a range of habitats and spatial scales is needed to identify potential disease hotspots and increase our understanding of the introduction and spread of paramoebiasis. For example, sampling tissues of deep-living sea urchins for presence of *P. invadens*, could establish whether amoebae are locally present in deep basins where bottom temperatures are at or above the lower tolerance limit (2 °C) established in laboratory experiments. The possibility of a resistant cyst stage also warrants further research in studies aimed at better understanding the physiological response of *P. invadens* to environmental variables such as temperature and salinity, particularly as winter temperatures in shallow coastal areas rise above the lower tolerance limit. Genetic markers of *P. invadens*, isolated from naturally infected sea urchins, could be used to effectively monitor the amoeba in water and sediment samples before, during and after a disease outbreak to gain insights into host-pathogen dynamics, factors affecting the spread of disease (e.g., sea urchin density, temperature, salinity, currents), and the fate of amoebae as temperatures drop. These genetic tools also would enable us to search broadly for source populations and explore dispersal mechanisms, such as advection and turbulent mixing by hurricanes, which potentially introduce *P. invadens* to the shallow coastal waters. Finally, a multiyear record of hurricane activity, surface temperature and occurrence of paramoebiasis in Nova Scotia, based on longitudinal studies and controlled field experiments, such the one presented here, is needed to critically test the Scheibling and Lauzon-Guay (2010) model. Further exploration of the mechanistic links between hurricanes, water temperature and spread of paramoebiasis will allow us to more accurately predict the magnitude and extent of epizootics that can profoundly affect the ecology of subtidal communities.

ACKNOWLEDGEMENTS

The authors thank the Ocean Biology Processing Group (Code 614.2) at the NASA Goddard Space Flight Center, Greenbelt, MD 20771, for the production and distribution of the MODIS/Aqua SST data, and Michael Brown for providing the processed imagery. This research has been continuously supported since 1982 by grants from the Natural Sciences and Engineering Research Council (NSERC) of Canada to RES.

REFERENCES

Beisner, B.E., Haydon, D.T. and Cuddington, K. (2003) Alternative stable states in ecology. *Frontiers in Ecology and the Environment*, 1, 376–382.

Bender, M.A., Knutson, T.R., Tuleya, R.E., Sirutis, J.J., Vecchi, G.A., Garner, S.T. and Held, I.M. (2010) Modeled impact of anthropogenic warming on the frequency of intense Atlantic hurricanes. *Science*, 327, 454.

Brady, S. and Scheibling, R.E. (2005) Repopulation of the shallow subtidal zone by green sea urchins (*Strongylocentrotus droebachiensis*) following mass mortality in Nova Scotia, Canada. *Journal of the Marine Biological Association of the United Kingdom*, 85, 1511–1517.

Caraguel, C.G., O'Kelly, C.J., Legendre, P., Frasca, S., Gast, R.J., Després, B.M., Cawthorn, R.J. and Greenwood, S.J. (2007) Microheterogeneity and coevolution: an examination of rDNA sequence characteristics in *Neoparamoeba pemaquidensis* and its prokinetoplastid endosymbiont. *Journal of Eukaryotic Microbiology*, 54, 418.

Dumont, C.P., Himmelman, J.H. and Russell, M.P. (2004) Size-specific movement of green sea urchins *Strongylocentrotus droebachiensis* on urchin barrens in eastern Canada. *Marine Ecology Progress Series*, 276, 93–101.

Feehan, C., Scheibling, R.E. and Lauzon-Guay, J.-S. (2012a) An outbreak of sea urchin disease associated with a recent hurricane: Support for the «killer storm hypothesis» on a local scale. *Journal of Experimental Marine Biology and Ecology*, 413, 159–168.

Feehan, C., Scheibling, R.E. and Lauzon-Guay, J.-S. (2012b) Aggregative feeding behavior in sea urchins (*Strongylocentrotus droebachiensis*) leads to gap formation and destructive grazing in a Nova Scotian kelp bed. *Marine Ecology Progress Series*, 444, 69–83.

Feehan, C., Johnson-Mackinnon, J., Scheibling, R.E., Lauzon-Guay, J.-S. and Simpson, A.G.B. (2013) Validating the identity of *Paramoeba invadens*, the causative agent of recurrent mass mortality of sea urchins in Nova Scotia, Canada. *Diseases of Aquatic Organisms*, 103, 209–227.

Feldman, G.C. and McClain, C.R. (2012) *Ocean Color Web, MODIS Reprocessing 2012.0*, NASA Goddard Space Flight Center (ed. by Kuring, N. and Bailey, S.W.). http://oceancolor.gsfc.nasa.gov/.

Filbee-Dexter, K. and Scheibling, R.E. (2012) Hurricane-mediated defoliation of kelp beds and pulsed delivery of kelp detritus to offshore sedimentary habitats. *Marine Ecology Progress Series*, 445, 51–64.

Flierl, G.R. and Wroeblewski, J.S. (1985) The possible influence of warm core Gulf Stream rings upon shelf water larval fish distribution. *Fishery Bulletin*, 83, 313–330.

Folke, C., Carpenter, S., Walker, B., Scheffer, M., Elmqvist, T., Gunderson, L. and Holling, C.S. (2004) Regime shifts, resilience, and biodiversity in ecosystem management. *Annual Review of Ecology and Systematics*, 35, 557–581.

Hart, M.W. and Scheibling, R.E. (1988) Heat waves, baby booms, and the destruction of kelp beds by sea urchins. *Marine Biology*, 99, 167–176.

Harvell, C.D., Kim, K., Burkholder, J.M., Colwell, R.R., Epstein, P.R., Grimes, D.J., Hofmann, E.E., Lipp, E.K., Osterhaus, A.D.M.E., Overstreet, R.M., Porter, J.W., Smith, G.W. and Vasta, G.R (1999) Emerging marine diseases–climate links and anthropogenic factors. *Science*, 285, 1505–1510.

Harvell, C.D., Mitchell, C.E., Ward, J.R., Altizer, S., Dobson, A.P., Ostfeld, R.S. and Samuel, M.D. (2002) Climate warming and disease risks for terrestrial and marine biota. *Science*, 296, 2158–2162.

Heath, R.A. (1973) *Variability of water properties and circulation of St. Margaret's Bay, Nova Scotia.* Fisheries and Research Board of Canada, Dartmouth, NS.

Himmelman, J.H., Cardinal, A. and Bourget, E. (1983) Community development following removal of urchins, *Strongylocentrotus droebachiensis*, from the rocky subtidal zone of the St. Lawrence Estuary, Eastern Canada. *Oecologia*, 59, 27–39.

Hooper, R. (1980) Observations on algal-grazer interactions in Newfoundland and Labrador. *Canadian Technical Reports of Fisheries and Aquatic Sciences*, 954, 120–124.

Jellett, J.F., Novitsky, J.A., Cantley, J.A. and Scheibling, R.E. (1989) Non-occurrence of free-living *Paramoeba invadens* in water and sediments of Halifax Harbour, Nova Scotia, Canada. *Marine Ecology Progress Series*, 56, 205–209.

Jellett, J.F. and Scheibling, R.E. (1988) Effect of temperature and prey availability on growth of *Paramoeba invadens* in monoxenic culture. *Applied and Environmental Microbiology*, 54, 1848–1854.

Jellett, J.F., Scheibling, R.E. and Wardlaw, A.C. (1988) Host specificity of *Paramoeba invadens*, a sea urchin pathogen. *Echinoderm biology* (ed. by Burke, R.D., Mladenov, P.V., Lambert, P. and Parsley, R.L.), pp. 755–761. Balkema, Rotterdam.

Johnson, C.R. and Mann, K.H. (1988) Diversity, patterns of adaptation, and stability of Nova Scotian kelp beds. *Ecological Monographs*, 58, 129–154.

Jones, G.M. (1985) *Paramoeba invadens* n. sp. (Amoebida, Paramoebidae), a pathogenic amoeba from the sea urchin, *Strongylocentrotus droebachiensis*, in eastern Canada. *Journal of Protozoology*, 32, 564–569.

Jones, G.M., Hebda, A.J., Scheibling, R.E. and Miller, R.J. (1985) Histopathology of the disease causing mass mortality of sea urchins (*Strongylocentrotus droebachiensis*) in Nova Scotia. *Journal of Invertebrate Pathology*, 71, 559–565.

Jones, G.M. and Scheibling, R.E. (1985) *Paramoeba* sp. (Amoebida, Paramoebidae) as the possible causative agent of sea urchin mass mortality in Nova Scotia. *Journal of Parasitology*, 71, 559–565.

Knowlton, N. (2004) Multiple 'stable' states and the conservation of marine ecosystems. *Progress in Oceanography*, 60, 387–396.

Krumhansl, K.A. and Scheibling, R.E. (2012a) Detrital subsidy from subtidal kelp beds is altered by the invasive green alga *Codium fragile* ssp. *fragile. Marine Ecology Progress Series*, 456, 73–85.

Krumhansl, K.A. and Scheibling, R.E. (2012b) Production and fate of kelp detritus. *Marine Ecology Progress Series*, 467, 281–302.

Lafferty, K.D., Porter, J.W. and Ford, S.E. (2004) Are diseases increasing in the ocean? *Annual Review of Ecology, Evolution, and Systematics*, 35, 31–54.

Lauzon-Guay, J.-S., Scheibling, R.E. and Barbeau, M.A. (2008) Formation and propagation of feeding fronts in benthic marine invertebrates: a modeling approach using kinesis. *Ecology*, 89, 3150–3162.

Lauzon-Guay, J.-S., Scheibling, R.E. and Barbeau, M.A. (2009) Modeling phase shifts in a rocky subtidal ecosystem. *Marine Ecology Progress Series*, 375, 25–39.

Lauzon-Guay, J.-S. and Scheibling, R.E. (2010) Spatial dynamics, ecological thresholds and phase shifts: modeling grazer aggregation and gap formation in kelp beds. *Marine Ecology Progress Series*, 403, 29–41.

Lessios, H. (1988) Mass mortality of *Diadema antillarum* in the Caribbean: What have we learned? *Annual Review of Ecology and Systematics*, 19, 371 – 393.

May, R.M. (1977) Thresholds and breakpoints in ecosystems with a multiplicity of stable states. *Nature*, 269, 471–477.

Miller, R.J. (1985) Succession in sea urchin and seaweed abundance in Nova Scotia, Canada. *Marine Biology*, 84, 275–286.

Miller, R.J. and Colodey, A.G. (1983) Widespread mass mortalities of the green sea urchin in Nova Scotia, Canada. *Marine Biology*, 73, 263–267.

Miller, R.J. and Nolan, S. (2000) *Management of the Nova Scotia Sea Urchin Fishery: A Nearly Successful Habitat Based Management Regime.* Canadian Stock Assessment Secretariat Research Document 2000/109 (41 pp.), Department of Fisheries and Oceans, Ottawa.

Miller, R.J. and Nolan, S.C. (2008) Management methods for a sea urchin dive fishery with individual fishing zones. *Journal of Shellfish Research*, 27, 929–938.

Moore, D.S. and Miller, R.J. (1983) Recovery of macroalgae following widespread sea urchin mortality with a description of the nearshore hard bottom habitat on the Atlantic coast of Nova Scotia. *Canadian Technical Reports of Fisheries and Aquatic Sciences*, 1230, vii-94.

Muelhstein, L. (1989) Perspectives on the wasting disease of eelgrass *Zostera marina. Diseases of Aquatic Organisms*, 7, 211–221.

MULLEN, T. E., RUSSELL, S., TUCKER, M. T., MARATEA, J. L., KOERTING, K., HINCKLEY, L., DE GUISE, S., FRASCA JR., S., FRENCH, R. A., BURRAGE, T. G. and PERKINS, C. (2004) Paramoebiasis associated with mass mortality of American lobster *Homarus americanus* in Long Island Sound, USA. *Journal of Aquatic Animal Health*, 16, 29–38.

MULLEN, T.E., NEVIS, K.R., O'KELLY, C.J., GAST, R. and FRASCA, Jr. S. (2005) Nuclear small-subunit ribosomal RNA gene-based characterization, molecular phylogeny and PCR detection of *Neoparamoeba* from western Long Island Sound lobster. *Journal of Shellfish Research*, 24, 719–731.

MYERS, R.M. and DRINKWATER, K.F. (1989) The influence of Gulf Stream warm core rings on recruitment of fish in the northwest Atlantic. *Journal of Marine Research*, 47, 635–656.

PETRAITIS, P.S. and HOFFMAN, C. (2010) Multiple stable states and relationship between thresholds in processes and states. *Marine Ecology Progress Series*, 413, 189–200.

ROBERTS-REGAN, D.L., SCHEIBLING, R.E. and JELLETT, J.F. (1988) Natural and experimentally induced lesions of the body wall of the sea urchin *Strongylocentrotus droebachiensis. Diseases of Aquatic Organisms*, 5, 51–62.

SAUCHYN, L.K., LAUZON-GUAY, J.-S. and SCHEIBLING, R.E. (2011) Sea urchin fecal production and accumulation in a rocky subtidal ecosystem. *Aquatic Biology*, 13, 215–223.

SCHEFFER, M., CARPENTER, S.R., FOLEY, J.A. and WALKER, B. (2001) Catastrophic shifts in ecosystems. *Nature*, 413, 591–596.

SCHEIBLING, R.E. (1984a) Echinoids, epizootics and ecological stability in the rocky subtidal off Nova Scotia, Canada. *Helgolander Wissenschaftliche Meeresuntersuchungen*, 37, 233–242.

SCHEIBLING, R.E. (1984b) Predation by rock crabs (*Cancer irroratus*) on diseased sea urchins (*Strongylocentrotus droebachiensis*) in Nova Scotia. *Canadian Journal of Fisheries and Aquatic Sciences*, 41, 1847–1851.

SCHEIBLING, R.E. (1986) Increased macroalgal abundance following mass mortalities of sea urchins (*Strongylocentrotus droebachiensis*) along the Atlantic coast of Nova Scotia. *Oecologia* 68, 186–198.

SCHEIBLING, R.E. (1988) Microbial control of sea urchins: Achilles' heel or Pandora's box? *Echinoderm biology* (ed. by BURKE, R.D., MLADENOV, P.V., LAMBERT, P. and PARSLEY, R.L.), pp. 745–754. Balkema, Rotterdam.

SCHEIBLING, R.E., FEEHAN, C. and LAUZON-GUAY, J.-S. (2010) Disease outbreaks associated with recent hurricanes cause mass mortality of sea urchins in Nova Scotia. *Marine Ecology Progress Series*, 408, 109–116.

SCHEIBLING, R.E. and HENNIGAR, A.W. (1997) Recurrent outbreaks of disease in sea urchins *Strongylocentrotus droebachiensis* in Nova Scotia: evidence for a link with large-scale meteorologic and oceanographic events. *Marine Ecology Progress Series*, 152, 155–165.

SCHEIBLING, R.E., HENNIGAR, A.W. AND BALCH, T. (1999) Destructive grazing, epiphytism, and disease: the dynamics of sea urchin-kelp interactions in Nova Scotia. *Canadian Journal of Fisheries and Aquatic Sciences*, 56, 2300–2314.

Scheibling, R.E. and Lauzon-Guay, J.-S. (2010) Killer storms: North Atlantic hurricanes and disease outbreaks in sea urchins. *Limnology and Oceanography*, 55, 2331–2338.

Scheibling, R.E. and Stephenson, R.L. (1984) Mass mortality of *Strongylocentrotus droebachiensis* (Echinodermata: Echinoidea) off Nova Scotia, Canada. *Marine Biology*, 78, 153–164.

Steneck, R.S., Graham, M.H., Bourque, B.J., Corbett, D., Erlandson, J.M., Estes, J.A. and Tegner, M.J. (2002) Kelp forest ecosystems: biodiversity, stability, resilience and future. *Environmental Conservation*, 29, 436–459.

Ward, J.R. and Lafferty, K.D. (2004) The elusive baseline of marine disease: Are diseases in ocean ecosystems increasing? *PLoS Biology*, 2(4): e120.

Wharton, W.G. and Mann, K.H. (1981) Relationship between destructive grazing by the sea urchin, *Strongylocentrotus droebachiensis*, and the abundance of American lobster, *Homarus americanus*, on the Atlantic coast of Nova Scotia. *Canadian Journal of Fisheries and Aquatic Sciences*, 38, 1339–1349.

LONG-TERM MONITORING OF SEA URCHIN POPULATIONS IN THE NW MEDITERRANEAN: INTEGRATING PROCESSES AND FACTORS ACTING AT DIFFERENT SPATIAL AND TEMPORAL SCALES

Bernat Hereu, Cristina Linares, David Diaz,
Enric Sala, Joaquim Garrabou, Mikel Zabala

CLIMATE CHANGE PERSPECTIVES FROM THE ATLANTIC:
PAST, PRESENT AND FUTURE
Jose María Fernández-Palacios, Lea de Nascimento, José Carlos Hernández,
Sabrina Clemente, Albano González & Juan P. Díaz-González (eds.)
Servicio de Publicaciones, Universidad de La Laguna – 2013

ISBN: 978-84-15910-54-1
pp. 389-410

Abstract

There is growing evidence that processes other than predation have a critical role in determining sea urchin populations, causing unexpected responses to existing top-down control models. Although the biology and ecology of sea urchins have been widely studied, the long term dynamics of their populations are still poorly understood. This lack of knowledge is caused mainly by the scarcity of monitoring studies that are long and frequent enough to integrate interannual variability with low-frequency processes, which can be essential in determining the structure and dynamics of sea urchin populations.
The aim of this study is to describe temporal variability in abundance and size-structure of the sea urchins *Paracentrotus lividus* and *Arbacia lixula* in rocky habitats in the north-western Mediterranean. Two long-term monitoring series of data in two different marine protected areas are compared: Medes Islands Marine Reserve and the nearby unprotected area (measured annually from 1991 to 2012) are compared with the Port-Cros National Park (measured annually from 1983-1984 and 1994-2003).
These series of data show how different processes, such as recruitment, predation or competition between both species, interact with other factors acting at different scales, such as a mass mortality episode that occurred in Port-Cros in 1982-1983, or the effects of an exceptional storm in Medes Islands in 2008, or the increase of sea temperature during the study period.

Keywords: Mediterranean, sea urchins, long term monitoring, population dynamics

INTRODUCTION

Changes in the abundance of key species can create alternative stable communities, which are only reversible by conspicuous shifts in their populations. Understanding the processes that regulate key species populations is crucial to understanding the mechanisms responsible for shifts in community types.

Although top-down models have been successfully applied to describe the dynamics of benthic algal communities, trophic cascades in which sea urchins play a major role have been demonstrated to be context dependent, varying as a function of regional and local scale environmental gradients (Micheli *et al.*, 2005; Shears *et al.*, 2008).

Moreover, physical factors, such as upwelling, water temperature (Wing *et al.*, 2003), sedimentation (Phillips and Shima, 2006; Walker, 2007; Shears *et al.*, 2008), wave action (Ebeling *et al.*, 1985; Harrold and Reed, 1985; Siddon and Witman, 2003; Micheli *et al.*, 2005), floods (Andrew, 1991; Witman and Grange, 1998; Fernandez *et al.*, 2006) or harvesting (reviewed by Andrew *et al.*, 2002; Gianguzza *et al.*, 2006) can also alter sea urchin abundance. Additionally, low-frequency disturbances such as disease outbreaks (Boudouresque *et al.*, 1980; Harrold and Reed, 1985; Andrew, 1991; Hughes, 1994; Scheibling and Hennigar, 1997; Lafferty, 2004; Lessios, 2005) can reduce sea urchins populations for decades after the event.

All of these processes may act simultaneously and on different time scales, from years to decades. Thus, a better understanding of the processes and factors controlling sea urchin populations on the appropriate spatial and temporal scales is a key issue for the management and conservation of subtidal temperate marine ecosystems. Since most studies encompass relatively limited spatial and short temporal scales, the dynamics of sea urchin populations at high spatial and especially on long temporal scales are still poorly understood (but see Micheli *et al.*, 2005, Shears *et al.*, 2008, Shears and Babckok, 2003; Babcock *et al.*, 2010).

In the Mediterranean, the sea urchin *Paracentrotus lividus* (Lamarck) is the most common sea urchin species (Boudouresque and Verlaque, 2001), and is considered a key species because of its grazing effect on algal communities (Verlaque and Nedelec, 1983; Verlaque, 1987; Sala *et al.*, 1998; Hereu *et al.*, 2008).

The other most abundant sea urchin species, *Arbacia lixula* (L.), is also distributed along the Mediterranean. It is more abundant in the southern areas of the Mediterranean, and is considered a thermophilic species (Kempf, 1962). It has been suggested that its population has recently increased as a consequence of SST due to climate change (Francour *et al.*, 1994).

The aims of this study are to analyze the different processes that act at different spatial and temporal scales, such as recruitment, predation, mortality, competition or environmental factors, and to determine their relative importance in determining the dynamics of sea urchins populations. For this, we monitored for a long period (19 and 24 years) the abundance and population size-structure of the sea urchins *P. lividus* and *Arbacia lixula* in shallow rocky habitats in two Mediterranean marine protected areas (Medes Islands and Port-Cros) in the northwestern Mediterranean. We compared the effects of small scale biotic processes and exceptional low recurrent perturbations, such as a mass mortality and an exceptional storm.

MATERIALS AND METHODS

The Medes Islands Marine Reserve (hereafter MIMR), where fishing has been prohibited since 1983 and densities of fish have remained high for decades (Garcia-Rubies and Zabala, 1990; Sala *et al.*, 2012), is located one kilometer offshore, opposite the town of L'Estartit (NE Spain, NW Mediterranean Sea) (Fig.

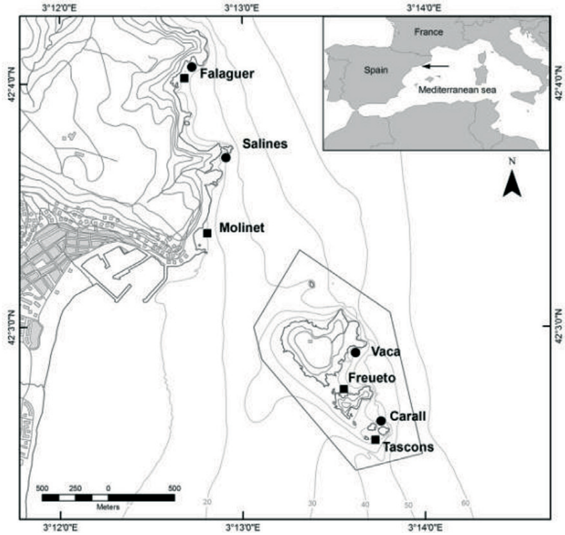

Figure 1. Study site. Medes Islands Marine Reserve. Locations of study sites inside and outside the reserve. The dotted line represents the limits of the Marine Reserve, where all fishing is prohibited. Squares boulder bottom stations. Circles: vertical walls.

1). Within this reserve, sea urchin populations were monitored annually for 20 years from its creation in 1991 to 2012, with a gap between 2006 and 2007 because of logistical constraints. To assess the effect of fishing pressure of fish predators on sea urchin populations, two sites inside the MIMR and two nearby sites on the non-protected coast were selected (Hereu *et al.*, 2012). Furthermore, to assess the role of topography in determining the structure of sea urchin populations through the accessibility of refuges, two different types of substrate were selected: large limestone boulders, and vertical walls without apparent spatial refuges (Fig. 1).

The abundance and population structure of *P. lividus* were studied by SCUBA diving along three transects (50 m^2 each) at a depth of 6 m at each study site for each type of substrate. Transects were divided into five 10 m^2 subtransects, and within each transect, *P. lividus* >1 cm in diameter were counted and their diameters (test without spines) were measured with a caliper. For analysis, the diameters were grouped into size classes with intervals of 1 cm, and at 0.5 cm after 2003. In 1995, *A. lixula* was added to the census; this species was monitored from 1995 to 2012 at the same sites and using the same methodology as applied to *P. lividus.*

In December 2008, a severe easterly storm occurred off the Catalan coast (NW Mediterranean) with winds surpassing 85 km/hour and waves over 7 m in

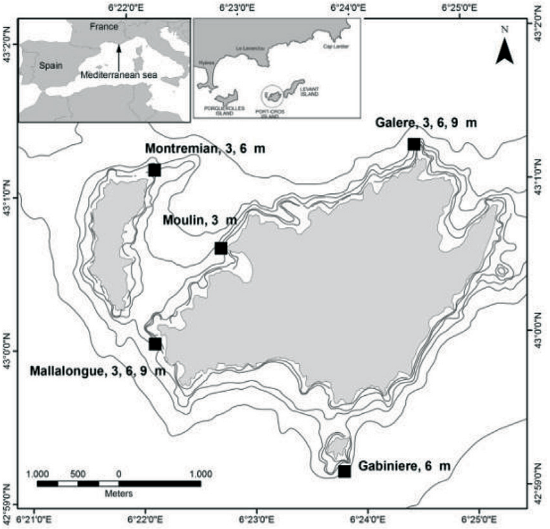

Figure 2. Port-Cros National Park. Location of the study sites and depths at each site.

significant height and up to 14.4 m in maximum height. No other comparably violent storm events had been recorded in the previous 50 years. This storm had profound impacts on benthic communities with substantial loss of benthic cover from abrasion and erosion (Garcia-Rubies *et al.*, 2009). MIMR and the nearby coast were affected by this storm, so the effects of this low-frequency event on sea urchin populations were also evaluated. After the storm, sea urchin recruits (<1 cm) were counted because we suspected that post-settlement mortality at the early stages could be important in determining the recovery of adult populations.

The level of sea urchin harvesting in this region is low, and thus, we hypothesized that it would not have a significant effect on the dynamics of the monitored sea urchin populations.

Port-Cros National Park (PCNP) encompasses two small islands of the Hyères archipelago (Northwestern Mediterranean, France), situated 5 miles offshore (Fig. 2). In this National Park, fishing has been regulated since 1963 and fish densities have also been high for decades (Francour and Harmelin, 1988). From 1979 to 1984, a mortality caused by the so-called bald-sea urchin disease (Jangoux, 1987) occurred along the NW Mediterranean coast (Boudoresque *et al.*, 1981; Hobaus *et al.*, 1981), where 53 to 86% of the population perished (Boudouresque *et al.*, 1980, 1981; Azzolina, 1987). The PCNP series of data began with controls in 1979 and two consecutive censuses in 1982 and 1983 were carried out by J. Harmelin and collaborators (Harmelin *et al.*, 1980, Hereu *et al.*, 2005). In that study, 6 permanent sites on rocky bottoms were monitored all around the island at three different depths: 3, 6 and 9 m when available (Fig. 2). Transects were performed on sloping bare rocks dominated by photophilic algae communities, with some accumulation of pebble and schist flagstones. At each site and depth, 2 permanent transects (60 m^2) were measured and marked with permanent tags. This series was interrupted in 1984 and restarted in 1994, when transects were extended to 200 m^2 (100 x 2 m^2). Densities of sea urchin populations were studied by SCUBA-diving once a year, and size-structure was measured beginning from 1993 to 2003, when the series was again interrupted. Transects were divided into 10 m^2 subtransects, and within each transect, *P. lividus* and *A. lixula* > 1 cm in diameter were counted and their diameters (test without spines) were measured with calipers. The diameters were grouped in size classes of 1 cm for analysis.

All censuses were performed once a year during late summer to avoid any possible effect of seasonality on our series.

Data analysis

To analyze the effect of different levels of protection, the abundance of each species in MIMR was compared using permutational multivariate analysis of variance (PERMANOVA, McArdle and Anderson, 2001) in areas temporarily and spatially replicated at each level of protection, type of bottom and year, based on the matrix of Euclidean distances between samples. The model was mixed with two fixed factors: protection (P) and bottom type (B). Year was used (T: 1995-2005 and 2009-2012 to have a complete design) as a random factor, as well as a site factor, which was random and nested in protection and bottom (Z(P*B)).

To test the ratio of the variances in inter-annual variability of sea urchin densities between the levels of protection in the two habitats (boulder bottoms and vertical walls), we used Fisher's F-test.

To analyze the variation of the abundance of each species in PCNP densities were compared between 1982 and 1984. Then, from 1994 to 2003, a permutational multivariate analysis of variance was performed (PERMANOVA, McArdle and Anderson, 2001) for each year only for sites at 6 m depth based on the matrix of Euclidean distances between samples. The model had two random factors: year (T: 1994-2003) and site. The PRIMER-E Ltd. (Anderson *et al.*, 2008) statistical package was used.

To determine density-dependent juvenile survival, least squares regression was applied to test for a positive association between the abundance of juveniles ≤20 mm in diameter (the average size of 1-year-old urchins) in each transect and the abundance of adults ≥20 mm from the following year. Juvenile and adult abundances were log-transformed to improve the distribution of residuals.

To determine the existence of a negative correlation between *P. lividus* and *A. lixula* densities, which would indicate a competition relationship between both species,

TABLE 1. Results of PERMANOVAs assessing the effects of Site, Protection, Type of bottom and Year for *Paracentrotus lividus* and *Arbacia lixula* densities in Medes Islands Marine Reserve.

	Paracentrotus lividus				*Arbacia lixula*			
Source	df	MS	Pseudo-F	P(perm)	df	MS	Pseudo-F	P(perm)
Year	14	27992	6,50	0,001	14	66,92	2,79	0,004
Protection	1	1,09E5	1,35	0,256	1	161,68	1,43	0,244
Habitat	1	3,14E5	0,52	0,032	1	1096,7	7,08	0,005
Year*Protection	14	6733,7	1,56	0,129	14	18,14	0,75	0,692
Year*Habitat	14	13460	3,12	0,001	14	47,22	1,97	0,034
Protection*Habitat	1	84452	1,07	0,372	1	6.2E-3	0,18	1
Site*(Prot*Hab)	4	77113	17,95	0,001	4	111,28	4,65	0,006
Year*Protection*Hab)	14	5929,7	1,37	0,196	14	21,08	0,87	0,573
Year*Site(Prot*Habitat)	56	4328,5	3,59	0,001	56	24,07	2,73	0,001
Res	1659	1203,3			1655	8,81		
Total	1778				1774			

we also applied least-square regression on MIMR data for each year and site from 1995 to 2005, and on PCNP data for each year, site and depth between 1994 and 2003.

We also applied least-square regression to determine the relationship between sea surface temperature and the abundance of recruits and adult *P. lividus* and *A. lixula*. Series of temperature data were obtained for MIMR by Josep Pascual (unpublished data) and from the T-MedNet network of long term high resolution temperature series in Mediterranean coastal waters (http://www.t-mednet.org)

RESULTS

Medes Islands Marine Reserve

P. lividus was the most abundant sea urchin species, with highly variable densities, especially on boulder bottoms (Figure 3). In MIMR, *P. lividus* densities showed a significant interaction between sites and years, indicating significant differences in density over the years at each site, and between the substrate types over time, where urchin densities on vertical walls were lower and less variable than on boulder bottoms (Table 1). However, mean density did not differ between the protected and the unprotected area, nor was there an interaction between habitat type and protection (Table 1).

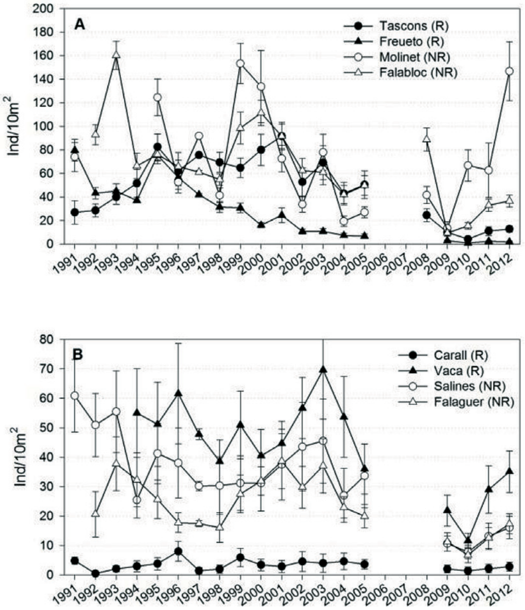

Figure 3. *Paracentrotus lividus* density over time in Medes Islands Marine Reserve. Number of *Paracentrotus lividus* (>1 cm diameter) per $10\ \text{m}^2$ (mean ±SE) over time at each site in MIMR on a) boulder substrates and (b) vertical walls. Solid symbols represent sites within the reserve (R); open symbols represent sites in the nearby unprotected area (NR). Note the different scales of both types of habitat.

Fisher's F-test showed higher variability in *P. lividus* density in boulder substrates outside the reserve compared to both the boulder and vertical wall habitats inside the reserve (Non Protected Boulders / Non Protected vertical $F = 12.72$, $p < 0.01$; Non Protected Boulders / Protected Boulders $F = 5.73$, $p < 0.01$; Non Protected Boulders / Protected Vertical $F = 6.058$, $p < 0.01$).

P. lividus densities on boulder bottoms dropped dramatically (82%, 84%, 59% and 56% in Falaguer, Molinet, Tascons and Freueto, respectively) in 2009 after the exceptionally severe storm in the winter of 2008, reaching the lowest values observed in the study period up to that point (Fig. 3a). The density declines were smaller on vertical walls, but with a significant drop of 78% at Salines (Fig. 3b). The size-frequency distribution showed that the larger size classes were the most affected by the storm.

Recruitment after the storm was very high in the Molinet population, in which a recruitment pulse occurred in 2010, with new individuals comprising 81% of the population, densities grew until 2012 when they reached similar values to those before the storm.

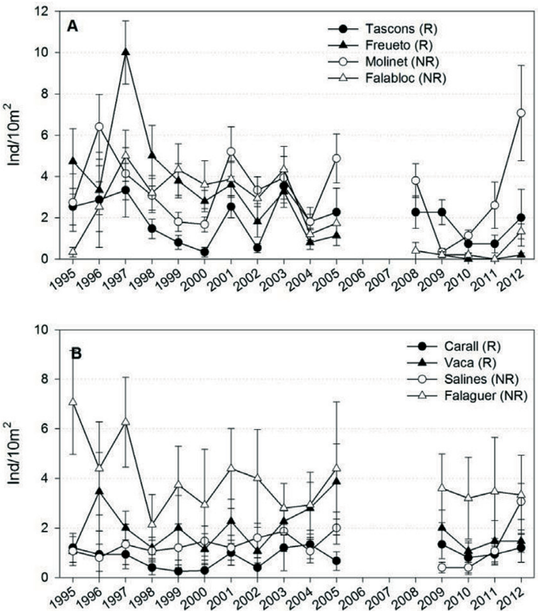

Figure 4. *Arbacia lixula* density over time in Medes Islands Marine Reserve. The number of *Arbacia lixula* (>1 cm diameter) per 10 m^2 (mean ± SE) over time at each site in the MIMR on a) boulder substrates and (b) vertical walls. Solid symbols represent sites within the reserve (R); open symbols represent sites in the nearby unprotected area (NR). Note the different scales of both types of habitat.

The numbers of adults (>2 cm diameter) and recruits (juveniles <2 cm) in the MIMR were positively correlated on both boulder bottoms and vertical walls ($r^2 = 0.85$, df = 24 $p<0.001$ and $r^2 = 0.84$, df = 24 $p<0.001$, respectively), while in the unprotected area no relationship was found ($r^2 = 0.104$, df = 24 $p = 0.108$ and $r^2 = 0.105$, df = 24 $p = 0.105$, respectively). On boulder bottoms, the *P. lividus* frequency-size distribution showed high variability, alternating between bimodal and unimodal distributions with conspicuous recruitment peaks. On vertical walls, *P. lividus* frequency-size distributions were more stable but also showed some high recruitment episodes.

Densities of *Arbacia lixula* in the MIMR were an order of magnitude lower than densities of *Paracentrotus lividus* (Fig. 4a) and were differently distributed, occupying more shaded and vertical habitats. *A. lixula* densities showed high variability over years within each site, and also between substrate type and time, but without effects of the level of protection (Table 1). On boulder bottoms, *A. lixula* densities also dropped dramatically in 2009 after the exceptionally severe

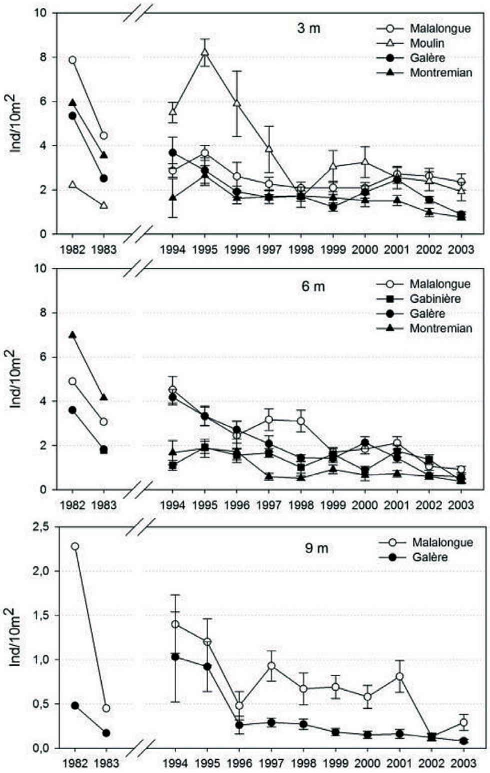

Figure 5. *Paracentrotus lividus* density over time in Port-Cros National Park. Number of *Paracentrotus lividus* (>1 cm diameter) per 10 m^2 (mean ±SE) over time at each site in PCNP at 3, 6 and 9 meters depth.

storm in the winter of 2008 (82%, 91% and 50% at Freueto, Molinet and Falaguer and remained constant at Tascons). On vertical walls, density declines were more variable (80%, 48% and 18% at Salines, Vaca and Falaguer, respectively, and an increase at Carall) (Fig. 4b). The size structure of *A. lixula* populations showed a unimodal distribution, with dominance of the 4 cm size class, and no recruitment pulses were observed, even after the 2008 storm.

P. lividus and *A. lixula* densities were not significantly correlated on either boulder bottoms or slope bare rock ($r^2 = 0.006$, df = 42, p = 0.87; $r^2 = 0.037$, df = 42, p = 0.209, respectively).

PORT CROS NATIONAL PARK

P.lividus is also the most common sea urchin in the infralittoral communities of PCNP. Their densities were highest at 3 m depth, and were very variable on both spatial and temporal scales at all depths (Fig. 5). In all sites

TABLE 2. Results of PERMANOVAs assessing the effects of Site and Year for *Paracentrotus lividus* and *Arbacia lixula* densities in Port-Cros National Park.

	Paracentrotus lividus				*Arbacia lixula*			
Source	df	MS	Pseudo-F	P(perm)	df	MS	Pseudo-F	P(perm)
Year	9	2272	5,37	0,004	9	27,15	0,737	0,66
Site	3	4765,3	12,41	0,001	3	424,94	12,198	0,001
Year*Site	27	436,46	4,75	0,001	27	37,08	2,9768	0,001
Res	581	91,74			702	12,45		
Total	620				741			

and depths, densities decreased between 1982 and 1984 due to the bald disease that occurred in this area (ANOVA $F_{2,47} = 4.762$, $p = 0.013$; $F_{2,33} = 9.493$, $p < 0.001$; $F_{2,18} = 4.459$, $p = 0.026$ at 3, 6 and 9 m respectively; also described by Harmelin *et al.*, 1980). When the series recommenced in 1994, densities were similar to 1984, except for Moulin, where densities were higher, mainly due to the high number of recruits (see below). After 1994, *P.lividus* populations in all stations suffered a gradual decrease until 2003, where the minimum values in 20 years of monitoring were reached, with less than the 10% of the original densities found in 1982 (Fig. 5).

At 6 m depth, there were significant differences between sites and in time (Table 2). After 1994, *P.lividus* densities at all sites have decreased since 2003, when the minimal values have been reached. As for size structure frequencies in Port-Cros, *P.lividus* populations varied from unimodal to bimodal, depending on the site studied, and in the frequency of recruitment episodes.

A. lixula is a common species on PCNP rocky bottoms, but less abundant than *P. lividus* (Fig. 6). This species is distributed in shadow habitats and is more abundant in sites with a major spatial heterogeneity, and at shallower depths. *A. lixula* was not affected by the mortality that occurred in the 1980s. Furthermore, in contrast to *P. lividus*, densities increased after 1983, and after 1994 their densities have been stable with some oscillations during the last 10 years at all studied sites (Fig. 6; Table 2).

In Port-Cros, the number of adults (ind >2 cm) and recruitment (i.e. number of juveniles <2cm in the following year) were correlated at all depths ($r^2 = 0.461$, $p < 0.001$; $r^2 = 0.135$, $p = 0.038$; $r^2 = 0.608$, $p < 0.001$ at 3, 6 and 9 m depth respectively). There was also a positive correlation between *P. lividus* and *A. lixula* at all depths (3m: $r^2 = 0.179$, df = 38, $p = 0.006$; 6m: $r^2 = 0.35$, df = 38, $p < 0.001$; 9m: $r^2 = 0.55$, df = 18, $p < 0.001$, respectively).

However, there was no positive correlation between mean sea surface temperature and density of *P.lividus* or *A. lixula* in any of the zones studied,

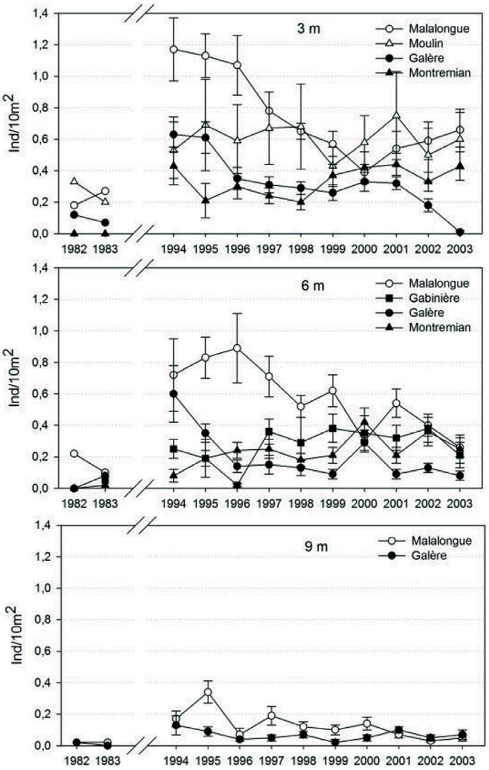

Figure 6. *Arbacia lixula* density over time in Port-Cros National Park. Number of *Arbacia lixula* (>1 cm diameter) per 10 m^2 (mean ±SE) over time at each site in PCNP at 3, 6 and 9 meters depth.

while both temperature series showed a slight increase in SST, sea urchins densities varied and even showed a decrease in both areas studied (*P.lividus*: $r^2 = 0.006$, $F = .097$, $p < .75$; $r^2 = 0.065$, $F = 0.48$, $p < 0.50$; *A.lixula*: $r^2 = 0.006$, $F = 0.006$, $p < .93$; $r^2 = 0.081$, $F = 0.97$, $p < 0.34$ for MIMR and PCNP respectively) (Fig. 7). The only correlation related to sea water temperature was found in the number of *P.lividus* recruits and the mean of the SST in April of each year ($r^2 = 0.26$, $F = 5.66$, $p < 0.03$).

DISCUSSION

These two long-term series of data show different trends in two sea urchin populations, and agree only partially with the expected results described by top-down deterministic models. Local factors may modify the intensity of some processes, and low-frequency historical factors only detectable through regular long-term monitoring may explain these deviations from theoretical models.

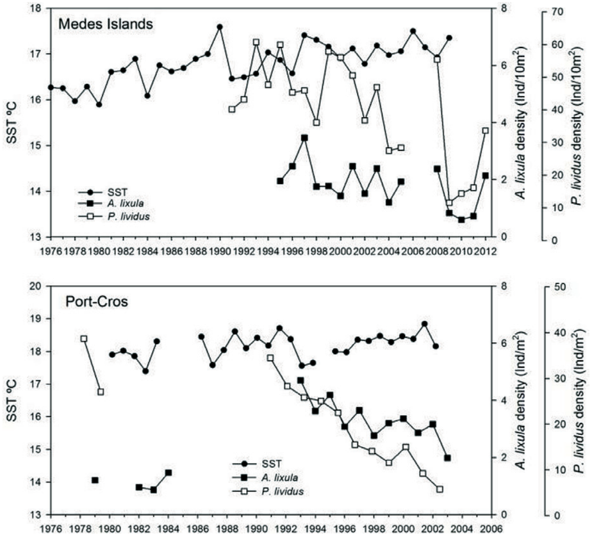

Figure 7. Density of *P. lividus* and *A.lixula* over time in Medes Islands Marine Reserve and Port-Cros National Park compared with the mean SST at each site.

MEDES ISLANDS

While fish densities remained high during the whole study period (more than 10 years) (Garcia-Rubies and Zabala, 1990; Sala *et al.*, 2012), sea urchin densities on MIMR were also high and did not show differences between the protected and the non-protected areas, evidencing the lack of control of predatory fish on sea urchin densities.

The series of data comparing the protected and the nearby non-protected areas showed a high yearly variability in sea urchin densities mainly caused by recruitment episodes. Although high settlement episodes have been observed both inside and outside MPA (Hereu *et al.*, 2004), recruitment peaks were more conspicuous outside the MPA. Thus, we observed predation control inside the MPA, where predators dampen high recruitment episodes stabilizing and potentially controlling sea urchin populations. This is more evident after the storm in 2008, where a high recruitment episode occurred outside the reserve, while inside the reserve the recruitment peak was attenuated.

The only clear factor in determining the density and structure of sea urchin populations was the topography. The absence of refuges on slope bare rocks (i.e. crevices and space between boulders) may cause a denso-dependent higher predation rate on juvenile sea urchins, thus the bimodal size structure is less affected by recruitment pulses. Contrarily, on boulder bottoms, with a high availability of refuges, juvenile mortality is density independent, indicating that the abundance of adults is more determined by pulses of recruitment. The population is denser, with a major proportion of juveniles and with frequent changes in size structure from bimodal to unimodal. Moreover, on boulder bottoms outside the MPA changes in size structure are more frequent because, in addition to refuge availability, predation rate is lower.

Port-Cros

In PCNP, sea urchin populations suffered conspicuous changes over the last decades.

In the Port-Cros Bay, an increase in sea urchin densities was described during the 1970s (Boudouresque *et al.*, 1980, 1981; Azzolina, 1987), reaching a maximum in 1979. After 1980, sea urchins densities declined abruptly due to the bald-sea-urchin disease, which reduced significantly sea urchin populations and afterwards they remained low, with a gradual but a constant decline. In 1980 Boudouresque *et al.*, (1980, 1981) described the bald-sea-urchin disease in a census on *Posidonia oceanica* meadows, where a progressive decline of 50% to 86% occurred until 1983, reaching the lowest density. On rocky bottoms a decline in sea urchin populations was not noticed until 1983 (Harmeiln *et al.*, unpublished data; this study).

Unfortunately, in 1984, the sea urchin monitoring was interrupted in PCNP. Nevertheless, despite the lack of data between 1984 and 1993, we assume that densities during this period never reached the levels of 1982. When we restarted the series in 1994, we observed values similar to those in 1983, which then decreased progressively in all sites until 2003, when they reached minimum values. Disregarding the effect of sea urchin fishing (as a National Park, the fishery is forbidden in PCNP) and the lack of evidence of recurrent episodes of the bald-sea-urchin disease (authors pers. obs.), low sea urchins densities could be caused by predation or recruitment limitation, or an interaction of both processes. Moreover, because of the dominance of schist rock, the majority of sites in PCNP are dominated by slope bare rock with limited refuges available, thus sea urchins are more vulnerable to fish predators.

We believe that mass mortality caused a shift in sea urchin population dynamics in Port-Cros, changing the role of different processes in maintaining populations. Before the mass mortality, sea urchin densities were high, probably following the same process as occurred in Medes Islands, where a density-dependent recruitment under high predation pressure exists. After the mass mortality, fish predators seem to exert a control together with low levels of recruitment, and thus sea urchin densities never again reach densities similar to those before the mortality outbreak.

Similar dynamics have been described in other sea urchin species around the world, such as *Diadema antillarum* in the Caribbean (Lessios, 2005), *Strongylocentrotus franciscanus* (Lafferty, 2004), *Stongylocentrotus droebachiensis* in Nova Scotia (Scheibling and Hennigar, 1997).

All this evidence and the present study suggest that punctual low frequency perturbations, such as diseases or storms, can exert an effective control on sea urchins populations, not only by reducing sea urchin populations, but also by changing their dynamics and the intensity of the processes that regulate them.

The bald-sea-urchin disease did not affect *A.lixula,* and after the *P. lividus* mass mortality, densities of *A.lixula* increased dramatically. This increase could suggest a competition role between both species as suggested by several authors (Benedetti-Cecchi *et al.*, 1998; Bulleri *et al.*, 1999). Nevertheless, the fact that after 1994 *A.lixula* populations decreased at almost all sites and depths does not support this hypothesis, which agrees with other authors that suggest complementary roles of both species (Privitera *et al.*, 2008; Gianguzza *et al.*, 2006; Bonaviri *et al.*, 2009, 2011).

EFFECTS OF GLOBAL WARMING ON MEDITERRANEAN SEA URCHIN POPULATIONS

Arbacia lixula is considered thermophilic (Kempf, 1962), and its abundance can vary in orders of magnitude depending on the regions. It is more abundant in the warmer southernmost parts of the Mediterranean (e.g., Palacín *et al.*, 1998; Pais *et al.*, 2007; Guidetti and Dulcik, 2007; Giancuzza *et al.*, 2006; Bulleri *et al.*, 1999; Bonaviri *et al.*, 2009), suggesting a biogeographical pattern. Due to its thermophilic affinity, *A.lixula* abundances have been suggested as an indicator of climate change (Francour *et al.*, 1994).

Some recent studies demonstrate that increasing water temperatures increase *A. lixula* larval production and survival (Ginguzza *et al.*, 2010, 2011; Privitera *et al.*, 2011), supporting the hypothesis of an increase in their populations in the Mediterranean as a consequence of climate change (Francour *et al.*, 1994).

Our long-term data do not support this hypothesis. Comparing the increase in SST and sea urchin abundance, we have only found an annual positive correlation between *P.lividus* recruitment and SST temperature in April, but not for *A.lixula,* and neither for a long-term decadal trend. In MIMR, *A.lixula* populations did not suffer any conspicuous change over 15 years; their densities were lower than those reported in Scandola by Francour *et al.*, (1994). In PCNP, between 1984 and 1993, we observed an increase in their densities of the same magnitude as Francour *et al.*, (1994) described in Corsica between 1985 and 1992. Nevertheless, after 1994, densities declined, and are similar to those reported in Scandola in the early 1990s (Francour *et al.*, 1994).

Moreover, other studies also show changes in *A. lixula* populations not attributable to climate change. For example, Kempf (1962) found densities greater than 10 indv. m^{-2} in Maresille (France) in the early 1960s (even 20-30 indv. m^{-2} as a maximum «rarely reached»), which suggest that long-term fluctuations in *A. lixula* abundance have occurred.

These results show high levels of variability in the biological and physical processes controlling sea urchin populations. Not only are physical factors important but low-frequency extreme events are important too. Only long-term monitoring programs with regular periodicity can integrate the effects of regulating factors that act at different temporal scales. Therefore, long temporal scales are needed to avoid misinterpreting processes or confusing factors. In contrast, short-term studies may attribute population trends to inappropriate causes, such as fish predation or climate change. Long-term studies, well-designed and regularly performed, are fundamental to understanding the functioning of natural ecosystems, as such studies provide evidence that cannot be detected by short-term experimental or space-for-time substitution studies (Babcock *et al.*, 2010).

REFERENCES

Anderson, M.J., Gorley, R.N., and Clarke, K.R. (2008) *PERMANOVA for PRIMER: Guide to Software and Statistical Methods* (214 pp.), Plymouth, UK.

Andrew, N.L. (1991). Changes in habitat structure following mass mortality of sea urchins in Botany Bay, New South Wales. *Australian Journal of Ecology*, 16, 353–362.

Andrew, N.L., Agatsuma, Y., Ballesteros, E., Bazhin, A.G. *et al.* (2002) Status and management of world sea urchin fisheries. *Oceanography and Marine Biology: an Annual Review*, 40, 343–425.

Azzolina, J.F. (1987) Evolution à long terme des populations de l'oursin comestible *Paracentrotus lividus* dans la vaie de Port-Cros (Var, France). *Proceedings of Colloque international sur Paracentrotus lividus et les oursins comestibles* (ed. by Boudouresque, C.F.), pp. 257–269. GIS Posidonie publ., Marseille, France.

Babcock, R.C., Shears, N.T, Alcala, A.C., Barrett, N.S., Edgar, G.J., Lafferty, K.D., Mcclanahan, T.R. and Russ, G.R. (2010) Decadal trends in marine reserves reveal differential rates of change in direct and indirect effects. *Proceedings of the National Academy of Sciences of the United States of America*, 107, 18256–18261.

Benedetti-Cecchi, L., Bulleri, F. and Cinelli, F. (1998) Density dependent foraging of sea urchins in shallow subtidal reefs on the west coast of Italy (western Mediterranean). *Marine Ecology Progress Series*, 163, 203–211.

Bonaviri, C., Vega Fernández, T., Badalamenti, F., Gianguzza, P., Di Lorenzo, M. and Riggio, S. (2009) Fish versus starfish predation in controlling sea urchin populations in Mediterranean rocky shores. *Marine Ecology Progress Series*, 382, 129–138.

Bonaviri, C., Gianguzza, P., Pipitone, C. and Hereu, B. (2012) Micropredation on sea urchins as a potential stabilizing process for rocky reefs. *Journal of Sea Research*, 73, 18–23.

Boudouresque, C.F., Nedelec, H. and Shepard, S.A. (1980) The decline of a population of the sea urchin *Paracentrotus lividus* in the Bay of Port-Cros (Var, France). *Travaux Scientifiques du Parc National de Port-Cros France*, 6, 243–251.

Boudouresque, C.F., Nedelec, H. and Shepherd, S.A. (1981) The decline of a population of the sea urchin *Paracentrotus lividus* In the Bay of Port-Cros (Var, France). *Rapports et Proces-Verbaux des Reunions - Commission Internationale pour l'Exploration Scientifique de la Mer Mediterranee*, 27, 223–224.

BOUDOURESQUE, C.F. and VERLAQUE, M. (2001) Ecology of *Paracentrotus lividus*. *Edible sea-urchins: biology and ecology - Developments in aquaculture and fisheries science* (ed. by Lawrence, J.M.), pp. 177–216. Elsevier, Amsterdam, The Netherlands.

BULLERI F., BENEDETTI, C.L. and CINELLI, F. (1999) Grazing by the sea urchins *Arbacia lixula* L. and *Paracentrotus lividus* Lam. in the North-Western Mediterranean. *Journal of Experimental Marine Biology and Ecology*, 241, 81–95.

EBELING, A.W., LAUR, D.R. and ROWLEY, R.J. (1985) Severe storm disturbances and reversal of community structure in a southern California kelp forest. *Marine Biology*, 84, 287–294.

FERNANDEZ, C., PASQUALINI, V., BOUDOURESQUE, C.F., JOHNSON, M., FERRAT, L., CALTAGIRONE, A. and MOUILLOT, M. (2006) Effect of an exceptional rainfall event on the sea urchin (*Paracentrotus lividus*) stock and seagrass distribution in a Mediterranean coastal lagoon. *Estuarine, Coastal and Shelf Science*, 68, 259–270.

FRANCOUR, P., BOUDOURESQUE, C.F., HARMELIN, G.J., HARMELIN-VIVIEN, M.L. and QUIGNARD, J.P. (1994). Are the Mediterranean waters becoming warmer? Information from biological indicators. *Marine Pollution Bulletin*, 28, 523–526.

FRANTZIS, A., BERTHON, J.F. and MAGGIORE, F. (1988) Relations trophiques entre les oursins *Arbacia lixula* et *Paracentrotus lividus* (Echinoidea Regularia) et le phytobrnthos infralittoral superficiel dans la baie de Port-Cros (Var, France). *Scientific Report of Port-Cros National Park*, 14, 81–140.

GARCIA-RUBIES, A. and ZABALA, M. (1990) Effects of total fishing prohibition on the rocky fish assemblages of Medes Islands Marine Reserve (NW Mediterranean). *Scientia Marina*, 54: 317–328.

GARCIA-RUBIES, A., MATEO, M.A., HEREU, B., COMA, R., TEIXIDO, N. *et al.* (2009) Preliminary assessment of the impact of an extreme storm on catalan mediterranean benthic communities. *Proceedings of the 11th Plinius Conference on Mediterranean Storms, 7–11 September 2009,* Barcelona, Spain.

GIANCUZZA, P., CHIANTORE, M., BONAVIRI, C., CATTANEO-VIETTI, R., VIELMINI, I. and RIGGIO, S. (2006) The effects of recreational *Paracentrotus lividus* fishing on distribution patterns of sea urchins at Ustica Island MPA (Western Mediterranean, Italy). *Fisheries Research*, 81, 37–44.

GIANGUZZA, P., AGNETTA, D., BONAVIRI, C., DI TRAPANI, F., VISCONTI, G., GIANGUZZA, F. and RIGGIO, S. (2011) The rise of thermophilic sea urchins and the expansion of barren grounds in the Mediterranean sea. *Chemistry and Ecology*, 27, 129–134.

GUIDETTI, P. and DULČIĆ, J. (2007) Relationships among predatory fish, sea urchins and barrens in Mediterranean rocky reefs across a latitudinal gradient. *Marine Environmental Research*, 63, 168–184.

HARMELIN, J.G., BOUCHON, C., DUVAL, C. and HONG, J.S. (1980) Les echinoderms de substrats durs de de l'ille de Port-Cros, Parc National (Méditerranée Nord-Occidental). Élement pour un inventaire quantitative. *Scientific Report of Port-Cros National Park*, 6, 25–38.

Harrold, C. and Reed, D.C. (1985) Food availability, sea urchin grazing and kelp forest community structure. *Ecology*, 66, 1160–1169.

Hereu, B., Linares, C., Diaz, D., Teixidor, N. and Zabala, M. (2005) *Diversité d'échinodermes dans les fonds marins de Porquerolles.* Scientific Report for the Port-Cros National Park (51 pp), Universitat de Barcelona, Spain.

Hereu, B., Zabala, M. and Sala, E. (2008) Multiple cotrols of community structure and dynamics in a sublittoral marine environment. *Ecology*, 89, 3423–3435.

Hereu, B., Zabala, M., Linares, C. and Sala, E. (2004). Temporal and spatial variability in settlement of the sea urchin *Paracentrotus lividus* in the NW Mediterranean. *Marine Biology*, 144, 1011–1018.

Hereu, B., Linares, C., Sala, E., Garrabou, J., Garcia-Rubies, A., Diaz, D. and Zabala, M. (2012) Multiple processes regulate long-term population dynamics of sea urchins on mediterranean rocky reefs. *PLoS ONE*, 7, e36901.

Hobaus, E., Fenaux, L. and Hignette, M. (1981) Premieres observations sur les lesions provoquees par une maladie affectant le test des oursins en Mediterranee occidentale. *Rapports et Proces-Verbaux des Reunions - Commission Internationale pour l' Exploration Scientifique de la Mer Mediterranee*, 27, 221–222.

Hughes, T.P. (1994) Catastrophes, phase shifts and large-scale degradation of a Caribbean coral reef. *Science*, 265, 1547–1551.

Jangoux, M. (1987) Diseases of Echinodermata. I. Agents microorganisms and protistans. *Diseases of Aquatic Organisms*, 2, 147–162.

Kempf, M. (1962) Recherches comparée sur *Paracentrotus lividus* (lmk) et *Arbacia lixula* (L). *Receuil des Travaux de la Station Marine d'Endoume*, 25: 47–115.

Lafferty, K.D. (2004) Fishing for lobsters indirectly increases epidemics in sea urchins. *Ecological Applications*, 14, 1566–1573.

Lessios, H.A. (2005) *Diadema antillarum* populations in Panama twenty years following mass mortality. *Coral Reefs*, 24, 125–127.

Micheli, F., Benedetti-Cecchi, L., Gambaccini, S., Bertocci, I., Borsini, C., Osio, G.C. and Romano, F. (2005) Alternate states, marine protected areas, and the structure of Mediterranean rocky-reef assemblages. *Ecological Monographs*, 75, 81–102.

McArdle, B.H. and Anderson, M.J. (2001) Fitting multivariate models to community data: a comment on distance based redundancy analysis. *Ecology*, 82, 290–297.

Pais A., Chessa, L.A., Serra, S., Ruiu, A., Meloni, G. and Donno, Y. (2007) The impact of commercial and recreational harvesting for *Paracentrotus lividus* on shallow rocky reef sea urchin communities in North-western Sardinia, Italy. *Estuarine Coast and Shelf Science*, 73, 589–597.

Palacin, G., Giribet, G., Carner, S., Dantart, L. and Turon, X. (1998) Low densities of sea urchins influence the structure of algal assemblages in the western Mediterranean. *Journal of Sea Research*, 39, 281–290.

Phillips, N.E. and Shima, J.S. (2006) Differential effects of suspended sediments on larval survival and settlement of New Zealand urchins *Evechinus chloroticus* and abalone *Haliotis iri*. *Marine Ecology Progress Series*, 314, 149–158.

Privitera, D, Chiantore, M., Mangialajo, L., Glavic, N., Kozul, W. and Cattaneo-Vietti, R. (2008) Inter- and intra-specific competition between *Paracentrotus lividus* and *Arbacia lixula* in resource-limited barren areas. *Journal of Sea Research*, 60, 184–192.

Sala, E., Boudouresque, C.F. and Harmelin-Vivien, M. (1998a) Fishing, trophic cascades, and the structure of algal assemblages: evaluation of an old but untested paradigm. *Oikos*, 82, 425–439.

Sala, E., Ribes, M., Hereu, B., Zabala, M., Alvà, V., Coma, R. and Garrabou, J. (1998*b*) Temporal variability in abundance of the sea urchins *Paracentrotus lividus* and *Arbacia lixula* in the northwestern Mediterranean: comparison between a marine reserve and an unprotected area. *Marine Ecology Progress Series*, 168, 135–145.

Sala, E., Ballesteros, E., Dendrinos, P., Di Franco, A., Ferretti, F. *et al.* (2012) The structure of Mediterranean rocky reef ecosystems across environmental and human gradients, and conservation implications. *PLoS ONE*, 7, e32742.

Scheibling, R.E., Hennigar, A.W. and Balch, T. (1999) Destructive grazing, epiphytism, and disease: the dynamics of sea urchin-kelp interactions in Nova Scotia. *Canadian Journal of Fisheries and Aquatic Sciences*, 56, 2300–2314.

Scheibling, R.E. and Hennigar, A.W. (1997) Recurrent outbreaks of disease in sea urchins *Strongylocentrotus droebachiensis* in Nova Scotia: evidence for a link with large-scale meteorologic and oceanographic events. *Marine Ecology Progress Series*, 152, 155–165.

Scheibling, R.E. and Robinson, M.C. (2008) Settlement behaviour and early post-settlement predation of the sea urchin *Strongylocentrotus droebachiensis*. *Journal of Experimental Marine Biology and Ecology*, 365, 59–66

Shears, N.T. and Babcock, R.C. (2003) Continuing trophic cascade effects after 25 years of no-take marine reserve protection. *Marine Ecology Progress Series*, 246, 1–16.

Shears N.T., Babcock, R.C. and Salomon, A.K. (2008) Context-dependent effects of fishing: variation in trophic cascades across environmental gradients. *Ecological Applications*, 8, 1860–1873.

Siddon C.E. and Witman, J.D. (2003) Influence of chronic, low-level hydrodynamic forces on subtidal community structure. *Marine Ecology Progress Series*, 261, 99–110.

Verlaque, M. (1987) Relations entre *Paracentrotus lividus* (Lamarck) et le phytobenthos de Méditerranée occidentale. *Proceedings of the Colloque international sur Paracentrotus lividus et les oursins comestibles* (ed. by Boudouresque, C.F.), pp. 5–36. GIS Posidonie Publications, Marseille, France.

Verlaque M. and Nedelec, H. (1983) Biologie de *Paracentrotus lividus* (Lamark) sur un substrat rocheur en Corse (méditerranée, France): alimentation des adultes. *Vie et Milieu*, 33, 191–201.

Walker, J.W. (2007) Effects of fine sediments on settlement and survival of the sea urchin *Evechinus chloroticus* in northeastern New Zealand. *Marine Ecology Progress Series*, 331, 109–118.

Wing, S.R., Botsford, L.W., Morgan, L.E., Diehl, J.M. and Lundquist, C.J. (2003) Inter-annual variability in larval supply to populations of three invertebrate taxa in the northern California Current. *Estuarine Coastal and Shelf Science*, 57, 859–872.

Witman J.D. and Grange, K.R. (1998) Links between salinity, rain and predation in a rocky subtidal community. *Ecology*, 79, 2429–2447.

PUSHING BOUNDARIES OF RANGE AND RESILIENCE: A REVIEW OF RANGE-EXTENSION BY A BARRENS-FORMING SEA URCHIN

Scott D. Ling

CLIMATE CHANGE PERSPECTIVES FROM THE ATLANTIC:
PAST, PRESENT AND FUTURE
Jose María Fernández-Palacios, Lea de Nascimento, José Carlos Hernández,
Sabrina Clemente, Albano González & Juan P. Díaz-González (eds.)
Servicio de Publicaciones, Universidad de La Laguna – 2013

ISBN: 978-84-15910-54-1
pp. 411-442

ABSTRACT

The barrens-forming sea urchin *Centrostephanus rodgersii* (Diadematidae) has undergone recent poleward range-extension to the Tasmanian coastline (SE Australia). By compiling field observations (including SST spanning >60yrs), broad-scale surveys and manipulative experiments conducted during the past decade, this review details knowledge on the response of this key sea urchin species to climate change and dually explores multiple processes influencing the ultimate ecological consequence of catastrophic-shift from productive kelp beds to urchin barrens, as now observed within the range-extension region. As a result of changing regional climate, eastern Tasmania has become increasingly suitable for *Centrostephanus* larval development with the timing of the sea urchins' arrival, age-structure and spatial distribution across the extension-region consistent with patterns in warming sea temperatures and current-driven dispersal potential. Furthermore, consistency in temperature dependency of larval development plus lack of genetic differentiation of the species across its entire range, confirm the critical role of changing climate in driving the range-extension.

Continued warming predicted for this region will favour increased larval survival, promoting ongoing population expansion and ultimately increased likelihood of populations reaching sufficient density to affect widespread overgrazing. As such, knowledge of patterns and mechanisms promoting overgrazing are also reviewed for the purpose of identifying kelp beds at greatest risk given climate trends, reef substratum types and predator abundance (chiefly spiny lobsters) as influenced by intense fishing pressure. Finally, this review shows how management of non-climatic local scale stressors can be used to increase resilience of kelp beds against overgrazing given large-scale climate-driven increases in key sea urchin populations.

KEYWORDS: Climate change, *Centrostephanus rodgersii*, kelp beds, sea urchin barrens, marine reserves, resilience.

INTRODUCTION

Global climate change is a mechanism that has already resulted in, and is predicted to further lead to widespread re-distribution of marine species ranges (e.g., Harley *et al.*, 2006; Poloczanska *et al.*, 2007). Consistent with the expectations of climate warming and effects on terrestrial systems, the general tide of change among marine species also involves pole-ward shifts in species distributions (reviewed by Przeslawski *et al.*, 2012). However, different to terrestrial systems, distributional patterns of marine organisms appear strongly coupled with ocean current systems that not only transport the species themselves, but also their respective thermal envelope (Sunday *et al.*, 2012). Thus shifts in the natural ranges of marine species appear heavily bound by dispersive capacity governed by ocean currents (Ling *et al.*, 2009a).

While there is a growing list of species documented to be on the move as a result of changing environmental conditions attributable to anthropogenic climate, an important feature of species re-distributions is that many documented range-shifters (e.g. Last *et al.*, 2010; Johnson *et al.*, 2011) seemingly either remain in a cryptic existence or never reach high abundance; either appearing as vagrants or establishing a presence in a novel area but being of negligible or inconspicuous consequence to overall ecosystem dynamics. Other species however, can be far more conspicuous in their arrival, not only because of their conspicuous size, shape or colour but because of their ecological function. Of profound consequence are shifts among species capable of directly or indirectly modifying habitats causing fundamental change within recipient ecosystems by impacting important species interactions and having flow-on effects to broader ecosystem dynamics (Ling, 2008).

In the southern hemisphere, the south eastern coast of Australia has been identified as a climate change hotspot (Poloczanska *et al.*, 2007; Ridgway, 2007). Here the East Australian Current (EAC) has strengthened resulting in greater poleward penetration of warm water over the past 60 years and an approximate quadrupling of ocean warming rates compared to the global ocean average (Ridgway, 2007). This pronounced change in the physical oceanography of the region, an approximate 350 km southward shift of a major current system, corroborates with a series of recent poleward range extensions (reviewed by Poloczanska *et al.*, 2007; Last *et al.*, 2010; Johnson *et al.*, 2011); with changes in both advective patterns and increased water temperature suggested as direct drivers of range extension in the world's oceans (e.g., Harley *et al.*, 2006). The physical and biological expression of changes in the dynamics of the EAC is clearly evident on the east coast of Tasmania where oceanographic data reveal rising water temperature and salinity due to this feature (Ridgway, 2007; Johnson *et al.*, 2011) and where species typical of warmer northern waters now occur (e.g., Edgar, 1997; Poloczanska *et al.*, 2007; Last *et al.*, 2010; Johnson *et al.*, 2011). Indeed the response of marine biota attributable to the changing climate of the region is striking with a documented 45 coastal fish species, (30%) of fishes in the region, considered to have shifted distribution southwards relative to historical records (Last *et al.*, 2010; reviewed by Johnson *et al.*, 2011). Here intertidal species have also been documented to have undergone similar rates of range-extension at southern margins (Pitt *et al.*, 2010).

Of all the species recently documented to have undergone range extension to eastern Tasmania, the sea urchin *Centrostephanus rodgersii* (Agassiz) is arguably the most conspicuous and ecologically important due to its ability to overgraze kelp beds and maintain an alternative and stable barrens habitat (Andrew and

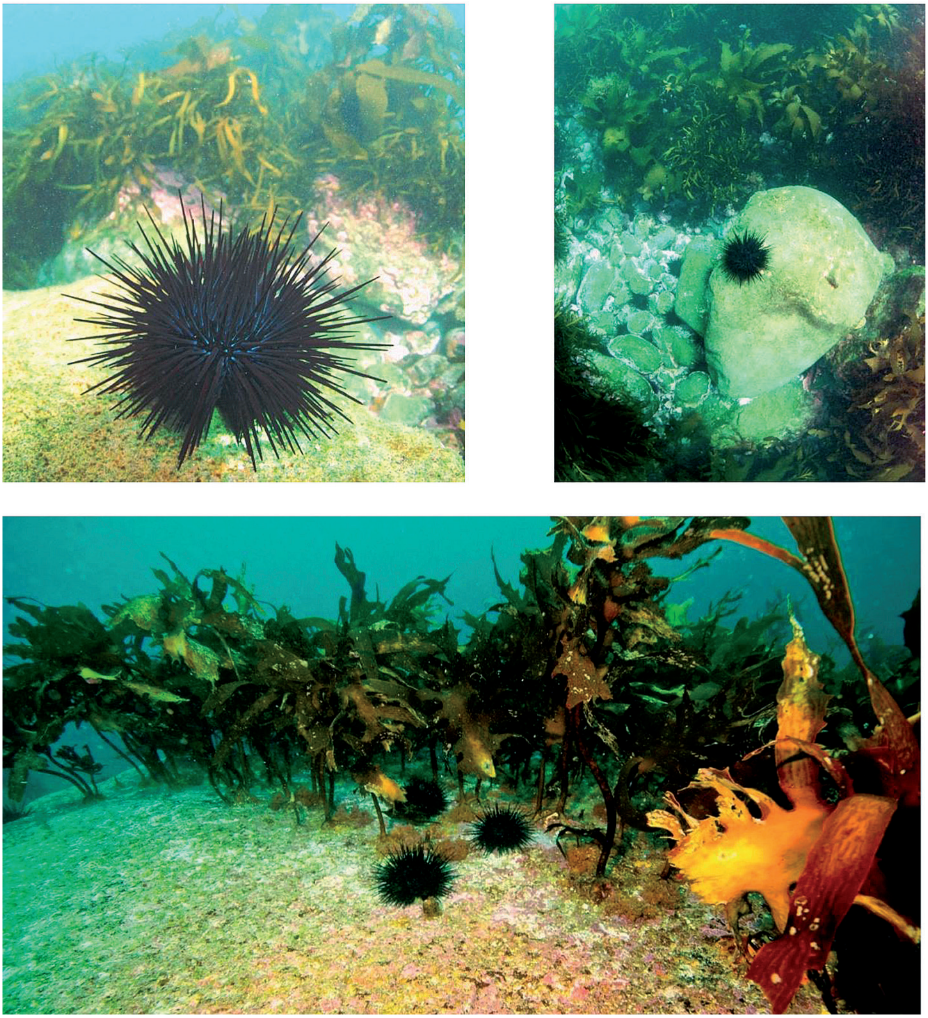

Figure 1. Patterns of overgrazing by the sea urchin *Centrostephanus rodgersii* in eastern Tasmania. Top left image is a close-up of *C. rodgersii* (test diam. of 100 mm) at a depth of 6 m at North Bay, south east Tasmania. Top right image is a planar view of a small incipient barrens patch (after Johnson *et al.*, 2005) grazed within an otherwise healthy kelp bed (dominated by *Ecklonia radiata*), North Bay. Lower image shows *C. rodgersii* grazing among kelp beds (*E. radiata*) at the edge of an extensive barrens ground (10^5 m^2 in size) ranging from 40 to 10 m depth at Sloop Rock, north east Tasmania, February 2011. Here, kelp beds have been documented to retreat (as a result of sea urchin overgrazing) by an average of ~1.25 metres over the period 2008 to 2011. Photography credits to the author.

Byrne, 2001; Hill *et al.*, 2003; Ling, 2008). Indeed within temperate Australia, no other benthic herbivore has as large an effect on shallow reef communities as *C. rodgersii* (Fletcher, 1987; Andrew, 1991; Andrew and Underwood, 1992; Ling, 2008).Thus its arrival to Tasmania is considered the single biggest threat to the structure and function of rocky reefs in Tasmania (Johnson *et al.*, 2005, 2011). In central and southern New South Wales (NSW) this species maintains barrens habitat over ~50% of shallow reef (Andrew and O'Neill, 2000) and observations from within Tasmania show that such levels of impact are now observable at some sites within the extended eastern Tasmanian range. Indeed, such is the impact of *C. rodgersii* on reef biodiversity that overgrazing by this single species results in localised losses of ~150 taxa that associate with Tasmanian kelp beds (Ling, 2008; see also Fig. 1). Thus population expansion and continued overgrazing by *C. rodgersii* within the range-extension region poses a major threat to rocky reef biodiversity generally (Ling, 2008) - particularly for those endemic species with very limited scope for migration given a lack of contiguous poleward landmass - but also specifically threatens lucrative commercial species dependent on kelp bed habitat including black-lip abalone and southern rock lobster (Andrew and Underwood, 1992; Andrew *et al.*, 1998; Worthington *et al.*, 1998; Johnson *et al.*, 2005; Strain and Johnson, 2009; reviewed by Johnson *et al.*, 2011).

Here I review the environmental, physiological and spatial context of the sea urchins' range extension to eastern Tasmania. Following the theme, "impacts of key sea urchin populations from larvae to ecosystems" this chapter first explores key features of the sea urchins early life history stages and moves toward the dynamics of kelp bed overgrazing and formation of extensive barrens ground. Finally, this review details how management of non-climatic stressors on rocky reefs can increase resilience of kelp beds against overgrazing given large-scale climate-driven increases in this key sea urchin population.

FEATURES OF A MARINE RANGE-EXTENDER

Belonging to a tropical sea urchin family the Diadematidae, the presence of C*entrostephanus rodgersii* in the cool temperate waters of Tasmania - where it is found grazing beneath *Macrocystis pyrifera* beds and adjacent to cold water bull 'kelp' *Durvillea potatorum* (Fucales) – may be considered anomalous. However, like its well-known tropical Diadematid relatives, the role of *C. rodgersii* as a key herbivore capable of effecting change at the scale of entire reef-scapes is by no means anomalous. Globally the distribution of *C. rodgersii* is constrained to the southwest Pacific where this large sea urchin (growing up to 133 mm TD and over 600 grams in wet weight) is conspicuously found on sub-tidal rocky reefs in south eastern Australia, Lord Howe Island, Norfolk Island, the Kermadec Islands (Schiel *et al.*, 1986) and in northern New Zealand (reviewed by Andrew and Byrne, 2007). Indeed this biogeographical distribution in itself hints to an important role of

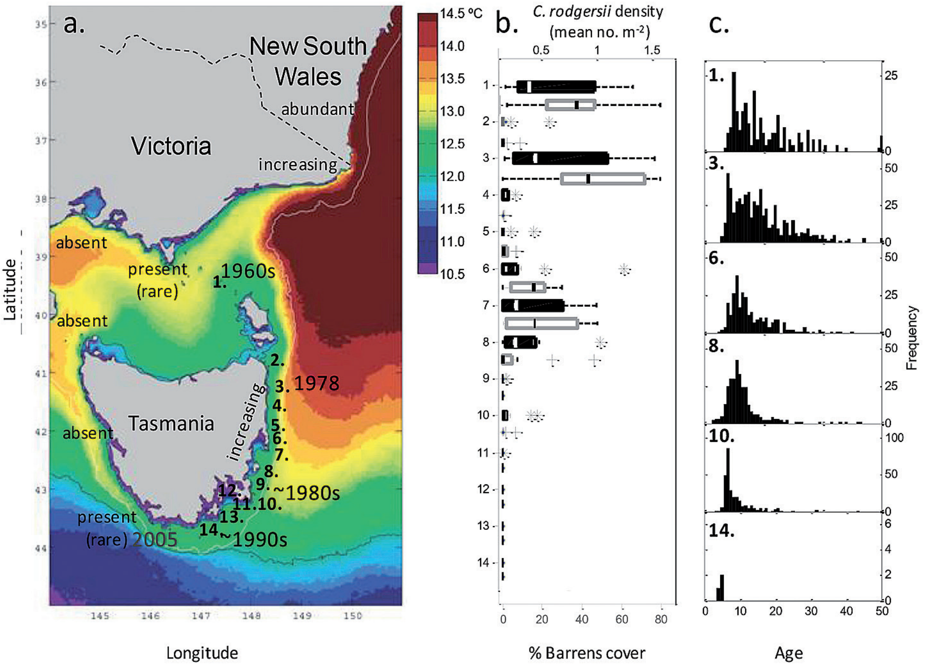

Figure 2. (a.) Map of south eastern Australia showing the dominant influence of the warm East Australian Current in eastern Tasmania during Austral winter (June-August averaged for the period 1993-2007) plus year of first discovery of *Centrostephanus rodgersii* along the coast is displayed as well as numbers showing sites (ordered north to south) where (b.) *C. rodgersii* density (black boxes) and barrens cover (grey open boxes) and (c.) age structure was assessed (survey of density and barrens conducted in 2000-2002 by Johnson *et al.*, 2005 and age assessment in 2005 by Ling *et al.*, 2009a). Both (b.) and (c.) reflect initial colonization in the north east and support the notion of recent range expansion mediated by increasing southward advection of larvae and heat.

the western boundary current, the East Australian Current (EAC), in defining the sea urchins range. Essentially the presence of *C. rodgersii* in south eastern Australia (Fig. 2a) and the south west pacific in general intuitively maps to where the various eddies of the EAC flow proximal to landmasses (Banks *et al.*, 2007).

Within Australia, the distribution of *C. rodgersii* is centred on the coast of NSW but the sea urchin is also found in high abundance in far eastern Victoria, on some of the eastern Bass Strait islands (i.e. Kent Group of Islands) and as is specifically reviewed here, the sea urchin has become progressively more abundant along the east coast of Tasmania (Johnson *et al.*, 2005). Notably, reports from abalone fishers also suggest a similar increase in *C. rodgersii* abundance in eastern Victoria and the population in northern New Zealand is also referred to as newly established (Pecorino, 2012; Pecorino *et al.*, 2013).

TIME-LINE OF DISCOVERY

Undergoing a poleward range extension from NSW, *C. rodgersii* was first recorded in the Kent Grp. in the late 1960s; north east mainland Tasmania in 1978; south eastern Tasmania in mid-1980s; and south western Tasmania in 2005 (Fig. 2). Since first detected in Tasmania (Dartnall, 1980), the sea urchins' abundance has increased and expansive barren areas now occur in some locations (Johnson *et al.*, 2005, 2011). Long-term observations in the Kent Grp. (Site 1, Fig. 2a) indicate initial establishment in the 1960s followed by a progressive spread to 2 of 7 survey sites in 1974; 3 of 9 sites in 1981 when urchin barrens were first recorded at a single site; to ultimately extensive urchin barren grounds being recorded at 7 of 7 sites surveyed in 2000 (Johnson *et al.*, 2005, 2011). A baseline survey in 2001/2002 confirmed the presence of *C. rodgersii* throughout eastern Tasmania revealing a patchy distribution but clear overall trend of decreasing abundance from north to south along this coastline (Johnson *et al.*, 2005; see Fig. 2a). But moreover the ecological effects of this sea urchin had become manifestly obvious with extensive barren grounds being found in the north east at St. Helens (site 3, Fig. 2a), the location where the sea urchin was first documented on mainland Tasmanian reefs 1978 (Edgar, 1997).

Across this extended range, the mean population age of *Centrostephanus rodgersii* becomes progressively younger towards the poleward range limit (Fig. 2). Such an age dynamic is consistent with the historical time-course of sequential poleward discoveries and expansion of *C. rodgersii* populations across eastern Tasmania, which has occurred at a rate of ~160 km decade^{-1} over the past 40 years (Ling *et al.*, 2009a, see Figure 2a-c). The sequential poleward discovery of the sea urchin, a pattern of declining age and a general poleward reduction in abundance along the eastern Tasmanian coastline is consistent with a model of range-extension driven by recent change to patterns of larval dispersal driven by change in the EAC. At the ecosystem level, the effects of grazing, as indicated by the percentage cover of sea urchin barrens, approximates the pattern in abundance of *C. rodgersii* along the eastern Tasmanian coast (Fig. 2b). Notably the described grazing impact is clearly due to grazing of the range-extending sea urchin *C. rodgersii* (Johnson *et al.*, 2005; Ling and Jacques, 2009) and not the native sea urchin *Heliocidaris erythrogramma* (Echinometridae) - which forms barrens on sheltered inshore reefs (Ling *et al.*, 2010) but constitutes negligible overall grazing impacts on fully exposed reefs in eastern Tasmania where *C. rodgersii* and its grazing impacts predominantly occur (Fig. 2b).

MECHANISMS OF RANGE-EXTENSION

While migration of benthic adult phases among sea urchins is generally very limited (*C. rodgersii* remain highly localised on rocky reefs whereby they undergo defined nocturnal homing movement [Andrew and Byrne, 2001; Williams *et al.*, 2009; Flukes *et al.*, 2012]), the key life-history stage facilitating long-distance dispersal of sea urchins is the larval phase. For the dioecious free-spawning *C. rodgersii*, adults spawn gametes into the water column where fertilisation occurs (King, 1992; Huggett *et al.*, 2005). Fertilised eggs then rapidly develop into a long-lived two-armed planktotrophic larval stage that exists in the water column for ~100 days before settling to reef substratum (Huggett *et al.*, 2005; reviewed by Byrne and Andrew, in press). This feature of the *C. rodgersii* life-cycle (indeed the common planktonic strategy among echinoids) facilitates long distance dispersal in oceanographic currents. Thus, logically it is likely that the southward incursion of *C. rodgersii* in eastern Tasmania has occurred due to increased larval dispersal driven by changes to patterns of the EAC (as originally raised by Dartnall, 1980).

Within the NSW range, *C. rodgersii* displays a seasonal cycle in gamete production with the major spawning activity occurring in winter (King *et al.*, 1994; Byrne *et al.*, 1998). Given the cooler water temperatures in eastern Tasmania (winter min. ~11 °C) relative to NSW (winter min. ~14°C), the ability of *C. rodgersii* to develop functional gonads, viable gametes and undergo normal larval development was thought to be compromised in the cooler Tasmanian environment. Indeed, Dartnall (1980) interpreted the discovery of *C. rodgersii* in north eastern Tasmania as perhaps a temporary range-extension at the southern distributional limit, clearly articulating that "We await evidence that this population is reproductively self-maintaining...". Thus a situation whereby *C. rodgersii* undergoes annual reproduction in eastern Tasmanian waters will likely facilitate a much more rapid population expansion and opportunity for secondary spread than if Tasmanian populations are only maintained by vagrant pulses of larvae brought south via the EAC (see Fig. 2). Hence initial research on the biology of *C. rodgersii* within the range extension region involved examining evidence for reproductive capability by sampling for the existence of a reproductive cycle, an ability to produce functional gametes and to undergo successful larval development.

REPRODUCTION ON THE EDGE

Demonstrating a clear annual reproductive cycle for *Centrostephanus rodgersii*, sampling of gonad somatic indices (GI) at 4 eastern Tasmanian locations over an 18 month period (Oct 2003 to March 2005, at a 2 month sampling interval) revealed a consistent and defined rise and fall in gonad condition (Fig. 3). As evidenced by a defined drop in GI and maximal response of populations to artificial spawn induction, spawning was isolated to occur during winter with major

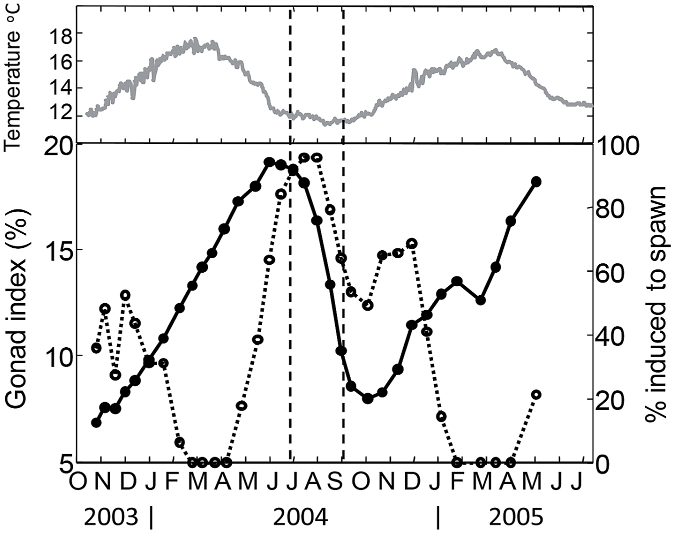

Figure 3. Reproductive cycle of *Centrostephanus rodgersii* as revealed by gonad index and the propensity of population to spawn (following artificial induction) in eastern Tasmania, Oct 2003 - Jun 2005. Smoothed cycles of gonad index (solid line) and % induced to spawn (dotted line) represent a 4 sample running mean calculated across 4 sites spanning the Tasmanian east coast (*after* Ling *et al.*, 2008). Gonad index was calculated from 30 individuals per sample, while propensity to spawn was calculated for each sample as the percentage of 10 individuals responding to spawn induction. Area within the dotted vertical lines indicates the major period of spawning. Top panel shows water temperature on the benthos throughout the sampling period (pooled across for 4 monitoring sites - St. Helens, Bicheno, Maria Is. and Tasman Peninsula; note temperature data prior to 23-Nov-2004 is daily mean for NE Tasmania only).

spawn-out occurring in the month of August (Fig. 3). In addition, the distribution of *C. rodgersii* sexes at each site and for eastern Tasmania as a whole did not deviate significantly from a 1:1 sex ratio (Ling *et al.*, 2008).

Given uncertainty surrounding viability of *Centrostephanus rodgersii* gametes spawned during the coldest month of the year at the cold range limit, fertilization trials were run to test gamete viability. Experiments revealed gametes to be viable, with eggs readily fertilised during the peak winter spawning period, with only a relatively subtle effect of temperature across the cooling gradient from 20 to 8°C (Fig. 4a). Embryonic and larval development for fertilized Tasmanian eggs was normal and the 2-arm pluteus stage was readily reached. While there was a small increase in fertilisation rate with increasing temperature (with 95-99 % fertilized), variation around this trend was large and thus temperature was

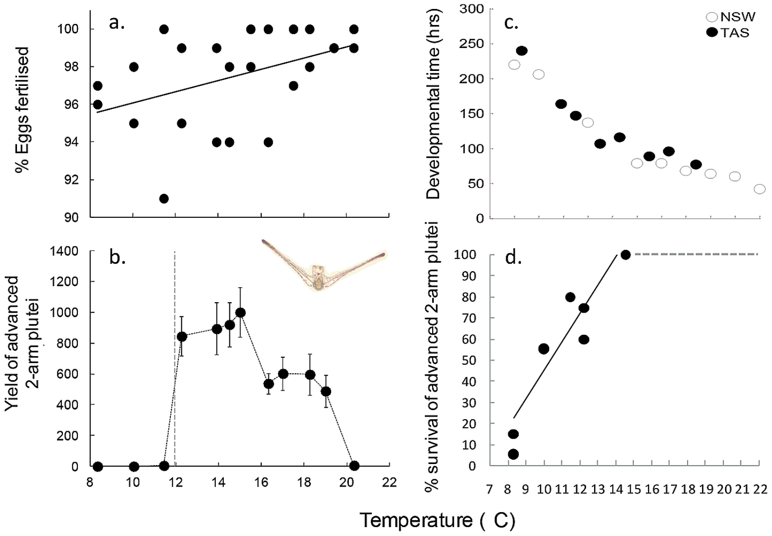

Figure 4. (a.) Temperature dependent fertilisation rates of Tasmanian *Centrostephanus rodgersii.* Data are means for 100 randomly selected eggs from 2 replicate trials, ± SE. While linear regression revealed a significant positive trend (treatment: $F_{1,10}$=18.29, P=0.0016), the fit was relatively poor (R^2=0.65) and the size of the effect small ($y = 0.297x + 93.10$); $F_{1,22}$= 5.26, P<0.05; $y = 0.30x + 93.10$; $R^2 = 0.19$. (b.) Temperature dependent yield of advanced 2-arm plutei of Tasmanian *Centrostephanus rodgersii.* Data are relative yields of advanced 2-arm plutei generated at each temperature treatment expressed as a percentage of the total number of advanced 2-arm plutei produced per trial (means ± SE of n=3 trials); image is of a 2-arm pluteus larva at 21 days post fertilisation (scale bar = 200µm). (c.) Development time to early 2-arm plutei versus water temperature for Tasmanian and NSW reared *Centrostephanus rodgersii* (after Ling *et al.*, 2008). (d.) Survival of 25 day old 2-arm pluteus larvae reared at 14.5°C and placed into a temperature gradient from 14.5 to 8.3°C; n= 2 replicate vials with 20 individual larvae per temperature, survival assessed at 17 days post assignment to temperature treatments (larval rearing as per Ling *et al.*, 2008); solid line is linear fit, $y = 13.52x - 90.36$, R^2 =0.85; $F_{1,8}$=46.93, P<0.001; dashed horizontal line extrapolates high survival across temperature range of 14 to 19°C, note that due to evidence of heat shock for the 20°C treatment (b.), this treatment was excluded from (c.) and hence 100% survival was not extrapolated beyond 19°C in (d.).

considered to have relatively small biological effect on fertilization success over the 8-20 °C range examined (Fig. 4a) – although could magnify greatly in absolute terms given the total number of eggs released into the water column per individual female during spawning; which is likely in the order of 10-100 million eggs as reported for other echinoids (e.g., McShane *et al.*, 1996). But much more striking was a clear threshold type response for the effect of water temperature on development, with essential no successful development to 2-arm plutei occurring in cultures below 12 °C (Fig. 4b).

The observation that Tasmanian *C. rodgersii* undertook spawning in water temperature below 12 °C in 2004 (Fig. 3) was intriguing given that gametes were released into a temperature environment unsuitable for successful larval development. Such a seemingly counter-productive strategy strongly suggested that *C. rodgersii* reproductive phenology had not undergone adaptive shift but was rather controlled by factors other than temperature. Such a notion was supported by research within the NSW range where consistencies in the timing of spawning of *C. rodgersii* occurred across 9 degrees in latitude even though large temperature gradients were present over this range (Byrne *et al.*, 1998). Photoperiod coinciding with the winter solstice appears as a likely proximate factor cuing the onset of spawning across this broad geographic range (Byrne *et al.*, 1998 and references therein), as has been found in other closely related echinoid species (e.g., Kennedy and Pearse, 1975; Coppard and Campbell, 2005). Not only indicating a lack of shift in phenology, a lack of acclimation for *C. rodgersii* within the extended range was also clearly indicated upon examination of the temperature dependency of larval development rate for Tasmanian and NSW larvae. That is, larvae from both NSW and eastern Tasmania showed no difference in developmental rates across temperature (Fig. 4c).

Simulating larvae spawned under normal winter conditions towards the southern margins of the NSW range, i.e. 14°C, advanced plutei larvae showed a pattern of reduced survival when transferred to cooler temperatures as anticipated to occur when larvae are advected south by the EAC to interact with cooler eastern Tasmanian coastal waters (Fig. 4d). That is, while larvae did not develop to advanced stages at temperatures < 12°C, larval survival of advanced plutei was also slightly compromised when larvae grown under warmer conditions, were exposed to cooler temperatures. Furthermore, while larvae were observed to develop to the advanced 2-arm stage above 12°C, survival of larvae grown at 14°C was indeed reduced (by ~20%) when these larvae, typical of NSW waters, were transferred to lower temperature (Fig. 4d). But note that given a 3 month planktonic developmental time, larvae spawned in conditions of 14°C during winter off NSW would likely interact with slightly warmer water (~13°C) relative to winter minima when arriving in eastern Tasmania by ~October.

Of note, recent work by New Zealand researchers identified the optimal temperature range for *C. rodgersii* larval development to be between ~17-23.5°C; which was essentially identical to that observed by the same researchers for *C. rodgersii* at Coffs Harbour in central NSW (Pecorino, *et al.*, 2013). Such a result seemingly contrasts with the above patterns of temperature dependency previously described for larvae from Tasmania and mid NSW whereby larvae were observed to develop to advanced plueti stage at temperatures as low as 12°C, albeit at a slower rate (Ling *et al.*, 2008). Notably, yields of Tasmanian 2-arm plutei crashed above 19 °C (Fig. 4b), suggesting the presence of heat shock at >~7 °C above ambient temperature. But moreover, for Tasmanian larvae, maximum yields were observed at ~15°C (Fig. 4b) and the optimal temperature range (as determined by rate of development) was ~15-19°C (Fig. 4c) indicating slight differences for development of early life history stages in cold environments. Importantly, while larval development occurs above 12°C, larval performance and survival of *C. rodgersii* larvae spawned within and advected to cooler Tasmanian waters (Fig. 4d) will indeed increase if winter sea temperatures warm above 12°C.

NO EVIDENCE FOR A GENETIC BOTTLENECK

Supporting the lack of difference observed for vital physiological rates of larval development between NSW and Tasmanian populations (Fig. 4c), investigation of *C. rodgersii* population genetics with allozyme and microsatellites revealed a lack of founder effect among the extended Tasmanian range as evidenced by low spatial genetic structure across the historical and range-extension zones (Johnson *et al.*, 2005, 2011; Banks *et al.*, 2010). That is, the range shift appears to be a poleward extension of the highly-connected range wide population of *C. rodgersii* involving continued advection and mixing of larvae from population centres within the native NSW range (Johnson *et al.*, 2005, 2011; Banks *et al.*, 2010). Suggesting that evidence for slight differences in thermal optima and heat shock responses between populations is phenotypic in nature (Ling *et al.*, 2008; see also Pecorino *et al.*, 2013). While there was a weak signal in genetic structuring across south east Australia, the underlying trend was for slightly reduced population-specific allele frequencies for the most southern populations in south-east Tasmania relative to central NSW populations (Banks *et al.*, 2010; Johnson *et al.*, 2005, 2011).

Genetic results therefore corroborate with the population age structure and patterns predicted from the vital physiological threshold for larval development across the extended range (Ling *et al.*, 2009a). That is, the broad range of *C. rodgersii* ages in north eastern Tasmania indicates that the range extension has not occurred as the result of a single, massive recruitment event. Rather, as supported by genetics (Johnson *et al.*, 2005, 2011; Banks *et al.*, 2010), age structure reveals multiple episodes of sea urchin recruitment with seemingly fewer and more recent recruitment events towards the southern limit of the extension-region (Fig. 2c). Thus combined, field, laboratory and genetic results support the recent nature of the *C. rodgersii* range-extension given that adaptive shifts to thermal tolerance would likely require many generations to evolve within the cooler Tasmanian environment. But moreover evidence for fixed temperature dependency of early development re-doubles the importance of environmental change in causing range-extension in this sea urchin species. That is, patterns of environmental change should largely determine the distribution and abundance of *C. rodgersii* and thus ultimately its abundance and propensity to cause widespread sea urchin barrens.

RESPONSE TO COASTAL WARMING

Long-term monitoring of sea surface temperature in eastern Tasmania has revealed an average warming of ~1.5 °C over the past 60 years, predominantly due to a greater influence of the EAC on this coast (Ridgway, 2007). Importantly, while the EAC is typically thought of as a summertime phenomenon, this warming trend in eastern Tasmania is also apparent during winter months, such that temperatures above the ~12 °C threshold for larval development are becoming frequent during the major spawning period (Fig. 5a) and are likely to arise with increasing frequency given anticipated ongoing coastal warming associated with global climate change (Cai *et al.*, 2005). Continued coastal warming will directly increase survival of *C. rodgersii* (Fig. 4d) plus also reduce overall larval development time (Fig. 4c) which may in turn enhance larval survival and increase the likelihood of self-recruitment of *C. rodgersii* within Tasmania due to decreased exposure to potentially hazardous planktonic conditions (e.g., Morgan, 1995).

Because eastern Tasmania represents the southern range extent where coastal waters are cold (~10–18 °C) relative to NSW (~13-25 °C), logically the observed distribution of *C. rodgersii* in Tasmania should track the moderating influence of the warm EAC along this coast (Ridgway, 2007; see Fig. 2a). Furthermore, any limiting effects of cold water on the development and survival of the sea urchin in Tasmania would most likely be felt during winter such that any temperature patterns driving distribution of *C. rodgersii* would likely manifest during winter. Indeed examination of *C. rodgersii* distribution with respect to winter water temperature revealed that the sea urchin generally occurs at sites existing above the 12°C threshold. That is, examination of mean SST for 41 eastern Tasmanian sites during the known *C. rodgersii* spawning period of August (winter), revealed that the sea urchin is generally limited to sites experiencing relatively warm winter temperatures in eastern Tasmania (Fig. 5b). However, variability in this signal across warmer winter sites suggests that factors other than temperature *per se* are important in determining patterns in abundance such as reef habitat quality (particularly high relief boulder habitat where *C. rodgersii* is found in higher abundance and where the risk of predation is lower, Ling and Johnson, 2012), or there exists local barriers to dispersal of sea urchin larvae.

At local-scales in eastern Tasmania, *C. rodgersii* is observed to be abundant on headland areas with examination of sea temperature profiles revealing warmer winter temperatures at the local-scale of these features which demonstrated a greater proportion of winters >12 °C relative to adjacent inshore sites where fewer or no *C. rodgersii* were established (Fig. 6a-c). Overall headlands expressed more moderate climates relative to inshore areas where seasonal temperature fluctuated with greater amplitude, with these shallower inshore environments appearing to be forced to a greater extent by seasonal atmospheric heating and cooling to become considerably warmer in summer but cooler in winter relative to headland sites (Fig. 6a-c). Closer to the EAC, headland sites were also more likely project

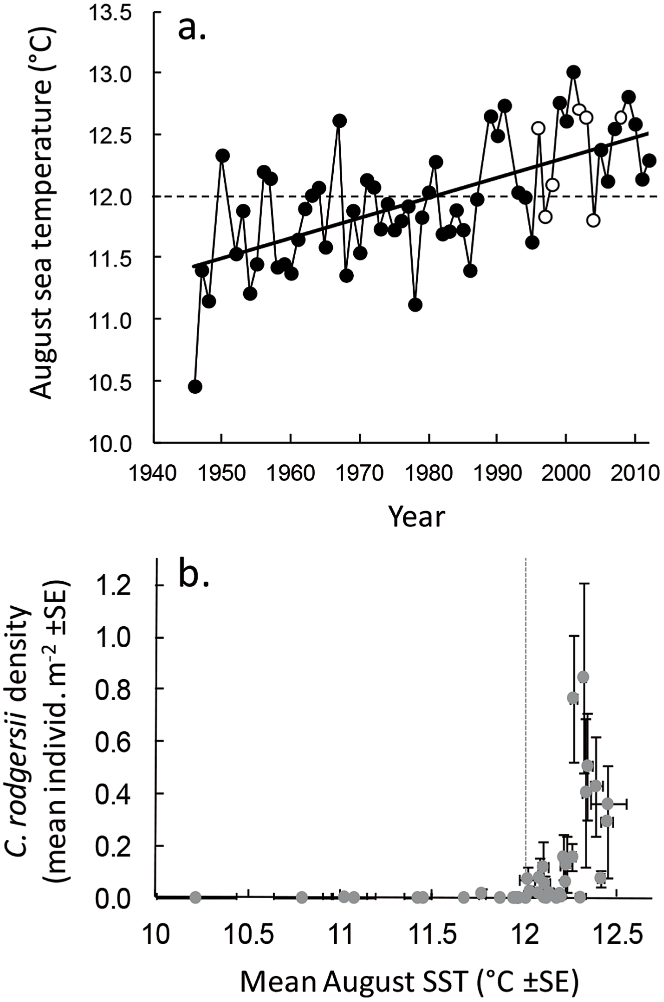

Figure 5. (a.) Long-term winter warming trend of coastal waters in eastern Tasmania, 1946-2012. Data are sea temperatures from the Maria Island coastal station (148° 13' E, 42° 36' S) averaged across depth (0-50 m) for August, i.e. the month of major spawning (data courtesy of CSIRO Marine & Atmospheric Research). Note that the water column is mixed across this depth range during August. Open symbols represent robust satellite derived estimates of sea surface temperature at the long-term station for recent years with missing *in situ* data (for demonstration of robust corroboration of SST with *in situ* temperature measurements *see* Ridgway, 2007). Dashed horizontal line at 12ºC indicates the approximate minimum larval development threshold for Tasmanian *Centrostephanus rodgersii.* (b.). Abundance of *C. rodgersii* as a function of mean winter temperature (mean SST derived from satellite images for the period 1993-2006) for 41 sites in eastern Tasmania.

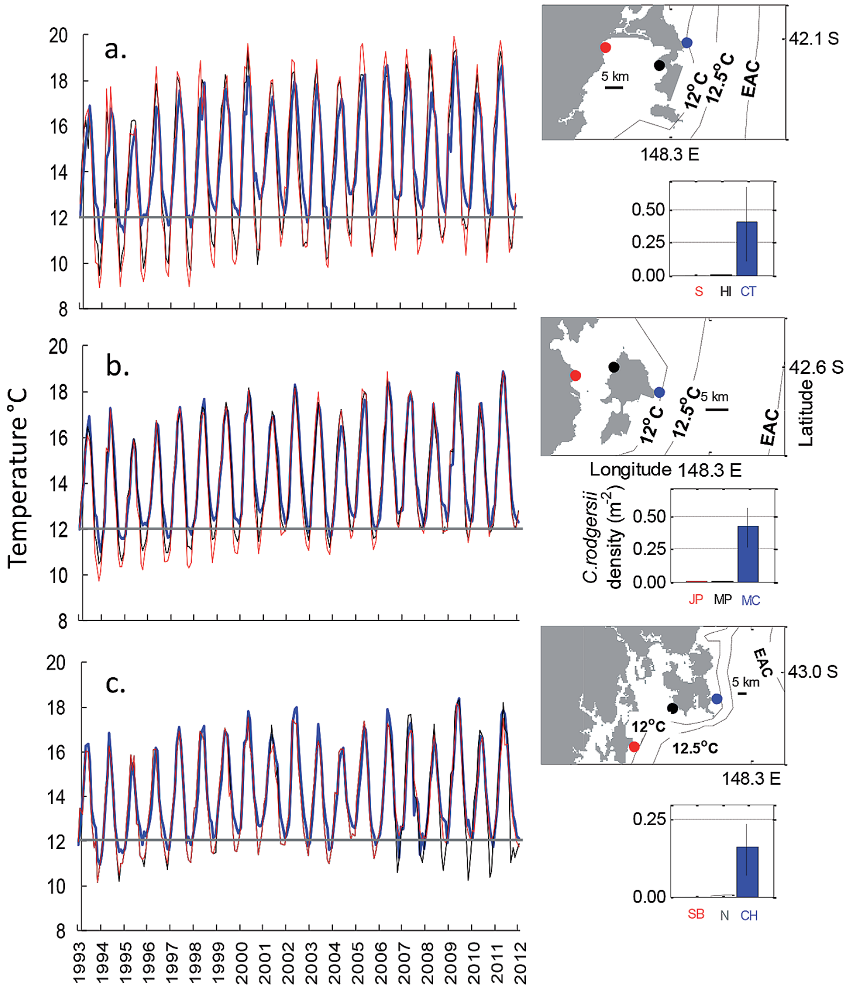

Figure 6. Seasonal temperature profiles and abundance of *Centrostephanus rodgersii* at 'headland' and adjacent inshore reefs. Data are SST for 1993-2012; thickened lines are data obtained from *in situ* temperature loggers. Horizontal bar on temperature plots indicates the lower temperature threshold (12 °C) for *C. rodgersii* larval development (after Ling *et al.*, 2008); numbers in parentheses below indicate proportion of winters > 12 °C at each site for 1993-2012. (a.) Freycinet Peninsula: CT=Cape Tourville (0.43); HI=Hazards Is. (0.00), S=Swansea (0.00); (b.) Maria Island: MC=Mistaken Cape (0.46), MP=Magistrates Pt. (0.00), JP=Johnson's Pt. (0.00); (c.) Tasman Peninsula: CH=Cape Huay (0.38), N=Nubeena (0.07), SB=South Bruny (0.07). For locations within Tasmania, refer to Figure 1. On maps, isotherms and western EAC margin represent mean positions for winter 1993-2006. *C. rodgersii* abundance data for HI and S, in panel (a.) courtesy of N. Barrett.

further beyond potential coastal boundary layers and so more frequently sample offshore currents (Ling *et al.*, 2009a). Thus, in eastern Tasmania the EAC appears to drive milder winters for offshore reefs and for north east Tasmanian reefs in general by having a greater influence on the thermal dynamics at such sites, essentially maintaining a temperature regime above the critical 12°C threshold for early development of *C. rodgersii.* Thus while the EAC is the chief vector for poleward transport of *C. rodgersii* larvae, as initially suggested by Dartnall (1980), purported by Edgar (1997) and concurred by Johnson and co-workers (2005, 2011) plus Banks and co-workers (2007, 2010), the dual role of this oceanic feature in providing a suitable thermal regime for *C. rodgersii* larval development is now also appreciated (Ling *et al.*, 2009a).

FUTURE TRENDS

Given that Tasmanian reared *C. rodgersii* displayed normal embryonic and larval development to the 2-arm pluteus stage within 12–20 °C (Fig. 4b), it is likely that the sea urchin successfully propagates larvae throughout its current Tasmanian range in years when the winter temperature during the major spawning period is ≥~12 °C. As evidenced from laboratory studies in NSW, Tasmania and New Zealand, overall larval performance would also appear poised to further increase as eastern Tasmanian coastal waters continue to warm above this critical temperature threshold as predicted by general climate change models and specifically for the SE Australian region. Combining a trend of increasing population size with reproductive capability, suggests that aided by a new thermal regime, *C. rodgersii* has established viable populations along the eastern Tasmanian coastline. Thus in highlighting links between *C. rodgersii* population trends and the physical environment across the Tasmanian extension-region, ongoing climate change appears poised to have further positive effects on *C. rodgersii* abundance by 1) increasing the extent of thermally suitable reef habitat as a direct result of atmospheric forced ocean warming (Fig. 7c); and 2) by driving further poleward supply of larvae and accelerating a warmer coastal regime as a result of ongoing intensification of the EAC (as predicted by Cai *et al.*, 2005; Cai, 2006).

Of note, ongoing climate change driven by anthropogenic increase in CO_2 emissions will not only continue to warm sea temperatures owing to the greenhouse effect and overall amplification of global weather systems including ocean currents, but will also alter sea water chemistry due to the process of ocean acidification (OA; e.g., Feely *et al.*, 2004). While OA appears particularly dire for calcium carbonate “shell-forming” invertebrates, there appears a great amount of variability in the response of different marine shell-forming invertebrates to this stressor (reviewed by Dupont *et al.*, 2010; Byrne *et al.*, 2011). Scenarios of OA have been investigated in the laboratory for *C. rodgersii* with the response of fertilization and early larval development processes to lower pH levels, as predicted

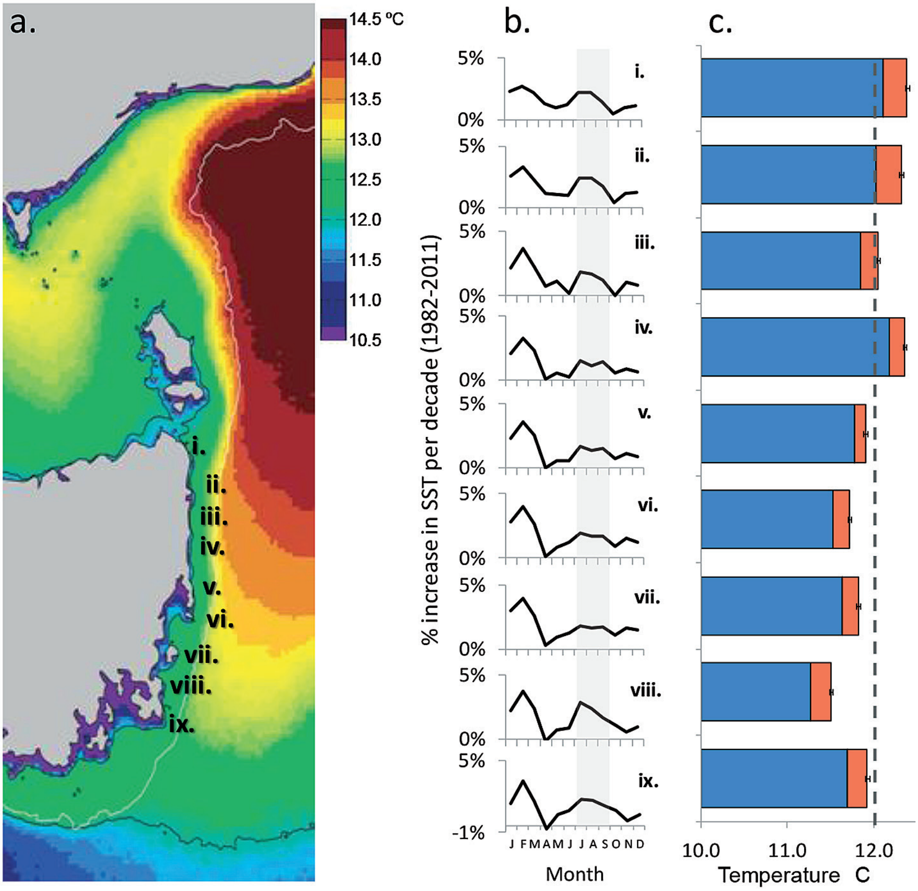

Figure 7. Spatial and seasonal patterns of sea warming across the Tasmanian east coast, 1982-2011. (a.) Map of eastern Tasmania showing sites (i-ix) examined for long-term SST change, SST map as per Fig. 1. (b.) Percent change in SST for each month of the year across eastern Tasmania revealing a clear pattern of summer and winter warming, grey band indicates the Austral winter (July-Sep) centred on the month of August when spawning by *Centrostephanus rodgersii* occurs. (c.) Mean August SST at each site during 2011, blue region of bar is SST in 1982 as back calculated (linearly) from observed level of warming (red region of bar) between 1982 and 2011. Dashed vertical line at 12°C indicates the approximate minimum larval development threshold for Tasmanian *C. rodgersii.* Coastal SST warming is based on the AVHRR V2 NOAA Optimum Interpolation 1/4 Degree Daily Sea Surface Temperature Analysis data (see Acknowledgments for data source).

for the year 2100, considered to be relatively robust compared to some other shell-formers and subtle relative to strong positive effects of ocean warming on rates of larval development (Byrne *et al.*, 2011; Pecornio, 2012; Foo *et al.*, 2012; reviewed by Byrne and Andrew, in press).

However inferring likely impacts of OA in nature is currently difficult as unlike the clear evidence of coastal warming and range-shift of *C. rodgersii* in eastern Tasmania (Figs. 5-7) there is at present a lack of field measurements of the current variability in pH levels across the distributional range of *C. rodgersii.* This is important as several coastal areas throughout the world show high urchin abundance yet demonstrate high daily variability in pH, with minimum pH readings often lower than that predicted to occur by the year 2100 (e.g., Hofmann *et al.*, 2011; J.C. Hernández, unpublished data). Given the potential for large spatial and temporal variability in pH, effects of OA are unlikely to be homogenous across the range of *C. rodgersii* and will not occur independently of changing thermal regimes with interactive effects between both these climate change stressors predicted to occur in the longer term (Foo *et al.*, 2012). Therefore a more complete understanding of current variability in pH across the distributional range of *C. rodgersii* (which clearly shows strong thermal variability) is required such that a firmer basis for predicting negative effects of OA at the individual (juvenile to adult stages), population and ultimately at the ecosystem level can be achieved.

While baseline surveys of *C. rodgersii* abundance conducted in eastern Tasmania in 2001/02 (Johnson *et al.*, 2005) have not been completely resurveyed, trained citizen scientists partially resurveyed all 9 baseline locations in eastern Tasmania in 2008/09 (on average 38% of all sites within a location were resurveyed). Importantly, there was no change in the rank abundances of *C. rodgersii* across locations between 2001/02 and 2008/09 with a slight, but not significant, overall increase in *C. rodgersii* abundance being observed (Ling and Jacques, 2009). The observed increase (while difficult to interpret given that not all sites within a location were re-surveyed) is consistent with an apparent gradual increase in sea urchin abundance within individual sites, which appeared largely accounted for by an apparent strong recruitment to the cryptic/ newly emergent size class (<70 mm TD) as such individuals became more frequently observed during 2008 at most sites (particularly among grazed rocky reef) that were regularly visited since 2001/02 (author's pers. obs.). Thus the anticipated pattern of population expansion is one of a gradual but steady increase in settlement, particularly for sites already containing the sea urchin, followed by emergence of sea urchins to the reef surface whereby such individuals can ultimately commence overgrazing once adequate size is attained (at ~ 7 years of age). Once such individuals become locally abundant then rates of grazing appear to become sufficient to overwhelm kelp beds and maintain widespread sea urchin barrens grounds. Indeed evidence from the age structure of populations in eastern Tasmania supports such a notion of gradual population building towards a critical transition in the rate of herbivory (Fig. 8).

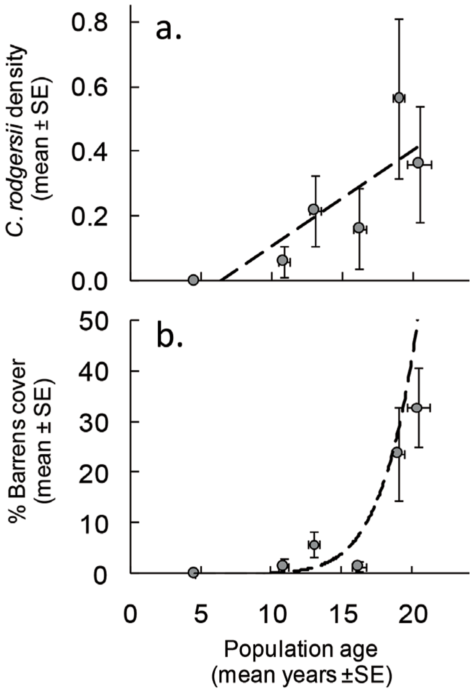

Figure 8. *Centrostephanus rodgersii* population density *versus* mean population age (a.), and percent cover of urchin barrens *versus* mean population age across the eastern Tasmanian range extension region. In (a.) linear fit described by y=0.029x - 0.187, R^2 = 0.70; in (b.) power curve described by y = 1E-09$x^{8.15}$; R^2 = 0.92.

RESILIENCE OF KELP BEDS TO OVERGRAZING

A gradual build-up of *Centrostephanus rodgersii* within kelp beds prior to a critical tipping point towards sea urchin barrens is further supported by data collected across eastern Tasmania whereby a range of sea urchin biomasses can be sustained by kelp beds but then a critical tipping point in grazing is reached and catastrophic phase-shift to urchin barrens occurs (Fig. 9). That is, the transition between kelp beds and *C. rodgersii* barrens provides an example of a classic non-linear 'catastrophic shift' between alternative and stable reef states with a strong hysteresis effect, as return to the kelp dominated state requires reducing sea urchin biomass to much lower levels than the critical 'tipping' point at which destructive overgrazing occurred in the first place (see alternative 'forward' and 'reverse' phase shift paths in Fig. 9). Ultimately, *C. rodgersii* overgrazing in eastern Tasmania causes the underlying ecosystem dynamic to shift to an alternative

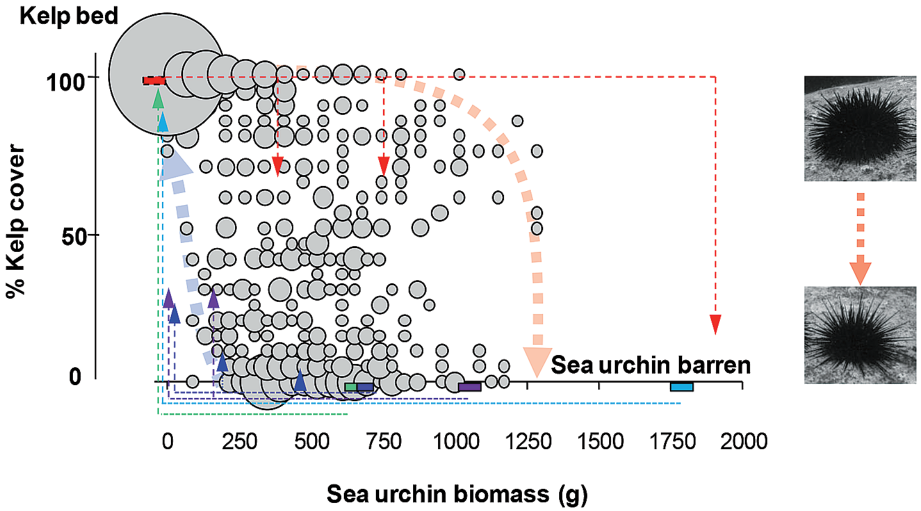

Figure 9. Catastrophic phase-shift between kelp beds and *Centrostephanus rodgersii* barrens. Bubble plot of kelp bed cover *versus* sea urchin biomass density per square metre for eastern Tasmania. Bubbles represent relative frequency of particular urchin density and seaweed cover combinations as measured in 575 individual 5 m^2 plots (data for 415 plots from Johnson *et al.*, 2005). Dashed arrows indicate magnitude and direction of ecosystem response to removals of *C. rodgersii* from a starting biomass density as indicated by rectangles; manipulated biomass density is where the arrow originating at rectangle takes a 90° turn from the x-axis, with the length of the arrow from the x-axis indicating the observed response in kelp cover after a given period of time (as specified below). Red rectangle/ arrows is that observed after ~5 months by Hill *et al.*, 2003 following additions of *C. rodgersii* to seaweed beds in NSW; dark blue is the response observed by Hill *et al.*, 2003 at ~5 months following sea urchin reductions on barrens in NSW; purple and light blue is response observed after 18 mths in NSW by Andrew and Underwood, 1993 and Andrew, 1998 respectively; light green is response after 18 mths observed in Tasmania by Ling, 2008. Broad dashed curves in background represent alternative «forward-shift» (kelp to barrens; red curve) and «reverse-shift» (barrens back to kelp) paths (after Scheffer *et al.*, 2001). Images of *C. rodgersii* show alternative morphologies associated with seaweed-beds (short-spines) and barrens (long-spines) (after Ling and Johnson, 2009).

domain of attraction characterized by the sea urchin barrens state which by definition has its own self-maintaining feedback mechanisms (Ling *et al.*, 2009b). Such non-linear or “catastrophic phase shift” (reviewed by Scheffer *et al.*, 2001) between desirable and undesirable ecosystem states are of particular concern to natural resource management as recovery of ecosystems appears exceedingly difficult to achieve once change has occurred.

Given the threat of climate-driven increases in *C. rodgersii* abundance and increasing risk of catastrophic shift of kelp beds to extensive sea urchin barrens grounds, a key research question was to examine mechanisms of resilience of kelp beds against the climate-driven stressor of increasing sea urchin abundance. Indeed, coincident with the arrival and expansion of *C. rodgersii* is heavy fishing of Tasmanian rocky reef systems including fishing down benthic species capable of preying on sea urchins. Previously, Pederson and Johnson (2006) demonstrated that the spiny lobster (*Jasus edwardsii* – Palinuridae) was an important predator of the native Tasmanian sea urchin *Heliocidaris erythrogramma* (Echinometridae), but lobsters were only an effective predator of adult sea urchins when lobsters were larger than the legal-size limit of 110 mm carapace length. Furthermore, labrids (wrasse) were also observed to consume *H. erythrogramma* but per capita predatory effects were considered much lower than that caused by lobsters (Pederson and Johnson, 2006).

Similar to patterns described for *Heliocidaris erythrogramma* (Johnson *et al.*, 2004; Pederson and Johnson, 2006), broad-scale *in situ* surveys spanning eastern Tasmania indicated a negative ceiling distribution between lobster abundance and *C. rodgersii* (Johnson *et al.*, 2005, 2011). To explicitly test the influence of predation on the range-extending *C. rodgersii*, multiple experiments were used utilising comparisons between long-term research reserves (where predators had recovered post cessation of fishing) with sites open to fishing and thus experiencing ongoing harvest of lobsters to examine the possibility that a reduction in predators has reduced resilience of kelp beds and increased the likelihood of widespread barrens formation by *C. rodgersii*. Initially, remote video surveillance inside no-take Marine Protected Areas (MPAs) identified that the lobster *Jasus edwardsii*, frequently predated tethered and non-tethered *C. rodgersii* and was a more important predator of *C. rodgersii* than fish (Table 1a). Furthermore, from a calibrated field-of-view, video monitoring, in combination with caging and laboratory experiments, revealed that only supra-legal sized lobsters (carapace length ~> 140 mm) were capable of effectively preying on *C. rodgersii* (Ling *et al.*, 2009b).

Predation rates on *C. rodgersii* were much higher inside no-take MPA boundaries (Fig. 10) which contained a high abundance of large lobsters (≥140 mm CL) compared to adjacent fished reef with nil large lobsters (Table 1b). Notably, there was no difference between protected and unprotected reef in the abundance of predatory fishes that could potentially prey on the sea urchin, albeit observed for small size-classes of sea urchin only (Table 1b). Because of intensive fishing, large lobsters are now functionally extinct along much of the coastline (Fig. 11) with the combined evidence suggesting strongly that removal of large (supra-legal) predatory-capable lobsters has effectively reduced resilience of macroalgal beds and increased the risk of wide-spread barrens formation by the range extending *C. rodgersii* (Ling *et al.*, 2009b). In addition, experimental results inside and outside Tasmanina marine reserves clearly show that both size and habitat specific factors define the survival of *C. rodgersii* which indicates that

TABLE 1. (a.) Summary of predator identity and diel timing of predation on *in situ Centrostephanus rodgersii* as observed by video monitoring inside marine reserves in eastern Tasmania. a(i). Video monitoring of tethered *C. rodgersii* inside marine reserves [Maria Island Marine Reserve (MIMR) and Crayfish Pt. Marine Reserve (CPMR) (12 and 33 years protection at time of experimentation respectively)]; predator identity was discernable for a total of 26 predation events observed by monitoring a total of 47 individual sea urchins over a total of 28 days and nights. a(ii). Video monitoring of non-tethered, non-tagged *C. rodgersii* housed in partial cages at CPMR (Dec - Jan 2006); a total of 4 predation events were witnessed over 8 days and nights; for lobsters and wrasse, large corresponds to ≥140 mm Carapace Length and >300 mm TFL respectively. (b.) Mean abundance of large lobsters and wrasse averaged for experimental reefs inside and outside reserves; mean values are averages across MIMR & CPMR and adjacent fished sites with the value of each site obtained using n=6 fifty metre long belt transects (4 m wide for lobsters and 10 m wide for fish) assessed *in situ* by divers (*see* Ling & Johnson 2012 for details).

a.	Predator	% of total predation events witnessed	
		Diurnal	Nocturnal
	i). Tethered *Centrostephanus rodgersii*		
	Large spiny lobster (*Jasus edwardsii*)	0 %	92 %
	Large Blue-throated wrasse (*Notolabrus tetricus*)	8 %	0 %
	ii). Partially caged *Centrostephanus rodgersii*		
	Large spiny lobster (*Jasus edwardsii*)	0 %	100 %

		Mean abundance 200m^{-2}	
b.	Predator	Reserve	Fished
	Large spiny lobster (*Jasus edwardsii*)	2.5 ± 0.9	0.0 ± 0.0
	Large blue-throated wrasse (*Notolabrus tetricus*)	± 0.3	0.9 ± 0.1

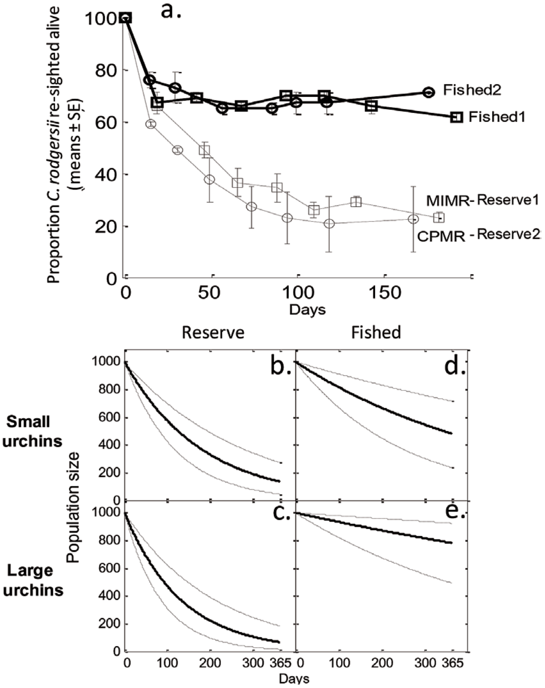

Figure 10. (a.) Percentage of tagged *Centrostephanus rodgersii* resighted through time at experimental reefs inside marine reserves (dotted lines; CPMR and MIMR) and at adjacent fished sites (solid lines) outside marine reserves, n=96 urchins per reef. Sites were located in Mercury Passage (Triangles); and the Derwent Estuary (circles). (b. - e.) Projection of annual population trajectories based on empirically observed mark-recapture survival rates applied to hypothetical populations of 1,000 small (b. - c.) and large (d. - e.) *C. rodgersii* 'invading' reef inside and outside marine reserves (after Ling and Johnson, 2012). Dotted lines indicate upper and lower 95% confidence intervals.

ecosystem impacts mediated by the climate driven range-extension of the sea urchin will be heterogeneous across different habitats, and that the likelihood and spatial extent of barrens will, all else being equal, be greater where urchin populations experience minimal predation risk within such novel systems (Ling and Johnson, 2012). That is, reefs protected from fishing, where the abundance of large predatory lobsters and predators in general (including labrids) is large, will maximise the resilience of kelp beds and reduce the likelihood and extent of catastrophic overgrazing.

While this clearly highlights the importance of predators for maximising resilience of kelp beds to overgrazing in the first instance, it is important to note

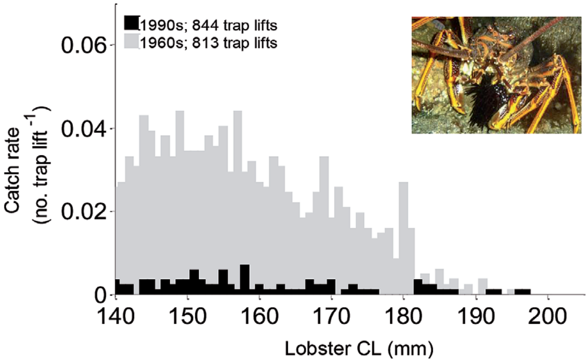

Figure 11. Change in size-frequency of the spiny lobster *Jasus edwardsii* pre- and post-intensive fishing in remote north eastern Tasmania for the large predatory capable size-class (CL ≥ 140 mm) observed to prey on *C. rodgersii* (data are for male lobsters which dominant larger size-classes, redrawn from Frusher, 1997). Inset image shows a large *J. edwardsii* (160 mm CL) preying on *C. rodgersii*; note prominent 1st pair of thoracic appendages used to grasp urchin.

that potential for predator driven recovery of barrens ground (once formed) appears to operate under a different dynamic due to the inherent hysteresis effect evident in this system (non-linear dynamics in the system). For example, take a starting sea urchin biomass of 850 g m^{-2} (~2 individuals m^{-2}) and assume strict adherence to the barrens formation ('forward-shift') and seaweed recovery ('reverse-shift') paths (Fig. 9). In the kelp bed dominated state, urchin biomass only needs to increase from ~1000 g m^{-2} to ~1250 g m^{-2} (an increase of 250 g m^{-2}) for the system to shift to the barrens state. Alternatively, assuming the same 1000 g m^{-2} starting biomass of urchins in the barrens state, and following the kelp recovery ('reverse-shift') path, urchin biomass must decrease to approx. < 125 g m^{-2} (a decrease of 875 g m^{-2}) for the system to return to the kelp dominated state. Thus conceptually, approx. 3.5 times as much urchin biomass must be consumed by predators to revert barrens to seaweed beds as that required to maintain the seaweed dominated state by keeping urchin density just below the 'forward-shift' threshold for barrens formation (Fig. 9).

Notably however, there appear other factors seemingly further stabilising the sea urchin barrens state once formed. That is, *C. rodgersii* on widespread barrens appear less vulnerable to predation as such individuals possess relatively long and more protective spines for a given test diameter (and age) compared to individuals observed within seaweed habitat where spines are frequently eroded by whiplash of robust seaweeds under the influence of ocean surge (Fig. 9). In addition, recruitment of juvenile sea urchins appears to be higher on urchin barrens compared to algal covered reef (e.g., Hernández *et al.*, 2010).

SUMMARY

The transition between the alternative seaweed dominated and sea urchin barrens states appears to be influenced by many processes operating across a wide spectrum of spatial and temporal scales. This includes oceanic processes affecting dispersal, larval development and settlement of urchins from the plankton (e.g., Hart and Scheibling, 1988; Ling *et al.*, 2008, 2009a); habitat preferences (e.g., Andrew, 1993; Ling and Johnson, 2012); storm events (e.g., Andrew, 1991); effects of sweeping macroalgae (e.g., Konar and Estes, 2003; Ling and Johnson, 2009); predation (e.g., Tegner and Levin, 1983; Estes and Duggins, 1995; Shears and Babcock, 2002; Ling *et al.*, 2009b; Ling and Johnson, 2012); and disease cycles (e.g., Lessios *et al.*, 1984; Scheibling and Hennigar, 1997). Thus, such reef assemblages are clearly complex and dynamic systems typified by high variability and shaped by interactions between physical and biological processes acting across multiple scales (e.g., Tegner and Dayton, 2000; Steneck *et al.*, 2002).

As evidenced from broad-scale field surveys, field manipulations and laboratory experiments the changing climate of eastern Tasmania has become increasingly suitable for *Centrostephanus rodgersii*. The timing of the sea urchins' arrival, age-structure and spatial distribution across the extension-region is consistent with patterns in warming sea temperatures and current-driven dispersal potential. Continued warming predicted for this region will favour increased larval survival, promoting ongoing population expansion and ultimately increased likelihood of populations reaching sufficient density to affect widespread overgrazing over a greater spatial extent of this coastline. Furthermore, heavy fishing of sea urchin predators also favours continuing population expansion and grazing impacts by the sea urchin. Thus while global climate change and overfishing may independently pose major threats to ecosystem dynamics, as reviewed here, the interaction between such broad scale perturbations demonstrates that it is the combined effects of multiple stressors that lead to unprecedented risk of catastrophic shifts in coastal ecosystems. Therefore, management of non-climatic local scale stressors, such as mediating the effects of heavy fishing on sea urchin predators, is an approach to increase resilience of kelp beds against overgrazing given climate-driven increases in this key sea urchin population.

ACKNOWLEDGEMENTS

The primary research literature by the author on *Centrostephanus rodgersii* in eastern Tasmania, as referred to in this review, was supported by the University of Tasmania (UTas), Tasmanian Abalone Council, and Fisheries Research and Development Corporation #2001/044 (to Craig Johnson); while undertaking these primary research activities the author received scholarship support from UTas and was a member of the UTas / Commonwealth Scientific and Industrial

Research Organization Joint PhD Program in Quantitative Marine Science. Katherine Jones and Pete Strutton assisted with extracting updated fine-scale SST trends for inshore and offshore sites in eastern Tasmania. Coastal SST warming trends for 1982 to 2011 were obtained from the Worldwide Coastal Warming Assessment project website at htttp://www.coastalwarming.org (2012).

REFERENCES

Andrew, N.L. (1991) Changes in subtidal habitat following mass mortality of sea urchins in Botany Bay, New South Wales. *Australian Journal of Ecology*, 16, 353–362.

Andrew, N.L. (1993) Spatial heterogeneity, sea urchin grazing, and habitat structure on reefs in temperate Australia. *Ecology*, 74, 292–302.

Andrew, N.L. and O'Neill, A.L. (2000) Large-scale patterns in habitat structure on subtidal rocky reefs in New South Wales. *Marine and Freshwater Research*, 51, 255–263.

Andrew, N.L. and Underwood, A.J. (1992) Associations and abundance of sea urchins and abalone on shallow subtidal reefs in southern New South Wales. *Australian Journal of Marine and Freshwater Research*, 43, 1547–1559.

Andrew, N.L. and Underwood, A.J. (1993) Density-dependent foraging in the sea urchin *Centrostephanus rodgersii* on shallow subtidal reefs in New South Wales, Australia. *Marine Ecology Progress Series*, 99, 89–98.

Andrew, N., Worthington, D.G., Brett, P.A. and Bentley, N. (1998) *Interactions between the Abalone Fishery and sea urchins in New South Wales.* Final Report to FRDC 1993/102 NSW Final Report Series No. 11.

Banks, S.C., Piggot, M.P., Williamson, J.E., Bové, U., Holbrook, N.J. and Beheregaray, L.B. (2007) Oceanic variability and coastal topography shape genetic structure in a long-dispersing sea urchin. *Ecology*, 88, 3055–3064.

Banks, S.C., Ling, S.D., Johnson, C.R., Piggott, M.P., Williamson, J.E. and Beheregaray, L.B. (2010) Genetic structure of a recent climate change-driven range extension. *Molecular Ecology*, 19, 2011–2024.

Byrne, M. and Andrew, N.L. (in press) The ecology of *Centrostephanus rodgersii. Edible Sea Urchins: Biology and Ecology.* (ed. by Lawrence, J.M.). Elsevier Science.

Byrne, M. (2011) Impact of ocean warming and ocean acidification on marine invertebrate life history stages: Vulnerabilities and potential for persistence in a changing ocean. *Oceanography and Marine Biology: An Annual Review*, 49, 1–42.

Byrne, M., Andrew, N.L., Worthington, D.G. and Brett, P.A. (1998) Reproduction in the diadematoid sea urchin *Centrostephanus rodgersii* in contrasting habitats along the coast of New South Wales, Australia. *Marine Biology*, 132, 305–318.

Cai, W.J., Shi, G., Cowan, T., Bi, D. and Ribbe, J. (2005) The response of southern annular mode, the East Australian Current, and the southern midlatitude ocean circulation to global warming. *Geophysical Research Letters*, 32, L23706.

CAI, W. (2006) Antarctic ozone depletion causes an intensification of the Southern Ocean super-gyre circulation. *Geophysical Research Letters*, 33, L03712.

COPPARD, S.E. and CAMPBELL, A.C. (2005) Lunar periodicities of diadematid echinoids breeding in Fiji. *Coral Reefs*, 24, 324–332.

DARTNALL, A.J. (1980) Tasmanian Echinoderms. *Fauna of Tasmania Handbook No. 3.* Hobart, Fauna of Tasmania Committee.

DAYTON, P.K., TEGNER, M.J., EDWARDS, P.B. and RISER, K.L. (1998) Sliding baselines, ghosts, and reduced expectations in kelp forest communities. *Ecological Applications*, 8, 309–322.

DUPONT, S., ORTEGA-MARTÍNEZ, O. and THORNDYKE, M. (2010) Impact of near-future ocean acidification on echinoderms. *Ecotoxicology*, 19, 449–462.

EDGAR, G.J. (1997) *Australian Marine Life.* Reed, Kew, Victoria.

ESTES, J.A. and DUGGINS, D.O. (1995) Sea otters and kelp forests in Alaska: generality and variation in a community ecological paradigm. *Ecological Monographs*, 65, 75–100.

FEELY, R.A., SABINE, C.L., LEE, K., BERELSON, W., KLEYPAS, J., FABRY, V.J. and MILLERO, F.J. (2004) Impact of anthropogenic CO_2 on the $CaCO_3$ system in the oceans. *Science*, 305, 362–366.

FLETCHER, W.J. (1987) Interactions among subtidal Australian sea urchins, gastropods and algae: effects of experimental removals. *Ecological Monographs*, 57, 89–109.

FLUKES, E., JOHNSON, C.R. and LING, S.D. (2012) Forming sea urchin barrens from the inside-out: an alternative model of overgrazing. *Marine Ecology Progress Series*, 464, 179–194.

FOO, S.A., DWORJANYN, S.A., POORE, A.G.B. and BYRNE, M. (2012) Adaptive capacity of the habitat modifying sea urchin *Centrostephanus rodgersii* to ocean warming and ocean acidification: performance of early embryos. *PloS One*, 7, e42497.

FRUSHER, S.D. (1997) *Stock assessment report: rock lobster. Government of Tasmania, Australia, Internal report No. 35.* Tasmanian Department of Primary Industry and Fisheries, Hobart.

HARLEY, C.D.G., HUGHES, R.A., HULTGREN, K.M., HULTGREN, K.M., MINER, B.G., SORTE, C.J.B., THORNBER, C.S., RODRIGUEZ, L.F., TOMANEK, L. and WILLIAMS, S.L. (2006) The impact of climate change in coastal marine systems. *Ecology Letters*, 9, 228–241.

HART, M.W. and SCHEIBLING, R.E. (1988) Heat waves, baby booms, and the destruction of kelp beds by sea urchins. *Marine Biology*, 99, 167–176.

HERNÁNDEZ, J.C., CLEMENTE, S., GIRARD, D., PEREZ-RUZAFA, A. and BRITO, A. (2010) Effect of temperature on settlement and postsettlement survival in a barrens-forming sea urchin. *Marine Ecology Progress Series*, 413, 69–80.

HILL, N.A., BLOUNT, C., POORE, A.G.B., WORTHINGTON, D. and STEINBERG, P. (2003) Grazing effects of the sea urchin *Centrostephanus rodgersii* in two contrasting rocky reef habitats: effects of urchin density and its implications for the fishery. *Marine and Freshwater Research*, 54, 691–700.

Hofmann, G.E., Smith, J.E., Johnson, K.S., Send, U., Levin, L.A., Micheli, F., Paytan, A., Price, N.N., Peterson, B., Takeshita, Y., Matson, P.G., Crook, E.D., Kroeker, K.J., Gambi, M.C., Rivest, E.B., Frieder, C.A., Yu, P.C. and Martz, T.R. (2011) High-frequency dynamics of ocean pH: a multi-ecosystem comparison. *PLoS One*, 6, e28983.

Huggett, M.J., King, C.K., Williamson, J.E. and Steinberg, P.D. (2005) Larval development and metamorphosis of the Australian diadematid sea urchin *Centrostephanus rodgersii. Invertebrate Reproduction and Development*, 47, 197–204.

Johnson, C.R., Valentine, J.P. and Pederson, H.G. (2004) A most unusual barrens: Complex interactions between lobsters, sea urchins and algae facilitates spread of an exotic kelp in eastern Tasmania. *Echinoderms: Munchen: Proceedings of the 11th International Echinoderm Conference, 6-10 October 2003, Munich, Germany*, pp. 213. Taylor & Francis.

Johnson, C.R., Ling, S.D., Ross, J., Shepherd, S. and Miller, K. (2005) *Establishment of the long-spined sea urchin (Centrostephanus rodgersii) in Tasmania: First assessment of potential threats to fisheries.* FRDC Final Report, Project No. 2001/044.

Johnson, C.R., Banks, S.C., Barrett, N.S., Cazzasus, F., Dunstan, P.K., Edgar, G.J., Frusher, S.D., Gardner, C., Helidoniotis, F., Hill, K.L., Holbrook, N.J., Hosie, G.W., Last, P.R., Ling, S.D., Melbourne-Thomas, J., Miller, K., Pecl, G.T., Richardson, A.J., Ridgway, K.R., Rintoul, S.R., Ritz, D.A., Ross, D.J., Sanderson, J.C., Shepherd, S., Slotwinski, A., Swadling, K.M. and Taw, N. (2011) Climate change cascades: shifts in oceanography, species' ranges and marine community dynamics in eastern Tasmania. *Journal of Experimental Marine Biology and Ecology*, 400, 17–32.

Kennedy, B. and Pearse, J.S. (1975) Lunar synchronization of the monthly reproductive rhythm in the sea urchin *Centrostephanus coronatus* Verrill. *Journal of Experimental Marine Biology and Ecology*, 8, 167–186.

King, C.K. (1992) The reproduction and development of the Echinoid *Centrostephanus rodgersii* - a potential bioassay organism. Honours thesis. University of Sydney, Sydney.

King, C.K., Hoegh-Guldberg, O. and Byrne, M. (1994) Reproductive cycle of *Centrostephanus rodgersii* (Echinoidea), with recommendations for the establishment of a sea urchin fishery in New South Wales. *Marine Biology*, 120, 95–106.

Konar, B. and Estes, J.A. (2003) The stability of boundary regions between kelp beds and deforested areas. *Ecology*, 84, 174–185.

Last, P.R., White, W.T., Gledhill, D.C., Hobday, A.J., Brown, R., Edgar, G.J. and Pecl, G. (2010) Long-term shifts in abundance and distribution of a temperate fish fauna: a response to climate change and fishing practices. *Global Ecology and Biogeography*, 20, 58–72.

Lessios, H.A., Cubit, J.D., Robertson, D.R., Shulman, M.J., Parker, M.R., Garrity, S.D. and Levings, S.C. (1984) Mass mortality of *Diadema antillarum* on the Caribbean coast of Panama. *Coral Reefs*, 3, 173–182.

Ling, S.D. (2008) Range expansion of a habitat-modifying species leads to loss of taxonomic diversity: A new and impoverished reef state. *Oecologia*, 156, 883–894.

Ling, S.D., Johnson, C.R., Frusher, S. and King, C.K. (2008) Reproductive potential of a marine ecosystem engineer at the edge of a newly expanded range. *Global Change Biology*, 14, 907–915.

Ling, S.D. and Jacques, M. (2009) *Subtidal reef monitoring and community awareness project: data report on the long-spined sea urchin.* A Tasmanian Government Fishwise Community Grant Project Final Report (69 pp.).

Ling, S.D. and Johnson, C.R. (2009) Population dynamics of an ecologically important range-extender: kelp bed versus barrens sea urchins. *Marine Ecology Progress Series*, 374, 113–125.

Ling, S.D., Johnson, C.R., Ridgway, K., Hobday, A.J. and Haddon, M. (2009a) Climate-driven range extension of a sea urchin: inferring future trends by analysis of recent population dynamics. *Global Change Biology*, 15, 719–731.

Ling, S.D., Johnson, C.R., Frusher, S. and Ridgway, K. (2009b) Overfishing reduces resilience of kelp beds to climate-driven catastrophic phase shift. *Proceedings of the National Academy of Sciences (USA)*, 106, 22341–22345.

Ling, S.D., Ibbott, S. and Sanderson, J.C. (2010) Recovery of canopy-forming macroalgae following removal of the enigmatic grazing sea urchin *Heliocidaris erythrogramma*. *Journal of Experimental Marine Biology and Ecology*, 395, 135–146.

Ling, S.D. and Johnson, C.R. (2012) Marine reserves reduce risk of climate-driven phase shift by restoring size and habitat specific trophic interactions. *Ecological Applications*, 22, 1232–1245.

McShane, P.E., Gerring, P.K., Anderson, O.W. and Stewart, R.A. (1996) Population differences in the reproductive biology of *Evechinus chloroticus* (Echinoidea: Echinometridae). *New Zealand Journal of Marine and Freshwater Research*, 30, 333–339.

Morgan, S.G. (1995) Life and death in the plankton: larval mortality and adaptation. *Ecology of marine invertebrate larvae* (ed. by McEdward, L.), pp. 279–322, CRC Press, Boca Raton, Florida.

Pecorino, D. (2012) Population biology and larval ecology of the sea urchin *Centrostephanus rodgersii* (Agassiz 1863) in New Zealand under the influence of Global Climate Change. PhD Thesis, University of Otago.

Pecorino, D., Lamare, M.D. and Barker, M.F. (2012) Growth, morphometrics and size structure of the Diadematidae sea urchin *Centrostephanus rodgersii* in northern New Zealand. *Marine and Freshwater Research*, 63, 624–634.

Pecorino, D., Lamare, M.D. and Barker, M.F. (2013) Reproduction of the Diadematidae sea urchin *Centrostephanus rodgersii* in a recently colonized area of northern New Zealand. *Marine Biology Research*, 9, 157–168.

Pederson, H.G. and Johnson, C.R. (2006) Predation of the sea urchin *Heliocidaris erythrogramma* by rock lobsters (*Jasus edwardsii*) in no-take marine reserves. *Journal of Experimental Marine Biology and Ecology*, 336, 120–134.

Pitt, N.R., Poloczanska, E.S. and Hobday, A.J. (2010) Climate-driven range changes in Tasmanian intertidal fauna. *Marine and Freshwater Research*, 61, 963–970.

Poloczanska, E.S., Babcock, R.C., Butler, A., Hobday, A.J., Hoegh-Guldberg, O., Kunz, T.J., Matear, R., Milton, D.A., Okey, T.A. and Richardson, A.J. (2007) Climate change and Australian marine life. *Oceanography and Marine Biology. An Annual Review*, 45, 409–480.

Przeslawski, R., Falkner, I., Ashcroft, M.B. and Hutchings, P. (2012) Using rigorous selection criteria to investigate marine range shifts. *Estuarine, Coastal and Shelf Science*, 113, 205–212.

Ridgway, K.R. (2007) Long-term trend and decadal variability of the southward penetration of the East Australian Current. *Geophysical Research Letters*, 34, L13613.

Scheffer, M., Carpenter, S., Foley, J.A., Folke, C. and Walker, B. (2001) Catastrophic shifts in ecosystems. *Nature*, 413, 591–596.

Scheibling, R.E. and Hennigar, A.W. (1997) Recurrent outbreaks of disease in sea urchins *Strongylocentrotus droebachiensis* in Nova Scotia: evidence for a link with large-scale meteorologic and oceanographic events. *Marine Ecology Progress Series*, 152, 155–165.

Schiel, D.R., Kingsford, M.J. and Choat, J.H. (1986) Depth distribution and abundance of benthic organisms and fishes at the subtropical Kermadec Islands. *New Zealand Journal of Marine and Freshwater Research*, 20, 521–535.

Shears, N.T. and Babcock, R.C. (2002) Marine reserves demonstrate top-down control of community structure on temperate reefs. *Oecologia*, 132, 131–142.

Steneck, R.S., Graham, M.H., Bourque, B.J., Corbett, D., Erlandson, J.M., Estes, J.A. and Tegner, M.J. (2002) Kelp forest ecosystems: biodiversity, stability, resilience and future. *Environmental Conservation*, 29, 436–459.

Strain, E.M.A. and Johnson, C.R. (2009) Competition between an invasive urchin and commercially fished abalone: effect on body condition, reproduction and survivorship. *Marine Ecology Progress Series*, 377, 169–182.

Sunday, J.M., Bates, A.E. and Dulvy, N.K. (2012) Thermal tolerance and the global redistribution of animals. *Nature Climate Change*, 2, 686–690.

Tegner, M.J. and Levin, L.A. (1983) Spiny lobsters and sea urchins: analysis of a predator-prey interaction. *Journal of Experimental Marine Biology and Ecology*, 73, 125–150.

Tegner, M.J. and Dayton, P.K. (2000) Ecosystem effects of fishing in kelp forest communities. *ICES Journal of Marine Science*, 57, 579–589.

Williams, S., Pizzaro, O., Jakuba, M., Ling, S.D. and Johnson, C.R. (2010). Repeated AUV surveying of urchin barrens in North Eastern Tasmania. *Proceedings of the IEEE International Conference on Robotics and Automatio*, Anchorage, pp. 293–299. Alaska, USA.

Worthington, D.G., Chick, R.C., Blount, C., Brett, P.A. and Gibson, P.T. (1998) A final assessment of the NSW abalone fishery in 1997. *NSW Fisheries Fishery Resource Assessment Series*, 5, 1–67.

TEMPORAL CHANGES IN THE SEA URCHIN *STRONGYLOCENTROTUS PURPURATUS* ALONG THE WEST COAST OF NORTH AMERICA

Thomas A. Ebert

CLIMATE CHANGE PERSPECTIVES FROM THE ATLANTIC:
PAST, PRESENT AND FUTURE
Jose María Fernández-Palacios, Lea de Nascimento, José Carlos Hernández,
Sabrina Clemente, Albano González & Juan P. Díaz-González (eds.)
Servicio de Publicaciones, Universidad de La Laguna – 2013

ISBN: 978-84-15910-54-1
pp. 443-460

ABSTRACT

The purple sea urchin *Strongylocentrotus purpuratus* has been studied at intertidal sites along the Pacific Coast of North America for many decades. Changes have been observed from southern California to central Oregon. At False Point, La Jolla, in southern California, sea urchin density has declined since 1969 and in 2007 sea urchins were gone from the site. The major cause has been human disturbance but sea surface temperature change shows more frequent episodes of stressful or lethal temperatures. Downward shifts in intertidal distribution from the 1980s have occurred at White Point on the Palos Verdes Peninsula, Los Angeles, and at Shelter Cove in northern California. Sea urchins have been studied at Sunset Bay, Oregon, since the early 1960s. Sea urchins in the Boulder Field disappeared following a census in 1995 and the most reasonable explanation is death due a record rain event that caused flooding into the bay from a small stream. Extensive clearcutting of timber in the watershed may have contributed to the magnitude of the flooding. All changes in sea urchins have been negative; no increases have been observed in the intertidal. Some changes have been directly due to human activity and some may have been caused by changes in severity of storms or sea surface and air temperatures. Changes may be transient pulses that have long recovery periods because of infrequent recruitment events but some may represent new stable states. All represent baselines to judge future changes in sea urchins along the Pacific coast.

KEYWORDS: baselines, population change, human disturbance, intertidal shifts, intertidal predation.

INTRODUCTION

In 1995 Daniel Pauly coined the term “shifting baseline syndrome” (Pauly, 1995). The general idea is that without historical records each new generation of scientists takes current conditions as a baseline on which they develop ideas of how a natural system works. Pauly had fisheries in mind but the same idea applies to all natural systems. I have worked with the purple sea urchin *Strongylocentrotus purpuratus* along the Pacific coast of North American for decades and observations I have made represent, for me, a baseline. The point of this paper is to provide these baseline observations so they can be used to calibrate “baselines” for others who examine sea urchins along the coast. I will include only those sites where I have observed change but there are other sites where change may be observed

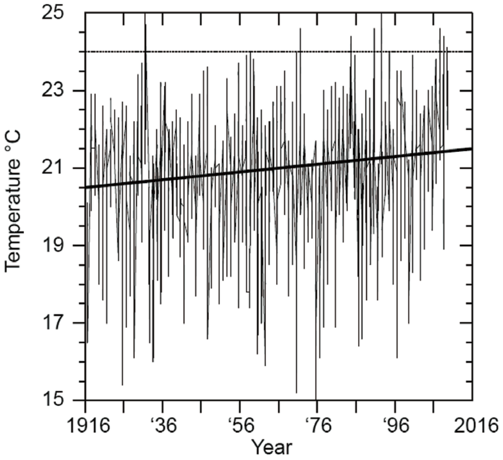

Figure 1. Sea surface temperature (SST) measured off the end of the pier at Scripps Institution of Oceanography, La Jolla, California, USA (32° 52.0' N, 117° 15.5' W; shorestation.ucsd.edu).

in the future. Additional documentation of the status of intertidal *S. purpuratus* populations is in Ebert (1968, 1983, 2010), Ebert *et al.* (2012), Russell (1987), Ebert and Russell (1988).

Climate related change along the coast is seen in the increase in sea surface temperature (SST) measured off the pier at Scripps Institution of Oceanography, La Jolla, California, USA (32° 52.0' N, 117° 15.5' W; shorestation.ucsd.edu). There is substantial year-to-year variation but also a significant upward trend since 1916 ($F_{1,2824} = 92.44$, $P<0.001$) with an increase of about 0.01 each year or 1°C since 1916 (Fig. 1). This rate is similar to the increase in temperature at Hopkins Marine Laboratory in Pacific Grove, California (36° 37.3' N, 121° 54.2' W; shorestation.ucsd.edu) since 1919 (Breaker, 2005). These trends are not smooth and are complicated by ENSO and decadal shifts but the overall trends are both positive and of similar magnitude. Breaker (2005) presents additional complications to long-term trends in sea surface temperatures along the Pacific coast.

Together with a general upward trend of SST at Scripps is an increase in frequency of temperatures exceeding 24°C; 25°C is lethal for *S. purpuratus* (Farmanfarmaian and Giese, 1963) and there is evidence that this species does not tolerate temperatures ≥22° C for prolonged periods (Ford *et al.*, 1976). Exposures at low tide resulting in internal temperatures of 25° or more for 3 to 5 hours result in death (Gonor, 1968). The SST changes in southern California indicate that periods of thermal stress are increasing for *S. purpuratus* (Fig. 1).

Figure 2. Locations where intertidal populations of the purple sea urchin *Strongylocentrotus purpuratus* have shown changes.

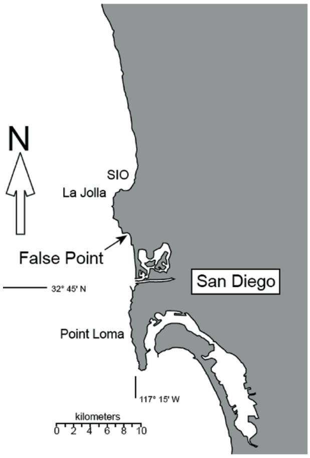

Figure 3. Locations of Scripps Institution of Oceanography and False Point, the intertidal area where sampling was done is on the south-facing shore.

SITES

Sites to be examined extend from southern California to central Oregon (Fig. 2) and study times are from the early 1960s (Sunset Bay, Oregon), the late 1960s (False Point, California), to sites visited in the 1980s. Presentation will be from south to north.

False Point, La Jolla, California, (32° 48’ 28” N; 117° 15’ 58” W) is located at the south end of a peninsula with Point La Jolla at the north end (Fig. 3) and was first sampled in October 1969. The location of sampling was south from the public access trail to the beach (Fig. 4A). The aerial photo was taken in spring 1971 and white lines indicate where sampling was done in October 1969 at about -0.1m below datum (MLLW). White lines delimit the east–west area where *S. purpuratus* was sampled as well as other echinoderms starting in 1971 (Muscat, 1975; Ebert, 1983; Addessi, 1994; Medeiros-Bergen and Ebert, 1995).

Density was determined by examining numbers of *S. purpuratus* under rocks. Rock surface area was estimated using the major and minor axes and assuming that rock shape was an ellipse. Sampling in spring 1971 was with students in a graduate class at San Diego State University. The same area was sampled in 1991 (Addessi, 1994) and again in 2003 (R. Presiado, pers. com., unpublished data). Numbers as a function of rock area (Fig. 4B) show an expected positive relationship between numbers and rock size. Adjusting for rock size (Table 1) shows the

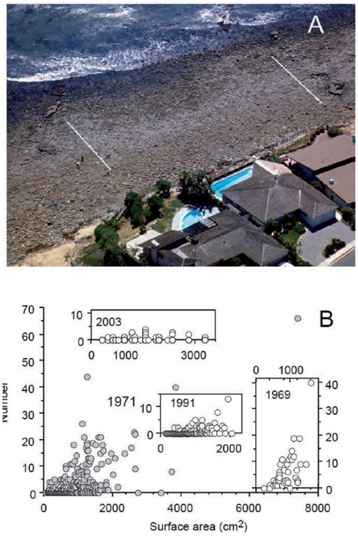

Figure 4. False Point. (A) Aerial photo looking south taken Spring 1971 (photo by T.A. Ebert); public access is down a trail and exits to the beach at the bottom left corner; white lines mark the east-west limits of area sampled in 1971 and again in 1991 (Addessi 1994), and in 2003 (R. Presiado, unpublished); sample of 24–26 October 1969 was in front of the rock ledge at the seaward tip of the white line on the left; (B) Number of sea urchins found under rocks with different surface areas; gray-filled circles are from February 22, 1971 to April 1971; 1991 samples gathered February 13–27 and 2003 samples from March 18–29; elevations from +0.1m to -0.3m relative to datum (MLLW).

TABLE 1. A) Analysis of number of sea urchins under rocks with rock area as a covariate and year as a categorical variable. B) Adjusted least significant mean number of sea urchins under a rock with mean area 1031.4 cm^2.

A. Source	SS	df	MS	F-ratio	P
surface area	1828.866	1	1828.866	145.047	<0.001
year	386.401	3	128.800	10.215	<0.001
year × area	3667.742	3	1222.581	96.963	<0.001
error	10364.402	822	12.609		
B. Year	Mean number	SE	N		
1969	9.34	0.65	42		
1971	4.40	0.21	294		
1991	0.98	0.32	175		
2003	0.13	0.21	319		

decline in numbers since 1969. The difference between 1969 and 1971 is best viewed as due to the very restricted location of samples in 1969 and much larger area in 1971. The site at False Point was visited again in 2007 and was searched by three experienced persons. The search was expanded west and about two hours spent around low tide. Only 2–3 sea urchins were found.

Although the major cause of loss of sea urchins at False Point probably is due to direct human activities of rolling rocks and general disturbance, combi-

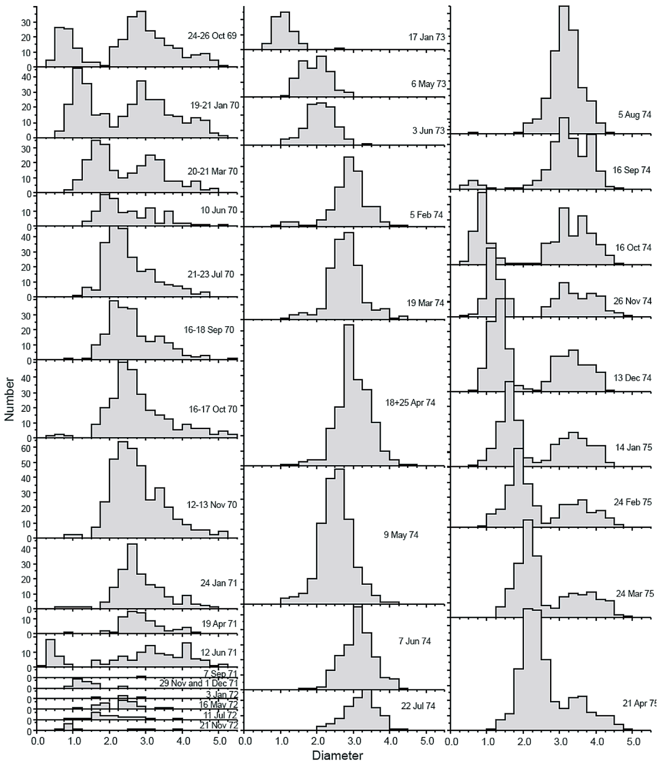

Figure 5. Size data for the purple sea urchin *Strongylocentrotus purpuratus* at False Point showing the major mortality event in September 1971 and rapid recovery by recruitment the following year.

nations of tide and weather conditions can cause mass mortality. Size-frequency distributions gathered from 1969 to 1975 (Fig. 5) show annual recruitment and with expected progression in size from month to month. Early in September 1971, low mid-day tides coupled with high temperatures and hot, dry winds appear to be the cause of a mass mortality of sea urchins as False Point. Large numbers of tests washed on to the beach and when visited on 7 September 1971, very few live sea urchins could be found. The size data (Fig. 5) suggest that large sea urchins may have suffered greater mortality than small individuals because in late November and early December sea urchins with diameters between 1.00 and 1.25 cm were found and none greater than 2.5 cm. Small individuals less than 1.0 cm were again observed in November 1972 and large numbers centered at 1.0 cm were found in January 1973. An event similar to that of 1971 was not observed from 1976 to 1997. The trend of density from 1969 to 2007 has shown a decline to zero or nearly so.

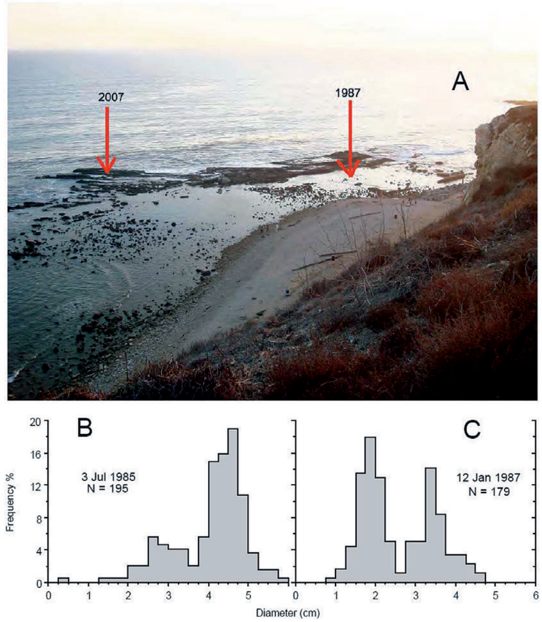

Figure 6. White Point, Palos Verdes Peninsula, Los Angeles, California. (A) photo with incoming tide to the east of the parking area of the County Park (photo by J. C. Hernández); sample of 1987 taken in area with cobbles and gravel; arrow for 2007 indicates area of channels that had sea urchins in 2007–2009; (B) size distribution gathered in 1985 in area to the right (west) of the photo in cobble/gravel area; (C) size distribution gathered approximately in area indicated by the arrow.

The second site that has shown change is White Point (Fig. 2) on the Palos Verdes Peninsula in Los Angeles, California (Fig. 6). Size data were collected in 1985 (33° 43' 02" N; 118° 19' 15" W) and in 1987 (33° 42' 56" N; 118° 19' 10" W). Both of these samples were in an area with gravel and small cobbles. Sea urchins were present in 1985 and 1987 in areas higher in the intertidal than where they occurred in 2007–2009. Field notes indicate that the 1985 site was similar to False Point but more exposed and at the west end of the bay in front of the County Park. The 1987 site was described as east of the main parking lot next to the dirt road (Fig. 6A). The size structures in both 1985 (Fig. 6B) and 1987 (Fig. 6C) show that the populations had persisted for at least several years. The first mode in the sample gathered 3 July 1985 at about 2.5 cm probably would have settled the previous summer if they grew according to the shifts in modes of sea urchins as False Point (Fig. 5). Sea urchins about 3.5 cm would have been two years old and larger individuals ≥4 years. Similarly, the first mode in the 12 January 1987 sample (Fig. 6B) probably is composed of individuals that settled the previous summer and so had survived both summer and fall weather conditions. The size data in 1987 (Fig. 6C) were collected in a 2 x 4m plot and so density was 22.3 m^{-1}.The significant point is that sea urchins were recruiting and surviving in the cobbles and gravel at White Point but were not seen in the 1987 area when the site was visited in 2007. The intertidal distribution appears to have shifted further down in the intertidal because *S. purpuratus* was abundant in channels close to

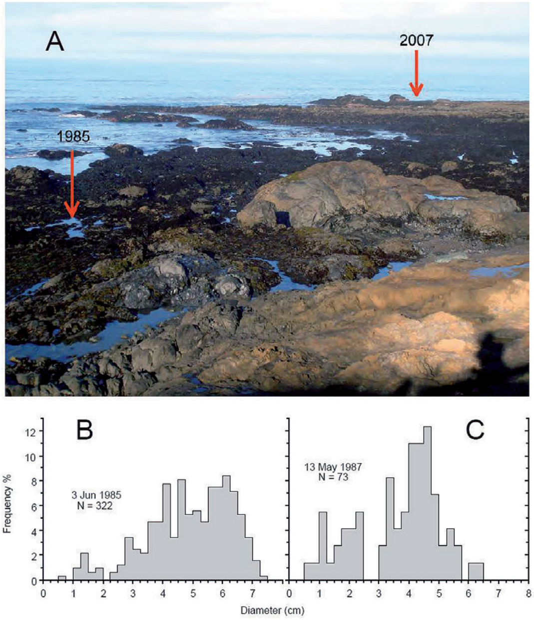

Figure 7. Shelter Cove, California (40° 01’ 18” N; 124° 04’ 11” W); (A) Intertidal area viewed from cliff by the Mal Coombs Park parking lot (photo by J. C. Hernández 2008); pool area where samples were gathered in 1985–’87 shown at the left; area sampled in 2007–2009 indicated out at the reef edge; (B) size data gathered in 1985; (C) size data gathered in 1987.

the reef edge in 2007–2009. White Point is visited by larger numbers of people and it is unknown whether direct human activity is the cause of disappearance in the cobble area, whether a change in temperature is responsible, or whether a transient mortality event similar to the 1971 event at False Point is the cause of loss.

Shelter Cove (Fig. 2) (40° 01’ 18” N; 124° 04’ 11” W) was first visited in 1985 and again in 1986 and ‘87. In 1985 (Fig. 7A) *S. purpuratus* was abundant in tidepools holding gravel and pebbles (Fig. 7B). Size structure indicated that the tidepools in the area had been occupied for many years. A similar pattern was found in 1986 but in 1987 there were large numbers of tests that appeared to have been broken within the past several days because test fragments still had color and attached spines. The cause of mortality is unknown but because of the large numbers that were killed it appeared to have been caused by people. Nevertheless, there still were some sea urchins in tidepools close to where collecting had been done in 1985 and ‘86 (Fig. 7C). In 2007, no sea urchins were found in the pools where they had been in 1985–’87 but were present in large numbers out near the reef edge where they also had been present in 1987. The cause of loss in pools nearer to shore is unknown but the downslope shift is similar to that seen at White Point.

Cape Blanco, Oregon, (Fig. 2) (42° 50’ 22” N; 124° 33’ 25” W) was visited on 4 June 1985. An elongated depression in the very low intertidal was selected and all sea urchins were measured (Fig. 8A). The total number of sea urchins was 472 and the area was about 2.27 m^2 so density was about 208 m^{-2}. The modal diameter was

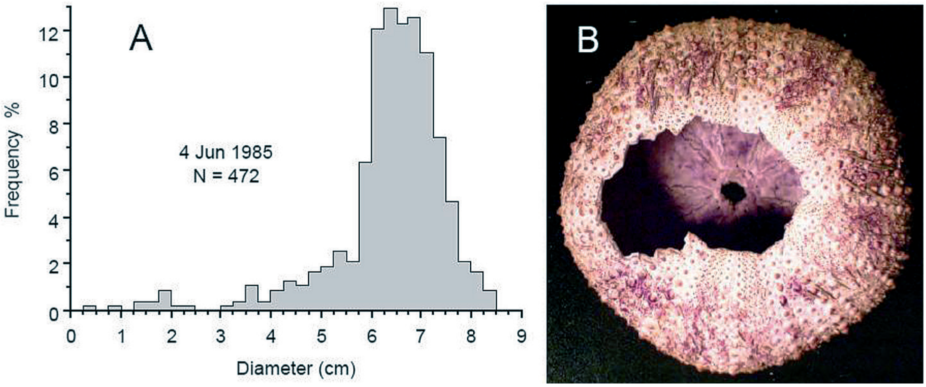

Figure 8. Cape Blanco, Oregon (42° 50' 22" N; 124° 33' 25" W). (A) Size frequency measured on 4 June 1985; (B) test showing typical attack by a raccoon.

about 6.7 cm and the largest individual had a diameter of 8.50 cm. When visited again in 1987, a low intertidal area was again selected and the largest sea urchin had a diameter of 8.39 cm. The sea urchin population at Cape Blanco had not shown any change and the size distribution of 1985 (Fig. 8A) shows that the area had been occupied for many years. When the low intertidal area was again visited in 2008, large individuals could not be found. The Cape Blanco site is relatively remote and direct human activity is unlikely. Physical changes in ocean conditions also are unlikely. Predation in the intertidal has been observed in the intertidal at Cape Blano by raccoons (*Procyon lotor*) that forage during low tide and tests have been found with a pattern of handling typical of raccoons (Fig. 8B). Although very low in the intertidal, predation by raccoons or black oyster-catchers (*Haematopus bachmani*) is possible and although not observed in the low intertidal at Cape Blanco, the sunflower star *Pycnopodia helioantoides* is capable of both consuming and panicking sea urchins (c.f. Grupe, 2006). Although in 1985 and 1987 it was clear that large *S. purpuratus* had occupied an area in the low intertidal at Cape Blanco for many years, the cause of the sudden loss is unknown and may be due to a transient event. The size structure (Fig. 8A) suggests that recruitment is very unusual and so any recovery will take many years.

Strongylocentrotus purpuratus has been observed at Sunset Bay, Oregon (43° 20' 3.8" N; 124° 22' 34" W), longer than at other sites along the coast. First observations were in 1962 and first size-frequency data gathered in 1964 (Ebert, 1968). Size data have been gathered at a number of sites on the south side of the bay, sometimes annually but often with breaks of many years. One site, called the Boulder Field (Ebert, 1968) is the focus of this presentation. Size data for *S. purpuratus* in the Boulder Field (Figs. 9 and 10) show that large sizes were found over the entire time period with very infrequent recruitment events. The largest recruitment occurred in 1963.

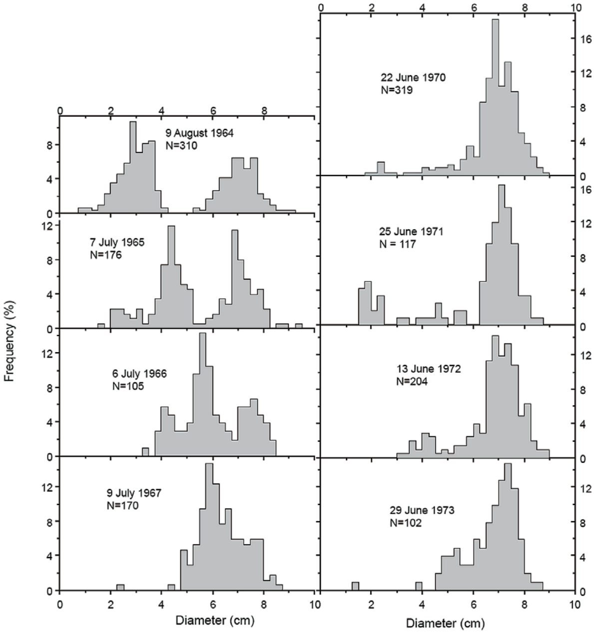

Figure 9. *Strongylocentrotus purpuratus* size frequency (%) in the Boulder Field, Sunset Bay, Oregon (43° 20’ 3.8” N; 124° 22’ 34” W) from 1964 to 1973.

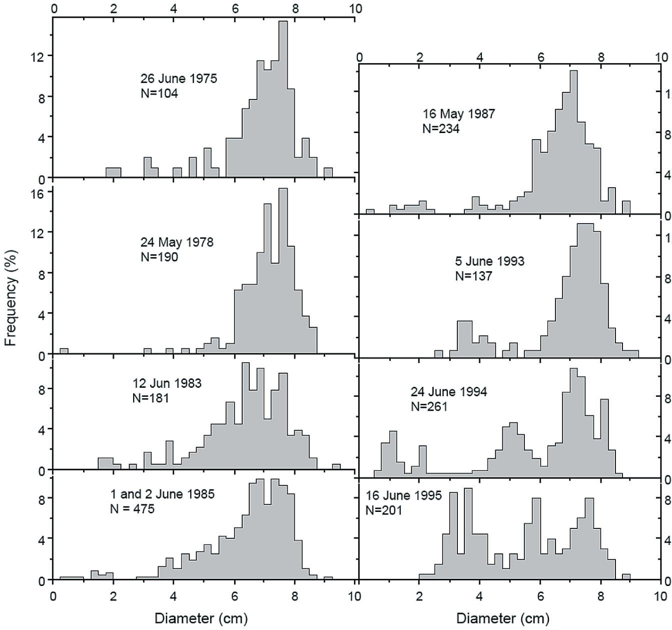

Figure 10. *Strongylocentrotus purpuratus* size frequency (%) in the Boulder Field, Sunset Bay, Oregon from 1975 to 1995

Figure 11. Sunset Bay, Oregon. (A) Vertical aerial view, 19 June 2002 (BLM), BF is the Boulder Field and BC is where Big Creek enters at the southeast corner of the bay; (B) the Boulder Field at low tide, March 1967; C: composite oblique aerial photo (1964) looking south showing Big Creek at upper left, the Boulder Field (BF) and locations of two other sites, the Postelsia Zone (PZ) and Surfgrass Area (SG) (photos B and C by T. A. Ebert).

Sunset Bay is protected on three sides with an opening to the northwest (Fig. 11A). The Boulder Field (BF) is on the south side of the bay and well inside the mouth. The substrate is large rocks (Fig. 11B) resting on more rocks or gravel. Other study sites in the bay have been called the Postelsia Zone (PZ) and Eelgrass Area (Ebert, 1968) although the proper name should be Surfgrass Area because the angiosperm that is present is *Phyllospadix scouleri* commonly called surfgrass. Sunset Bay has a small stream, Big Creek (BC) that enters from the southeast. A cursory examination in 2004 failed to find sea urchins in the Boulder field and a more thorough search in 2007 revealed only a few individuals. Ben Grupe suggested a major rain event may have caused the loss and it appears at this time to be the best explanation (Ebert and Grupe, 2008).

A major rain event occurred on 18–19 November 1996 when warm, moist air came up from the south and encountered a cold air mass from the north. The rainfall was intense and set a 24 hour record at North Bend airport (Figs. 12B and 12C). Runoff from Big Creek described by a local resident to B. Grupe (pers. comm.) was that picnic tables from Sunset Bay campground washed into the bay. November 18–21 was during spring tides (Fig. 12A) so flushing in the bay would have been reduced. No salinity measurements were made in the bay so it is unknown to what level salinity dropped or how long it remained low. Salinities ≤ 24‰ are lethal after five days under laboratory conditions (Giese and Farmanfarmaian, 1963). At 20‰ most die by the second day.

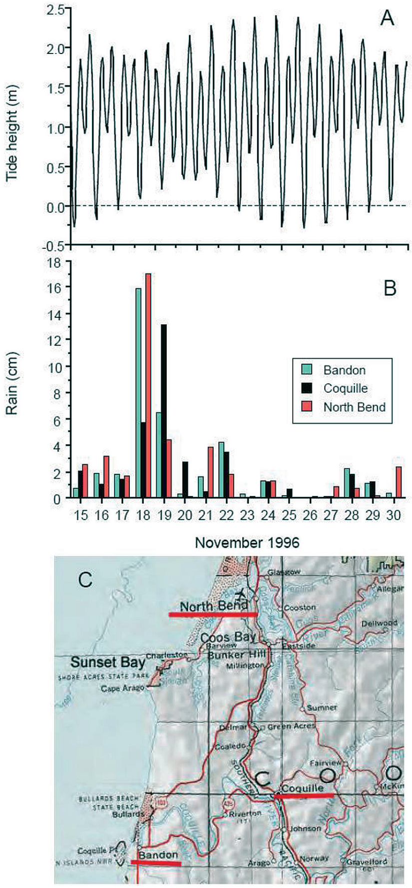

Figure 12. Environmental conditions surrounding the major rain even of 18–19 November 1996; (A) semidiurnal tides showing spring tides during the major rain event; (B) daily rainfall at three weather stations near Sunset Bay; (C) map showing positions of weather stations at North Bend, Coquille, and Bandon; red underlines drawn on a National Geographic TOPO map.

Although rainfall intensity was unusual an additional factor that probably contributed to runoff was logging in the Big Creek watershed. The Big Creek wateshed is small (Fig. 13A) and the dominant forest is Douglas fir (*Pseudostuga menziesii)* that is harvested on roughly a 40 year cycle. Logging is by clearcutting, and many clearcuts are visible in the aerial photograph taken on 27 May 1994 (Fig. 13B). Harvesting from 1990 to September 1996 (Fig. 14) was about 1200 hectares with major effort in 1995. Terrain that has been clearcut has greater runoff following rain than does soil covered by vegetation (e.g., Harr, 1986, Jones, 2000).

It must be emphasized that the cause of loss of *S. purpuratus* in the Boulder Field at Sunset Bay is unknown and the rain event of 18–19 November as the primary agent of loss is speculation. What is known is that sea urchins disappeared in the Boulder Field sometime between 16 June 1995 and 2004. Sea urchins in

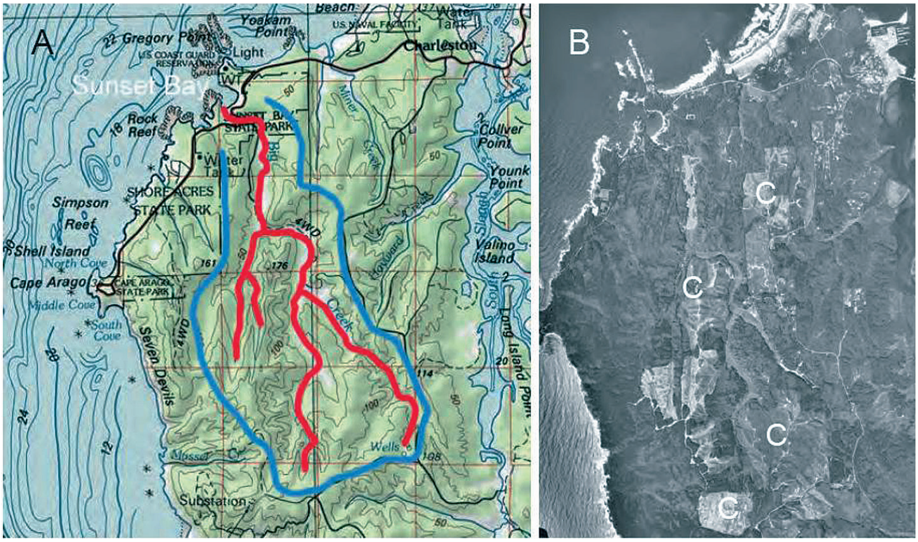

Figure 13. (A) map showing Big Creek (red) and the watershed that drains into Big Creek (outlined in blue) (lines drawn on a National Geographic TOPO! map); (B) vertical aerial photo 27 May 1994 (05-27-94 NAPP 7173-223) of the Big Creek watershed showing recent clearcuts, some labeled C.

the other sites at Sunset Bay such as the Postelsia Zone or Surfgrass Area (Fig. 11C) were unaffected. These sites are closer to the open sea and also are higher in the intertidal than the Boulder Field and so would be expected to have had better flushing with seawater. At present, the unusual 1996 rain event seems to be the best explanation for loss in the Boulder Field.

DISCUSSION

Changes in the distribution and abundance of the purple sea urchin *Strongylocentrotus purpuratus* have been observed at intertidal sites along the west coast of North America from southern California to Oregon. All changes that have been observed have been declines; no increases have been observed. There also, however, have been many sites where no changes have been observed. Many sites from Mexico to Canada were first visited in the 1980s (Russell, 1987; Ebert and Russell, 1988; Ebert, 2010) and a selection of these sites still have abundant sea urchins (e.g., Ebert, Hernández, and Russell 2012). The most dramatic changes have been at False Point, La Jolla, California, and at Sunset Bay, Oregon. The primary cause of change at False Point appears to be due to direct human dis-

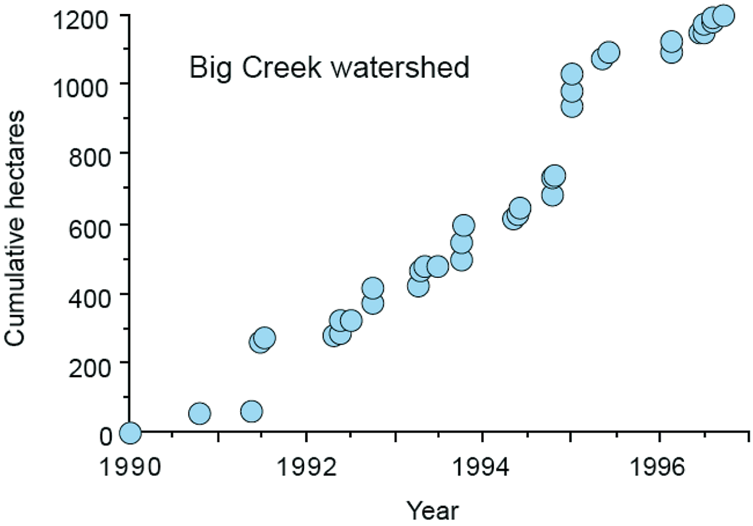

Figure 14. Cumulative hectares logged in the Big Creek watershed for the period 1990 to mid September 1996.

turbance although lack of small individuals suggests that either settlement has declined or early post-settlement mortality has increased. Neither of these is likely to be directly related to human disturbance and so the trend of increased incidence of elevated temperatures may play an important role.

The loss of sea urchins in the Boulder Field at Sunset Bay, Oregon, seem best explained by a drop in salinity due to flooding into the bay from an unusual rain event and possibly exacerbated by logging in the Big Creek watershed. The rain event was one of the largest single day storms in the past 100 years (Wiley 2000) and over the three day period from 17–19 November 1996 rainfall was 23.1cm (Coe et al. 2011). To what degree this might relate to climate change is, of course, unknown.

Loss of sea urchins in the intertidal areas is not new along the coast. E. F. Ricketts at Pacific Grove, California, kept file cards on intertidal invertebrates. In 1926 or ‘27 he wrote on a card for *S. purputatus* (Ricketts, ca. 1946): “well distributed over the entire region, wherever it finds surf beaten rock tidepools exposed only on ultra-low tide. Great beds are to be found at Arch Rock and elsewhere. The most numerous big marine animal of our region.” In late 1946, however, he wrote: “I wouldn’t know where to go now to pick up even 100 specimens in the immediate region.” The loss had not been recent and Ricketts says that they had been rare in the Arch Rock region for many years. He suggested a combination of collecting and inroads of civilization.

A storm event during 1983 destroyed sea urchins living in the lowest parts of a boulder field at Ellwood Pier, Santa Barbara, California. Following the storm the site was colonized by a tube-building sabellid polychaete *Phragmatopoma californica*, which has monopolized space and sea urchins have not returned. The *Phragmatopoma* reef has become a stable system and subsequent wave damage or heavy rains have not tipped the system back to one with sea urchins (S. Schroeter, pers. comm.).

Other dramatic losses of intertidal sea urchins have included ones due to freshwater in southern California (MacGinitie, 1939; Littler and Littler, 1987; Hendler, 2013) and elevated temperature in Oregon (Gonor, 1968). An important point is that catastrophic mortality events occur in the intertidal and, in general, populations of *S. purpuratus* recover. Long-period trends, however, such as seen at False Point and the stable state change at Ellwood pier indicate more permanent conditions. It seems unlikely that the loss of large sea urchins at Cape Blanco or at Sunset Bay represent a shift to a new stable state but may appear so because of the very infrequent major settlement events. Baselines have shifted and may or may not return to previous conditions.

ACKNOWLEDGEMENTS

A large number of people contributed to this work. In alphabetical order: S. W. Adair, L. C. Addessi, S. L. Baker, S. Clemente, C. A. Ebert, L. K. Ebert, T. A. Ebert, P. W. Frank, B. M. Grupe, J. C. Hernández, B. A. Miller, A. M. Muscat, N. T. Richmond, M. P. Russell, C. D. White, J. A. Wolfe, and students in the spring 1971 Advanced Invertebrates class. A copy of E. Ricketts' file card was sent to me by J.S. Pearse. Aerial photos were obtained from the Map Library, University of Oregon, Eugene. Data on logging in the Big Creek watershed were supplied by the Oregon Department of Forestry Coos Bay District. Funding at various times was from the Ocean Sciences Division Biological Oceanography of the US National Science Foundation grants OCE-0623934, OCE75-10442, OCE 84-01415 and GA-30899 (to P. W. Frank). Finally, I thank José Carlos Hernández for inviting me to submit this manuscript and to him and Sabrina Clemente for taking care of me during my stay in La Laguna. I greatly appreciate all of the help and support I have received.

REFERENCES

Addessi, L. (1994) Human disturbance and long-term changes on a rocky intertidal community. *Ecological Applications*, 4, 786–797.

Breaker, L.C. (2005) What's happening in Monterey Bay on seasonal to interdecadal time scales. *Continental Shelf Research*, 25, 1159–1193.

Coe, J.A., Michael, J.A. and Burgos, M.M. (2011) *Map of debris flows caused by rainfall during 1996 in parts of the Reedsport and Deer Head Point quadrangles, Douglas County, southern Coast Range, Oregon* (9 pp. pamphlet), U.S. Geological Survey Open File Report 2011–1150.

Ebert, T.A. (1968) Growth rates of the sea urchin *Strongylocentrotus purpuratus* related to food availability and spine abrasion. *Ecology*, 49: 1075–1091.

Ebert, T. A. (1983) Recruitment in echinoderms. *Echinoderm Studies Vol. 1* (ed. by Jangoux, M. and Lawrence, J.M.), pp 169–203. A.A. Balkema, Rotterdam, The Netherlands.

Ebert, T.A. (2010) Demographic patterns of the purple sea urchin *Strongylocentrotus purpuratus* along a latitudinal gradient, 1985–87. *Marine Ecology Progress Series*, 406, 105–120.

Ebert, T.A. and Grupe, B.M. (2008). Sudden loss of sea urchins at Sunset Bay, Oregon, following documented presence for 40 years. *Proceedings of the 93rd Ecological Society of America Annual Meeting*, Milwaukee, Wisconsin. (http://esameetings.allenpress.com/2008/P10301.HTM).

Ebert, T.A., Hernández, J.C. and Russell, M.P. (2012) Ocean conditions and bottom-up modifications of gonad development in the sea urchin *Strongylocentrotus purpuratus* over space and time. *Marine Ecology Progress Series*, 467, 147–166.

Ebert, T.A. and Russell, M.P. (1988) Latitudinal variation in size structure of the west coast purple sea urchin: A correlation with headlands. *Limnology and Oceanography*, 32, 286–294.

Farmanfarmaian, A. and Giese, A.C. (1963) Thermal tolerance and acclimation in the western purple sea urchin, *Strongylocentrotus purpuratus. Physiological Zoölogy*, 36, 237–243.

Ford, R.F., Foreman, D.G., Grubbs, K.J., Kroll, C.D. and Watts, D.G. (1978) Effects of thermal effluent on benthic marine invertebrates determined from long-term simulation studies. *Energy and environmental stress in aquatic systems* (ed. by Thorp, J.H. and Gibbons, J.W.), pp. 546–568, CONF-771114. Tech. Information Center. U.S. Dept. Energy.

GIESE, A.C. and FARMANFARMAIAN, A. (1963) Resistance of the purple sea urchin to osmotic stress. *Biological Bulletin*, 124, 182–192.

GONOR, J. J. (1968) Temperature relations of central Oregon marine intertidal invertebrates: a pre-publication technical report to the Office Naval Res. Dept. Oceanogr, Oregon St Univ. Data Rpt No. 34. Ref. 68-38. http://ir.library.oregonstate.edu/dspace/handle/1957/6591.

GRUPE, B.M. (2006) *Purple sea urchins (Strongylocentrotus purpuratus) in and out of pits: The effects of microhabitat on population structure, morphology, growth and mortality.* MS Thesis (261 pp.), University of Oregon, Eugene, USA. http://www.uoregon.edu/~ashanks/Ben%20Grupe/Ben%20Grupe_files/Ben%20Grupe%20Thesis_1.pdf

HARR, R.D. (1986) Effects of clearcutting on rain-on-snow runoff in Western Oregon: A new look at old studies. *Water Resources Research*, 22, 1095–1100.

HENDLER, G. (2013) Recent mass mortality of *Strongylocentrotus purpuratus* (Echinodermata: Echinoidea) at Malibu and a review of purple sea urchin kills elsewhere in California. *Bulletin of the Southern California Academy of Sciences*, 112, 19–37.

JONES, J.A. (2000) Hydrologic processes and peak discharge response to forest removal, regrowth, and roads in 10 small experimental basins, western Cascades, Oregon. *Water Resources Research*, 36, 2621–2642.

Littler, M.M. and Littler, D.S. (1987) Effects of stochastic processes on rocky-intertidal biotas: an unusual flash flood near Corona del Mar, California. Bulletin *of the Southern California Academy of Sciences*, 86, 95–106.

MACGINITIE, G.E. (1939) Some effects of fresh water on the fauna of a marine harbor. *American Midland Naturalist*, 21, 681–686.

MEDEIROS-BERGEN, D.E. and EBERT T.A. (1995) Growth, fecundity and mortality rates of two intertidal brittlestars (Echinodermata: Ophiuroidea) with contrasting modes of development. *Journal of Experimental Marine Biology and Ecology*, 189, 47–64.

MUSCAT, A.M. (1975*) Reproduction and growth in the ophiuroid Ophionereis annulata*. MS Thesis (83 pp.), San Diego State University, San Diego, CA USA.

PAULY, D. (1995) Anecdotes and the shifting baseline syndrome of fisheries. *Trends in Ecology & Evolution*, 10, 430.

RICKETTS, E.F. (ca. 1946) Notes on *Strongylocentrotus purpuratus* File card. Hopkins Marine Station library, Pacific Grove, California.

RUSSELL, M.P. (1987) Life history traits and resource allocation in the purple sea urchin *Strongylocentrotus purpuratus* (Stimpson). *Journal of Experimental Marine Biology and Ecology*, 108, 199–216.

WILEY, T.J. (2000) Relationship between rainfall and debris flows in western Oregon. *Oregon Geology*, 62, 27–43.

DIRECT IMPACTS OF NEAR-FUTURE OCEAN ACIDIFICATION ON SEA URCHINS

Sam T. Dupont and Mike S. Thorndyke

CLIMATE CHANGE PERSPECTIVES FROM THE ATLANTIC:
PAST, PRESENT AND FUTURE
Jose María Fernández-Palacios, Lea de Nascimento, José Carlos Hernández,
Sabrina Clemente, Albano González & Juan P. Díaz-González (eds.)
Servicio de Publicaciones, Universidad de La Laguna – 2013

ISBN: 978-84-15910-54-1
pp. 461-485

ABSTRACT

Anthropogenic CO_2 emissions are acidifying the world's oceans. A growing body of evidence demonstrates that this ocean acidification can impact survival, growth, development and physiology in marine invertebrates. A few years ago, a global analysis of the literature revealed that echinoderms were surprisingly robust to ocean acidification (Dupont *et al.,* 2010a). An updated semi-quantitative analysis of the literature confirms that sea urchins are resilient to near-future ocean acidification. Direct impacts of ocean acidification on sea urchins are mostly negative but sub-lethal. These include slower somatic and gonadal growth and reflect a shift in energy budgets linked to additional costs of pHe and pHi regulation rather than a direct impact on calcification. This highlights the plasticity of this taxonomic group at levels from molecular to whole organism physiology when facing a changing environment. All life-history stages can be impacted but juveniles are the most sensitive to near-future ocean acidification. Sea urchins also show evidence of acclimation and adaptation potential. However, despite some resilience to ocean acidification in adult and larval stages, strong negative carry-over effects between adult, larval and juvenile stages are likely to compromise the sustainability of some urchin populations. Most of the published evidence are based on short term analyses and focus on single life-history stages, neglecting key processes such as carry-over effects between different life-history stages and generations. As a consequence, the vast majority of published evidence probably underestimates the real impact of ocean acidification. Recommendations for experimental design and future research priorities are discussed.

KEYWORDS: Ocean Acidification, Sea Urchins, CO_2, Life History Stages, Climate Change, Physiology

INTRODUCTION

Since the beginning of the industrial revolution and the extensive use of fossil fuels, global atmospheric CO_2 concentration has increased from 280 to 400 ppm and is expected to double by 2100 with well described consequences for climate (global warming, increase in extreme events frequency, etc.) The ocean represents a major sink for CO_2 and absorbs half of the excess of this gas. Continued uptake of CO_2 alters the carbonate chemistry of the ocean and increases the concentration of hydrogen ions, thereby reducing pH, a phenomenon called ocean acidification (Caldeira and Wickett, 2003). An increasing body of evidence suggests that ocean acidification is a major threat for marine species and ecosystems, possibly leading to species extinctions within a few decades (e.g., Dupont *et al.*, 2008, 2010a, b).

CO_2 dissolution in seawater changes the equilibrium between bicarbonate and carbonate, depleting the available carbonate pool and increasing the rate of dissolution of deposited calcium carbonates. As a consequence, it is often suggested that marine calcifiers will be highly sensitive to near-future ocean acidification. Under this paradigm, sea urchins were identified early on as a primary target for ocean acidification research and are today one of the most studied models in this field. In a previous review, we concluded that echinoderms were surprisingly robust to ocean acidification (Dupont *et al.*, 2010a). We also highlighted some key modulating factors such as the time of exposure, the life-history stage, and strategies, genetic diversity, etc.

The aim of this chapter is to update this review and revise our conclusions in the light of new findings. We will focus on sea urchins, a vital component of the marine environment with representatives in virtually every ecosystem, strong socio-economic value (0.2% of global landings; Branch *et al.*, 2012) and used as model species in several scientific disciplines including developmental biology and ecotoxicology.

METHODS

Several strategies can be used to synthesize the available scientific information including narrative reviews and meta-analysis. Meta-analyses are believed to provide a more objective and informative alternative. However, the assumption that a meta-analysis represents the final and accurate viewpoint in an area of research is not always warranted. This is true for ocean acidification research where contrasting methodologies are used (Dupont *et al.*, 2010b). In consequence, we have decided to use a semi-quantitative strategy, quantifying the number of species or articles showing a similar response in similar experimental conditions and highlighting the more informative studies.

We compiled 49 research articles available to date (November 2012) investigating the impact of CO_2-driven ocean acidification on sea urchins using perturbation experiments. Studies that do not fully mimic the changes in carbonate chemistry expected from ocean acidification (e.g. manipulation of pH by addition of strong acids without manipulation of the alkalinity) were excluded. We considered all studies using at least one realistic ocean acidification scenario predicted for the end of the century (max $\Delta pH = 0.5$ units).

RESULTS AND DISCUSSION

SEMI-QUANTITATIVE LITERATURE DESCRIPTION

Most published studies use atmospheric pCO_2 to define their control measures instead of the carbonate chemistry in the species' habitat. The pH classically used as control is ~8.05 with future scenarios of ΔpH around -0.4 units. The aver-

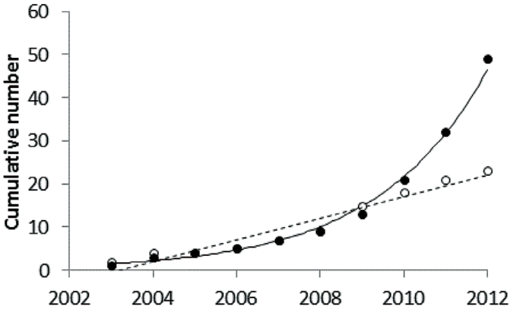

Figure 1. Cumulative number of published articles on the impact of ocean acidification on sea urchins (black circles) and studied sea urchin species (open circles) since 2003.

age number of pH treatments is 3.5 but ranges between 2 and 7. Only a few studies consider local environmental pH and its variability and use sufficient treatments to cover both today and future variability (see McElhany and Busch, 2012).

The cumulative number of articles increases exponentially with time while the number of studied species follows a linear relationship (Fig. 1). In consequence and compared to 2 years ago, information per species is increasing with time while less effort is invested in studying new species. For example, since the publication of our previous review on the impact of ocean acidification on echinoderms in 2010 (Dupont *et al.*, 2010a), only 8 new species of sea urchins were investigated (35% of all studied species) while 36 new articles were published (73% of all articles). This represents a species-article ratio of ~1:5 in the last 2 years compared to a ratio of ~1:1 before 2010.

Some species are more extensively studied than others (Fig. 2). The vast majority of species are only used as models in 1 to 3 articles. However, 3 species can now be considered as classic models in ocean acidification research due to their increasing and wider use by the community: (i) the green urchin *Strongylocentrotus droebachiensis* (6 articles; Box 1); (ii) the purple urchin *S. purpuratus* (7 articles; Box 2); and (iii) *Heliocidaris erythrogramma* (6 articles; Box 3).

General impact of ocean acidification on sea urchins

According to current evidence, the impact of ocean acidification on sea urchin fitness is either negative, through increased mortality, decreased fecundity or reduced fertilization success (29% of published articles; Fig. 3), a sublethal decreased growth rate (29%), or neutral (40%). A positive effect is only marginally observed (2%) and includes an increase in sperm swimming speed (Caldwell

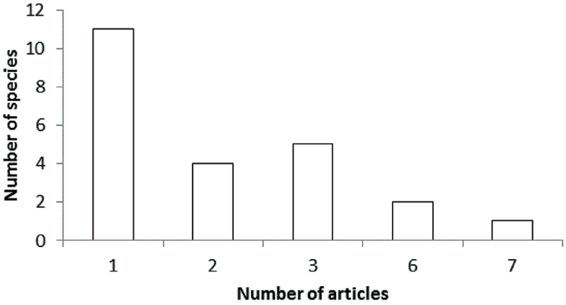

Figure 2. Relationship between the number of species and the number of research articles on impacts of ocean acidification on sea urchins in which they are used as model.

Box 1 – Ocean acidification top model #1: *Strongylocentrotus droebachiensis*

The green sea urchin *S. droebachiensis* is a widely distributed species that plays a key ecological and economical role in boreal coastal ecosystems. For example, on European coasts, grazing by this urchin is central in structuring marine benthic communities leading to two stable states: abundant kelp forests with a high biodiversity and species-depleted sea urchin barrens (Norderhaug and Christie, 2009). In some areas, the green sea urchin has been considered a pest as intensive grazing destroyed kelp habitats and limited the production of commercial species such as cod. On the other hand, it is fished and now cultured for roes in the Northern Atlantic and Northeast Pacific (Vadas *et al.*, 2000).

Impact of ocean acidification on adults is only sub-lethal. No increased mortality was observed in adult *S. droebachiensis* exposed to near-future OA (ΔpH=-0.4 unit) for up to 16 months (Dupont *et al.*, 2012). When an individual is exposed to lower pH, an extracellular acidosis is first observed (Spicer *et al.*, 2011) but is fully compensated within a few days (Dupont and Thorndyke, 2012; Stumpp *et al.*, 2012a). This acidosis is associated with an increase in coelomocyte in the extra-cellular fluid (Dupont and Thorndyke, 2012). The extracellular pH compensation is possible by accumulation of bicarbonate (Stumpp *et al.*, 2012a). Adult exposure to ocean acidification also resulted in a shift in energy budget, leading to a reduced somatic and reproductive growth (Siikavuopio *et al.*, 2007; Dupont *et al.*, 2012; Stumpp *et al.*, 2012a). Ammonium excretion increased suggesting an enhanced protein metabolism to support ion homeostasis by increasing net acid extrusion (Stumpp *et al.*, 2012a). However, the negative effect on fecundity observed after <4 months exposure was no longer observed in individuals acclimated for 16 months suggesting that the green sea urchin can fully acclimate to their new environment and are able to replenish their energy stores for reproduction (Dupont *et al.*, 2012).

The planktotrophic pluteus larvae of the green sea urchin are unable to compensate for an extracellular acidosis resulting from an exposure to ocean acidification. Sea urchin larvae have a leaky integument and the extracellular fluid conforms to the surrounding seawater pH. However, the calcifying primary mesenchyme cells are able to fully compensate an induced intracellular acidosis using a bicarbonate buffer mechanism involving secondary active Na^+-dependent membrane transport proteins (Stumpp *et al.*, 2012b). This is likely to be associated with an enhanced costs leading to modification in larval energy budget and negative impact on growth (Dupont *et al.*, 2012). Larval and juvenile survival is not directly impacted by ocean acidification. However, a strong carry-over between adults, larvae and juveniles is observed: when adults, larvae and juveniles are raised in ocean acidification conditions, a 100 time increase in juvenile mortality is observed (Dupont *et al.*, 2012).

In conclusion, despite some resilience to ocean acidification in adult and larval stages, strong negative carry-over effects between adult, larval and juvenile stages are likely to compromise *S. droebachiensis* population sustainability.

Box 2 - Ocean acidification top model #2: *Strongylocentrotus purpuratus*

The purple urchin *S. purpuratus* is an abundant long lived species and key component of the intertidal and sub-tidal zone of the Eastern Pacific coast, with a distribution range from Mexico to Alaska (Biermann *et al.*, 2003) and an important fishery resource. It is an important grazer of macroalgae, particularly kelp, where it competes with other grazers. It is a food source for many predators including sea otters (Steneck *et al.*, 2002).

Despite 7 articles published on this species, information on the impact of ocean acidification on the purple sea urchin is restricted to embryos and planktotrophic larval stages. When grown under ocean acidification conditions ($\Delta pH=0.5$), no difference is observed in the dynamic of the first cell division (Place and Smith, 2012). However, after several days, larvae are smaller in the ocean acidification treatments (Stumpp *et al.*, 2011a, b; Yu *et al.*, 2011) and suffer from a developmental delay (Stumpp *et al.*, 2011a, b). Larval respiration rates are increased at low pH while feeding rate remains unaffected. Ocean acidification has no direct effect on mortality but lead to a shift in energy budget with less energy available for somatic growth (Stumpp *et al.*, 2011b).

Thanks to a genome fully sequences, the purple sea urchin was one of the first species investigated using genomics tools. Impact of ocean acidification on embryos and larval transcriptomics was assessed using both microarrays (Todgham and Hofmann, 2009) and qPCR (Stumpp *et al.*, 2011a; Hammond *et al.*, 2012). However, only subtle differences in gene expression were documented.

In conclusion, the only documented negative effect of ocean acidification on *S. purpuratus* is a delay in development. However, the observed difference in larval growth rate can translate into a 2 time increase in mortality due to predation (Dupont *et al.*, 2010b).

Box 3 - Ocean acidification top model #3: *Heliocidaris erythrogramma*

The sea urchin *H. erythrogramma* is restricted to the south of Australia from Shark Bay on the west coast to Port Stephens in New South Wales on the eastern coast. The species is also known in Tasmania. It lives exclusively in the littoral zone and down to a depth of 35 m. It has large eggs and a rapid lecithotrophic development. About four to five days after fertilization it sinks to the bottom. More tube-feet, spines and pedicellariae emerge, and after about 23 days the juvenile begins to feed.

Most of the literature documenting the impact of ocean acidification on *H. erythrogramma* focuses on fertilization. Contrasting results from no effect (Byrne *et al.*, 2009, 2010a-b) to negative effect (Havenhand *et al.*, 2008) are described and were attributed to differences in experimental design. However, a recent study highlights the key role of inter-individual variations leading to a range of responses from positive to negative effects (Schlegel *et al.*, 2012).
H. erythrogramma is also one of the few species used to investigate the interaction between ocean acidification and increased temperature. Ocean acidification and temperature had no effect on fertilization success (Byrne *et al.*, 2010a, b) but it was shown that temperature but not ocean acidification has a negative impact on the percentage of gastrulation (Byrne *et al.*, 2009). The percentage of normal juveniles decreased in response to OA and increased temperature (Byrne *et al.*, 2011).
In conclusion, the combination of OA and temperature are likely to have negative impacts on *H. erythrogramma* juveniles.

et al., 2011) and moderately increased fertilization success in some individuals (Schlegel *et al.*, 2012).

No clear pattern in response is observed between studied areas (Fig. 3). However, the vast majority of studied species (78%) are temperate and entire geographical regions remain totally unexplored (e.g., Africa, South America, Polar regions). As a consequence, there is not enough data to draw any conclusion on sea urchin sensitivity and geographical locations (e.g., temperate vs. tropical vs. polar; coastal vs. deep sea). However, other parameters are well known to modulate a species' response to ocean acidification including (i) life-history stages and carry-over effects between subsequent stages and generations; (ii) the duration of exposure (e.g., acute vs. chronic) and intra-specific variability (potential for acclimation and adaptation).

Life-history stages

Most sea urchin species goes through three major transitions during the life cycle: (1) a first ecological transition occurs when adults release gametes (eggs or sperm) into the water column to ensure fertilization. This transition between benthic and pelagic environment is also associated with complex developmental changes (fertilization, embryo and larval development); (2) the second ecological transition (settlement from pelagic to benthic environment) occurs at about the same time as anatomical changes during the metamorphosis of the larva into a young juvenile; and (3) the post-metamorphic anatomical transition between the juvenile and the adult. A semi-quantitative evaluation of the literature (Fig. 4) suggests a higher resilience to ocean acidification in adults and gametes (fertilization) compared to embryos/larvae and juveniles. Negative effects on fitness is observed in more than 85% of the published studies for embryos/larvae and

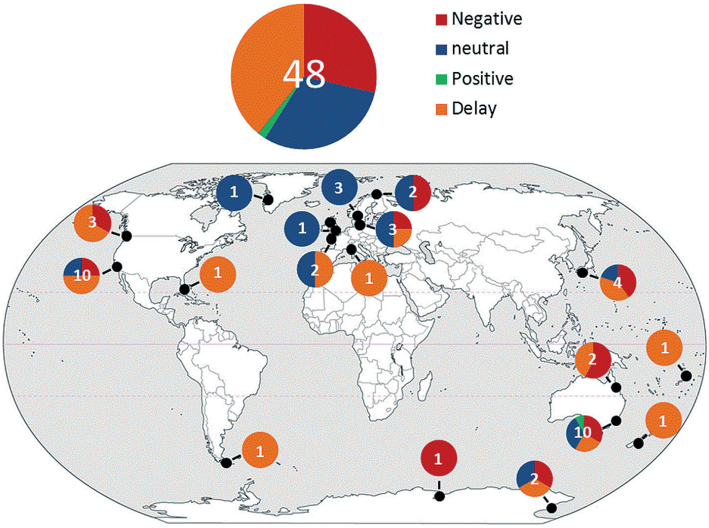

Figure 3. Proportion of published articles showing negative, neutral, positive or sublethal (delay in development or decreased growth rate) impacts of ocean acidification on sea urchin fitness in different geographic areas. Number of published article per location in indicated in each pie chart.

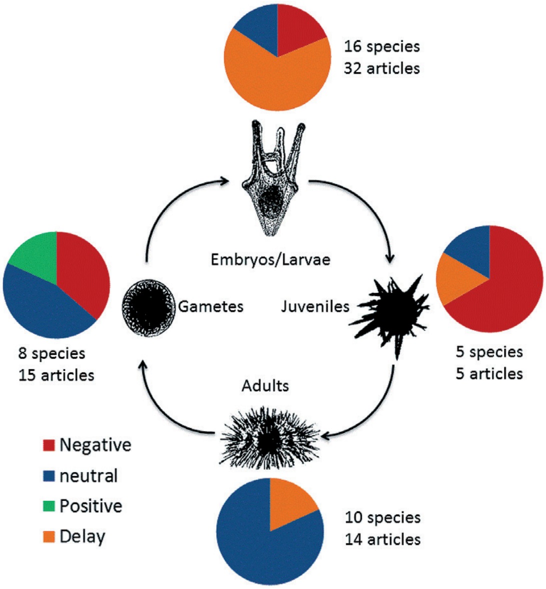

Figure 4. Proportion of published articles showing lethal (negative, neutral, positive) or sublethal (delay in development or decreased growth rate) impacts of ocean acidification on fitness related parameters in sea urchin life-history stages.

juveniles compared to 30-35% for gametes and adults. For a discussion on the modulating role of life-history strategies in echinoderms, see Dupont *et al.*, 2010c.

A part of the variability observed between studies investigating similar processes/stages is likely to be a consequence of contrasting experimental design. For example, using similar pH changes and working on the same species (*H. erythrogramma*), Byrne *et al.*, (2009; 2010a, b) showed no effect on fertilization while Havenhand *et al.*, (2008) showed a negative effect. This may partly reflect differences in experimental design (polyandry vs. single male-female crosses, sperm concentration, stability of pH, use of different sperm:egg ratios, sperm-egg contact time, etc.; e.g., Reuter *et al.*, 2011) but also individual variability in reproductive success (Schlegel *et al.*, 2012), a parameter only now beginning to be considered.

In 78% of all studied species, information is only available for 1 or 2 life-history stages (Table 1). Information on 3 life-history stages is available for 4 species (*Heliocidaris erythrogramma, Hemicentrotus pulcherrimus, Paracentrotus lividus* and *S. droebachiensis*) and information on the 4 life history stages is only available for the urchin *Echinometra mathaei* (Box 4).

Life-history stages form a continuum and an environmental change leading to a disturbance in one stage can carry-over into the following stage (Podolsky and Moran, 2006). Only two studies of the impact of ocean acidification on sea urchins, from the 49 published to date, considered these carry-over effects. Exposure of adult *E. mathaei* to ocean acidification for 7 weeks had no effect on larval response to ΔpH=-0.5 (no carry-over effect, Uthicke *et al.*, 2012). However, a clear and strong negative carry-over was observed in *S. droebachiensis* (Dupont *et al.*, 2012). Taken individually, each life-history stage (larval, juvenile and adult) appears to be quite resilient to ocean acidification. However, when adults were exposed to ΔpH=-0.4 for 4 months, 5 to 9 times less larvae produced by gametes from those adults reached the juvenile stage. Moreover, an additional negative carry-over effect was observed on juvenile survival when both larvae and juveniles were raised under ocean acidification conditions leading to a total of 100 times less eggs surviving the first 4 months of development (Dupont *et al.*, 2012). Thus, considering only single life-history stages can lead to an underestimation of the real impact of ocean acidification.

Duration of the exposure

In our previous review on impacts of ocean acidification on echinoderms, we already highlighted the importance of long-term exposure times (Dupont *et al.*, 2010a). Surprisingly, the time of exposure in perturbation experiments is not increasing in the published literature (Fig. 5). The average duration time is 37±12 days but varies with life-history stages (Larvae: 9±3 days; Juveniles: 135±36 days; Adults: 63±2 days).

TABLE 1. Number of published articles investigating the impact of ocean acidification on a given life-history stage (gametes, embryos/larvae juveniles or adults) for 23 species of sea urchins.

Species	Gametes	Embryos/Larvae	Juveniles	Adults
Arachnoides placenta	1	1	.	.
Arbarcia drufresnei	.	1	.	.
Arbarcia punctulata	1	.	.	1
Brissopsis lyrifera	.	.	.	1
Centrostephanus rodgersii	.	3	.	.
Cystechinus sp.	.	.	.	1
Denstraster excentricus	.	1	.	.
Echinocardium cordatum	.	.	.	1
Echinometra mathaei	**1**	**2**	**1**	**1**
Eucidaris tribuloides	.	.	.	1
Evechinus chloroticus	.	1	.	.
Heliocidaris erythrogramma	5	2	1	.
Hemicentrotus pulcherrimus	1	2	1	.
Lytechinus pictus	.	1	1	.
Paracentrotus lividus	3	2	.	1
Psammechinus miliaris	.	.	.	1
Pseudechinus huttoni	.	1	.	.
Sterechinus neumayeri	2	3	.	.
Strongylocentrotus franciscanus	1	2	.	.
Strongylocentrotus droebachiensis	.	1	1	5
Strongylocentrotus purpuratus	.	7	.	.
Tripneuste gratilla	.	2	.	.

BOX 4 - OCEAN ACIDIFICATION TOP MODEL #4: *ECHINOMETRA MATHAEI*

The burrowing urchin *E. mathaei* is found on reefs in tropical parts of the Indo-Pacific Ocean at depths down to 139 m. Its range extends from Madagascar, the East African coast and the Red Sea to Hawaii. *E. mathaei* uses its spines and teeth to dig itself into the calcareous rock where it lives causing coral reef erosion. It emerges from these hollows at night to graze on algae.

E. mathaei is the only sea urchin species with all the life-history stages investigated in the context of ocean acidification. While fertilization and embryos development were robust under near-future ocean acidification conditions, a delay in development was observed in the planktotrophic pluteus larvae (Kurihara and Shirayama, 2004; Uthicke *et al.*, 2012). Both growth and survival were negatively impacted in juveniles exposed to ΔpH<0.1 for up for 6 months (Shirayama and Thornton, 2005). Following a 6 weeks acclimation to ocean acidification, adults exhibit a slight decline of growth and an associated reduced respiration. This acclimation did not affect female spawn ability but had a negative effect on male spawning ability (Uthicke *et al.*, 2012). In conclusion, negative effects of ocean acidification through reduced larval growth rate and juvenile increased mortality is then possible.

A key question for ocean acidification research is how «long» is «long enough» to evaluate the real impact of near-future ocean acidification on a given specie. For example, it was demonstrated that ocean acidification induced a 4.5 fold decrease in female fecundity exposed for 4 months during the reproductive conditioning period in the sea urchin *S. droebachiensis*. In contrast, no impact on fecundity was observed for the same species after 16 months exposure to ocean acidification (Dupont *et al.,* 2012). This suggests that more than 4 months exposure is needed for some adult urchin species to be fully acclimated to their new environmental conditions. As a consequence, experiments considering exposure times shorter than 4 months may over-estimate the real impact of ocean acidification.

Individual variability and adaptation potential

Differences in tolerance to ocean acidification have been observed within the same species. Some of these differences can be attributed to differences in experimental design (see above for discussion on fertilization success in *H. erythrogramma*). However, genuine intraspecific differences have been observed between (Carr *et al.*, 2006; Moulin *et al.*, 2010) and within populations of the same species (Chan *et al.*, 2011, 2012; Sunday *et al.*, 2011; Foo *et al.*, 2012; Schlegel *et al.*, 2012). Understanding the genetic contribution to this observed variation is of vital importance if we are to be able to estimate the potential of a given species to adapt to ocean acidification. For sea urchins, only two studies have attempted to quantify adaptation capacity and rates of evolutionary adaptation in response to ocean acidification (Sunday *et al.*, 2011; Foo *et al.*, 2012). For example, using a full-factorial breeding design, Sunday *et al.* (2011) showed that the sea urchin *Strongylocentrotus franciscanus* has a high level of phenotypic and genetic variation for larval size when exposed to ΔpH=-0.4 together with a potential for fast evolutionary response within 50 years.

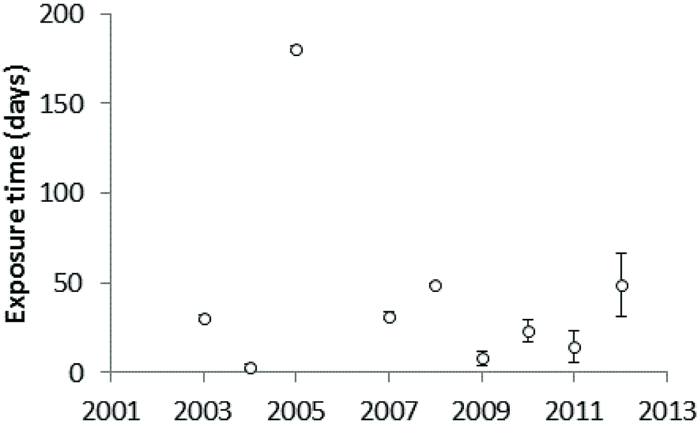

Figure 5. Evolution through time of the average (±standard error of mean) exposure time (days) in perturbation experiments studying the impact of ocean acidification on sea urchins.

A NEED FOR A BETTER MECHANISTIC UNDERSTANDING

One of the challenges of ocean acidification research is to provide realistic projections of the potential impacts on marine species and ecosystems at the global and local levels. While studies of the impacts of individual marine stressors such as ocean acidification have matured, in the real world ocean acidification acts in concert with other global (e.g., warming, de-oxygenation) and local (over-fishing, eutrophication, pollution) stressors. For sea urchins, temperature is the only other stressor that has been evaluated in interactions with ocean acidification (8 articles; Sheppard Brennand *et al.*, 2010; Byrne *et al.,* 2010a, b, 2011; Caldwell *et al.*, 2011; Catarino *et al.*, 2012; Ericson *et al.*, 2012; Foo *et al.*, 2012). From this limited dataset, it appears that interaction between temperature and ocean acidification is complex and can include temperature being the main driver of change or temperature amplifying or diminishing the negative effects of ocean acidification. For example, in adult *Paracentrotus lividus,* oxygen uptake was increased under ocean acidification at 10°C but not at 16°C (Catarino *et al.*, 2012) but warming diminished the negative effect of acidification on *Tripneuste gratilla* larval growth (Sheppard Brennand *et al.*, 2010).

Moreover, experimental studies often neglect local environmental variability of pH but also other important environmental parameters and stressors that may have important adaptive impacts on endemic populations. As a consequence, the combined impacts of ocean acidification in the context of multiple stressors and their natural variability are largely unknown. This is complicated by the fact that impacts of ocean acidification are species-, population- and even individual-specific. It is then practically impossible to evaluate the impact of ocean acidification experimentally on the numerous populations of the 950 species of sea urchins in all locally relevant environmental conditions.

Rather than *stamp collecting* by testing one species after the other, another approach is to develop a mechanistic understanding of the observed responses. Sea urchins provide a powerful model to investigate the mechanisms underlying responses to ocean acidification. They are among the best studied marine animals with considerable resources available including full genome sequences and an in-depth understanding of gene regulatory networks (Sodergren *et al.*, 2006).

A range of techniques are classically used in sea urchin ocean acidification research. Fitness related processes such as survival (13 studies), fecundity (5 studies), growth (28 studies) and abnormalities (8 studies) are classically measured using simple techniques such as microscopy and morphometry. Response at the transcriptome level has been investigated using qPCR (5 studies) or microarrays (2 studies). Less effort has been invested in measuring physiological parameters such as oxygen consumption (4 studies), feeding (3 studies), swimming behavior (1 study), acid-base regulation (6 studies) and calcification/skeletal integrity (8 studies).

Mortality/Abnormality

Surprisingly, mortality/survival is not systematically considered in studies investigating the impact of ocean acidification on sea urchins. Nevertheless, available data suggest that adults are resilient to medium (<4 months; Dashfield *et al.*, 2008; Dupont and Thorndyke, 2012; Dupont *et al.*, 2012; Stumpp *et al.*, 2012b) and long term exposure (16mo; Dupont *et al.*, 2012) with no impact of ocean acidification on mortality. No increased mortality is documented in larval stages reared under near-future ocean acidification conditions (up to 21 days exposure; Clark *et al.*, 2009; Stumpp *et al.*, 2011; Chan *et al.*, 2012; Gonzalez-Bernat *et al.*, 2012). This is consistent with the lack of strong effects of ocean acidification on % of embryo/larval abnormality (Ericson *et al.*, 2010; Sheppard Brennand *et al.*, 2010; Catarino *et al.*, 2011; Stumpp *et al.*, 2011b) with only a small % increase in abnormality observed in 2 species (Ericson *et al.*, 2012; Uthicke *et al.*, 2012). The bottleneck is the juvenile stage showing an increase % of abnormalities (5 days; Byrne *et al.*, 2010) and mortality (26 weeks; Shirayama and Thornton, 2005) that can reach 100 times increased mortality over 3 months when carry-over effects are considered (Dupont *et al.*, 2012). Similarly a doubling of abnormalities during juvenile development was observed.

Growth

The most studied parameter is growth. Embryo development is not significantly impacted by ocean acidification (Kurihara *et al.*, 2004; Byrne *et al.*, 2009; Ericson *et al.*, 2010; Foo *et al.*, 2012; Place and Smith, 2012). With a few exceptions (no effect on growth, Clark *et al.*, 2009; Moulin *et al.*, 2010), negative effects on growth (reduced size at a given time and/or delayed development) is the rule for sea urchin larvae (Kurihara and Shirayama, 2004; Kurihara *et al.*, 2004; O'Donnell *et al.*, 2010; Sheppard Brennand *et al.*, 2010; Catarino *et al.*, 2011; Chan *et al.*, 2011; Martin *et al.*, 2011; Stumpp *et al.*, 2011a, b; Sunday *et al.*, 2011; Doo *et al.*, 2012; Gonzalez-Bernat *et al.*, 2012; Uthicke *et al.*, 2012). For example, a 2 day delay in development was observed in the sea urchin *S. purpuratus* when raised in ΔpH=-0.4 (Stumpp *et al.*, 2011b). A negative effect on growth was also observed in juvenile urchins (Shirayama and Thornton, 2005; Albright *et al.*, 2012) with negative impact on growth observed in *E. mathaei* exposed for 26 weeks (Shirayama and Thornton, 2005). Only one study considered the impact of ocean acidification on adult urchins and revealed a negative effect on growth at ΔpH<0.5 (Stumpp *et al.,* 2012b).

Fecundity

When exposure time is <4 months, the impact of ocean acidification on sea urchin fecundity is negative (but see Catarino *et al.*, 2012 showing no effect on RNA:DNA ratio after 19d exposure): decreased gonadal growth (56d, Siikavuopio *et al.*, 2007; 45d, Stumpp *et al.*, 2012b), reduced male spawning response (7 weeks, Uthicke *et al.*, 2012) and egg production (4 months, Dupont *et al.*, 2012). Gonads can be considered the most plastic body compartment in adult sea urchins and are often used as an energy storage that can be filled or depleted depending on conditions. The observed decreased fecundity is likely to reflect the increased energy costs needed for survival in a more challenging environment. However, the negative effect observed on fecundity after 4 months of exposure in the sea urchin *S. droebachiensis* disappeared after 16 months exposure (Dupont *et al.*, 2012). This suggests that impacts on fecundity are transient and that adults were able to replenish their energy stores for successful reproduction after full acclimation.

Molecular level

Transcriptomics approaches have so far only used on early life-history stages. Two microarray and two qPCR studies showed altered gene expression in embryos and early pluteus stages exposed to ocean acidification conditions including a down-regulation of genes related to biomineralization (Todgham and Hofmann, 2009; O'Donnell *et al.,* 2010; Hammond and Hofmann, 2012; Kurihara *et al.,* 2012), cell stress responses, metabolism and apoptosis (Todgham and Hofmann, 2009). However, these studies did not consider the direct effect of ocean acidification on developmental rate and part of the observed effect may be attributed to a delay of development rather than a direct effect of gene expression (see Pörtner *et al.*, 2010 for a discussion on experimental design). When corrected for developmental delay, an up-regulation of genes related to metabolism and down-regulation of genes related to biomineralization were observed (Stumpp *et al.*, 2011a). Overall, transcriptomics data reveal plasticity at the gene expression level that allows a normal, but delayed, development under ocean acidification conditions (Martin *et al.*, 2011).

Physiology

When acutely exposed to ocean acidification conditions, both larval and adult sea urchins experience extracellular acidosis. In adults, this acidosis can remain uncompensated for a few days (Miles *et al.*, 2007; Spicer *et al.*, 2011, 2012) but can be fully compensated during medium- to long-term exposure (Catarino *et al.*, 2012; Dupont and Thorndyke, 2012; Stumpp *et al.*, 2012a) by accumulation of bicarbonate in the extracellular fluids. In pluteus larvae, extracellular fluid remains uncompensated but calcifying primary mesenchyme cells are able to fully compensate the intracellular acidosis by mechanisms involving bicarbonate buffering (Stumpp *et al.,* 2012a).

In juveniles and adults, ocean acidification exposure for up to 45 days has been shown to have only subtle positive or negative effects on metabolic rates (Catarino *et al.*, 2012; Stumpp *et al.*, 2012b; Uthicke *et al.*, 2012). In contrast, pluteus larvae of *S. purpuratus* increased their respiration rates by up to 100% under ocean acidification (Stumpp *et al.*, 2011b).

Calcification, one of the processes widely predicted to be affected by ocean acidification, is also poorly investigated. Overall, calcification seems fairly resilient to ocean acidification. Only one study investigates the impact of ocean acidification on adults showing contrasting responses between two species (positive in *Arbarcia punctulata,* no effect in *Eucidaris tribuloides*; Ries *et al.*, 2009). In juveniles of *Lytechinus variegatus,* subtle skeletal malformation and/or dissolution was observed after 89d of ΔpH=-0.3 (Albright *et al.*, 2012). Ocean acidification had no direct impact on *Paracentrotus lividus* pluteus larval calcification rates until ΔpH<-0.75 (Martin *et al.*, 2011). However, apparent degradation of the skeletal fine structure was observed in two sea urchin species (*Sterechinus neumayeri* and *Tripneuste gratilla*; Clark *et al.*, 2009).

Adult feeding is negatively impacted by ocean acidification (Siikavuopio *et al.*, 2007; Stumpp *et al.*, 2012b) while pluteus larval feeding remains unaffected (Stumpp *et al.*, 2011b).

TABLE 2. Summary of the impact of ocean acidification on sea urchin physiology. +, increased; =, neutral; -, decreased.

	Adult	Juvenile	larvae
Growth	-	-	= / -
Feeding	-	?	=
Respiration	=	?	+
Reproduction	-	.	.
Calcification	= / +	?	=
Acid-base	+	?	+

The only behavioral studies on sea urchin published so far, investigated the swimming behavior of the sand dollar *Denstraster excentricus* reared under ocean acidification conditions. Pluteus larvae developed narrower bodies but without any impact on swimming speed (Chan *et al.*, 2011).

Surprisingly, regarding the key role of immunity in fitness, the impact of ocean acidification on sea urchin immunity is neglected. Dupont and Thorndyke (2012) showed an intriguing relationship between coelomic fluid acidosis and an increase in phagocyte numbers, cells playing a key role in cellular immune-response. However, no study has yet considered the immune response functionally, from the perspective of fitness and resource allocation.

Energy budget

Mechanistic understanding of the impact of ocean acidification on sea urchins is in its infancy and little information is currently available on the physiological processes involved (Table 2). However, based on the limited information available, we can propose conceptual models for sea urchin responses to ocean acidification based on shifts in energy budget:

(i) In adults, acute exposure to ocean acidification induces acidosis in coelomic fluid. Urchins are able to compensate fully for this acidosis leading to an increased energy cost needed for maintenance. Ocean acidification also directly impacts feeding ability and thus the total amount of energy available. The increased energy needs for maintenance combined with a decreased amount of resources (energy) available leads to a significant decrease in energy available for other processes, such as somatic and gonadal growth (Fig. 6). However, under long-term exposure (>4 months), adults urchins

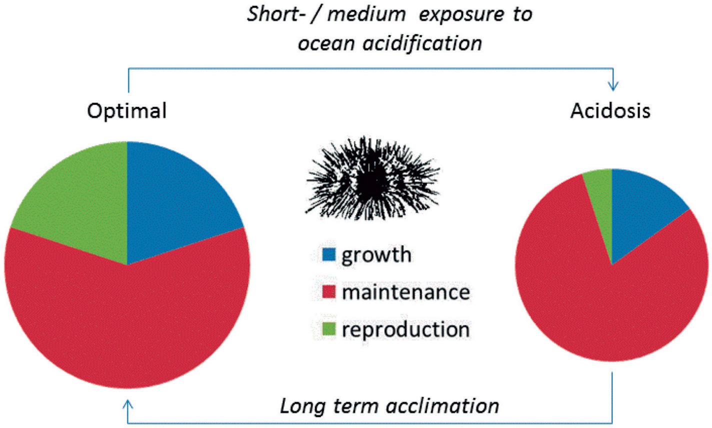

Figure 6. Adult energy budget under control and ocean acidification conditions. The size of the pie chart is proportional to the amount of energy available.

are able to acclimate (e.g. developing a more efficient pH regulatory system) and restore their initial energy budget (Dupont *et al.*, 2012).

(ii) Similarly, pluteus larvae are able to cope quickly with extracellular acidosis by fully compensating at the intracellular level. The associated cost of pHi regulation combined with no direct effect of ocean acidification on energy acquisition (feeding) leads to a shift in energy budget with less energy available for growth (delayed growth rate; Fig. 7).

Surprise surprise

The field of ocean acidification is maturing and is moving from an exploratory to a hypothesis-driven phase. However, we predict that it is very likely that some unexpected effects will be observed in coming years. For example, it was recently shown that ocean acidification can induce high-frequency budding (release of blastula-like structures) in *S. purpuratus* larval stages (Chan *et al.*, 2012; Fig. 8) leading to new hypotheses regarding the potential physiological and ecological tradeoffs between short-term and long-term costs in the face of ocean acidification.

CONCLUSIONS

Direct impacts of ocean acidification on sea urchins are generally negative but mostly sublethal. Effects include slower somatic and gonadal growth and reflect a shift in energy budgets linked to the additional costs for increased pHe

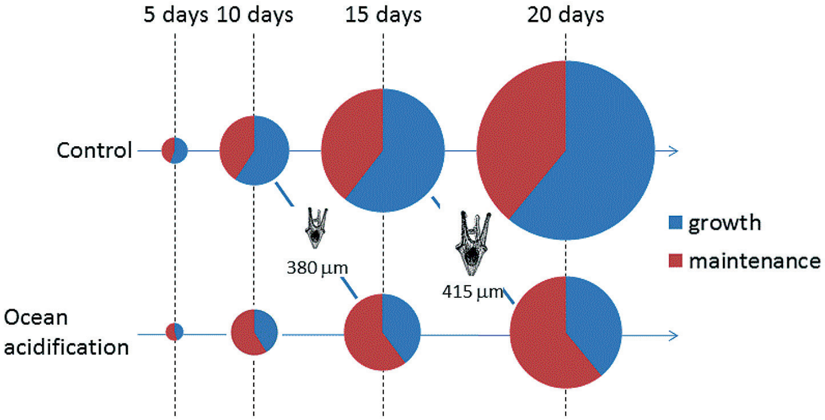

Figure 7. Pluteus larvae energy budget under control and ocean acidification conditions (calculated from Stumpp *et al.*, 2011b for *Strongylocentrotus purpuratus*). The size of the pie chart is proportional to the amount of energy available.

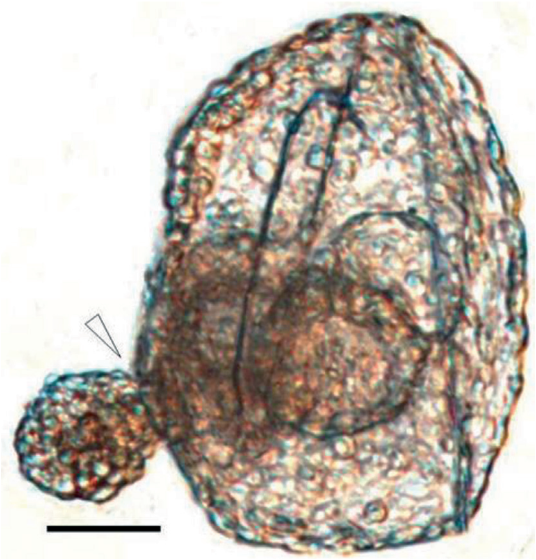

Figure 8. Seven days old larval *S. purputatus* actively budding when cultured in ocean-acidification conditions (ΔpH<-0.2). The arrow indicates the site of constriction leading to bud formation. Scale = 50µm

and pHi regulation rather than direct impacts on calcification. This highlights the plasticity of this taxonomic group at all levels from molecular to whole organism physiology when facing a changing environment.

However, most studies published to date have probably under-estimated the real impacts of ocean acidification on sea urchins. To better estimate these impacts, future experimental design should allow long term-exposure and consider multiple subsequent life-history stages to include acclimation, adaptation and carryover effects. Tested scenarios should also consider local environmental pH, its variability and sufficient treatments to cover both today and future (predicted) variability.

Our recommendations include:

- All life-history stages, transitions between these stages and carry-over effects should be considered. Partial information on all life-history stages is only available for 1 species (Box 4) and ironically the most-sensitive life-history stage (juveniles) is the less studied.
- More physiology and a better mechanistic understanding of sea urchin responses to ocean acidification is needed. It is not possible to test all species in all relevant environmental conditions (including variability, micro-environments and multiple stressors). Understanding the physiology and physiological tipping points in a range of environmental conditions would allow us to highlight unifying principles underlying sea urchin responses to ocean acidification and develop our predictive capability.
- There is a real need to better understand the relative contributions of the different processes (e.g. calcification) to the energy budget and how these tradeoffs are impacted by ocean acidification.
- Some key fitness-related processes such as the immune-response should be better investigated.
- Some regions of the world are neglected (e.g. Polar, Africa, South America) and should be considered for selection of new model species and populations.

This chapter focused on the impact of ocean acidification on sea urchins at the organismal level. However, it is also critical to understand impacts at the ecosystem level and how ecological interactions (e.g. competition, food quantity and quality, chemical ecology, pathogens etc.) modulate individual responses. For example, a few days delay in development during larval development can translate into a significant mortality due to predation (Dupont *et al.*, 2010b).

Over the last 10 years and thanks to its key role as model species in many scientific disciplines, sea urchins have been instrumental in understanding the impacts of ocean acidification on invertebrate species, in identifying key biological aspects modulating a species response and in guiding best practice for experimental design. There is no doubt that sea urchins will continue to play a key role in ocean acidification research.

REFERENCES

Albright, R., Bland, C., Gilette, P., Serafy, J.E., Langdon, C. and Capo, T.R. (2012) Juvenile growth of the tropical sea urchin *Lytechinus variegatus* exposed to near-future ocean acidification scenarios. *Journal of Experimental Marine Biology and Ecology,* 426–427, 12–17.

Biermann, C.H., Kessing, B.D. and Palumbi, S.R. (2003) Phylogeny and development of marine model species: strongylocetrotid sea urchins. *Evolution and Development,* 5, 360–371.

Byrne, M., Ho, M, Wong, E, Soars, N.A., Selvakumaraswamy, P., Shepard-Brennand, H., Dworjanyn, S.A. and Davis, A.R. (2011) Unshelled abalone and corrupted urchins: development of marine calcifiers in a changing ocean. *Proceedings of the Royal Society B, Biological Sciences,* 278: 2376–2383.

Byrne, M., Ho, M., Selvakumaraswamy, P., Nguyen, H.D., Dworjanyn, S.A. and Davis, A.R. (2009) Temperature, but not pH, compromises sea urchin fertilization and early development under near-future climate change scenarios. *Proceedings of the Royal Society part B Biological sciences,* 276, 1883–1888.

Byrne, M., Soars, N, Selvakumaraswamy, P., Dworjanyn, S.A. and David, A.R. (2010a) Sea urchin fertilization in a warm, acidified and high pCO_2 ocean across a range of sperm densities. *Marine Environmental Research,* 69, 234–239.

Byrne, M., Soars, N.A., Ho, M.A., Wong, E., McElroy, D., Selvakumaraswamy, P., Dworjanyn, S.A. and Davis, A.R. (2010b) Fertilization in a suite of coastal marine invertebrates from SE Australia is robust to near-future ocean warming and acidification. *Marine Biology*, 157, 2061–2069.

Caldeira, K. and Wickett, M.E. (2003) Anthropogenic carbon and ocean pH. *Nature,* 425, 365.

Caldwell, G.S., Fitzer, S., Gillespie, C.S., Pickavance, G., Turnbull, E. and Bentley, M.G. (2011) Ocean acidification takes sperm back in time. *Invertebrate Reproduction and Development*, 4, 217–221.

Carr, R.S., Biedenbach, J.M. and Nipper, M. (2006) Influence of potentially confounding factors on sea urchin porewater toxicity tests. *Archives of Environmental Contamination and Toxicology,* 51, 573–579.

Catarino, A.I., Bauwens, M. and Dubois, P. (2012) Acid-base balance and metabolic response of sea urchin *Paracentrotus lividus* to different seawater pH and temperatures. *Environmental Science and Pollution Research*, 19, 2344–2353.

Catarino, A.I., De Ridder, C., Gonzalez, M., Gallardo, P. and Dubois, P. (2011) Sea urchin *Arbacia dufresnei* (Blainville 1825) larvae response to ocean acidification. *Polar Biology*, 35, 455–461.

Chan, K.Y., Grünbaum, D., Arnberg, M., Thorndyke, M. and Dupont, S.T. (2012) Ocean acidification induces budding in larval sea urchins. *Marine Biology*, DOI: 10.1007/s00227-012-2103-6.

Chan, K.Y.K., Grünbaum, D. and O'Donnell, M.J. (2011) effects of ocean-acidification-induces morphological changes on larval swimming and feeding. *The Journal of Experimental Biology*, 214, 3857–3867.

Clark, D., Lamare, M. and Barker, M. (2009). Response of sea urchin pluteus larvae (Echinodermata: Echinoidea) to reduced seawater pH: a comparison among a tropical, temperature, and a polar species. *Marine Biology,* 156, 1125–1137.

Dashfield, S.L., Somerfield, P.J., Widdicombe, S., Austen, M.C. and Nimmo, M. (2008) Impacts of ocean acidification and burrowing urchins on within-sediment pH profiles and subtidal nematode communities. *Journal of Experimental Marine Biology and Ecology,* 365, 46–52.

Doo, S.S., Dworjanyn, S.A., Foo, S.A., Soars, N.A. and Byrne, M. (2012) Impacts of ocean acidification on development of the meroplanktonic larval stage of the sea urchin *Centrostephanus rodgersii. ICES Journal of Marine Sciences*, 69, 460–464.

Dupont, S. and Thorndyke, M. (2012) Relationship between CO_2-driven changes in extracellular acid-base balance and cellular immune response in two polar echinoderm species. *Journal of Experimental Marine Biology and Ecology,* 424–425, 32–37.

Dupont, S., Dorey, N. and Thorndyke, M. (2010b) What meta-analysis can tell us about vulnerability of marine biodiversity to ocean acidification? *Estuarine, Coastal and Shelf Science*, 89, 182–185.

Dupont, S., Dorey, N., Stumpp, M., Melzner, F. and Thorndyke, M. (2012) Long-term and trans-life-cycle effects of exposure to ocean acidification in the green sea urchin *Strongylocentrotus droebachiensis. Marine Biolog,* DOI 10.1007/s00227-012-1921-x.

Dupont, S., Lundve, B. and Thorndyke, M. (2010c) Near future ocean acidification increases growth rate of the lecithotrophic larvae and juvenile of the seastar *Crossaster papposus. The Journal of Experimental Zoology part B*, 314B, 382–389.

Dupont, S., Ortega-Martinez, O. and Thorndyke, M. (2010a) Impacts of near-future ocean acidification on echinoderms. *Ecotoxicology,* 19, 449–462.

Ericson, J.A., Ho, M.A., Miskelly, A., King, C.K., Virtue, B., Tilbrook, B. and Byrne, M. (2012) Combined effects of two ocean change stressors, warming and acidification, on fertilization and early development of the Antarctic echinoids *Sterechinus neumayeri. Polar Biology,* 35, 1027–1034.

Ericson, J.A., Lamare, M.D., Morley, S.A. and Barker, M.F. (2010) The response of two ecologically important Antarctic invertebrates (*Sterechinus neumayeri* and *Parborlasia corrugatus*) to reduced seawater pH: effects on fertilisation and embryonic development. *Marine Biology*, 157, 2689–2702.

Foo, S.A., Dworjanyn, S.A., Poore, A.G.B. and Byrne, M. (2012) Adaptive capcity of the habitat modifying sea urchin *Centrostephanus rodgersii* to ocean warming and ocean acidification: performance of early embryos. *PloS One,* 7, e42497.

Gonzalez-Bernat, M.J., Lamare, M., Uthicke, S. and Byrne, M. (2012) Fertilisation, embryogenesis and larval development in the tropical intertidal sand dollar *Arachnoides placenta* in response to reduced seawater pH. *Marine Biology*, DOI 10.1007/s00227-012-2034-2.

Hammond, L.M. and Hofmann, G.E. (2012) Early developmental gene regulation in *Strongylocentrotus purpuratus* embryos in response to elevated CO_2 seawater conditions. *The Journal of Experimental Biology,* 215, 2445–2454.

Havenhand, J.N., Butler, F-R., Thorndyke, M.C. and Williamson, J.E. (2008) Near-future levels of ocean acidification reduce fertilization success in a sea urchin. *Current Biology*, 18, R651–R652.

Kurihara, H. and Shirayama, Y. (2004) Effects of increased atmospheric CO_2 on sea urchin early development. *Marine Ecology Progress Series,* 274, 161–169.

Kurihara, H., Shimode, S. and Shirayama, Y. (2004) Sub-lethal effects of elevated concentration of CO_2 on planktonic copepods and sea urchins. *Journal of Oceanography*, 60, 743–750.

Kurihara, H., Takano, Y., Kurosawa, D. and Akasaka, K. (2012) Ocean acidification reduces biomineralization-related gene expression in the sea urchin, *Hemicentrotus pulcherrimus. Marine Biology,* 159, 2819–2826.

Martin, S., Richier, S., Pedrotti, M-L., Dupont, S., Castejon, C., Gerakis, Y., Kerros, M-E., Oberhänsli, F., Teyssié, J-L., Jeffree, R. and Gattuso, J-P. (2011) Early development and molecular plasticity in the Mediterranean sea urchin *Paracentrotus lividus* exposed to CO_2-driven acidification. *The journal of Experimental Biology*, 214, 1357–1368.

McElhany, P. and Busch, S.D. (2012) Appropriate $p\mathrm{CO}_2$ treatments in ocean acidification experiments. *Marine Biology.* DOI 10.1007/s00227-012-2052-0.

Miles, H, Widdicombe, S, Spicer, J.I. and Hall-Spencer, J. (2007) Effects of anthropogenic seawater acidification on acid-base balance in the sea urchin *Psammechinus miliaris. Marine Pollution Bulletin,* 54, 89–96.

Moulin, L, Catarino, A.I., Claessens, T. and Dubois, P. (2010) Effects of seawater acidification on early development of the intertidal sea urchin *Paracentrotus lividus* (Lamarck 1816). *Marine Pollution Bulletin,* 62, 48–54.

Norderhaug, K.M. and Christie, H.C. (2009) Sea urchin grazing and kelp re-vegetation in the NE Atlantic. *Marine Biology Research,* 5, 515–528.

O'Donnell, M., Hammond, L.M. and Hofmann, G.E. (2009) Predicted impact of ocean acidification on a marine invertebrate: elevated CO_2 alters response to thermal stress in sea urchin larvae. *Marine Biology*, 156, 439–446.

O'Donnell, M.J., Todgham, A.E., Sewell, M.A., Hammond, L.M., Ruggiero, K., Fangue, N.A., Zippay, M.L. and Hofmann, G.E. (2010) Ocean acidification alters skeletogenesis and gene expression in larval sea urchins. *Marine Ecology Progress Series,* 398, 157–171.

Place, S.P. and Smith, B.W. (2012) Effects of seawater acidification on cell cycle control mechanisms in *Strongylocentrotus purpuratus* embryos. *PloS One*, 7, e34068.

Podolsky, R.D. and Moran, A.L. (2006) Integrating function across marine life cycles. *Integrative and Comparative Biology,* 46, 577–586.

Pörtner, .H.O, Dupont, S., Melzner, F. and Thorndyke, M. (2010) Laboratory experiments and benthic mesocosm studies. *Guide to best practices for ocean acidification research and data reporting* (ed. by Riebesell, U., Fabry, V.J., Hansson, L. and Gattuso, J-P.), pp. 167–180. Publications Office of the European Union, Luxembourg.

Reuter, K.E., Lotterhos, K.E., Crim, R.N., Thompson, C.A. and Harley, C.D. (2011) Elevated pCO_2 increases sperm limitation and risk of polyspermy in the red urchin *Strongylocentrotus franciscanus. Global Change Biology,* 17, 163–171.

Ries, J.B., Cohen, A.L. and McCorkle, D.C. (2010) Marine calcifiers exhibit mixed responses to CO_2-induced ocean acidification. *Geology,* 37, 1131–1134.

Schlegel, P., Havenhand, J.N., Gillings, M.R. and Williamson, J.E. (2012) Individual variability in reproductive success determines winners and losers under ocean acidification: a case study with sea urchins. *PloS One,* 7, e53118.

Sheppard Brennand, H., Soars, N, Sworjanyn, S.A., David, A.R. and Byrne, M. (2010) Impact of ocean warming and ocean acidification on larval development and calcification in the sea urchin *Tripneuste gratilla. PloS One,* 5, e11372.

Shirayama Y. and Thornton, H. (2005) Effects of increased atmospheric CO_2 on shallow water marine benthos. *Journal of Geophysical Research,* 110, c09S08.

Siikavuopio, S.I., Mortensen, A., Dale, T. and Foss, A. (2007) Effects of carbon dioxide exposure on feed intake and gonad growth in green sea urchin, *Strongylocentrotus droebachiensis. Aquaculture,* 266, 97–101.

Sodergren, E., Weinstock, G.M., Davidson, E.H., Cameron, R.A., Gibbs, R.A., Angerer, R.C. *et al.* (2006) The genome of the sea urchin *Strongylocentrotus purpuratus. Science,* 314, 941–952.

Spicer, J.I. and Widdicombe, S. (2012) Acute extracellular acid-base disturbance in the burrowing sea urchin *Brissopsis lyrifera* during exposure to a similated CO_2 release. *Science of the Total Environment*, 427–428, 203–207.

Spicer, J.I., Widdicombe, S., Needham, H.R. and Berge, J.A. (2011) Impact of CO_2-acidified seawater on the extracellular acid-base balance of the northern sea urchin *Strongylocentrotus dröebachiensis. Journal of Experimental Biology and Ecology*, 407, 19–25.

Steneck, R.S., Graham, M.H., Bourque, B.J., Corbett, D., Erlandson, J.M., Estes, J.A. and Tegner, M.J. (2002). Kelp forest ecosystems: biodiversity, stability, resilience and future. *Environmnental Conservation,* 29, 436–459.

Stumpp, M., Dupont, S., Thorndyke, M.C. and Melzner, F. (2011a) CO_2 induces seawater acidification impacts sea urchin larval development II: gene expression patterns in pluteus larvae. *Comparative Biochemistry and Physiology, Part A,* 160, 320–330.

Stumpp, M., Hu, M.Y., Melzner, F., Gutowska, M.A., Dorey, N., Himmerkus, N., Hotmann, W.C., Dupont, S.T., Thorndyke, M.C. and Bleich, M. (2012). Acidified seawater impacts sea urchin larvae pH regulatory systems relevant for calcification. *Proceedings of the National Academy of Sciences of the USA,* 189, 18192–18197.

Stumpp, M., Trübenbach, K, Brennecke, D, Hu, M.Y. and Melzner, F. (2012) Resource allocation and extracellular acid-base status in the sea urchin *Strongylocentrotus droebachiensis* in response to CO_2 induced seawater acidification. *Aquatic Toxicology,* 110–111, 194–207.

Stumpp, M., Wren, J., Melzner, F., Thorndyke, M.C. and Dupont, S.T. (2011b) CO_2 induced seawater acidification impacts sea urchin larval development I: Elevated metabolic rates decrease scope for growth and induce developmental delay. *Comparative Biochemistry and Physiology, Part A,* 160, 331–340.

Sunday, J.M., Crim, R.N., Harley, C.D.G. and Hart, M.W. (2011) Quantifying rates of evolutionary adaptation in response to ocean acidification. *PloS One,* 6, e22881.

Todgham, A.E. and Hofmann, G.E. (2009) Transcriptomic response of sea urchin larvae *Strongylocentrotus purpuratus* to CO_2-driven seawater acidification. *The Journal of Experimental Biology,* 212, 2579–2594.

Uthicke, S., Soars, N., Foo, S. and Byrne, M. (2012) Effects of elevated *p*CO2 and the effect of parent acclimation on development in the tropical Pacific sea urchin *Echinometra mathaei. Marine Biology,* DOI 10.1007/s00227-012-2023-5.

Vadas, R.L., Beal, B., Dowling, T. and Fegley, J.C. (2000) Experimental field tests of natural algal diets on gonad index and quality in the green sea urchin, *Strongylocentrotus droebachiensis*: a case for rapid summer production in post-spawned animals. *Aquaculture.* 182, 115–135.

Yu, P.C., Matson, P.G., Martz, T.R. and Hofmann, G.E. (2011) The ocean acidification seascape and its relationship to performance of calcifying marine invertebrates: laboratory experiments on the development of urchin larvae framed by environmentally-relevant pCO_2/pH. *Journal of Experimental Marine Biology and Ecology,* 400, 288–295.

SEA URCHINS, NATURAL EVENTS AND BENTHIC ECOSYSTEMS FUNCTIONING IN THE CANARY ISLANDS

José Carlos Hernández, Carlos Sangil, Sabrina Clemente

CLIMATE CHANGE PERSPECTIVES FROM THE ATLANTIC:
PAST, PRESENT AND FUTURE
Jose María Fernández-Palacios, Lea de Nascimento, José Carlos Hernández,
Sabrina Clemente, Albano González & Juan P. Díaz-González (eds.)
Servicio de Publicaciones, Universidad de La Laguna – 2013

ISBN: 978-84-15910-54-1
pp. 487-512

ABSTRACT

Sea urchin population outbreaks frequently cause ecological disequilibrium. Destructive urchin grazing causes serious depletion of macroalgae beds: a situation observed in many places around the world. Urchin hyper-abundance results in unproductive barren grounds, which are highly persistent and result in economic losses. Although barren grounds are widespread, the factors that control urchin outbreaks are still poorly understood.

Large populations of *Diadema africanum* occur in the East Atlantic Archipelagos (Madeira, Salvajes and Canarias). Sea urchin densities over 4 indv · m^{-2} reduce macroalgae cover to under 30%. However, there is a high spatial variability of population abundances. Sites with low wave action, as found on the leeward side of the Islands, or with high habitat complexity lead to high urchin densities and the depletion of conspicuous macroalgae. Another important factor determining spatial variability is the presence of key predators. Macroalgae beds with less fishing activity or more fishing restrictions implemented, and where these predators are naturally present, show higher resilience, lower urchin densities and smaller barren extensions. The key role of predators has been recently highlighted by two contrasting natural experiments. The first case is a submarine eruption in the Mar de Las Calmas (El Hierro) that has triggered a severe mass mortality of fishes. The mortality of predators of the sea urchin allowed an unprecedented massive recruitment of *D. africanum*. The second case involves four years of fishing restrictions in La Palma Marine Reserve that have promoted the recovery of key predator populations and reduced the extension of barren grounds.

Another underlying natural event that has recently been detected to influence urchin populations is the increase in seawater temperatures. Data on population dynamics collected over a 10 yr period (2002-2012) have shown how temperatures above 24°C induced important settlement pulses and higher post-settlement survival rates in barren areas but not in predator-dominated systems. Assuming climate change predictions are correct, the strong positive relationship between thermal history and post-settlement survival of this ecologically important species suggests that barren grounds will become more extensive in the future as seawater temperatures warm. However, maintaining high numbers of predators seems to increase the resilience of benthic systems and prevent barren formations. In addition, recently detected urchin mortalities originated by bacterial pathogens, probably facilitated by high seawater temperatures, will also play an important role in controlling urchin densities, as has been observed in other parts of the world.

KEYWORDS: *Diadema africanum*, population dynamics, sea water warming, sea urchin outbreak, mortality.

INTRODUCTION

Sublittoral rocky reefs are among the most diverse and economically important ecosystems on earth, due to their large extension worldwide and the number of biological and ecological processes they support. Protecting these ecosystem processes is imperative, not only to conserve the system, but also to maintain the subset of ecological functions that are directly relevant to humans and provide valuable services (De Groot *et al.*, 2002; Worm *et al.*, 2006). In many benthic coastal ecosystems worldwide, sea urchin grazing is recognized as a major determinant of plant community structure and organization, driving the transition from productive erect macroalgal beds to impoverished encrusted algae barren grounds (Sala *et al.*, 1998; Tegner and Dayton, 2000; Hernández *et al.*, 2008a; Ling, 2008).

In the Canary Islands, we have found extensive barren grounds, with almost 12 ind · m^{-2}. Later, we discovered that these kinds of remarkable situations are also observed in Madeira and the Selvage Islands (Alves *et al.*, 2001; A. Brito pers. com.). These large densities of the sea urchin *Diadema africanum* are known to cause the direct elimination of erect algal beds and result in the prevalence of rocky unvegetated bottoms in the rocky subtidal zone. The disappearance of these algal beds greatly limits benthic primary production, as well as the amount of food and shelter these algal habitats provide for associated invertebrates and fishes, which clearly exacerbates the deterioration of marine biodiversity in the shallow subtidal waters of a region greatly affected by human activities (Hernández *et al.*, 2008a). We started wondering, as John Lawrence (1975) did before: (1) what the causes were that can lead to such high concentrations of sea urchins and result in barrens, and (2) if they were natural phenomena or due to recent processes arising from human activity leading to changes in the characteristics of marine environments. Although these questions have been partially answered in some regions (Lessios, Scheibling *et al.*, Ebert, Ling, Bernat *et al.*, chapters in this book), they remain valid today, since processes that mediate transition between states are highly complex and require further research efforts.

Several natural events and habitat features are known to influence the dynamics of sea urchin populations. There are positive relationships that increase echinoid densities, such as the recent increase in sea water temperature (Ling *et al.*, 2008; Hernández *et al.*, 2010) or the severe overfishing of natural predators (Sala *et al.*, 1998; Clemente *et al.*, 2010) and negative effects that tend to keep sea urchin abundances under control, for example disease outbreaks (Lessios, 1998; Lauzon-Guay and Scheibling, 2007; Clemente *et al.*, in prep). Above all, the most worrying factor is the trend of global warming with its global scale of influence and potential positive effect on sea urchin abundance, which, in turn, have implications for the decline in benthic productivity and ecosystem services (e.g. algae carbon sink/sequestration function, fishing resources, diving activities, among others).

Despite the wealth of information on barren grounds in the region of the Canary Islands, understanding how anthropogenic climate changes are affecting these benthic ecosystems is still a challenge, given the complex interplay of factors involved in regulating sea urchin populations and the lack of baseline data. Therefore, in this paper, we can only offer potential scenarios to explain how these algae-urchin systems will change over this century based on recent data that describe urchin population responses to natural events (sea water warming, underwater volcanic eruptions) or fishing restrictions on the main sea urchin predators (MPA enforcement, which has been used as natural, large scale experiments). The work presented here summarizes the information we started collecting 11 years ago, around the Canary Islands. We put special emphasis on the population dynamics of the key herbivore *D. africanum* and the effects of natural and human-induced events, as well as the implications for the functioning of the entire benthic ecosystem.

HOW OLD IS THE PRESENCE OF *DIADEMA* POPULATIONS IN THE CANARY ISLANDS?

Many factors, including natural events and fluctuations of oceanographic parameters, are thought to be involved in the recent fluctuations of *Diadema africanum* populations. Despite the observed inter-annual variability of urchin abundances in recent years (Hernández *et al.*, 2008a), the occurrence of high abundances of the species has been known for much longer. Mortensen (1943) provided one of the first references to the species in the Canary Islands, pointing out the presence of long-spined black sea urchins during his visit to the island of Gran Canaria at the beginning of the 1930s. Reports, several decades ago, from other naturalists mentioned the large densities of this sea urchin in the shallow rocky subtidal zone of the Canary Islands. The species (misidentified as *Centrostephanus longispinus*) was appointed as the cause of the lack of algae in this subtidal zone through overgrazing around the island of Lanzarote (Johnston, 1969).

Therefore urchin barren grounds have been present in the Canary Islands for almost 50 years. But, what was the situation further back? In order to answer this question we need to use genetic analysis as Lessios and collaborators have done (Lessios *et al.*, 2001; Garrido 2003). Their studies showed that *Diadema* arrived at the Islands two million years ago and has evolved into a new species; recently morphological described and named as *Diadema africanum* (Fig. 1) (Rodríguez *et al.*, 2013). Lessios has also studied the mismatched distribution of haplotypes, which gives us an idea of when changes in population size occurred. It has been shown that a considerable increase in population density occurred between 80,000 and 125,000 years ago (Lessios *et al.*, 2001). Studies on mollusc fossils on Fuerteventura Island have shown that the Canary Islands were warmer in that

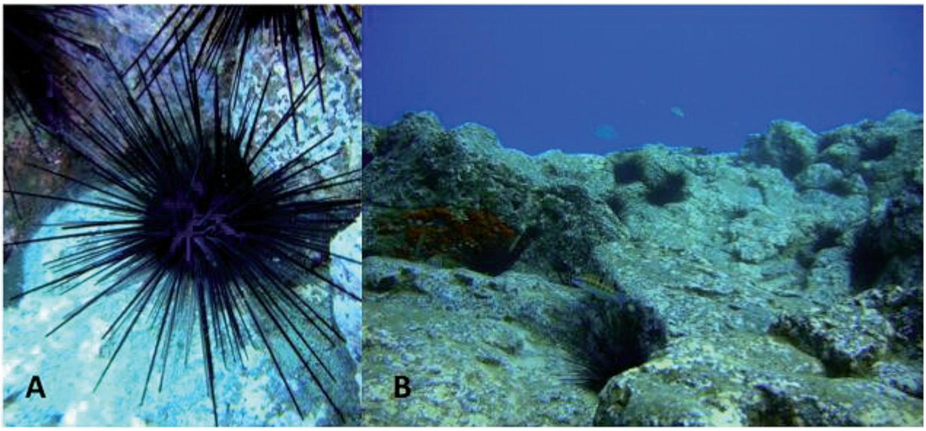

Figure 1. (A) Recently described sea urchin *Diadema africanum* (Rodríguez *et al.*, 2013). (B) View of a sea urchin barren in Tenerife Island, Canary Islands.

period; this warmer environment is known as the isotopic period 5e (Carracedo *et al.*, 2005) and was characterized by the presence of more tropical species, such as the coral *Siderastrea* and the mollusc *Strombus* (for more information regarding this topic see the Paleoclimatic section of this book). Therefore, the first expansion of *Diadema* occurred long before the humans arrived on the Islands and was related to past warmer temperature regimes.

DIADEMA AFRICANUM: A KEY HERBIVORE ON EASTERN ATLANTIC ROCKY REEFS

The influence of echinoid grazing activity on rocky reef communities of the eastern Atlantic oceanic islands, particularly in the Canary Islands, has been well studied (Alves *et al.*, 2001; Tuya *et al.*, 2004a; Hernández *et al.*, 2008a). Several species are known to generate barrens at this latitude: relatively small barren grounds are created by *Paracentrotus lividus* especially in tidepools, and by *Arbacia lixula* on shallow bottoms and around artificial jetties (authors' pers. obs.). However, barrens caused by the intense grazing activity of *Diadema africanum* are more extensive and commonly spread throughout the entire region (Hernández *et al.*, 2008a). These persistent barrens reach up to 50 m in depth and cover about 75% of the total littoral rocky bottoms of the Canary Islands (Barquín *et al.*, 2004). *D. africanum* is a thermophilus species, which probably constitutes a competitive advantage for its population proliferation at the sublittoral latitude of the Canary Islands, in contrast to sea urchins of temperate affinities which also occur in the region, such as *P. lividus*. This has been especially relevant over

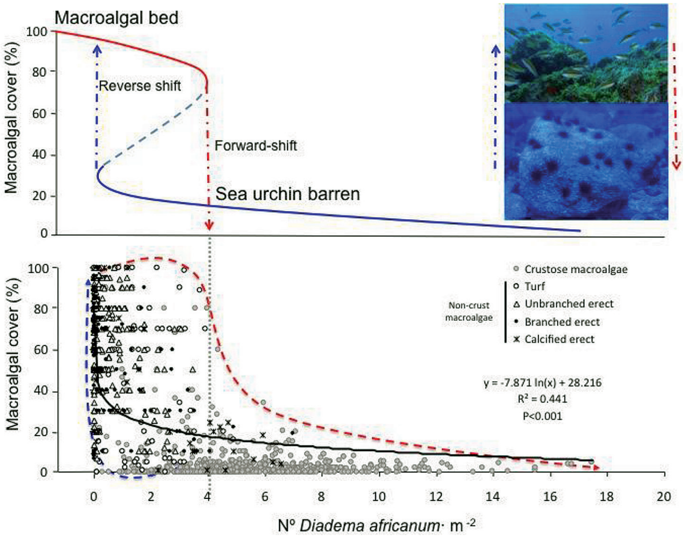

Figure 2. Log-linear relationship between sea urchins (*Diadema africanum*) abundances and macroalgae cover. Four ind · m^{-2} is the threshold that promote forward shift to urchin barren (red line); reverse shifts (blue line) have only been observed in La Palma MPA after four years of protection enforcement (Sangil *et al.*, 2012) and at some sites by complete experimental removal of sea urchins (Hernández *et al.*, unpublished data).

the last few decades, when a trend of progressive seawater warming has occurred in the region as a consequence of global climate change processes (Brito, 2008; Hernández *et al.*, 2010).

As a major herbivore, *D. africanum* is recognized as having a key ecological role that threatens the resilience of algae systems in the eastern Atlantic, with the subsequent establishment of undesired conservation states (Hernández *et al.*, 2008b). The consequences of these sea urchin hyper-abundances are the depletion of the main ecosystem engineers: the macroalgae beds. At sea urchin densities of 4 ind · m$^{-2,}$ macroalgae cover is greatly reduced and always remains below 30% (Fig. 2). *D. africanum* is a key herbivore in the rocky subtidal systems of the Canary Islands and is able to significantly modify macroalgae richness and diversity (Fig. 3) (Sangil *et al.*, in press). This altered situation also affects the upper levels of the ecosystem, such as the macroinvertebrates (Ortega *et al.*, 2009) and vertebrates (Tuya *et al.*, 2004a; Clemente *et al.*, 2010). Loss of macroalgal beds due to *D. africanum* grazing activity leads not only to lower species diversity, but also to a lack of habitats suitable for fish feeding and reproduction (Tuya *et al.*, 2005; Clemente, 2007) and

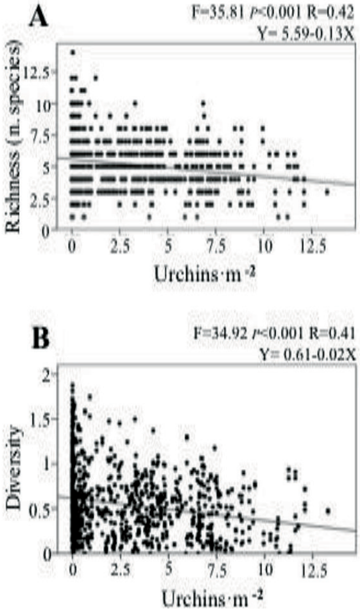

Figure 3. Relationships between *Diadema africananum* density and macroalgal (A) richness and (B) diversity.

severe depletion of local fishing resources (Fig. 4) (Tuya *et al.*, 2004a; Clemente *et al.*, 2010). Macroalgae constitute a major energy source that maintains the food web, and are the main biological engineers on rocky reefs at this latitude, which lie between tropical and temperate waters and have no coral reefs. Consequently, algal cover provides a habitat that maintains the whole system, and, thus, constitutes a well-known indicator of benthic conservation status (Hernández *et al.*, 2008b).

The reported increasing frequency of overgrazing events, concomitant with loss of associated ecosystem goods and services, generates a serious environmental problem that threatens coastal marine ecosystems and the local communities of the Islands (Hernández *et al.*, 2013). Hence, the need for managing the populations of *D. africanum* to prevent overgrazing has become evident, especially in areas of the Canary Islands where algae-associated services (such as fish stocks) are important for livelihood and sustenance.

DYNAMICS OF ALTERNATIVE STATES: SEA URCHIN BARREN GROUNDS AND MACROALGAE BEDS

Due to their biological and ecological features, such as size, mobility, feeding preferences or longevity, several urchin species play a key role (see Ling, Scheibling *et al.*, and Bernat *et al.*, chapters in this book), even more important

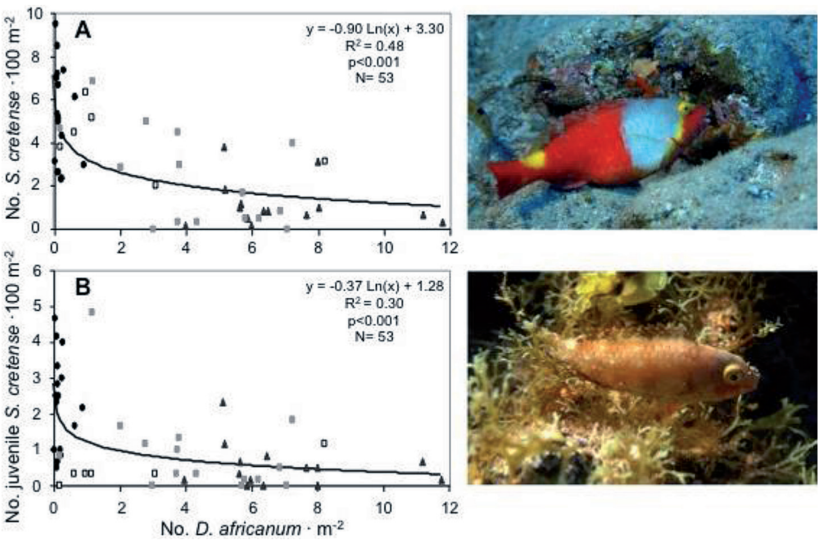

Figure 4. Log-linear relationships between *Diadema africanum* density and (A) population density of *Sparisoma cretense* (an indicator species of local fisheries resources) and (B) abundance of juvenile *S. cretense* (<20 cm total length). Circles: El Hierro Island; triangles: Tenerife Island; open squares: La Palma; solid squares: Lanzarote Island and northern islets. Source: Clemente *et al.*, 2010.

than other herbivores, in controlling epibenthic communities and, in turn, in the overall structure of coastal communities. In the Canary Islands, we simultaneously found two alternative states of the rocky bottoms: *Diadema africanum* barren grounds and macroalgae beds. Algal stands are very restricted in space and have shown a temporal regression related to the demographic explosion of the sea urchin over recent years, mainly in the eastern islands (Hernández *et al.*, 2008a; Clemente *et al.*, 2011). High percentage cover is usually attained only in shallow water stands at exposed sites, where hydrodynamics prevent urchin activity (Alves *et al.*, 2001; Tuya *et al.*, 2007; Hernández *et al.*, 2008a); in certain marine protected areas (Clemente, 2007; Hernández *et al.*, 2008b); or at barely perturbed areas associated with lower anthropogenic development, such as isolated and less populated islands (Clemente *et al.*, 2009). Examples of this are El Hierro and La Palma islands where there is higher cover of erect seaweeds (Hernández *et al.*, 2008a, b) (Fig. 5).

Alternation of ecosystem states has been observed in both directions. At the Alegranza Islet, to the north of Lanzarote Island, an alternation of systems from macroalgae to barren grounds occurred during the 90s (Fig. 6) (Hernández *et al.*, 2008a; Hernández *et al.*, in prep). However, we have also, very recently,

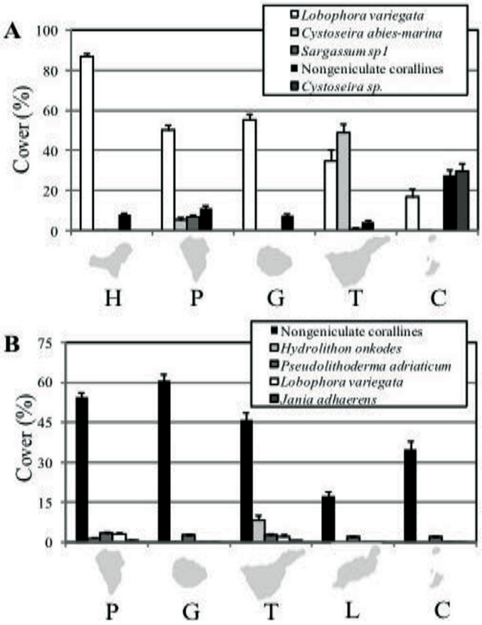

Figure 5. Mean percent cover (±SE) per studied island of the five most abundant macroalgae taxa at (A) upright seaweed beds (with *Diadema africanum* mean densities <2.5 sea urchins·m^{-2}), and at (B) urchin barrens (sea urchin density >2.5 urchins·m^{-2}). H: El Hierro Island; P: La Palma Island; G: La Gomera Island; T: Tenerife Island; L: Lanzarote Island; and C: Chinijo northern islets.

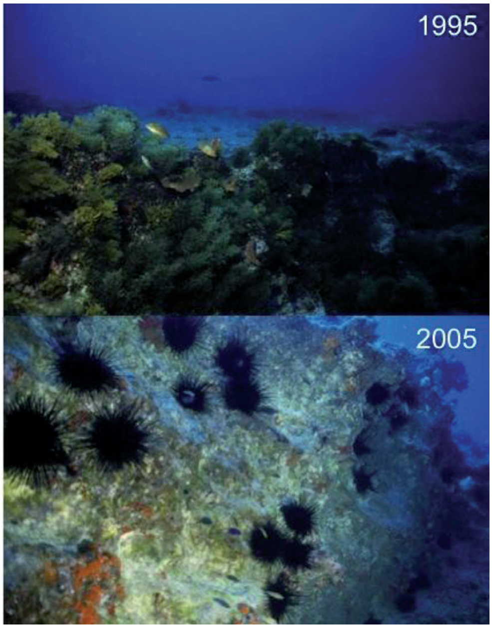

Figure 6. Comparison of the benthic assemblages at the Veril de Las Agujas site (Alegranza, Chinijo northern islets) between years 1995 and 2005 showing the recent expansion of *Diadema africanum* barren state. Pictures: Herrera *et al.*, 2005.

observed a shift from urchin barren ground to a macroalgae bed inside the La Palma MPA (Sangil *et al.*, 2012). This is the fastest reported recovery from a barren state after MPA enforcement. Other examples of state shifts due to fishing restrictions have been reported at Maria Island (Pacific Ocean), New Zealand and Kenya (Babcock *et al.*, 2010).

Similar to that found for other species worldwide (Andrew and Byrne, 2001; Johnson *et al.*, 2011; Flukes *et al.*, 2012), this species' capacity to maintain high density populations by switching to alternative food sources and reduce its body size is unparalleled in any other benthic herbivore in the eastern Atlantic Archipelagos, and, thus, greatly compromises the structure of macroalgae assemblages. Field monitoring and experimental manipulations of sea urchin densities have shown its major effects on algal communities (Hernández *et al.*, 2008 unpublished data). However, monitoring has also shown that at moderate densities, sea urchins coexist with high species diversity, playing an integral part of ecosystem dynamics (Fig. 3) (Sangil *et al.*, 2012). Compared to typical urchin barrens elsewhere in the world (Chapman, 1981; Pearse and Hines, 1987; Valentine and Johnson, 2005; Guidetti and Dulčić, 2007), barrens generated by *Diadema africanum* in the eastern Atlantic appear to be maintained by relatively low numbers of sea urchins (starting at 2 ind · m^{-2}) (Fig. 2). Probably, the oligotrophic condition of waters surrounding the Archipelago provides limited nutrient resources that are not sufficient to maintain extremely high urchin densities. Additionally, species movement and food consumption rates, which involve grazing large areas of rocky substrate at night (Tuya *et al.*, 2004b), is enough to maintain a barren habitat denuded of most erect macroalgae biomass with comparatively lower urchin densities.

POPULATION BIOLOGY OF *DIADEMA AFRICANUM*

It is very difficult to fully understand what regulates urchin populations. Urchins have complex life cycles, from planktonic larval stages to the benthic phases of post-settlement and adult stage. In order to study these processes, we have addressed some factors that can potentially determine the spatial and temporal dynamics of sea urchin reproduction, settlement, recruitment and adult densities. We have identified several factors controlling several pre-settlement processes: sea urchin reproduction output is greatly controlled by the benthic productivity (bottom up processes) (Hernández *et al.*, 2006); larvae survival is higher when sea water temperature is above 24ºC (Fig. 7) (Hernández *et al.*, 2010); physical parameters at meso- and micro-scale, such as island leeward areas and high benthic complexity facilitate larvae retention (Hernández and Clemente, 2011; Hernández *et al.*, 2012; Hernández *et al.*, in prep). Among post-settlement processes, we have detected that predation, habitat complexity, sedimentation, wave exposure and disease all interplay to determine the abundances of *Diadema africanum* (Clemente *et al.*, 2007; Hernández *et al.*, 2008a; Clemente *et al.*, in prep).

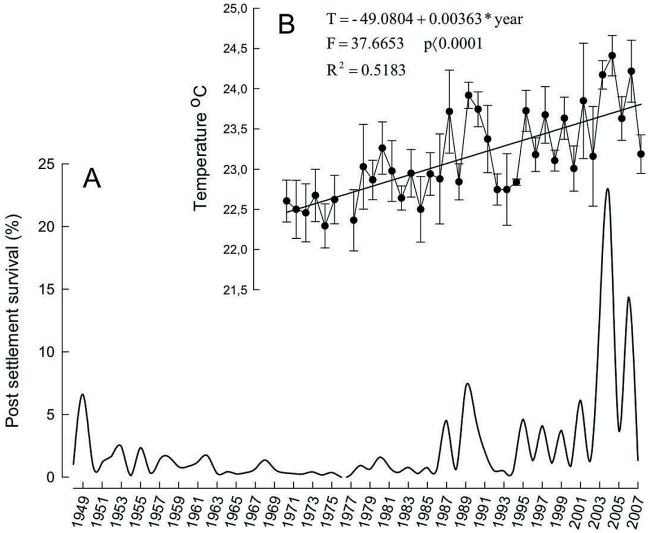

Figure 7. (A) Reconstructed postsettlement survival pattern (PS) of *Diadema africanum* from 1948 to 2007 using historical sea surface temperature (SST) data. The previously obtained relationship between SST and PS (PS = 8.3565E – 24 $2^{.3045 \times T}$) was used to reconstruct the historical PS pattern. (B) Long-term summer warming trend of coastal waters in the Canary Islands from 1970 to 2007. Sea temperatures were obtained from Kalnay *et al.* (1996) reanalysis and averaged across settlement months (August–October). Source: Hernández *et al.*, 2010.

Gonad maturation in *D. africanum* coincides with increases in benthic macroalgae cover (Hernández *et al.*, 2006). Spawning occurs during June-August (Hernández *et al.*, 2011), when daylight decreases, and which is coupled with waning moon and new moon phases (González *et al.*, 2012). We hypothesise that during these moon phases, a higher fertilization percentage and egg survival is assured due to high water movement and strong tides at new moon. Darker nights may also limit predation on eggs by planktonic organisms. Therefore, the planktotrophic larvae of the sea urchin are in the water during the thermocline of the warm season, which coincides with low abundances of planktonic predators (Hernández, 2006). Settlement takes place during the months of maximum seawater temperature, August-October (Hernández *et al.*, 2006; Hernández *et al.*, 2010) and, in general, at three to four months from spawning, we can observe the first recruits in the benthos, so population renewal is fast.

A long-term study has recently detected a clear relationship between sea surface temperature and *D. africanum* settlement in the Canary Islands (Hernández *et al.*, 2010). This study was based on a historical compilation of seawater surface temperature data from 1948 to the present and a continuous collection of data on sea urchin settlement, recruitment and densities from 2001 to 2008. Urchin settlement was higher during warmer years. Temperatures above 24°C produced major settlement pulses and higher post-settlement survival rates in barren areas, despite some variability across habitats. While seawater temperature was a major factor influencing *D. africanum* density in urchin barrens, since it enhances post-settlement survival, specific factors in macroalgal beds constrained settlement by increasing post-settlement mortality and limiting sea urchin populations (Hernández *et al.*, 2010). The study showed that warmer summer temperatures during the settlement period of the species have been more frequent since the early 1980s, with a parallel increase in urchin population densities mainly in the eastern part of the Archipelago (Hernández *et al.*, 2008a), where specific urchin predators are scarce (Clemente *et al.*, 2011). A synergy between the detected seawater warming and the low functional diversity of urchin predators is, therefore, proposed as a causative factor for the observed depletion of macroalgae in extensive parts of the Archipelago (Hernández *et al.*, in prep) (Fig. 6).

PATTERNS ARISING FROM SPATIO-TEMPORAL MONITORING OF URCHIN POPULATIONS

HABITAT PREFERENCES AND PREDATORS

Urchin barrens occur all around the Canary Islands except on the island of El Hierro (Fig. 8). There is an archipelagic variation in urchin abundances and barren extension, so there are islands, such as Tenerife, La Gomera, Lanzarote and islets with mean densities around 5 ind · m^{-2}, while El Hierro island show abundances below 1 ind · m^{-2} (Hernández *et al.*, 2008a).

Comparisons of the spatial distribution of *Diadema africanum* show that the species is not well adapted to support intense water movement. This results in a general pattern in the rocky reefs of the eastern Atlantic Ocean in which wave exposure and island slope, which limit wave energy, are major environmental factors determining densities of this herbivore (Hernández *et al.*, 2008a). Southern and south-eastern coasts of the islands have calmer waters, which promote retention of urchin larvae (Hernández, 2006), and barrens occur on these sheltered coasts within the first few meters of depth. In contrast, areas with higher hydrodynamics, on the northern sides of the islands, show urchin barrens at deeper waters (15-20 m) just below the algal stand (Fig. 9) (Hernández *et al.*, 2008a). Therefore, the population age structure found around different parts of the islands is determined by different wave regimens, with leeward sides of the islands characterized by higher population renewal and younger populations, and

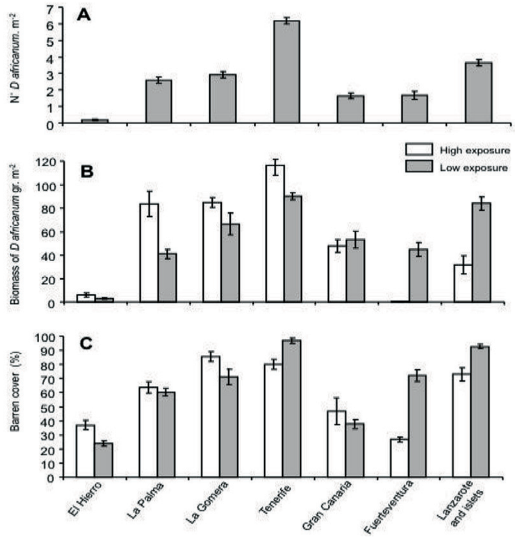

Figure 8. (A) Comparison of mean sea urchin (*Diadema africanum*) abundances (± SE) among islands of the Canarian Archipelago. (B) and (C) comparisons of mean urchin biomass and percentage of barren cover (± SE) among islands at different wave exposures regimes.

northern and north-western coasts characterized by older urchins (Hernández *et al.*, 2012). According to wave action restrictions, there is higher larvae settlement at depths of over 10 m, since larvae are wiped out from shallow turbulent waters (Hernández, 2006). So factors reducing wave action seem very important for promoting settlement of this species on different spatial scales (Hernández and Clemente, 2011).

Several anthropogenic factors, such as the number of islanders and tourists per coastal perimeter, the number of operational fishing boats and the overfishing of sea urchins' natural predators have been associated with higher abundances (Hernández *et al.*, 2008a; Clemente *et al.*, 2009, 2011). Regulation of sea urchin populations has been shown to depend, to some extent, on the strength of certain trophic interactions. Experimental studies have identified key fish species that successfully prey upon *D. africanum* as having the potential to control urchin populations (Clemente *et al.*, 2010). The implications for coastal management are evident. By controlling herbivore densities, and thus the amount of intact macroalgal cover, predatory fish indirectly aid in preserving ecosystem services or capacity to provide locally important fishing resources and maintain coastal productivity in sublittoral rocky reefs. The identified predatory fish are mainly species very susceptible to fishing (Clemente *et al.*, 2010). Consequently, increased

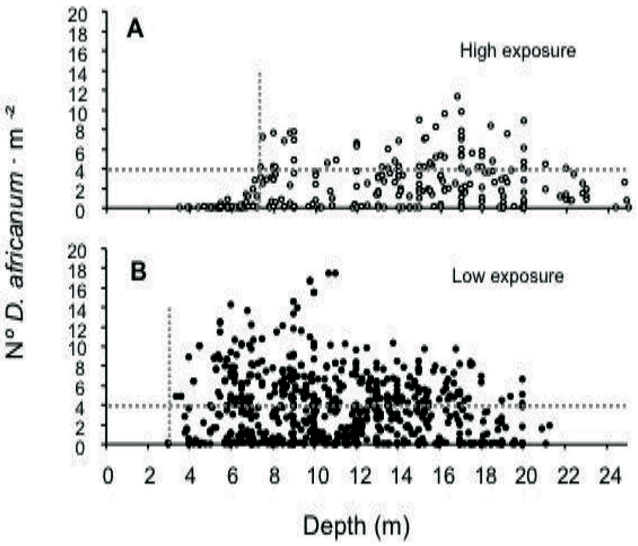

Figure 9. Dispersion diagrams illustrating abundances of *Diadema africanum* in the depth range studied (0.5–25 m), in conditions of high and low wave exposure. Dashed lines show the starting depth of urchin barrens.

fishing activities have been associated with lower numbers of these predatory species and higher urchin densities in the Canary Islands (Clemente *et al.*, 2009, 2011) and elsewhere (Sala *et al.*, 1998; Shears and Babcock, 2002; Guidetti 2006; Guidetti and Dulčić, 2007). Additionally, fishing decreases the mean size of fish, which adds to the loss of fish sizes capable of consuming large sea urchins, resulting in a smaller escape size from predation that favours their proliferation (Fig. 10). The removal of fish predators by severe overfishing in most areas of the Canarian Archipelago have led to an urchin population outbreak driven only by settlement and recruitment in the absence of any kind of predatory control (Hernández, 2006; Clemente, 2007). This ecological disequilibrium, mediated by trophic cascade processes, has major consequences for the structure and function of the entire benthic community, as has been previously highlighted for many other regions (Sala *et al.*, 1998; Shears and Babcock, 2002; Guidetti, 2006).

As top-down effects on *D. africanum* in the eastern Atlantic archipelagos depend on specific predatory species and their abundances within the food web, preserving the diversity of fish predators must be a priority for conservation efforts (Clemente *et al.*, 2010). Marine protected areas in which fishing restrictions are implemented to allow stocks to recover (Hernández *et al.*, 2008a) are recognised as effective management tools that can indirectly contribute to the

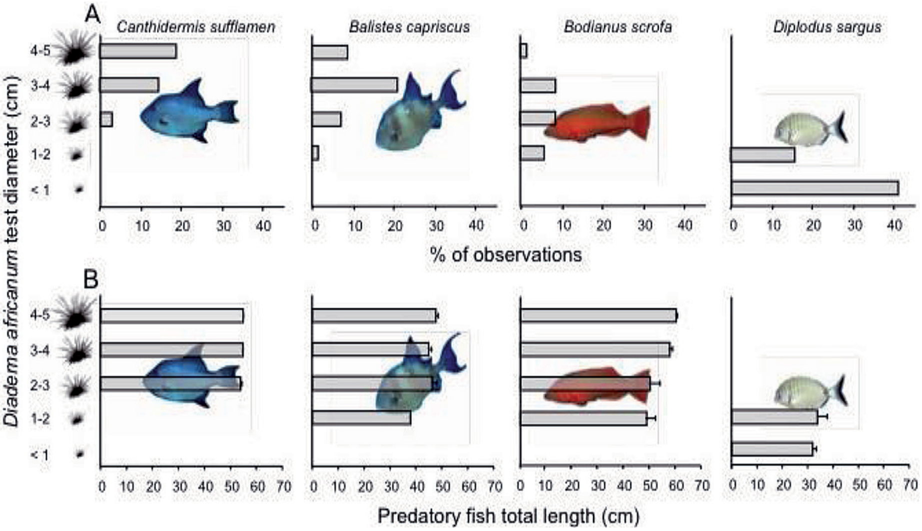

Figure 10. Consumption performance variables of predatory fish *Canthidermis sufflamen*, *Balistes capriscus*, *Bodianus scrofa* and *Diplodus sargus*: (A) percentage of observations of predation and (B) total fish body length (mean ± SE) displayed for each size class of the sea urchin prey *Diadema africanum*. Source: Clemente *et al.*, 2010.

control of sea urchin populations, as observed in other areas of the world (Sala *et al.*, 1998; Babcock *et al.*, 1999; McClanahan *et al.*, 1999; Guidetti, 2006). Studies in the Canary Islands have stressed the value of marine protected areas as a tool for ecosystem restoration (Hernández *et al.*, 2008a; Clemente *et al.*, 2009, 2011; Sangil *et al.*, 2012). In fact, the three marine protected areas within the Canary Islands support higher densities of fish predators and higher levels of predation intensity on *D. africanum* compared to equivalent non-protected locations (Fig. 11) (Clemente *et al.*, 2011). However, recent studies have shown the importance not only of protection measures but also of the environmental context to enhance the strength of predatory fish activity. Biogeographical differences in fish communities across the oceanographic gradient of the Canarian Archipelago have been related to the variations in the response of predation to the establishment of fishing restrictions (Clemente *et al.*, 2011). Therefore, regional and local-scale environmental gradients should not be overlooked as a factor affecting the occurrence and magnitude of predatory interactions in benthic marine communities, especially in systems that are markedly variable on small scales, such as the Canary Islands. Regardless of the complexity of factors involved, controlling overpopulation of *D. africanum* may be achieved by aiding the recovery of the predatory fish community with appropriate fishing bans and protection

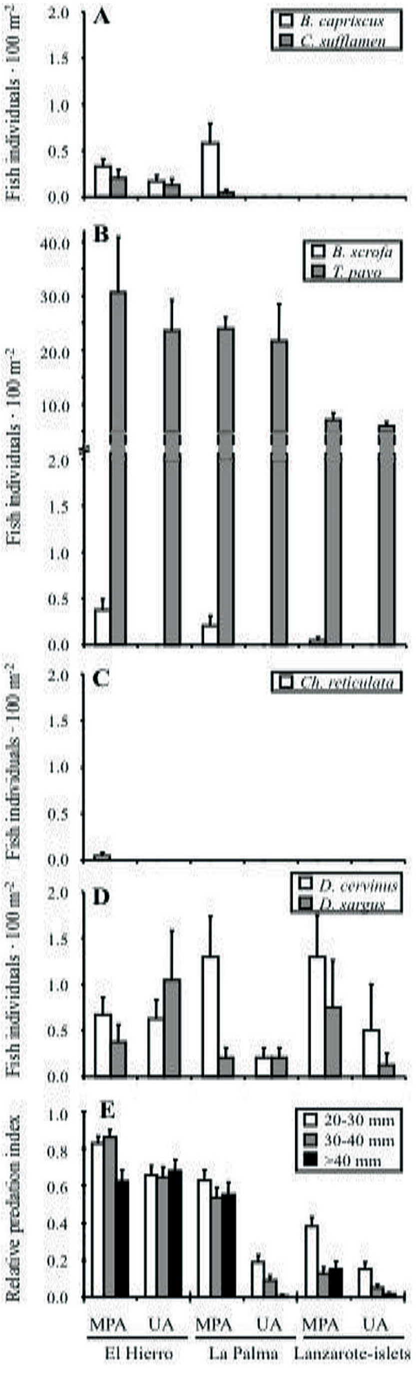

Figure 11. Mean densities (± SE) of predatory fish species of *Diadema africanum* within the marine protected (MPAs) and unprotected areas (UAs) on 3 islands off the Canary Islands: (A) the balistids *Balistes capriscus* and *Canthidermis sufflamen*, (B) the labrids *Bodianus scrofa* and *Thalassoma pavo*, (C) the diodontid *Chilomycterus reticulata*, and (D) the sparids *Diplodus cervinus* and *Diplodus sargus.* (C) Mean relative predation index (± SE) upon 3 sea urchin size classes obtained in predation experiments within MPAs and UAs on the 3 islands in the Canary Islands. Source: Clemente *et al.*, 2011.

measures. Current knowledge about the species' population dynamics adds to a growing body of research suggesting that the incidence of barrens and their associated impacts are related to human disturbance (Levitan, 1992; Sala *et al.*, 1998; Babcock *et al.*, 1999; McClanahan *et al.*, 1999; Steneck *et al.*, 2002; Guidetti, 2006; Ling *et al.*, 2009).

Global warming, disease outbreaks and catastrophes

By analysing long datasets of seawater temperature, we have detected a positive and significant trend of increasing temperatures, similar to other areas in the world (see other chapters of this book by Scheibling *et al.*, Ling *et al.*, and Bernat *et al.*). This increase in water temperature is highly and positively correlated with post-settlement survival of *Diadema africanum.* In fact, more frequent pulses of urchin recruitment have occurred since the 80s and 90s (Fig. 7) (Hernández *et al.*, 2010), coinciding with the appearance and expansion of barrens in the easternmost islands (Fig. 6) (R. Herrera pers. com.). Summer temperatures over 24ºC promote higher settlement rates; however, there is a spatial variation on post-settlement survival. There are islands like Tenerife, where an increment in settlement due to warming promotes higher recruitment, whereas around other islands, like El Hierro, high settlement does not result in increased recruitment and the system shows higher resilience (Hernández *et al.*, 2010).

Other consequences of global warming are less favourable to urchin populations. Early evidence of the effects of climate change have shown an increase in numbers of thermophile species of littoral fish and an expansion in their geographical range, facilitated by seawater warming. These species have reached the Canary Islands by their own means (Brito *et al.*, 2005). The triggerfish *Canthidermis sufflamen* was first noticed in 1994 in El Hierro Island (Brito *et al.*, 1995), and the following year the species was found to have successfully reproduced. Nowadays, this fish species constitutes a new and important fishing resource in the western Islands of the Archipelago. It also represents an important element in those Islands as a key predator of the sea urchin *D. africanum*, as recently reported by Clemente *et al.* (2010)

A sea urchin mortality event was detected in November 2009 in Madeira Island, (F. Alves pers. com.) which reached the Canary Islands in February 2010. An overall reduction of ~50% of sea urchin populations due to the die-off was documented (Fig. 12). We identified that the disease symptoms were similar to those described for the «bald sea urchin disease» and the pathogens involved were identified as *Vibrio algynoliticus* and *Neoparamoeba brachiphila* (Dyková *et al.*, 2011; Clemente *et al.*, in prep). Given that *Neoparamoeba* can act as a host, as occurs in other world areas (Scheibling *et al.*, in this book), further studies are needed to elucidate whether bacteria or amoebae were the primary agents of the disease or, alternatively, there was a synergy of both free-living agents. The

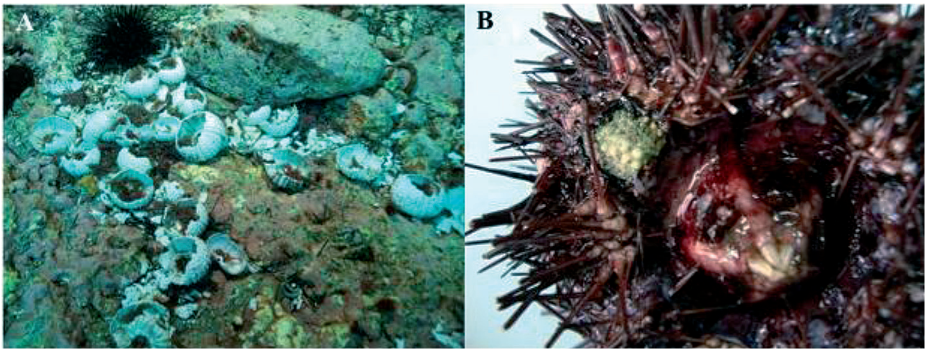

Figure 12. (A) Sea urchin mortality event detected in the Canary Islands during October 2009 (B) Detail of an infected sea urchin showing the bald sea urchin disease.

seawater temperature records since the 1950s have shown that the disease developed during the highest winter temperatures ever-registered both in Madeira and the Canary Islands. Knowing that these infections typically exhibit strong temperature dependence, it is probable that the mortality events were related to the unusually high seawater temperatures (Fig. 13).

Natural disturbances create opportunities for species to claim previously utilized space and resources. The widespread and massive disturbance caused by catastrophic events provides ideal conditions for the rapid recruitment and spread of certain species. El Hierro Island has recently been subjected to an underwater volcanic eruption starting in October 2011 and coinciding with the annual settlement peak of the key herbivore sea urchin, *Diadema africunum*. Despite the eruption being at a depth of ~100 m off the southwest coast of the island, it triggered severe mass mortalities of many organisms due to the release of gasses that changed seawater chemistry. A spatio-temporal analysis of *D. africanum* recruit densities showed significant differences before and after the eruption in the area closest to the impact, while unimpacted sites showed no variation in recruit numbers over time. Population size distributions, as well as the abundance and composition of urchin predatory fish, significantly differed from pre-eruption levels at the most impacted sites in comparison to non-affected sites. We attribute this recruitment pulse to a release of urchins from predation control during the post-settlement and recruitment stage, related to the disturbance of the benthic systems (Clemente *et al.*, 2012). Results suggest that sea urchins will mostly comprise the dominant component of the fauna in the early stages of the successional response to the disturbance, and once large sizes are achieved, they will more easily escape from predation of slower growing fish predators. Given the greater echinoid grazing activity, this may have long-lasting structural consequences for the community.

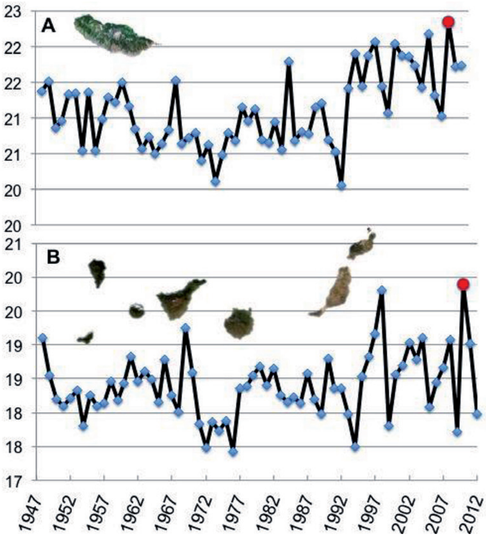

Figure 13. Long-term winter SST trend of coastal waters in (A) Madeira and in (B) the Canary Islands from 1947 to 2012. Red circles show high winter temperatures registered during *Diadema africanum* mortality events at each region. Sea temperatures were obtained from Kalnay *et al.* (1996) reanalysis.

FUTURE PREDICTIONS: TRAJECTORIES IN RESPONSE TO CLIMATE CHANGE.

In the Canary Islands, sea water temperatures have increased by ~1°C since the year 1985 (AEMET 2008), and this rising trend is predicted to continue in the future (Fig. 7) with some variability between colder and warmer years. At the same time, an increment in CO_2 concentrations and seawater acidification levels have been detected, giving an overall rate of pH reduction of 0.002 pH units/year (QUIMA, Universidad de Las Palmas de Gran Canaria). The sensitivity of sea urchins to the combined effects of rising ocean temperatures and decreasing pH regimes predicted for climate change scenarios has started to be documented (Hernández *et al.*, unpublished data). Assuming climate change predictions (IPCC 2007) for the future are correct, the strong positive relationship between thermal history and post-settlement survival of this ecologically important species suggests that barren grounds will become more extensive in the future, as seawater temperatures warm in relation to anthropogenic activities. On the other hand, the first mortality event of the species recorded during 2010 (Clemente *et al.*, 2011) has shown that these events could become more frequent in the future due to warmer winter waters, as other authors have previously noticed (Lafferty *et al.*, 2004; Girard *et al.*, 2012; Scheibling *et al.*, in this book). These events may constitute a self-regulating mechanism of extremely high population densities. Therefore, the seawater-warming trend in the Canarian Archipelago will probably increase the frequency of these mortality events in the future and will probably aid the alternation between algae beds and barren grounds. Until now there has been a high persistence of these alternative systems, macroalgae beds and sea urchin barrens, in the Canary Islands but as the water warms there will be higher frequencies of alternation of these system states by means of massive recruitments and more frequent mortality events. However, sites where the sea urchin predators are naturally abundant will show higher buffering capacity to tolerate any expected change due to warming effects. Therefore, protecting predatory species and promoting the enforcement of marine protected areas may be a more effective way to ensure the continuity of productive macroalgae beds.

ACKNOWLEDGEMENTS

We would like to acknowledge Rodrigo Trujillo, «Vicerrector de Internacionalización y Excelencia» of the «Universidad de La Laguna», for supporting the organization of this International Workshop within the framework of the «Campus de Excelencia Tricontinental de La Universidad de La Laguna y la Universidad de Las Palmas de Gran Canaria». This international event has resulted in the publication of this book on Climate Change and aided in promoting international research collaborations that have led to the development of a trending topic opinion paper on these issues. We are greatly in debt with all participants as well as with all the students that helped in the organization of the event (Yasmina Díaz, Eliseba García, Celso Hernández, Cataisa López, David Martínez, José Carlos Mendoza, Alejandro Pérez-San Juan, Adriana Rodríguez and Oceania student organization).

REFERENCES

Alves, F.M.A., Chícharo, L.M., Serrao, E. and Abreu, A.D. (2001) Algal cover and sea urchin spatial distribution at Madeira Island (NE Atlantic). *Scientia Marina* 65, 383–392.

Andrew, N. and Byrne, M. (2001) The ecology of *Centrostephanus rodgersii. Edible sea urchins: biology and ecology* (ed. by Lawrence, J.M.), pp. 149–160. Elsevier Science, Amsterdam, The Netherlands.

Babcock, R.C., Kelly, S., Shears, N.T., Walker, J.W. and Willis, T.J. (1999) Changes in community structure in temperate marine reserves. *Marine Ecology Progress Series,* 189, 125–134.

Babcock, R.C., Shears, N.T., Alcala, A.C., Barret, N.S., Edgar, G.J., Lafferty, K.D., McClanahan, T.R. and Russ, G.R. (2010). Decadal trends in marine reserves reveal differential rates of change in direct and indirect effects. *Proceedings of the National Academy of Sciences of the United States of America,* 107, 18256–18261.

Barquín, J., Gil-Rodríguez, M.C., Del Arco Aguilar, M.J., González, G., Domínguez-Álvarez, S., González, R., Aldanondo-Ariztizabal, N., Rodríguez, M., Cruz-Reyes, M.A., Herrera-Lopez, G., Sancho, A., Cruz, T., O'dwyer, J., Martin, L. and Cansado, S, (2004) La Cartografia bionomica del litoral de Tenerife: resultados preliminaries. *Proceedings of the XIII Simposio Ibérico de Estudio del Bentos Marino.* Las Palmas de Gran Canaria, Canary Islands, Spain.

Brito, A. (2008) Influencia del calentamiento global sobre la biodiversidad marina de las Islas Canarias. *Naturaleza amenazada por los cambios en el clima Actas de la III Semana Científica Telesforo Bravo* (ed. by Afonso-Carrillo, J.), pp. 141–161. Instituto de Estudios Hispánicos de Canarias, Puerto de La Cruz, Canary Islands, Spain.

Brito, A., Falcon, J.M. and Herrera, R. (1995) Ocurrence of the ocean triggerfish in the Eastern Atlantic (Canary Islands). *Journal Fish Biology,* 47, 1099–1101.

Brito, A., Falcón, J.M. and Herrera, R. (2005) Sobre la tropicalización reciente de la ictiofauna litoral de las islas Canarias y su relación con cambios ambientales y actividades antrópicas. *Vieraea,* 33, 515–525.

Carracedo, J.C., Pérez, F.J. and Meco, J. (2005) La gea: análisis de una isla en estado post-erosivo de desarrollo. *Patrimonio natural de la isla de Fuerteventura* (ed. by. Rodríguez, O.), pp. 27–44. Cabildo de Fuerteventura-Consejería de Medio Ambiente y Ordenación Territorial del Gobierno de Canarias-Centro de la Cultura Popular Canaria. Santa Cruz de Tenerife, Canary Islands, Spain.

Chapman, A.R.O. (1981) Stability of sea urchin dominated barren grounds following destructive grazing of kelp in St. Margaret's Bay, eastern Canada. *Marine Biology*, 62, 307–311.

Clemente, S. (2007) *Evolución de las poblaciones del erizo Diadema aff. antillarum en Canarias y valoración de la depredación como factor de control*. Ph.D. Thesis (421 pp.), Universidad de La Laguna, Tenerife, Canary Islands, Spain.

Clemente, S., Hernández, J.C., Toledo, K. and Brito, A. (2007) Predation upon *Diadema* aff. *antillarum* at barrens grounds in the Canary Islands. *Scientia Marina*, 71, 745–754.

Clemente, S., Hernández, J.C. and Brito, A. (2009) Evidence of the top–down role of predators in structuring sublittoral rocky-reef communities in a marine protected area and nearby areas of the Canary Islands. *ICES Journal of Marine Science*, 66, 64–71.

Clemente, S., Hernández, J.C., Rodríguez, A. and Brito, A. (2010) Identifying keystone predators and the importance of preserving functional diversity in sublittoral rocky bottoms. *Marine Ecology Progress Series*, 413:55–67

Clemente, S., Hernández, J.C. and Brito, A. (2011) Context-dependent effects of marine protected areas over predatory interactions. *Marine Ecology Progress Series*, 437, 119–133.

De Groot, R.S., Wilson, M.A. and Boumans, R.M.J. (2002) A typology for the classification, description and valuation of ecosystem functions, goods and services. *Ecology and Economics*, 41, 393–408.

Dyková, I., Lorenzo-Morales, J., Kostka, M., Valladares, B. and Pecková, H. (2011) *Neoparamoeba branchiphila* infections in moribund sea urchins *Diadema* aff. *antillarum* in Tenerife, Canary Islands, Spain. *Diseases of Aquatic Organisms*, 95, 225–231.

Flukes, E.B., Johnson, C.R. and Ling, S.D. (2012) Forming sea urchin barrens from the inside out: an alternative pattern of overgrazing. *Marine Ecology Progress Series*, 464, 179–194.

Garrido, M. (2003) *Contribución al conocimiento de Diadema antillarum Philippi 1845, en Canarias*. Ph.D. Thesis, Universidad de Las Palmas de Gran Canaria, Canary Islands, Spain.

Girard, D., Clemente, S., Toledo, K., Brito, A. and Hernández, J.C. (2012) A mass mortality of subtropical intertidal populations of the sea urchin *Paracentrotus lividus*: analysis of potential links with environmental conditions. *Marine Ecology – An Evolutionary Perspective*, 33, 377–385.

González-Domínguez, R., Díaz, Y., Mendoza, J.C., Clemente, S. and Hernández J.C. (2012) Sea urchins also howl together at the moon. *Proceedings of the 14th International Echinoderm Conference, 20-24 August 2012*. Brussels, Belgium.

Guidetti, P. (2006) Marine reserves reestablish lost predatory interactions and cause community effects in rocky reefs. *Ecological Applications*, 16, 963–976.

Guidetti, P. and Dulčić, J. (2007) Relationships among predatory fish, sea urchins and barrens in Mediterranean rocky reefs across a latitudinal gradient. *Marine Environmental Research*, 63, 168–184.

Hernández, J.C. (2006) *Estrategia reproductiva de la población canaria del erizo Diadema aff. antillarum, Phillipi, 1845: maduración gonadal, asentamiento larvario y reclutamiento.* Ph.D. Thesis (242 pp.), Universidad de La Laguna, Tenerife, Canary Islands, Spain.

Hernández, J.C. and Clemente, S. (2011) La complejidad del hábitat determina el reclutamiento de *Diadema* aff. *antillarum* en zonas libres de depredadores. *Proceedings of the 1º Congreso Latinoamericano de Echinodermos, November 13-18, 2011.* Puerto Madryn, Argentina.

Hernández, J.C., Brito, A., García, N., Gil-Rodríguez, M.C., Herrera, G., Cruz-Reyes, A. and Falcón, J.M. (2006) Spatial and seasonal variation of the gonad index of *Diadema antillarum* (Echinodermata: Echinoidea) in the Canary Islands. *Scientia Marina*, 70, 689–698.

Hernández, J.C., Clemente, S., Sangil, C. and Brito, A. (2008a) The key role of the sea urchin *Diadema* aff. *antillarum* in controlling macroalgae assemblages throughout the Canary Islands (eastern subtropical Atlantic): a spatio-temporal approach. *Marine Environmental Research*, 66, 259–270.

Hernández, J.C., Clemente, S., Sangil, C. and Brito, A. (2008b) Actual status of the sea urchin *Diadema* aff. *antillarum* populations and macroalgal cover in marine protected areas compared to a highly fished area (Canary Islands-eastern Atlantic Ocean). *Aquatic Conservation: Marine and Freshwater Ecosystems*, 18, 1091–1108.

Hernández, J.C., Clemente, S., Girard, D., Pérez-Ruzafa, A. and Brito, A. (2010) Effect of temperature on settlement and post -settlement survival in a barrens-forming sea urchin. *Marine Ecology Progress Series*, 413, 69–80.

Hernández, J.C., Clemente, S. and Brito, A. (2011) Effects of seasonality on the reproductive cycle of *Diadema* aff. *antillarum* in two contrasting habitats: implications for the establishment of a sea urchin fishery. *Marine Biology*, 158, 2603–2615.

Hernández, J.C., Clemente, S., Sangil, C., Rodríguez, A. and Eebrt, T.A. (2012) Population dynamics of a barren forming sea urchin: influence of island shelter and algae assemblage on population age structure. *Proceedings of the 14th International Echinoderm Conference,* 20-24 August, 2012. Brussels, Belgium.

Hernández, J.C., Clemente, S., Tuya, F., Pérez-Ruzafa, A., Sangil, C., Moro-Abad, L. and Bacallado, J.J. (2013). Echinoderms of the Canary Islands, Spain. *Echinoderms Research and Diversity in Latin America* (ed. by Alvarado, J.J. and Solis, F.), pp. 471–510. Springer, Berlin, Heidelberg.

IPCC (2007) The fourth assessment report of the IPCC. Cambridge University Press, Cambridge, United Kingdom.

Johnson, C.R., Banks, S.C., Barrett, N.S., Cazzasus, F., Dunstan, P.K., Edgar, G.J., Frusher, S.D., Gardner, C., Helidoniotis, F., Hill, K.L., Holbrook, N.J., Hosie, G.W., Last, P.R., Ling, S.D., Melbourne-Thomas, J., Miller, K., Pecl, G.T., Richardson, A.J., Ridgway, K.R., Rintoul, S.R., Ritz, D.A., Ross, D.J., Sanderson, J.C., Shepherd, S., Slotwinski, A., Swadling, K.M. and Taw, N. (2011) Climate change cascades: shifts in oceanography, species' ranges and marine community dynamics in eastern Tasmania. *Journal of Experimental Marine Biology and Ecology*, 400, 17–32.

Johnston, C.S. (1969) Studies on the ecology and primary production of Canary Islands marine algae. *Proceedings of the International Seaweed Symposium*, 6, 213–222.

Kalnay, E., Kanamitsu, M., Kistler, R., Collins, W. *et al.* (1996) The NCEP/NCAR 40-year reanalysis project. *Bulletin the American Meteorological Society*, 77, 437–471.

Lafferty K.D., Porter J.W. and Ford S.E. (2004) Are diseases increasing in the ocean? *Annual Review of Ecology, Evolution, and Systematics*, 35, 31–54.

Lauzon-Guay, J.S. and Scheibling, R.E. (2007) Seasonal variation in movement, aggregation and destructive grazing of the green sea urchin (*Strongylocentrotus droebachiensis*) in relation to wave action and temperature. *Marine Biology*, 151, 2109–2118.

Lawrence, J.M. (1975) On the relationships between marine plants and sea urchins. *Oceanography and Marine Biology: An Annual Review*, 13, 213–286.

Lessios, H.A. (1988) Mass mortality of *Diadema antillarum* in the Caribbean: what have we learned? *Annual Review of Ecology Evolution and Systematics*, 19, 371–379.

Lessios, H.A., Kessing, B.D. and Pearse, J.S. (2001) Population structure and speciation in tropical seas, global phylogeography of the sea urchin *Diadema. Evolution*, 55, 955–975.

Levitan, D.R. (1992) Community structure in time past: influence of human fishing pressure on algal-urchin interactions. *Ecology*, 73, 1597- 605.

Ling, S.D. (2008) Range expansion of a habitat-modifying species leads to loss of taxonomic diversity: a new and impoverished reef state. *Oecologia*, 156, 883–894.

Ling, S.D., Johnson, C.R., Frusher, S. and King, C.K. (2008) Reproductive potential of a marine ecosystem engineer at the edge of a newly expanded range. *Global Change Biology*, 14, 907–915.

Ling, S.D., Johnson, C.R., Frusher, S.D. and Ridgway, K.R. (2009) Overfishing reduces resilience of kelp beds to climate driven catastrophic phase shift. *Proceedings of the National Academy of Sciences of the United States of America*, 106, 22341–22345,

McClanahan, T.R., Muthiga, N.A., Kamukuru, A.T., Machano, H. and Kiambo, R.W. (1999) The effects of marine parks and fishing on coral reefs of northern Tanzania. *Biological Conservation*, 89, 161–182.

Mortensen, T. (1943) *A Monograph of the Echinoidea. III. 3. Camarodonta. II. Echinidæ, Strongylocentrotidæ, Parasaleniidæ, Echinometridæ.* CA Rietzel, Copenhagen.

Ortega, L., Tuya, F. and Haroun, R. (2009) El erizo de mar *Diadema antillarum* Phillipi, 1845 influye sobre la diversidad y composición de la comunidad de mega-invertebrados vágiles en fondos rocosos del Archipiélago Canario. *Revista de Biología Marina y Oceanografía*, 44: 489–495.

Pearse, J.S. and Hines, A.H. (1987) Long-term population dynamics of sea urchins in a central California kelp forest: rare recruitment and rapid decline. *Marine Ecology Progress Series*, 39, 275–283.

Rodríguez, A., Hernández, J.C., Clemente, S. and Coppard, S.E. (2013) A new species of *Diadema* (Echinodermata: Echinoidea: Diadematidae) from the eastern Atlantic

Ocean and a neotype designation of *Diadema antillarum* (Philippi, 1845). *Zootaxa*, 36361, 144–170.

Sala, E., Boudouresque, C.F. and Harmelin-Vivien, M. (1998) Fishing, trophic cascades, and the structure of algal assemblages: evaluation of an old but untested paradigm. *Oikos*, 82, 425–439.

Sangil, C., Clemente, S. and Hernández J.C. (2012) No take areas as an effective tool to restore urchin barrens on subtropical rocky reefs. *Estuarine, Coastal and Shelf Science*, 112, 207–215.

Sangil, C., Sansón, M., Clemente, S., Afonso-Carrillo, J. and Hernández, J.C. (in press). Structure and spatial variation of subtidal rocky assemblages mediated by sea urchin populations: from upright seaweed beds to barrens in subtropical islands. *Marine Environmental Research.*

Shears, N.T. and Babcock, R.C. (2002) Marine reserves demonstrate top-down control of community structure on temperate reefs. *Oecologia*, 132, 131–142.

Steneck, R.S., Graham, M.H., Bourque, B.J., Corbett, D., Erlandson, J.M., Estes, J.A. and Tegner, M.J. (2002) Kelp forest ecosystems: biodiversity, stability, resilience and future. *Environmental Conservation*, 29, 436–459.

Tegner, M.J. and Dayton, P.K. (2000) Ecosystem effects of fishing in kelp forest communities. *ICES Journal of Marine Science*, 57, 579–589.

Tuya, F., Boyra, A., Sánchez-Jerez, P., Haroun, R.J. and Barberá, C. (2004a) Relationships between rocky reef fish assemblages, the sea urchin *Diadema antillarum* and macroalgae throughout the Canarian Archipelago. *Marine Ecology Progress Series*, 278, 157–169.

Tuya, F., Martín, J.A. and Luque, A. (2004b) Patterns of nocturnal movement of the long-spined sea urchin *Diadema antillarum* (Philippi) in Gran Canaria (the Canary Islands, central East Atlantic Ocean). *Helgoland Marine Research*, 58, 1–26.

Tuya, F., Boyra, A., Sánchez-Jerez, P. and Haroun, R.J. (2005) Influence of fishing and functional group of algae on sea urchin control of algal communities in the eastern Atlantic. *Marine Ecology Progress Series*, 287, 255–260.

Tuya, F., Cisneros-Aguirre, J., Ortega, L. and Haroun, R.J. (2007) Bathymetric segregation of sea urchins on reefs of the Canarian Archipelago: role of flow-induced forces. . *Estuarine, Coastal and Shelf Science*, 73, 481–488.

Valentine, J.P. and Johnson, S.R. (2005) Persistence of sea urchin (*Heliocidaris erythrogramma*) barrens on the east coast of Tasmania: inhibition of macroalgal recovery in the absence of high densities of sea urchins. *Botanica Marina*, 48, 106–115.

Worm, B., Barbier, E.B., Beaumont, N., Duffy, J.E., Folke, C., Halpern, B.S., Jackson, J.B.C., Lotze, H.K., Micheli, F., Palumbi, S.R., Sala, E., Selkoe, K.A., Stachowicz, J.J. and Watson, R. (2006) Impacts of biodiversity loss on ocean ecosystem services. *Science*, 314, 787–790.

ABSTRACTS

SEA URCHIN RECRUITMENT FAILURE IN WARMER COASTAL WATERS IN NORWAY

Camilla With Fagerli, Kjell Magnus Norderhaug, Hartvig C. Christie,
Morten Foldager Pedersen, Stein Fredriksen

Abstract

Sea urchin (*Strongylocentrotus droebachiensis*) populations are declining and kelp forests (*Laminaria hyperborea*) recovering in the southern parts of a 2 000 km^2 area on the Norwegian coast formerly overgrazed by sea urchins. Approximately 500 km^2 kelp forests have recovered since the 1990s. Reductions in sea urchin populations might be related to climate change, as *S. droebachiensis* larval development is restricted to cold waters. Increasing temperatures might also facilitate northern range extensions for potentially important sea urchin predators. Predation on juvenile sea urchins has so far been given little attention in the NE Atlantic.

Field sampling showed low sea urchin settlement in the area where kelp had recovered, compared to barren areas further north. Tethering experiments in the field and laboratory feeding experiments showed that crabs, and in particular the edible crab *Cancer pagurus* were efficient sea urchin predators. The abundance of this species has increased substantially in the kelp recovery area in mid-Norway during recent years.

URCHIN BARRENS AND CLIMATIC CHANGES IN JAPAN

Daisuke Fujita

Abstract

How will climate changes affect sea urchin populations at barrens? In Japan, mass mortalities have been documented for a temperate species, *Strongylocentrotus nudus*, at high sea water temperatures (≈30°C) on the central Sea of Japan off coast of Honshu in summer of 1984; for the tropical species *Diadema* spp. at low water temperatures below 12 °C on the central Pacific coast of Honshu in winter of 2002; and in both temperate and tropical species at low salinities recorded at sites in Honshu and Hokkaido. Furthermore, abundances of *S. nudus* were significantly reduced probably due to extremely strong drawback at least in two large tsunamis (1983, 2011) in northern Japan. As a result of these events, algal beds flourished. In addition to these natural events, recent periodical discharge of wastewater and sediments has also affected the population of *S. nudus* along the coast of the Sea of Japan. Since climate change processes predict increasing extreme conditions, rather than a simple elevation of seawater temperature, all of the above processes should be considered to forecast the expansion of urchin barrens. However, more complex patterns should be considered in Japan due to the increase of coastal engineering (already achieving 40% of the national shoreline) proportional to the magnitude of natural events.

THERMOPHILOUS SEA URCHINS AND THE FUTURE OF MEDITERRANEAN ROCKY REEFS

Owen S. Wangensteen, Xavier Turon, Creu Palacín

Abstract

Marine ecosystems are ever changing, prompted by a wide range of natural or human-driven processes and disturbances. Introduction of new species is one of the most critical changes, particularly if they are structural species that strongly impact the landscape physiognomy by producing catastrophic shifts between alternative states. Much research has been undertaken on invasive species, which are a major element of global change, but not all invasion events are directly attributable to human intervention. Species can colonize new regions driven by distribution range expansions, which may occur by natural changes in climate, geographic or ocean circulation patterns, in a manner that can be greatly influenced by ecological, behavioral or historical processes. When a natural colonization by a structural species occurred many years ago, it eventually becomes abundant and ecologically significant in the new ecosystem. Consequently, one may tend to consider the species as a well-established and native element from the new geographic area, and the recentness of the colonization can easily be overlooked. This could have been the case of the sea urchin *Arbacia lixula* in the Mediterranean, one of the most abundant macroinvertebrates in rocky reefs of the region, and thus widely regarded as a typical representative of its fauna. However, the species has been considered by some authors as a thermophilous sea urchin of tropical origin. We recently studied the phylogeographic and past demographic patterns of *A. lixula* using molecular tools, which, consistently with the lack of its appearance in the Mediterranean fossil record, lead us to suggest that the species may have colonized the Mediterranean from the tropical Eastern Atlantic as recently as during the last interglacial period (100-130 thousand years ago). By means of studying the reproductive cycle of *A. lixula* in Northwestern Mediterranean during a period of four years, we gathered evidence of its thermophilic nature. Small increments in mean sea surface temperature seem to boost the species reproductive potential, by increasing several times its gonadosomatic index. Experiments currently in progress suggest that warmer water temperatures also increase survival rates of *A. lixula* larvae and that the expected values for ocean acidification would not represent a serious threat for its development in the near future. Therefore, we can expect that Mediterranean populations of *A. lixula* would suffer a significant demographic expansion in the coming decades. In fact, some records of *A. lixula* population densities prove that it has already become more abundant in the Northwestern Mediterranean along the last fifty years, an increase that has been attributed to rising sea temperatures. Considering its great potential to impact shallow rocky reef ecosystems triggering the development of subtidal barren zones, and the recent finding of its omnivorous behavior, *A. lixula* should be considered as potential threat for these ecosystems. Monitoring of its populations is highly recommendable as a management tool for protecting the threatened Mediterranean shallow water habitats in the near future.

EFFECTS OF OCEAN ACIDIFICATION AND GLOBAL WARMING ON *PARACENTROTUS LIVIDUS* FERTILIZATION AND LARVAE DEVELOPMENT AT ITS SOUTHERN MOST LIMIT OF DISTRIBUTION

Eliseba García, Mishal Cohen-Rengifo, Sabrina Clemente,
Celso Hernández, José Carlos Hernández

Abstract

In a context of climate change, increasing values of atmospheric carbon dioxide (CO_2) are tilting the delicate balance of the ocean chemistry towards seawater acidification. Likewise, increasing seawater temperatures constitutes an important stressor of marine populations that may induce migrations and even local extinctions. Sea urchins are key herbivores and act as important grazers in benthic communities. In this study, we have evaluated, on the one hand, the separated effects of low predicted pH levels as a consequence of increased concentrations of atmospheric CO_2, as well as those of warming temperatures, on fertilization and early development stages of the sea urchin *Paracentrotus lividus*. We used experimental ranges of pH including current values for the region of the Canary Islands and simulated predictable values of the parameter for future conditions due to climate change processes. On the other hand, we assessed the effects of each seawater acidification condition on larvae development until settlement. In the first part, we examined fertilization rates, cleavage rates (proportion of cells in a given cleavage stage), developmental speed, and early pluteus larval morphology (overall length, post-oral arm length and body length) at different times before insemination as well as at three contrasting ranges of pH and temperature. A clear pattern was exhibited among pH treatments showing an important delay on cleavage, as well as on larval development, as pH decreased. In contrast, fertilization rate showed a slight but significant increase with higher seawater temperatures. In the second part, we cultured *P. lividus* larvae at starting densities of 2 per ml, which were distributed in 3 seawater tables with controlled pH conditions. Individuals were fed with *Rhodomona lens* in concentrations of 2000 cells/ml and daily monitoring was carried out to assess larvae development and growth. Larvae were able to survive in all pH treatments. A significant decrease of post-oral arm length and a reduced overall growth were detected at the most acidic conditions. Mean post-oral arm lengths after 25 days of treatments were L(pH:8) = 0.506 mm; L(pH:7.7) = 0.538 mm and L(pH:7.4) = 0.373 mm, at each treatment respectively. These results suggest that for moderate pH

changes, such as those predicted for the year 2100, the larvae of *P. lividus* would be able to develop normally, whereas extreme seawater pH values, as those predicted for 2300, would limit larvae development and the achievement of a competent stage would then be compromised. Despite the clear implications of these results for predicting climate change effects over key species, further experimental research to assess larval survival and settlement under longer pH exposures would be desirable.

FROM FIELD TO BENCH AND FROM BENCH TO FIELD: MARINE BIODIVERSITY AND TROPICAL MEDICINE RESEARCHERS WORKING TOGETHER

Jacob Lorenzo-Morales

Abstract

Collaboration between the Department of Animal Biology and the University Institute of Tropical Diseases and Public Health of the Canary Islands, University of La Laguna started in 2010. Researchers from both areas decided to collaborate in a mass mortality event of sea urchins in the coast of Tenerife island, Canary Islands, Spain. Moreover, the free living amoebae group at the University Institute of Tropical Diseases and Public Health of the Canary Islands was aiming to isolate amoebae from echinoderms and thus also asked for collaborations from this department. Therefore, cellular and molecular tools were applied in a case of mass mortality of sea urchins in order to evaluate possible infectious agents as the cause of this event (from field to bench). Collected specimens of three species of sea urchins were examined for the presence of opportunistic free living amoebae (from bench to field). The obtained results indicated that sea urchins were suffering from the sea urchin bald disease and bacteria belonging to *Vibrio* genus (characterized by growing in TB agar and PCR/DNA sequencing) were isolated from the lesions and coelomic fluid from dead and moribund sea urchins. Thus, the mortality event was assumed to be caused by this agent. In parallel, sea urchins from the same three species (healthy and diseased ones) were also collected and the coelomic fluid was also examined for the presence of free living amoebae. From these samples, eight strains of amoebae were established and characterized by morphological and molecular methods as *Neoparamoeba brachiphila*. Results of this second study together with data on sea urchins mortalities reported to date justify the hypothesis that free-living amoebae play an opportunistic role in the mortality of sea urchins in the studied area. In our opinion, the future study of sea urchin bald disease should consider a possible synergy of both free-living agents, bacteria and amoebae.

ACIDIFICATION EFFECTS OF THE RECENT VOLCANIC ERUPTION OF EL HIERRO IN THE ISLAND MARINE BIOTA

Ricardo Haroun, Teba Gil Díaz, Séfora Betancor,
Rubén Rámirez, Fernando Tuya

Abstract

The large emissions of CO_2 from different antrophogenic sources are promoting the acidification of the marine waters with concomitant pH reductions and unstable balance of carbon. Thus, in the scenarios of global change for the next decades, one of the main environmental issues arising is acidification process of the marine realm, particularly its effects in species and marine ecosystems with large carbonate structures.

Between 19th of October 2011 and 7th of March 2012, a major submarine volcanic eruption took place near the coast of El Hierro Island, the southwestern most island of the canarian archipelago. During the eruption period, several oceanographic expeditions were conducted, but unfortunately very restricted access was allowed for coastal assessment of benthic populations. In November 2011, March and July 2012 research trips were done to El Hierro Island to collect biological samples from different coastal stations along a gradient of enviromental conditions, with the pH as major physical driver. The targed species were two brown macroalgae, limpets and other gastropods species. Another coastal station was studied as an external control in Gran Canaria Island during the same sampling period with similar environmental characteristics.

In this contribution we shall present the main results of the comparative analysis performed in *Padina pavonica*, a carbonated macroalgae which is the dominant species in turf assemblages along the intertidal rocky shores of the canarian archipelago. The calcification degree and physiological performance of this brown algae showed large plasticity, with clear detrimental effects during the period of coastal water acidification (eruption period) and quick recovery aftermath.

UNDERWATER VOLCANIC ERUPTION WEAKENS TROPHIC CASCADES

Sabrina Clemente, José Carlos Mendoza, José Carlos Hernández

Abstract

Natural disturbances create opportunities for species to claim previously utilized space and resources. The widespread and massive disturbance caused by catastrophic events provides ideal conditions for rapid recruitment and spread of certain species. This study was conducted across El Hierro (Canary Islands), an island impacted by an underwater volcanic eruption starting on October 2011 and coinciding with the annual settlement peak of the key herbivore sea urchin *Diadema africanum*. Despite the eruption was ~100 m deep off the southwest of the island, it triggered severe mass mortalities of many organisms due to the release of gasses that changed seawater chemistry with severe pH reductions. We present data on the recruitment dynamics of *D. africanum* in relation to the disturbance caused by the eruption and the relative abundance of its predators at the first 2 months post-eruption. A spatio-temporal analysis of recruits' densities showed significant differences before and after the eruption at the area closer to the impact, while sites within the east and north of the island showed no variation in recruits' numbers through time. Population size distributions, as well as the abundance and composition of urchin predatory fish, significantly differed from pre-eruption levels at the most impacted sites in comparison to non-affected sites, while no significant changes in adult urchin densities were detected. We show that this recruitment pulse may be due to a release from predation control during the post-settlement and recruitment stage related to the disturbance of the benthic systems. Results suggest that sea urchins will mostly comprise the dominant component of the fauna in the early stages of the successional response to the disturbance. Given the echinoid major grazing activity, this may have long-lasting structural consequences for the community.

EFFECTS OF A VOLCANIC ERUPTION OVER THE INTERNAL CALCAREOUS STRUCTURES OF THE SEA-CUCUMBER *HOLOTHURIA SANCTORI* (DELLE CHIAJE, 1823) [ECHINODERMATA: HOLOTHUROIDEA]

Pablo G. Navarro, Juan M. Barrio, Sara García-Sanz, Fernando Tuya

Abstract

Studies describing how ocean acidification may impact on the marine biota have been restricted to laboratory experiments over a few species, while only a few studies have taken advantage of direct observations near volcanic spots, where pH levels are drastically reduced. To date, no study has assessed the way severe changes of pH levels may affect the morphology of holothurians. A submarine eruption started off El Hierro Island, Canary Islands, on October 10th 2011. Individuals of *Holothuria sanctori* were collected, on December 2011, on two shallow-water reef locations adjacent to the eruption off El Hierro Island (pH ranged between 7.12-7.83) and on a reef location off Gran Canaria Island as a control (pH 8.13). A microscopic analysis of the ossicles in the dorsal area of their bodies and in the calcareous ring was undertaken to determine if there were differences between locations directly affected by the eruption and the control. The mean width, diameter and number of holes of button, table and rod-type ossicles were measured using an ocular micrometer. Button and table-type ossicles showed significantly narrower structures off El Hierro Island than those from Gran Canaria. Significant differences were found also on table and rod-type ossicle mean diameter between locations. Table-type ossicles showed significant differences on mean number of holes between locations. In conclusion, lowered pH levels off El Hierro Island caused significant changes in the internal calcareous structures of *H. sanctori*, and therefore highlight the consequences of sea water acidification over holothurians.

WORKSHOP PICTURES

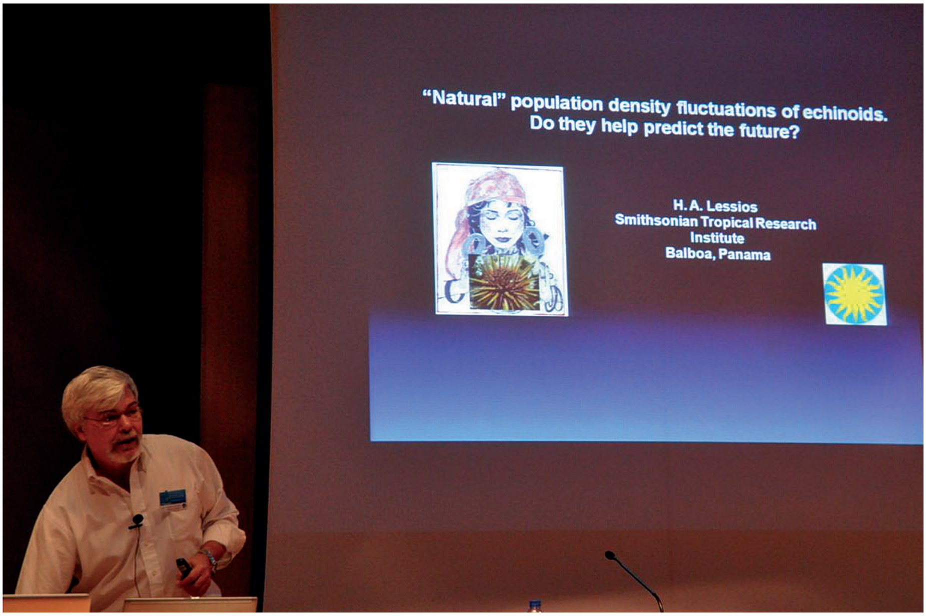

“Natural” population density fluctuations of echinoids.
Do they help predict the future?

H. A. Lessios
Smithsonian Tropical Research
Institute
Balboa, Panama

Harilaos Lessios’ Presentation, Universidad de La Laguna, Tenerife.

Climate change, disease and dynamics of a
kelp-bed ecosystem

Bob Scheibling
Dalhousie University

Robert Scheibling’s presentation, Universidad de La Laguna, Tenerife.

Bernat Hereu's presentation, Universidad de La Laguna, Tenerife.

Scott Ling's presentation, Universidad de La Laguna, Tenerife.

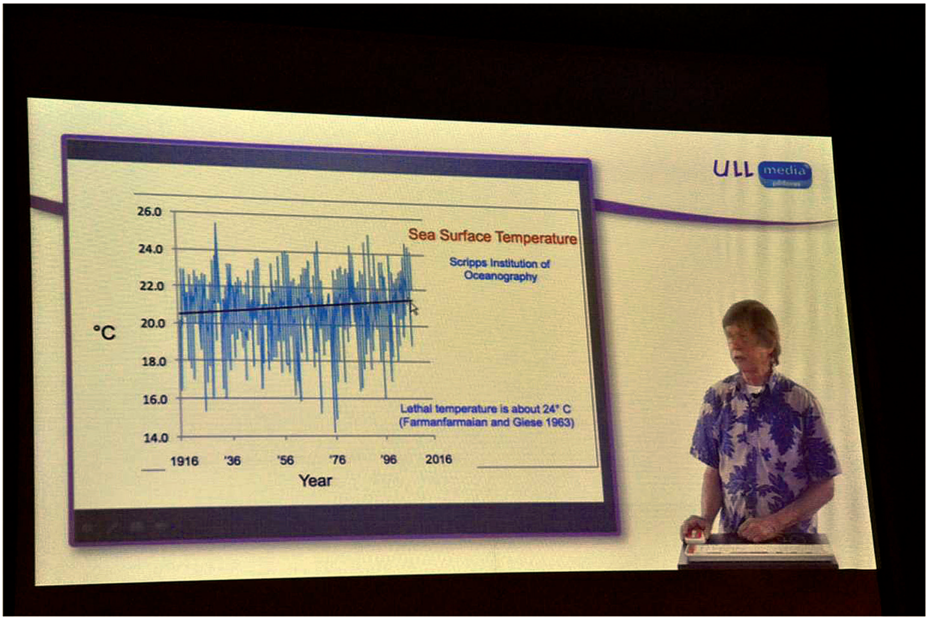

Thomas A. Ebert's presentation, Universidad de La Laguna, Tenerife.

Sam Dupont's presentation, Universidad de La Laguna, Tenerife.

José Carlos Hernández's presentation, Universidad de La Laguna, Tenerife.

Oceania student organization, Universidad de La Laguna, Tenerife.

Workshop Opening at the Aula Magna of the Facultad de Física, Universidad de La Laguna by José Carlos Hernández and Rodrigo Trujillo.

Las Cañadas del Teide National Park, Tenerife.

Las Cañadas del Teide National Park, Tenerife.

Abades dive, Tenerife.

Las Eras lunch, Tenerife.

La Restinga, El Hierro Island.

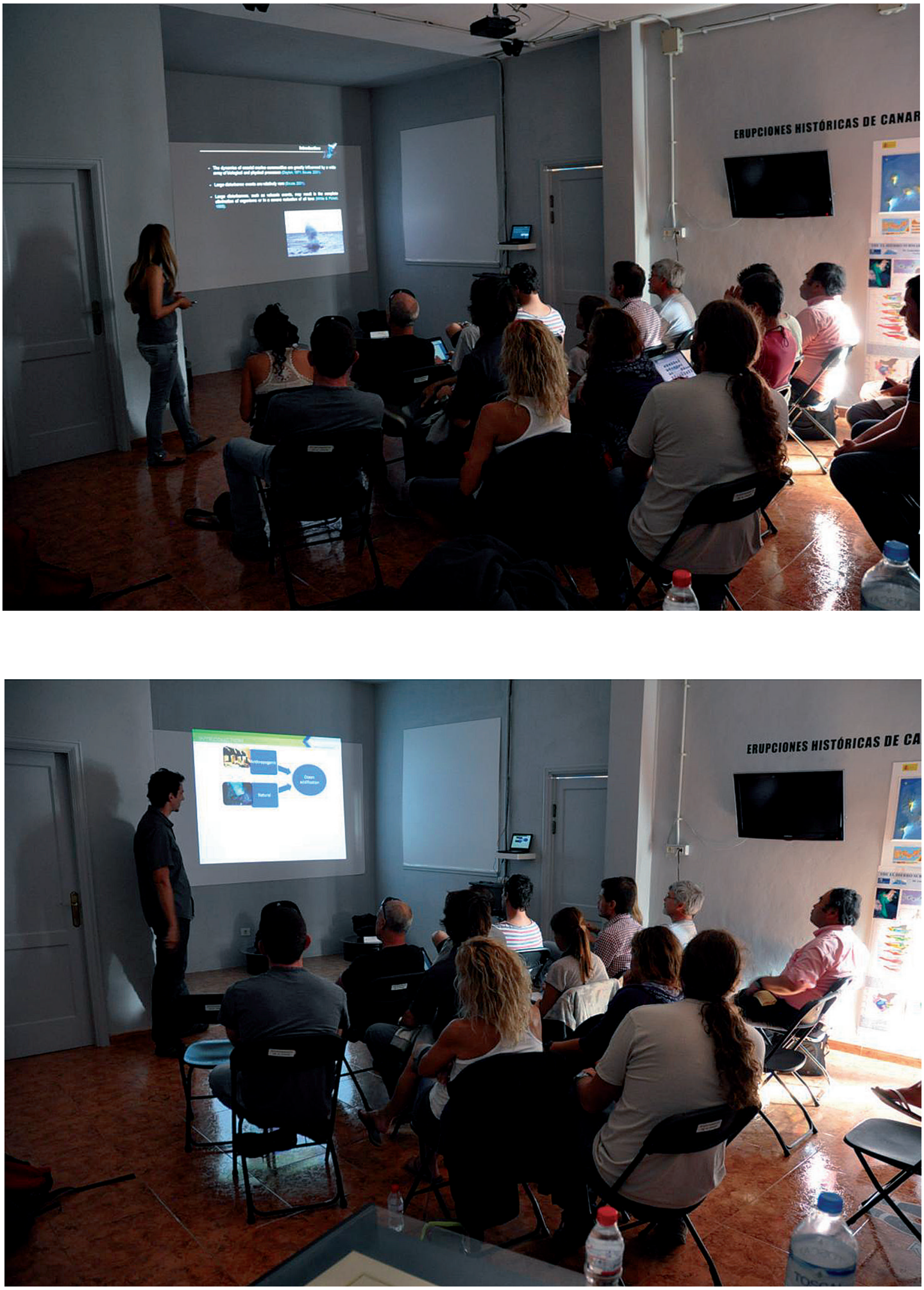

Sabrina Clemente's and Pablo González's presentations at the Restingolita Museum, La Restinga, El Hierro.

FUTURE:
CORDEX WEATHER RESEARCH AND FORECASTING

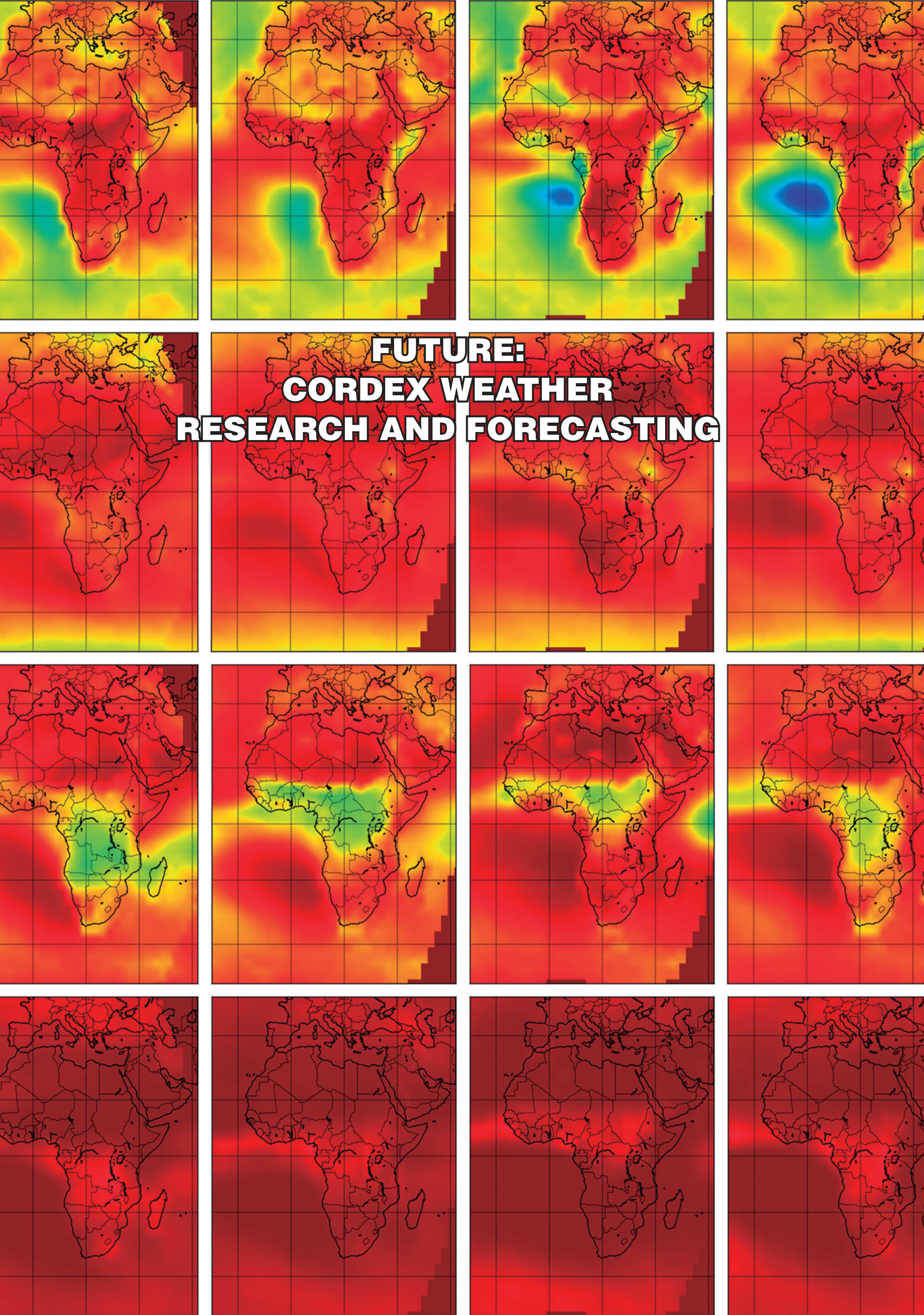

LIST OF AUTHORS

D. Argüeso
Climate Change Research Centre, University of New South Wales, Sydney, Australia.

Juan Pedro Díaz
Grupo de Observación de la Tierra y la Atmósfera. University of La Laguna, 38203 Canary Islands. Spain..

Jason P. Evans
Climate Change Research Centre, University of New South Wales, Sydney, Australia.

F. J. Expósito
Grupo de Observación de la Tierra y la Atmósfera. University of La Laguna, 38203 Canary Islands. Spain.

L. Fita
Climate Change Research Centre, University of New South Wales, Sydney, Australia.

Albano González
Grupo de Observación de la Tierra y la Atmósfera. University of La Laguna, 38203 Canary Islands. Spain.

K. Görgen
Meteorologisches Institut der Universität Bonn, Rheinische Friedrich-Wilhems-Universität Bonn, 53115 Bonn, Germany.

P. Hadjinicolaou
Energy, Environment and Water Research Center, The Cyprus Institute, Nicosia, 2121, Cyprus..

K. Hamilton
International Pacific Research Center, School of Ocean and Earth Science and Technology, University of Hawaii at Manoa, Honolulu, HI 96822, USA.

A. Henríquez
Grupo de Observación de la Tierra y la Atmósfera. University of La Laguna, 38203 Canary Islands. Spain.

Bruce Hewitson
Climate Systems Analysis Group. University of Cape Town. South Africa.

Fei Ji
New South Wales State Government Office of Environment and Heritage.

T. Karacostas
Department of Meteorology and Climatology, Aristotle University of Thessaloniki, Thessaloniki, 54124, Greece.

E. Katragkou
Department of Meteorology and Climatology, Aristotle University of Thessaloniki, Thessaloniki, 54124, Greece.
E-mail: katragou@auth.gr

A. Lauer
International Pacific Research Center, School of Ocean and Earth Science and Technology, University of Hawaii at Manoa, Honolulu, HI 96822, USA.

Chris Lennard
Climate Systems Analysis Group. University of Cape Town. South Africa.

J. Lelieveld
Energy, Environment and Water Research Center, The Cyprus Institute, Nicosia, 2121, Cyprus.
Department of Atmospheric Chemistry, Max Planck Institute for Chemistry, Mainz, 55020, Germany.

F. Marougianni
Laboratory of Atmospheric Physics, Aristotle University of Thessaloniki, Thessaloniki, 54124, Greece.

Jon Padgham
Global Change System for Analysis and Training. Washington. USA

J. C. Pérez
Grupo de Observación de la Tierra y la Atmósfera. University of La Laguna
38203 Canary Islands. SPAIN.
E-mail: jcperez@ull.es

I. PYTHAROULIS
Department of Meteorology and Climatology, Aristotle University of Thessaloniki, Thessaloniki, 54124, Greece.

A. SARR
Département Climat et Applications, Agence Nationale de la Météorologie (ANACIM), Dakar, 16688 Dakar- Fann, Senegal.
E-mail: layesarr@voila.fr

SILVINA A. SOLMAN
Centro de Investigaciones del Mar y la Atmósfera (CIMA/ CONICET-UBA), DCAO/FCEN, UMI IFAECI/CNRS, Ciudad Universitaria, Pabellón II Piso 2, Buenos Aires (C1428EGA), Argentina.
E-mail: solman@cima.fcen.uba.ar

J. SWEENEY
Department of Geography, National University of Ireland, Maynooth, Co Kildare, Ireland.

D. TAIMA
Grupo de Observación de la Tierra y la Atmósfera. University of La Laguna 38203 Canary Islands. Spain.

RODNEY F. TECK
Department of Geography, National University of Ireland, Maynooth, Co Kildare, Ireland.
E-mail: Rodney.Teck@nuim.ie

I. TEGOULIAS
Department of Meteorology and Climatology, Aristotle University of Thessaloniki, Thessaloniki, 54124, Greece.

R. VAUTARD
Laboratoire des Sciences du Climate et de l'Environnement, IPSL, CEA/CNRS/ UVSQ, Gif sur Yvette, France.

YU QUING WANG
International Pacific Research Center, School of Ocean and Earth Science and Technology, University of Hawaii at Manoa, Honolulu, HI 96822, USA.
E-mail: Yuqing@hawaii.edu

K. Warrach-Sagi
Institut für Physik und Meteorologie, Universität Hohenheim, Garbenstr. 30, 70599 Stuttgart, Germany.
E-mail: kirsten.warrach-sagi@uni-hohenheim.de

P. Zanis
Department of Meteorology and Climatology, Aristotle University of Thessaloniki, Thessaloniki, 54124, Greece.

C.X. Zhang
International Pacific Research Center, School of Ocean and Earth Science and Technology, University of Hawaii at Manoa, Honolulu, HI 96822, USA.

G. Zittis
Energy, Environment and Water Research Center, The Cyprus Institute, Nicosia, 2121, Cyprus.
E-mail: g.zittis@cyi.ac.cy

CORDEX-AFRICA – ANALYSING CORDEX DATA FOR INTEGRATION INTO THE IMPACTS COMMUNITY

Chris Lennard, Bruce Hewitson and Jon Padgham

CLIMATE CHANGE PERSPECTIVES FROM THE ATLANTIC:
PAST, PRESENT AND FUTURE
Jose María Fernández-Palacios, Lea de Nascimento, José Carlos Hernández,
Sabrina Clemente, Albano González & Juan P. Díaz-González (eds.)
Servicio de Publicaciones, Universidad de La Laguna – 2013

ISBN: 978-84-15910-54-1
pp. 541-561

ABSTRACT

The Cordex-Africa campaign has been developed to analyze downscaled regional climate data over the African domain of Cordex, train young climate scientists in climate data analysis techniques and engage users of climate data in sector specific applications. The campaign has run four training and analysis workshops over an 18 month period each of which had specific objectives. During the first three regional analysis teams were formed and preliminary analyses were run on the Cordex data. During the second workshop regional analysis objectives were refined. During the third, climate data analysis continued and additionally each analysis group was linked with impact scientists to understand and address the types of climate related questions these sectors have. The fourth workshop focused on writing up the work of the previous workshops and four articles were submitted in time to qualify for review in the IPCC AR5. A separate workshop engaged health sector practitioners to understand their needs with respect to climate information and representatives of each Cordex-Africa regional analysis team was present. Achievements of the campaign so far include the formation of competent teams to assess the impacts of climate change at the regional scale, published four journal articles and engaged successfully with the climate impacts community. The campaign will continue as downscaled CMIP5 future projection data become available through Cordex during 2013. Dependent on funding, the analysis groups will both assess the climatological data as well as engage with the impacts community to distil the implications of these changes at the regional scale.

KEY WORDS: Cordex-Africa, analysis, impacts, engagement

INTRODUCTION

The CORDEX (Coordinated Regional Downscaling Experiment) program was initiated by the World Climate Research Program (WCRP) to develop downscaled regional climate change projections at user-relevant scales for all terrestrial regions of the world. Africa was identified at the outset as the priority region in urgent need of attention, and the CORDEX first phase of activities thus focused on model downscaling for Africa from the CMIP-5 suite of Global Climate Models. However, the WCRP-CORDEX program is focused on model simulation tasks, and as such has no explicit analysis agenda. In response, the CORDEX-Africa analysis program was established to address the acute climate data analysis and relevant capacity development needs for Africa. The activities of CORDEX-Africa is spearheaded by the Climate Systems Analysis Group (CSAG) at the University of Cape Town in partnership with global change System for Analysis Research and Training (START), World Climate Research Programme (WCRP), Climate and Development Knowledge Network (CDKN), the International Centre for Theoretical Physics (ICTP), the Swedish Meteorological-Hydrological Institute (SMHI), and the UNDP- Africa Adaptation Program (UNDP-AAP).

CORDEX-Africa has three overarching objectives: (1) to analyse downscaled evaluation run data (Era-Interim reanalysis) as well as downscaled CMIP5 projections runs, (2) to advance the skill base within Africa in climate data analysis across diverse fields including atmospheric science/climatology, hydro-meteorology and relevant bio-physical and social sciences, and (3) to foster inter-disciplinary investigations of climate data through engaging users of climate information to transform climate data into useful, usable climate information. These intertwined objectives aim to further the understanding of climate processes over Africa as well as to foster collaboration and knowledge sharing between research, policy and practitioner communities. Within these objectives a guiding ethos was developed to frame the analysis process. This can be summarised with the acronym A-F-R-I-C-A:

A –Analysis: developing methods and tools to analyse atmospheric processes over Africa and how these may change into the future
F –Foci: addressing key meteorological and impacts knowledge gaps
R –Regional messages: presenting information for key regions of the continent
I –Integrated approach: bringing together climate and vulnerability-impact-adaptation scientists to identify and address key climate vulnerabilities
C –Capacity development: long-term collaboration between African scientists and key global institutions for career development
A –Application and Adaptation: bridging the science-society divide through transforming climate data into actionable information

STRATEGY

During 2011 a series of 3 workshops were held with the above objectives in mind. The first two were primarily climate data analysis workshops and the third included the integration of the vulnerability-impact-assessment (VIA) community. A fourth workshop held in February 2012 was a «writeshop» in which the analyses performed in the previous workshops was written up for climate journals.

This chapter serves primarily to describe the workshop activities and outcomes of Cordex-Africa Analysis campaign so far. Each workshop will be considered sequentially and some results will presented as appropriate. Also discussed are future activities of the Cordex-Africa initiative in the light of downscaled

CMIP5 data and engagement of the VIA community. The chapter will conclude with a presentation of plans for activities in 2013 and 2014.

WORKSHOP 1

The first workshop was held on 25th to 26th March 2011 at the Abdus Salam International Centre for Theoretical Physics (ICTP) in Trieste, Italy. This two day workshop was preceded by the four day International Conference on the Coordinated Regional Climate Downscaling Experiment which was a useful grounding for the workshop delegates who had not been exposed to Cordex before.

Twenty four participants from across Africa, representing a mix of scientists from the atmospheric science and a small group from climate impact communities were invited to this workshop. This was the first of a planned series of three workshops with the aim of leveraging data output from the CORDEX downscaling activities for benefit in regional climate change adaptation and decision making. The primary goal of the workshop was to train delegates in techniques of climate data analysis using data from the CORDEX simulations over the African domain to better understand the regional details of climate processes and projected change. In addition to this, skill development through the formulation of regional research questions that directed the subsequent analysis activities.

Participants divided into regional analysis teams, namely West, East and southern Africa to design an initial analysis framework for the remainder of the workshops, with special focus on societal relevant questions. A series of presentations were held which framed the objectives of the Cordex-Africa analysis and introduced resource tools available to the project. During breakout sessions key regional climate issues were identified and articulated by each team which formed the launch point for team discussions that continued throughout the workshop. Key knowledge gaps identified by the participants could be placed into three sub-groupings: (1) meta-questions dealing with uncertainties in the observation data, circulation changes, (2) precipitation questions - such as changes in rainfall characteristics like onset, cessation, dry spell duration, long term trends and controls and (3) questions about extremes e.g. the definition of extremes, intra-seasonal events and variability, trends, changes in frequency of events. Most of the questions were regionally specific e.g. convection in the ITCZ, tropical cyclones in the Mozambique Channel, the West African Monsoon. At the end of the workshop each team gave a presentation of their analysis framework.

Together with the knowledge gap identification exercise, five training sessions for a total time of 6 hours were dedicated to the diagnosis of the CORDEX outputs. The objective was to explore the datasets and report on the ability of the regional climate models (RCMs) to reproduce the observed climatology of precipitation and temperature over the African domain as well as at regional scale. The R-statistical software was used to assess the interannual and seasonal

TABLE 1. Region climate models used in the Cordex-Africa Analysis campaign.

Modeling Centre	Regional model
Centre National de Recherches Météorologiques, France	CNRM-ARPEGE51
Danmarks Meteorologiske Institut, Danmar	DMI-HIRHAM
Abdus Salam International Centre for Theoretical Physics, Italy	ICTP-REGCM
CLM community (www.clm- community.eu)	IES-CCLM
Koninklijk Nederlands Meteorologisch Instituut, Netherlands	KNMI-RACMO2.2b
Max Planck Institute, Germany	MPI-REMO
Sveriges Meteorologiska och Hydrologiska institut, Sweden	SMHI-RCA35
University of Cape Town, South Africa	UCT-PRECIS
Universidad de Cantabria, Spain	UC-WRF311
University of Murcia, Spain	UM-MM5
Université du Québec à Montréal, Canada	UQAM-CRCM5

variability in rainfall and temperature. Downscaled temperature and rainfall data from the ERA-interim reanalysis over the period 1989-2008 were provided by 14 regional modelling groups. Prior to performing the analyses, the raw data from the modelling groups were checked to demonstrate the need for a quality assessment of data. Metadata and data of NetCDF files containing monthly mean precipitation and temperature at 2 meters were checked with ready made scripts and information such as the dimensions and units were extracted and diagnosed. From this preliminary diagnostic, inconsistencies in some RCM outputs were identified and on this basis it was decided to exclude the outputs from 3 RCMs for the workshop activities. This left data from 11 RCMs that could be used in the analysis and are listed in Table 1.

Participants computed and mapped the annual mean and quantified the biases in the modelled annual mean over the African domain as well as over various targeted regions. At monthly scale, the wet/dry and warm/cold biases were quantified and the annual cycle of precipitation and temperature over targeted regions (e.g. Sahel) were derived. During the last training session inter-annual variability of annual and monthly mean precipitation and temperature over the targeted regions. Results from these analyses showed that generally the models were generally able to reproduce the inter-annual variability of temperature but for precipitation, however, some of the models poorly reproduce the year to year variation. Similarly, at the inter-annual scale, models generally reproduced the inter-annual variability of temperature but for precipitation some of the models poorly reproduce the year to year variation Delegates presented their preliminary results at the end of the meeting. All scripts and datasets that were prepared beforehand were made available to the delegates.

There was a strong desire expressed for daily and sub-daily data and a number of desired metrics were proposed by delegates that would require these data. These were largely related to rainfall and agriculture and included metrics like onset and cessation of rain, rainfall intensities and dry spell duration. However, in terms of developing capacity within Africa for rigorous climate analysis, the analysis was structured so that participants would gain the appropriate groundwork on baseline aspects of the data, and the essential framing concepts. These analysis diagnostics introduced participants to a stepwise, incremental approach to evaluating RCM datasets, to assess the general capability of the models to reproduce some well-known features of the precipitation and temperature climatology, and introduce flexible software tools for analysis.

On the whole, the goals of the workshop were achieved. The workshop facilitated the formation of the regional groups and training (capacity development) through analysing the data was achieved. Some results from the workshop were presented by representatives from each group at WCRP Open Science conference in Denver during 2011.

Workshop 2

The second workshop of CORDEX Africa programme was convened in Cape Town in early July as a follow-up action to the workshop held at ICTP in Trieste, Italy. The main purpose of this workshop was to engage a smaller group of participants (particularly the leaders and more senior members of the group) to further develop analytical and interpretive skills related to CORDEX as well as discuss strategies to include the VIA sector within Cordex-Africa. Priority analysis questions (dominated by seasonal rainfall onset) were identified and matched against the available data to scope the analysis possibilities.

The participants demonstrated a strong understanding of climate systems theory, climate change and its potential impacts, and regional climate models. This facilitated further skills training with software analysis tools and resulted in a move from the theoretical discussions of the first workshop through to hand-on analysis of the data. Instructors partnered one-on-one with participants to help with the implementation of the analyses use of the relevant software.

The participants engaged in a number of analyses that included assessments of precipitation and temperature biases. The West African group divided the region into 5 sub-regions and assessed the ability of the regional models to reproduce the annual cycle of precipitation using the GPCC data as reference (Fig. 1). The models generally captured the annual cycle including the uni-modal

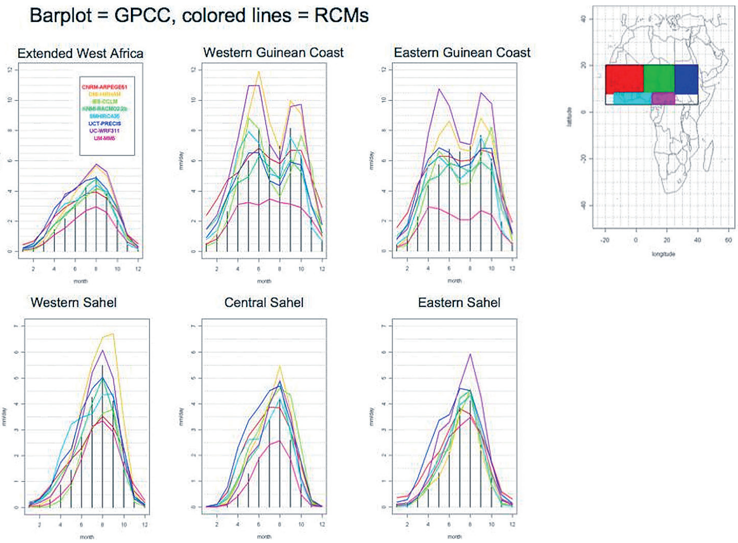

Figure 1. Annual cycle of rainfall in 5 sub-regions of the West African as simulated by 8 RCMs.

precipitation distribution in the Sahelian region and the bimodal rainfall distribution in the two Guinean regions. However, results varied between models e.g. rainfall was generally under (over)-simulated by the MM5 (WFR, HIRAM) models and ensemble average outperformed the individual ensemble members. The spatial characteristics of the rainfall simulated by each of the models indicated that the individual model biases varied significantly across the RCMs. A common feature among the RCMs is the underestimation of the simple daily index (rainfall intensity) over the Sahel and along the Guinea Coast and the ensemble mean did not improve the individual RCM members for this metrics (Fig 2).

The southern African group assessed biases in the seasonal rainfall cycle against the GPCC precipitation data. Individual models showed unique and shared biases in different regions with the ensemble mean looking most like the observed (Fig. 3). Most models displayed dry biases over Mozambique and a wet bias over the higher lying regions around Lesotho. The group divided the region into 3 sub-regions (each sub-region represents a different rainfall regime) to assess the ability of the models to reproduce the seasonal cycle (Fig. 4). In the northern most region the annual cycle was well represented by all models in the rainy season; in the central region the start of the rainy season is captured but with a strong wet bias (SON) which extends into DJF; in the western Cape region the rainy season (JJA) is poorly represented (dry bias) and the observed rainfall falls outside the model spread in August and September. Correlations between

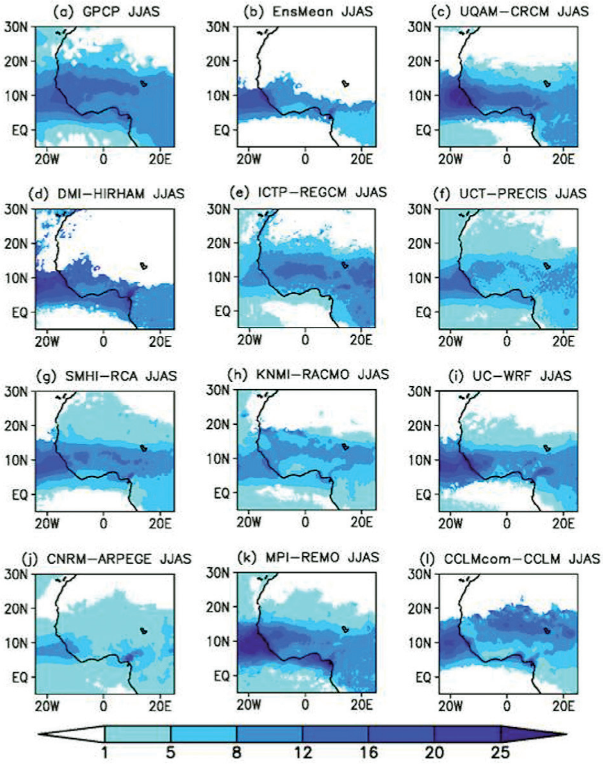

Figure 2. Mean intensity of daily rainfall (mm/day) during the rainy season (JJAS) from the Cordex models over West Africa for the period 1989-2008. From Klutse et al. (in review).

modelled and GPCC rainfall indicate a similar growth in bias from the northern to southern parts of the region (Fig. 5).

In the East African region the rainfall regime consists of two rainy seasons (JJAS and OND). Although most models were able to reproduce the desired double peaks in the area-averaged annual cycle, spatially there large biases in individual models. As seen in the other regions the ensemble mean outperformed the individual members (Fig. 6).

During the workshop both goals of continued training in analysis tools and as well as the production of the first results were attained. In addition, plans were set in place for the third workshop to be held at the end of 2012 which would see the production of an analysis product that could be written up for publication (one paper for each region) as well as how best to engage the VIA sector at this meeting.

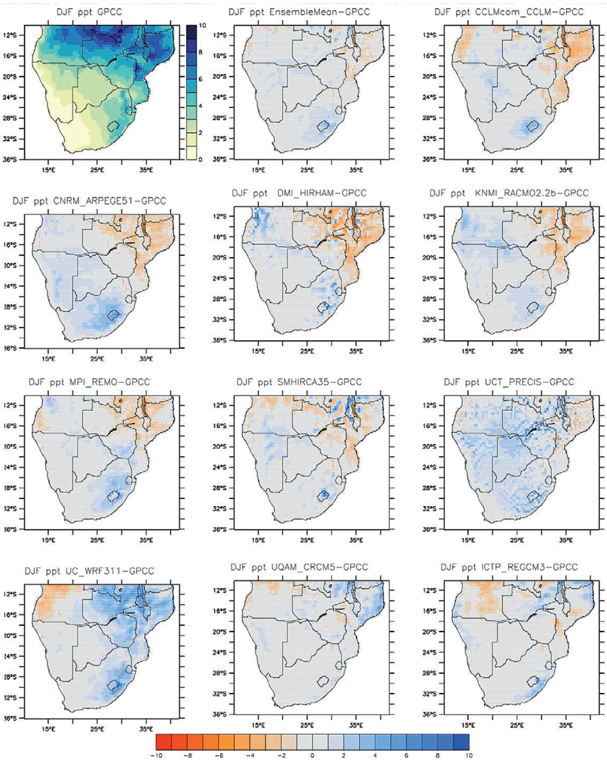

Figure 3. Rainfall biases in the regional models compared to the GPCC dataset.

WORKSHOP 3

The third workshop of CORDEX Africa programme was convened in Cape Town in late November 2011 as the official follow-up workshop to the initial workshop held at ICTP during March 2011. Based on the mid-year meeting a number of measurable goals were set for the workshop:

1. To identify key, regionally specific atmospheric processes and how these may change into the future using reanalysis and climate projection data
2. To continue the collaborative training of African scientists for capacity building and career development and address issues identified during the mid-year meeting
3. To identify key vulnerability-impact-adaptation questions and assess the climate data with these in mind

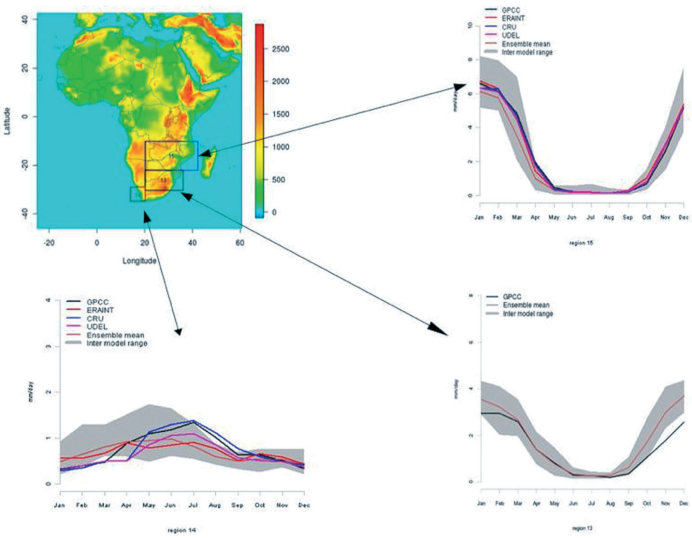

Figure 4. Seasonal cycle of three southern African regions as simulated by the regional models (grey band represents the spread of the results) compared to several observational data sets.

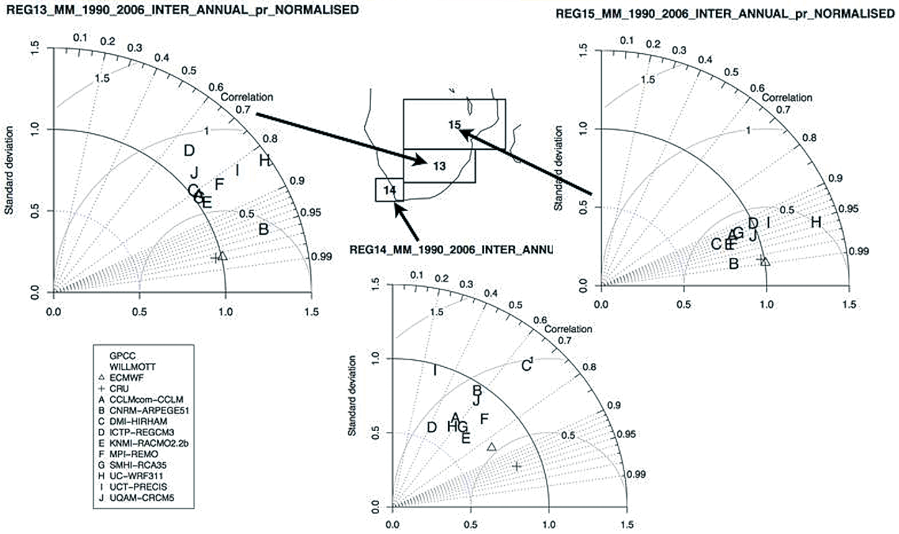

Figure 5. Taylor diagrams for each southern Africa regions showing the correlation with GPCC rainfall data as well as the standard deviation (a measure of variability) and RMSE. (From Kalognomou et al., in review.)

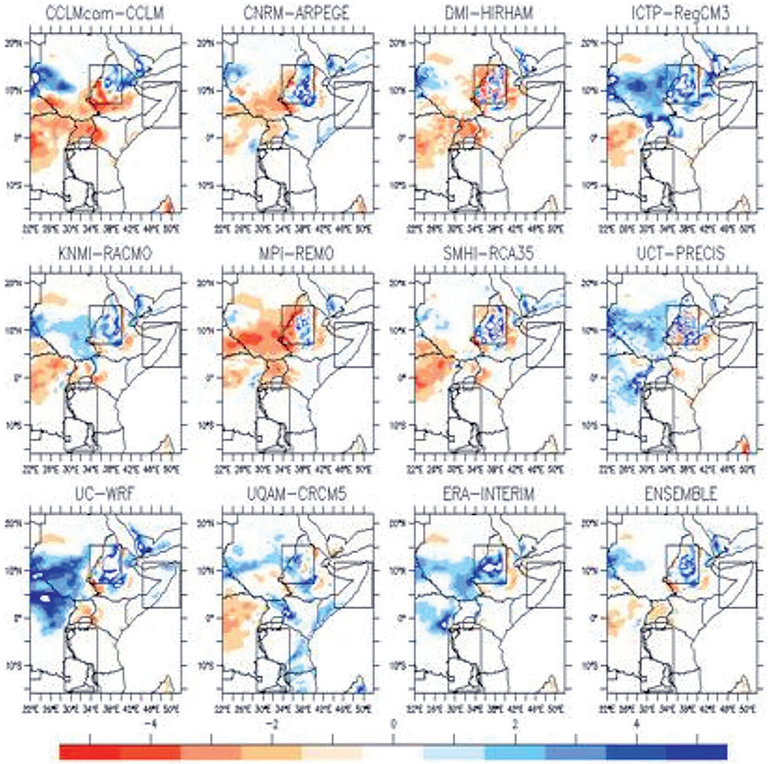

Figure 6a. Rainfall biases of each model as well as the ensemble mean during JJAS (top) and OND (bottom). From Seid et al. (in review).

4. To develop the structure and content of journal papers to be submitted in time for consideration by the IPCC 5th assessment report.

The workshop content was divided into three distinct streams. The first stream was designed for experienced scientists who could immediately begin with complex analysis of climate data. The second stream catered for the training of early career climate scientists in methods and tools of climate analysis using the CORDEX data. The third stream was designed for vulnerability-impact-adaptation (VIA) scientists who would be able to identify and articulate questions concerning VIA issues in Africa. A key aims of this workshop were to (1) produce analyses that could be written up for publication before the IPCC AR5 submission deadline of 31 July 2012 and (2) have climate scientists and VIA scientists work together to identify and understand the key African climate vulnerabilities, their causes and consequences in a changing climate.

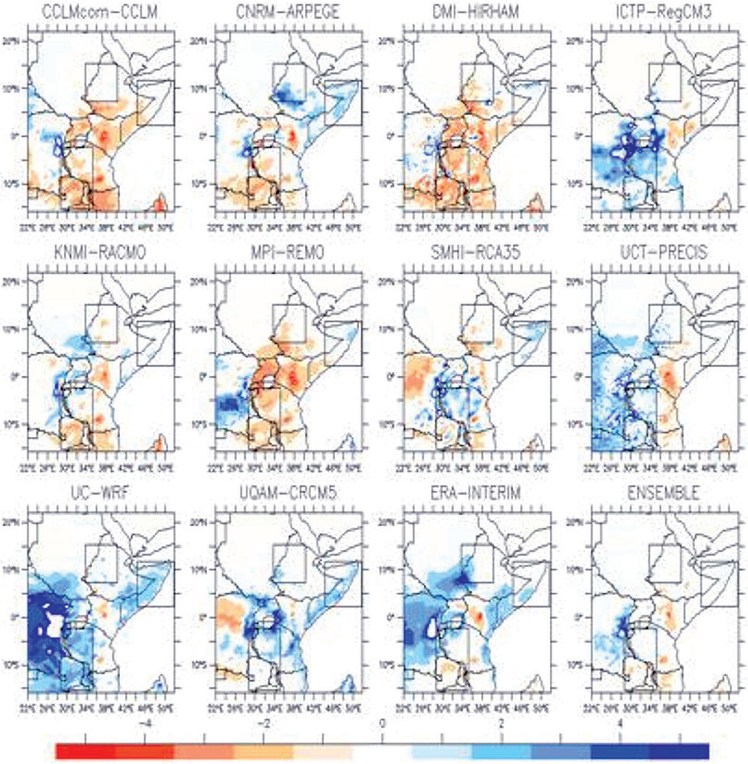

Figure 6b. Rainfall biases of each model as well as the ensemble mean during JJAS (top) and OND (bottom). From Seid et al. (in review).

In the first and second streams regional groups self-organised and worked well to produce results by the end of the workshop and assist those in the groups who were not as advanced in climate analysis. The west African group further characterised rainfall and temperature biases in the regional models, assessed the model's ability to simulate the Sahara heat low as well as the West African Monsoon. For the monsoon assessment most models were able to produce a monsoon jump, however, the intensity of rainfall in the monsoon varied between models (Fig. 7). The southern African group developed higher order statistics and fitted a parametric Generalized Extreme Value (GEV) model to the RCMs and GPCC data. Ten-year return values estimates show a realistic pattern with more intense over the north-eastern parts (Mozambique Channel) and low over the south west Benguela system (Fig. 8). The East African group assessed the ability

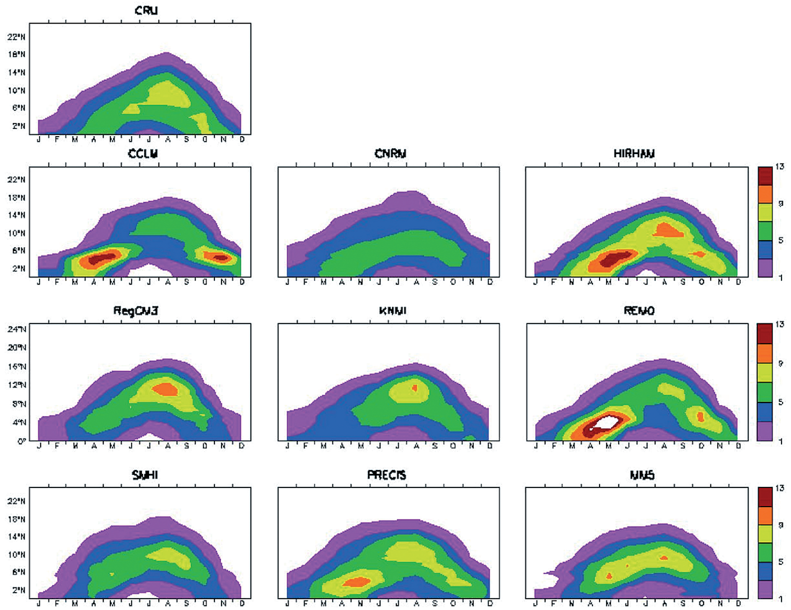

Figure 7. Simulations of the West African Monsoon using a Hovmoller plot between 10 degrees west and 10 degrees east showing the northward and southward tracking of the ITCZ. Units are in mm per day. From Gbobaniyi et al. (in review).

of the models to propagate teleconnections like ENSO and IOD into the domain as these exert strong controls on the regional rainfall. During LaNina (El Nino) JJAS is generally wetter (drier) and OND is drier (wetter). Using a composite analysis it was shown that the models were able to propagate these signals into the domain to a greater or lesser degree (Fig 9).

The third stream consisted of only 3 core VIA people instead of the 8 invited and represented sectors were agriculture, ecology and water resource management. The VIA programme was adapted for this small group and a number of sector-specific vulnerabilities were identified. In the case of agriculture questions posed by the this community concerned the onset of the rainy season, rain season length, intra-seasonal seasonal rainfall and temperature variation, frequency of threshold exceedences and incidences of pest outbreaks. Information needed in ecological management / ecosystem services sector concerned threshold exceedences, changes in temperature ranges, within season rainfall characteristics including extreme rainfall and scales of available information in time and space (e.g. monthly data at 0.44 degrees vs 6 hourly data at the basin

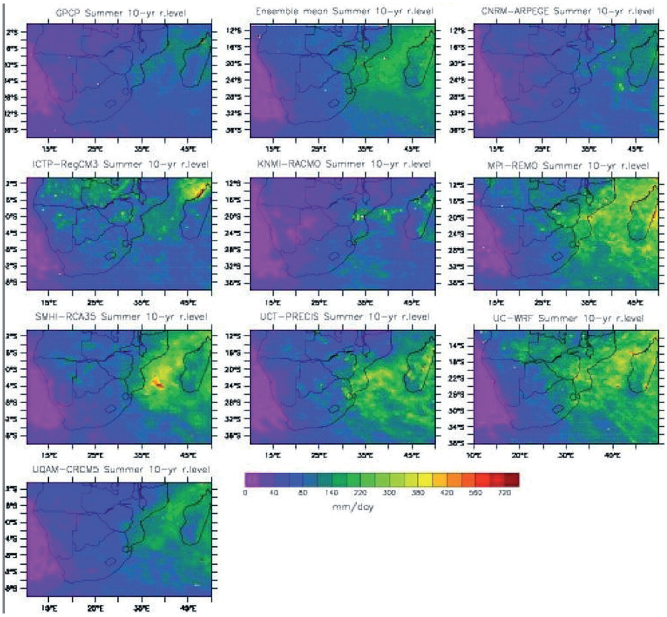

Figure 8. Spatial representation of ten year return values over the southern African domain as simulated by each model.

scale). Water resource management sector were primarily concerned with information about changes in the characteristics of extreme rainfall (frequency and intensity) and frequencies of threshold exceedences. Other questions raised by this group concerned reliability of the models and dealing with uncertainty in the downscaled results and how to interpret results of an impact model using the downscaled climate data. An entire day of the 5-day workshop was given to the joint consideration of these issues by the climate and VIA communities which resulted in modification of some of the analyses undertaken by the climate stream.

Workshop 4

This workshop was convened during February 2012 and was held in Trieste, Italy. The workshop was positioned as a «writeshop» where the goal was to have by the end of the week long process, a detailed structure of at least one journal article per regional group based on the analyses performed during the previous 3 workshops. A deadline for the submission of the papers to journals was set for the 31 July 2012 in order to be eligible for consideration in the IPCC 5th assess-

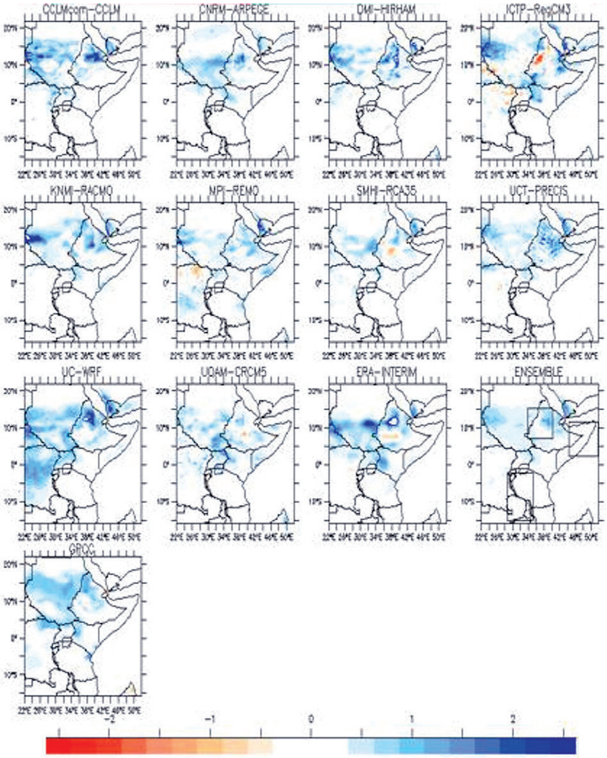

Figure 9a. Rainfall anomalies during La Niña in the East African domain in JJAS (top) and OND (bottom). From Seid et al. (in review).

ment. Both senior and junior scientists form each of the three regional groups were invited to the event to expose the more junior scientists to the experience of writing a scientific paper.

The activities of the week were conducted either with all participants together («plenary») or in their regional groupings (west, east, southern Africa). During the first plenary the objectives of the week were discussed and these were agreed to by all of the participants. The first outcome set was to produce an outline of each paper being written that included the relevant section titles, section sub-titles if possible, and either a list of figures to be used or proposed number of figures to be used. These were then presented in plenary and discussed. From this exercise it was realised that some participants had never authored an academic paper so some theory on the structure and content of a paper was needed.

The second day began in plenary with a presentation on how to write a journal article that included thoughts about the take-home message of the jour-

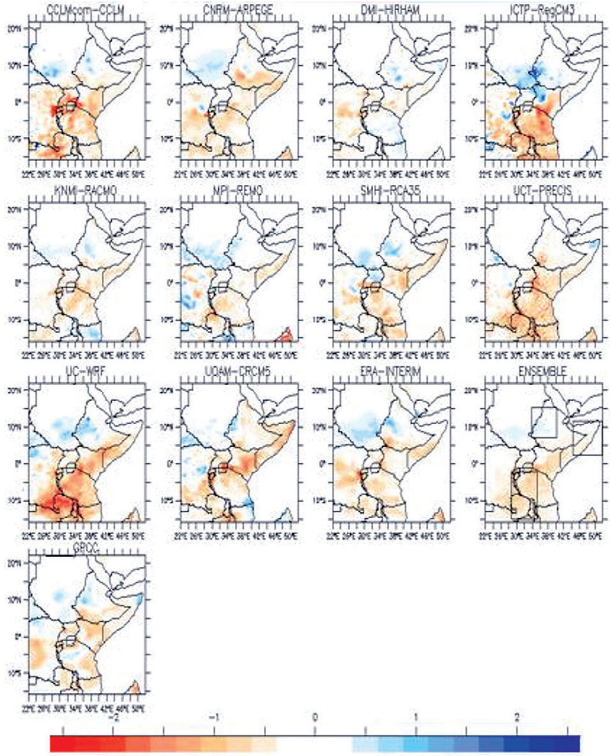

Figure 9b. Rainfall anomalies during La Niña in the East African domain in JJAS (top) and OND (bottom). From Seid et al. (in review).

nal article, the importance of the Introduction and the paper from the reviewer perspective. Thereafter each group was set the task to write the Introduction for each of the papers. Given the analyses had already been done the participants were asked to develop and Introduction in which the purpose for and goals of the paper were clearly stated. These were then submitted later in the day for internal review by organisers of the workshop and the comments were fed back to the groups in plenary at the end of the day. The reviews generally dealt with the need to focus the Introduction in terms of the objectives and outcomes of the paper. As the feedback was given in plenary the participants were also able to give input into each others papers.

Given the properly constructed Introduction and paper framework, it was decided that a day would be given to the production of figures and tables to be included in the papers. Although it was not the goal of this workshop to make any more analyses of the Cordex Africa downscaled data, the focused Introductions facilitated a succinct and rapid production of the figures required. The figures each groups produced were reviewed in a plenary session at the end of the day by all the participants and the refinements made.

On the fourth day of the workshop the participants were required to write the Conclusion section of the paper in which it was required to demonstrated that the goals set out in the Introduction had been achieved. These were then submitted for internal review and it was observed that most groups provided only a summary of the work and did not actually make any conclusions or link with the Introduction. This was addressed in a plenary session and appropriate content was inserted.

On the last day the process of taking the papers through to completion without meeting again in a workshop setting was discussed. Each team appointed a co-ordinating lead author (CLA - similar to the IPCC structure) whose responsibility included making sure individuals in the teams followed through with what they committed to do. Each team also selected a lead author whose responsibility was to write the bulk of the paper with input from the team. Teams thus consisted of a CLA, lead author and co-authors. The final activity of the week was to develop a detailed work plan to be followed in order to complete the papers before the IPCC AR5 deadline. This included and assessment of the status, as a percentage complete, of each of the sections of each of the papers. Firm dates for completion of sections were also set and agreed to by all members of the teams. Most papers were on average 70% complete and two were closer to 90% complete. Although six papers were mentioned as a best case scenario, each group committed to producing one paper before this deadline and developed the work plan accordingly.

All participants were asked to review the «writeshop», its workings and effectiveness. Overwhelmingly the responses were positive and several more senior participants requested this type of focused, paper writing activity to be repeated. It appears a focused and dedicated time for the purpose of paper writing is highly desired amongst the Cordex-Africa scientists.

ACHIEVEMENTS

Formation of the analysis teams

The formation of the three analysis teams, who continue to work together remotely, was a major achievement of the Cordex-Africa campaign. In these teams are a mix of senior and junior scientists and researchers who are now able to assess climate data for both applied and pure science purposes. Each team has a strong facilitator who ensures the smooth running of the group and communicates with other facilitators and co-ordinators of the Cordex-Africa Analysis effort. The teams engage in the analysis of Cordex Africa data both in a core scientific context to more completely understand African climate as well as for the provision of useful and relevant climate information to user communities. Furthermore team members have participated in side events at COP 17 in Durban, and they have become an important intellectual resource for agencies engaged in the assessment of climate change impacts in Africa e.g. START and CDKN.

Papers

By midnight of 31 July 2012, the submission deadline for an article to be considered in the IPCC's 54th assessment report, two papers had been submitted to the Journal of Climate and one to JGR. The lead authors were all first time lead authors on a climate related paper and the papers are currently in review. A fourth paper (from the West African team) will be submitted to JGR before the end of 2012.

Engagement with VIA community

Although it was initially difficult to engage with the VIA community, Cordex-Africa has succeeded in establishing relationships with people in key sectors such as agriculture, water management, human and animal health and urban flood risk management. During a number of separate workshops arranged by agencies such as START, members of the regional analysis groups worked alongside the users of the climate data identify key climate information needs. In facilitated settings, key sector specific climate related questions were identified and articulated and collectively answered by VIA scientists and climate experts. Such a co-exploration of the issues facing the various sectors proved a new and valuable experience for all parties involved. In addition, non-climate practitioners at these meetings were trained in the nuances of exploring climate information. These training techniques centred around key topics such as (1) an assessment of current climate-related vulnerabilities and thresholds which if crossed might alter response strategies, (2) dealing with uncertainty in the climate data, and (3) the importance of assessing multiple lines of evidence instead of just one source of data/information. Furthermore, the training and research methods received by the participants could be implemented at their home institutions together with the support of the analysis group members.

FUNDING AND INTELLECTUAL SUPPORT

Such activities cannot take place without funding from sponsors who are concerned about this type of research and capacity development within Africa. To this end the institutions contributed time and finances to the activities of Cordex-Africa are:

The World Climate Research Programme (WCRP)
The global change System for Analysis, Research and Training (START)
The Climate and Development Knowledge Network (CDKN)
The Climate System Analysis Group (CSAG)
The International Centre for Theoretical Physics (ICTP)
The Swedish Meteorological-Hydrological Institute (SHMI)
The UNDP African Adaptation Programme (UNDP-AAP)

FUTURE PLANS

CORDEX has come to be viewed by many in the decision making community as the leading source of new climate change information for Africa, and expectations are high. As downscaled CMIP5 projection data continue become available during 2013 through Cordex it is incumbent on the Cordex-Africa teams to continue to develop analysis techniques to assess multi-model downscaled data as well as engage with a user community that requires climate information for medium and long term planning. To this end three further workshops are planned for 2013 and 2014. The first two workshops will be analysis workshop where downscaled CMIP 5 data will be analysed by the climate teams in each region. This will be followed by a second writeshop during which the findings of the analyses will be written up for journal publication. Thereafter it is envisioned that these climate teams will engage with the VIA and user communities in their respective regions to investigate sector-specific regional impacts climate change and possible adaptation or mitigation strategies.

The running of these important workshops, however, is in no way guaranteed. Current funding has come to an end and we are actively seeking means to bring the climate groups together in a co-ordinated effort to undertake these essential investigations. We are optimistic that once funding is made available to the Cordex-Africa analysis initiative we will contribute greatly to the understanding of the climate and the effects of climate change on the peoples of the Africa.

REFERENCES

Endris, H., P. Omondi, S. Jain, L. Chang'a, J. Awange, P. Ketiem, L. Tazalika, C. Lennard, B. Hewitson, A. Dosio, G. Nikulin, H. Panitz, M. Büchner, In review. Assessment of the performance of CORDEX regional climate models in simulating eastern Africa rainfall.

Gbobaniyi, E., A. Sarr, M. Sylla, I. Diallo, A. Dhiédiou, A Kamga, A. Abdou , N. Klutse, B. Lamptey, C. Lennard, B. Hewitson, C. Jones, G. Nikulin, A. Dosio, In Review. Climatology, annual cycle and interannual variability of precipitation and temperature in CORDEX regional climate models simulation over West Africa.

Kalognomou, E., C. Lennard, M. Shongwe, I. Pinto, M. Kent, B. Hewitson, A. Dosio, G. Nikulin, H. Panitz, M. Büchner, In review. A diagnostic evaluation of precipitation in CORDEX models over southern Africa.

Klutse, N., M. Sylla, A. Sarr, A. Dhiédiou, A. Kamga, A. Abdou , B. Lamptey, E. Gbobaniyi, K. Owusu, C. Lennard, B. Hewitson, C. Jones, G. Nikulin, A. Dosio, In Review. Daily characteristics of West African monsoon rainfall in CORDEX regional climate models.

DYNAMICAL DOWNSCALING OF REGIONAL CLIMATE FOR THE HAWAIIAN ISLANDS: AN OVERVIEW

Y. Wang, C. Zhang, and A. Lauer

CLIMATE CHANGE PERSPECTIVES FROM THE ATLANTIC:
PAST, PRESENT AND FUTURE
Jose María Fernández-Palacios, Lea de Nascimento, José Carlos Hernández,
Sabrina Clemente, Albano González & Juan P. Díaz-González (eds.)
Servicio de Publicaciones, Universidad de La Laguna – 2013

ISBN: 978-84-15910-54-1 pp. 563-597

ABSTRACT

This chapter provides an overview of current efforts in dynamical downscaling of regional climate for the Hawaiian Islands in the International Pacific Research Center (IPRC) at University of Hawaii at Manoa (UHM), USA. The configuration of the Weather Research and Forecasting (WRF) model V3.3 as a dynamical downscaling tool for the Hawaiian region is introduced. The results of a one-year continuous simulation forced by observed boundary conditions with 3-km horizontal grid spacing in the inner nested domain are presented. Future directions for the detailed evaluation of the model performance and application to the assessment of global climate change on Hawaiian regional climate are also briefly discussed.

KEYWORDS Dynamical downscaling, regional climate, the Hawaiian Islands, trade wind inversion, pseudo-global-warming (PGW) method.

INTRODUCTION

The Hawaiian Islands, situated in the middle of the Pacific Ocean, are the most isolated landmass in the world, which range from Kanemilohai in the northwest to the Island of Hawaii in the southeast, a span of 1,591 miles. There are eight main islands from Niihau to Hawaii (Fig. 1). The Island of Hawaii, at 8,150 km^2 and often referred to as the Big Island, comprises nearly 2/3 of the total land area of the State of Hawaii. The Island of Kahoolawe, the smallest of the eight, is 125 km^2 and is not inhabited. In addition to being home to 1.3 million residents, islands are home to unique ecosystems and some endemic species that provide economic opportunities, nourishment, and cultural value to island communities.

The state of Hawaii still relies heavily on groundwater replenished by trade wind-introduced rainfall for the bulk of its fresh water. Perhaps nothing is as critical to life in the islands as rain. Among the eight main islands, only five of them (Kauai, Oahu, Molokai, Maui, and Hawaii) are high enough to receive orographic rainfall by lifting moist air in the prevailing northeast trade winds and generate perennial streams on the windward side of the islands. These streams present the freshwater ecosystem and are home to native stream animals. Changes in rainfall

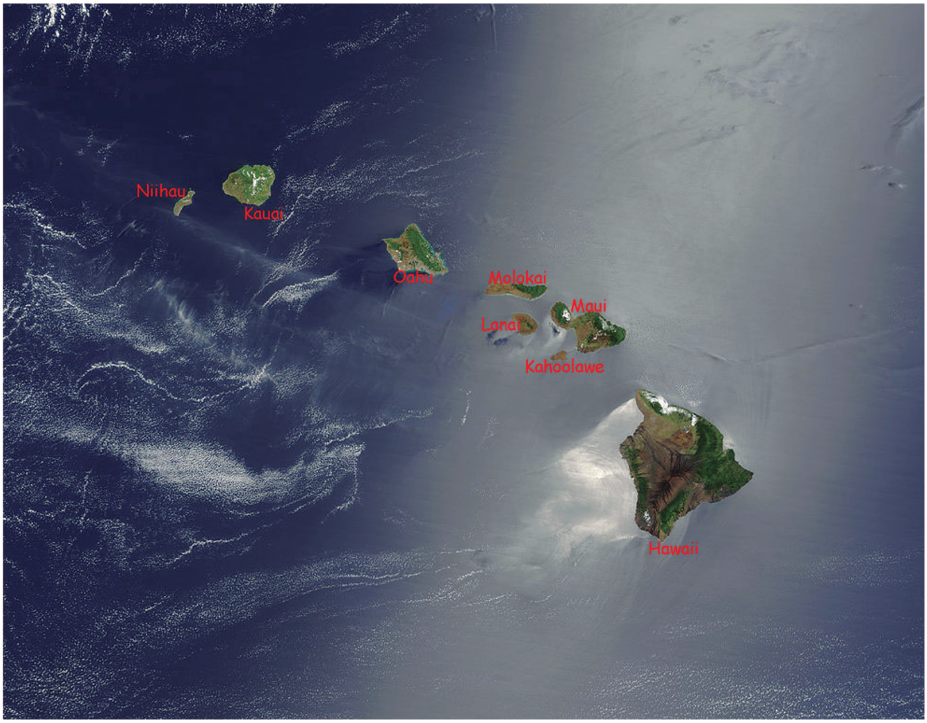

Figure 1. Satellite image of the main Hawaiian Islands (http://www.mauihawaii.org/maui-pictures/hawaii-satellite-space.htm), showing the geographic locations, fine landscape, and names of main Hawaiian Islands.

has major implications for not only Hawaii's 1.3 million people, but also its native ecosystems, including about one quarter of all federally listed threatened and endangered species in the US. The distribution of the freshwater ecosystems is closely related to rainfall and drought patterns. Shifting rainfall patterns and higher temperatures have direct and indirect consequences for plants and animals. Changes in sea level, temperature, and the acidity of coastal waters could threaten the stability and functioning of these ecosystems.

The effects of global warming are evident in Hawaii: air temperature is rising, rainfall and stream flow have decreased, rain intensity has increased, sea level and sea surface temperatures have increased, and the ocean is acidifying. Hawaii's recorded precipitation has experienced a 5-20% decrease between 1901 and 2005 with a more dramatic decline (27%) in winter months since 1970, while a slightly increase in summer months. If these trends continue, growing impacts to

Hawaii's water resources and forests, coastal communities and environments, and marine ecology would be anticipated. Therefore it is desired to assess potential future changes of the regional climate in the Hawaiian region. Such an assessment could be used by various communities to estimate the potential impacts of climate change on the regional agriculture and ecosystems and by decision-makers to plan the need for future infrastructure. The assessment of potential climate change has been heavily based on climate simulations and projections with various climate change scenarios using the global climate models.

Because of their small dimensions and their steep topography, the Hawaiian Islands are not well resolved in current state-of-the-art global coupled models (GCMs) used for long-term climate simulations/projections. It is thus necessary to downscale the global model results to regional climate at local and island scales. There are two downscaling approaches currently in use: statistical downscaling and dynamical downscaling. The statistical downscaling approach often uses regression to treat regional scale variable (often at stations) as predictand (such as station precipitation or air temperature) and large-scale circulation patterns or indices as predictors. The dynamical downscaling approach is to run a nested high-resolution model with both the initial and lateral boundary conditions as large-scale forcing obtained from observations or global model simulations/projections. The regional model can represent finer scale surface forcing and finer scale response to given large scale forcing. Previous studies on downscaling climate change in the Hawaiian region have been based on the statistical downscaling approach (Chu et al. 2010; Elison Timm et al. 2011, 2013). Their results show that some islands are projected to experience decreases in precipitation, while others may increases.

When applying the statistical downscaling method to assess climate projections, the predictor-predictand relationship is assumed stationary and can be used to generate point data, such as station temperature, precipitation measurements. It is also assumed that the predictors are physically meaningful and reflect processes responsible for climate variability, and that GCMs can accurately reproduce their statistics. Dynamical downscaling approach using high-resolution regional climate models (RCMs) has been widely used for regional climate studies since its first demonstrations by Dickinson *et al.* (1989) and Giorgi and Bates (1989). The principle behind the approach is that given detailed representations of physical processes and high spatial resolution that resolve regional forcing (such as complex topography, land-sea contrast, and land use), a RCM can generate realistic regional climate information consistent with the driving large-scale circulation supplied by either global reanalysis data, or a general circulation model (GCM). So far, the majority of efforts using the dynamical downscaling approach have been limited to continental areas with model resolutions ranging between 20 and 50 km. Although this resolution is marginally acceptable for the large-scale and synoptic systems in the Hawaiian region, it is far from that required to resolve the fine-scale geographical variations and the local and small scale features that control the microclimates in the Hawaiian Islands.

Some previous studies have used 1.5 km to 3 km horizontal grid spacings but mainly for short-term (several days to several months) simulations/forecasts (Zhang *et al.* 2005a and b; Chen and Feng 2001; Feng and Chen 2001; Nguyen *et al.* 2010) for the Hawaiian Islands. The short-term integrations by Zhang *et al.* (2005b) showed that the 1.5 km resolution Mesoscale Spectral Model (MSM) provided a better simulation of surface variables than the 10 km resolution. They also demonstrated that further improvements were achieved by coupling the atmospheric model with a land surface model (LSM). The Advanced Research Weather Research and Forecasting (WRF–ARW) model has been widely used in dynamical downscaling in recent years (Leung *et al.* 2006; Bukovsky and Karoly 2009; Zhang *et al.* 2009; Jiménez *et al.* 2010). With the increasing capacity of computing facilities, some long-term high-resolution simulations have been attempted recently. For example, Jiménez *et al.* (2010) performed a 14-year simulation over complex topography in Spain with 2 km horizontal grid spacing and showed that the WRF model with high-resolution can be used for dynamical downscaling in a region with complex terrain.

In the last few years, researchers at the International Pacific Research Center (IPRC) at the University of Hawaii have been engaged in development and application of a regional atmospheric model appropriate for fine resolution dynamical downscaling and regional climate simulations for the Hawaiian Islands. A nested version of the Advanced Weather Research and Forecasting (WRF–ARW) model release 3.3 (V3.3) with high resolution has been configured to cover the Hawaiian region with improved land surface specifications (albedo, land use/cover type, soil type, green vegetation fraction) for the Hawaiian Islands, as well as the improved model physics to better simulate the climate in the Hawaiian region (Zhang et al. 2012a, b). The behavior of the model system when it was run in doubly-nested mode with an inner nest grid spacing of 3 km for a 13-month continuous simulation from October 2005 to November 2006 forced by observed SSTs and lateral boundary conditions from reanalysis data was recently documented in Zhang *et al.* (2012b). Note that the first month is considered as spin-up period and thus discarded in the analysis. Current efforts are being devoted to conduct 20 year simulations for the present and projected future climates under several global warming scenarios.

In this chapter, the climate settings in the Hawaiian region will be briefly discussed as a basis of our regional climate downscaling efforts. Model configuration and results from a one-year continuous simulation detailed in Zhang et al. (2012b) will be highlighted to demonstrate the potential applications of the newly configured model for the Hawaiian region. Strategies using the dynamical downscaling approach for the assessment of global warming impact on the regional climate over the Hawaiian Islands will be then described. The chapter will end with a brief discussion on future directions.

WEATHER AND CLIMATE SETTINGS IN THE HAWAIIAN REGION

CLIMATOLOGICAL SETTINGS

Located in the central North Pacific between 18.9°N and 22.2°N, the Hawaiian Islands are affected year round by prevalent trade winds. The climate in the Hawaiian Islands is characterized by two seasons: «summer,» between May and October, and «winter», between October and April. Despite being located in a region of large-scale mean subsidence in the subtropics, rainfall over the Hawaiian Islands is frequent and abundant mainly because of the strong interaction between the orography and prevailing trade winds (Schroeder 1993). On average about 82% of all days in the Hawaii region are trade wind inversion (TWI) days as defined by Cao *et al.* (2007). The trade wind inversion height (Chen and Feng 1995, 2001) and trade wind strength (Esteban and Chen 2008; Carlis *et al.* 2010) have a close relation to precipitation over the Hawaiian Islands. The trade wind–induced rainfall along the windward sides of mountains accounts for most of the statewide rainfall (Lyons 1982), as can be seen from the climatological mean rainfall in Fig. 2, which is developed based on rainfall measurements taken at over 1,000 stations as the principal source of information (Giambelluca et al. 211).

In winter the climatological North Pacific subtropical high retreats southward to the latitude range 25-30ºN, only several degrees to the north of the Hawaiian Islands (Fig. 3a). The midlatitude westerlies extends southward with a large-scale trough located north of the Hawaiian Islands (Fig. 3a). Although the Hawaiian region are still controlled by the easterly trade winds, the trade winds may be interrupted for days or weeks by frontal systems or migratory cyclones from the midlatitudes and by Kona storms (Kona storms are extratropical cyclones usually formed in winter resulting in westerly winds, «Kona» in Hawaiian, see the next subsection). Therefore, winter in Hawaii is the season of more frequent heavy rainstorms (Schroeder *et al.* 1977).

In summer the subtropical high is generally strengthened and shifts northward with its ridge to the north of 35ºN. The Hawaiian Islands are located in the deep easterlies south of subtropical high (Fig. 3b). The intertropical convergence zone (ITCZ) in summer is several degrees north of its winter latitudes. As a result, tropical disturbances originating in the ITCZ can influence the Hawaiian Islands and very occasionally cause severe precipitation events (Chu and Clark 1999). Sometimes, the local sea breeze can also bring heavy showers to the Hawaiian Islands, especially over the Big Island (Schroeder 1981; Chen and Nash 1994).

Furthermore, the variety of valleys and ridges, broad and steep slopes, and land-sea contrasts, gives the Hawaiian Islands a diversity of climates which are quite different from climate over the surrounding oceans. Hawaii possesses 11 of the 13 climatic zones, each with a unique ecosystem and weather feature, depending on altitude, barometric pressure, rainfall, temperature, wind and topography. The microclimates in the Hawaiian Islands range from tropical hu-

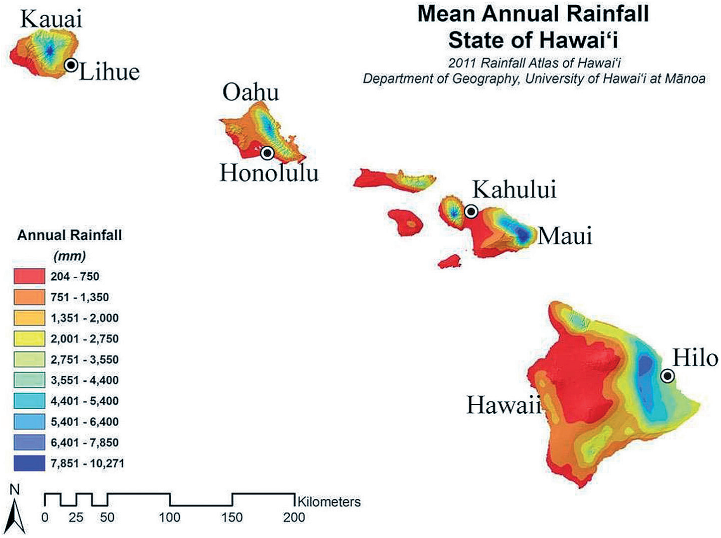

Figure 2. Climatology of annual mean rainfall over the Hawaiian Islands (Giambelluca *et al.* 2011). Rainfall measurements taken at over 1,000 stations were used as the principal source of information in the development of the rainfall maps.

mid forest climate on windward (northeast) flanks to arid and semi-arid climate on leeward (southwest) areas, often with remarkable differences within short distances (Giambeluca and Schroeder 1986).

In addition to the trends mentioned in the introduction, the climate in the Hawaiian Islands also experiences strong variability on various time scales. For example, Hawaii rainfall shows both interannual and interdecadal variations (Lyons 1982; Taylor 1984; Chu 1995; Mantua et al. 1997; Chu and Clark 1999; Chu and Chen 2005). On the interannual time scale, Hawaii tends to be dryer than average during most El Niño winters. This occurs because during El Niño winter, the upper-tropospheric jet stream extends eastward and Hawaii is located in the right exit region of the jet stream, namely in an area of upper-level convergence and anomalous sinking motion. Such a situation inhibits both the development and maintenance of subtropical cyclones over Hawaii and the southeastward propagation of strong frontal systems into the island chain (Chu 1995). On the interdecadal time scale, Hawaii winter rainfall is negatively correlated with the Pacific decadal oscillation (PDO) index (Mantua et al. 1997).

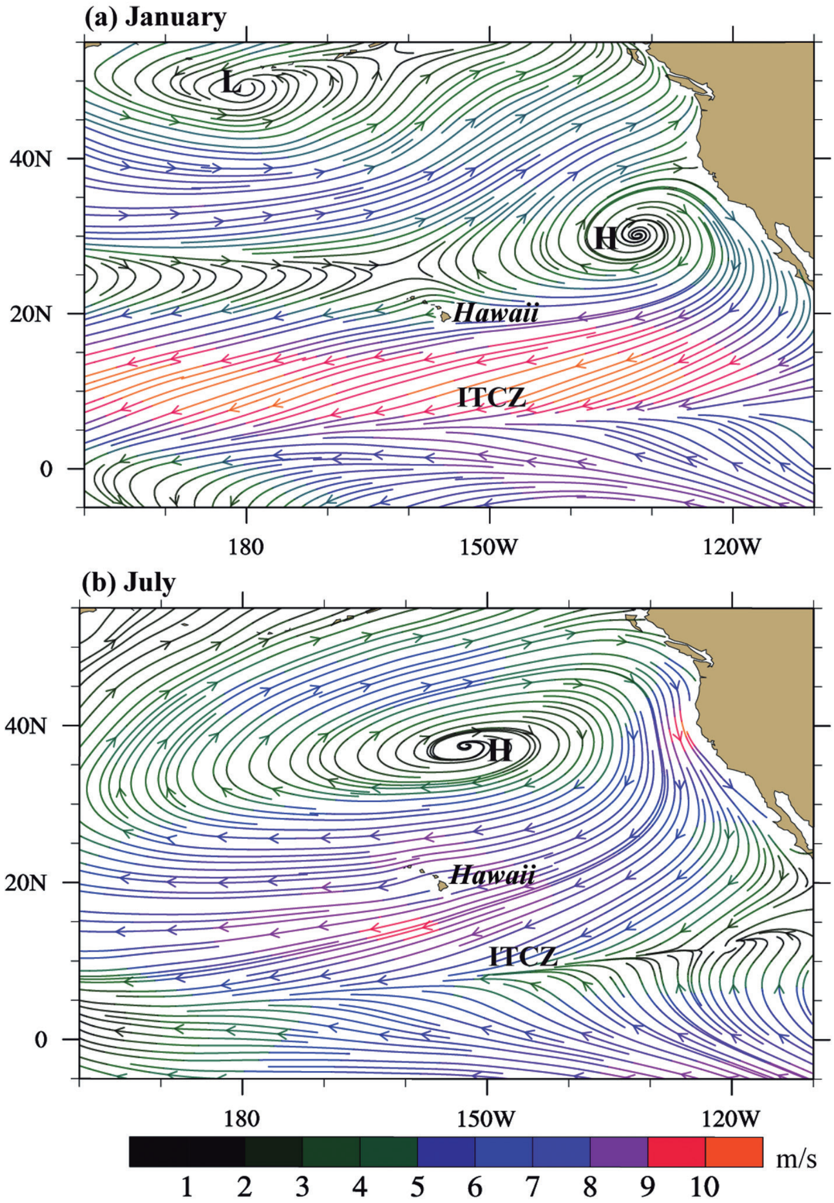

Figure 3. The 20–year (1990-2009) surface wind climatology from MERRA analysis data over the Northeast Pacific for January (a) and July (b), respectively. The streamlines are colored by wind speed. Labels L and H indicate the centers of cyclonic and anticyclonic circulations, respectively and ITCZ indicates the intertropical convergence zone in the Pacific.

Weather systems

Kodama and Businger (1998) provided an overview of weather systems and forecasting challenges in the Pacific region. As they schematically showed there are four major synoptic systems that may cause significant wind and rainfall in the Hawaiian region (Fig. 4). These weather systems are usually only observed in specific seasons of the year and they are not only challenges to short-weather forecasts but also challenges to long-term regional climate modeling.

In the Hawaiian Islands, on average there are nine cold fronts per year passing through the entire island chain (Worthley 1967). Heavy rains and flash flooding are often associated with such cold fronts (Fig. 4a). The duration of the rains depends, in part, on the propagation speed of the front. Because of traveling over the ocean, the cold fronts affecting the Hawaiian region are generally not very strong and are characterized by a wind discontinuity with cyclonic shear (known as shear line) on the poleward side of the cold front. Both cold fronts and shear lines can bring hazardous wind and rain events to the Hawaiian Islands.

Strong cyclones can develop in the Hawaiian region particularly during the cool season. This type of weather system is the subtropical cyclone and also known as «Kona storm» (Simpson 1952; Fig. 4b). The Hawaiian word «Kona» means leeward, in reference to the western slopes of the islands in the prevailing trade winds. These systems often originate from either occluded cyclones that become trapped in the low latitudes by blocking from a warm high-pressure cell or strengthening of an upper-tropospheric disturbance that gradually penetrates downward and causes a synoptic low-pressure system to develop at the surface. Once formed, these systems are usually very persistent, can last up to two weeks and often produce heavy rain, strong winds, and high surf.

Another synoptic-scale system is the upper-tropospheric cold core low (Fig. 4c). These cold core lows occur mainly in the warm season and have their largest cold temperature anomalies at 300 hPa and strongest circulation at around 200 hPa (Kelley and Mock 1982). Their formation is often related to the tropical upper-tropospheric trough (TUTT) (Sadler 1976). Downward penetration of the cold core low can induce a cyclonic circulation at the surface, resulting in enhanced convection and rain to the east and southeast of the low (Whitfield and Lyons 1992).

In summer, the Hawaiian Islands can be affected by tropical disturbances, including tropical depressions, tropical storms or hurricanes, originating in the ITCZ (Fig. 4d). A notable example is Hurricane Iniki (1992), which caused damages of about 2 billion US dollars to the State of Hawaii. In the central North Pacific, the tropical cyclone frequency is much lower than in the eastern and western North Pacific, with an annual average of 3.5 cyclones with tropical storm intensity or greater. Indeed, most of them (~70%) form and intensify in the eastern North Pacific. In most cases, cyclones that move into the central North Pacific from the eastern North Pacific are past the peak intensity and are

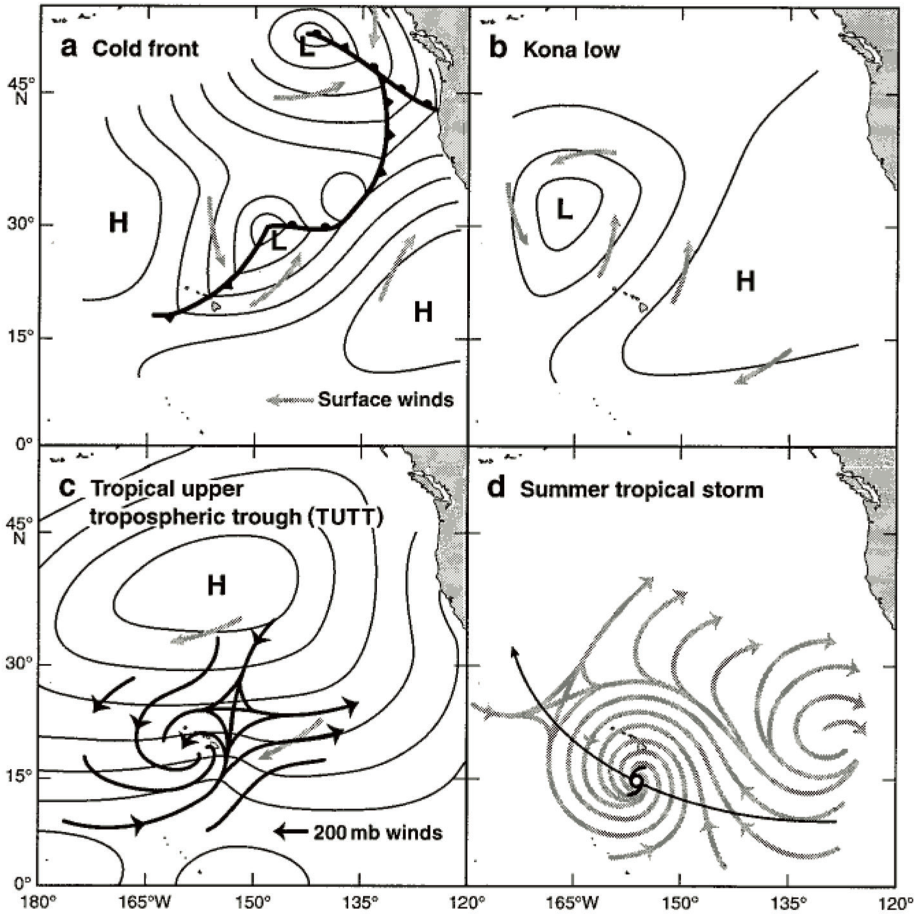

Figure 4. Conceptual diagram of four types of synoptic-scale weather systems that affect the Hawaiian Islands. Solid lines show idealized surface isobars. Shaded arrows indicate surface flow, bold arrows in (c) indicate 200-hPa flow. The solid arrow in (d) indicates the tropical cyclone track. (From Kodama and Businger 1998).

in the stage of weakening. These dissipated systems are not a high wind or storm surge threat, but they can produce significant rain. Most of the tropical cyclones that either form in or move into the central Pacific pass south of the Hawaiian Islands (Fig. 4d). There is also a tendency for more tropical cyclones to form in or move into the central North Pacific under the global warming background (Chu and Clark 1999).

THE NESTED MODEL SYSTEM FOR THE HAWAIIAN REGION

Very high model resolution is necessary to resolve the detailed surface forcing and to model the microclimates in the Hawaiian region. Given the large-scale forcing, as discussed in the previous section, such models should be able to simulate the statistics of weather systems affecting the regional climate and its change of the Hawaiian Island. In the last few years, researchers at IPRC have developed an infrastructure using a nested version of the WRF–ARW model release 3.3 (V3.3) for fine resolution dynamical downscaling of regional climate for the Hawaiian Islands. For this purpose land surface specifications (albedo, land cover type, soil type, green vegetation fraction) for the Hawaiian Islands have been improved. This version also includes improved model physics to better capture trade wind inversion and cloud systems (Zhang *et al.* 2012a). This newly configured WRF model is now referred to as Hawaiian Regional Climate Model (HRCM).

Configuration of the WRF model for the Hawaiian region

The WRF–ARW version 3.3 (Skamarock *et al.* 2008) was configured with one-way nesting for three meshes (Fig. 5) of 15 km, 3 km, and 1 km horizontal grid spacings, respectively. The model atmosphere is divided into 31 full terrain-following σ–levels in the vertical (14 levels below 700 hPa) with the model top at 10 hPa for all meshes, the same as those used in Zhang *et al.* (2012a, b). The outermost mesh (D1) has 260 grid points in the east-west direction and 320 grid points in the north-south direction, which is large enough to cover both the ITCZ and the subtropical region in the central North Pacific. The second mesh (D2) has 276 by 186 grid points covering the main Hawaiian Islands with enough area for the upstream trade winds in the nested domain. The innermost mesh has 154 by 112 grid points only covering the Island of Maui, which is designed for later sliced dynamical downscaling to 1 km resolution at island scale. There is a buffer zone with 15 grid points normal to the lateral boundary in domain D1 (D2), which provides the lateral boundary conditions for D2 (D3). Note that similar third nests of 1 km resolution are also being applied to the Islands of Oahu and Kauai (not shown), respectively.

The model physics are optimally selected for applications in the Hawaiian region. The single-moment WSM6 microphysics scheme with 6 prognostic cloud variables is used for grid-scale cloud microphysics processes (Hong and Lim 2006). In order to better reproduce observed trade wind clouds, the autoconversion and accretion rates in the original WSM6 cloud scheme (Tripoli and Cotton 1980; Hong and Lim 2006) are replaced with the parameterizations from Khairoutdinov and Kogan (2000). The latter is found to perform better for the region particularly in very high-resolution simulations such as in the nested domains D2 and

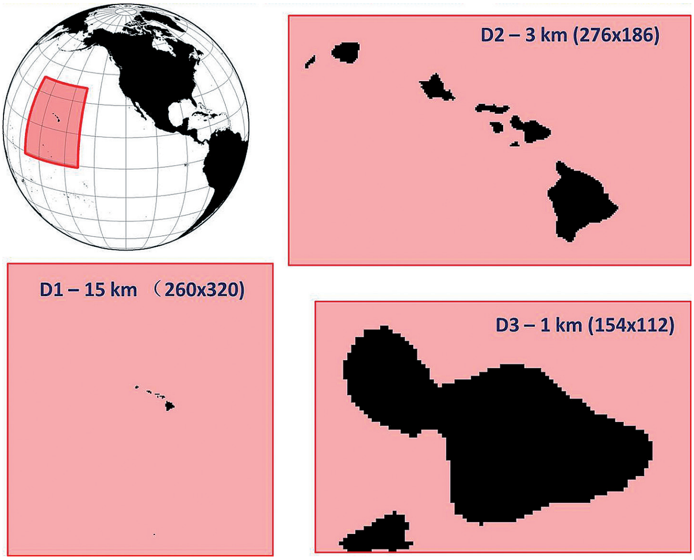

Figure 5. Triply-nested model mesh configuration for the Hawaiian region.

D3. In addition, the cloud droplet number concentration is reduced from 300 cm^{-3} in the original code to 55 cm^{-3}, which is more representative for the clean maritime conditions, typical of the Hawaii region. The shortwave and longwave radiation fluxes are calculated by the Community Atmospheric Model Version 3 radiation scheme (CAM3, Collins *et al.* 2004). Cloud fraction is diagnosed by grid-scale cloud ice and cloud water mixing ratios and relative humidity (Xu and Randall 1996). The Mellor-Yamada-Janjićplanetary boundary layer scheme (Janjić 1990, 1996, 2002, hereafter MYJ) is used for the subgrid scale vertical mixing and the Noah land surface model (LSM) is used for the land surface processes (Chen and Dudhia 2001). The modified Tiedtke scheme (Wang *et al.* 2003, 2004) is used for the cumulus parameterization in the outermost domain, which has been shown to be able to skilfully simulate trade wind inversion and associated low-level clouds (Zhang *et al.* 2012a). No cumulus parameterization is applied in the nested domains. Since the trade wind inversion height and trade wind strength have a close relation to precipitation over the Hawaiian Islands, realistic simulation of trade winds and TWI is critical for dynamical downscaling of the Hawaiian regional climate.

In addition, the Hawaiian Islands have a complex landscape with various surface properties (Fig. 1). The Noah LSM requires the land surface properties, including land cover/use, surface albedo, vegetation types/fraction, and soil types, as input parameters (Chen and Dudhia 2001). However, the Hawaiian region is

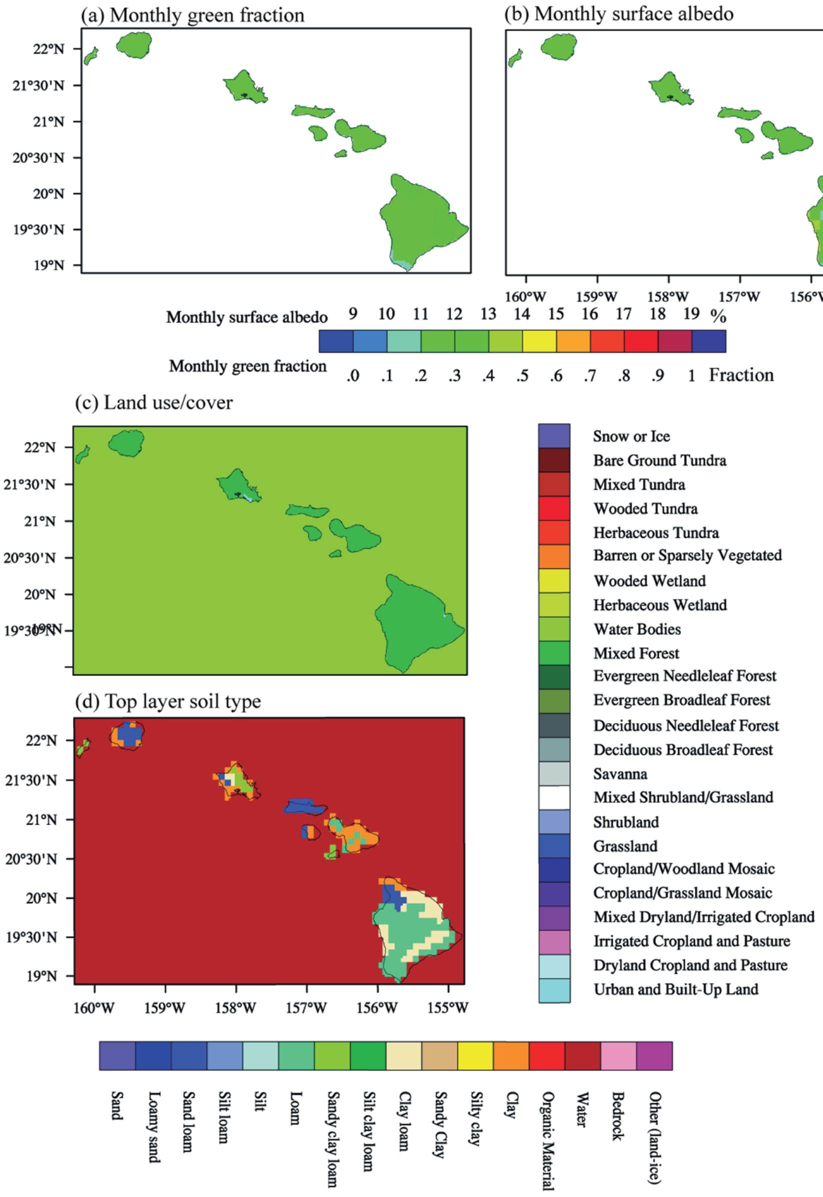

Figure 6: The land surface categories from WRF preprocessing system (WPS) geographical input data set, including monthly vegetation fraction in January (a), monthly surface albedo in January (b), land surface use/cover with 24 USGS categories with vertical color bar (c), and top layer soil type with 16 categories with horizontal color bar (d).

not well represented in the land surface datasets of the official WRF model release. The poor representation of the land surface properties is mainly caused by the low resolution datasets or poorly retrieved datasets (land cover/use) for the Hawaiian Islands (Fig. 6). Since land surface properties affect regional climate in various ways, the first priority thus was to improve the land surface data for the region, which was done based on the USGS (United States Geological Survey) data and other sources, as documented in Zhang et al. (2012b). Figure 7 shows the model land surface data newly constructed for the HRCM. Details for the construction of the new land surface dataset can be found in Zhang *et al.* (2012b).

A ONE-YEAR CONTINUOUS SIMULATION

The HRCM described above was run in doubly-nested mode with an inner nest grid spacing of 3 km for a 12-month continuous simulation from October 2005 to November 2006 forced by observed SSTs and lateral boundary conditions from reanalysis data. The results were discussed in details in Zhang *et al.* (2012b). Here the key procedures and the major results are highlighted.

Experimental design

The model initial and lateral boundary conditions for the model atmosphere were obtained from the MERRA (Modern-Era Retrospective Analysis for Research and Applications) reanalysis from National Aeronautical and Space Administration (NASA), which covers the satellite era from 1979 to the present and has achieved significant improvements in precipitation and water vapor climatology (Rienecker et al. 2011). The MERRA data have a horizontal resolution of 0.5°×0.6667° latitude by longitude and are available at 32 pressure levels from 1000 hPa to 10 hPa at 6-h intervals. The sea surface temperature (SST) is given and updated daily using the 0.25°×0.25° global analysis provided by National Oceanic and Atmospheric Administration (NOAA, Reynolds et al. 2010). The ERA-INTERIM data from the European Centre for Medium-Range Weather Forecasts (ECMWF) provides the initial conditions for soil temperature and moisture (Dee et al. 2011). The diurnal SST variation is calculated based on the surface energy budget with the method from Zeng and Beljaars (2005).

The model was initialized at 00 UTC 1 OCT 2005 and integrated continuously till 00 UTC 1 Nov 2006. The first month is considered as the model spin-up and excluded from further analysis. While soil moisture usually requires a considerably longer spin-up period, our analysis showed that the soil moisture for the Hawaiian Islands after the 1-month spin-up does not differ too much from the one obtained at the end of the 1-year simulation. The model evaluation discussed below covers one year from 1 Nov 2005 to 31 Oct 2006. For the evaluation of the

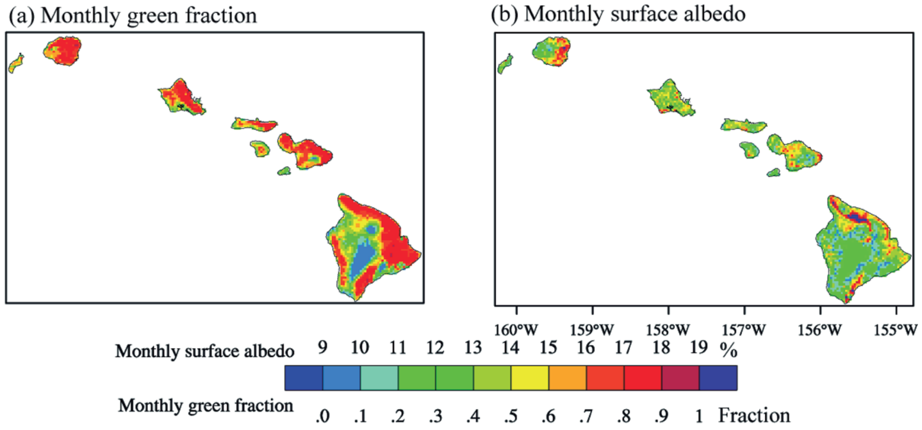
(a) Monthly green fraction

(b) Monthly surface albedo

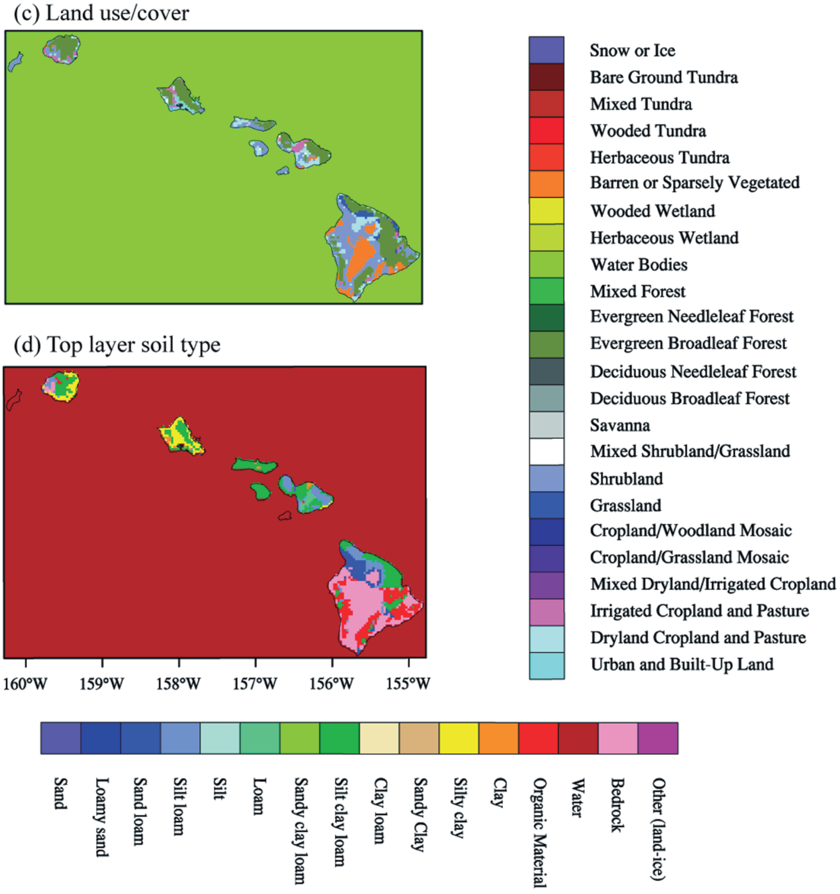
(c) Land use/cover

(d) Top layer soil type

Figure 7. Same as Figure 6, but for new land surface data.

large scale circulation, two seasons are considered, namely, the winter season from 1 Nov 2005 to 30 Apr 2006 and the summer season from 1 May 2006 to 31 Oct 2006. This year included an exceptional period of heavy rainfall over much of the main Hawaiian Islands from mid-February to the end of March (http://www.ncdc.noaa.gov/oa/climate/research/2006/mar/mar06.html). Two different inner domain runs were conducted with the original land surface data provided by the official WRF release (hereafter OLD) and the new land surface data developed for the Hawaiian Region (hereafter NEW, see section 2b) to demonstrate the improvements of the simulation with the new land surface dataset. Note that in both runs, the outer model domain is identical with the new land surface data, e.g., the boundaries for both D2 runs were forced by results from identical D1 integrations by disabling any feedbacks from D2 onto D1.

DATA FOR EVALUATION AND ANALYSIS METHODS

In addition to the MERRA reanalysis data used to drive the HRCM, more data are used for verification of the model simulation. The simulated surface winds are compared with the monthly mean surface winds from Quick Scatterometer (QuikSCAT) measurements over the ocean, which has a resolution of 25 km provided by the Remote Sensing Systems (http://www.ssmi.com/qscat/qscat_browse.html). The MODIS level-3 monthly mean cloud data, which have a resolution of 1°×1° for each month and are available at http://climserv.ipsl.polytechnique.fr/cfmip-obs/, are used for verification of simulated clouds.

There are two sounding stations in the Hawaiian Islands: Lihue (21.97°N, 159.33°W) on the Island of Kauai and Hilo (19.72°N, 155.05°W) on the Island of Hawaii. Twice-daily (0000 and 1200 UTC) sounding data since 1973 to the present were taken from the University of Wyoming's weather data website (http://weather.uwyo.edu/upperair/sounding.html). The TWI base height (TWIBH) is calculated based on the observations at 1200 UTC daily. The algorithm for identifying the inversion follows the method of Guo *et al.* (2011) with some modifications to take into account the different vertical resolutions as documented in Zhang *et al.* (2012b).

Three surface observational accumulated precipitation datasets for the Hawaiian region are used in our verification of the simulated rainfall. The first one is the NCDC cooperative monthly precipitation data (http://www.ncdc.noaa.gov/oa/ncdc.html), which includes observations from about 190 stations. The second one is the USGS daily precipitation data (http://hi.water.usgs.gov/recent/index.html). The observations at about 30 stations are averaged to get monthly means. The third one is from the Hydronet system, which began collecting 15-minute rainfall data in July 1994 (http://www.prh.noaa.gov/hnl/hydro/hydronet/hydronet-data.php). Currently the data are collected from 70 rain gauges located throughout the Hawaiian Islands. After a basic quality control, we have used data from 65 stations and converted the 15-minute rainfall data to hourly and monthly precipitation values. In our analysis, to verify the simulated seasonal mean horizontal distribution of precipitation, a gridded precipitation dataset for all Hawaiian Islands was generated using the Cressman objective analysis (Cressman 1959) on WRF native grids. The analysis radii are 0.2, 0.12, 0.06, 0.03 degrees in sequence. The first guess field is from TRMM-3B43 (Huffman et al. 1995). All NCDC, USGS and Hydronet data are ingested into the objective analysis.

The spatial correlation coefficient (SC) between a simulated (m) and an observed (o) quantity *a* is defined as

$$SC = \frac{\sum_i \sum_j (a_{i,j}^m - \overline{a_{i,j}^m})(a_{i,j}^o - \overline{a_{i,j}^o})}{\left[\sum_i \sum_j (a_{i,j}^m - \overline{a_{i,j}^m})^2 \sum_i \sum_j (a_{i,j}^o - \overline{a_{i,j}^o})^2\right]^{1/2}} \quad , (1)$$

where subscripts *i, j* are the horizontal grid point indices in the zonal and meridional directions, respectively. The overbar denotes the spatial average over the HRCM model grids. The temporal correlation coefficient (TCR) between a simulated (m) and an observed (o) quantity *a* is defined as

$$TCR = \frac{\sum(a_t^m - \overline{a^m})(a_t^o - \overline{a^o})}{\sqrt{\sum(a_t^m - \overline{a^m})^2 \cdot \sum(a_t^o - \overline{a^o})^2}}, \quad , (2)$$

where the subscript *t* is the given time, and the overbar denotes the time average. We noticed that evaluation of simulations at regional and local scales is complicated by the smaller ratio of the signal to the internal variability and the climate itself is poorly known on regional scales because of the sparse observational data in the Hawaiian region. These may be kept in mind when the model performance is evaluated in the following.

Verification of simulation

The «summer» (May-October) and «winter» (November-April) averaged large-scale circulations in D1 from the HRCM simulation are first compared with those observed. The 500 hPa geopotential height (GHT) and mean sea level pressure (MSLP) biases are shown in Figs. 8a and 8b, respectively. The biases are calculated as the difference between the HRCM simulation and MERRA reanalysis. In both winter and summer, the GHT bias in most of the domain is less than 10 m and less than 5 m around the Hawaiian Islands, with spatial pattern being similar in summer and winter. The positive bias in MSLP is centered around the Hawaiian Islands in winter, while the positive MSLP bias is centered northwest of the Hawaiian Islands in summer, with the maximum MSLP biases being less than 1 hPa in both seasons. The HRCM simulated seasonal-mean 10-m height

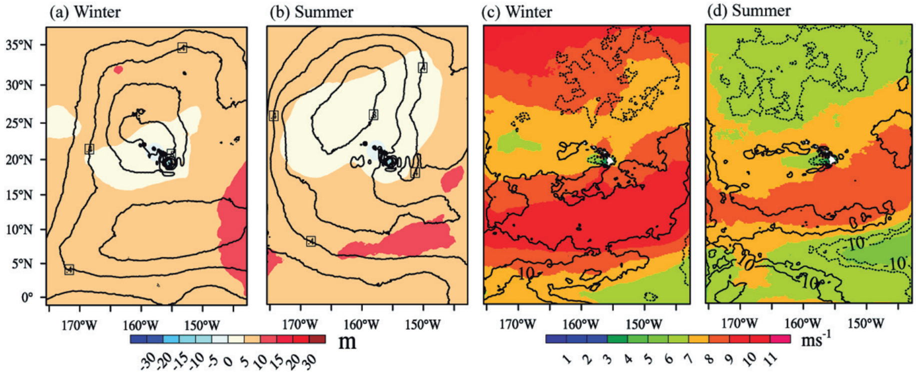

Figure 8. The biases of the simulated 500 hPa geopotential height (shaded) and mean sea level pressure (contours) in the outer model domain for winter (a) and summer (b) with contour interval of 0.2 hPa; and the simulated surface wind speed (shaded) and its bias ratio (contours, 5% intervals, negative biases are dashed) for winter (c) and summer (d) in the outer model domain. Observations are from QuikSCAT. The bias ratio is calculated as simulated surface wind speed minus observed wind speed, divided by observed wind speed. (From Zhang et al. 2012b).

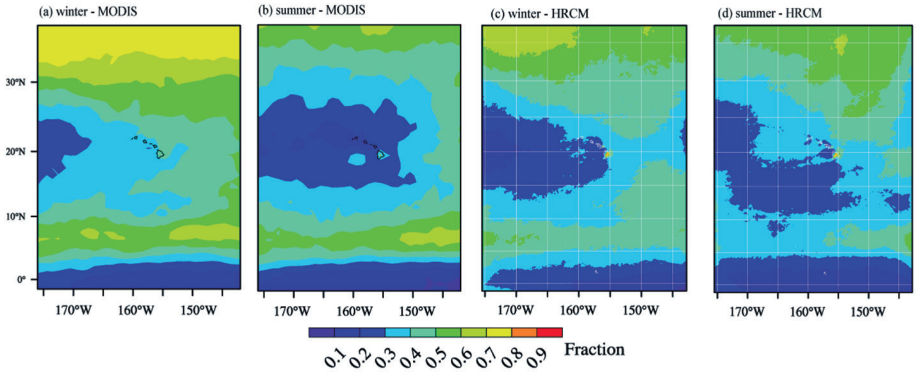

Figure 9. MODIS retrieved and model simulated total cloud fraction for winter (a, c) and summer (b, d). (From Zhang et al. 2012b)

wind speed and its bias ratio are shown in Figs. 8c and 9d, respectively. The bias ratio is defined as the bias divided by the QuikSCAT surface wind speed. The 10-m height wind speed bias ratio around the Hawaiian Islands in both winter and summer are generally less than 5% with the actual bias less than 0.5 m s^{-1}. The negative bias north of the Hawaiian Islands and the positive bias south of the Hawaiian Islands are generally larger, but still less than 15%.

Figure 9 compares the simulated and the MODIS retrieved total cloud fractions for both summer and winter. The SC between the simulated and the MODIS cloud fractions is 0.74 in winter and 0.75 in summer, indicating that the model can capture the spatial pattern of the seasonal mean total cloud fraction. In winter, the simulated total cloud fraction is about 10-20% lower in most of domain D1 in winter and close to or about 10% higher north of 15°N in summer than that observed. The model underestimates the total cloud fraction in the ITCZ in both seasons. The HRCM simulated total cloud fraction around the Hawaiian Islands is between 20% and 40%, while the MODIS retrieved total cloud fraction is generally less than 10% in summer, except for the Island of Hawaii. We note that MODIS cannot resolve the trade cumuli well in the Hawaiian region due to its coarse spatial resolution and the thresholds used in the retrieval algorithm (Pincus et al. 2011). Nevertheless, the results suggest that the HRCM has promising skills in reproducing the cloud distribution at large scale around the Hawaiian Islands.

The HRCM reproduces the observed seasonal mean precipitation reasonably well on the windward sides of the Islands of Hawaii and of Haleakala on Maui, but underestimates precipitation over Oahu in winter, which is mainly a result of the underestimation of the mean precipitation for all the islands in winter (Fig. 10). This is mainly because the model does not reproduce the heavy rain events in March 2006 well when a synoptic-scale low-pressure system lingered west of the Hawaiian Islands. Even though the model captures this storm, the location of the storm is deviated to the west by 1-2 degree longitudes (not shown). This clearly indicates the challenges of simulating heavy precipitation events due to individual storms even though the model is forced by observed lateral boundary conditions. Nevertheless, the SC between the simulated and observed seasonal mean precipitation is as high as 0.8, suggesting that the model reproduces well the spatial distribution of the observed precipitation over the Hawaiian Islands.

One of the main features of the trade wind region is the trade wind inversion (TWI), which is highly correlated with precipitation (Chen and Feng 1995). Figure 11 shows the HRCM simulated and the observed TWI at the two Hawaiian sounding stations (Hilo and Lihue). At Lihue, 283 days with the TWI were observed at 12 UTC and 262 days and 283 days were simulated in D1 and D2, respectively. The mean TWI height at Lihue simulated in D1 is 2411 m, which is about 400 m higher than that in observations. The mean TWI height at Lihue simulated in D2 is only about 175 m higher than that in observations. At Hilo, 303 TWI days were simulated in D1, which is close to the observed 291 TWI day, and the simulated mean TWI height of 2499 m in D1 is about 300 m higher than the observed. In D2, 327 TWI days were simulated at Hilo in D2, where the simulated mean TWI height is only about 8 m higher than the observed. The results thus suggest that the high resolution can improve the simulated vertical structure of the atmosphere and the TWI in the Hawaiian region.

An important benchmark for the performance of a regional climate model is its capability to reproduce the synoptic variability and probability density func-

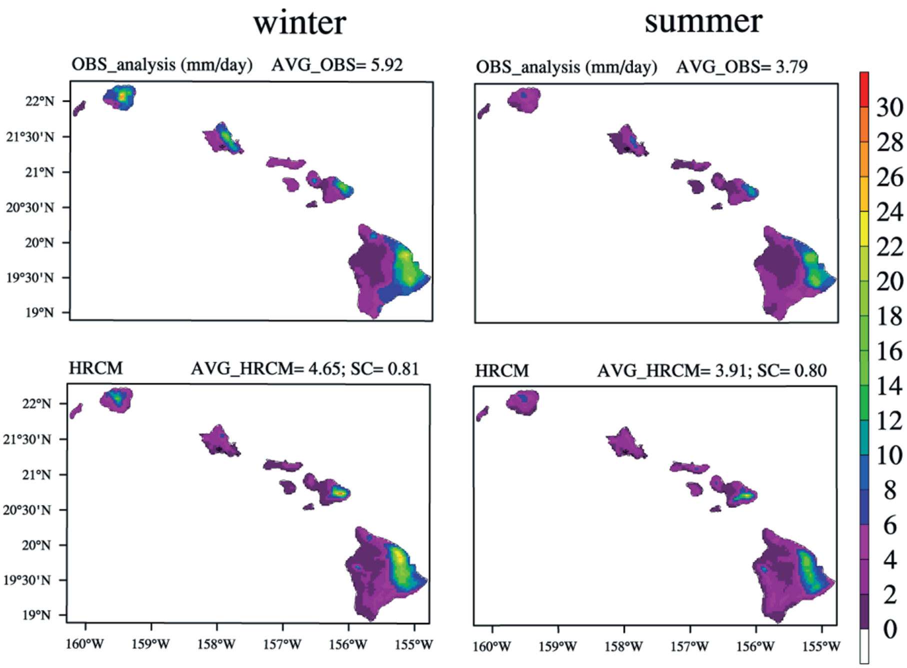

Figure 10. The observed and the HRCM inner domain simulated seasonal mean precipitation for winter (left) and summer (right). The numbers above the plots give the domain average for all islands (AVG) and spatial correlation coefficient of model results with observations (SC). (From Zhang et al. 2012b)

tion (PDF). We examined the synoptic variation of precipitation based on the pentad mean island-scale precipitation data, which was created island by island with the gridded precipitation data. Figure 12 shows the pentad mean precipitation for each island from the model and the observation. The HRCM captures most of the precipitation events reasonably well except for some events in March over the Islands of Oahu and Maui. This is caused mainly by a bias in the location of the simulated synoptic-scale storm as mentioned earlier. The temporal correlation coefficients reach 0.65, 0.50, 0.53, and 0.58 Kauai, Oahu, Maui, and Hawaii, respectively. The relatively high temporal correlation coefficients for the island-averages suggest that the model has skills in reproducing the synoptic variability of precipitation in the Hawaiian region.

The PDFs for daily precipitation intensity averaged over the 4 main Hawaiian Islands from observations and the model simulation are shown in Fig. 13. The simulated rainfall intensity PDFs over the Islands of Kauai and Oahu are similar to that observed except that the model slightly underestimates light rain

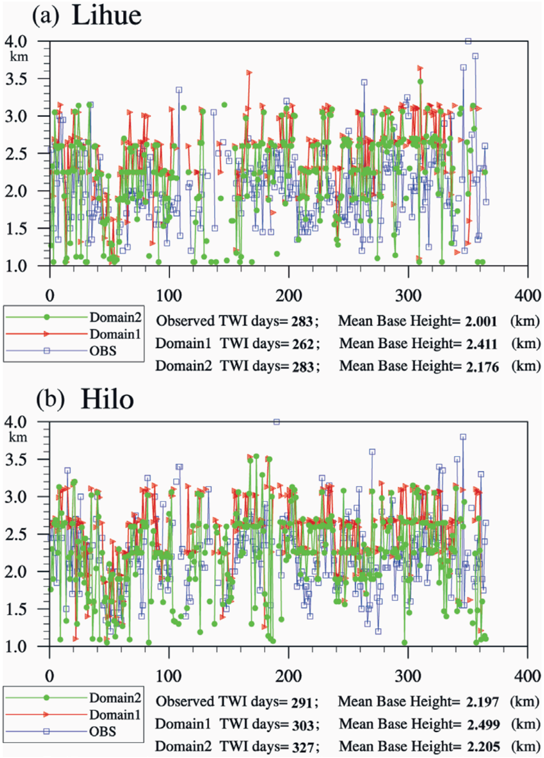

Figure 11. The observed and the HRCM simulated trade wind inversion (TWI) days and heights for Lihue, Kauai (a) and Hilo, Hawaii (b). (From Zhang et al. 2012b).

over Kauai (Fig. 13a) and overestimates light rain over Oahu (Fig. 13b) and Maui (Fig.13c). The model slightly underestimates precipitation below 3 mm/day and slightly overestimates precipitation between 3-9 mm/day for the Island of Hawaii. In general, the HRCM tends to simulate slightly more light rain (less than 3mm/day) except for the Island of Kauai.

Another important benchmark for the performance of a regional climate model is its capability to reproduce the diurnal cycle. The Hydronet rainfall data at 65 observational stations are used to study the rainfall diurnal cycle over the Hawaiian Islands for TWI days. That means that periods with mid-latitude or tropical disturbances were excluded and the analysis focuses on the trade wind regime in the Hawaiian region and. The rainfall intensity peak is defined as the hour with the maximum observed hourly rainfall averaged over all TWI days and the rainfall frequency peak is defined as the hour when rainfall occurs

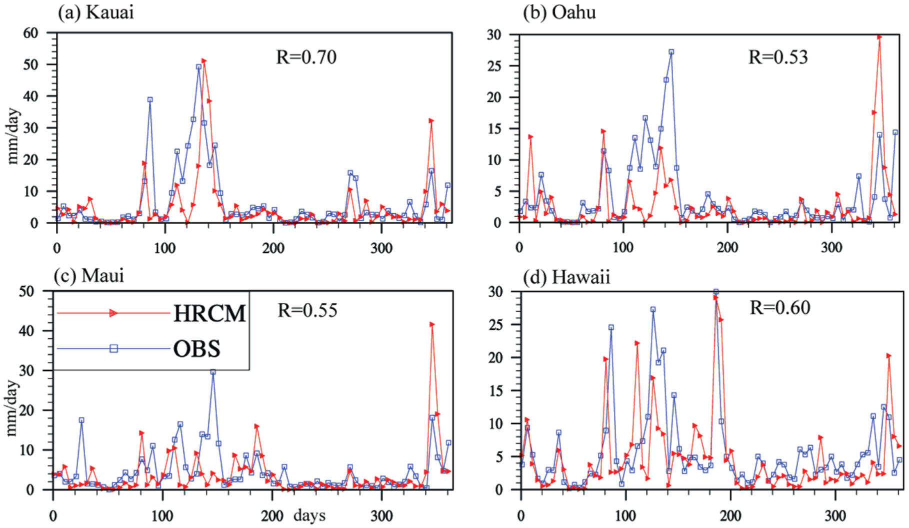

Figure 12. The time series of the 5-day mean precipitation over the island of Kauai (a), Oahu (b), Maui (c) and Hawaii (d) from observations (OBS) and simulation in D2 (HRCM). R is the temporal correlation coefficient between OBS and HRCM.

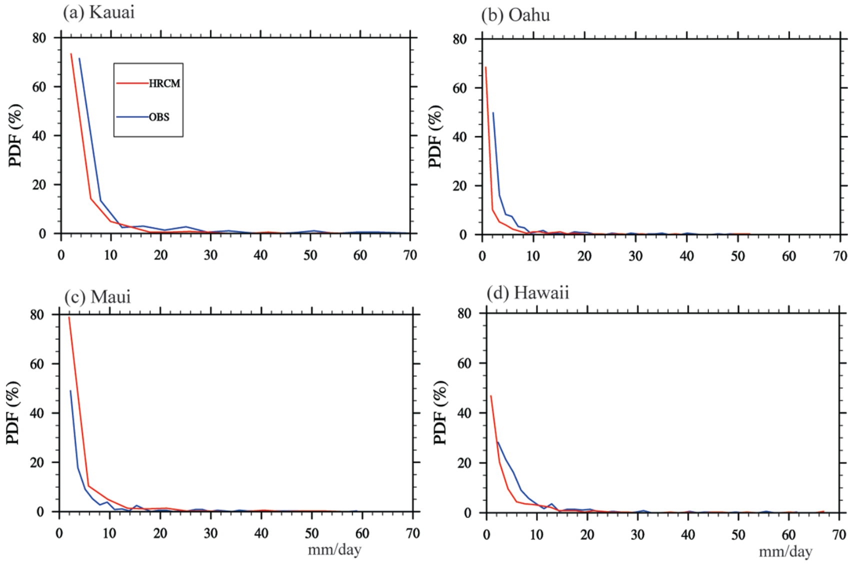

Figure 13. The daily precipitation probability density functions (PDFs) over the island of Kauai (a), Oahu (b), Maui (c) and Hawaii (d) from observations (OBS) and simulation in D2 (HRCM).

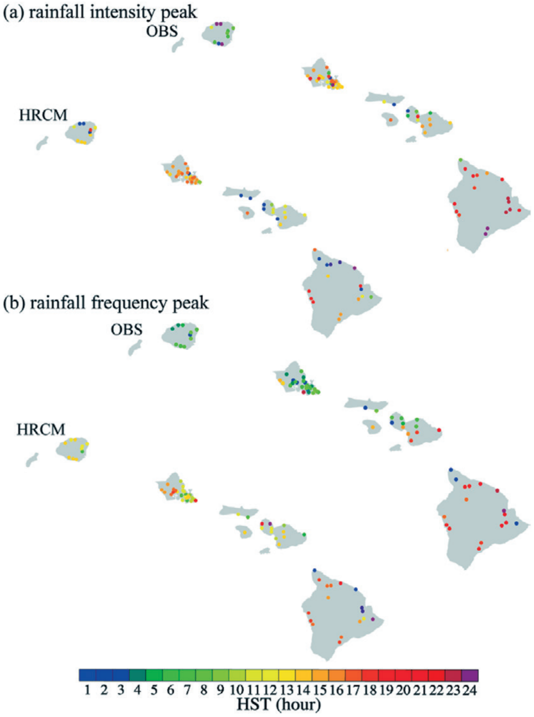

Figure 14. The rainfall intensity peak (a) and frequency peak (b) from observations (OBS) and the simulation in D2 (HRCM). HST means Hawaiian Standard Time (UTC-10).

most frequently. The rainfall intensity at each station was normalized by the daily rainfall amount before the averaged rainfall intensity was calculated island by island. As we can see from Fig. 14, each island has a unique rainfall diurnal cycle. The rainfall intensity peak from the observations shows a large diversity among different islands. Over most of the islands the rainfall intensity peak is consistent with the frequency peak or within a few hours at the most except for the island of Oahu where the intensity peak occurs in the afternoon while the frequency peak occurs in the early morning (Fig. 14).

The model didn't capture the rainfall peak very well for the Island of Kauai. Most stations on Kauai show the peak between midnight and early morning in observation, while the HRCM simulates rainfall peak in the late morning to mid-afternoon. The observations show an early morning frequency peak over Oahu, while the simulated frequency peaks in the afternoon at many stations. However, the simulated frequency peaks in the early morning at some stations in southeast Oahu, consistent with the observations. The simulated rainfall frequencies between 9 am and 4 pm over the Island of Kauai are relatively close to the observations. The model captures the afternoon rainfall intensity peak over Maui and reproduces the rainfall intensity and frequency peaks over the Island of Hawaii well (Fig. 14). Despite there are some biases, the model simulates a clear precipitation diurnal cycle and its variation among different islands.

STRATEGIES FOR DYNAMICAL DOWNSCALING OF THE PROJECTED FUTURE CLIMATE CHANGE

An overview of downscaling strategies

There are different strategies for dynamical downscaling of the projected future climate change. There are two main categories: the direct global warming (DGW) dynamical downscaling method and the pseudo global warming (PGW) dynamical downscaling method. The DGW method is a traditional approach and has been widely used to dynamically downscale regional climate change (Giorgi and Mearns, 1991; Mearns *et al.* 1999; Leung *et al.* 2003; Wang *et al.* 2004; Plummer *et al.* 2006). Dynamical downscaling with the DGW method can be done by performing the following regional climate model (RCM) simulations:

(i) A single RCM-downscaled climate change simulation using results from a selected coupled general circulation model (CGCM) for current and projected climate;
(ii) An ensemble of RCM-downscaled climate change simulations using results from various CGCMs for current and projected climate;
(iii) A single RCM-downscaled climate change simulation of the ensemble of current and projected climate simulated from various CGCMs;
(iv) An ensemble of multi-RCMs climate change simulations downscaling results from a single CGCM current and projected climate simulations;
(v) An ensemble of multi-RCM climate change simulations downscaling results from various individual CGCM current and projected climate simulations;
(vi) An ensemble of multi-RCM climate change simulations downscaling results from an ensemble of various CGCM simulations for current and projected climate.

The DGW downscaling method is straightforward. It can take into account the potential changes in seasonal/intraseasonal and interannual variabilities under the projected climate as well as the forcing of synoptic disturbances through the lateral boundaries. The major weakness of the DGW downscaling method is that CGCM biases could substantially affect the downscaled regional climate (Liang *et al.* 2008). Furthermore, the current state-of-the-art CGCMs still have low skills in reproducing the observed variabilities at various time scales and thus giving a low confidence in the projected changes in those variabilities.

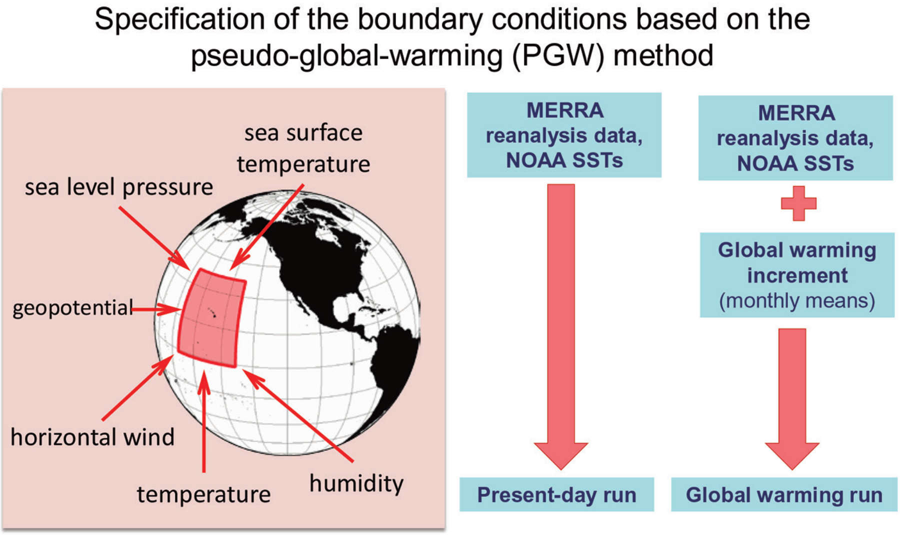

Figure 15. Schematic diagram showing the pseudo-global-warming (PGW) dynamical downscaling method.

In the PGW approach, a RCM is used to downscale a high quality global reanalysis at relatively coarse resolution for current climate. A similar RCM simulation is done adding monthly mean global warming increments to the same reanalysis, as schematically shown in Fig. 15. This method was first proposed by Kimura and Kitoh (2007) and has been used in various studies (Sato *et al.* 2007; Hara *et al.* 2008; Knutson *et al.* 2008; Kawase *et al.* 2008, 2009; Lauer *et al.* 2010, 2012). The scientific basis of the PGW method is the assumption that the projected climate change is a small perturbation to the current climate so that a linear coupling of the global warming increment can be used as a good approximation. This also neglects the possible interactions between the climate change and the interannual variations of the regional climate system. It is also assumed that the variability of the synoptic-scale forcing from outside of the regional domain of interest does not change under the new climate. The PGW method can be done by the following RCM simulations:

(i) A single RCM-downscaled climate change simulation with the global warming increments from a selected coupled general circulation model (CGCM);
(ii) An ensemble of RCM-downscaled climate change simulations with the global warming increments from various CGCMs;
(iii) A single RCM-downscaled climate change simulation with ensemble global warming increments from various CGCMs;

(iv) An ensemble of multi-RCM-downscaled climate change simulations with the global warming increments from a single CGCM;

(v) An ensemble of multi-RCM-downscaled climate change simulations with the global warming increments from various CGCMs;

(vi) An ensemble of multi-RCM-downscaled climate change simulations with ensemble global warming increments from various CGCMs.

Compared with the DGW downscaling method, the PGW downscaling method has several advantages. First, since only the global warming increments are obtained from the CGCM current and projected climate simulations, theoretically the impact of the CGCM systematic biases on the RCM downscaled climates is largely reduced. Second, since most CGCMs have low skills in simulating the statistics of synoptic disturbances and intraseasonal and interannual variabilities, it might not be a bad assumption to keep these variabilities at its present-day level when providing the lateral boundary conditions for the future regional climate simulations. Indeed how the global warming may modulate variabilities at various time scales itself is a hot topic of current research.

Another advantage of using the PGW downscaling method is the computationally low cost. As shown by Kawase *et al.* (2009) for the summer rainfall in East Asia, the algorithms (ii) and (iii) of the PGW downscaling method can produce very similar results. Our recent results demonstrated that this is also the case for the Hawaii region in our HRCM simulations (Lauer et al. 2013). We found that a single RCM-downscaled climate change can be conducted with ensemble global warming increments from various CGCMs instead of using global warming increments from many individual CGCMs. This will largely reduce the computational costs. Nevertheless, some limitations should be kept in mind when the PGW downscaling method is adopted, such as the unchanged intraseasonal and interannual variabilities and the same level of synoptic forcing through the lateral boundaries.

SUMMARY AND FUTURE DIRECTIONS

A nested version of the WRF–ARW model release 3.3 (V3.3) with high resolution has been configured to cover the Hawaiian region with improved land surface specifications (albedo, land cover type, soil type, green vegetation fraction) for the Hawaiian Islands. This version includes the modified Tiedke convective parameterization introduced into the WRF model system by IPRC researchers (Zhang *et al.* 2012a), which was shown to have a good performance for trade wind regime cloud simulations. In addition, some modifications were made to the cloud microphysics package to improve the cloud and precipitation processes in the maritime conditions for the Hawaiian region as documented in Zhang *et al.* (2012b).

The behavior of the HRCM when it was run in doubly-nested mode with an inner nest grid spacing of 3 km for a 13-month continuous simulation from October 2005 to November 2006 forced by observed SSTs and lateral boundary conditions from reanalysis data was recently documented in Zhang *et al.* (2012b) and highlighted here. Results show the model has relatively small biases for large-scale circulation and can simulate realistically the frequency of the trade wind inversion, time-mean rainfall and surface variables on relatively small scales over the Hawaiian Islands. The model also captured the observed synoptic time-scale variations of the island-averaged rainfall. Encouraged by these results, we have recently completed a 20-year continuous simulation with the same model configuration. In addition to assessing the model performance in reproducing the observed climatological mean state, main efforts are to examine the model skill in capturing the interannual variability, and statistics of various climate variables, and extreme climate events.

Methods currently used by research community for dynamical downscaling of projected future climate change have been summarized as well. In particular, the advantages and disadvantages of the DGW and PGW downscaling methods are discussed. Because of the importance of both interannual variability and synoptic scale forcing to the regional climate in the Hawaiian region, which are poorly represented in most CGCMs, the PGW downscaling method is now being applied to evaluate the possible regional climate changes over other Pacific Islands. We note that the impacts of anticipated anthropogenic climate change over the coming decades are of great concern for the Pacific Islands as they are particularly vulnerable due to their small, geographically isolated ecosystems and economies as well as their susceptibility to extensive inundation from rising sea levels. In contrast to most other regions in the world, the Pacific Islands have also received only limited attention from the climate modeling community.

A notable recent development has been the work supported by the Australian government's Pacific Climate Change Science Program (PCCSP) which includes an analysis of global CGCM results as well as high-resolution regional atmospheric model simulations. The PCCSP focuses mostly on the southern and western areas of the tropical Pacific. An important recent development has been a new project focusing on climate projections for the US-affiliated Pacific islands sponsored by The Department of Interior Pacific Islands Climate Science Center (PICSC) and we are planning to continue our research on regional climate projections for other Pacific islands.

ACKNOWLEDGEMENTS

This study was supported in part by USGS PICCC/PICSC grant G12AC20501, by DOE Regional and Global Climate Modeling (RCGM) Program grant ER64840, by the NOAA Climate Adaptation Partnership for the Pacific (CAPP) via a subcontract to the International Pacific Research Center from the East-West Center and by the US Fish and Wildlife Service. Additional support was provided by the Japan Agency for Marine-Earth Science and Technology (JAMSTEC) for its sponsorship of the International Pacific Research Center. We would like to acknowledge the Hawaii Open Supercomputer Center for providing access to their facilities.

REFERENCES

Bukovsky, M.S., and Karoly, D.J., (2009) Precipitation simulations using WRF as a nested regional climate model. *Journal of Applied Meteorology and Climatology, 48,* 2152–2159.

Cao, G., Giambelluca, T.W., Stevens, D.E., and Schroeder, T.A., (2007) Inversion variability in the Hawaiian trade wind regime. *Journal of Climate, 20,* 1145–1160.

Carlis, D.L., Chen, Y.-L., and Morris, V., (2010) Numerical simulations of island-scale airflow and the Maui vortex during summer trade-wind conditions. *Monthly Weather Review, 138*, 2706-2736.

Chen, F., and Dudhia, J., (2001) Coupling an advanced land-surface/ hydrology model with the Penn State/NCAR MM5 modeling system. Part i: Model description and implementation. *Monthly Weather Review, 129*, 569–585.

Chen, Y.-L., and Nash, A.J., (1994) Diurnal variation of surface airflow and rainfall frequencies on the Island of Hawaii. *Monthly Weather Review, 122,* 34–56.

Chen, Y.-L., and Feng, J., (1995) The influences of inversion height on the precipitation and airflow over the island of Hawaii. *Monthly Weather Review, 123,* 1660-1676.

Chen, Y.-L., and Feng, J., (2001) Numerical simulations of airflow and cloud distributions over the windward side of the island of Hawaii. Part i: The effects of trade-wind inversion. *Monthly Weather Review, 129*, 1117-1134.

Chu, P.-S., (1995) Hawaii rainfall anomalies and El Niño. *Journal of Climate, 8,* 1697–1703.

Chu, P.-S., Nash, A.J., and Porter, F.-Y., (1993) Diagnostic studies of two contrasting rainfall episodes in Hawaii: Dry 1981 and wet 1982. *Journal of Climate, 6,* 1457–1462.

Chu, P.-S., and Clark, J.D., (1999) Decadal variations of tropical cyclone activity over the Central North Pacific. *Bulletin of American Meteorological Society, 80*, 1875–1881.

Chu, P.-S., and Chen, H., (2005) Interannual and interdecadal rainfall variations in the Hawaiian Islands. *Journal of Climate, 18*, 4796-4813.

Chu, P.-S., Chen Y.R, and Schroeder T.A., (2010) Changes in Precipitation Extremes in the Hawaiian Islands in a Warming Climate. *Journal of Climate, 23,* 4881–4900.

Collins, W.D., and Co-authors, (2004) Description of the NCAR Community Atmosphere Model (CAM3.0), NCAR Technical Note, NCAR/TN-464+STR, 226pp.

Dee, D.P., and Co-authors, (2011) The ERA-Interim reanalysis: Configuration and performance of the data assimilation system. *Quarterly Journal Royal Meteorological Society, 137*, 553-597.

DICKINSON, R.E., ERRICO, R.M., GIORGI, F., and BATES, G.T., (1989) A regional climate model for the western United States, *Climatic Change, 15*, 383–422.

ELISON TIMM, O., DIAZ H. F., GIAMBELLUCA T.W., and TAKAHASHI M., (2011) Projection of Changes in the Frequency of Heavy Rain Events over Hawaii Based on Leading Pacific Climate Modes. *Journal of Geophysical Research – Atmosphere, 116*, D041.

ELISON TIMM. O., TAKAHASHI M., GIAMBELLUCA T. W., and DIAZ H. F., (2013) On the relation between large-scale circulation pattern and heavy rain events over the Hawaiian Islands: Recent trends and future changes, *Journal of Geophysical Research – Atmosphere, 118*, 1-13. doi:10.1002/jgrd.50314.

ESTEBAN, M.A., and CHEN, Y.-L., (2008) The impact of trade-wind strength on precipitation over the windward side of the Island of Hawaii. *Monthly Weather Review, 136*, 913-928.

FENG, J., and CHEN, Y.-L., (2001) Numerical simulations of airflow and cloud distributions over the windward side of the island of Hawaii. Part II: Nocturnal flow regime. *Monthly Weather Review*, *129*, 1135-1147.

Giambelluca, T.W., SCHROEDER, T.A., (1986) *rainfall Atlas of Hawaii.* Department of Land and Natural Resources Hawaii, Rep. R76, 267pp.

GIAMBELLUCA, T.W., CHEN, Q., FRAZIER, A.G., PRICE, J.P., CHEN, Y.-L., CHU, P.-S., EISCHEID, J., and DELPARTE, D., (2011) The Rainfall Atlas of Hawai'i. http://rainfall. eography.hawaii.edu.

GIORGI, F., and MEARNS, L.O., (1991) Approaches to the simulation of regional climate change: a review. *Review of Geophysics, 29*, 191-216.

GIORGI, F., and BATES, G.T., (1989) The climatological skill of a regional model over complex terrain, *Monthly Weather Review, 117*, 2325–2347.

GUO, P., KUO, Y.-H., SOKOLOVSKIY, S.V., and LENSCHOW, D.H., (2011) Estimating atmospheric boundary layer depth using COSMIC radio occultation data, *Journal Atmospheric Sciences*, *68*, 1703–1713.

HARA, M., YOSHIKANE, T., KAWASE, H., and KIMURA, F., (2008) Estimation of the impact of global warming on snow depth in Japan by the pseudo-global-warming method. *Hydrological Research Letters*, *2*, 61-64, doi:10.3178/hrl.2.61.

HONG, S.-Y., and LIM, J., (2006) The WRF single-moment 6-class microphysics scheme (WSM6). *Journal of Korean Meteorological Society*, *42*, 129–151.

JANJIC, Z.I., (1990) The step-mountain coordinate: physical package, *Monthly Weather Review, 118,* 1429–1443.

JANJIC, Z.I., (1996) The surface layer in the NCEP Eta Model, *Eleventh Conference on Numerical Weather Prediction*, Norfolk, VA, 19–23 August; *Amer. Meteor. Soc.,* Boston, MA, 354–355.

JANJIC, Z.I., (2002) Nonsingular Implementation of the Mellor–Yamada Level 2.5 Scheme in the NCEP Meso model, *NCEP Office Note*, No. 437, 61 pp.

JIMÉNEZ, P.A., and Co-authors, (2010) Surface wind regionalization over complex terrain: Evaluation and analysis of a high-resolution WRF simulation. *Journal of Applied Meteorology and Climatology*, *49,* 268–287.

Kawase, H., Yoshikane, T., Hara, M., Ailikun, B., Kimura, F., and Yasunari, T., (2008) Downscaling of the climatic change in the Maiu rainband in East Asia by a pseudo climate simulation method. *Scientific Online Letters on the Atmosphere, 4*, 73-76, doi:10.2151/sola.20080-19.

Kawase, H., Yoshikane, T., Hara, M., Kimura, F., Yasunari, T., Ailikun, B., Ueda, H., and Inoue, T., (2009) Intermodel variability of future changes in the Baiu rainband estimated by the pseudo global warming downscaling method. J*ournal of Geophysical Research, 114*, D2411, doi:10.1029/2009JD011803.

Kelley, W. E., and Mock, D.R., (1982) A diagnostic study of upper tropospheric cold lows over the western North Pacific. *Monthly Weather Review, 110*, 471–480.

Khairoutdinov, M., and Kogan, Y., (2000) A New Cloud Physics Parameterization in a Large-Eddy Simulation Model of Marine Stratocumulus. *Monthly Weather Review*, 1*28*, 229–243.

Kimura, F., and Kitoh, A., (2007) Downscaling by pseudo global warming method. Final Report, pp. 43-46, ICCAP, Research Institute for Humanity and Nature, Kyoto, Japan.

Kodama, K.R., and Businger, S., (1998) Weather and forecasting challenges in the Pacific region of the National Weather Service. *Weather and forecasting, 13*, 523-546.

Knutson, T.R., Sirutis, J.J., Gamer, S.T., Vechi, G.A., and Held, I.M., (2008) Simulated reduction in Atlantic hurricane frequency under twenty-first-century warming conditions. *Nature Geoscience, 1*, 359-364, doi:10.1038/ngeo202.

Lauer, A., Hamilton, K.P., Wang, Y., Phillips, V.T., and Bennartz, R., (2010) The impact of global warming on marine boundary layer clouds over the eastern Pacific – A regional model study. *Journal of Climate, 23*, 5844-5863.

Lauer, A., Bennartz, R., Hamilton, K., and Wang, Y., (2012) Modeling the response of subtropical marine boundary layer clouds to global warming: The impact of subgrid scale precipitation formation. *Journal of Climate, 25*, 6610–6626.

Lauer, A., Zhang, C.-X., Elison-Timm, O., Wang, Y., and Hamilton, K., (2013) Downscaling of climate in the Hawaii region using CMIP5 results: On the choice of the forcing fields. *Journal of Climate,* (in press).

Leung, L.R., Mearns, L.O., Giorgi, F., and Wilby, R.J., (2003) Regional climate research. *Bulletin of the American Meteorological Society, 84*, 89-95.

Leung, L.R., Kuo, Y.-H., and Tribbia, T., (2006) Research needs and directions of regional climate modeling using WRF and CCSM. *Bulletin of American Meteorological Society, 87*, 1747–1751.

Liang, X.Z., Kunkel, K.E., Meehl, G.A., Jones, R.G., and Wang, J.X.L., (2008) Regional climate models downscaling analysis of general circulation models present climate biases propagation into future change projections. *Geophysical Research Letter, 35*, L08709, doi:10.1029/2007GL032849.

Lyons, S.W., (1982) Empirical orthogonal function analysis of Hawaiian rainfall. *Journal of Applied Meteorology, 21*, 1713–1729.

Mantua, N. J., Hare, S.R., Zhang, Y., Wallace, J.M., and Francis, R.C., (1997) A Pacific interdecadal climate oscillation with impacts on salmon production. *Bulletin of American Meteorological Society, 78*, 1069–1079.

Mearns, L.O., Bogardi, I., Giorgi, F., Matyasovszky, I., and Palecki, M., (1999) Comparison of climate change scenarios generated from regional climate model experiments and statistical downscaling. *Journal of Geophysical Research – Atmosphere, 104*, 6603-6621.

Meehl, G.A., Covey, C., Delworth, T.L., Latif, M., McAveney, B., Mitchell, J.F.B., Stouffer, R.J., and Taylor, K.E., (2007) The WCRP CMIP3 multimodel dataset: A new era in climate change research. *Bulletin of the American Meteorological Society, 88*, 1383–1394, doi:10.1175/BAMS-88-9-1383.

Nguyen, H.V., Chen, Y.-L., and F. Fujioka, F., (2010) Numerical simulations of island effects on airflow and weather during the summer over the Island of Oahu. *Monthly Weather Review, 138*, 2253–2280.

Otkin, J.A., and Martin, J.E., (2004) A synoptic climatology of the subtropical Kona storm. *Monthly Weather Review, 132*, 1502–1517.

Pincus, R., Platnick, S., Ackerman, S.A., Hemler, R.S., and Hofmann, R.J.P., (2012) Reconciling simulated and observed views of clouds: MODIS, ISCCP, and the limits of instrument simulators. *Journal of Climate, 25*, 4699-4720.

Plummer, D.A., Caya, D., Frigon, A., Côté, H., Giguère, M., Paquin, D., Biner, S., Harvey, R., and de Elía, R., (2006) Climate and climate change over North America as simulated by the Canadian Regional Climate Model. *Journal of Climate, 19*, 3112-3132.

Reynolds, R.W., Gentemann, C.L., and Corlett, G.K., (2010) Evaluation of AATSR and TMI Satellite SST Data. *Journal of Climate, 23*, 152-165.

Rienecker, M.M., and Co-authors, (2011) MERRA: NASA's Modern-Era Retrospective Analysis for Research and Applications. *Journal of Climate, 24*, 3624–3648.

Sadler, J.C., (1976) A role of the tropical upper tropospheric trough in early season typhoon development. *Monthly Weather Review, 104*, 1266–1278.

Sato, T., Kimura, F., and Kitoh, A., (2007) Projection of global warming onto regional precipitation over Mongolia using a regional climate model. *Journal of Hydrology. 333*, 144-154.

Schroeder, T.A., (1981) Characteristics of local winds in Northwest Hawaii. *Journal of Applied Meteorology, 20*, 874–881.

Schroeder, T.A., (1993) Climate controls. Prevailing Trade Winds: Weather and Climate in Hawai'i, M. Sanderson, Ed., University of Hawai'i Press, 12–36.

Schroeder, T.A., Kilonsky, B.J., and Meisner, B.N., (1977) Diurnal variation in rainfall and cloudiness. VH-MET 77-03, Dept. of Meteorology, University of Hawaii at Manoa, 67 pp. [Available from Dept. of Meteorology, University of Hawaii at Manoa, 2525 Correa Rd., Honolulu, HI 96822.]

Simpson, R.H., (1952) Evolution of the kona storm: A subtropical cyclone. *Journal of Meteorology,* 9, 24–35.

Skamarock, W.C., Klemp, J.B., Dudhia, J., Gill, D.O., Barker, D.M., Wang, W., and Powers, J.G., (2008) A description of the Advanced Research WRF Version 3. NCAR Tech Notes-475+STR, 113pp.

Taylor, G. E., (1984) Hawaiian winter rainfall and its relation to the Southern Oscillation. *Monthly Weather Review, 112*, 1613-1619.

Tripoli, G.J., and Cotton, W.R., (1980) A numerical investigation of several factors contributing to the observed variable intensity of deep convection over south Florida. *Journal of Applied Meteorology, 19*, 1037-1063.

Wang, Y., Sen, O.L., and Wang, B., (2003) A highly resolved regional climate model (IPRC_RegCM) and its simulation of the 1998 severe precipitation events over China. Part i: Model description and verification of simulation. *Journal of Climate, 16*, 1721-1738.

Wang, Y., Xie, S.-P., Xu, H., and Wang, B., (2004) Regional model simulations of marine boundary layer clouds over the Southeast Pacific off South America. Part i: Control experiment. *Monthly Weather Review, 132*, 274-296.

Wang, Y., Leung, L.R., McGreger, J.L., Lee, D.-K., Wang, W.-C., Ding, Y., and Kimura, F., (2004) Regional climate modelling: progress, challenges, and prospects. *Journal of Meteorological Society of Japan, 82*, 1599-1628.

Whitfield, M.B., and Lyons, S.W., (1992) An upper-tropospheric low over Texas during summer. *Weather and Forecasting, 7*, 89–106.

Worthley, L.E., (1967) Weather phenomena in Hawaii. Part I. Synoptic climatology of Hawaii. Hawaii Institute of Geophysics, University of Hawaii, 40 pp. [Available from Dept. of Meteorology, University of Hawaii, 2525 Correa Rd., Honolulu, HI 96822.]

Xu, K.-M., and Randall, D.A., (1996) A semiempirical cloudiness parameterization for use in climate models. *Journal of the Atmospheric Sciences, 53*, 3084-3102.

Yang, Y., Chen, Y.-L., and Fujioka, F.M., (2005) Numerical simulations of the island-induced circulation over the island of Hawaii during HaRP. *Monthly Weather Review, 133*, 3693-3713.

Zeng, X., and Beljaars, A., (2005) A prognostic scheme of sea surface skin temperature for modeling and data assimilation. *Geophysical Research Letter, 32*, L14605, 10.1029/2005GL023030.

Zhang, C., Wang, Y., and Hamilton, K., (2011) Improved Representation of Boundary Layer Clouds over the Southeast Pacific in ARW-WRF Using a Modified Tiedtke Cumulus Parameterization Scheme. *Monthly Weather Review, 139*, 3489–3513.

Zhang, C., Wang, Y., Lauer, A., Hamilton, K., and Xie, F., (2012a) Cloud base and top heights in the Hawaiian region determined by satellite and ground-based measurements. *Geophysical Research Letters, 39*, L15706, doi:10.1029/2012GL052355.

Zhang, C., Wang, Y., Lauer, A., and Hamilton, K., (2012b) Configuration and evaluation of the WRF model for the study of Hawaiian regional climate. *Monthly Weather Review, 140*, 3259-3277.

ZHANG, Y.-X., DULIÈRE, V., MOTE, P.W., and SALATHÉ, E.P., (2009) Evaluation of WRF and HadRM Mesoscale Climate Simulations over the U.S. Pacific Northwest. *Journal of Climate*, *22*, 5511–5526.

ZHANG, Y.-X., CHEN, Y.-L., and KODAMA, K., (2005a) Validation of the coupled NCEP Mesoscale Spectral Model and an advanced Land Surface Model over the Hawaiian Islands. Part II: A high wind event. *Weather and Forecasting*, *20*, 873-895.

ZHANG, Y.-X., CHEN, Y.-L., HONG, S.-Y., JUANG, H.-M. H., and KODAMA, K., (2005b) Validation of the coupled NCEP Mesoscale Spectral Model and an advanced Land Surface Model over the Hawaiian Islands. Part I: Summer trade wind conditions and a heavy rainfall event. *Weather and Forecasting*, *20*, 847-872.

NARCLIM: NSW | ACT REGIONAL CLIMATE MODELLING PROJECT

Lluis Fita, Jason P. Evans, Daniel Argüeso and Y. Li

CLIMATE CHANGE PERSPECTIVES FROM THE ATLANTIC:
PAST, PRESENT AND FUTURE
Jose María Fernández-Palacios, Lea de Nascimento, José Carlos Hernández,
Sabrina Clemente, Albano González & Juan P. Díaz-González (coords)
Servicio de Publicaciones, Universidad de La Laguna – 2013

ISBN: 978-84-15910-54-1 pp. 599-613

Abstract

NARCliM (NSW/ACT Regional Climate Modelling project) is a regional climate modelling project for the Australian area. It will provide a comprehensive dynamically downscaled climate dataset for the CORDEX-AustralAsia region at 50km, and South-East Australia at a resolution of 10km. NARCliM data will be used by the NSW and ACT governments to design their climate change adaptation plans.

NARCliM uses WRFv3.3 regional climate model (RCM) to perform an ensemble of simulations for the present and the projected future climate. WRF is run in three different model configurations, using four different GCMs from CMIP3, over three 20-year time periods (1990-2009, 2020-2039 and 2060-2079). The methodology chosen to select the 4 GCMs and the 3 different physical configurations of the WRF model are presented. First preliminary results from the control period runs (1950-2009) using NCEP re-analysis are also shown.

NARCLIM PROJECT OVERVIEW

NARCliM project (http://www.ccrc.unsw.edu.au/NARCliM) will produce an ENSEMBLE of projected climatologies over Australia in a two domain configuration. WRF v3.3 with clWRF and CCRC modifications (Fita *et al.*, 2010) is used. Spectral nudging for the large scales in the outer domain is also used. The project will produce 12 members for each period covered. This ensemble will be used for planning purposes by the NSW (New South Wales) and ACT (Australia Capital Territory) governments. The data can be directly compared to CORDEX (http://cordex.dmi.dk/joomla/) data-base, since the outer domain corresponds with the Austral-Asia CORDEX domain (AUS-44).

Steering committee of the NARCliM project is constituted by researchers (in charge of the model runs) and stake holders of both governments. In this way, it ensured that the requirements of end-users are meet, and utility of the project will be maximised. At this stage of the project, different experiments have been designed by the agencies and they cover a large variety of aspects such as: water resources management, rainfall erosivity, flooding, fire, biodiversity, coastal erosion, changes in salt Marshes and Mangroves, air quality and public health.

TABLE 1: Summary of model assessments.

Assessment region		Australia							MDB		SE Australia	
Model	Fractional Demerit	A	B	C	D	E	F	G	H	I	J	K
UKMO-HadCM3	0	0	Yes	6	608							179
CSIRO-Mk3.5	0						5	1				207
GFDL-CM2.1	0.111	0	Yes	2	672	Yes			No	Yes	0.72	184
GFDL-CM2.0	0.125	0	Yes	2	671	Yes			No	Yes		252
MIROC3.2 (hires)	0.125	0	Yes	7	608		12	9	Yes			201
CSIRO-Mk3	0.182	1	No	7	601	Yes	1	2	Yes	No	0.73	214
UKMO-HadGEM1	0.2	0	No	2	674							163
ECHAM5/MPI	0.222	0	Yes	1	700	Yes			No	No	0.79	173
MIUB-ECHO-G	0.222	0	No	4	632	Yes			Yes	No	0.78	174
INM-CM3.0	0.222	1	No	7	627		9	11		Yes	0.75	192
NCAR CCSM3	0.273	0	No	2	677	No	4	6	No		0.68	245
CNRM-CM3	0.286	0	No	4	542					No	0.73	196
FGOALS-G1.0	0.3	2	No	2	639	No	8	4	Yes		0.66	251
MIROC3.2 (medres)	0.364	2	Yes	7	608	Yes	11	3	Yes	No	0.6	255
CCCM3.1(T63)	0.375	1		10	478		2	7	No		0.72	241
MRI-CGCM2.3.3	0.455	1	No	3	601	No	10	12	Yes	Yes	0.41	437
CCCM3.1(T47)	0.455	1	No	8	518	No	3	10	Yes	No	0.77	186
GISS-ER	0.5	0	No	8	515	Yes	6	5	No	No		238
BCCR-BCM2.0	0.5	5		5	590	Yes			No			485
GISS-AOM	0.667	1	No	8	564	No	7	13	Yes		0.6	326
IPSL-CM4	0.8	2	No	14	505	No	13	8	Yes		0.48	394
NCAR PCM	0.833	3	No	11	506						0.64	309
GISS-EH	1	5	No	14	304		14	14				487

CHOOSING GCMS

GCM EVALUATION

The first step in choosing the GCMs to provide the driving data for the WRF simulations was a review of the literature that analysed the performance of CMIP3 GCMs over Australia. Many studies have evaluated the performance of GCMs over south-east Australia using different variables and metrics. Here we build on the meta-analysis of Smith and Chandler (2010). First, more recent evaluations over Australia, not covered in Smith and Chandler (2010) are added to the analysis for a total of 11 studies (see Table 1). Then a fractional demerit point was calculated to indicate the models over-all performance. The lower the fractional demerit the better the performance (see Table 1) with A: number of rainfall criteria failed (Smith and Chandler, 2010), B: satisfied ENSO criteria (Min *et al.*, 2005; van Oldenborgh *et al.*, 2005), C: demerit points based on criteria for rainfall, temperature and MSLP (Suppiah *et al.*, 2007), D: M-statistic representing goodness of fit at simulating rainfall, temperature and MSLP over Australia (Watterson, 2008), E: satisfied criteria for daily rainfall over Australia (Perkins *et al.*, 2007), F: order of model based on the total skill scores for each rainfall metric (Kirono *et al.*, 2010), G: order of model based on the total skill scores for each of rainfall and PET metric (Kirono *et al.*, 2010), H: satisfied criteria for daily rainfall over MDB region (Maximo *et al.*, 2008), I: satisfied criteria for MSLP over MDB region (Charles *et al.*, 2007), J: combination of RMSE of mean annual rainfall across south-east Australia and mean NSE (rainfall > 1mm) comparing GCM-simulated and observed daily rainfall distribution with equal weights (Vaze *et al.*, 2011), K: RMSE of mean annual rainfall over south-east Australia (Chiew *et al.*, 2009)

Demerit points are added to a GCM in two ways. For evaluations which provided a binary pass/fail outcome any fail equals one demerit point. For evaluations that provide a continuous measure, any GCM that falls in the 25% worst performing GCMs receives one demerit point. All demerit points across the published studies are totalled for each GCM. Since not every GCM was present in every study this demerit total is then divided by the total number of studies the GCM appeared in to calculate the fractional demerit. In this way fractional demerit scores of 0.5 or above indicate that the GCM was amongst the 25% worst GCMs at least half of the time. These consistently worst performers were then removed from further analysis.

GCM Independence

In the method of Abramowitz and Bishop (2010) the model independence is defined based on the correlation of model errors. For precipitation, mean temperature, the daily time series for each event is bias corrected using the gridded observational dataset from the Bureau of Meteorology's (BoMs) Australian Water Availability Project (AWAP, Jones *et al.*, 2009), to produce an anomaly time series. These time series are then used to create the model error covariance matrix. Abramowitz and Bishop (2010) are able to show that the coefficients of a linear combination of the models that optimally minimises the mean square error depends on both model performance and model dependence. The solution of this minimisation problem can be written in terms of the covariance matrix already constructed. The size of the coefficients assigned to each model reflects a combination of model performance and independence. That is, the models with the largest coefficients are the best performing/most independent models in the ensemble.

TABLE 2: The absolute GCM independence coefficient for each model.

Models	Temperature	Precipitation	Average	Rank
miroc3_2_medres	0.3525	0.0364	0.3889	1
ukmo_hadgem1	0.1361	0.0694	0.2055	2
inmcm3_0	0.1605	0.0436	0.2041	3
gfdl_cm2_0	0.0729	0.1078	0.1807	4
mpi_echam5	0.0704	0.0921	0.1625	5
mri_cgcm2_3_2a	0.0624	0.0847	0.1470	6
miub_echo_g	0.0868	0.0414	0.1282	7
gfdl_cm2_1	0.0290	0.0799	0.1090	8
cccma_cgcm3_1	0.0233	0.0733	0.0966	9
ukmo_hadcm3	0.0331	0.0602	0.0932	10
csiro_mk3_5	0.0059	0.0860	0.0919	11
csiro_mk3_0	0.0398	0.0503	0.0901	12
ncar_ccsm3_0	0.0091	0.0726	0.0817	13
cnrm_cm3	0.0061	0.0513	0.0575	14

These coefficients are calculated for each variable and then averaged to give the overall performance/independence of each model (see Table 2).

GCM Future Change

The projected future changes of all the reasonably well performing GCMs are considered equally probable future changes. As such we want to choose models that sample from this future change space, while being as independent as possible.

Based on these criteria the ideal GCM choice would be: MIROC (1), HadGEM (2), GFDL 2.0 (4), MRI (6). Due to many groups not keeping all the required data to run the WRF model, alternative choices have to be made. The GCM choice used in practise is: MIROC (1), ECHAM5 (5), CCCMA (9) and CSIRO mk3.5 (11)

CHOOSING THE RCMS TO PERFORM THE DOWNSCALING

The Weather Research and Forecasting (WRF) modelling system (Skamarock *et al.*, 2008) v3.3 is used to perform the climatological regionalisation. This system facilitates the use of many *'RCMs'* by allowing all model components to be changed and hence many structurally different RCMs can be built. The aim of this methodology is to choose three RCMs from a large ensemble of adequately performing RCMs, such that they retain as much independent information as possible while spanning the uncertainty range found in the full ensemble. Due to computational limitations, the RCM performance and independence is evaluated based on a series of event simulations rather than using multi-year simulations.

Evaluate RCM performance for a series of important precipitation events

By limiting the evaluation period to a series of representative events for NSW, a much larger set of RCMs can be tested. In this case an ensemble of 36 RCMs will be created by using various parameterisations for the Cumulus convection scheme, the cloud microphysics scheme, the radiation schemes and the Planetary Boundary Layer (PBL) scheme. Each of these RCMs will be used to simulate a set of 7 representative storms that cover the various NSW storm types discussed in the literature (Shand *et al.*, 2010; Speer *et al.*, 2009). An eighth event focused on a period of extreme fire weather will also be analysed. In each case a two week period is simulated centred around the peak of the event. Subsequent analysis then includes pre and post-event climate as well as the event itself.

Evaluation will be performed against daily precipitation, minimum and maximum temperature from AWAP. Evaluation will also be performed against the mean sea level pressure and the 10m winds obtained from BoMs MesoLAPS analysis (Puri *et al.*, 1998). Any RCMs that perform consistently poorly will be removed from further analysis. The overall spread in these results provides a measure of the uncertainty due to the choice of RCM.

The RCMs are evaluated in terms of simulating temperature, MSLP, wind speed and rain, various metrics were calculated and combined using four different methods. The metrics used for the ranking are RMSE, MAE and R for Tmin, Tmax, MSLP and wind speed. The FSS score was used for the rainfall totals. These metrics are calculated for all 8 events and combined as described in Evans *et al.* (2011). Two overall metrics are calculated. One metric characterizes the climatology (clim) and the other is dominated by the most extreme events (impact).

RCM Independence

Abramowitz and Bishop (2010) method of evaluation of the level of independence between the RCMs is used to choose that WRF configuration that contribute the most independent information.

The three most independent/best performing models of the 30 model ensemble are given in Table 3.

TABLE 3: Most performing WRF configurations. Pbl: planetary boundary layer, sfl: surface layer physics, cu: cumulus physics, mp: microphysics, s/lrad: Shortwave/Longwave radiation physics.

Ensemble member	pbl / sfl	cu	mp	s/l rad
R1	MYJ / Eta similarity	KF	WDM 5 class	Dudhia / RRTM
R2	MYJ / Eta similarity	BMJ	WDM 5 class	Dudhia / RRTM
R3	YSU / MM5 similarity	KF	WDM 5 class	CAM / CAM

REANALYSIS DRIVEN RCM SIMULATIONS

The three RCMs have been run using boundary conditions from the NCEP/NCAR reanalysis. The reanalysis component of NARCliM is focused on assessing the RCMs ability to simulate the recent climate of the region. From which a robustness test on the WRF ability to simulate the climate will be obtained, and the retrieval of derived variables that will be used to drive impact models used for evaluation and/or calibration of the government agencies involved in the project.

It is well know, that the period covered by the reanalysis experiments 1950-2009 encompass the Australian wet periods in the 1950s and 1970s, as well as the very dry period in the 2000s. This ensures that the natural variability of the climate of the region is well covered.

The WRF simulations overestimate precipitation along the Eastern coastal zone. This might be related to an orographic enhancing effect recognised in other studies (Fig. 1). There is an improvement in precipitation simulated in the higher resolution domain. Best results are obtained with the R2 run. WRF configuration R1 and R3 overestimate precipitation on the tropical North coastal region.

Simulated minimum temperature climatologies show a mixture of under/overestimation pattern (Fig. 2). A clear North-South bias pattern is also shown in the R1 and R2 simulations. Higher resolution domain shows a small improvement in comparison with the coarser domain. Configuration R3 shows a different sign in the bias in comparison with the other two. The topography does not strongly influence the distribution of the bias.

There are no significant differences among the three WRF configurations on maximum temperature (Fig. 3). There is no substantial difference between higher and coarser resolution domains. In general there is an underestimation in all the climatologies over the continent except the Northern tropical coastal-line.

In order to analyse in more detail the differences between simulations, a spatial average over a SE section (lon/lat box of S 38.45, 139.9631 W x S 27.77, 153.7956 W) of the continent (common in all the experiments) are calculated. Temporal evolution of the differences between spatial averages are plotted and filtered with a running average of 12-month.

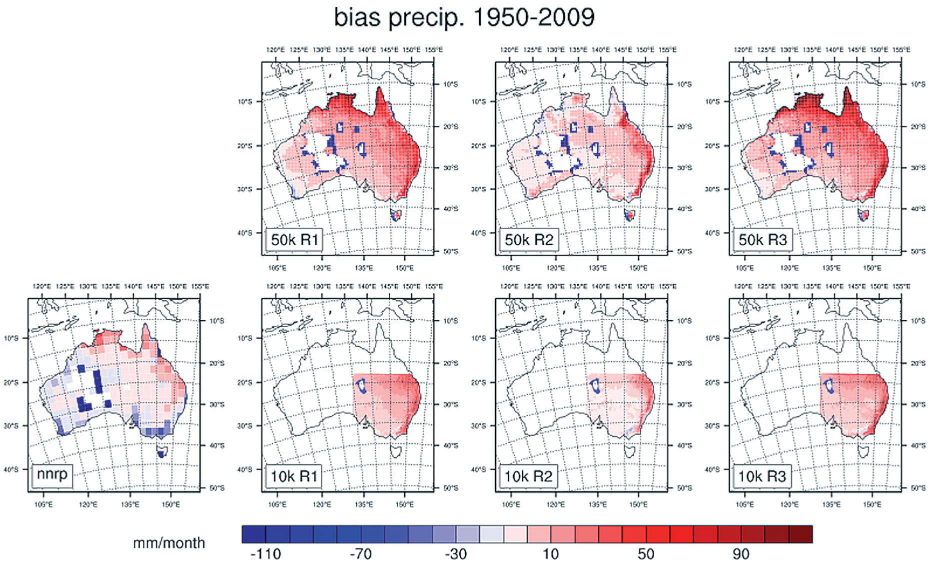

Figure 1. Bias of mean daily precipitation over the period 1950-2009 with respect AWAP gridded data. For the R1, R2, R3 and both domains 50km (top), 10km (bottom). Results for NCEP re-analysis (nnrp) are also shown (bottom left).

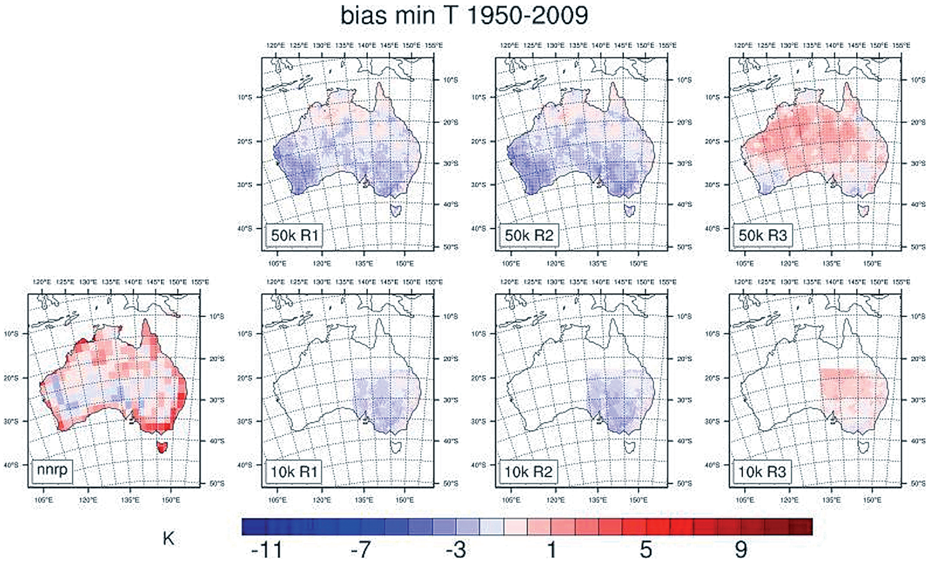

Figure 2. As in Fig. 1, but for the minimum daily temperature.

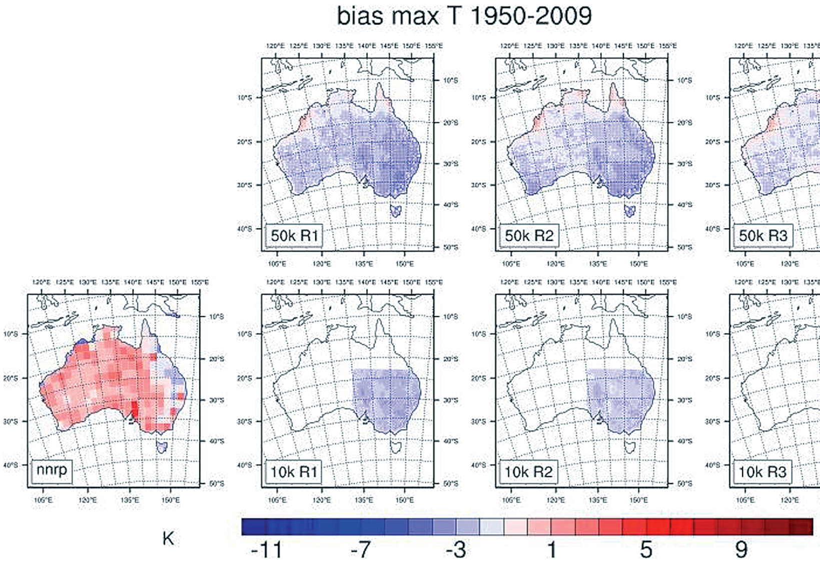

Figure 3. As in Fig. 1, but for the maximum daily temperature.

Temporal evolutions of the differences of spatial averages between simulations and AWAP data do not show domain sensitivity (Figs. 4 to 6). There is a significant difference between the NCEP re-analysis and WRF experiments. The smallest differences are found for the minimum temperature (tasmin) and the highest for precipitation (pracc, up to a 130%).

Temporal evolutions of the differences in precipitation (Fig. 4) show a small increasing trend with respect AWAP gridded observations. All WRF driven climatologies exhibit a similar evolution of the differences, with most often an overestimation. WRF R2 configuration shows the lowest differences with respect AWAP observed values.

Differences for minimum temperature are the lowest for the R3 WRF configuration (Fig. 5). There is no significant difference between R1 and R2. A light improvement along the period of simulation is observed in all the simulations (broadly differences are -2.5 K to a -1.5 K)

Differences for maximum temperature are higher in all the WRF simulations being very low for the NCEP re-analysis (Fig. 6). Although R3 configuration shows smaller differences and R1 the highest with AWAP. Differences do not change through the period and they present a wider variability in comparison with minimum temperature.

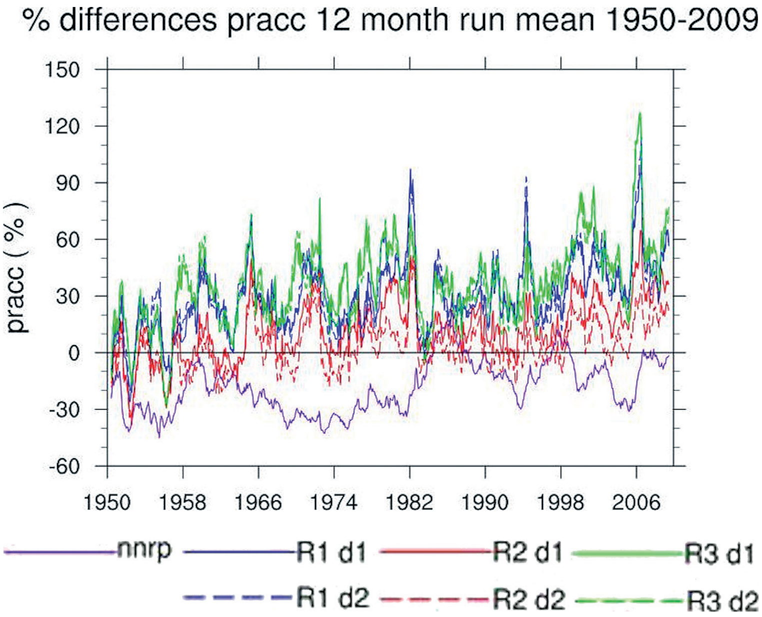

Figure 4. Temporal evolution of the percent differences in daily precipitation between spatial averages of the simulations over the SE (see text) of Australia and AWAP spatial average.

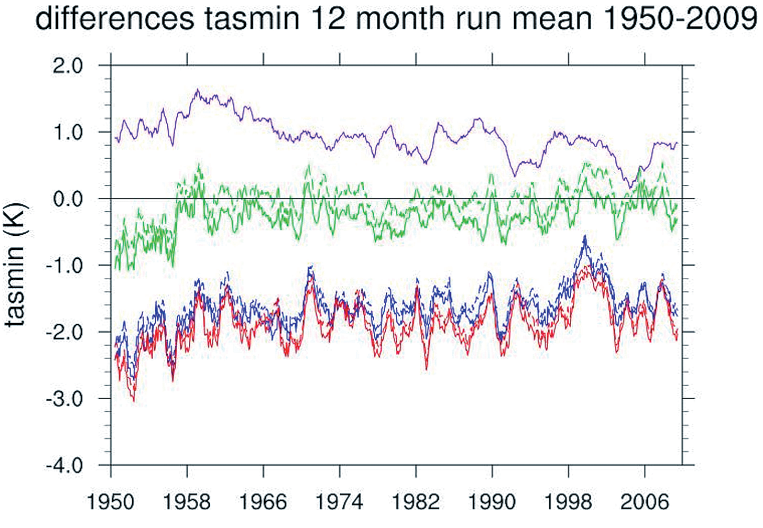

Figure 5. As in Fig. 4, but for the minimum temperature.

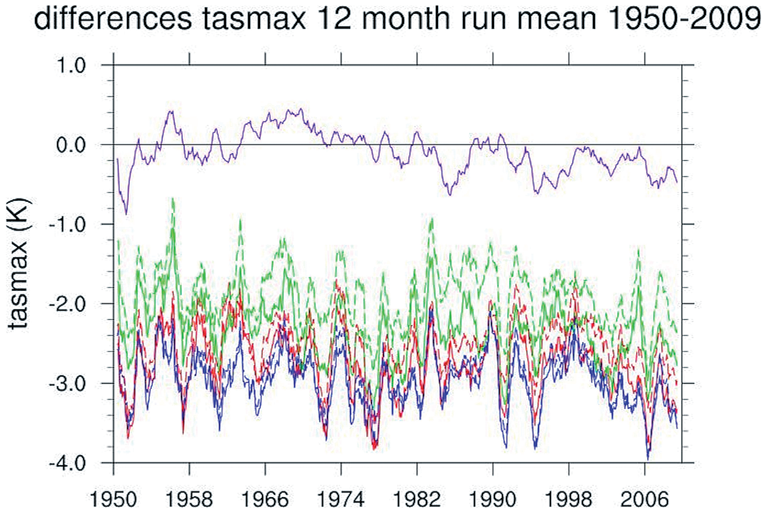

Figure 6. As in Fig. 4, but for the maximum temperature.

CONCLUSIONS

Different particularities of NARCliM project provide an innovation in the way a dynamical downscaling climatological project is carried out. These particularities encompass different stages and aspects of the project, such us: data management, science and application.

NARCliM has been designed/implemented and it is currently going on under the supervision of a steering committee which is formed by scientists and stakeholders of both states which founded the project: New South Wales and Australia Capital Territory. In this way, it is certainly true that the gap between scientists (who are in charge of the model runs and their evaluation) and stakeholders (who will use the outcomes of the project) is reduced. Access to the project data will fit end-users requirements. At the same time, continuous feed-back between members of the committee has simplified the building of a common working space, as well as the acquisition of necessary knowledge for both parts. As an example, this has had a positive impact on the planning and design of the studies of the governmental agencies with advise from the climate scientists.

Development of an ensemble of climate simulations will provide a wider description of the climatology in the area. Using independence criteria when choosing GCM driving conditions and WRF configurations, should ensure that the climate richness of Australia is well encompassed within the ensemble. All these aspects will be tested and evaluated as the project progresses.

Preliminary analyses based on mean values, shows an acceptable performance of the WRF model for the area of study. Precipitation differences with observed values exhibit similar patterns to those in older similar studies. However, this is an achievement of the WRF model, since climatology in Australia is very rich with tropical, semi-arid, Mediterranean and other climatological regimes spread around the continent.

However, a significant and systematic underestimation of the maximum temperature in all the WRF configurations and, in lesser extend for the minimum. This is a well know result from numerical models like WRF (García-Díez *et al.*, 2012) which usually they are not able to reproduce the extreme regimes of the temperature field.

WRF simulations provide a significant improvement with respect to the NCEP re-analysis (except for maximum temperature). WRF climatologies show a good agreement with observed gridded values, however, no WRF configuration performs the best in all the AWAP variables. Preliminary results suggest that Betts-Miller-Janjic (BMJ) cumulus scheme (R2) performs better for Australia precipitation regimes than Kain-Fritsch (KF). YSU/MM5 pbl configuration performs the best in all the Australian climatological regimes for the temperature extremes.

A future detailed seasonal-based study will provide better insights in all the climatological characteristics of the model outputs. The computation of a series of different statistical measurements and methodologies will also provide a deeper and better description about the goodness and robustness of the NARCliM ensemble.

By the end of the simulated period (end of 2014), it is planned to build a web portal (CliMDDIR website, www.climddir.org) which will provide open access to all the data of the NARCliM project.

ACKNOWLEDGEMENTS

NARCliM is funded through a consortium of project partners including NSW Office of Environment and Heritage (OEH), ACT Environment and Sustainable Development Directorate, Sydney Water, Sydney Catchment Authority, Hunter Water, NSW Department of Transport, NSW Department of Primary Industry, NSW Office of Water

REFERENCES

Abramowitz, G., and C. Bishop, (2010): Defining and weighting for model dependence in ensemble prediction. AGU Fall meeting, San Francisco, USA.

Charles, S., M. Bari, A. Kitsios, and B. Bates, (2007): Effect of GCM bias on downscaled precipitation and runoff projections for the Serpentine catchment, Western Australia. *International Journal of Climatology*, 27, 1673–1690, doi:10.1002/joc.1508.

Chiew, F.H.S., J. Teng, J. Vaze, and D.G.C. Kirono, (2009): Influence of global climate model selection on runoff impact assessment. *Journal of Hydrology*, 379, 172–180.

Evans, J.P., M. Ekstrom, and F. Ji (2011) Evaluating the performance of a WRF physics ensemble over South-East Australia, accepted 3 Nov 2011, *Climate Dynamics.*

Fita, L., Fernández, J., and García-Díez, M., (2010)*:* CLWRF: WRF modifications for regional climate simulation under future scenarios, Poster, 11th WRF Users' Workshop, Boulder, USA.

M. García-Díez, J. Fernández, L. Fita, and C. Yagüe*,* (2012): Seasonal dependence of WRF model biases and sensitivity to PBL schemes over Europe, *Q. J. of Roy. Met. Soc.*

Jones, D.A., W. Wang, and R. Fawcett, (2009): High-quality spatial climate data-sets for Australia. *Australian Meteorological Magazine*, 58, 233–248.

Kirono, D.G.C., F.H.S. Chiew, and D.M. Kent, (2010): Identification of best predictors for forecasting seasonal rainfall and runoff in Australia. *Hydrological Processes*, 24, 1237–1247.

Maxino, C.C., B.J. McAvaney, A.J. Pitman, and S.E. Perkins, (2008): Ranking the AR4 climate models over the Murray-Darling Basin using simulated maximum temperature, minimum temperature and precipitation. *International Journal of Climatology*, 28, 1097–1112.

Min, S.-K., S. Legutke, A. Hense, and W.-T. Kwon, (2005): Internal variability in a 1000-yr control simulation with the coupled climate model ECHO-G - II. El niño Southern Oscillation and North Atlantic Oscillation. *Tellus Ser. A Dyn. Meteorol. Oceanogr.*, 57, 622–640.

Perkins, S.E., A.J. Pitman, N.J. Holbrook, and J. McAneney, (2007): Evaluation of the AR4 climate models' simulated daily maximum temperature, minimum temperature, and precipitation over Australia using probability density functions. *Journal of Climate*, 20, 4356–4376.

Puri, K., G. Dietachmayer, G. Mills, N. Davidson, R. Bowen, and L. Logan, (1998): The new BMRC limited area prediction system, LAPS. *Australian Meteorological Magazine*, 47, 203–223.

Shand, T.D., I.D. Goodwin, M.A. Mole, J.T. Carley, I.R. Coghlan, M.D. Harley, and W.L. Peirson, (2010): NSW Coastal Inundation Hazard Study: Coastal Storms and Extreme Waves. UNSW Water Research Laboratory, Sydney, Australia.

Skamarock, W.C., and Coauthors, (2008): A Description of the Advanced Research WRF Version 3. NCAR, Boulder, CO, USA.

Smith, I., and E. Chandler, (2010): Refining rainfall projections for the Murray Darling Basin of south east Australia-the effect of sampling model results based on performance. *Climatic Change*, 102, 377–393, doi:10.1007/s10584-009-9757-1.

Speer, M., P. Wiles, and A. Pepler, (2009): Low pressure systems off the New South Wales coast and associated hazardous weather: establishment of a database. *Australian Meteorological and Oceanographic Journal*, 58, 29–39.

Suppiah, R., K. Hennessy, P.H. Whetton, K. McInnes, I. Macadam, J. Bathols, J. Ricketts, and C.M. Page, (2007): Australian climate change projections derived from simulations performed for the IPCC 4th Assessment Report. *Australian Meteorological Magazine*, 56, 131–152.

van Oldenborgh, G.J., S.Y. Philip, and M. Collins, (2005): El Niño in a changing climate: a multi-model study. *Ocean Sci.*, 1, 81–95.

Vaze, J., J. Teng, and F.H.S. Chiew, (2011): Assessment of GCM simulations of annual and seasonal rainfall and daily rainfall distribution across south-east Australia. *Hydrological Processes*, 25, 1486–1497.

Watterson, I.G., (2008): Calculation of probability density functions for temperature and precipitation change under global warming. *Journal of Geophysical Research*, 113.

COMPARISON OF OBSERVATIONAL, REANALYSIS AND SIMULATED CLOUD COVER DATABASES IN THE AFRICAN CORDEX DOMAIN

Juan C. Pérez, Albano González, Juan P. Díaz, Francisco J. Expósito,
David Taima and Aaron Henríquez

CLIMATE CHANGE PERSPECTIVES FROM THE ATLANTIC:
PAST, PRESENT AND FUTURE
Jose María Fernández-Palacios, Lea de Nascimento, José Carlos Hernández,
Sabrina Clemente, Albano González & Juan P. Díaz-González (coords)
Servicio de Publicaciones, Universidad de La Laguna – 2013

ISBN: 978-84-15910-54-1
pp. 615-639

Abstract

Comparisons between cloud cover data obtained from ISCCP and CRU databases, reanalysis of NCEP/DOE AMIP-II, ERA-40 and ERA-Interim data, and different simulation results from GCMs included in the Coupled Model Intercomparison Project Phase 5 (CMIP5) have been conducted, to evaluate the skills of models to reproduce the climatological behavior of cloud cover over the African continent during approximately two decades, 1984 to 2005. The behavior of all the models is very similar, they underestimate the total cloud cover but show a good space-time correlation with satellite data, with values between 0.7 - 0.8. However, the separate analysis of low, mid and high cloud cover produces worse results, revealing an important underestimation of low clouds. One of the areas that show important differences corresponds to marine boundary layer clouds near the coast of Namibia. The trends from the observational and reanalysis data are analyzed for different African climate zones.

Keywords: ISCCP, CMIP5, Cloud cover, CORDEX, climate.

INTRODUCTION

Clouds are one of the most important regulators of climate due to their influence on the Earth's hydrological cycle, regulation of latent heat fluxes and their interaction with short-wave (SW) and long-wave radiation (LW), having a profound effect on the radiation budget of the planet (IPCC, 2007). At any time, they approximately cover 68% of the Earth's surface, but their distribution is very irregular over time and space (Stubenrauch *et al.*, 2013). Their climate effects depend on cloud height, thickness, horizontal extent, horizontal variability, water content, phase and the size distributions of droplets and crystals, as well as on other factors of the climate system, such as albedo and temperature of the underlying surface or time of day (diurnal cycle). Therefore, it is necessary to evaluate the characteristics of the different types of clouds. For example, marine stratus and stratocumulus (MSC) have an albedo of 30-40% while maintaining a cloud-top temperature not much colder than the sea surface temperature (SST) (Randall *et al.*, 1984; Eastman *et al.*, 2011). MSC have a negative cloud radiative effect (CRE), i.e. produce a cooling effect on climate. Randall *et al.* (1984) estimated that a 4% increase in marine stratocumulus clouds (MSC) cover could offset a 2 - 3 °C global temperature rise. Moreover, high clouds (cirriform) are thinner and colder, so their longwave effect predominates over the scattering processes in the shortwave range, giving a positive CRE. Loeb *et al.* (2009) have estimated that the global mean cloud radiative effect (CRE) is 29.5 Wm^{-2} in the LW, –46.6 Wm^{-2} in the SW, and that the net CRE is –17.1Wm^{-2}, using the Clouds and the Earth's Radiant Energy System (CERES)-Energy Balanced and Filled (EBAF) top of atmosphere (TOA) fluxes.

Beside determining the micro- and macro-properties (over space and time), a critical point is the determination of the underlying mechanisms of cloud formation and the cloud-climate feedback processes. Due to the multiple aspects of this problem, a systematic and detailed combination of model and observation is necessary.

Due to the influence of clouds on both the water balance of the atmosphere and the Earth's radiation budget, small cloud variations can alter climate response associated with changes in greenhouse gases, aerosols or any other factor associated with global change-(Stephens, 2005). In fact, the response of clouds to increasing greenhouse gases is one of the greatest uncertainties in model predictions of climate sensitivity (IPCC, 2007).

Ground based observations of cloud cover are routinely performed by meteorological observers in many stations around the world (often in units of eighths, or oktas) and they constitute the longest time series of data. The main drawback of this kind of observation is its inhomogeneous spatial coverage, with few observation sites in the oceans and in polar regions, and a variable density in land areas. However, some efforts have been made to create gridded and homogenized datasets from these observations, such as those produced by the Climatic Research Unit (CRU) at the University of East Anglia (Mitchell and Jones, 2005). Another archive of land-based, surface-observed cloud characteristics is the Extended Edited Cloud Report Archives (EECRA). This database is created using cloud data from weather stations worldwide and from reports taken aboard ships (Eastman and Warren, 2012).

On the other hand, Earth observation satellites estimate cloud cover from radiometric measurements, and constitute the main data source for cloud studies on global or synoptic scales. In this way, considerable effort has been devoted to developing global cloud climatologies from various instruments on board satellites, and at least nine of these instruments are currently available (Stubenrauch *et al.*, 2009; 2013). For example, the International Satellite Cloud Climatology Project (ISCCP), which has provided cloud data since 1983 at an intermediate spatial resolution, is one of the most comprehensive cloud climatological databases (Schiffer and Rossow, 1983; Rossow and Schiffer, 1999). Other datasets, such as those obtained from MODIS instruments on board Terra and Aqua satellites, provide cloud cover data at higher spatial resolutions, but their time series are too short for climate-related studies.

Global analyses of atmospheric fields also provide cloud cover gridded data on a global scale. Reanalysis datasets are obtained by the assimilation of observational data using methods based on variational analyses. Each reanalysis product uses the same assimilation method for the entire period of coverage to avoid inhomogeneities in the produced dataset due to changes in model assumptions. Some of the most widely used reanalysis data are those from the NCEP/NCAR (National Centers for Environmental Prediction/National Center for Atmospheric Research), NCEP-DOE (Department of Energy), ERA-15, ERA-40 or ERA-Interim. The ERA datasets are provided by the European Centre for Medium-range Weather Forecasts (ECMWF). Although reanalysis products have been applied in many research areas related to climate, it must be taken into account that observational cloud data are not used in assimilation procedures, so that cloud related quantities are only loosely constrained in the resulting analyses (Pincus *et al.*, 2008).

Furthermore, numerical weather and global climate models have rapidly evolved since the first simple model developed in 1950. This evolution has been possible thanks to improved numerical models and parameterizations, which describe physical processes, and to the increasing performance of computers. However, some drawbacks exist in cloud modeling mainly associated with the different scales of the cloud processes, 100 to 250 m, and the Global Circulation Model (GCM) resolutions, usually hundreds of kilometers. This implies the use of different parameterizations to take into account the sub-grid scale processes. Although multiple parameterizations have been developed, there is not a general consensus as to which provide the most reliable results.

The four above-mentioned databases provide cloud cover data, but the values arise from different points of views: clouds seen from below (surface observations), seen from above (satellites) and using overlap assumptions (numerical models used in reanalyses and GCMs). This fact complicates the comparison of different cloud cover databases (Weare 2000; 2004). Even comparisons between two datasets of the same type can present some discrepancies, such as satellite data obtained by different sensors (Pincus *et al.*, 2012) or different procedures (Stubenrauch *et al.*, 2013). One way to bridge the gap between the properties of the clouds that may be observed by satellite instruments and those evaluated from models is through instrument simulators, defined as a diagnostic code applied to model variables that reduces the influences of inconsistencies between the ways clouds are observed and the ways they are modeled (Bodas-Salcedo *et al.*, 2011). By mimicking the observational process in a simplified way, the simulator attempts to compute what a satellite would retrieve if the real-world atmosphere had the clouds from the model.

The aims of this work are to study the main characteristics of cloudiness in the African region based on different sources of observational (CRU, ISCCP, etc.) and reanalysis data and to compare them with the features of cloudiness obtained from models participating in the CMIP5. In the next section, the observational, reanalysis and modeling datasets are described. In the third section, the main features of the total cloud cover (TCC) and of low, mid and high clouds are discussed, as well as the TCC trends obtained from the observational and reanalysis datasets. Also in this section the main results of the intercomparison of the CMIP5 simulations are analyzed, using the historical experiment versus ISSCP D2 data. Section 4 presents the main conclusions.

OBSERVATIONAL AND MODELING DATASETS.

Observational and reanalysis databases

In the present study, two observational and three reanalysis cloud cover datasets, summarised in Table 1, have been used to analyze the cloudiness in Africa. The study area has been selected to include the African continent and uses the boundaries suggested in the Coordinated Regional climate Downscaling Experiment (CORDEX) (Giorgi *et al.*, 2009) for this region, which has been defined as a key area for developing regional climate studies. Thus, the results presented in this paper could be used in future works of climate regionalization for the African region.

The International Satellite Cloud Climatology Project (ISCCP) was established in 1982, as part of the World Climate Research Program (WCRP) to analyze satellite imagery to estimate the global distribution of clouds, their macro and microphysical properties and their temporal variations. D1 and D2 products have been used in this study, from the whole set of data provided by the ISCCP project. The D1 product is produced by summarizing the pixel-level results obtained from different satellites every three hours on an equal-area grid with 280 km resolution. The D2 data product is obtained by averaging the D1 data over each month. In this case, the data used are the products regridded to a 2.5° x2.5° spatial resolution. The D1 dataset is not included in Table 1 because it has only been used to perform auxiliary computations, as explained below, and not to obtain the cloud cover. Among many other variables, D2 provides cloud cover data for different cloud top pressures and cloud optical thicknesses, allowing us to distinguish between several types of clouds. These data have been combined to generate just five variables, corresponding to total cloud cover and cloud cover of four cloud types: low, middle, high and deep convective, as defined in Rossow and Schiffer (1999). ISCCP data are based on measurements of many satellites, which have been replaced during the project development and whose orbits and instrument properties have varied over their lifetimes. Thus, some authors suggest that the ISCCP cloud time series contain artifacts due to changes in satellite view angles (Campbell, 2004; Evan *et al.*, 2007). To check the dependence of the ISCCP cloud cover on the changes in observation angles, the cosines of satellite zenith angle (mue) have been obtained from the D1 dataset and the

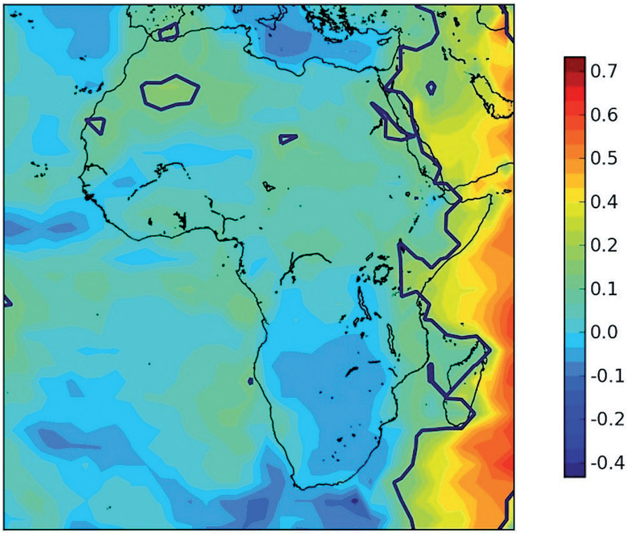

Figure 1. Map of the coefficients of the regression between 1/mue and total cloud cover. The thick line corresponds to p-value = 0.01.

monthly mean values have been computed. To determine the regions that are more affected by the changes in observation conditions, regressions between 1/mue and total cloud cover time series for each grid point have been calculated. Fig. 1 shows a map of the correlation coefficients for the study area. The higher correlations are located in the eastern part of the map, over the Indian Ocean and the Arabian Peninsula. The thick contour lines bound areas where the regression is statistically significant (p value lower than 0.01) based on a two- tailed t-test and 238 degrees of freedom. As can be seen, most of the African continent is not significantly affected by changes in the observation angles of the satellites.

Climate Research Unit Time Series 2.1 (CRU TS 2.1) is a database of monthly climate observations from meteorological stations (Mitchell and Jones, 2005) and was constructed at the University of East Anglia, UK. The dataset used in this study has a 0.5° spatial resolution. One of the main problems of this database is the lack of ground observations in the study area, as will be discussed later.

For completeness of this study, cloud information for the three reanalysis data has been included in the analysis of the cloud fraction (total and by type: top, medium and low). ERA-40 (Uppala *et al.*, 2005) and ERA-Interim (Dee *et al.*, 2011) databases are provided by the European Centre for Medium-range Weather Forecasts (ECMWF). ERA-40 data have been generated using a 3D-variational analysis and an spectral T159 (triangular truncation) model resolution, corresponding to approximately 125 km. ERA-Interim is the latest global atmospheric reanalysis produced by ECMWF and uses a 4D-variational analysis on a spectral grid with triangular truncation T255, which corresponds to approximately 79 km. For this study, both datasets have been obtained from ECMWF data server on fixed grids with resolutions of 2.5° and 1.5°, respectively. The ERA-Interim reanalysis is produced from the ECMWF Integrated Forecast System (IFS), which incorporates a forecast model with three fully coupled components for the atmosphere, land surface, and ocean waves. A history of changes introduced in the IFS since 1985 is maintained at http://www.ecmwf.int/products/data/operational system/evolution. ERA-Interim is based on IFS release Cy31r2, used for operational forecasting at ECMWF from 12 December 2006 until 5 June 2007. Several modifications to the model's physics were introduced with potentially significant impact on the representation of the hydrological cycle. The cloud scheme was also substantially revised in Cy25r3. Using ISCCP observations as a reference, the following features have improved regarding ERA-40: Marine stratocumulus cloud cover increases by 15-25%, Tropical ocean total cloud cover decreases by 5-15%, Tropical land cloud cover increases by 20-30% and Midlatitude ocean (low- and medium-height) cloud cover increases by about 5% (Dee *et al.*, 2011).

NCEPDOE AMIP-II reanalysis (R-2) data (Kanamitsu *et al.*, 2002) were generated by the National Centers for Environmental Prediction (NCEP) at the National Energy Research Supercomputing Center (NERSC) of the Department of Energy (DOE) for the NCEP-DOE Atmospheric Model Intercomparison Project (AMIP-II). NCEP-DOE was created as an update (not as a next-generation reanalysis) for the NCEP-NCAR R1 reanalysis and includes new physics and observations, an improved assimilation procedure based on 4D-variational assimilation and has a horizontal spectral resolution of T62 (approximately 209 km). Relevant improvements to the model's physics consist of a new SW radiation scheme (Chou, 1992; Chou and Lee, 1996) to remove excess surface insolation found in R1, updated cloud-tuning coefficients for stratus clouds, and radiation calculations performed on a full Gaussian grid at every hour as opposed to every 3 hours in R1. Cloud fraction in R2 is diagnosed from an empirical relative humidity-cloud cover relationship and is assumed to be randomly overlapped. A more accurate system description and evaluation of R2 is documented in Kanamitsu (2002). The corresponding datasets have been obtained from NOAA/OAR/ ESRL PSD (National Oceanic. and Atmospheric Administration / Outstanding Accomplishments in Research / Earth System Research Laboratory - Physical Science Division).

In order to facilitate comparison between databases, the higher resolution grids have been degraded to the lowest resolution, that is 2.5° x 2.5°, and the period for the study was selected to include 2 decades, from 1981 to 2000. However, not all the datasets can fill this period, as shown in Table 1. Furthermore, all the datasets have been converted to the same temporal resolution, computing the monthly mean values for those with higher frequency (ERA-Interim and NCEP-DOE).

TABLE 1. Summary of observational and reanalysis datasets used in this study.

		Temporal coverage	
Dataset	Spatial resolution	Available	Used
ISCCP-D2	2.5º x 2.5º	1983-2008 (monthly)	1984-2000
CRU TS 3.1	0.5º x 0.5º	1901-2009 (monthly)	1981-2000
ERA40	2.5º x 2.5º	1958-2001 (monthly)	1981-2000
ERA-Interim	1.5º x 1.5º	1989-present (6-hours)	1989-2000
NCEP/DOE AMIP-II	Global T62 Gaussian grid (192x94)	1979-2011 (6-hours)	1981-2000

Coupled Model Intercomparison Project 5 (CMIP5) Data

The main purposes of the CMIP5 project are to address outstanding scientific questions that arose as part of the IPCC AR4 (IPCC, 2007) process, to improve the understanding of climate and to provide climate data and estimates for future climate change that will be useful to the scientific community (Taylor *et al.*, 2012). In this work, the «Historical Experiment», which imposes changing conditions consistent with observations and simulates the climate system since 1850 to, at least, 2005, has been selected.

As previously mentioned, the use of a satellite simulator avoids ambiguities in the comparisons between model variables and satellite retrievals and also puts model intercomparison on a firmer basis by minimizing the impacts of how clouds are defined in different parameterizations (Bodas-Salcedo *et al.*, 2011). The Cloud Feedback Model Intercomparison Project (CFMIP) community has developed an integrated satellite simulator, the CFMIP Observation Simulator Package (COSP). COSP is a flexible software tool that enables the simulation from model variables of data from several satellite-borne active and passive sensors. It facilitates the use of satellite data to evaluate models in a consistent way. The main objective of CFMIP-2 is to make an improved assessment of climate change cloud feedbacks. Among the main activities of this project, the following should be highlighted: Incorporating COSP in a subset of the proposed mandatory CMIP-5 experiments and expanding the set of CMIP-5 experiments to include some that will help isolate the role of cloud processes and feedbacks.

From the whole set of available data, two variables have been used: the Total Cloud Fraction (clt), which indicates the percentage of the grid-cell that is covered by any kind of cloud, and the ISCCP Cloud Area Fraction (clisccp), where the cloud cover is specified for different atmospheric levels and optical thicknesses, facilitating the comparison with ISCCP satellite data. The models

TABLE 2. CMIP5 models used in this study. The number of runs used for each model is specified in the two last columns for total cloud fraction (clt) and ISCCP cloud fraction simulations, respectively.

Model identification	Institution (Country)	Atmospheric resolution	Ensemble size	
			clt	isccp
CanESM2	Canadian Centre for Climate Modeling and Analysis (Canada)	1.9º x 1.9º	1	
CCSM4	National Center for Atmospheric Research (USA)	0.9º x 1.25º	6	
CSIRO-Mk3.6	Commonwealth Scientific and Industrial Research Organization (Australia)	1.875º x 1.875º	10	
GFDL-CM3	NOAA Geophysical Fluid Dynamics Laboratory (USA)	200km	5	
GFDL-ESM2G			1	
GFDL-ESM2M			1	
GISS-E2-H	NASA Goddard Institute for Space Studies (USA)	2º x 2.5º	15	
GISS-E2-R	2º x2.5º	16		
HadGEM2-CC	Met Office (UK)	1.875º x 1.25º	3	
HadGEM2-ES		1.875º x 1.25º	4	
IPSL-CM5A-MR	Institut Pierre Simon Laplace (France)	1.25º x 2.5º	1	
IPSL-CM5A-LR		1.9º x 3.75º		5
MIROC-ESM-CHEM	University of Tokyo, Japan Agency for Marine-Earth Science and Technology, and National Institute for Environmental Studies (Japan)	2.8º x 2.8º	1	1
MIROC-ESM		2.8º x 2.8º	3	3
MIROC5		1.4º x 1.4º	4	3
MPI-ESM-LR	Max Planck Institute for Meteorology (Germany)	1.8º x 1.8º	3	1
MPI-ESM-P		1.8º x 1.8º	3	
MRI-CGCM3	Meteorological Research Institute (Japan)	280km	5	1
NorESM1-M	Norwegian Climate Centre (Norway)	1.9º x 2.5º	1	
INM-CM4	Institute for Numerical Mathematics (Russia)	2º x 1.5º	1	

used in this study are listed in Table 2. All the datasets, from satellite and models, have been regridded to a common grid (2.5° x 2.5°), and the mean annual cycle has been computed by monthly averaging each variable over 22 years to obtain 12 maps, one for each month.

As previously mentioned, the representation of clouds by climate models is a major challenge in the modeling of the Earth's climate. The ISCCP data and ISCCP simulator have been applied for over a decade in model assessments, which have allowed common biases in the climate models of clouds properties to be established: 1) the underestimation of total cloud, 2) the overestimation of optically thick cloud, and 3) the underestimation of low-level cloud (Kay *et al.*, 2012). Recent works, mainly using COSP and different satellite datasets (CALIPSO, PARASOL, MODIS, CERES, ...) find measurable improvements from CMIP3 to CMIP5 both in the cloud properties and cloud radiative effect (CRE). However, some problems remain mainly associated with the underestimation of the low-cloud cover and the overestimation of its optical thickness (Nam *et al.*, 2012). Further analysis of the tropical region shows that the good model simulations of tropical mean CREs are a result of compensating errors over different dynamical regimes.

INTERCOMPARISON OF OBSERVATIONAL DATA VERSUS MODELING CMIP5 DATASET

Total cloud cover in Africa

As previously mentioned, the comparison of different cloud cover databases is a difficult task because the values arise from different points of views. So, some differences between satellite data, ground observations and analysis results are due to this fact. Fig. 2 shows, in the first row, the mean annual and seasonal total cloud cover (TCC) values obtained from ISCCP data for the period 1984-2000. The full time period map shows a strong latitudinal dependence of the cloudiness over the continent. The TCC is higher in the equatorial area, and the effects of the Intertropical Convergence Zone (ITCZ) can be observed in seasonal maps, since the high values of TCC shifts latitudinally in response to the position of the maximum solar radiation throughout the seasons. Another area with high cloudiness, in the southern part of the study area, is associated with midlatitude cyclones. The region over the ocean, off the west coast of Namibia, also shows high TCC values, which will be explained below.

The total cloud cover differences between ISCCP and the other databases are also summarized in Fig. 2, lower rows. These differences have been computed, for each grid point, as the bias of the corresponding time series. Important differences, both positive and negative, can be observed in some areas and to facilitate their interpretation, the ISCCP cloud cover values classified by cloud types are shown in Fig. 3.

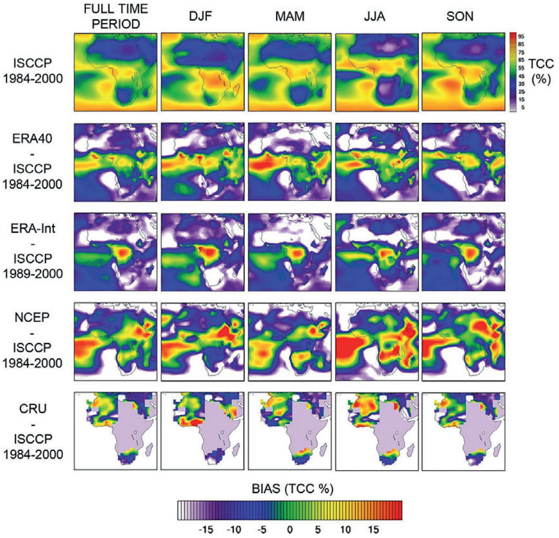

Figure 2. Annual and seasonal climatologies of TCC from ISCCP database (upper row) and the biases between the other datasets (ERA-40, ERA-Interim, NCEP-DOE and CRU TS 2.1) and ISCCP.

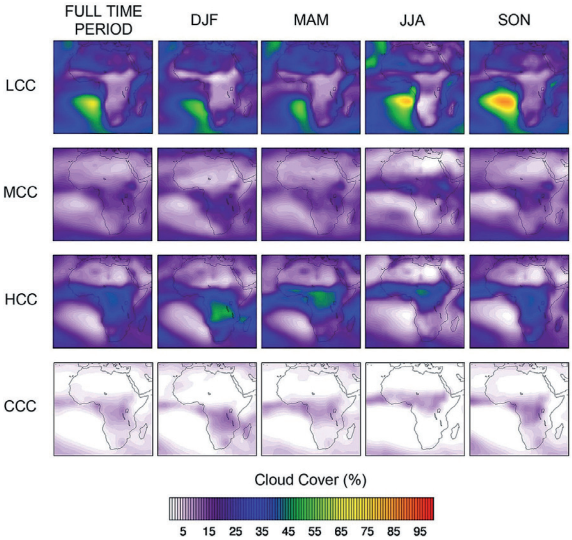

Figure 3. Annual and seasonal climatologies, obtained from ISCCP database, of different cloud types coverage: low, mid, high and convective clouds.

As can be observed from Figs. 2 and 3, ERA-40 data overestimate the cloud cover in the convective zone in the tropics. This behavior has been partially corrected in the ERA-Interim reanalysis, at least over the ocean, because over land the bias is higher than for ERA-40 data due to the improved representation of the deep convective triggering (Dee *et al.*, 2011). The overestimation of TCC in the Inter-Tropical Convergence Zone (ITCZ) could be due to the different sensitivities to thin cirrus detection; this kind of cloud is very difficult to detect from satellite data used in ISCCP (Stubenrauch *et al.*, 2013). ERA-40 data considerably underestimate the low cloud cover in two areas, the Canary Islands region and, mainly, off the Namibian coast, where important boundary layer cloud decks are formed due to the large-scale subsidence in the subtropical region and coastal upwelling-induced cold sea surface temperature. This underestimation has been considerably diminished, or even eliminated, in the ERA-Interim data probably due to the implementation of a new moist boundary-layer scheme (Köhler *et al.*, 2011). The TCC values are very low in the desert region of the northern African continent, but both databases, ERA-40 and -Interim analyses, underestimate them, producing lower values than those observed by satellites.

NCEP-DOE reanalysis largely overestimates cloud cover in the Atlantic Ocean region, where lower TCC values are measured by satellites, and at the same time, underestimates the marine boundary clouds, as in the case of ERA-40. It also overestimates the cloudiness in the region of the Horn of Africa and underestimates it in the storm track area. As previously mentioned, the number of ground stations available in the African continent to generate CRU TS 2.1 is very low, leaving many areas without adequate coverage. For this reason, in the last row of Fig. 2 the bias between CRU and ISCCP data is only shown in those grid points for which the CRU values have been computed from at least one ground station that belongs to their influence area. Due to this fact, the interpretation of the differences with ISCCP is very difficult.

For each grid point, the correlation between the time series of ISCCP and the other databases has also been computed. In Fig. 4, the corresponding values for the correlation coefficient are presented for the full time period and for the four seasons. In the latter case, only the months corresponding to each season were considered to create the time series from the different databases. Furthermore, Table 3 summarizes these results for the whole study area, indicating the percentage of grid points whose correlation coefficient is larger than 0.7 for each dataset and season. For CRU, the percentage of pixels with correlation higher than 0.7 was calculated using only those grid points considered in Fig. 4. ERA-Interim data present good correlations in practically all areas and seasons, more than 80% of the grid points have a correlation coefficient greater than 0.7 in the annual time series. ERA-40 cannot reproduce the marine boundary layer cloud cover variations measured in ISCCP project during the season of maximum coverage (SON), and NCEP-DOE reanalysis has a similar behavior but for all the four seasons. For these three databases, the lower percentage of grid points with

TABLE 3. Percentage of grid cells in the study area with r>0.7, for each database compared with ISCCP.

	ISCCP vs. ERA-40	ISCCP vs. ERA-Int.	ISCCP vs. NCEP	ISCCP vs. CRU TS 2.1	
	1984-	1989-	1984-	1984-	1996-
	2000	2000	2000	1995	2000
Annual	61.73	81.73	37.49	91.21	50.30
DJF	47.97	74.63	14.98	46.15	8.58
MAM	50.65	72.12	23.64	63.74	34.02
JJA	21.20	49.44	11.17	46.15	31.66
SON	45.97	59.05	31.52	81.91	56.21

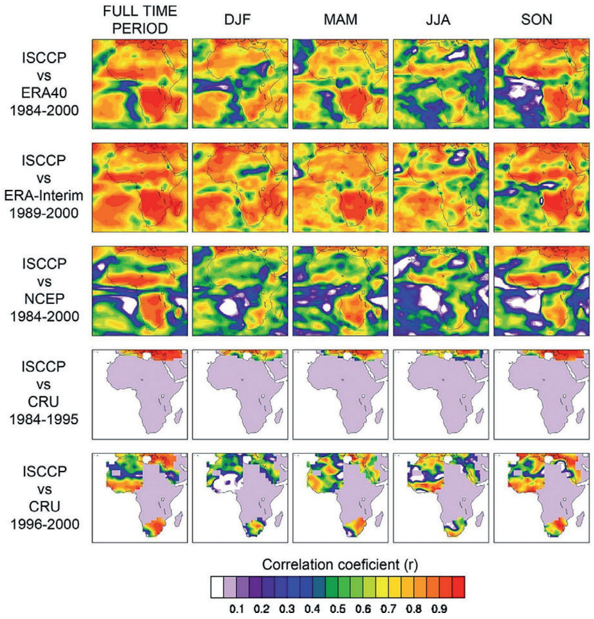

Figure 4. Correlation map of TCC from ISCCP and from the other datasets (ERA-40, ERA-Interim, NCEP-DOE and CRU TS 2.1).

TABLE 4. Percentage points in the study area with rms<15%, for each database compared with ISCCP.

	ISCCP vs. ERA-40	ISCCP vs. ERA-Int.	ISCCP vs. NCEP	ISCCP vs. CRU TS 2.1	
	1984-2000	1989-2000	1984-2000	1984-1995	1996-2000
Annual	66.15	61.47	44.42	78.02	81.36
DJF	72,90	68,57	51,08	89,01	74,85
MAM	59,39	57,84	49,09	64,83	81,36
JJA	66,93	66,23	50,04	87,91	71,60
SON	69,52	64,07	51,17	74,73	78,11

correlation coefficients larger than 0.7 occur during the northern hemisphere summer. CRU data were divided into two periods, 1984-1995 and 1996-2000, to show the evolution in the number of ground based cloud cover measurements included in the CRU TS 2.1 dataset. It can be observed that, in the Mediterranean area, where the ground measurements are denser, the correlation is higher than in other regions with sparse measurement stations. In fact, the percentage of points with $r>0.7$ is over 90% for the annual time series and for the period 1984-1995. The lower correlations occur at the north of the Guinean Gulf during DJF season, when high clouds are the prevalent cloud type measured by satellites. This low correlation between both databases could be partially due to different points of views used for observations: from the top of the atmosphere and from the ground. In this case, the percentage of grid points with $r>0.7$ is lower than 10%.

The root mean square (rms) errors, for each grid point, between ISCCP and the selected databases have been also computed. Table 4 summarises the percentage of these points with rms lower than 15% for each dataset. The lower errors correspond to the CRU database, at least in those locations where cloud cover measurements are computed from real ground observations. The behavior of the ECMWF databases is very similar, and better than the results of the NCEP.

TOTAL CLOUD COVER TRENDS

Africa is a large continent with regions of different geological, biological and climate characteristics. For this reason, the cloudiness trends have been studied for particular regions and not for the whole area. As previously analyzed,

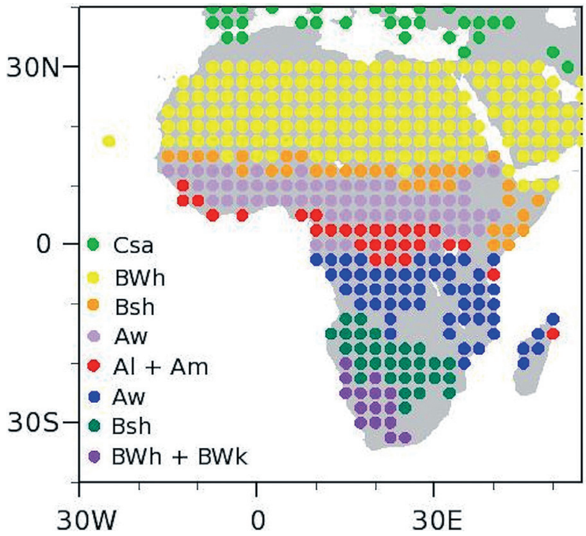

Figure 5. Climate areas used in this study.
See text for explanation.

there is a clear effect of the latitude on the cloud cover, so the total study area could be divided into several zones at different latitudes. However, the use of a well-defined climate classification map was preferred, specifically an update of the widely used Köppen-Geiger climate classification map based on the precipitation data provided by CRU (Kottek *et al.*, 2006). The main areas used for this study are represented in Fig. 5, where the corresponding grid points have been labelled using the same nomenclature used in the original map. These areas are: Csa (warm temperate climate with dry and hot summer), BWh (desert climate, hot and arid), BSh (steppe climate, hot and arid), Aw (equatorial savannah with dry winter), Al (equatorial rainforest, fully humid), Am (equatorial monsoon) and BWk (desert climate, cold and arid).

The monthly means of cloud cover have been averaged for each climate region, creating a time series for each of them. Then, the overall trends of these new time series have been computed by least square linear fitting, checking that the significance of all of them are over the 95% level. An example of the time series for the region labelled as Csa, located in the northern part of the study area, is plotted in Fig. 6. It shows the time series and the corresponding linear trend for each database. The trends have been computed for the minimum common time period available, in order to make the results comparable. The trends for the different defined areas and each dataset are given in Table 5. If two regions have the same climate characteristics, for example there are two Bsh regions

TABLE 5. Trends of total cloud cover (%/decade)
for each dataset and each climate area represented in Figure 5.

	ERA40	ERA-Int.	ISCCP	NCEP	CRU
Csa	-1.03%	-2.12%	-4.82%	-0.31%	0.19%
BWh	-1.39%	0.30%	-2.87%	0.27%	-
Bsh(N)	-2.20%	3.94%	-1.66%	-1.88%	-
Aw(N)	-6.72%	-0.38%	-0.87%	-1.19%	-
Al+Am	-3.15%	-0.38%	-2.69%	0.77%	-
Aw(S)	-3.41%	-1.21%	-1.30%	0.95%	-
Bsh(S)	-0.67%	2.15%	-1.47%	5.13%	-
BWh+BWk	0.38%	-1.18%	-1.97%	4.75%	-

due to the relative symmetry with respect to the equator, they have been labeled as (N) or (S) depending on whether they belong to the northern or southern hemispheres. Satellite data from ISCCP present negative trends in every climate area, according to studies on global trends in TCC using ISCCP data for the same period (e.g. Norris and Slingo, 2009), however, trends obtained from ground observations or even other satellites are positive (Norris and Slingo, 2009; Wylie *et al.*, 2005). Some authors argue that this negative trend is due to some artifacts in ISCCP data, although, as explained previously, the African continent is not strongly affected by variations in the observational angles.

ERA-Interim also has negative trends in many areas, except in those where the differences with ISCCP are larger (Fig. 2). However, the analysed differences between ERA-40 and ISCCP are larger and the trends are negative in all areas except one. As can be expected, the NCEP trends are the most different from ISCCP, as occurred with the analysis of TCC maps. For the CRU dataset, the cloud cover trend has only been computed for the northern climate area, as for the other regions the time series are too short.

CMIP5 INTERCOMPARISON VERSUS ISCCP DATA

For the Total Cloud Cover (TCC), the mean bias, the centered root mean square error and the correlation between each model's results and ISCCP measurements have been computed over the twelve monthly mean maps, weighting each grid cell by the corresponding fraction of the total area. The results have been summarized using a Taylor diagram (Fig. 7) as suggested, for example,

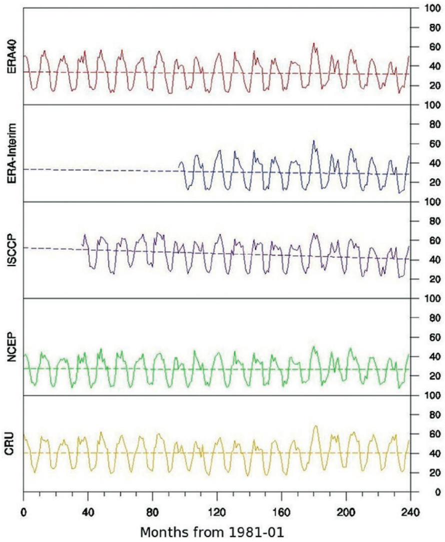

Figure 6. TCC time series for the northern climate area and each database.

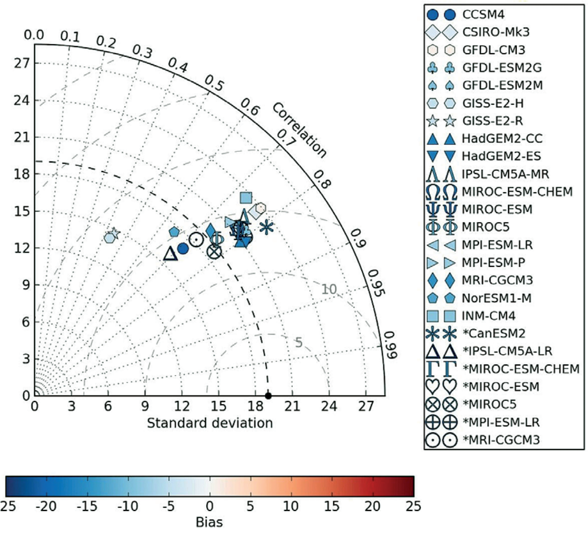

Figure 7. Taylor diagram of TCC, comparing the CMIP5 models and ISCCP data. Models marked with * correspond to TCC computed using an ISCCP simulator.

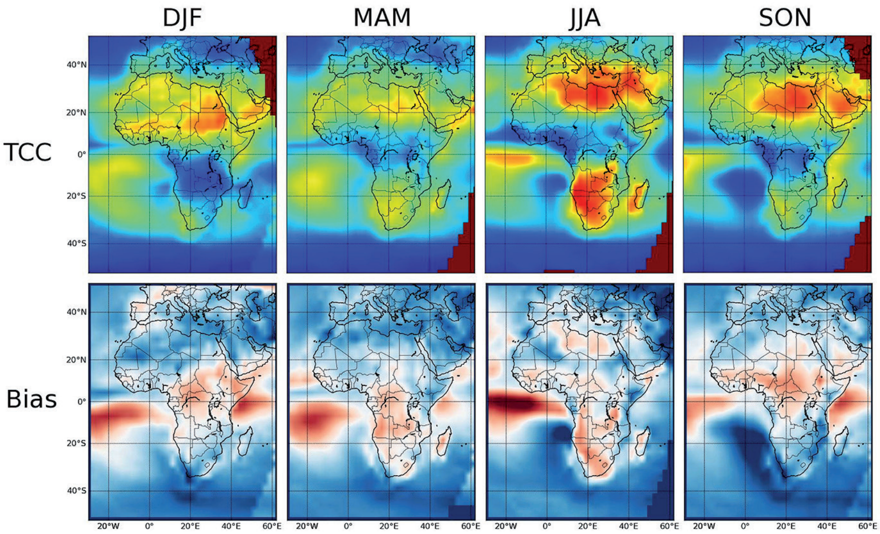

Figure 8. TCC from ISCCP data (upper row) and mean bias of CMIP5 models for each season.

in Pincus *et al.* (2008). As can be observed, the results are very similar for the studied models, except for the GISS models, which show worse results. It is also noticeable that all the models, except GFDL-CM3, show a negative bias when they are compared to ISCCP data, which means that they produce lower cloud covers from their simulations. To check the spatial distribution, the seasonal biases have been computed for each model and then the mean bias of the models has been calculated. This is shown in Fig. 8 together with the seasonal TCC obtained from ISCCP data. Examining Figs. 3 and 8, the general underestimation of TCC can be observed, the larger biases corresponding to those areas where the formation of marine boundary layer clouds is more important, specially the area off the Namibian coast. The models also overestimate TCC near the equator in those areas where ISCCP data show low TCC values, probably due to the lack of detection of very thin cirrus clouds by the satellites used to create the ISCCP dataset. Similar statistical analysis have been performed for the three types of clouds for those CMIP5 models which provide the ISCCP model outputs as prescribed by CFMIP-2, and their results are shown in Fig. 9. The results for low, mid and high clouds covers are significantly worse than for TCC, indicating that the models can simulate the cloud cover, but not their vertical position in the atmosphere. However, the errors in the cloud top determination from satellite data must be also taken into account.

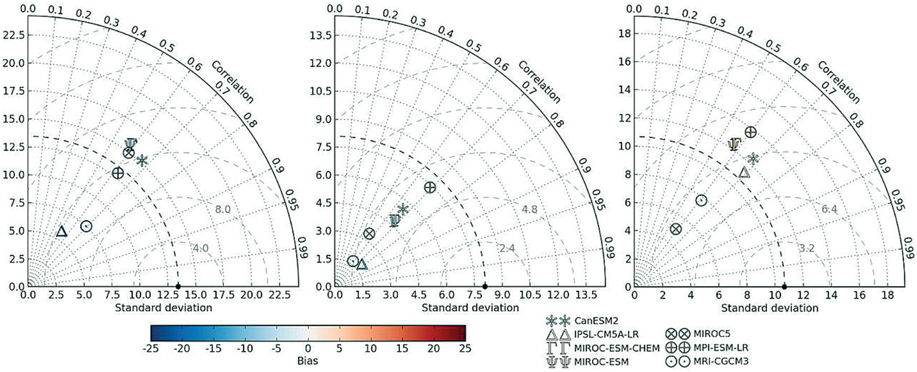

Figure 9. Taylor diagram for low (LCC), mid (MCC) and high (HCC) cloud cover, comparing the CMIP5 models and ISCCP data.

From the CMIP5 models, the lower-tropospheric stability (LTS), defined by the difference in potential temperature between 700 and 1000 hPa levels, has also been calculated for the Namibian low cloud region and compared to the stability computed from NCEP reanalysis data. The stability in this region is underestimated by the models, which can be one of the causes of the underestimation of low cloud cover. A relationship between worse model estimation of stability and worse cloud cover results was also observed. However, further analyses are necessary to investigate other possible causes of the observed deviations between models and satellite data.

SUMMARY AND CONCLUSIONS

The IPCC 2007 confirms that substantial progress has been made in the goal of improving the modeling of clouds in climate models. Cloud feedbacks have been confirmed as a primary source of the remaining uncertainties, with low clouds making the largest contribution. Using observational and reanalysis data (ISCCP, CRU, ERA-40, ERA-Interim and NCEP R2), this work has assessed the simulated multi-year mean of total cloud cover by CMIP5 models over the African CORDEX Domain. Table 1 and Table 2 summarize the observational/reanalysis and CMIP5 databases characteristics, respectively.

In general the databases in Table 1 underestimate the ISCCP TCC value. By season, all the TCC values are underestimated. The best correlation coefficients both for the global period and by season are obtained by the ERA-Interim database (see Table 3). The worst period is the second half of the year. The NCEP-R2 shows the worst correlation values. ERA-40 presents the best RMS values (see Table 4), although the ERA-Interim shows very similar RMS values.

The evaluation of the TCC trends from observational datasets, both from ground-based and from satellite measurements are quite controversial because of the important uncertainties associated with each dataset. The artifacts associated with ISCCP data have been studied in depth, but even when view angle artifacts associated with changes in the number and position of geostationary satellites are statistically removed, other apparently spurious variability remains. For example, coincident variations in cloud amount are seen across the entire view area of a geostationary satellite (Norris, 2000). From the Extended Edited Cloud Reports Archive (EECRA, Hahn *et al.*, 2009, updated 2012), which is available online at the Carbon Dioxide Information Analysis Center: http://cdiac.ornl.gov/epubs/ndp/ndp026c/ndp026c.html and from the information available at http://www.atmos.washington.edu/CloudMap/, Warren *et al.* (2007) have estimated a global average trend of total cloud cover over land of –0.7%/decade, offsetting the small positive trend that had been found for the ocean, and resulting in no significant trend for the land–ocean average. Later studies have shown a global average trend of cloud cover in the order of –0.4 % per Decade. Declining clouds in middle latitudes at high and middle levels appear responsible for this trend. ISCCP data analyzed in this study showed trends in the range –4.82 to –0.87 %/decade depending on the climate area defined in Table 5.

Comparing the CMIP5 TCC values with those obtained from ISCCP there is a general tendency of the models to underestimate the TCC. There are remarkable differences between models depending on the different parameterizations that each model uses. To better understand these differences, the cloud types, as defined in the ISCCP product, have been compared. The low clouds are systematically underestimated (a slight underestimation for the medium clouds is also observed) and the high clouds are overestimated. The situation associated with the low clouds has been widely reported in the literature. The so-called «too few, too bright» problem associated with an underestimation of the low cloud cover and an overestimation of the cloud optical depth were detected in the CMIP3 project and remains in CMIP5 (Nam *et al.*, 2012). The correlations for the TCC are between 0.7 - 0.8 and between 0.6 - 0.7 if calculated for low, mid and high clouds.

It is of interest to evaluate other cloud properties such as cloud top pressure, liquid and ice water paths, diurnal cycle and the relation of these properties with environmental parameters such as lower tropospheric stability or the 500 hPa vertical velocity. Future studies are planned to evaluate the influence of the spatial resolution on the modeling of cloud properties using dynamic downscaling with the Weather Research and Forecasting (WRF) modeling system. The increase of the spatial resolution over Africa (aprox. 50 km) and over the Canary Islands (aprox. 5 km) allows different parameterizations (i.e. microphysics, planetary boundary layer, land-surface, etc.) of the components of the climate system with mesoscale resolution to be tested. To make projections over the 21st century of cloud properties, it is essential that climate models reproduce the actual climatology with a high confidence.

ACKNOWLEDGEMENTS.

The authors acknowledge the MEC (Ministry of Education and Science, Spain) for the following support: projects CGL2008-04740/CLI, CGL2010-22158-C02-01 and CGL2010-21366-C04-01. They also acknowledge the World Climate Research Programme's Working Group on Coupled Modeling, which is responsible for CMIP, and the climate modeling groups (listed in Table 1) for producing and making available their model output. For CMIP the U.S. Department of Energy's Program for Climate Model Diagnosis and Intercomparison which provides coordinating support and led the development of software infrastructure in partnership with the Global Organization for Earth System Science Portals. The ISCCP D2 data were obtained from the International Satellite Cloud Climatology Project web site (http://isccp.giss.nasa.gov) maintained by the ISCCP research group at the NASA Goddard Institute for Space Studies. Finally thanks to all institutions and researchers involved in the generation of the reanalysis databases: NCEP/DOE AMIP-II, ERA-40 and ERA-Interim.

REFERENCES

Bodas-Salcedo, A., Webb, M.J., Bony, S., Chepfer, H., Dufresne, J.L., Klein, S.A., Zhang, Y., Marchand, R., Haynes, J.M., Pincus, R. and John, V.O., 2011. COSP Satellite simulation software for model assessment. *Bulletin of the American Meteorological Society,* 92(8).

Campbell, G., 2004. View angle dependence of cloudiness and the trend in ISCCP cloudiness. *13th AMS Conference on Satellite Meteorology and Oceanography.* 20-23 September Norfolk, VA, USA.

Chou, M.D., 1992. A Solar-Radiation Model for use in Climate Studies. *Journal of the Atmospheric Sciences,* 49(9).

Chou, M.D. and Lee, K.T., 1996. Parameterizations for the absorption of solar radiation by water vapor and ozone. *Journal of the Atmospheric Sciences,* 53(8),.

Dee, D.P., Uppala, S.M., Simmons, A.J., Berrisford, P., Poli, P., Kobayashi, S., Andrae, U., Balmaseda, M.A., Balsamo, G., Bauer, P., Bechtold, P., Beljaars, A.C.M., Van De Berg, L., Bidlot, J., Bormann, N., Delsol, C., Dragani, R., Fuentes, M., Geer, A.J., Haimberger, L., Healy, S.B., Hersbach, H., Holm, E.V., Isaksen, L., Kallberg, P., Koehler, M., Matricardi, M., Mcnally, A.P., Monge-Sanz, B.M., Morcrette, J.-., Park, B., Peubey, C., De Rosnay, P., Tavolato, C., Thepaut, J.-. and Vitart, F., 2011. The ERA-Interim reanalysis: configuration and performance of the data assimilation system. *Quarterly Journal of the Royal Meteorological Society,* 137(656).

Eastman, R., Warren, S.G. and Hahn, C.J., 2011. Variations in Cloud Cover and Cloud Types over the Ocean from Surface Observations, 1954-2008. *Journal of Climate,* 24(22).

Eastman, R. and Warren, S.G., 2012. A 39-Year Survey of Cloud Changes from Land Stations Worldwide 1971-2009: Long-Term Trends, Relation to Aerosols, and Expansion of the Tropical Belt. *Journal of Climate.*

Evan, A.T., Heidinger, A.K. and Vimont, D.J., 2007. Arguments against a physical long-term trend in global ISCCP cloud amounts. *Geophysical Research Letters,* 34(4), pp. L04701.

Giorgi, F., Jones, C. and Asrar G.R., 2009. Addressing climate information needs at the regional level: the CORDEX framework. *WMO Bulletin* 58(July):175–183

IPCC, 2007. *Climate Change 2007: The Physical Science Basis. Contribution of Working Group I to the Fourth Assessment Report of the Intergovernmental Panel on Climate Change [Solomon, S., D. Qin, M. Manning, Z. Chen, M. Marquis, K.B. Averyt, M.Tignor and H.L. Miller (eds.)].* Cambridge, United Kingdom and New York, NY, USA: Cambridge University Press.

Kanamitsu, M., Ebisuzaki, W., Woollen, J., Yang, S.K., Hnilo, J.J., Fiorino, M. and Potter, G.L., 2002. NCEP-DOE AMIP-II reanalysis (R-2). *Bulletin of the American Meteorological Society,* 83(11).

Kay, J.E., Hillman, B.R., Klein, S.A., Zhang, Y., Medeiros, B., Pincus, R., Gettelman, A., Eaton, B., Boyle, J., Marchand, R. and Ackerman, T.P., 2012. Exposing Global Cloud Biases in the Community Atmosphere Model (CAM) Using Satellite Observations and Their Corresponding Instrument Simulators. *Journal of Climate,* 25(15).

Köhler, M., Ahlgrimm, M. and Beljaars, A., 2011. Unified treatment of dry convective and stratocumulus-topped boundary layers in the ECMWF model. *Quarterly Journal of the Royal Meteorological Society,* 137(654).

Kottek, M., Grieser, J., Beck, C., Rudolf, B. and Rubel, F., 2006. World map of the Koppen-Geiger climate classification updated. *Meteorologische Zeitschrift,* 15(3),.

Loeb, N.G., Wielicki, B.A., Doelling, D.R., Smith, G.L., Keyes, D.F., Kato, S., Manalo-Smith, N. and Wong, T., 2009. Toward Optimal Closure of the Earth's Top-of-Atmosphere Radiation Budget. *Journal of Climate,* 22(3).

Mitchell, T.D. and Jones, P.D., 2005. An improved method of constructing a database of monthly climate observations and associated high-resolution grids. 25.

Nam, C., Bony, S., Dufresne, J. and Chepfer, H., 2012. The 'too few, too bright' tropical low-cloud problem in CMIP5 models. *Geophysical Research Letters,* 39, pp. L21801.

Norris, J.R., Slingo, A., 2009. Trends in observed cloudiness and Earths radiation budget: what do we not know and what do we need to know? In: Heintzenberg J., Charlson R.J. (eds) Clouds in the Perturbed Climate System, MIT Press, pp 17–36.

Norris, J.R., 2000. What can cloud observations tell us about climate variability? *Space Science Reviews,* 94(1-2).

Pincus, R., Batstone, C.P., Hofmann, R.J.P., Taylor, K.E. and Glecker, P.J., 2008. Evaluating the present-day simulation of clouds, precipitation, and radiation in climate models. *Journal of Geophysical Research-Atmospheres,* 113(D14), pp. D14209.

Pincus, R., Platnick, S., Ackerman, S.A., Hemler, R.S. and Hofmann, R.J.P., 2012. Reconciling Simulated and Observed Views of Clouds: MODIS, ISCCP, and the Limits of Instrument Simulators. *Journal of Climate,* 25(13).

Randall, D.A., Coakley, J.A., Fairall, C.W., Kropfli, R.A. and Lenschow, D.H., 1984. Outlook for Research on Sub-Tropical Marine Stratiform Clouds. *Bulletin of the American Meteorological Society,* 65(12).

Rossow, W.B. and Schiffer, R.A., 1999. Advances in understanding clouds from ISCCP. *Bulletin of the American Meteorological Society,* 80(11).

Schiffer, R.A. and Rossow, W.B., 1983. The International-Satellite-Cloud-Climatology-Project (Isccp) - the 1st Project of the World-Climate-Research-Programme. *Bulletin of the American Meteorological Society,* 64(7).

Stephens, G.L., 2005. Cloud feedbacks in the climate system: A critical review. *Journal of Climate,* 18(2).

STUBENRAUCH, C., KINNE, S. and TEAM, C.A., 2009. Assessment of Global Cloud Climatologies. *GEWEX Newsletter* 19(1), 6–7.

STUBENRAUCH, C.J., ROSSOW W. B., KINNE S., ACKERMAN S., CESANA G., CHEPFER H., DI GIROLAMO L., GETZEWICH B., GUIGNARD A., HEIDINGER A., MADDUX B., MENZEL P., MINNIS P., PEARL C., PLATNICK S., POULSEN C., RIEDI J., SUN-MACK S., WALTHER A., WINKER D., ZENG S. and ZHAO G., 2013. Assessment of Global Cloud Datasets from Satellites. submitted to *Bulletin of American Meteorological Society.*

TAYLOR, K.E., STOUFFER, R.J. and MEEHL, G.A., 2012. An Overview of Cmip5 and the Experiment Design. *Bulletin of the American Meteorological Society,* 93(4),.

UPPALA, S.M., KALLBERG, P.W., SIMMONS, A.J., ANDRAE, U., BECHTOLD, V.D., FIORINO, M., GIBSON, J.K., HASELER, J., HERNANDEZ, A., KELLY, G.A., LI, X., ONOGI, K., SAARINEN, S., SOKKA, N., ALLAN, R.P., ANDERSSON, E., ARPE, K., BALMASEDA, M.A., BELJAARS, A.C.M., VAN DE BERG, L., BIDLOT, J., BORMANN, N., CAIRES, S., CHEVALLIER, F., DETHOF, A., DRAGOSAVAC, M., FISHER, M., FUENTES, M., HAGEMANN, S., HOLM, E., HOSKINS, B.J., ISAKSEN, L., JANSSEN, P.A.E.M., JENNE, R., MCNALLY, A.P., MAHFOUF, J.F., MORCRETTE, J.J., RAYNER, N.A., SAUNDERS, R.W., SIMON, P., STERL, A., TRENBERTH, K.E., UNTCH, A., VASILJEVIC, D., VITERBO, P. and WOOLLEN, J., 2005. The ERA-40 re-analysis. *Quarterly Journal of the Royal Meteorological Society,* 131(612).

WEARE, B.C., 2000. Near-global observations of low clouds. *Journal of Climate,* 13(7),.

WEARE, B.C., 2004. A comparison of AMIP II model cloud layer properties with ISCCP D2 estimates. *Climate Dynamics,* 22(2-3).

WYLIE, D., JACKSON, D.L., MENZEL, W.P. and BATES, J.J., 2005. Trends in global cloud cover in two decades of HIRS observations. *Journal of Climate,* 18(15).

REGIONAL CLIMATE MODELING ACTIVITIES OVER SOUTH AMERICA: FROM EARLY EFFORTS TO CORDEX

Silvina A. Solman

CLIMATE CHANGE PERSPECTIVES FROM THE ATLANTIC:
PAST, PRESENT AND FUTURE
Jose María Fernández-Palacios, Lea de Nascimento, José Carlos Hernández,
Sabrina Clemente, Albano González & Juan P. Díaz-González (coords)
Servicio de Publicaciones, Universidad de La Laguna – 2013

ISBN: 978-84-15910-54-1 pp. 641-664

Abstract

This review summarizes the progress achieved during the last decade on regional climate modeling activities over South America. From the early efforts at the beginning of the 2000s, simulations with Regional Climate Models (RCMs) have been performed for several purposes over the region. This paper describes the most outstanding contributions from the isolated efforts to the on-going coordinated RCM activities in the framework of the CLARIS-LPB and CORDEX initiatives, which represent a major endeavor to produce ensemble climate-change projections at regional scales. The remaining challenges in modeling South American climate features are also discussed.

Keywords: Regional Climate Models, South America, CORDEX

INTRODUCTION

One of the main motivations for developing Regional Climate Models has been the need for producing climate information at the regional level to assess the impacts of climate change. It is a well known fact that, to date, Atmosphere-Ocean Global Models (AOGCMs) are the only tools available to predict the future evolution of the climate system in response to anthropogenic forcings, such as increases in greenhouse gas (GHG) concentrations. During the last decades, coupled global models have been continuously improved, mostly due to increasing computational capacity and improved representation of different components of the climate system: the atmosphere, the oceans and the land-surface. However, the most updated global models within the suit of the CMIP5 initiative (Stouffer *et al.*, 2011) operate on horizontal resolutions of the order of a hundred of kilometers (Taylor *et al.*, 2011).

The lack of regional detail in current AOGCMs limits their capability in capturing regional scale processes forced by topographic features or other regional scale forcings. These regional scale forcings are responsible of modulating the large scale circulation features that determine the regional climate. Moreover, coarse resolution also limits the applicability of global model outputs for impact studies that demand information on much finer spatial scales. Since the early 90s, Regional Climate Models (RCMs) became the most widespread methodology to add further detail to

Figure 1: Topographic features of the South American continent.

global climate simulations. After the pioneering work by Giorgi and Mearns (1991), the development of regional climate models has led to increased resolution, longer model simulations, and developments towards regional climate system models. During recent years, coordinated efforts for several regions of the world have started to emerge to further improve not only the quality of the RCM results but also to explore the associated uncertainty of the regional climate model products. The CORDEX initiative (Giorgi *et al.*, 2009) is an excellent example of a coordinated effort all around the world which aims to further advance the state-of-the-art in regional climate modeling and to provide valuable information for the impact community.

South American climate and its variability are affected by remote, regional and local forcings. Owing to its considerable meridional extension and prominent orography, South America exhibits diverse patterns of weather and climate, including tropical, subtropical and extratropical features The most important feature of the regional geography is the complex Andes chain, which extends all along the western coast and is characterized by a narrow barrier channeling the flow in the central part of the continent (Fig.1). The Andes not only act as a climatic wall with dry conditions to the west and moist conditions to the east at tropical/subtropical latitudes (the pattern reverses in midlatitudes) but they also foster tropical–extratropical interactions, especially along their eastern side.

The seasonal migration of the Inter-tropical convergence zone (ITCZ) largely controls climate conditions over the northern part of the continent. During the austral summer season the large scale circulation at upper levels is characterized by a high pressure centre over the Altiplano, a trough extending from northeast Brazil towards subtropical latitudes over the Atlantic Ocean and westerly circulation over subtropical and higher latitudes. At low levels, the semi-permanent subtropical highs over the Atlantic and Pacific oceans, dominate the large scale features. Easterly flow from the Atlantic Ocean is channeled southward by the Andes mountains into the Chaco low, which represents the main source of moisture over southern Brazil and the subtropical plains of southern South America. One of the major components of the continental warm season precipitation regime over tropical and subtropical latitudes is the South American Monsoon system (SAMS) (Vera *et al.*, 2006a). Over the southern part of the continent, synoptic activity is dominated by the presence of the Pacific storm-track and its interaction with the Andes.

During winter the recurrent passages of cold fronts progressing northeastward east of the Andes from subpolar latitudes and the upper level troughs propagating eastward at subtropical latitudes are the triggering factors for strong cyclogenesis over eastern South America. The presence of the Pacific subtropical high, its seasonal meridional shift and the sea surface temperature over the subtropical Pacific Ocean define the seasonal cycle of precipitation west of the Andes.

The variability of the South American climate from intraseasonal to interdecadal time-scales results from the superposition of several large-scale phenomena: El Niño-Southern Oscillation (ENSO); the control exerted by anomalous sea surface temperature (SST) over subtropical Atlantic and Pacific Oceans, mainly over sub-tropical latitudes; SST anomalies over the tropical North Atlantic Ocean which affect climate variability over the Amazonia and North-eastern Brazil; high-latitude forcing, such as by the Antarctic Oscillation (AAO) and the North Atlantic Oscillation (NAO) also play a role in climate variability over South America. A thorough review of the main characteristics of the South American climate and its variability can be found in Garreaud *et al.* (2008) and references therein.

Owing to the variety of dynamical mechanisms controlling South American climate and its variability, modeling regional climate seems to be a challenging goal. Regional climate modeling efforts over the South American continent have been increasingly developed during the last decade. This article presents an overview of the development of regional climate modeling activities over South America during the last 10 years, with the aim of highlighting the major achievements and shortcomings. Two outstanding initiatives led to an enormous progress on producing valuable information for impact assessment studies. These are the CLARIS Project (Boulanger *et al.*, 2010) - CLARIS-LPB Project (Boulanger *et al.*, 2011) and CORDEX (Giorgi *et al.*, 2009). Progress in modeling the South American climate within these major coordinated initiatives is described in Section 3. On-going activities within the CORDEX-South America framework are presented together with the expected outcomes in Section 4. Outstanding questions associated with remaining challenges are reviewed in Section 5. This review of modeling activities over South America is far for being complete but the most relevant results leading to further improvements are mentioned. The references provided are not exhaustive and the discussion regarding main achievements does not venture into deep detail.

REVIEW OF REGIONAL CLIMATE MODELING ACTIVITIES OVER SOUTH AMERICA

As stated in the introduction, the early developments in regional climate modeling were focused on simulating North-American climate during the early 90s (Dickinson *et al.*, 1989; Giorgi, 1990). The pioneering studies using RCMs over South America focused mainly on seasonal scale simulations. The first study was published by Menéndez *et al.* (2001) who developed a numerical nesting system to simulate wintertime climate of the eastern South Pacific-South America-western South Atlantic region, using a limited area model (the Limited Area Hibu Model-LAHM) driven by the LMDZ GCM. A similar study was performed by Nicolini *et al.* (2002) who simulated ten separate 30-day simulations for both January and July, nesting the CSIRO Division of Atmospheric Research limited area model (DARLAM) into the CSIRO GCM. Though these very first efforts lead to encouraging results, the regional model domains covered only the southern part of the South American continent and they were both limited due to computational constraints.

Nobre *et al.* (2001) and Misra *et al.* (2002; 2003) performed several seasonal scale simulations focused mainly on the northern part of South America with the aim of evaluating the capability of the nesting modeling system to reproduce the interannual variability signal associated with ENSO. Precipitation and circulation features for two extremes ENSO events (La Niña and El Niño) were evaluated and discussed.

All these preliminary efforts were focused mainly on evaluating the capability of RCMs in improving the description of climatic features compared with the driving GCMs.

After these preliminary results, several studies devoted to assess the sensitivity of RCM simulations to model configuration came out. Examples of these studies can be found in Seth and Rojas (2003) and Rojas and Seth (2003) who performed seasonal-scale simulations using the RegCM model nested into both reanalysis and GCMs. They discussed the sensitivity of seasonal simulations to domain-size, to changes in surface forcing (local land-use over the Amazon and soil moisture) and to the quality of the driving GCM. The focus of these studies was mainly on the tropical South American region and the model domain covered the tropics and extended to the sub-tropical areas. Seth *et al.* (2004) explored the capability of the RegCM3 RCM to reproduce daily rainfall statistics on sub-seasonal timescales over several South American regions. Rojas (2006) analyzed a triply-nested two-way-interacting domains centered over the eastern South Pacific and the western coast of southern South America, with horizontal grid intervals of 135, 45, and 15 km, respectively, using the MM5 model driven by reanalysis. This study was concentrated on exploring to what extent increasing resolution influences the simulation of precipitation processes over a region of complex topography.

It is worth to recall the study by Fernandez *et al.* (2006) in which a preliminary RCM intercomparison exercise was performed. These authors performed simulations of the summertime climate over tropical South America with the RegCM3 and the climate version of the CPTEC Eta model. The aim of this work was to evaluate the capability of the two models in simulating the mean climatological features of the summer quasi-stationary circulations over South America. As for the previous studies, the length of the simulations was limited to the seasonal scale and the domain covered partially the South American continent. Moreover, the authors highlighted common shortcomings on the simulations performed with two RCMs and recommended that tuning the regional models was necessary on order to improve the capability of the models in reproducing the mean climatic conditions over several regions of South America.

Taking into account the individual modeling efforts described, most of them focused on the assessment of model performance for mean climatic conditions, mainly for precipitation and temperature, for individual seasons and particular regions. However, not all the modeling exercises covered the same domain neither the simulations covered the same time-period, consequently it was not able to look for agreement or disagreement among models' behavior. Moreover, the metrics employed for evaluating model performance were diverse, mainly due to each of the studies aimed to evaluate the model capability to reproduce different features of the South American climate.

During the early 2000's regional climate modeling activities over other regions of the word, mostly over North America and Europe were already examining extended simulations, from one to three decades. The aims of these studies were twofold. First, to evaluate regional climate models' behavior in reproducing present climate conditions nesting the RCMs either into perfect-boundary conditions (reanalysis) or AOGCMs (Giorgi, 1990; Giorgi *et al.*, 2004a; Leung *et al.*, 2003; Liang *et al.*, 2004 and references therein). Second, to assess the regional climate change signal simulated by a RCM nested within time-slice atmospheric AOGCM experiments (Giorgi *et al.*, 2004b; Räisänen *et al.*, 2001 and references therein). These studies were mostly devoted to evaluate the added value of RCMs and to explore the projected changes in mean climate under specified emission scenarios.

These advances in the regional climate modeling community motivated further studies over South America in which the simulated period was enlarged to several decades (Seth *et al.*, 2007; Rauscher *et al.*, 2007; Solman *et al.*, 2008; da Rocha *et al.*, 2009; Reboita *et al.*, 2010a and 2010b; Silvestri *et al.*, 2009, Pesquero *et al.*, 2009, among others). These studies were mostly focused on evaluating the capability of RCMs in reproducing different aspects of the South American climate, nesting the models into either reanalysis or GCMs. The regional models mostly used in these studies were the RegCM3; MM5, ETA and REMO. References about the models can be found in the referred articles.

The first set of RCM simulations devoted to produce high-resolution climate change scenarios over the South American region was performed by Nuñez *et al.* (2009).They nested the MM5 RCM into the Hadley Center Atmospheric Global Model (HadAM3) and simulated three 10-year periods representing present and future climate conditions for the end of the twenty first century, respectively, under two emission scenarios: A2 and B2. The domain in their simulations spanned from the subtropics to the southern tip of South America. Garreaud *et al.* (2009) evaluated the regional climate change signal over the western coast of the continent from a 30-year simulation using the PRECIS RCM nested into the HADAM3 AGCM. Their domain was centered on central Chile and extended from the subtropics to the southern tip of South America and from the eastern Pacific to central Argentina. Marengo *et al.* (2009) and Marengo *et al.* (2011) performed a 30-year simulation but using the PRECIS and the ETA RCMs, respectively, both RCMs were nested into the HADAM3 AGCM. They focused mainly on evaluating the regional climate change signals over tropical South America. Urrutia and Vuille (2009) performed a similar analysis using the PRECIS model nested into the HADAM3 AGCM but focusing on the tropical Andes region. Sorensson *et al.* (2010) assessed the responses of precipitation seasonal means and extremes over South America in a warmer climate using the Rossby Centre Regional Atmospheric Model (RCA) and evaluated the likelihood of occurrence of severe extreme rainfall events and dry spells over the La Plata Basin, northeastern Brazil and the Amazon basin under the A1B scenario.

All these regional efforts lead to the assessment of the regional climate change patterns. Though the regional climate change projections available for South America were produced with a variety of RCMs driven mostly by the same AGCM, there was no coordination among the groups performing the simulations. The model domains were different in all the referred studies, however, several common features concerning the regional climate change signal could be identified and an «ensemble of opportunities» could be built. The «ensemble of opportunities» is not expected to produce quantitative information, but taking into account each individual regional climate change projection, it is possible to evaluate qualitatively the agreement or disagreement of the projected changes among individual modeling exercises. Moreover, common shortcomings could also be identified in terms of the capability of the models in reproducing observed climate features.

Schematically, Fig. 2 highlights the areas in which common features arise from the available downscaling exercises considering projected changes for both temperature and precipitation. Most of the models agree on a generalized warming all over the continent, with several hot-spots where the temperature increase projected for the end of the twenty first century under the A2 scenario is larger than 4°C (large red arrows in Fig. 2), namely the Amazon and the Andean regions. Hot-spots for the projected precipitation changes show a consistent precipitation

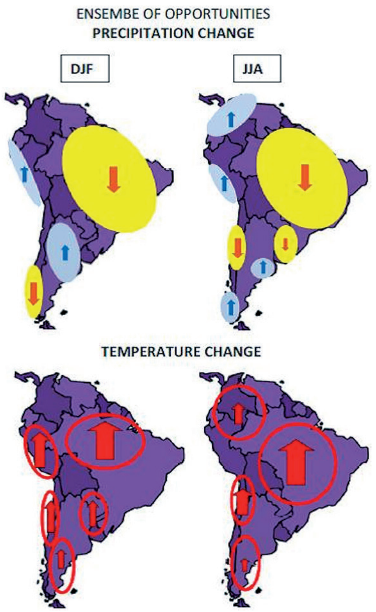

Figure 2: Qualitative changes projected at the end of the XXI century under the A2 emission scenario from an «ensemble of opportunities»: Precipitation changes (upper panels) and temperature (lower panels). The size of the arrows indicates the magnitude of the projected changes.

decrease over the western coast of South America and the Amazon region and increases over southeastern South America.

Though the ensemble of opportunities may provide common results, the regional climate model simulations are sensitive to model configuration and experimental design (Laprise *et al.*, 2012; Rauscher *et al.*, 2006). Consequently, results for un-coordinated modeling efforts may not provide robust results. It is important to bear in mind that all RCMs included in the ensemble of opportunities were driven by the same AGCM and is a well known fact that the climatic response to a given radiative forcing is model-dependent. Vera *et al.* (2006b) explored projected precipitation changes over South America from a sub-set of CMIP3 AOGCMs and found a general consensus among models on the precipitation changes, particularly an increase of summer precipitation over South America and a reduction of precipitation in all seasons along the southern Andes.

COORDINATED RCM EXPERIMENTS OVER SOUTH AMERICA: CLARIS-LPB CONTRIBUTION

All individual modeling efforts described in the previous section, were based on results from a single model realization, either using one driving GCM or one RCM, which is insufficient to provide a measure of uncertainty needed for a comprehensive evaluation of potential climate change and the associated uncertainty. In recent years, several studies have shown that regional climate simulations are affected by several sources of uncertainty (Dequé *et al.* 2007 and references therein) and the spread among different climate realizations should be taken into account before drawing conclusions about the significance of the regional climate responses to the external forcings.

The sources of uncertainty in regional climate change projections can be due to: 1) the inherent uncertainty of the climate system triggered by differences in the initial conditions, referred to as internal variability; 2) the uncertainty due to models, both RCMs and GCMs and 3) the scenario uncertainty. Exploring all these sources of uncertainty is a very demanding task, as it requires performing a large amount of RCM simulations with different RCMs nested into different GCMs for different emission scenarios and different realizations with the same model but changing the initial conditions. In a recent study, Solman and Pessacg (2011) explored the relative relevance of different uncertainty sources, namely internal variability, regional model configuration and choice of model's physics in seasonal scale simulations over South America. Their results showed that the internal variability represents the lowest level of uncertainty; the uncertainty due to the choice of model physics arises as the most important uncertainty, particularly for temperature and precipitation. They also shown that the spatial pattern of the uncertainty is invariant with respect to the source of uncertainty explored. Though this study was focused on quantifying the level of uncertainty in regional climate simulations over South America, it did not account for the full range of uncertainty sources associated with the regional climate change projections.

In order to provide useful information for impact studies the broad range of uncertainties should be considered. This requires the generation of ensembles of simulations performed with different RCMs nested into different GCMs for different emission scenarios in order to explore the full range of uncertainty sources. This approach has been followed by several international efforts, such as the PRUDENCE project (Christensen *et al.*, 2007) and ENSEMBLES project (Hewitt, 2005) for Europe; the NARCAPP project for North America (Mearns *et al.*, 2009), and CORDEX (Giorgi *et al.*, 2009) among others.

The preliminary collaborative initiative for producing ensembles of RCM simulations over the South American continent was initiated within the EU-FP6 CLARIS project (A Europe-South America Network for Climate Change Assessment and Impact Studies). Several South American and European institutions participating in this collaborative project agreed on a set of coordinated experiments using different RCMs to produce the first coordinated ensemble for the region. In a first stage, three case studies of 1-month length simulations corresponding to anomalous rainfall conditions over south-eastern South America were simulated with 6 RCMs. All the models were nested into ERA40 reanalysis. The most outstanding results were published in Menéndez *et al.* (2010a); (2010b). These studies explored the uncertainty associated with the variety of RCMs and the dependence of the level of uncertainty on the simulated period. The analysis was focused not only on the uncertainty in simulating the mean climatic conditions but also on simulating extreme rainfall events. At a second stage, a subset of 4 RCMs driven also by ERA40 reanalysis was used to perform multiyear simulations covering the period from 1991 to 2000. With this set of simulations Carril *et al.* (2012) evaluated the capability of simulating the major characteristics of seasonal mean climate for South America and the associated uncertainties. They found that the models displayed a considerable precipitation biases especially in tropical and Andean areas. Moreover, the relatively good performance of the multi-model annual precipitation average over La Plata Basin results from the cancelation of offsetting errors in the individual models. A systematic warm bias was identified over southeastern South America. This coordinated modeling effort allowed identifying common shortcomings and strengths of regional climate models behavior over the region.

A similar initiative was implemented in Brazil by means of the CREAS project (Regional Climate Change Scenarios for South America – Marengo and Ambrizzi, 2006). In this framework, three regional models were used: the ETA RCM, the PRECIS RCM and the RegCM3 RCM, all nested in one AGCM (HADAM3). This initiative certainly represented an important step forward in characterizing the uncertainty in regional climate change projections over South America (Chou *et al.*, 2011; Marengo *et al.*, 2010).

More recently, under the support of the EU-FP7, the CLARIS-LPB project (A Europe-South America Network for Climate Change Assessment and Impact studies in La Plata Basin; http://www.claris-eu-org) has developed an unprecedented effort for designing a coordinated experiment using different RCMs over South America, with the goal of providing ensemble projections of climate change over South America and their underlying uncertainties. The modeling strategy was built for two purposes. First, to provide a framework to evaluate model performance; second, to produce climate projections for use in impact and adaptation studies. The model evaluation framework was designed following the CORDEX protocol, so as to contribute to the CORDEX initiative for the South American domain.

The experimental set up follows the CORDEX protocol Phase I (http://wcrp.ipsl.jussieu.fr/SF_RCD_CORDEX.html) (Giorgi *et al.*, 2009). Every model has been configured to cover the South American-CORDEX domain, from 60°S to 15° N and from 90°W to 20 °W, shown in Fig. 3. All models were integrated on a horizontal grid of roughly 50 km (around 0.44° to 0.48 °) resolution. For the evaluation framework, a set of 7 RCMs simulations nested into ERA-Interim reanalysis (Uppala *et al.*, 2008) for the period 1990-2008 were performed. The models participating in this initiative were: RegCM3/USP, Universidade de Sao Paulo, Brazil; RCA/SMHI, from Rossby Centre, Swedish Meteorological and Hydrological Institute, Sweeden; MM5/CIMA from Centro de Investigaciones del Mar y la Atmósfera (CIMA), Argentina; REMO/MPI from Max-Planck-Insti-

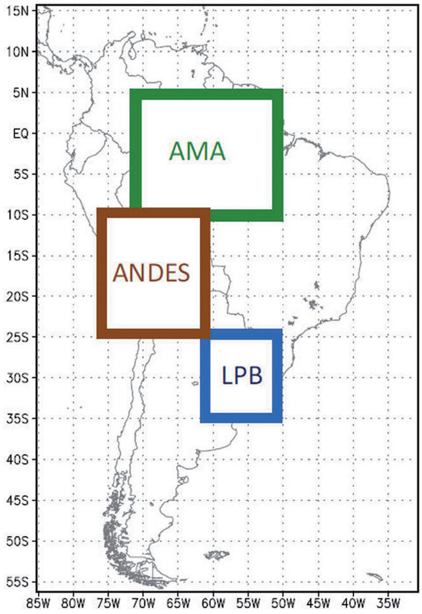

Figure 3: CLARIS–LPB model domain. Regions selected for area-averages. AMA for Amazon, LPB for La Plata Basin and ANDES for central Andes region.

tute for Meteorology, Hamburg, Germany; PROMES/UCLM, from Grupo MOMAC, Universidad Castilla-La Mancha, Toledo, Spain; LMDZ/IPSL, from IPSL (Institute Pierre-Simon Laplace), París France and ETA/INPE, from Instituto Nacional de Pesquisas Espaciais (INPE), Brazil. A thorough description of each model configuration is described in Solman *et al.* (2013) and references therein.

The analysis of the simulations allowed evaluating the capability of the participating RCMs in reproducing several basic characteristics of the mean observed climate over South America and also characterizing the uncertainty associated with RCMs only. The preliminary evaluation of the RCM ensemble can be found in Solman *et al.* (2013). The evaluation of RCM's performance showed that all RCMs are able of capturing the main features of the seasonal mean precipitation and temperature over South America. However, some systematic biases were identified, such as an overestimation of temperature and underestimation of precipitation over the La Plata basin (LPB) region. Individual model's biases over tropical areas of South America were diverse, depending on the model. The Andean region was characterized by a strong underestimation of temperature and overestimation of precipitation mainly over the Andean slopes, a common shortcoming of every modeling effort. However, it is important to bear in mind that also that the quality of observational datasets over areas with complex topography is critical for evaluating model performance, as pointed out by several authors (e.g. Rauscher *et al.*, 2010; Urrutia and Vuille, 2009).

TABLE 1. Matrix of GCM/RCM combinations of regional climate change simulations over the South America domain performed within the CLARIS-LPB project.

RCM/Institution	ERA-Interim (1990-2008)	GCM	Present climate (1961-1990)	Near future (2011-2040)	Far future (2071-2100)	Continuous run (1961-2100)
RegCM3/USP	X	HadCM3-Q0	X	X	X	
		EC5OM-R1	X	X	X	
RCA/SMHI	X	EC5OM-R1				X
		EC5OM-R2				X
		EC5OM-R3				X
MM5/CIMA	X	HadCM3-Q0	X	X		
REMO/MPI	X	EC5OM-R3	X	X	X	
PROMES/UCLM	X	HadCM3-Q0				X
LMDZ/IPSL	X	IPSLA1B				X
		HadCM3-Q0				X
ETA/INPE	X	HadCM3-Q0	X	X	X	

The availability of a set of coordinated RCM simulations allowed also exploring the degree of agreement or disagreement among individual RCMs and thus characterizing the uncertainty in simulating regional climate. Overall, it was found that he uncertainty in simulating the main characteristics of climate over the LPB region were generally lower compared with tropical regions of the South American continent. Though several systematic biases were identified, the reliability of the simulations is generally good for the LPB region. The ensemble of RCMs systematically improves the quality of the simulated climate compared with any individual model.

In the climate change framework seven RCMs were nested into different GCMs under the SRES A1B emission scenario in order to account for the uncertainty due to both RCMs and GCMs. The matrix of GCM/RCM simulations performed under the CLARIS-LPB project is shown in Table 1. This matrix allows exploring the most relevant sources of uncertainty in regional climate change projections over South America.

Taking advantage of the set of different realizations performed by some of the participating RCMs, a set of 11 simulations are available for both the present climate and the near future climate, and 10 simulations are available for the far future climate.

Inspection of the projected changes showed that though the RCM ensemble gives a good indication of the uncertainty in climate scenarios it is also important to bear in mind that it does not cover the whole range of uncertainty sources. All simulations were performed under the SRESA1B emission scenario; consequently the uncertainty associated with the emission scenario has not been explored within the CLARIS-LPB initiative.

CORDEX SOUTH AMERICA: ON-GOING ACTIVITIES AND EXPECTED OUTCOMES

The CLARIS-LPB contribution to CORDEX- South America has allowed making an unprecedented advance in producing high quality RCM products for impact assessment studies over the South American continent. Moreover, the coordinated framework allowed also to critically assess the strength and shortcomings of the state-of-the-art RCMs for the region. However, as noted previously, the number of institutions performing the RCM simulations was limited to those participating in the project. Besides that, the GCMs selected to drive the RCMs were from the CMIP3 generation and only the SRESA1B emission scenario was selected for the climate change projections.

In recent years, the World Climate Research Program (WCRP) has recognized the relevance of providing a conceptual framework for organizing a coordinated international effort to assess and intercompare dynamical and statistical downscaling techniques. This approach was initially coordinated by a Task Force on Regional Climate Downscaling (TFRCD) in 2009 who designed the Coordinated Regional Climate Downscaling Experiment (CORDEX) sponsored by the WCRP. CORDEX was envisaged on the basis of recognizing the relevance of regional downscaling as both an important research topic and an opportunity to engage a broader community of climate scientists in its activities.

The CORDEX initiative has two main purposes. In first place, to provide a framework in which downscaling methodologies can be inter-compared through standardized experiment protocols. Second, to provide a coordinated set of downscaled regional climate simulations both dynamical and statistical for the historical past and future periods of CMIP5 GCM simulations for use in impact and adaptation studies. Besides these two main aims, CORDEX seeks for facilitating the communication with the Impact and Vulnerability (IAV) community.

The CORDEX protocol includes the definition of common domains covering the majority of land areas around the world and several general aspects of RCM configuration, such as horizontal resolution. In order to encourage the broad scientific community to contribute to this initiative, the standard horizontal resolution for CORDEX simulations has been decided to be around 50 km, though simulations with resolutions of 22 km and 11 km are also planned for some domains.

For the evaluation framework CORDEX has agreed to utilize the ERA-Interim reanalysis (Uppala *et al.*, 2008) covering the period 1989-2008. For the climate

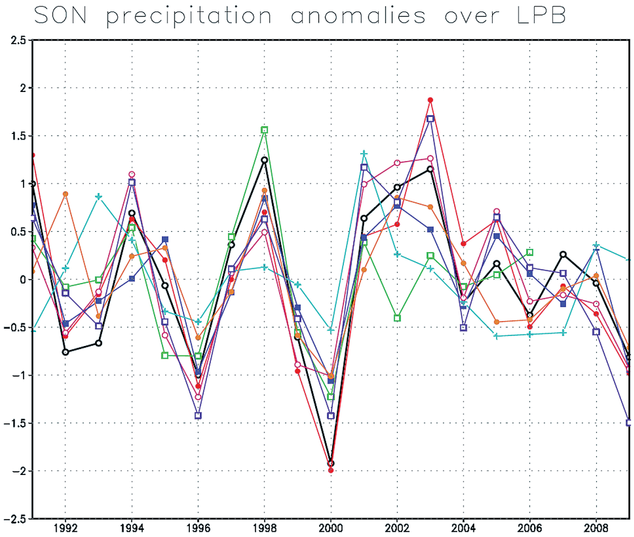

Figure 4: Time series of seasonal September-October-November (SON) precipitation anomalies over LPB. Black line corresponds to CRU data. Color lines correspond to each individual model for the CLARIS-LPB/ CORDEX coordinated experiment.

change framework, the new generation of scenarios is used. These scenarios are based on prescribed greenhouse-gas concentration pathways throughout the 21st century, corresponding to different radiative forcing stabilization levels by the year 2100, the so-called Representative Concentration Pathways (RCPs). Four RCPs have been selected, with stabilization levels at 2.6, 4.5, 8.5 and 11.2 W/m2 (referred to as RCP2.6, RCP4.5, RCP8.5 and RCP11.2, respectively), being the highest-priority simulations selected to be the RCP4.5 and RCP8.5, in agreement with the CMIP5 priorities. The simulations will cover the historical period, from 1950 to 2005 and the future period from 2006 to 2100. Continuous RCM simulations from 1950 to the end of the twenty first century will be performed. A complete description of the CORDEX framework can be found in Giorgi *et al.* (2009).

For the model evaluation framework, besides the CLARIS-LPB project contributions, several other groups have contributed performing the ERA-Interim driven simulations for the CORDEX-South American domain. The list of the participating models and groups is detailed in Table 2.

A preliminary inspection of the ERA-Interim driven simulations is summarized in Figs. 4 to 6, which show examples of the results obtained. In these figures the interannual variability of rainfall as depicted by each individual RCM participating in the CLARIS-LPB/CORDEX evaluation framework is displayed

TABLE 2. List of the RCM simulations driven by the ERA-Interim reanalysis performed over the CORDEX-South America domain. (*) Personal communication.

RCM/Institution-Country
RegCM3/USP-Brazil
RCA3/SMHI-Sweeden
REMO/MPI-Germany
LMDZ/IPSL-France
PROMES/UCLM-Spain
MM5/CIMA-Argentina
ETA/INPE-Brazil
COSMO/ IACS-Switzerland(*)
WRF/IPSL-France (*)
PRECIS/Met Off-Hadley Centre (*)

for several regions of South America: the LPB region, the Amazon region and the Andes region (indicated in Fig. 3). Note that the temporal evolution of seasonal precipitation anomalies for the LPB region from the Climate Research Unit data set is well reproduced by every individual RCM. The RCMs are able to reproduce the interannual variability of rainfall anomalies considering both the timing and the magnitude of the anomalies. Over the Amazon region, though the models are still able to capture the year-to-year variability of rainfall anomalies, the dispersion among individual models is larger compared with that for the LPB region. Finally, over the Andes regions the RCMs tend to show a weaker agreement with the observations both in terms of the magnitude of the anomalies but also in terms of temporal evolution of the seasonal rainfall anomalies. This figure is a good example for the need of both model improvements but also high quality datasets to evaluate model performance.

For the climate change framework, several groups have already started to perform the 150-year simulations under several RCPs. The larger the number of RCM/CGM/RCPs combination will allow exploring the full range of sources of uncertainty affecting regional climate change projections which will provide valuable climate change information to guide future impact, adaptation and vulnerability assessments towards defining choices for coping with climate variability and change across South America.

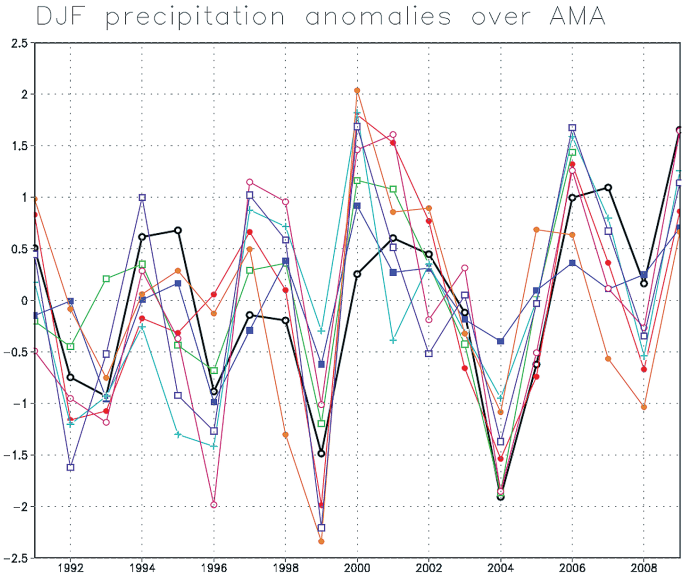

Figure 5: Same as Fig. 4 but for December-January-February (DJF) precipitation anomalies over AMA.

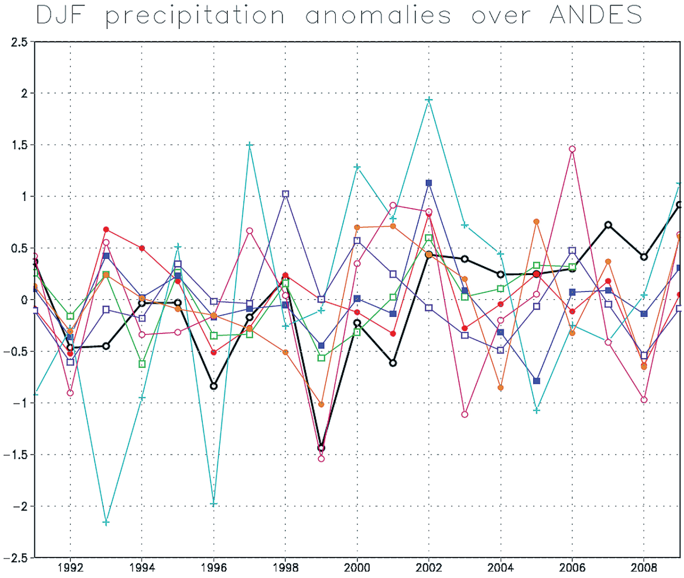

Figure 6: Same as Fig. 5 but for ANDES.

SUMMARY AND CONCLUSIONS

In this article a review of the more outstanding efforts on regional climate modeling over the South American continent has been presented. The development of regional-scale climate modeling over the region has developed during the last 10 to 12 years and an enormous progress has been made up to date. An example of this progress can be seen from Fig. 7 which shows the number of research articles published on peer-review journals per year. This count has been made taking into account publications based on regional climate modeling studies over South America from the SCOPUS database.

Early efforts, initiated during the beginning of the 2000s were conducted by isolated initiatives and a reduced number of modeling groups. These early efforts were mostly focused on evaluating the capability of a particular RCM on reproducing some basic aspects of the seasonal climate. From 2002 to 2007 several groups started performing simulations with different RCMs and focused on evaluating model performance, sensitivity of the RCMs on technical issues, such as model configuration and process studies. Though the modeling efforts were increased there was still no coordination among the modeling groups. From 2008 most of the efforts were focused on producing regional climate change scenarios. In these studies the regional climate simulations were extended from 10 to 30 years and the modeled climatologies were compared with observational datasets, focusing on different features of South American climate. The preliminary studies were based on results from a single RCM.

The CLARIS and CLARIS-LPB projects represented an enormous progress in this regard, due to the coordinated framework designed to provide regional climate change scenarios over the South American continent. The coordinated framework allowed to explore the major shortcomings and strengths of the state-of-the-art RCMs over South America but also to characterize the uncertainty in simulating regional climate and regional climate change projections over the region. This unprecedented effort has been the major contribution to CORDEX over the South American region.

Though the progress on regional climate modeling activities over South America has been enormous, it is important to highlight that all the RCMs used for simulating South American climate have been originally developed for other regions of the world, mainly Europe and USA. No single RCM has been developed within South American institutions. Conversely, the RCMs have been evaluated over South America and sensitivity experiments were carried on in order to attain an optimal model set up to get a good model performance. However, the general quality of the RCM simulations over the South American continent is not as good as those for Europe and North America. Even when some of the models used to simulate the South American climate are the same as those used for other regions, the biases are larger. Moreover, some of the most recent studies based on ensembles of RCM have identified several systematic biases shared by almost

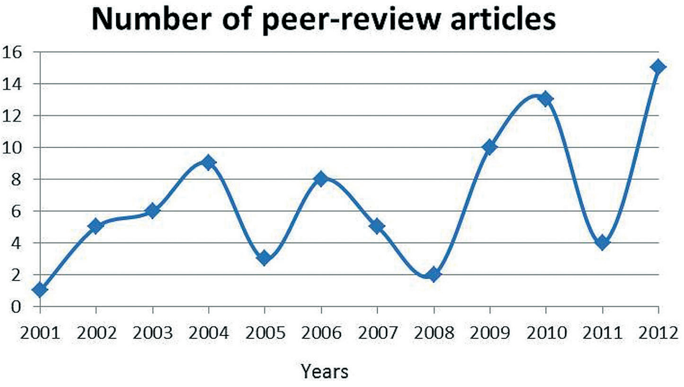

Figure 7: Number of peer-review articles published on the literature devoted to Regional Climate modeling studies over South America since 2000 to 2012. Source: SCOPUS.

every RCM: the systematic overestimation of temperature over central Argentina during the austral summer months and the underestimation of rainfall over South Eastern South America during the austral winter months. Though the reasons for these biases are still unknown, models still need to be improved in order to increase their reliability on simulating South American climate features.

Though CORDEX will allow exploring the full range of uncertainty sources characterizing regional climate change projections, there are still some important issues that should be addressed. Almost all the most updated RCM simulations performed or planned over South America are on grids of roughly 50 km resolution. Up to date, the major challenges in regional climate modeling over South America are related with model improvement, increasing resolution and increasing the ensemble size. These tracks will certainly allow improving the interpretation of model results for use in impact and adaptation studies.

ACKNOWLEDGEMENTS

This review has been made under the support of the European Community's Seventh Framework Programme (FP7/2007-2013) under Grant Agreement B°212492 (CLARIS LPB A Europe- South America Network fir Climate Change Assessment and Impact Studies in La Plata Basin). This work has also been supported by UBACyT Grant Y028 and Conicet Grant PIP 112-201101-00189.

REFERENCES

Boulanger J.P., G. Brasseur, A.F. Carril, M. de Castro, N. Degallier, C. Ereño, H. Le Treut, J. Marengo, C.G. Menendez, M.N. Nuñez, O. Penalba, A. Rolla, M. Rusticucci, R. Terra (2010): A Europe–South America network for climate change assessment and impact studies. *Climatic Change*, 98: 307–329 DOI 10.1007/s10584-009-9734-8.

Boulanger J.P., S. Schlindwein and E. Gentile (2011): CLARIS LPB WP1: Metamorphosis of the CLARIS LPB European project: from a mechanistic to a systemic approach. CLIVAR Exchanges No. 57, Vol. 16, No.3, 7–10.

Carril, A., C. Menéndez, A. Remedio, F. Robledo, A. Sörensson, B. Tencer, J.P. Boulanger, M. de Castro, D. Jacob, H. Le Treut, L. Li, O. Penalba, S. Pfeifer, M. Rusticucci, P. Salio, P. Samuelsson, E. Sanchez and P. Zaninelli (2012): Assessment of a multi-RCM ensemble for South Eastern South America, *Climate Dynamics.*

Chou, S.C., Marengo, J.A., Lyra, A., Sueiro, G., Pesquero, J., Alves, L.M., Kay, G., Betts, R., Chagas, D., Gomes, J.L., Bustamante, J., Tavares, P. (2011). Downscaling of South America present climate driven by 4-member HadCM3 runs, *Climate Dynamics.* DOI 10.1007/s00382-011-1002-8.

Christensen, J.H., T.R. Carter, M. Rummukainen and G. Amanatidis (2007): Evaluating the performance and utility of regional climate models: the PRUDENCE project. *Climatic Change,* 81, 1–6.

da Rocha, R.P., C.A. Morales, S.V. Cuadra, T. Ambrizzi (2009) Precipitation diurnal cycle and summer climatology assessment over South America: An evaluation of Regional Climate Model version 3 simulations. *Journal of Geophysical Research,* 114:1-19. doi:10.1029/2008JD010212.

Déqué M., D.P. Rowell, D. Luthi, F. Giorgi, J.H. Christensen, B. Rockel, D. Jacobson, E, Kjellstrom, M. de Castro and B. van der Hurk (2007): An intercomparison of regional climatic simulations for Europe: assessing uncertainties in model projections. *Clim. Change* 81:53–70.

Dickinson, R.E., Errico, R.M., Giorgi, F. and Bates, G.T. (1989) A regional climate model for the western United States. *Climatic Change* 15, 383–422.

Fernandez, J.P.R., S.H. Franchito, and V.B. Rao (2006), Simulation of the summer circulation over South America by two regional climate models. Part I: Mean climatology, Theor. *Appl. Climatol.*, 86, 247 – 260, doi:10.1007/s00704-005-0212-6.

Garreaud, R.D., *et al.*, (2008). Present-day South American climate, Paleogeogr. Palaeoclimatol. Palaeoecol., doi:10.1016/j.palaeo.2007.10.032.

Garreaud, R. and M. Falvey (2009) The coastal winds off western subtropical South America in future climate scenarios. *Int. J. of Climatology*, 29, 543-554. doi: 10.1002/joc.1716.

Giorgi, F. (1990) On the simulation of regional climate using a limited area model nested in a general circulation model. *J Climate* 3:941–963.

Giorgi, F., Bi, X., Pal, J. (2004a) Mean, interannual variability and trends in a regional climate change experiment over Europe i. Presentday climate (1961–1990). *Clim Dyn* 22:733–756.

Giorgi, F., Bi, X. and Pal, J. (2004b): Mean, interannual variability and trends in a regional climate change experiment over Europe. ii: climate change scenarios (2071–2100). *Climate Dynamics* 23: 839–858 DOI 10.1007/s00382-004-0467-0.

Giorgi, F. and L.O. Mearns (1991): Approaches to the simulation of regional climate change: a review. *Reviews of Geophysics*, 29, 191–216.

Giorgi, F., C. Jones, and G. Asrar (2009) Addressing climate information needs at the regional level: The CORDEX framework. *WMO Bull.,* 58, 175–183.

Hewitt, C.D. (2005) The ENSEMBLES project: providing ensemblebased predictions of climate changes and their impacts. *EGGS Newslett* 13:22–25.

Laprise, R., D. Kornic, M. Rapaic, L. Separovic, M. Leduc, O. Nikiema, A. Di Luca, E.P. Diaconescu, A. Alexandru, Ph. Lucas-Picher, R. de Elia, D. Caya and S. Biner, 2012: Considerations of domain size and large-scale driving for nested Regional Climate Models: Impact on internal variability and skill at developing small-scale details. In: Climate Change: Inferences from Paleoclimate and Regional Aspects, Proceedings of the Milutin Milankovitch 130th Anniversary Symposium. Belgrade, 22-25 September 2009. Springer, Editors: A. Berger, F. Mesinger and Dj. Sijacki, Part 4, 181-199, DOI: 10.1007/978-3-7091-0973-1_14.

Leung, L.R., Qian, Y., Bian, X. (2003) Hydroclimate of the western United States based on observations and regional climate simulation of 1981–2000. Part I: seasonal statistics. *J Climate* 16:1892–1911.

Liang, X.Z., Li, L., Kunkel, K. (2004) Regional climate model simulation of US precipitation during 1982–2002. Part I: annual cycle. *J Climate* 17:3510–3528.

Marengo, J.A., Chou, S.C., Kay, G., Alves, L., Pesquero, J.F., Soares, W.R., Santos, D.C., Lyra, A.A., Sueiro, G., Betts, R., Chagas, D.J., Gomes, J.L., Bustamante, J.F., Tavares, P. (2011). Development of regional future climate change scenarios in South America using the Eta CPTEC/HadCM3 climate change projections: Climatology and regional analyses for the Amazon, São Francisco and the Parana River Basins. *Clim Dyn,* DOI 19.1007/s00382-011-756 1155-5.

Marengo, J.A., R. Jones, L.M. Alves, and M.C. Valverde (2009). Future change of temperature and precipitation extremes in South America as derived from the PRECIS regional climate modeling system. *International Journal of Climatology,* 15, 2241-2255.

Marengo, J.A., Ambrizzi, T. (2006). Use of regional climate models in impacts assessments and adaptations studies from continental to regional and local scales: The CREAS (Regional Climate Change Scenarios for South America) initiative in South America. Proceedings of 8 ICSHMO, Foz do Iguaçu, Brazil, pp. 291-296.

Marengo, J.A., T. Ambrizzi, R.P. Rocha, L.M. Alves, S.V. Cuadra, M.C. Valverde, S.E.T. Ferraz, R.R. Torres, and D.C. Santos (2010). Future change of climate in South America in the late xxi Century: Intercomparison of scenarios from three regional climate models, *Climate Dynamics*, 35:1073-1097, DOI 10.1007/s00382-009-0721-6.

Mearns, L., Gutowski, W.J., Jones, R., Leung, L., McGinnis, S., Nunes, A.M.B., Qian, Y. (2009) A regional climate change assessment program for North America. Eos Trans Amer Geophys Unio, 90:311–312.

Menéndez, C.G., Saulo A.C., Li Z.X. (2001). Simulation of South American wintertime climate with a nesting system. *Climate Dynamics*, 17, 219–231.

Menéndez, C.G., M. de Castro, J.P. Boulanger, A. D'Onofrio, E. Sanchez, A.A. Sörensson, J. Blazquez, A. Elizalde, D. Jacob, H. Le Treut, Z.X. Li, M.N. Núñez, S. Pfeiffer, N. Pessacg, A. Rolla, M. Rojas, P. Samuelsson, S.A. Solman, C. Teichmann, (2010a). Downscaling extreme month-long anomalies in southern South America. *Climatic Change*, 98, 379-403, DOI 10.1007/s10584-009-9739-3.

Menéndez, C.G., M. de Castro, A.A. Sörensson, J.P. Boulanger and participating CLARIS Modeling Groups (2010b). CLARIS Project: towards climate downscaling in South America. *Meteorol.* Z., 19, 357-362. DOI 10.1127/0941-2948/2010/0459.

Misra, V., Dirmeyer, P.A., Kirtman, B.P., Juang, H.M., Kanamitsu, M. (2002). Regional simulation of interannual variability over South America. *J Geophys Res* 107(D20) doi: 10.1029/2001JD900216.

Misra, V., Dirmeyer, P.A., Kirtman, B.P. (2003) Dynamic downscalling of seasonal simulations over South America. *J Climate*, 16:103–117.

Nicolini, M., Salio, P., Katzfey, J., McGregor, J.L., Saulo, A.C. (2002). January and July regional climate simulation over South America. *J Geophys Res.*, 107(D20) doi: 10.1029/2001JD000736.

Nobre, P., A.D. Moura, and L. Sun (2001). Dynamical downscaling of seasonal climate prediction over Nordeste Brazil with ECHAM3 and NCEP's Regional Spectral Models at IRI. *Bull. Amer. Meteor. Soc.,* 82, 2787–2796.

Nuñez, M. Solman, S. and Cabré, S. (2009): Regional Climate change experiments over southern South America. II: Climate Change scenarios in the late twenty first century. *Climate Dynamics*, DOI 10.1007/s00382-008-0449-8). Vol 32, N°7-8, 1081–1095.

Pesquero, J.F.; Chou, S.C.; Nobre, C.A.; Marengo, J.A. (2009) Climate downscaling over South America for 1961-1970 using the Eta Model. *Theoretical and Applied Climatology*. DOI: 10.1007/s00704-009-0123-z.

Räisänen, J., Rummukainen, M., Ullerstig, A. (2001). Downscaling of greenhouse gas induced climate change in two GCMs with the Rossby Centre regional climate model for northern Europe. *Tellus A* 53:168–191.

Rauscher, S.A., A. Seth, J.H. Qian, and S.J. Camargo (2006), Domain choice in a nested modeling prediction system for South America, *Theor. Appl. Climatol.*, 86, 229– 246, doi:10.1007/s00704-006-0206-z.

Rauscher, S., A. Seth, B. Liebmann, J. Qian, and S. Camargo (2007). Regional climate model–Simulated timing and character of seasonal rains in South America, *Mon. Weather Rev.*, 135, 2642 – 2657, doi:10.1175/MWR3424.1.

Reboita, M.S.; R.P. da Rocha, T. Ambrizzi, S. Sugahara (2010a). South Atlantic Ocean cyclogenesis climatology simulated by regional climate model (RegCM3). *Clim Dyn* 35:1331-1347 (doi: 10.1007/s00382-009-0668-7).

Reboita, M.S., da Rocha, R.P., Ambrizzi, T., Caetano, E. (2010b). An assessment of the latent and sensible heat flux on the simulated regional climate over Southwestern South Atlantic Ocean. *Clim Dyn* 34: 873–889.

Rojas, M. (2006). Multiply Nested Regional Climate Simulation for Southern South America: Sensitivity to Model Resolution. *Mon. Wea. Rev.*, 134, 2208–2223. doi: http://dx.doi.org/10.1175/MWR3167.1

Rojas, M., and A. Seth (2003), Simulation and sensitivity in a nested modeling system for South America. Part II: GCM boundary forcing, *J. Clim.*, 16, 2454 – 2471, doi:10.1175/1520-0442.

Seth, A., Rojas, M. (2003) Simulation and sensitivity in a nested modeling system for South America. Part I. Reanalysis boundary forcing. *J Climate* 16:2437–2453.

Seth, A., M. Rojas, B. Liebmann, and J.H. Qian (2004), Daily rainfall analysis for South America from a regional climate model and station observations, *Geophys. Res. Lett.*, 31, L07213, doi:10.1029/ 2003GL019220.

Seth, A., S.A. Rauscher, S.J. Camargo, J.H. Qian, and J.S. Pal (2007), RegCM3 regional climatologies for South America using reanalysis and ECHAM global model driving fields, *Clim. Dyn.*, 28, 461 – 480, doi:10.1007/s00382-006-0191.

Silvestri, G., C. Vera, D. Jacob, S. Pfeife and C. Teichmann (2009): A high-resolution 43-year atmospheric hindcast for South America generated with the MPI regional model *Clim Dyn* 32:693–709 DOI 10.1007/s00382-008-0423-5.

Solman, S., Nuñez, M. and Cabré, M.F. (2008): Regional Climate change experiments over southern South America. I: Present Climate. *Climate Dynamics*, Vol. 30, 533–552.

Solman, S., Sanchez, E., Samuelsson, P., da Rocha, R.P., Li, Marengo, J.A., Pessacq, N.L., Remedio A.R., Chou, S.C., Berbery, H., Le Treut, H., de Castro, M., Jacob, D., (2013) Evaluation of an ensemble of regional climate model simulations over South America driven by the ERA-Interim reanalysis: Models' performance and uncertainties, *Climate Dynamics*. DOI: 10.1007/s00382-013-1667-2.

Solman, S. and Pessacg, N. (2011): Evaluating uncertainties in Regional Climate simulations over South America at the seasonal scale. *Clim Dyn*, DOI 10.1007/s00382-011-1219-6.

Sorensson, A.A., C.G. Menéndez, R. Ruscica, P. Alexander, P. Samuelsson, and U. Willén, (2010). Projected precipitation changes in South America: a dynamical downscaling within CLARIS. *Meteorologische Zeitschrift*, 19 (4), 347–355.

Stouffer, R.J., K.E. Taylor and G.A. Meehl (2011). CMIP5 Long-term experimental Design. CLIVAR Exchanges No. 56, Vol. 16, No.2, 5–7.

Taylor, K.E., R.J. Stouffer and G.A. Meehl (2011). An overview of CMIP5 and the experiment design. *Bull. Amer. Meteorol. Soc.*, submitted.

Uppala, S., D. Dee, S. Kobayashi, P. Berrisford and A. Simmons (2008) Towards a climate adapt assimilation system: status update of ERAInterim, *ECMWF Newsletter*, 115, 12–18.

Urrutia, R., and M. Vuille (2009), Climate change projections for the tropical Andes using a regional climate model: Temperature and precipitation simulations for the end of the 21st century, *J. Geophys. Res.*, 114, D02108, doi:10.1029/2008JD011021.

Vera, C., Higgins, W., Amador, J., Ambrizzi, T., Garreaud, R., Gochis, D., Gutzler, D., Lettenmaier, D., Marengo, J., Mechoso, C.R., Nogues-Paegle, J., Silva Diaz, P.L., Zhang, C., (2006a). Towards a unified view of the American Monsoon System. *J. Climate* 19, 4977–5000.

Vera, C., G. Silvestri, B. Liebmann and P. González (2006b). Climate change scenarios for seasonal precipitation in South America from IPCC-AR4 models, *Geophys. Res. Lett.*, 33, L13707, doi:10.1029/2006GL025759.

EXPERIENCES WITH WRF IN EURO-CORDEX

Kirsten Warrach-Sagi, Klaus Görgen and Robert Vautard

CLIMATE CHANGE PERSPECTIVES FROM THE ATLANTIC:
PAST, PRESENT AND FUTURE
Jose María Fernández-Palacios, Lea de Nascimento, José Carlos Hernández,
Sabrina Clemente, Albano González & Juan P. Díaz-González (coords)
Servicio de Publicaciones, Universidad de La Laguna – 2013

ISBN: 978-84-15910-54-1
pp. 665-684

ABSTRACT

For the Coordinated Downscaling Experiment in Europe (EURO-CORDEX) an ensemble of regional climate model simulations on 0.11°, 0.22° and 0.44° has been completed in 2012. The Weather and Research Forecast (WRF) model belongs to the regional climate models that within CORDEX for the first time were applied to a long term climate model ensemble outside of North America. Due to its suite of possible set-ups WRF was and is applied in multiple configurations, contributing significantly to the multi-model ensemble. So far three WRF simulations were completed at 0.11° for the 1989-2008 simulation in Europe. For Europe the gridded data set EOBS of precipitation and temperature observations, which had been compiled at 0.25° in the European ENSEMBLES project, is still the highest resolved long-term gridded data set for Europe. This data set does not resolve the fine scale structures of the EURO-CORDEX simulations at 0.11°. For Germany a 1 km resolution gridded precipitation data set from the German Weather Service is available for the simulation period for evaluation. The observational data is gridded to the 0.11° simulation grid to compare and evaluate the three 0.11° WRF simulations in this sub-region. The three simulations suggest that the microphysics scheme, one-way double nesting, vertical layer distribution and combined effect of microphysics-convection parameterization deserve more attention. In Germany in spring and summer WRF in the three analyzed simulations has a stronger wet bias than in autumn and winter. A closer look into the convection parameterization and into the land surface – atmosphere exchange is suggested.

KEYWORDS: Europe, Germany, precipitation, parameterizations

INTRODUCTION

Climate change will induce not only modifications of temperature statistics and trends but also of the water cycle. This will result in spatial and temporal changes of soil, cloud, and precipitation patterns. Policy makers and end users like e.g. hydrologists require an appropriate accuracy of these changes in order to react and to adapt to climate change.

For Europe the performance of regional climate models (RCMs) to successfully reproduce the observed regional climate characteristics was extensively assessed within the last decades. In the EU projects ENSEMBLES and PRUDENCE, ensemble simulations of RCMs were executed and analyzed with a grid resolution of the order of 25 km and 50 km (e.g. Christensen and Christensen, 2007; Christensen *et al.*, 2007). These models were able to reproduce the pattern of temperature distributions reasonably well but a large scatter was found with respect to the simulation of precipitation. The results of ENSEMBLES and PRUDENCE are in accordance with a variety of studies of RCMs in Europe at the order of 25 to 50 km (e.g. Kotlarski *et al.*, 2005; Beniston *et al.*, 2007; Déqué *et al.*, 2007; Jacob *et al.*, 2007; Jaeger *et al.*, 2008).

In the past decade RCMs with even higher grid resolutions of 10-20 km were developed and extensively verified e.g. in Germany. Feldmann *et al.* (2008) and Früh *et al.* (2010) studied the consortia runs of the climate version of the COSMO model (COSMO-CLM) of the German Weather Service (DWD) and the REMO model of the Max Planck Institute for Meteorology. However, even at this resolution, several systematic errors were remaining. For instance, the «windward-lee effect» (Schwitalla *et al.*, 2008; Wulfmeyer *et al.*, 2008) is visible at mountain ranges showing a strong overestimation of precipitation on the windward side and an underestimation on the lee side. Heikkilä *et al.* (2011) studied the impact of grid resolution on simulation results of precipitation in Norway applying the Weather Research and Forecasting (WRF) model (Skamarock *et al.*, 2008) Version 3.1.0 forced with ERA-40 reanalysis on 0.33° and 0.11°. Despite the inaccuracies of the coarse forcing data that were transferred to the results, all simulations indicated a gain from high resolution due to better resolution of orographic effects.

WRF has great potential in the application for regional climate simulations. This is due to the fact that this model has advanced description of physical processes such as land-surface-vegetation-atmosphere interaction, dynamical processes, and it can be operated down to the convection-permitting scale. WRF offers multiple parameterizations for microphysics, turbulence, land surface processes, convection, radiation transfer and boundary layer physics. So the best set of a combination of state of the art parameterizations can be chosen for each model domain WRF is applied to. Alternatively, a multi-physics ensemble of WRF simulations can be run with different combinations of parameterizations.

So far, the NCEP, ERA-15 and ERA-40 reanalysis had been downscaled over Europe. Recently the third generation of the ECMWF reanalysis, ERA-interim (Dee *et al.*, 2011; Simmons *et al.*, 2007; Uppala *et al.*, 2008) became available. The ERA-interim reanalysis corrects some of the errors of the ERA-40 reanalysis and is available on a T255 spectral grid (i.e. approx. 0.75°). The World Climate Research Program (WCRP) initiated the COordinated Regional climate Downscaling EXperiment (CORDEX) in order to provide high-resolution ensembles and comparisons of regional climate simulations for the preparation of the fifth assessment report of the Intergovernmental Panel on Climate Change (IPCC AR5) (Giorgi *et al.*, 2009). For each model participating in CORDEX with a climate projection, the results of a verification run must be submitted. This verification run is performed for a 20-year period (1989-2008) driven by the ERA-interim data.

For CORDEX in Europe (EURO-CORDEX, http://www.euro-cordex.net) an ensemble of RCM simulations on 0.11°, 0.22° and 0.44° has been completed in

2012 and is currently under evaluation (e.g. Vautard *et al.*, 2013; Klaus Keuler and Sven Kotlarski, pers. comm.). WRF belongs to the RCMs that within CORDEX for the first time were applied to a long term climate model ensemble. Due to its suite of possible set-ups WRF was and is applied in multiple configurations and by this adds significantly to the multi-model ensemble.

Different from previous sensitivity studies with WRF, the multiple WRF simulations were now all carried out for 20 years, so both, normal and extreme years are included in many regions. Therefore an in depth analysis of all model results will provide more insight in the parameterizations, and in the abilities and deficiencies of WRF in a climate simulation in Europe.

The analyses of the EURO-CORDEX ensemble results are subject to other publications and here only an overview will be given. The evaluation of the multiple WRF simulations at 0.44°, 0.22° and 0.11° is still preliminary since many simulations only finished within the past months prior to the first CORDEX-WRF workshop held by CORWES (CORDEX-WRF-España) in October 2012 in Tenerife. Therefore, here only the precipitation results from the three 0.11° WRF simulations in Germany are shown.

Germany has been the focus of weather forecasts (e.g. Bauer *et al.*, 2011, Schwitalla *et al.*, 2011) and climate studies (e.g. Feldmann *et al.*, 2008; Früh *et al.*, 2010; Warrach-Sagi *et al.*, 2013) due to 1) its interesting orography, 2) readily available high quality observational data, 3) its vulnerability to floods, and 4) its importance for agriculture and industry. For Germany the German Weather Service compiled a high resolution gridded data set of daily precipitation since 1961, which is an ideal basis for the analysis of the 0.11° simulations.

This chapter describes the simulations set up in EURO-CORDEX, followed by a description of the WRF simulations. Then the observational data set for Germany is described, followed by the comparison between the three WRF model precipitation simulations. The chapter closes with a discussion of the results.

SIMULATIONS SET UP IN EURO-CORDEX

Models in EURO-CORDEX

According to EURO-CORDEX (www.euro-cordex.net) so far, twenty-one verification simulations (i.e. forced with reanalyses data) were completed for CORDEX in Europe using seven models (ARPEGE V5.1, Déqué (2010); CCLM, Rockel *et al.* (2008), http://www.cosmo-model.org; RCA, Samuelsson *et al.* (2011); REGCM, Giorgi *et al.* (2012); REMO, Jacob *et al.* (2012); WRF (Version 3.3.1, Skamarock *et al.* (2008); RACMO, Meijgaard *et al.* (2008)). Seven simulations were carried out with high resolution (0.11° or about 12 km), one with 0.22° (i.e. approx. 25 km) and thirteen with a low resolution (0.44° or about 50 km) on rotated grids (Fig. 1). Among these two sets, five simulations were made with

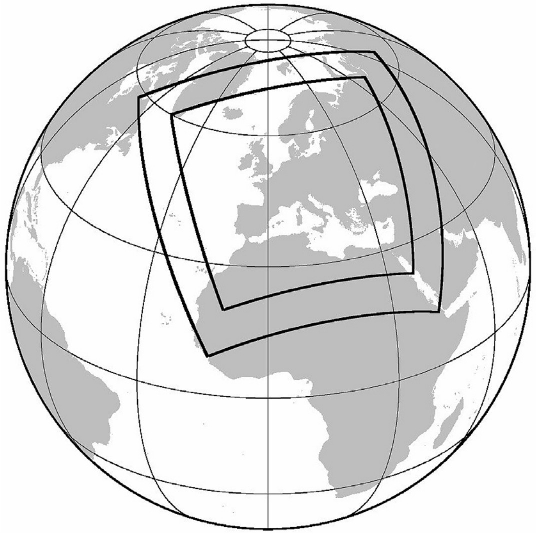

Figure 1. Domain of CORDEX Europe on a rotated grid.

the same model and similar setups (ARPEGE, CCLM, RCA, and WRF) at high and low resolutions. In the case of REMO at high resolution, a different model version was used which also includes rain advection. This change can be seen as adding a new process relevant on the small scale.

ERA-interim data is used for model initialization and as lateral boundary forcing. The ERA-interim data set is the latest ECMWF global atmospheric reanalysis of the period 1989 to present using a 12-hour 4D-Var data assimilation system as described in Simmons *et al.* (2007) and Uppala *et al.* (2008). Dee *et al.* (2011) give a detailed description and analysis of the ERA interim data. Among the main advances in the ERA-interim data assimilation compared to ERA-40 are the T255 horizontal resolution, a new humidity analysis, improved model physics and improvements in bias handling.

The simulations cover at least the period 1989 – 2008 as initially imposed in the EURO-CORDEX project. However, in 2011 ERA-interim data became available since 1979, so recently some groups started their WRF simulations earlier.

All models used the 6-hourly ERA-Interim meteorological re-analysis as forcing data at the boundaries, with different nesting methods depending on the model. Simulations were generally carried out over a larger grid than the official EURO-CORDEX grid to account for boundary imbalance effects, and a «relaxation region» of various widths (a few hundred kilometers in general) was used.

The evaluation of the EURO-CORDEX ensemble is subject to other publications, so in the following only the precipitation results from the three WRF simulations at 0.11° in Germany are shown.

TABLE 1. Differences in the set-up of the WRF Version 3.3.1 simulations at 0.11° for EURO-CORDEX. All simulations are forced with ERA-Interim reanalysis data.

Institute/contact	Vert. levels / TOA	Period	Microphys.	Cumulus	Radiation (SW+LW)	Nesting/ Domain
CRP-GL K. Görgen	50L / 20hPa	1989-2009	WRF Single Moment 6-class (Hong and Lim, 2006)	Kain-Fritsch (Kain, 2004)	CAM3 (Collins *et al.*, 2004)	0.44° to 0.11° (one-way)/ 10 grid cell enlarged
IPSL R. Vautard	32L / 50hPa	1989-2009	WRF Single Moment 6-class (Hong and Lim, 2006)	Grell-Devenyi (Grell and Devenyi, 2002)	RRTMG (Iacono *et al.*, 2008)	No/ 10 grid cell enlarged
Univ. of Hohenheim K. Warrach-Sagi	Modified 50L / 20hPa	1987-2009	Morrison-double-moment (Morrison *et al.*, 2009)	Kain-Fritsch (Kain, 2004)	CAM3 (Collins *et al.*, 2004)	No/ 30 grid cells enlarged

WRF IN EURO-CORDEX

Version 3.3.1 of the WRF model has been applied to Europe on a rotated latitude-longitude grid with a horizontal resolution of 0.11° and 0.44° respectively. So far at 0.11° three WRF simulations are completed: 2 simulations (WRFUHOH, WRFIPSL) at 0.11° forced with ERA-interim, 1 simulation forced with ERA-interim one-way nested, in a double nesting at 0.44° and 0.11° simulation (WRFCPRGL). Further simulations at 0.22° and 0.44° are completed by different institutes. Table 1 summarizes the differences in the set-ups of the WRF simulations at 0.11°. All simulations use the NOAH land surface model (Chen and Dudhia, 2001a; 2001b), the MM5 similarity scheme for the surface layer (Skamarock *et al.*, 2005) and the YSU atmospheric boundary layer parameterization (Hong *et al.*, 2006). Different from previous sensitivity studies with WRF, the multiple WRF simulations were now all carried out for 20 years, so both, normal and extreme years are included in many regions. The results between all WRF simulations in Europe in many regions differ significantly (e.g. Vautard *et al.*, 2013), so an in depth analysis will be carried out in the near future.

For vegetation type and soil texture the following data sets included in the pre-processing package of WRF are used. For the soil outside of North America the 5 min. UN/FAO data is given.

STUDY AREA AND PRECIPITATION DATA

Germany

Germany has a typical mid-latitude moderate climate, characterized by a westerly flow with rainfall associated with frontal systems in winter and more convective precipitation in summer (Wulfmeyer *et al.*, 2011). The North Sea and Baltic Sea further influence the climate in northern Germany. Germany is characterized by its flat terrain in the north, the low mountain ranges of the Harz and Thüringer Wald in the center and the mountain ranges of the Black Forest, Swabian Jura, Bavarian Forest and the Alps in the south. Mixed Forests, needle leaf forests, cultivated grasslands and croplands characterize the landscape.

Precipitation

For Germany, the German Weather Service (DWD) processed a consistent 1 km^2 gridded dataset of daily precipitation (REGNIE = Regionalisierung von Niederschlagsdaten) from 1961 to 2009. REGNIE is generated from about 1200 precipitation measurement stations interpolated on a 1×1 km^2 grid over Germany. During the interpolation, also the station elevation and exposition are considered. Richter (1995) gives the climatological (1961-1990) monthly mean undercatch of the german precipitation gauges used in the REGNIE data. It is between 5.6% in July in very protected locations below 1000 m in southern Germany up to 33.5% in February below 700m at non-protected gauges in eastern Germany. The annual mean precipitation between 1961 and 2009 varied between 584 mm in 1976 and 1005 mm in 2002.

To compare the REGNIE dataset with simulation results, the observations were interpolated to the model grid using a bilinear interpolation algorithm of the climate data operators (CDOs, Schulzweida *et al.*, 2012).

COMPARISON OF WRF 0.11° PRECIPITATION RESULTS

Three WRF simulations in EURO-CORDEX were completed at 0.11°. WRFCPRGL, WRFIPSL and WRFUHOH were set up for EURO-CORDEX with different sets of parameterizations, vegetation data and vertical levels (see table 1). Different from WRFUHOH and WRFIPSL, WRFCPRGL was applied in a one-way double-nesting approach at 0.44° and 0.11°. WRFIPSL and WRFCPRGL were started in 1989 while WRFUHOH was started in 1987 to allow for a spin-up period. With respect to the chosen parameterizations, WRFCPRGL and WRFUHOH differ in the microphysics scheme. While WRFCPRGL was carried out with the WRF Single Moment 6-class scheme (Hong and Lim, 2006), WRFUHOH applied the Morrison double-moment scheme (Morrison *et al.*, 2009). WRFIPSL differs from WRFCPRGL in the choice of the cumulus parameterization (here WRFIPSL applies Grell and Devenyi (2002), while WRFCPRGL and WRFUHOH apply Kain-Fritsch (Kain, 2004)) and the radiation transfer scheme (WRFIPSL applies the RRTMG scheme (Iacono *et al.*, 2008) while WRFCPRGL and WRFUHOH apply the CAM3 scheme (Collins *et al.*, 2004)).

Dependent on the season, the three model set ups differ significantly in the precipitation results. Since the simulations were only recently completed only a preliminary analysis can be given here. However, the results invite for an in depth analysis in the future.

Europe

The EURO-CORDEX ensemble evaluation against the ECA&D gridded data set E-OBS (version 6, Haylock *et al.*, 2008) (Klaus Keuler and Sven Kotlarski, pers. comm.) shows a wet bias of WRFIPSL and WRFUHOH in most seasons and regions (WRFCPRGL is not yet included in their evaluation). Note that the EOBS data may have a dry bias though, since the precipitation gauge data usually shows an undercatch depending on wind, exposition and temperature (e.g. Sevruk, 1982; Richter, 1995).

In winter (DJF) and spring (MAM) WRFIPSL and WRFUHOH show a wet and dry bias, respectively, in the same regions. The biases of WRF-IPSL exceed those of WRF-UHOH. In winter, the southern Iberian Peninsula shows a dry bias; in France, Germany and the British Islands both simulations show a good agreement with the EOBS data. In spring all regions except Portugal and southern Spain show a wet bias in both simulations. Like in winter, the dry bias in spring on the Iberian Peninsula is larger in WRFIPSL. Summer (JJA) is the only season where WRFIPSL and WRFUHOH show a different bias pattern. The whole Mediterranean Region shows a wet bias in both simulations, but WRFUHOH has a much larger bias. In Central Europe, on the British Islands and most of Scandinavia WRFIPSL has a wet bias while WRFUHOH agrees well with EOBS (dry and wet biases 0-20 mm/month). In autumn (SON) both the simulated precipitation agrees well with EOBS in Germany, France, BeNeLux states and British Islands. On the Iberian Peninsula WRFIPSL has a dry bias, in the remainder wet and dry biases. WRFUHOH has a wet bias in southern Italy and in South East Europe.

The mean seasonal precipitation differences between WRFCPRGL, WRFIPSL and WRFUHOH are displayed in Figs. 2, 3, 4 and 5. In winter (Fig. 2) WRFUHOH is drier than WRFIPSL mainly on the central European mountain ranges. WRFCPRGL is wetter than WRFIPSL and WRFUHOH. In spring (Fig. 3) WRFUHOH and WRFIPSL agree well, only in the Eastern Mediterranean WRFUHOH is wetter than WRFIPSL and drier in the southern Alps. WRFCPRGL is wetter throughout the domain except in Germany, Poland and north eastern

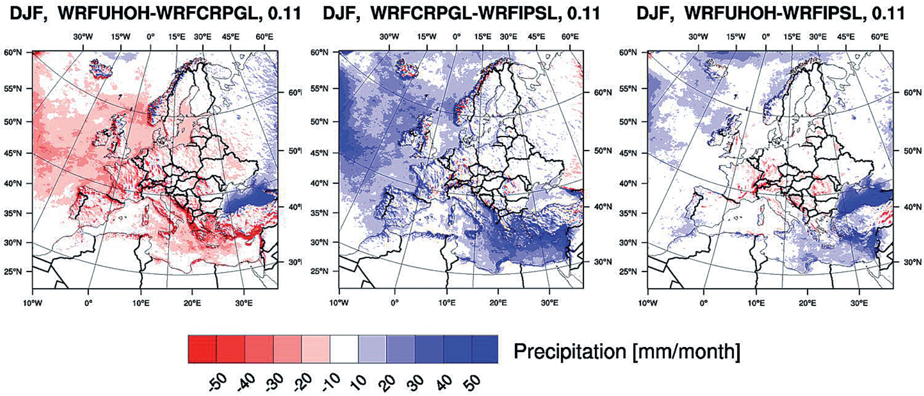

Figure 2. Mean winter (December, January, February) precipitation differences between WRFCPRGL, WRFIPSL and WRFUHOH in Europe.

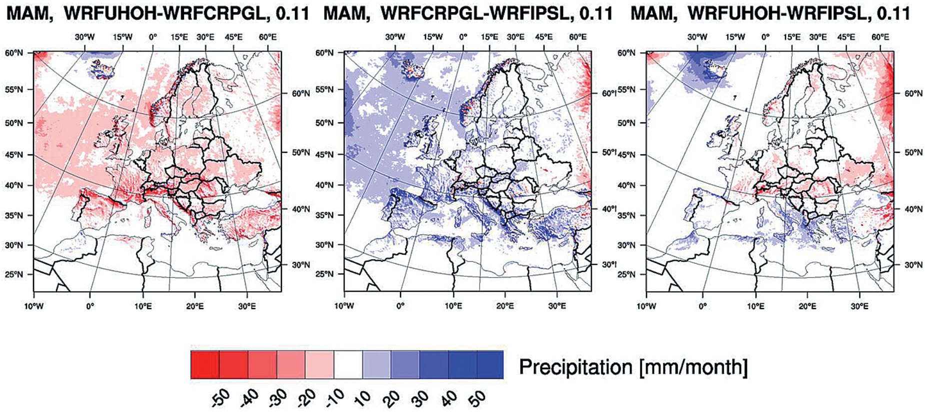

Figure 3. Mean spring (March, April, May) precipitation differences between WRFCPRGL, WRFIPSL and WRFUHOH in Europe.

Europe, where the 3 simulations agree well with each other, i.e. have a similar wet bias. In summer (Fig. 4) WRFUHOH differs from WRFIPSL and WRFCPRGL. North of 45°N WRFCPRGL and WRFIPSL both are wetter than WRFUHOH, while it is vice versa in the Mediterranean part of the domain. WRFCPRGL is wetter than WRFIPSL except for the Iberian Peninsula and the western Mediterranean where both agree. In autumn (Fig. 5) WRFUHOH and WRFCPRGL are wetter than WRFIPSL in the Mediterranean and in the Atlantic coastal areas of Spain and France. North of 45° WRFUHOH is drier than WRFCPRGL and WRFIPSL.

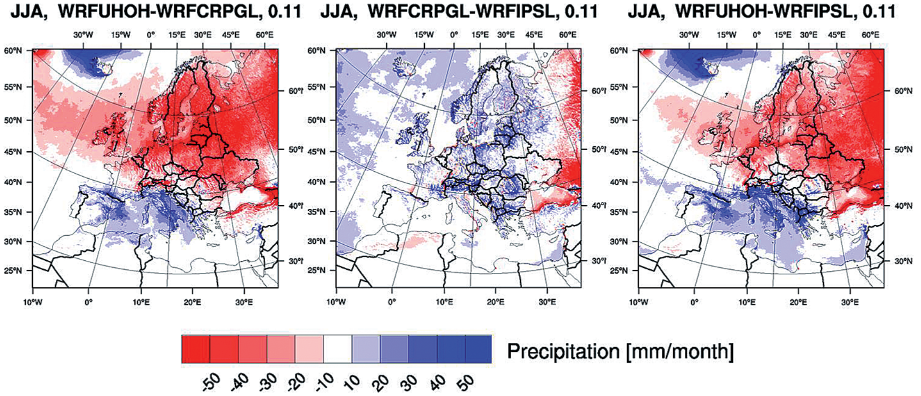

Figure 4. Mean summer (June, July, August) precipitation differences between WRFCPRGL, WRFIPSL and WRFUHOH in Europe.

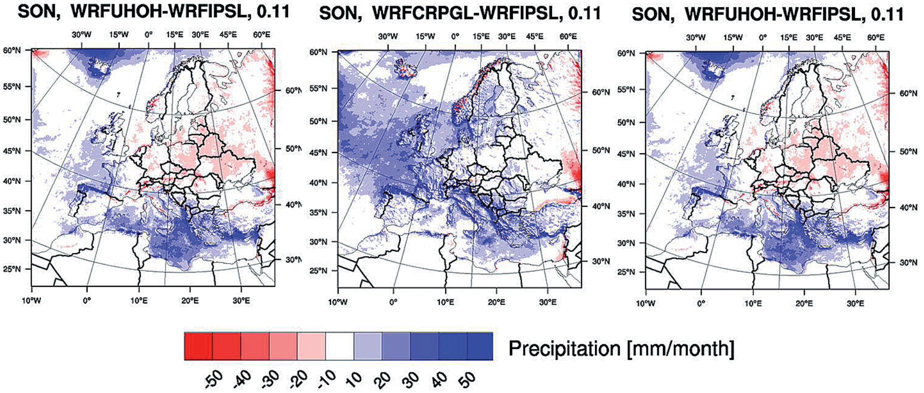

Figure 5. Mean autumn (September, October, November) precipitation differences between WRFCPRGL, WRFIPSL and WRFUHOH in Europe.

GERMANY

The mean seasonal precipitation for Germany is displayed in Figs. 6, 7, 8, 9 and 10. The simulated precipitation is evaluated against the REGNIE observational data, which has a larger resolution than the EOBS data. Fig. 6 shows the observed precipitation of the four seasons.

In winter (Fig. 7) the observed precipitation in Northeastern and most of southern Germany is between 20 and 60 mm/month. Western Germany is char-

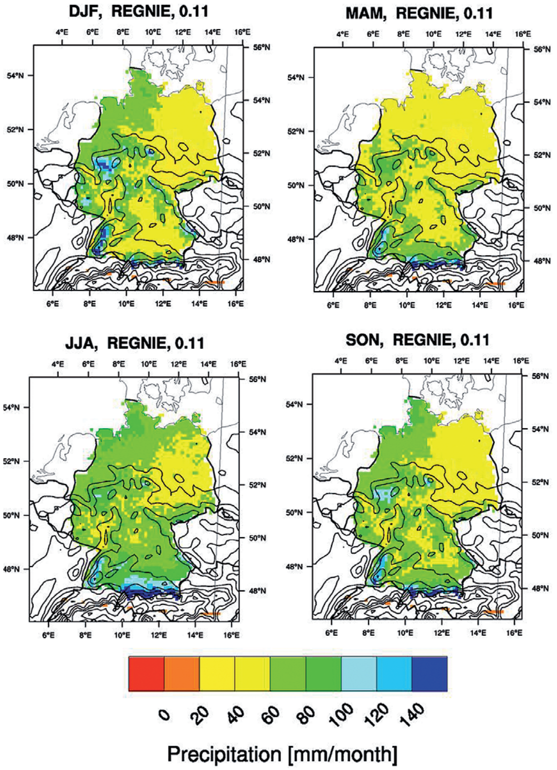

Figure 6. Mean seasonal observed precipitation from the gridded REGNIE data set interpolated to the 0.11° model grid.

acterized by precipitation between 60 and 80 mm/month and values above 120 mm/month in the mountainous regions. WRFUHOH agrees with the observation within +/-10 mm/month in most of Germany except in the mountainous regions the wet bias is up zo 50 mm and in the drier lowlands of north eastern Germany it is up to 20 mm/month. WRFIPSL shows a wet bias in most of Germany, however in most regions the bias is below 20 mm/month. This differs from WRFCPRGL which has the largest wet biases in most of the domain.

In spring (Fig. 8) precipitation of 40-60 mm/month is observed in most of Germany. All simulations show a larger wet bias than in winter. WRFUHOH has the lowest bias with less than 20 mm/month in most of the domain and less than 40 mm/month in the mountainous regions. WRFCPRGL has a wet bias of 20-40 mm/month in most of the domain and larger biases in the mountainous regions.

In summer (Fig. 9) WRFIPSL and WRFCPRGL both show a wet bias throughout Germany above 30 mm/month and 40 mm/month respectively. WRFUHOH shows a dry bias in parts of the North-West of 10-20 mm/month (approx. 15%) and a wet bias in the southern half of Germany mostly in the order of 10-30 mm/month and more in the windward side of the mountain ranges.

In autumn (Fig. 10) WRFIPSL agrees very well with REGNIE while WRFUHOH shows a dry bias between 10 and 30 mm/month in the South-East and in the West. Again WRFCPRGL has a wet bias in a lot of regions, however it is smaller than in the other seasons.

All in all WRFUHOH in Germany is the driest and WRFCPRGL the wettest simulation. All simulations perform best in autumn and worst in spring.

DISCUSSION

Precipitation differences between the model setups are significant and will need a more in depth investigation. In Europe WRF shows a systematic wet bias in most regions and seasons. However, since observational precipitation data may be showing a systematic dry bias, this needs to be done with care and in conjunction with a bias analysis of observational data.

The main differences between WRFCPRGL and WRFUHOH are:

- the microphysics scheme
- no nesting versus one-way double nesting
- modified vertical layer distribution (more layers in the lower PBL in WRFUHOH)

The main differences between WRFCPRGL and WRFIPSL are:

- the convection parameterization
- the radiation transfer model
- no nesting versus one-way double nesting
- vertical layer distribution and top of the atmosphere
- vegetation map and parameters

The main differences between WRFUHOH and WRFIPSL are:

- the microphysics scheme
- the convection parameterization
- the radiation transfer model
- vertical layer distribution and top of the atmosphere
- vegetation map and parameters

The three model runs suggest that the microphysics scheme, the one-way double nesting, vertical layer distribution and the combined effect of microphysics-convection parameterization deserves more attention.

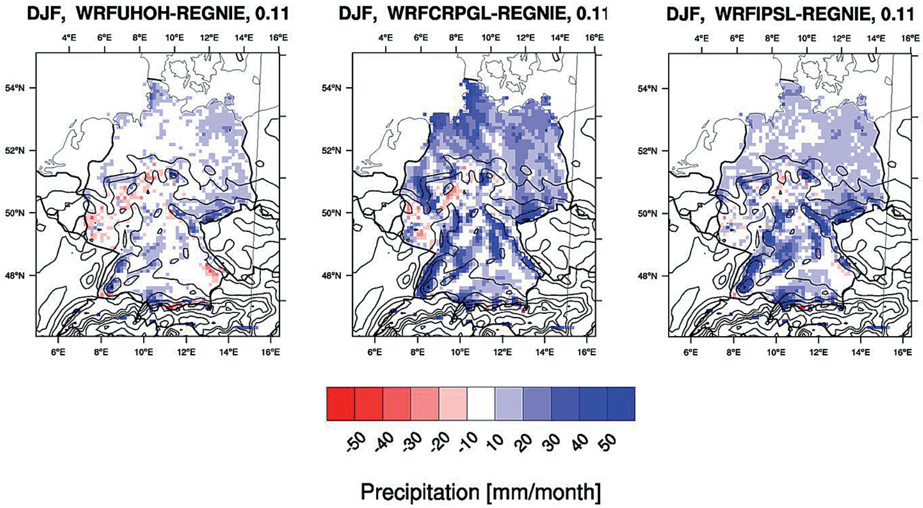

Figure 7. Mean winter (December, January, February) precipitation differences between WRFCPRGL, WRFIPSL and WRFUHOH in Germany.

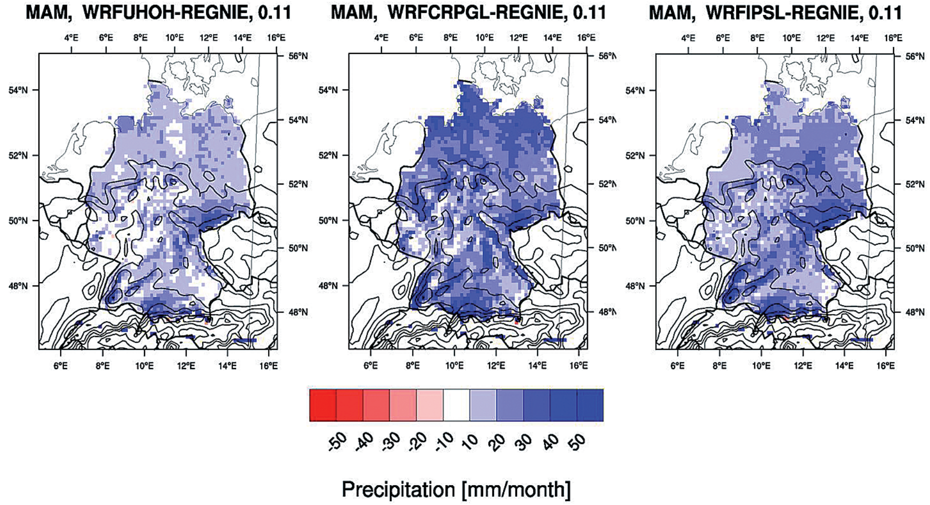

Figure 8. Mean spring (March, April, May) precipitation differences between WRFCPRGL, WRFIPSL and WRFUHOH in Germany.

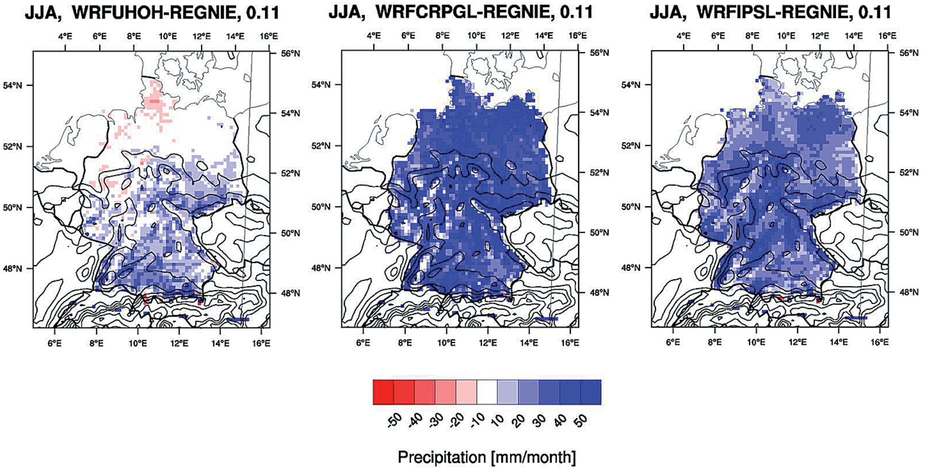

Figure 9. Mean summer (June, July, August) precipitation differences between WRFCPRGL, WRFIPSL and WRFUHOH in Germany.

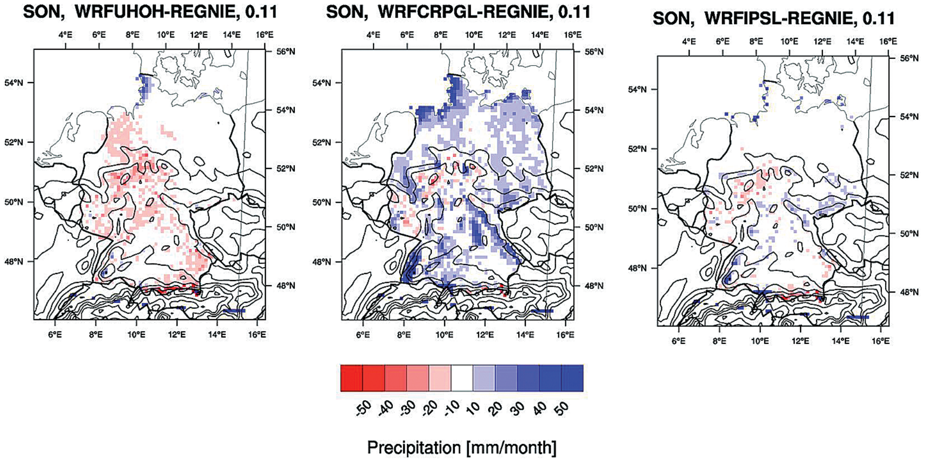

Figure 10. Mean autumn (September, October, November) precipitation differences between WRFCPRGL, WRFIPSL and WRFUHOH in Germany.

In Germany in spring and summer WRF in the three analyzed simulations has a stronger wet bias than in autumn and winter. A closer look into the convection parameterization but also into the land surface – atmosphere exchange will be worth.

Further, the precipitation biases show a large intra-annual variability. So a sensitivity study would be needed for at least a couple of years. Here EURO-CORDEX with the ERA-interim forced simulations provides an ideal test bed, since 20 year data are now available from multiple model runs for analysis. The models of the EURO-CORDEX ensemble show different biases, so the results might help to investigate the reasons for the biases. On the other hand EURO-CORDEX shows that a multi-model ensemble is useful for the end users since it gives a reasonable mean value including a possible spread. So in case of ensemble simulations the hindcast runs of EURO-CORDEX show that projections with this ensemble will be useful for the end users such as hydrologists who force their models with the results of the regional climate models for future planning.

Since many end-users are highly interested in precipitation, and since precipitation is one of the few widely measured quantities in time and space, this variable was chosen first for an analysis. However, it is a diagnostic variable. To better understand the differences between the model set-ups it will be necessary to study the atmospheric variables like pressure, temperature, humidity, wind and radiation in dependence of the set-ups.

ACKNOWLEDGEMENTS

Kirsten Warrach-Sagi thanks the German Science Foundation for her funding within the frame of the integrated research project PAK 346/FOR 1695 «Structure and function of agricultural landscapes under global climate change – Processes and projections on a regional scale». We acknowledge the E-OBS dataset from the EU-FP6 project ENSEMBLES (http://ensembles-eu.metoffice.com) and the data providers in the ECA&D project (http://www.ecad.eu). Further we acknowledge the REGNIE data from the German Weather Service.

REFERENCES

Bauer, H.-S., Weusthoff, T., Dorninger, M., Wulfmeyer, V., Schwitalla, T., Gorgas, T., Arpagaus, M., and Warrach-Sagi, K. (2011) Predictive Skill of a Subset of the D-PHASE Multi-Model Ensemble in the COPS Region. *Q. J. R. Meteorol. Soc.*, 137, 287-305, doi:10.1002/qj.715.

Beniston, M., and co-authors (2007) Future extreme events in European climate; an exploration of Regional Climate Model projections. *Climate Change*, 81, 71–95.

Chen, F., and Dudhia, J. (2001a) Coupling an advanced landsurface/ hydrology model with the Penn State NCAR MM5 modeling system. Part i: Model implementation and sensitivity. *Mon. Weather Rev.*, 129, 569–585.

Chen, F., and Dudhia, J. (2001b) Coupling an advanced landsurface/ hydrology model with the penn state NCAR MM5 modeling system. Part ii: Preliminary model validation. *Mon. Weather Rev.*, 129, 587–604.

Christensen, J.H., and Christensen, O.B. (2007) A summary of the PRUDENCE model projections of changes in European climate by the end of this century. *Climate Change*, 81, 7–30.

Christensen, J.H., Carter, T.R., Rummukainen, M., and Amanatidis, G. (2007) Evaluating the performance and utility of regional climate models: the PRUDENCE project. *Climate Change*, 81, 1–6.

Collins, W.D., and co-authors (2004) Description of the NCAR Community Atmosphere Model (CAM 3.0). NCAR Technical Note, NCAR/TN-464+STR, 226pp.

Dee, D.P., and co-authors (2011) The ERA-Interim reanalysis: configuration and performance of the data assimilation system. *Q. J. R. Meteorol. Soc.*, 137, 553–597.

Déqué, M., and co-authors (2007) An intercomparison of regional climate simulations for Europe: assessing uncertainties in model projections. *Climate Change*, 81, 53–70.

Déqué, M., (2010) Regional climate simulation with a mosaic of RCMs. *Meteorolog. Z.*, 19, 259-266, doi : 10.1127/0941-2948/2010/0455.

Feldmann, H., Früh, B., Schädler, G., Panitz, H.-J., Keuler, K., Jacob, D., and Lorenz, P. (2008) Evaluation of the Precipitation for South-western Germany from High Resolution Simulations with Regional Climate Models. *Meteorol. Z.*, 17, 455–465.

Früh, B., Feldmann, H., Panitz, H.-J., Schädler, G., Jacob, D., Lorenz, P., and Keuler, K. (2010) Determination of precipitation return values in complex terrain and their evaluation. *J. Climate*, 23, 2257–2274, doi:10.1175/2009JCLI2685.1.

Giorgi, F., Jones, C., and Asrar, G. (2009) Addressing climate information needs at the regional level: The CORDEX framework. *WMO Bull.*, 58, 175–183.

Giorgi, F., Coppola, E., Solmon, F., Mariotti, L., Sylla, M.B., Bi, X., Elguindi, N., Diro, G.T., Nair, V., Giuliani, G., Cozzini, S., Güttler, I., O'Brien, T.A., Tawfik, A.B., Shalaby, A., Zakey, A.S., Steiner, A.L., Stordal, F., Sloan, L.C., and Brankovic, C. (2012) RegCM4: Model description and preliminary tests over multiple CORDEX domains. *Climate Research,* 52, 7–29.

Grell, G.A., and Devenyi, D. (2002) A generalized approach to parameterizing convection combining ensemble and data assimilation techniques. *Geophysical Research Letters,* 29, doi:10.1029/2002GL015311.

Haylock, M.R., Hofstra, N., Klein Tank, A.M.G., Klok, E.J., Jones, P.D., and New, M. (2008) A European daily high-resolution gridded dataset of surface temperature and precipitation. *J. Geophys. Res (Atmospheres)*, 113, D20119, doi:10.1029/2008JD10201.

Heikkilä, U., Sandvik, A., and Sorteberg, A. (2011) Dynamical downscaling of ERA-40 in complex terrain using the WRF regional climate model. *Climate Dyn.*, 37, 1551-1564, doi: 10.1007/s00382-010-0928-6.

Hong, S.-Y., and Lim, J.-O.J. (2006) The WRF single-moment 6-class microphysics scheme (WSM6). *J. Korean Meteor. Soc.*, 42, 129–151.

Hong, S.Y., Noh, Y., and Dudhia, J. (2006) A new vertical diffusion package with an explicit treatment of entrainment processes. *Mon. Weather Rev.*, 134, 2318–2341.

Iacono, M.J., Delamere, J.S., Mlawer, E.J., Shephard, M.W., Clough, S.A., and Collins, W.D. (2008) Radiative forcing by long-lived greenhouse gases: Calculations with the AER radiative transfer models. *J. Geophys. Res.*, 113, D13103, doi:10.1029/2008JD009944.

Jacob, D., and co-authors (2007) An inter-comparison of regional climate models for Europe: Design of the experiments and model performance. *Climatic Change,* 81, 31–52.

Jacob, D., Elizalde, A., Haensler, A., Hagemann, S., Kumar, P., Podzun, R., Rechid, D., Remedio, A.R., Saeed, F., Sieck, K., Teichmann, C., and Wilhelm, C. (2012) Assessing the Transferability of the Regional Climate Model REMO to Different Coordinated Regional Climate Downscaling Experiment (CORDEX) Regions. *Atmosphere,* 3, 181-199. DOI:10.3390/atmos3010181.

Jaeger, E.B., Anders, I., Lüthi, D., Rockel, B., Schär, C., and Seneviratne, S.I. (2008) Analysis of ERA40-driven CLM simulations for Europe. *Meteorol. Z.*, 17, 349–367.

Kain, J.S. (2004) The Kain-Fritsch convective parameterization: An update. *J. Appl. Meteorol.*, 43, 170–181.

Kotlarski, S., Block, A., Böhm, U., Jacob, D., Keuler, K., Knoche, R., Rechid, D., and Walter, A. (2005) Regional climate model simulations as input for hydrological applications: evaluation of uncertainties. *Adv. in Geosci.*, 5, 119–125.

Meijgaard, E. van, Ulft, L.H. van, Berg, W.J. van de, Bosveld, F.C., Hurk, B.J.J.M. van den, Lenderink, G., and Siebesma, A.P., (2008) The KNMI regional atmospheric climate model RACMO, version 2.1. *KNMI Technical Report,* 302, 43 pp. Available from KNMI, Postbus 201, 3730 AE, De Bilt, The Netherlands.

Morrison, H., Thompson, G., and Tatarskii, V. (2009) Impact of cloud micrpohysics on the development of trailing stratiform precipitation in a simulated squall line: Comparison of one- and two-moment schemes. *Mon. Weather Rev.*, 137, 991–1007.

Richter, D. (1995) Ergebnisse methodischer Untersuchungen zur Korrektur des systematischen Messfehlers des Hellmann-Niederschlagsmessers. *Berichte des Deutschen Wetterdienstes*, 212, 93pp.

Rockel, B., Will, A., and Hense, A., eds. (2008) Special issue Regional climate modelling with COSMO-CLM (CCLM), *Meteorolog. Z.*, Vol. 17.

Samuelsson P., Jones, C., Willen, U., Gollvik, S., Hansson, U. and coauthors. (2011) The Rossby Centre Regional Climate Model RCA3: model description and performance. *Tellus*, 63A, 4–23.

Schulzweida, U., Kornblueh, L., and Quast, R. (2012) CDO User's Guide. Available at: https://code.zmaw.de/embedded/cdo/1.5.5/cdo.html (accessed October 2012).

Schwitalla, T., Zängl, G., Bauer, H.-S., and Wulfmeyer, V. (2008) Systematic errors of QPF in low-mountain regions. Special Issue on Quantitative Precipitation Forecasting. *Meteorol. Z.*, 17, 903-919. doi:10.1127/0941-2948/2008/0338.

Schwitalla, T., Bauer, H.-S., Wulfmeyer, V., and Aoshima, F. (2011) High-resolution simulation over Central Europe: Assimilation experiments with WRF 3DVAR during COPS IOP9c. *Q. J. R. Meteorol. Soc.*, 137, 156-175. doi:10.1002/qj.721.

Sevruk, B. (1982) Methods of correction for systematic error in point precipitation measurement for operational use. *WMO Operational Hydrology Report,* 21, 92 pp.

Simmons, A.J., Uppala, S.M., Dee, D.P., and Kobayashi, S. (2007) ERA-Interim: New ECMWF reanalysis products from 1989 onwards. *ECMWF Newsletter,* 110, 25–35.

Skamarock, W.C., Klemp, J.B., and Dudhia, J. (2005) A description of the advanced research WRF version. *Technical Note TN-468+STR, NCAR, Boulder, CO, NCAR.*

Skamarock, W.C., Klemp, J.B., Dudhia, J., Gill, D., Barker, D.O., Duda, M.G., Wang, W., and Powers, J.G. (2008) A Description of the Advanced Research WRF Version 3. *NCAR Technical Note TN-475+STR. Boulder, CO, NCAR*, 125 pp.

Uppala, S.M., Dee, D.P., Kobayashi, S., Berrisford, P., and Simmons, A.J. (2008) Towards a climate data assimilation system: Status update of ERA Interim. *ECMWF Newsletter,* 115, 12–18.

Vautard, R., and co-authors (2013) The simulation of European heat waves from an ensemble of regional climate models within the EURO-CORDEX project. *Clim. Dyn.*, doi: 10.1007/s00382-013-1714-z.

Warrach-Sagi, K., Schwitalla, T., Wulfmeyer, V., and Bauer, H.-S. (2013) Evaluation of a CORDEX-Europe simulation based on the WRF-NOAH Model System: precipitation in Germany. *Clim. Dyn.*, doi: 10.1007/s00382-013-1727-7.

Wulfmeyer, V., and co-authors (2008) The Convective and Orographically-induced Precipitation Study: A Research and Development Project of the World Weather Research Program for improving quantitative precipitation forecasting in low-mountain regions. *Bull. Amer. Meteor. Soc.*, 89, 1477-1486, DOI:10.1175/2008BAMS2367.1.

WULFMEYER, V., and co-authors (2011) The Convective and Orographically Induced Precipitation Study (COPS): The Scientific Strategy, the Field Phase, and First Highlights. *Q. J. R. Meteorol. Soc.*, 137, 3-30. doi:10.1002/qj.752.

ABSTRACTS

PREDICTABILITY OF DRY SEASON EXTREME EVENTS OVER WESTERN AFRICA: ASSESSING WRF SIMULATION OF 2002 CASE OVER SENEGAL

A. Sarr

CLIMATE CHANGE PERSPECTIVES FROM THE ATLANTIC:
PAST, PRESENT AND FUTURE

Jose María Fernández-Palacios, Lea de Nascimento, José Carlos Hernández,
Sabrina Clemente, Albano González & Juan P. Díaz-González (coords)
Servicio de Publicaciones, Universidad de La Laguna – 2013

ISBN: 978-84-15910-54-1

pp. 687-697

ABSTRACT

West Africa climate and mainly its northern part known as Sahel has experience the longest and most devastating drought ever recorded in the 70s and 80s. A lot of attention has been given to this climate shift characterized by rainfall deficit during the monsoon season. This trigged many studies focusing at different time scales on climate features modulating rain producing systems but also large scale factors controlling rainfall variability. This study investigates less known features like off season rains occurring out of the rainy season period over Sahel. The Weather and Research Forecast model (WRF ARW version 3.2) is use to simulate an extreme case which occurred in January 2002 on the western coast around the land/ocean interface and caused huge damages in Senegal and Mauritania. A nesting strategy with three domains is carried out to have a higher resolution of 10km in the inner domain while the mother domain covering a large area is at 90 km. The model was able to reasonably simulate the event and its intensity 2 to 3 days in advance, demonstrating the usefulness of such tools for early warning system (EWS) which could help mitigate the impacts. The location of rain band was closer to the observed situation in higher resolution domains. The study showed key dynamic and thermodynamic conditions associated with the event. Precipitable water (PW) evolution played a central role on the intensity due to north-east transport from the Inter Tropical Convergence Zone (ITCZ) over the Ocean near the Equator.

KEYWORDS: Regional climate model, off season rain, extreme event, jet.

INTRODUCTION

The major climate features, over West Africa Sahel, on which all attention is focused, occur during the monsoon season. Rainfall is mainly recorded during this period and corresponds to rainfed agriculture activities and last from May to October north of 10°N. Over Western Africa Sahel, rainfall occurring from November to April over Western Africa is not well documented. In recent years a few studies have been done on these systems using observational (Gaye and Fongang, 1997; De Félice, 1999; Thorncroft and Flocas, 1997) and modelling studies (Meier and Knippertz, 2008).

This is a common feature occurring over western Sahel and affects mainly Cape Verde, Senegal and Mauritania between late October and March considered as dry season as opposed to the monsoon season. They are very well known

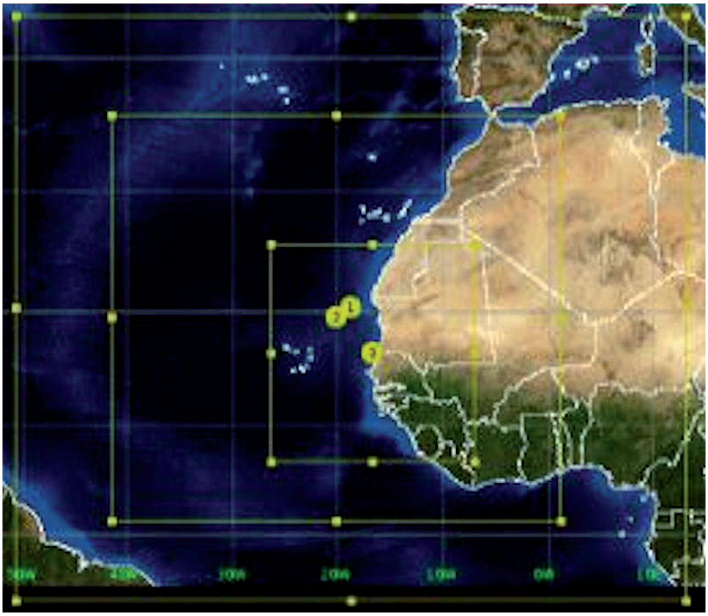

Figure 1. Map showing the 3 domains at respectively 90km for the d01, 30 for d02 and 10km horizontal resolution for d03.

by local population who name them «heug» or «mago rain» in Senegal. In most cases only light rain lasting hours with cloud structure dominated by midlevel clouds altocumulus or altostratus. When the system is strong enough convective clouds giving moderate to heavy rains are observed.

Other important elements, associated with these weather types, are cold waves and dust conditions. As they occur during a harvest and transaction period, they cause damages of different forms.

In this study, we focus on the extreme case which occurred in January 2002, causing tremendous damages on livestock in Senegal and Mauritania.

In section 2, we present the model configuration and data. Section 3) the typical mechanism and structure of these weather types is highlighted before the validation of simulation results in sections 4 and 5 with an emphasis on large scale dynamic and precipitation. Summary and conclusion are presented in section 6.

MODELLING STRATEGY AND DATA

Predictability for early warning is essential in order to mitigate the high impacts weather and climate systems.

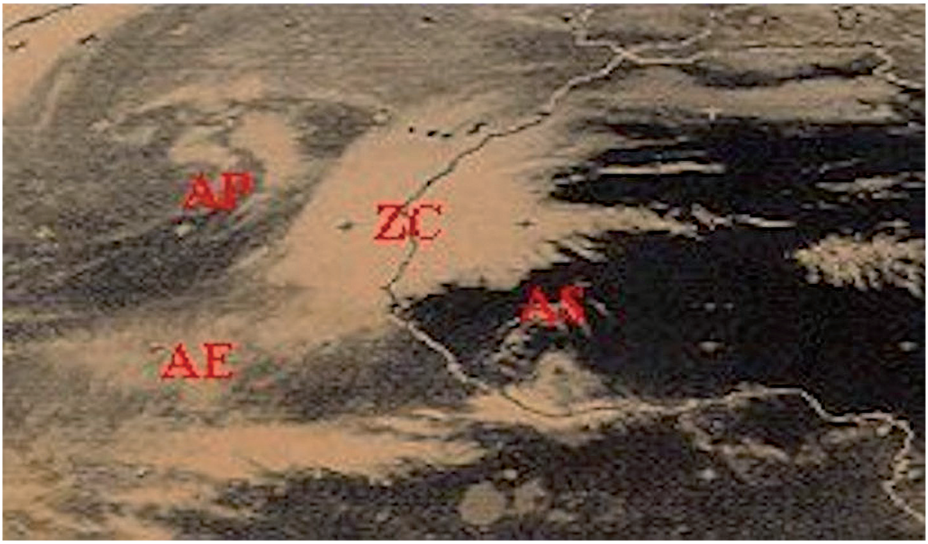

Figure 2. Satellite image of an off season case with continent in black, area of cloud is in white and the different air masses contributing to the system formation AP (polar air) AE (equatorial air), AS (Saharan air) and ZC the confluence zone.

In the study, a nesting strategy using the Weather Research and Forecasting model (WRF ARW version 3.2 Skamarock *et al.*, 2008), to simulate the case adopted. Two nest domains and a parent domain are configured for simulation at respectively 90, 30 and 10 km horizontal resolutions (Fig. 2).

The model is initialized by NCEP reanalysis 1&2 (Kalnay *et al.,* 1996) January 7, 2002 at 00Z and the simulation lasted 8 days in order to assess the predictability of such kind of events. Meier and Knippertz (2008) used the GME model at 40km horizontal resolution to simulate the event and found skills in predicting the event 7 days ahead even though the precipitation location was not well simulated. Data used to validate the model outputs are the ARC2 which combine gauge and satellite estimation datasets and TRMM (only estimation) as well as gauge rainfall from stations in Senegal. They are at high resolutions close to those of the nested domains. Large scale environment using key variables from model outputs are analysed in order to understand the mechanism and dynamic which lead to the formation of the system. The most difficult aspect to predict is certainly the heavy precipitation which occurred in 3 consecutive days and caused damages on livestock, crops and people. Beside the predictability, a lot of questions were raised about the intensity, the duration and the cold wave which exacerbated the disaster.

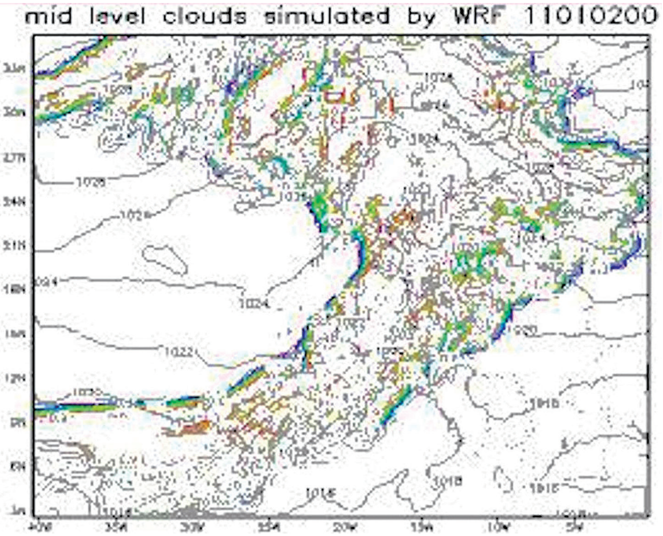

Figure 3. Mid level clouds simulated by WRF model and extracted
from domain 1the contour lines represent sea level pressure for 11 January 2012.

MECHANISM AND SCHEMATIC

Off season rains represent a typical climate interaction case between temperate and tropical regions. They are mainly due to air masses «conflict» or an area of confluence, above the region depicted earlier. Polar air (AP) coming through a trough, equatorial air (AE) transported by the subtropical jet and Saharan air (AS) from the continent as shown in Fig. 1. A large band of clouds is then observed around the ZC area and generate rainfall of different intensity. To investigate these kinds of weather events, a large area, covering continent and ocean, has to be considered. We tried to identify the schematic describe above in model outputs using model clouds at midlevel (Fig. 3). The results are consistent with this behaviour with cloud band with comma shape showing the cloud band structure with a comma structure. This indicates potential ability of WRF model in simulating off season systems.

LARGE SCALE ENVIRONMENT

The vertical structure of the atmosphere is analysed mainly low, mid and high levels of the troposphere to better understand the formation of these disturbances over Western Africa and mainly in this case what could explain the intensity of the event.

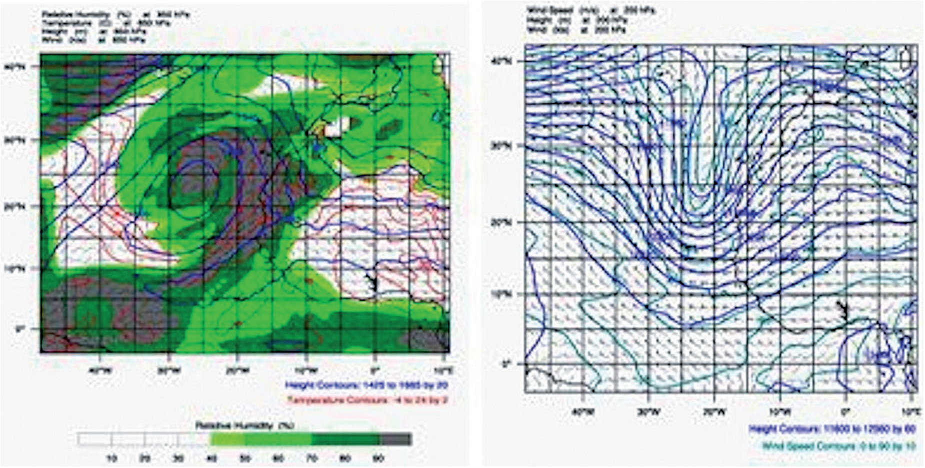

Figure 4. Wind barbs over d01 at 850 hPa, January 10 at 06Z, with shaded relative humidity in %, geopotential height blue contours and temperatures red contours in °C (left); Geopotential height and wind (kts) at 200hPa on January 10, 2002 from wrf forced by reanalysis 2(wrf_r2) (right).

The cold air from mid Atlantic Ocean reaching the lower latitudes through a trough created the formation of a cut off low off the coat of North-West Mauritania. On January the 7th at 00Z, the vertical structure exhibit at 850 hPa a low off the coast of northern Mauritania with an area of temperature ranging from 6-8°C and cyclonic winds around the low geopotential height with relative humidity above 90%. At 700, the low persists surrounded by strong winds with a west-south-west component and speed reaching 35kt. At 500 and 200hPa the low located south of Canary Islands directing strong westerly winds over Western parts of Mauritania and Senegal. On the 8th, the low at 850hPa extends a southwest trough toward Northern Cape Verde Islands with winds shifting slightly west-south-west up to 500 hPa. At 200hPA the subtropical jet with a western component has speeds reaching 90kts over Senegal. On the 9th, the low is deeper at all level with high values of relative humidity at 850 hPa and winds having a south-west component even at 200hPa. The low centered now 23°N26°W deepen again on the 10th of January Fig. 4a, and exhibit a large band of relative humidity between 80 and 100% from the Equator to Canary Islands. At 700hPa, strong south-westerly winds of 45kts are observed over Cape Verde, Senegal and Mauritania East of the deep low. The same configuration remains at upper levels (500 and 200hPa). On the 11th the trough at 200hPa moved eastward and is located off the coast of Mauritania with north-west winds over Cape Verde turning west to south-west over Senegal. On

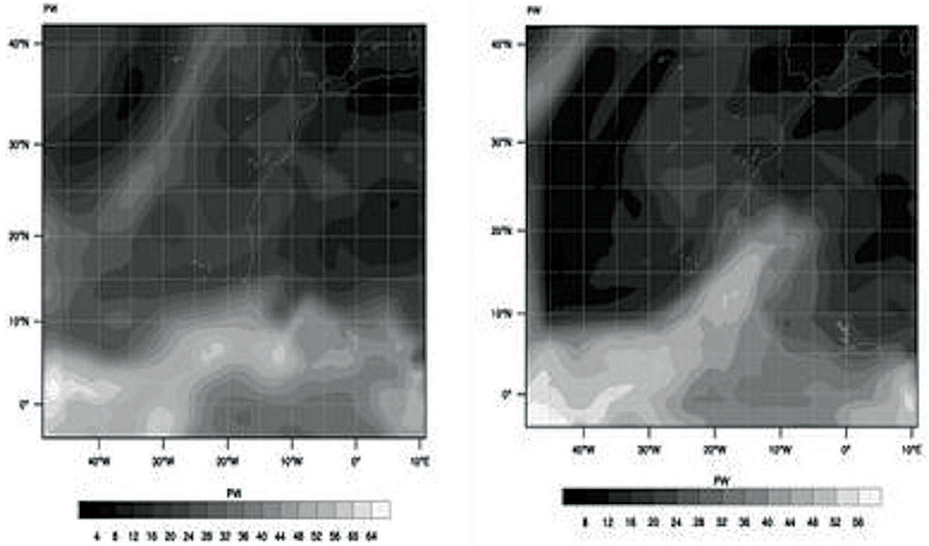

Figure 5. Precipitable water (PW) simulated by the model on the 8th (left) and January 10, 2002 (right) showing PW attracted of pushed with a south-west/North-east component.

the 12th, wind at 200hPa with the northward shift of the low centered 35°N 23°W became westerly with speeds of 40 to 60kts over Senegal.

When considering domain d03 at higher temporal and space resolution, the peak rainfall between 10 and 11 January 2002 Fig. 4 better depict the structure of parameter discussed above using d01. At 850 hPa a broad band of high relative humidity of more than 90% and south-western wind are observed at all levels up to 200 hPa. At 200hPa a broad subtropical jet with very strong south-westerly winds in observed.

The Hovmöller plot of precipitable water (PW) (not show) demonstrates its time evolution from the equatorial region of the ITCZ, southwest of the domain, towards the area of confluence. On January 07, 2002 (Fig. 5), precipitable water (PW) chart shows high values between the equator and 10°N corresponding to the position of the ITCZ. At this time of the year with the retreat of the monsoon, it corresponds to the dry season over Sahel while Guinea coast region which has a bimodal regime is experiencing the first part of their bimodal regime. Another elongated band of high values of PW goes from 22°N 50°W to 43°N 25°W with a core around 45. With time the second band move southeast weakening while the ITCZ band seems attracted northward with a core reaching southern Senegal on the 8th at 1200Z . From January 9 at 12 a broad band of high PW going from southwest corner of the domain to northern Senegal/south Mauritania is observed and reached Canaries Islands on the 10 at 1200Z (not shown). The location of the core of maximum PW area corresponds to the area where the maximum precipitation has been recorded. On the 12 the link between the ITCZ and the lower PW over Senegal is observed. Even the cloud band is still present the rainfall stopped, showing the importance of the feeding role of the main ITCZ core.

PRECIPITATION

A comparison of model output from R1 and R2 exhibit differences on the rainfall band location. Both runs are able to simulate the system with the intensity but outputs from R1 (wrf_r1) are mainly located off the coast of Senegal in domain 1, 2 and 3 (not shown). For R2 (wrf_r2) in both domains mainly d02 and d03 the inland position is closer to observed situation.

Intensity is better simulated in d02 while d03 slightly overestimates the intensity over Mauritania with reference to ARC2 and TRMM (Fig. 6). Care should be taken on rainfall amount validation between the different sources of information. The observed values from rain gages are from 06Z to 06Z the previous days, while here from TRMM and ARC the 24 hours is from 00Z to 24Z. We don't have rain gages information in Mauritania to better assess the model output which seems giving more rain.

In terms of rainfall the system lasted 3 to 4 days but the cold wave a big drop of surface temperature contribute to increasing the negative impacts of the event. The official statistics reported 8 people dead, more than 100,000 bovine, 350,000 ovine, 64,000 goats, 2,867 flooded new rice plants, 3,488 tons of rice production destroyed.

SUMMARY AND CONCLUSION

Western Africa Sahel, from Cape Verde to Senegal and Mauritania, experience in January 2002 an off season rain extreme event witch cause huge damages to affected countries. The statistics for Senegal are catastrophic demonstrating vulnerability to such events. To better understand the system and prospect predictability we use a modelling approach with the Weather Research and Forecast model WRF ARW force by NCEP reanalysis R1 and R2. A nesting strategy to have high resolution (10km) surrounding the targeted area, the parent domain covering a large area being at 90 km. We showed differences between wrf_r1 and wrf_r2 in reproducing the system 2 to 3 days in advance. In both domains wrf_r1 simulated the event but rainfall band was located mainly off the coast of Senegal, while for wrf_2 the simulated rainfall is closer to the observed situation over land. The analyse of large scale environment in the troposphere helped understand the

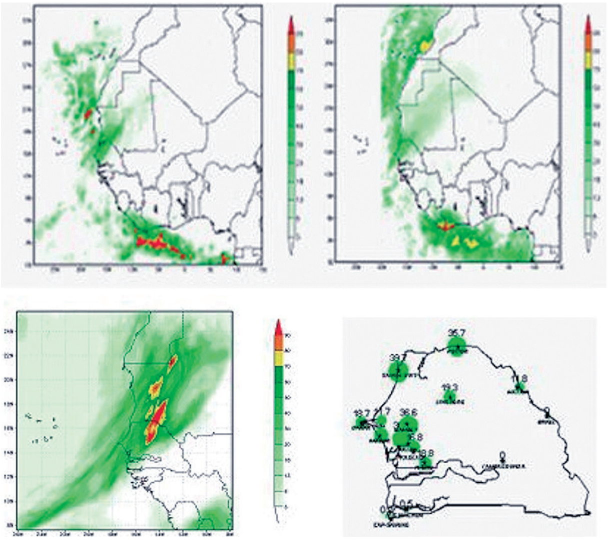

Figure 6. Rainfall from two estimated datasets ARC2 and TRMM (top panel) and WRF model domain 03 (bottom left) and rain gage observation over Senegal on January 10, 2002.

role played by the ITCZ through precipitable water (PW) when attracted and/or propagated from southwest to northeast. The study shown that modelling is a forecasting tool which could help for early warning in case of extreme events to mitigate the impacts, mainly on highly vulnerable countries in Sahel region.

ACKNOWLEDGEMENT

This work was supported by the ICTP Associate scheme.

REFERENCES

De Félice P. (1999) *La pluie au Sahel. Ecologie et agronomie appliquée, l'*Harmattan, pp. 144.

Gaye A.T. and S. Fongang (1997*) Some aspects of interactions between tropical region and temperate zones in northern hemisphere winter season. Proceedings 22nd conference on hurrican and tropical meteorology,* 19-23 may 1997,Colorado, 232-233.

Kalnay, E., (1996) *The NCEP/NCAR 40-years Reanalysis Project. Bull.* Amer. Meteor. Soc., 77, 437–471.

Meier F. and Knippertz P. (2008) Dynamics and predictability of a heavy dry season precipitation event over West Africa: Sensitiviy studies with a global model. Mon. Wea. Rev., 137, 189–206.

Skamarock W.C. and coauthors (2008) *A Description of the Advanced Research WRF Version 3. NCAR technical note NCAR/TN–475+STR.*

Thorncroft C.D. and H.A. Flocas (1997) *A case study of Saharan Cyclogenesis.* Mon. Wea. Rev., 125, 1147–1165.

REGIONAL CLIMATE MODELLING FOR IRELAND USING A REPRESENTATIVE CARBON PATHWAYS APPROACH

R.F. Teck and J. Sweeney

CLIMATE CHANGE PERSPECTIVES FROM THE ATLANTIC:
PAST, PRESENT AND FUTURE
Jose María Fernández-Palacios, Lea de Nascimento, José Carlos Hernández,
Sabrina Clemente, Albano González & Juan P. Díaz-González (coords)
Servicio de Publicaciones, Universidad de La Laguna – 2013

ISBN: 978-84-15910-54-1
pp. 699-708

Keywords: EC-EARTH, WRFV3.1.1, CLWRF.

INTRODUCTION

A key limitation of Global Climate Models (GCM's) is the fairly coarse horizontal resolution, typically 3.75° by 2.5° (500 km x 300 km). For practical planning, countries require information on a much smaller scale than GCM's are able to provide. One of the solutions is to dynamically downscale the output from the GCM using a Regional Climate Model (RCM).

Climate and forecasting applications share a common ancestry and also build on the same physical principles. Nevertheless, climate research and forecasting are commonly seen as different applications. The concept of «seamless prediction» (cf. WCRP) is emerging to forge forecasting and climate change into a joint topic.

The need for an Earth System model is recognized by various ECMWF Member States (MS). A consortium with representatives from 11 MS is formed in which the seasonal forecast system of ECMWF (system 3) is developed into an earth system model. The project, which is named EC-EARTH, has a general objective to develop a global Earth System model consisting of the: European Centre for Medium Range Weather Forecasts (ECMWF) atmospheric general circulation model, the Nucleus for European Modelling of the Ocean (NEMO) developed by the institute Pierre Simon Laplace (IPSL) as the ocean component, a sea-ice model, a land model, and an atmospheric chemistry model (see http://ecearth.knmi.nl).

The aim of this work is to provide dynamically downscaled RCM output data for use in other disciplines such as: biodiversity mapping, forestry pest and disease control, water resource management etc. and to use the output of the most up to date (2012) CMIP5 European Global Climate Model, 'EC-EARTH'.

Met-Eireann the Irish Meteorological Service, which is a member of the EC_EARTH consortium and ICHEC, the Irish Centre for High End Computing have provided us with the Representative Carbon Pathway (RCP) EC_EARTH output data. This has been dynamically downscaled to a scale more use-

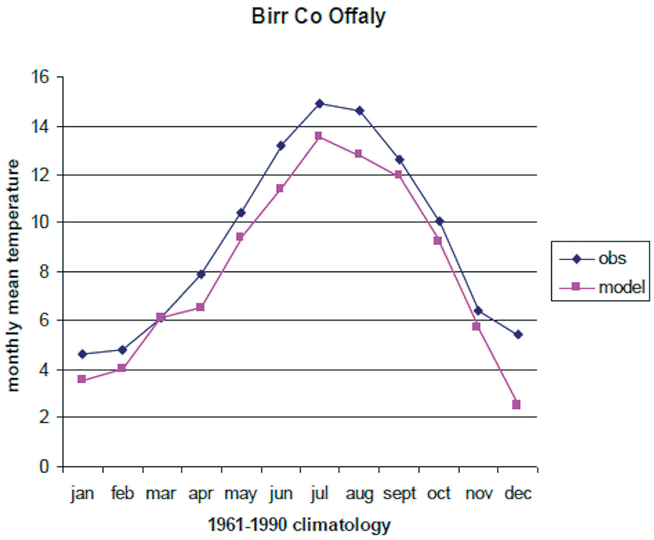

Fig. 1. This is a comparison between observed mean temperature at Birr Co Offaly Ireland (1961-1990) and EC_EARTH – CLWRF modelled 1961-1990 mean temperature for the same location.

ful to the local environment (10km x 10km) through the use of a Regional Climate Model (RCM). The model is the Weather Research Forecasting Model (WRFV3.1.1).

In the past GCM's have relied upon hypothetical scenarios, Special Report on Emission Scenarios (SRES) based on four future predictions of world development: A1, A2, B1, B2. The SRES scenarios, however, do not encompass the full range of possible futures: emissions may change less than the scenarios imply, or they could change more? Current thinking within the Intergovernmental Panel on Climate Change (IPCC) has resulted in a new approach to scenarios: choosing a handful of emission trajectories, known as Representative Carbon Pathways (RCP's). The RCP's then became the basis for a series of new climate runs in the latest climate models, such as the EC-EARTH GCM. The new choice of scenarios has five emission trajectories to focus on and have labeled them based on how much heating they produce at the end of the 21st century – Four future runs (2005 -2100): 8.5, 6, 4.5 and 2.6 watts per meter squared (Wm^{-2}) and an Historical run (1870-2005). At the high end, by the end of the 21st century in the case of the 8.5 Wm^{-2} RCP, carbon dioxide levels rise to 1,300 parts per million.

The present research has sought to dynamically downscale the Historical (RCP) output from the EC- EARTH GCM for the period 1961 – 1990 for Ireland and the UK. As all models (regional and global) suffer from systematic error, climate change is evaluated by comparing the future simulations against the same models run in the current climate (i.e. over a reference period). The period 1961-1990 is usually taken as the reference and is used here as the climatological baseline for the 8.5 Wm^{-2} RCP 2041-2100 future predictions. This was carried out using The National Center for Atmospheric Research (NCAR's) Weather Research and Forecasting Model (WRFV3.1.1) as a regional climate model (RCM).

MODEL DESCRIPTION AND DETAILS

The version of WRFV3.1.1 used in this research encompassed the modification by CLWRF *SantanderMetGroup* (Fernandez *et al.,* 2011). The 1961- 1990 and 2041-2100 simulations utilized in the research used one domain with a 10km x 10km grid space with 28 vertical and 4 soil levels. The initial fields were obtained from the EC-EARTH ECMWF model and used for the lateral boundary conditions.

Precipitation processes on the grid scale are represented by the explicit moisture scheme WRF Single-Moment Class 3 (WSM3) following Hong *et al.* (2004). A major difference from other approaches is the diagnostic relationship for ice number concentrations that is based on ice mass content rather than temperature. Deep moisture convection is represented in the model by the Kain-Frisch parameterization (Kain and Fritsch, 1993). The scheme removes Convective Available Potential Energy (CAPE) which is calculated using the traditional, parcel-ascent method through vertical reorganization of mass. Cumulus parameterizations are theoretically valid for coarser grid scales (e.g. greater than 10km), where they are necessary to properly release latent heat on realistic time scales in the convective columns. In this research release times between cumulus physics calls are set to 5 minutes.

The Land-Surface model Noah LSM was developed by jointly by NCAR and NCEP, and is used in the operational North American Mesoscale Model (NAM). This is a 4-layer soil temperature and moisture model with canopy moisture and snow cover prediction. The scheme provides sensible and latent heat fluxes to the boundary-layer scheme Yonsei University (YSU) PBL (Hong *et al.,* 2006).

The YSU scheme has an explicit treatment of the entrainment layer at the top of the Planetary Boundary Layer and is responsible for vertical sub-grid-scale fluxes due to eddy transport in the whole atmospheric column, not just the boundary layer. YSU PBL produces a well-mixed boundary-layer profile. Sea surface temperature are based on the initial analysis fields provided in the EC-EARTH GCM and are updated within the analysis fields provided by NEMO to the EC- EARTH model. Both short and longwave-radiative effects are accounted for where clouds are explicitly represented in the model. Surface radiative fluxes are provided by the RRTM and Dudhia schemes, (Dudhia, 1989).

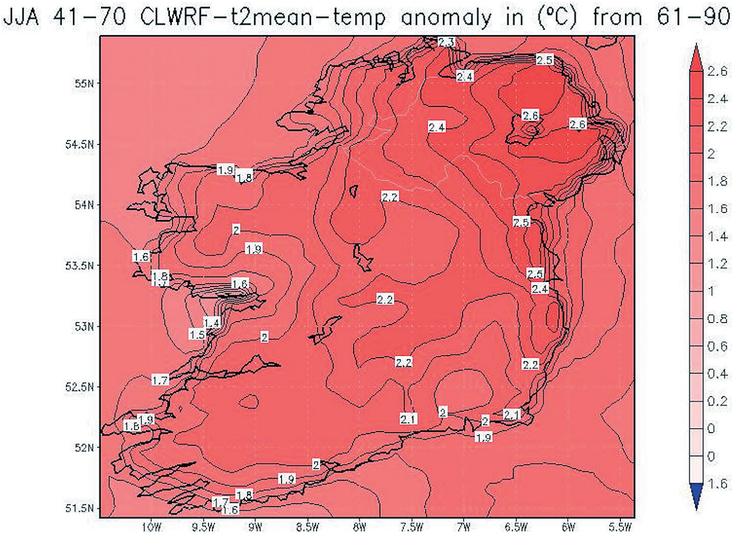

Figure 2. This is the 30 year CLWRF t2mean temperature anomaly 2041–2070 minus the CLWRF 1961-1990 temperature climatology for Ireland.

RESULTS

WRFV3.1.1 results by members of the modelling community in Ireland (Mooney *et al.*, Poster Presentation NCAR Tutorial, 2011). They observed that WSM5 together with LSM parameterization produced less bias in the summer period than WSM3 micro-physics scheme. Whilst Birr is close to the centre of Ireland, other observing stations close to the west coast Valentia and Belmullet show similar biases in the summer period. The conclusion being that the present parameterization schemes within the model results in the model having a 2° degree cool bias in the summer months, over the 1961-1990 period and a 1° to 1.5° cool bias in spring and autumn. Spatially there appears to be a good degree of correlation between the observed and model output.

Future 2041-2070 Mean Temperature Divergence from 1961-1990 Monthly T2mean

Fig. 2 shows a marked positive temperature differential between the north-east and south-west of Ireland between 2.6 and 1.8 °C for the 30 years 2041-2070, relative to the 1961-1990 temperature climatology. An increase of this magnitude

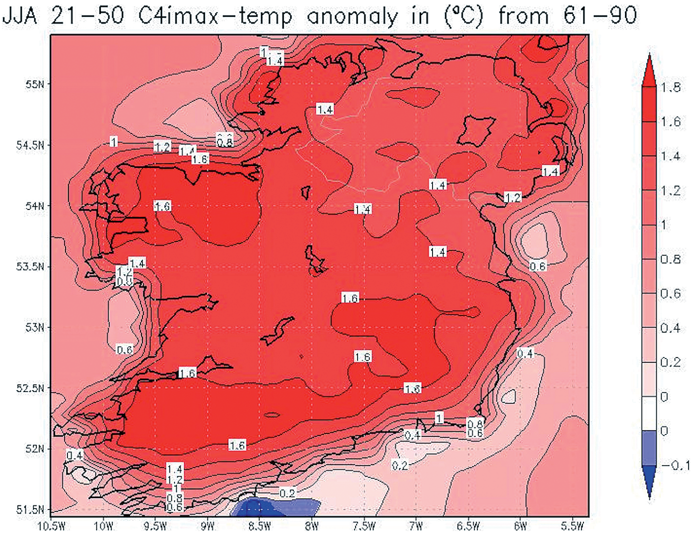

Fig. 3. 30 years 2021-2050 ECHAM5 and C4i RCA3 output minus the current 40 year RCA3 1961-2000 temperature anomalies. See http://www.c4i.ie.

would result in summer temperatures at Birr Co Offaly experiencing mean temperatures during the mid-century of 17 °C, an increase of 2.1°C.

The model shows greater bias from observed temperatures in summer (JJA) than either spring (AMJ) or autumn (SON). Similar biases have been observed in

Previous Modelling using ECHAM-5 C4i Data.

Previous modelling was undertaken by the Met-Eireann modelling group C4i using ECHAM-5 GCM data and RCA3 regional climate model. This focused on simulations of 1961-2000 and 2021-2100 using ECHAM5 A2 emission scenarios.

As can be seen, the mid-century climate is warming, particularly in the summer and also in the autumn (1.2 - 1.6 °C) with further increases up to 3.4 °C towards the end of the century (not shown). The warming is greatest in the south and east of the country. As compared with Fig. 2, the spatial distribution is south and east whereas Fig. 2 mid-century warming is from north-east to south west and of a greater magnitude (reflecting the difference between the A2 SRES scenario and 8.5 Wm^{-2} RCPs).

Fig. 4. Hylobius Abietis (Pine Weevil).

CHANGING CLIMATE: CONSEQUENCES FOR IRISH FORESTRY.

Forestry is an important commodity for Ireland's economy. Considerable investment has been made not only by the Irish state body Coillte but also by many small private investors. Forestry also plays a large part in Ireland meeting its commitments under the Koyoto agreement. Therefore, it is vital that forests are protected and well managed. It is important that pests and disease which threaten to destroy forestry are understood and measures taken to combat them. Understanding how temperatures and precipitation will change in the future is a key element to pest and disease control. One such pest is the Pine Weevil (*Hylobius Abietis*). This is the most damaging pest for young Irish conifer plantations. They feed on the bark of young trees and typically can kill 30%-100% of unprotected new plantings. Activity starts in the early spring when temperatures reach 8-9 °C and become very active at 13 - 16 °C. The development process can accelerate if temperatures become warmer in the early spring and carry forward into autumn. Weevils can consume five times as much tree bark at 20 °C than at 10 °C, therefore climate variability is an important aspect of their life- cycle and ultimately the forests.

ACKNOWLEDGEMENTS

This work is supported by: Intergrated Management of forest Pests Addressing Climate Trends (IMPACT). The Ireland-Wales Council, (2007-2013) and the European Regional Development Fund.

REFERENCES

DUDHIA, J., 1989: Numerical study of convection observed during the Winter Monsoon Experiment using a mesoscale two-dimensional model. *J. Atmos. Sci.,* 46, 3077–3107.

FERNANDEZ J. *et al.,* (2011), Coordinated regional climate downscaling using WRF: A contribution to the CORDEX initiative by the Spanish WRF community (CORWES). International Conference on the Coordinated Regional Climate Downscaling Experiment, Trieste, Italy.

HONG, S.-Y., J. DUDHIA, and S.-H. CHEN, 2004: A Revised Approach to Ice Microphysical Processes for Bulk Parameterization of Clouds and Precipitation, *Mon. Wea. Rev.,* 132, 103–120.

HONG, S,-Y., Y. NOH, and J. DUDHIA, 2006: A new vertical diffusion package with an explicit treatment of entrainment processes. *Mon. Wea. Rev.,* 134, 2318–2341.

KAIN, J.S., and FRITSCH J.M., 1993: Convective parameterization for mesoscale models: the Kain-Fritsch scheme. The Representation of Cumulus Convection in Numerical Models, Meteor. Monogr., No. 46, *Amer. Meteor. Soc.*, 165–170.

MOONEY, P, *et al.* 2011: Poster Presentation NCAR 2011: Sensitivity of surface temperature and precipitation to a selection of parameterization schemes.

EURO-CORDEX REGIONAL CLIMATE SIMULATIONS: HINDCAST 1990-2008

E. Katragkou, P. Zanis, I. Pytharoulis,
I. Tegoulias, T. Karacostas

CLIMATE CHANGE PERSPECTIVES FROM THE ATLANTIC:
PAST, PRESENT AND FUTURE
Jose María Fernández-Palacios, Lea de Nascimento, José Carlos Hernández,
Sabrina Clemente, Albano González & Juan P. Díaz-González (coords)
Servicio de Publicaciones, Universidad de La Laguna – 2013

ISBN: 978-84-15910-54-1 pp. 709-714

Abstract

We present results from the hindcast simulation 1990- 2008 performed with the WRF3.3.1 model within the framework of the EURO-CORDEX initiative. Model results are compared with the E-OBS observational dataset for two key climatic variables, 2m temperature and precipitation. First results are discussed thoroughly and compared with higher resolution (10 Km) regional climatic simulations performed over south-east Europe with the climate model RegCM3.
The WRF model has been forced by the ERA- INTERIM reanalysis (Simmons *et al.,* 2006). Table 1 presents the setup used for the WRF EURO-CORDEX simulation. Figure 1 shows the mean summer (JJA) 2m temperature averaged over the hindcast period (1990- 2008). The spatial variations are captured relatively well as compared to the observational dataset (Fig. 2). There seems to be some negative bias, especially over northern Europe during the summer and winter months.

Keywords: Regional climate, WRF, hindcast

ACKNOWLEDGMENTS

We acknowledge the Research Committee of AUTH for the financial support, the Scientific Computing Center of AUTH for the technical support and the EGI and HellasGrid infraestructures for the provision of computational resouces.

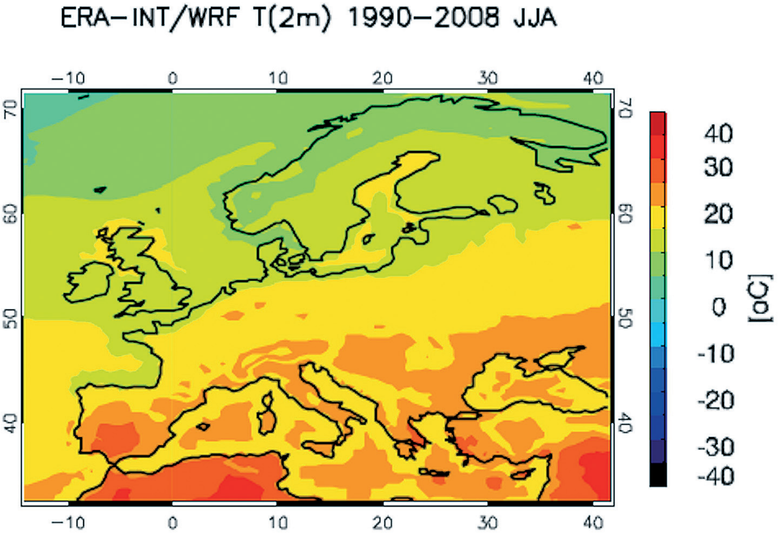

Figure 1. ERA-INT/WRF simulated mean summer (JJA) 2m temperatures for the hindcast period 1990-2008.

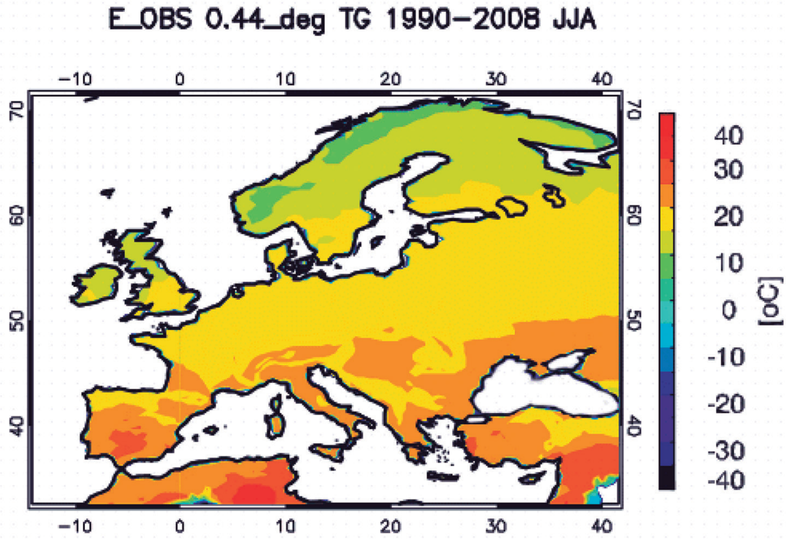

Figure 2. Mean summer (JJA) E-OBS temperature (TG) for the hindcast period 1990-2008.

TABLE 1. WRF3.3.1 set up for the COREX EUR-0.44 simulations

Phs/Dyn Options	Scheme
Microphysics	WRF-single moment 6-class
Radiation (SW/LW)	CAM
Surface Layer	MM5-Similarity
Land surface	NOAH LSM
Planetary BL	Yonsei University
Cumulus paramet	Kain-Fritsch

REFERENCES

Simmons, A., Uppala, S., Dee, D. and Kobayashi, S., 2006. ERA-Interim: new ECMWF reanalysis products from 1989 onwards. *ECMWF Newslett.*, 110, 25–35.

DYNAMICAL DOWNSCALING IN THE EASTERN MEDITERRANEAN AND THE MIDDLE EAST USING PRECIS REGIONAL CLIMATE MODEL

G. Zittis, P. Hadjinicolaou and J. Lelieveld

CLIMATE CHANGE PERSPECTIVES FROM THE ATLANTIC:
PAST, PRESENT AND FUTURE
Jose María Fernández-Palacios, Lea de Nascimento, José Carlos Hernández,
Sabrina Clemente, Albano González & Juan P. Díaz-González (coords)
Servicio de Publicaciones, Universidad de La Laguna – 2013

ISBN: 978-84-15910-54-1

pp. 715-724

Keywords: Dynamical down-scaling, climate change, feedbacks.

INTRODUCTION

The Eastern Mediterranean and the Middle East (EMME) are likely to be greatly affected by climate change, associated with increases in the frequency and intensity of droughts and heat waves. Since the region is socio-economically diverse and extreme climate conditions already common, the impacts will be disproportional. The variable topography (land alternating with major water bodies) and steep orography (from deserts to mountains several Km high) make the EMME a complex region hard to be well represented in the current Atmosphere-Ocean General Circulation Models (AOGCM) resolutions. In addition, this part of the world is an atmospheric circulation crossroad (influenced by North Atlantic and South Asian flows) so it is essential to create simulations using mesoscale - regional models of finer resolution, where local weather features can be simulated more realistically.

We performed simulations using the PRECIS (Providing Regional Climates for Impact Studies) regional climate model, based on the United Kingdom (UK) Met Office Hadley Centre HadRM3P model (Jones *et al.,* 2004) for the 20th and 21st centuries. PRECIS is freely available and has been ported to run on a PC (under Linux) with a simple user interface, so that experiments can easily be set up over any region of the globe. It applies the same formulation of the climate system as its parent AOGCM, HadCM3 (Collins *et al.,* 2005), which is also used to provide the lateral boundary conditions, and is driven by the IPCC SRES A1B emissions scenario. PRECIS accounts for the radiative forcing by changing concentrations of greenhouse gases, including ozone, and sulfate aerosols, and for interactions with the surface and deep soils. Results presented here are obtained from a PRECIS run over the period 1950–2099, applying a horizontal resolution of 0.22° latitude and longitude (about 25 km) and 19 vertical levels (Fig. 1).

In this paper we briefly present some of the future climate projections from our simulation with focus in temperature and precipitation. Moreover, trying to understand better the feedback mechanisms that may contribute to

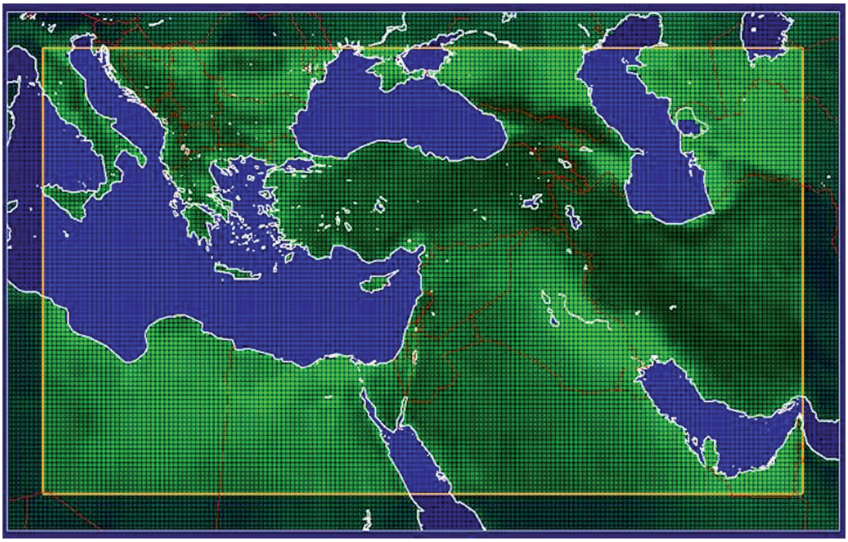

Figure 1. Geographic area and 0.22° latitude/longitude grid coordinates of the PRECIS regional cimate model, applied for the period 1950–2099. The outer eight rows of grid cells are a "buffer zone" (not included in our analysis) to circumvent inconsistencies between the global and regional models. The EMME domain.

these regional climate changes we have explored the role of soil moisture in the warming of the region.

We evaluate the model output with meteorological observations from the Climatic Research Unit (CRU) TS3.0 data (http://badc.nerc.ac.uk/data/cru/). This dataset offers the most complete, consistent and updated compilation of gridded precipitation and temperature data at the global scale in general and for the Middle East in particular (Tanarhte *et al.*, 2011). The 0.5° resolution data cover the period 1901-2006. The monthly time series of various climate variables include air temperature, precipitation, and vapor pressure, interpolated from surface observations.

A comparison between the PRECIS and CRU 30- year (1961-1990) climatology is presented in figures 2 and 3. The upper panels of Fig. 2 show the mean summer (JJA) maximum temperature (TX). In general, the model represents sufficient the CRU climatology. PRECIS overestimates summer TX mostly in the Arabic peninsula. The lower panels depict the mean winter (DJF) TN for the 1961-1990 period. Again the spatial patterns of the model and the observational dataset are very similar. Though, a small underestimation of the model for winter TN is observed in the Arabian Peninsula.

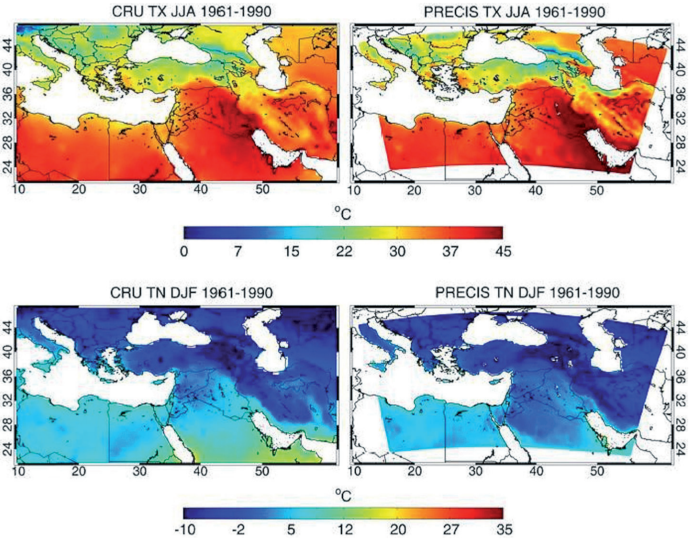

Figure 2. Patterns of the mean summer maximum (JJA, top) and mean winter minimum (DJF, bottom) temperatures. TX and TN respectively. The left panels are based on CRU data and the right panels on PRECIS output (Lelieveld *et al.*, 2012a).

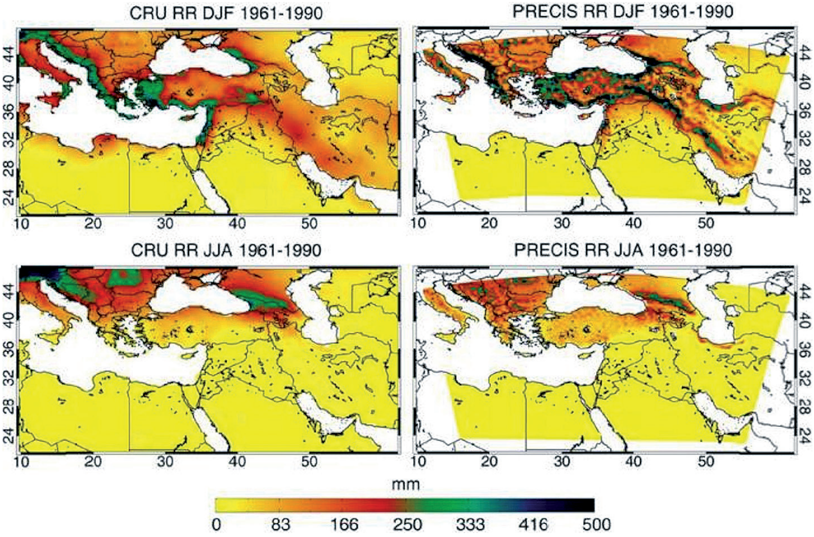

Figure 3. Patterns of the mean summer (JJA, top) and mean winter (DJF, bottom) precipitation (RR). The left panels are based on CRU data and the right panels on PRECIS output (Lelieveld *et al.*, 2012a).

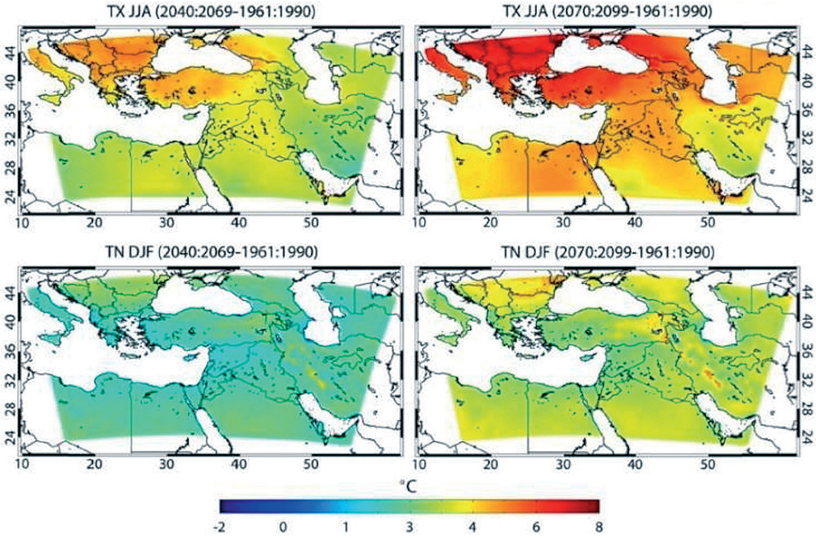

Figure 4. Patterns of changing mean summer maximum and mean winter minimum temperatures, TX (top) and TN (bottom), respectively. The left panels show the mean changes for 2040-2069 and the right panels for 2070-2099 relative to the 1961-1990 control period (Lelieveld *et al.*, 2012a).

More extensive comparison of the PRECIS output against point observations in the EMME and ensemble model output for the European part of the domain, with a focus on temperature, precipitation and weather extremes can be found in Lelieveld *et al.*, (2012a) and (2012b).

Average winter and summer precipitation (RR) are presented in Fig. 3. During winter PRECIS is wetter than CRU. Because of the paucity of rain gauge data in many mountainous regions, however, it is not certain to what extent PRECIS overestimates RR. For most of the region summers are dry. Only in some continental locations in the Balkans and the Caucasus convective storms in summer contribute significant amounts of rain. In the southern part of the domain, rainfall deficits and summer droughts are commonplace.

Future climate projections from PRECIS model are presented in the following figures. Summer TX warming ranges from 3-5 °C in the mid-century period (2040-2069) to 3.5-7 °C by the end of the century (2070- 2099). Winter TN warming is less in this region with a maximum 3-4 °C by the end of the century. In each period, this warming is more spatially uniform for winter TN, while for TX it is most pronounced at latitudes north of 36-38 °N (reaching 6-7 °C in the Balkans, Turkey and the Caucasus by 2070-2099) and

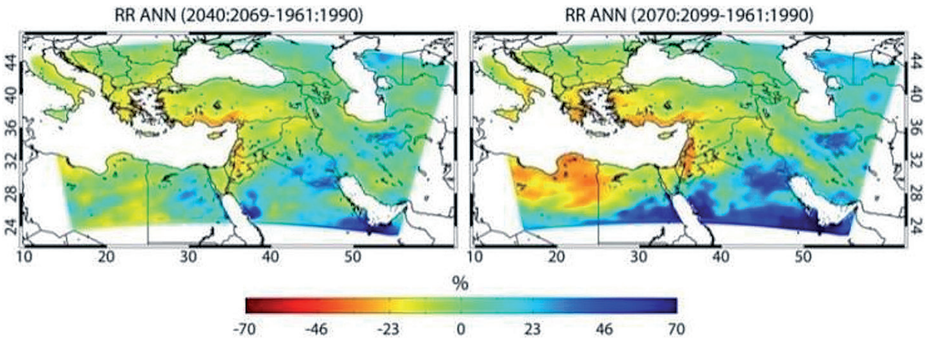

Figure 5. Same as Fig. 4 for mean annual precipitation (Lelieveld *et al.*, 2012a).

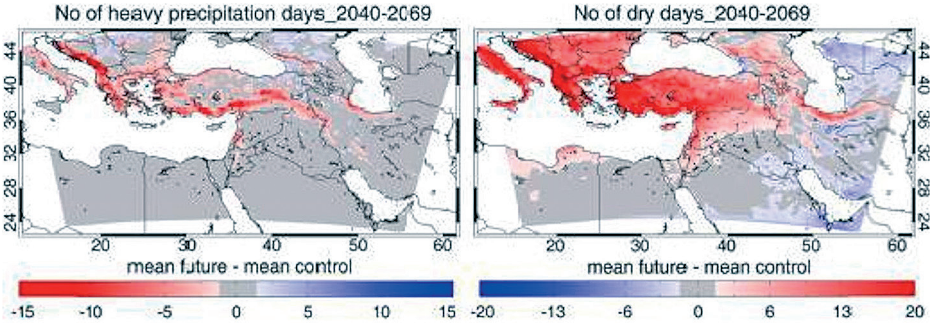

Figure 6. Patterns of changing number of days per year with heavy precipitation (RR>10mm, left panel) and number of dry days (RR<1mm, right panel), calculated from PRECIS output, showing the mean changes for 2049-2069 relative to the control period 1961-1990 (Lelieveld *et al.*, 2012a).

weaker in the southern EMME (~3.5 °C in Libya, western Saudi Arabia and southern Iran).

The modeled changes in precipitation exhibit a large variability in space (Fig. 5). The strongest drying is projected around the eastern Mediterranean, the coastal Levant and North Africa (−10% to −25% in 2040-2069 and −25% to −35% in 2070-2099). Another notable feature is the projected, statistically significant, strong increase in precipitation throughout the southeastern part of the domain, related to the northward expansion of moisture from the tropical rain belt. Note, however, that these relative changes should not be over- interpreted since rainfall during the control period in the southern EMME is minor.

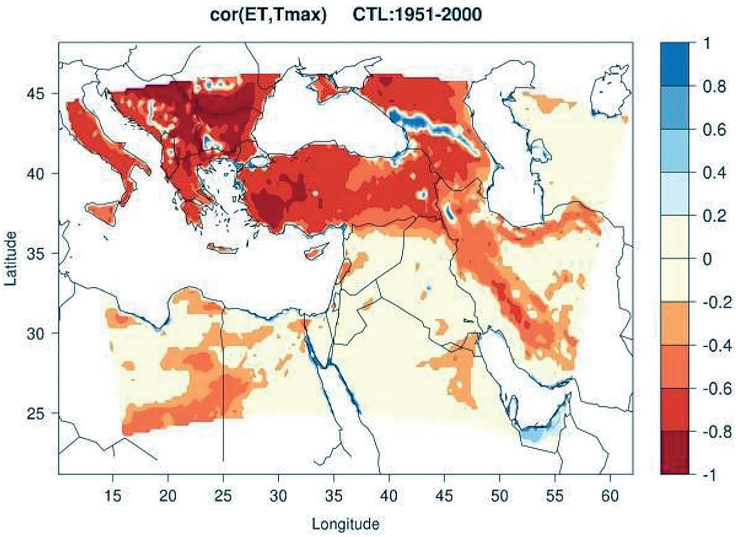

Figure 7. Correlation coefficients between maximum temperature and evapotranspiration for the 1951-2000. Significant correlations (95% confidence level) are colored red and blue (Zittis *et al.*, 2012).

The annual number of days with less than 1 mm precipitation for the 1961-1990 period exceeds 300 over the southern and eastern part of the domain (not shown), demonstrating the near-absence of rainfall. In future (Fig. six – right panel) this is not expected to change much apart from a small decrease in the number of dry days (up to ~10 days/year) around the Persian Gulf. In the northern EMME, mainly in the Balkans, Turkey, Cyprus, Lebanon and Israel, the number of dry days may increase (10-20 days/year).

The number of days with heavy precipitation (>10 mm/day) is expected to decrease in the high- elevation areas of the EMME (Fig. 6 – left panel).

Trying to attribute the north-south gradient of climate warming (Fig. 4 – top panels) we explored the connection between soil moisture and temperature. Regions of higher warming concur with regions of more pronounced drying considering precipitation amounts (not shown) and not percentages. Such regions occur in northern EMME. A well-known type of feedback involves soil moisture – atmosphere interactions. When the soil water content and evapotranspiration are decreased, as our projections suggest for north EMME, near surface air temperatures may be enhanced due to reduced evaporative cooling.

We present here a common diagnostic of the land- atmosphere coupling, the correlation coefficient between evapotranspiration (ET) and near surface air temperature (Seneviratne *et al.*, 2010; Jaeger and Seneviratne, 2011). When ET is

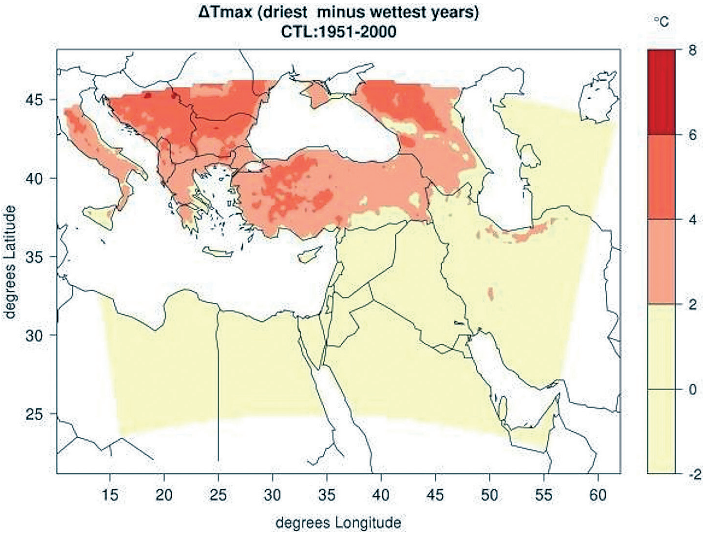

Figure. 8. Composite analysis of TX. The difference between the ten driest and ten wettest years is shown for the period 1951-2000 (Zittis *et al.*, 2012).

controlled by soil moisture a strong anti- correlation is expected. On the other hand, when there is abundant soil moisture and evaporation is controlled by atmospheric conditions the correlation is positive. Low correlations indicate no coupling. Fig. 7 depicts the correlation coefficients between summer ET and TX for the 1951-2000 period. Significant negative correlations that indicate strong connection are found in the regions that may experience higher warming (Italy, Balkans, Anatolia, Caucasus).

In addition, we created composite maps of TX (Fig. 8) trying to highlight the effect of extreme dry and wet years. The mean TX difference for the ten driest minus the ten wettest years has high positive values again in the northern part of our study area indicating there that during years of soil moisture deficits TX is enhanced.

ACKNOWLEDGEMENTS

The research leading to these results has received funding from the European Research Council under the European Union’s Seventh Framework Programme (FP7/2007-2013) / ERC grant agreement n° 226144 (C8 Project).

REFERENCES

Collins M., Booth B.B.B., Harris G.R., Murphy J.M., Sexton D.M.H., Webb M.J. (2005) Towards quantifying uncertainty in transient climate change. *Clim. Dyn.* 27:127–147.

Jones R.G., Noguer M., Hassell D.C., Hudson D., Wilson S.S., Jenkins G.J., Mitchell J.F.B. (2004) Generating high resolution climate change scenarios using PRECIS. Met Office Hadley Centre, Exeter.

Lelieveld J., Hadjinicolaou P., Kostopoulou E., Chenoweth J., El Maayar M., Giannakopoulos C., Hannides C., Lange M.A., Tanarhte M., Tyrlis E., Xoplaki E. (2012a). Climate change and impacts in the Eastern Mediterranean and the Middle East. *Clim. Change* 114:667-687. doi: 10.1007/s10584-012-0418-4.

Lelieveld J., Hadjinicolaou P., Kostopoulou E., Giannakopoulos C., Tanarhte M., Tyrlis E. (2012b) Extreme heat in the eastern Mediterranean and Middle East. *Reg. Env. Change* (submitted).

Seneviratne S.I., Corti T., Davin E.L., Hirschi M., Jaeger E.B., Lehner I., Orlowsky B., Teuling A.J. (2010) Investigating soil moisture–climate interactions in a changing climate: A review. *Earth Sci. Rev.* 99(3-4):125-161. doi:10.1016/j.earscirev.2010.02.004.

Tanarhte M., Hadjinicolaou P., Lelieveld J. (2012) Intercomparison of temperature and precipitation datasets based on observations in the Mediterranean and the Middle East. *J. Geophys. Res.* 117: D12102. doi:10.1029/2011JD017293.

Zittis G., Hadjinicolaou P., Lelieveld J. (2012) Role of soil moisture in the amplification of climate warming in the Eastern Mediterranean and the Middle East. Clim Dyn. (under submission).

WORKSHOP PICTURES

Visit to ITER (Institute of Technology and Renewable Energies),
3rd October 2012

Visit to ITER (Institute of Technology and Renewable Energies), 3rd October 2012

Visit to Teide National Park, 3rd October 2012.

SERVICIO DE PUBLICACIONES
UNIVERSIDAD DE LA LAGUNA

ULL Universidad de La Laguna

CAMPUS ATLÁNTICO TRICONTINENTAL
CANARIAS 2010/2015
CAMPUS DE EXCELENCIA DE ÁMBITO REGIONAL